

Proceedings of the TensiNet Symposium 2023

TENSINANTES2023

**Membrane architecture: the seventh established
building material. Designing reliable and sustainable
structures for the urban environment**

7-9 June 2023

Nantes Université

ISBN 9789464787313

Copyright © 2023 by the authors

Published by TensiNet Association and Nantes Université.

Peer-review under responsibility of the TensiNet Association.

Proceedings of the TensiNet Symposium 2023

TENSINANTES2023

Membrane architecture: the seventh established building material. Designing reliable and sustainable structures for the urban environment

7-9 June 2023

Nantes Université, Nantes, France

Editors

Evi Corne, Marijke Mollaert, Carol Monticelli, Bernd Stimpfle,
Jean-Christophe Thomas

Scientific Committee

Prof Adriana Angelotti, Ass Prof Paolo Beccarelli, Dipl Ing Arch Katja Bernert,
Dr Alexis Bloch, Prof Heidrun Bögner-Balz, Dr Stéphanie Bonnet, Dr Rabah Bouzidi,
Roberto Canobbio, Dr Mathilde Chevreuil, Prof John Chilton, Prof Jan Cremers,
Prof Lars De Laet, Dr Olivier Flamand, Prof Gunther Filz, Dr Ing Ann-Katrin Goldbach,
Dr Laurent Gornet, Prof Peter Gosling, Prof Anh Le Van, Prof Josep Llorens,
Prof Marijke Mollaert (coordinator), Prof Arch Carol Monticelli (coordinator),
Prof Nicolas Pauli, Ass Prof Arno Pronk, Dr Monica Rychtáriková, Prof Franck
Schoefs,

Dipl Ing Bernd Stimpfle, Prof Natalie Stranghöner, Ass Prof Martin Tamke,
Prof Patrick Teuffel, Dr Jean-Christophe Thomas (coordinator), Dr Ing Jörg Uhlemann,
Adjunct Prof Salvatore Viscuso, Prof Alessandra Zanelli

Sponsors

Platinum



Gold



Silver



Copper



Support

TENSINANTES2023 is financially supported by Nantes Université & Nantes Métropole



Proceedings of the TensiNet Symposium 2023

TENSINANTES2023

**Membrane architecture: the seventh established
building material. Designing reliable and sustainable
structures for the urban environment**

7-9 June 2023

Nantes Université

The 7th International TensiNet Symposium "Membrane architecture: the seventh established building material. Designing reliable and sustainable structures for the urban environment" took place at Nantes Université (France) from Wednesday 7th till Friday 9th June 2023.

TENSINANTES 2023 focuses on the significance and potential of fabrics and foils as established building materials and promotes the use of tensile structures in a world of constant change and adaptation. The optimal use of materials, the realisation of a Eurocode, sustainability and reuse are some of the topics which are covered, ranging from research over practical experiences to realisations.

This three-day event allows prominent experts from the world of architecture and engineering to present inspiring projects, to demonstrate the multitude of possibilities offered by lightweight structures, as well as to show recent research results in the domain of fabrics and foils.

The symposium is organised around 3 main topics including 5 keynote lectures & 47 lectures held in plenary and parallel sessions

- **Structural membrane:** contemporary, innovative, adaptive daring and impactful solutions
- **Tensioned membrane structures:** the seventh building material
- **Structural membrane:** an answer to issues of the 21st century

The papers have been brought together by topic and in the order in which they were presented.

Proceedings of the TensiNet Symposium 2023

TENSINANTES2023

Table of content

Structural membrane: contemporary, innovative, adaptive daring and impactful solutions

Bouncing Bridge: ephemeral, autonomous and self-supporting pneumatic temporary structure11
<i>Grégoire Zündel and Ramon Sastre</i>	
Advanced tools for futuristic skins – ETFE12
<i>Massimo Maffeis, Antonio Diaferia, Nicola Todesco</i>	
Modeling of impacts on tensile structures21
<i>Adam Bown, Adrian Cabello, Artem Holstoi</i>	
Porto Pi shopping center's floating pergolas33
<i>Juan García-Lastra Zorrilla, Juan Rey-Rey, Alejandro Minguez</i>	
PumpItUp, gite mobile for the European cultural capital Esch-sur-Alzette 202245
<i>Bernd Stimpfle</i>	
The integration of CAD and FEA for lightweight design and analysis57
<i>Ann-Kathrin Goldbach, Kai-Uwe Bletzinger</i>	
Swatch Omega Headquarters-Multifunctional ETFE-modules in the building envelope	65
<i>Karsten MORITZ, Koffi Alate</i>	
Temporary structure Grand Palais Éphémère77
<i>Patrick Vaillant, Beatriz Arnaiz, Feike Reitsma</i>	
Affine minimal surfaces: an intuitive family of shapes for tensile architecture84
<i>Cyril Douthe, Rémi Belloc, Ken'ichi Kawaguchi</i>	
Value enhancement of the roof of the CC Le Polygone Montpellier93
<i>Fabián Ascaso, Beatriz Arnaiz, Ramon Julián, Feike Reitsma</i>	
Optimisation of tensegrity systems with tensioned fabrics	...102
<i>Fevzi Dansik, Meltem Sahin, Caglar Samat</i>	
Retractable membrane roofs as urban shading device	...114
<i>Liu Dongyuan, Gregor Grünkorna, Julian Lienhard, Ata Chokhachian, Thomas Auer</i>	
Use of Parametric Design in Design to Production Process of a Membrane Façade	...127
<i>Milan Dragoljevic, Roberto Canobbio</i>	
Corolla, the soft-robotic coworking pod	...141
<i>Paolo Beccarelli, Ofir Albag, Martin Huba, Roberto Maffei</i>	
The Wave Pavilion from 2014 to 2023: origins, realization and reuse	...151
<i>Mathieu Lemunier</i>	
TensyDome: A pavilion combining tensegrity ring and tensile architecture	...161
<i>Nicolas Pauli</i>	
Beyond bending: tension. Membrane structures 1	...173
<i>Josep Ignasi de Llorens Duran</i>	

Tensioned membrane structures: the seventh building material

Computational design workflow for a complex cable network	...186
<i>Jef Rombouts, Oriane Guidet, Ludovic Regnault, Klaas De Rycke</i>	
Development and validation of an experimental methodology for the characterization and FEM analysis of fibre-reinforced architectural meshes	...195
<i>Salvatore Viscuso, Carol Monticelli, Alessandra Zanelli, Alberto Fiorenzi</i>	
Parametric workflow approach in membrane design, from details to construction	...208
<i>Rémi Journo</i>	
Simulation of functionally graded CNC-knitted membranes	...220
<i>Yuliya Sinke, Martin Tamke, Mette Ramsgaard Thomsen</i>	
Testing Parameters for uniaxial short-term tensile tests of ETFE foils and their connections	...234
<i>Dominik Runge, Jörg Uhlemann, Natalie Stranghöner</i>	
Living in the 7th element: Hans-Walter Müller's pneumatics	...246
<i>Katja Bernert</i>	
Finite element modelling of inflatable beams up to the ultimate stability phase	...254
<i>Laurent Gornet, Jean-Christophe Thomas</i>	
Analytical, numerical and experimental study of inflatable panels	...261
<i>Paul Lacorre, Anh Le van, Rabah Bouzidi, Jean-Christophe Thomas</i>	
The calculation of large cable reinforced gas storage systems	...273
<i>Jürgen Holl</i>	
Textile covers of biogas storage tanks - Interaction between Membrane behaviour and Operation of the Gas Membrane	...282
<i>Rosemarie Wagner, Kai Heinlein</i>	
Design and execution of membrane structures acc. to CEN/TS 19102	...291
<i>Jörg Uhlemann, Bernd Stimpfle, Natalie Stranghöner</i>	
Determination of ULS values of ETFE membrane structures acc. to Eurocode using tensile strength measurements in quality control of production	...303
<i>Torsten Balster, Carl Maywald, Lazarev Delche</i>	
On the design of membrane structures with the partial safety factor concept – a parameter study on the influence of structural and probabilistic properties	...312
<i>Martin Fueeder, Max Teichgraber, Daniel Staub, Kai-Uwe Bletzinger</i>	
Characterization of polyethylene structure membrane	...322
<i>Sherryl Patton</i>	
Practical application of a stress-ratio dependent adaptive material model in the structural analysis of textile structures	...334
<i>Jörg Uhlemann, Mehran Motevalli, Natalie Stranghöner, Daniel Balzan</i>	

Structural membrane: an answer to issues of the 21st century

- Textile Architecture with or versus today challenges in built environment** ...345
Rosemarie Wagner
- The Pathways to Zero Carbon for Tensioned Membrane Architecture: ongoing actions and next steps** ...355
Bruce Danziger and Carol Monticelli with Beatriz Ferreyra Vargas and Nathaly Michelle Rodriguez Torres
- Integrating sustainability aspects in the teaching of lightweight structures and their comparison with common structures** ...356
Heidrun Bögner-Balz, Sarah Von Der Weth, Karsten Moritz
- The environmental performance of membrane structures** ...367
Zehra Eryuruk, Marijke Mollaert
- A comparative LCA between a Textile Façade Retrofit and conventional solutions** ...380
Giulia Procaccini, Carol Monticelli
- ATLAS architectural membrane as a core element for larger and energy efficient air domes** ...392
Alexandra Sonnenberg
- T-shade: experimental case study conducted to reuse t-shirts as a tensile-shading system** ...406
Amirhossein Ahmadnia, Gergely Mátyás Jelinek Jelinek, Aina Radovan, Salvatore Viscuso, Alessandra Zanelli
- Comparison of PE coated PE weave to PVC coated PES weave** ...417
Rogier Houtman
- Advancing the Design of Sustainable ETFE Membrane Structures: Insights from the Lighten Consortium Project** ...423
Mohammad Hosein Nejabatmeimandi, Alessandro Comitti, Luis Seixas, Adrian Cabello, Adam Bown
- Lightweight ideas for a built environment beyond concrete** ...435
Katja Bernert
- How lightweight architecture contribute to sustainability & decarbonization strategy.**447
Thomas Bonneville
- 6dTEX - Sustainable Composite Structures from 3D Print on 3D Textile** ...454
Claudia Lueling, Sascha Biehl, Roxana Tennert, Gözdem Dittel, Marina Chernychova, Thomas Gries
- Architecture for pigs** ...467
Maxime Durka
- An innovative solar shading device for outdoor thermal comfort** ...476
Adriana Angelotti, Alara Kutlu, Salvatore Viscuso, Andrea Alongi, Alessandra Zanelli
- Suntex: weaving solar energy into building skin** ...486
Rogier Houtman, Ahmed Mohamed Ahmed, Pauline van Dongen, Mariana Popescu
- Integration of the Fog water harvesting system in lightweight structure design for emergency camps** ...499
Maria Giovanna Di Bitonto, Nathaly Michelle Rodriguez Torres, Alara Kutlu, Nicolò Elio Giorgiotti, Alessandra Zanelli
- Challenges of measuring sound absorption of ETFE membranes in a laboratory** ...512
Yannick Sluyts, Monika Rychtarikova, Christ Glorieux
- Greentexx: Advanced tensile architectural membranes for active and passive cooling of the outdoor & indoor environments via vertical gardens** ...522
Benny Picke

TOPIC 1
Structural membrane:
contemporary, innovative, adaptive daring and impactful
solutions



Bouncing Bridge: ephemeral, autonomous and self-supporting pneumatic temporary structure

Grégoire Zündel*, Ramon Sastre**

*Atelier Zündel Cristea, Paris, France

**Retired Prof., Universitat Politècnica Catalunya, Spain

Abstract

Our lecture is about the genesis of the Bouncing Bridge project as well as a few other inflatable structure projects, born from this first experience.

The Bouncing Bridge project consists of three tubular pneumatic 3D rings, 30 m diameter, with a trampoline in their interior. Each ring has a double symmetrical 3D ring with two lower points touching the water and the other two high points, at the middle, of the ring. Once the concept achieved, the architects started to look for a firm who could build the project. Eventually, they decided to order a variant of the project to a Catalan firm, near the French border, "T&P Construcció Tèxtil s.c.p." whose CEO was Ton Miserachs, an industrial man who, through years, became a friend. During the detailed studies we had to change the initial shape. We sacrificed the double symmetry to gain stability. The ring passed from a double symmetry to a single symmetry, creating a piece of tube straight instead of the lower points, allowing to maintain better stability. The higher points stayed.

Keywords: Trampoline, tube, pressure, welding, equilibrium, patterning



Figure 1: General view. Original project.



Figure 2: General view. Model 10 m.

References

- [1] AZC, Paris, *Peace Pavillion*, London, Project, Analysis, R. Sastre, 2013.
- [2] T&P, *Movable Inflatable Construction*, analysis R. Sastre, 2006
- [3] Q.-T. Nguyen, J.-C. Thomas, and A. Le Van. "Inflation and bending of an orthotropic inflatable beam". *Thin-Walled Structures*, 88 (0), 2015, 129 - 144.



tensinantes2023 : TensiNet Symposium 2023 at Nantes Université

Membrane architecture: the seventh established building material. Designing reliable and sustainable structures for the urban environment.

Proceedings of the Tensinet Symposium 2023

TENSINANTES2023 | 7-9 June 2023, Nantes Université, Nantes, France

Jean-Christophe Thomas, Marijke Mollaert, Carol Monticelli, Bernd Stimpfle (Eds.)

Advanced tools for futuristic skins - ETFE

Massimo Maffeis*, Antonio Diaferia^a, Nicola Todesco^b

*CEO Maffeis Engineering, via Mignano, 26, 36020 Solagna, Italy, m.maffeis@maffeis.it

^a Lead Designer Maffeis Engineering, via Mignano, 26, 36020 Solagna, Italy

^b Senior Designer Maffeis Engineering, via Mignano, 26, 36020 Solagna, Italy

Abstract

A large experience with textile architecture with the large number of requests of challenging design are the base to create interesting tools related each other to develop and control the entire process of design. In Maffeis this has been our first mission dedicating and investing time with a team that step by step have recognised what the process needs. A series of specific digital tools integrated each other were developed to fulfil the expectation of the clients at each level of design (from concept design stage to a construction design stage). Built the idea, value engineering, real-time structural analysis within parametric model is the most important action where we have focused our effort to optimize at the best time, cost and expectation of the client. Following case studies are presented: Veronafiére Marble Plaza and Google Sidewalk as projects focused on ETFE that are the reference of the design approach above specified. Marble Plaza at Veronafiére is the new shading structure for the exhibition centre of Verona, Italy. Featuring an iconic design, the roof is composed by Voronoi-shaped modules of ETFE cushions supported by 45m height tree-shaped steel columns. Google Sidewalk in Toronto. A "raincoat" designed by architecture studio Partisans. The new prototypes are intended to respond to the harsh weather endured in the city's winter months. "It's cold," said Sidewalk Labs in a project description. "The weather plays a big role in determining how much time we spend outdoors." With much of the Sidewalk Toronto development intended to be wooden construction as part of its environmental and sustainable strategy – these adjustable and protective structure are intended to protection to the buildings, as well as pavements.

Keywords: pneumatic structures, ETFE, lightweight structures, performance, conceptual design, construction design, form finding, optimization, parametric design, manufacturing.

1. Introduction

Textile architecture has always represented innovation. From tools to structures, all those who have ventured to learn about it and use it, improving it, have appreciated its enormous versatility. Its evolution, in terms of quality and use, is the challenge par excellence; and challenges are well suited to young people who better than others are predisposed to seek new points of view and new stimuli. Design, in a vision of the near future will be increasingly linked

Membrane architecture: the seventh established building material. Designing reliable and sustainable structures for the urban environment.

to the search for optimization with the goal of innovative, simple and economical solutions. The parameterization of the design process is only the beginning of what will become our business, and textile architecture will always be the great protagonist. It will be so because the power of computational methods will push it to cover larger and larger surfaces and overcome greater lengths; improvements in processing methods will increasingly refine its resistant qualities and the evolution of equipment will make it easy to use.

It is with parameterization that the methods of artificial intelligence will also enter our world; parameterization that may concern not only actual structural aspects but extend to architecture and the use of materials in a context of absolute freedom. These were the prerequisites of the design of Veronafiore Marble Plaza in Verona and Google Sidewalk in Toronto, and all the works that we now design in the world with a young and highly motivated team.

The freedom of design understood as expansion to the improbable of possible solutions allows us to develop more and more critique of the finished product, never surrendering to an acceptable solution, always pushing further and further toward achieving the best solution.

The design process will no longer be an activity linked to experience alone but will involve professionalism, skills, energy and enthusiasm by linking different knowledge and ages, and it is with these criteria that it is now possible to imagine a future in our profession.

Until a few years ago, it was unthinkable to be able to conceive, study and build very light and strong structures for covering large areas without imposing investments in engineering and technology. Today, operational availability and acquired knowledge allow us to see almost no limits to our potential with the knowledge that only competence and shared choices can guarantee us a future.

2. Veronafiore Marble Plaza

The “New Entrance Re Teodorico” plaza on the south side of the Veronafiore Trade Show grounds in Verona, an international leader in the agriculture and agro-food sector, hosting 45% of Italian trade shows in the two fields.



Figure 1: Veronafiore Marble Plaza - Completed project

Membrane architecture: the seventh established building material. Designing reliable and sustainable structures for the urban environment.

The project is a steel roof structure, L-shape in plan, that extends over an area of 6,750 square meters. The design is based on merging the two concepts of an undulating veil and an organic surface. The wavy effect was created with high and low points in the structure, that are required for drainage. The organic shape was created by using a Voronoi pattern highlighting diversity as a visual effect. The macro modules with each one low point were repeated several times to facilitate fabrication and mitigate cost but from the visual side this is not noticeable. Repetition is a key effect of the structure, but the observer's eye cannot catch this repetition thanks to the different arrangement of the columns.



Figure 2: Views of the project

The 17m high steel columns are designed to represent trees in the woods with their tapered upper columns. At the top of the columns diagonal members project to support the roof, mimicking tree branches. The columns are located under the low point of the canopy and the drainage of the Voronoi occurs through the columns core into the ground. The steel columns are painted in different brown Pantone tonalities to resemble the effect of being in the woods, with brighter colours at the entrance and slightly darker colours as you move further down the Plaza.

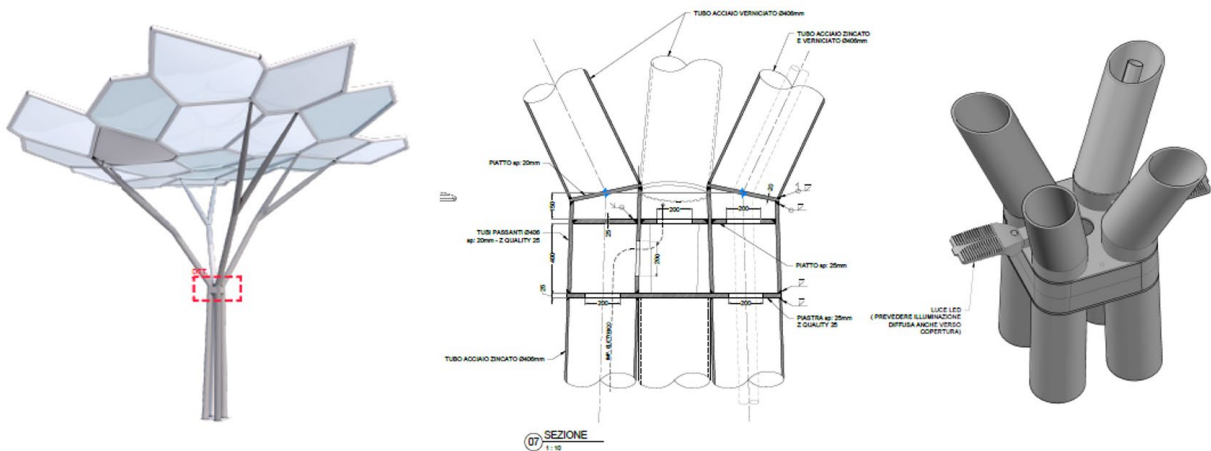


Figure 3: Details of the columns

Membrane architecture: the seventh established building material. Designing reliable and sustainable structures for the urban environment.

For the Canopies, three different shades of fritted ETFE were used in a 2-layer composition to emphasise the differentiation between the macrostructures. The ETFE cushions are representing an undulating veil from the top and from underneath representing tree leaves. The different shading options were analysed with an environmental analysis tool to create a comfortable area in winter and summer for the visitors. Outdoor comfort is complex to assess. Unlike what happens in indoor environment, people are exposed to a multitude of variables when spending time outdoors. These variables are difficult to foresee and to control without transforming the outdoor space into an indoor area. Light was controlled by defining the amount of dark and light fritted pillows. The necessary light transmission as well as heat gain on the ground during the warm season was also influenced by the fritted ETFE. A translucent canopy has Mean Radiant Temperature a little higher than Dry Bulb Temperature.

The whole canopy structure weighs 495 tons of steel welded on site due to structural and cost reasons. The macro modules were lifted onto the column trees via mobile cranes and then were welded to each other. There is no bolted connection on the project.

2.1. Design process

The main objective was to demonstrate a high-level steel structure controlled by computational design in all stages from design to analysis and construction details. The Voronoi pattern is generated with Grasshopper software in Rhino3D by a set of given points. The process started with the identification of the optimum insertion points for the tree shaped columns through structural analysis. Following that, a set of points were generated around the column to create the tree shape block of Voronoi module panels.

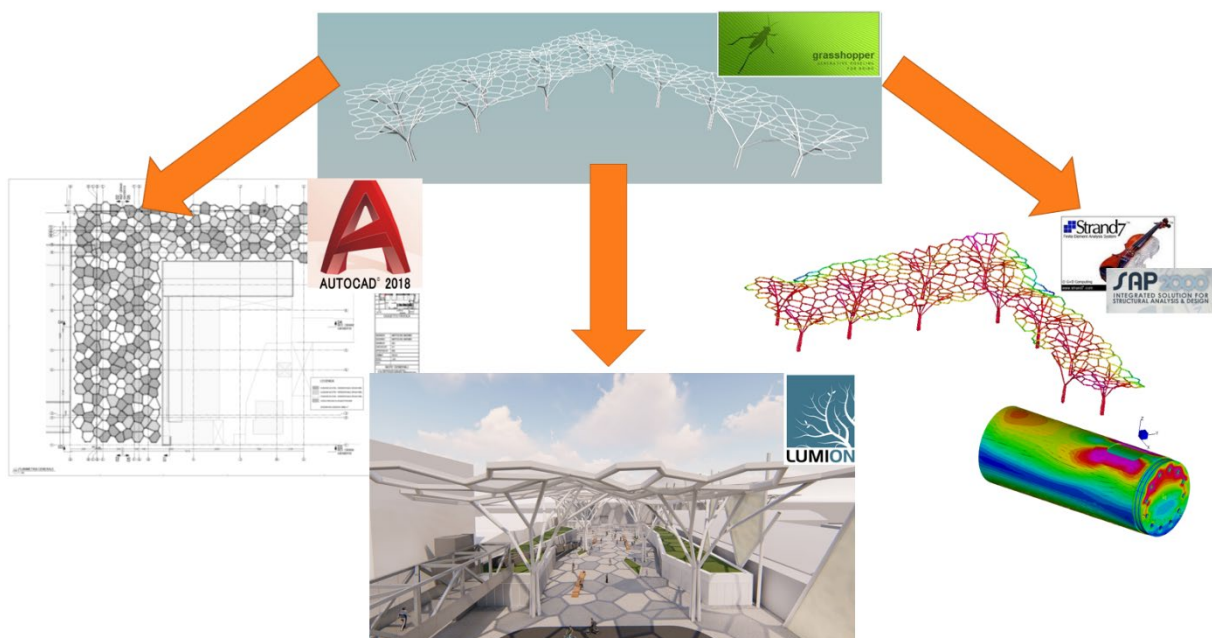


Figure 4: Grasshopper parametric model to share geometrical information with other software

Membrane architecture: the seventh established building material. Designing reliable and sustainable structures for the urban environment.

2.2. Parametric tools

The architectural intent is to create a roof with voronoi, typically random geometries that appear not to repeat themselves, supported by columns with asymmetrical tree-like geometries. The roof must provide slopes to allow rainwater to drain away, which will then be conveyed within the branches of the tree-columns in the most concealed manner possible.

For the roof, we started with the target dimensions of the voronoi-cushions, which had to remain as much as possible confined in a 6m circumference for structural reasons. The challenge then was to repeat these voronoi as much as possible, creating a macro-module of 36 cushions that could be copied as many times as necessary to cover the entire intervention area.

For this purpose, we started with a perfectly symmetrical starting mesh, and with the help of parametric software we modified the reference points of the voronoi mesh until we obtained a geometry that satisfied us aesthetically. The mesh then was projected into a concave pyramidal geometry (impluvium) to obtain the correct water drainage slope to the central voronoi, which instead of being an ETFE cushion, is a water collection basin with a syphonic drainage system.

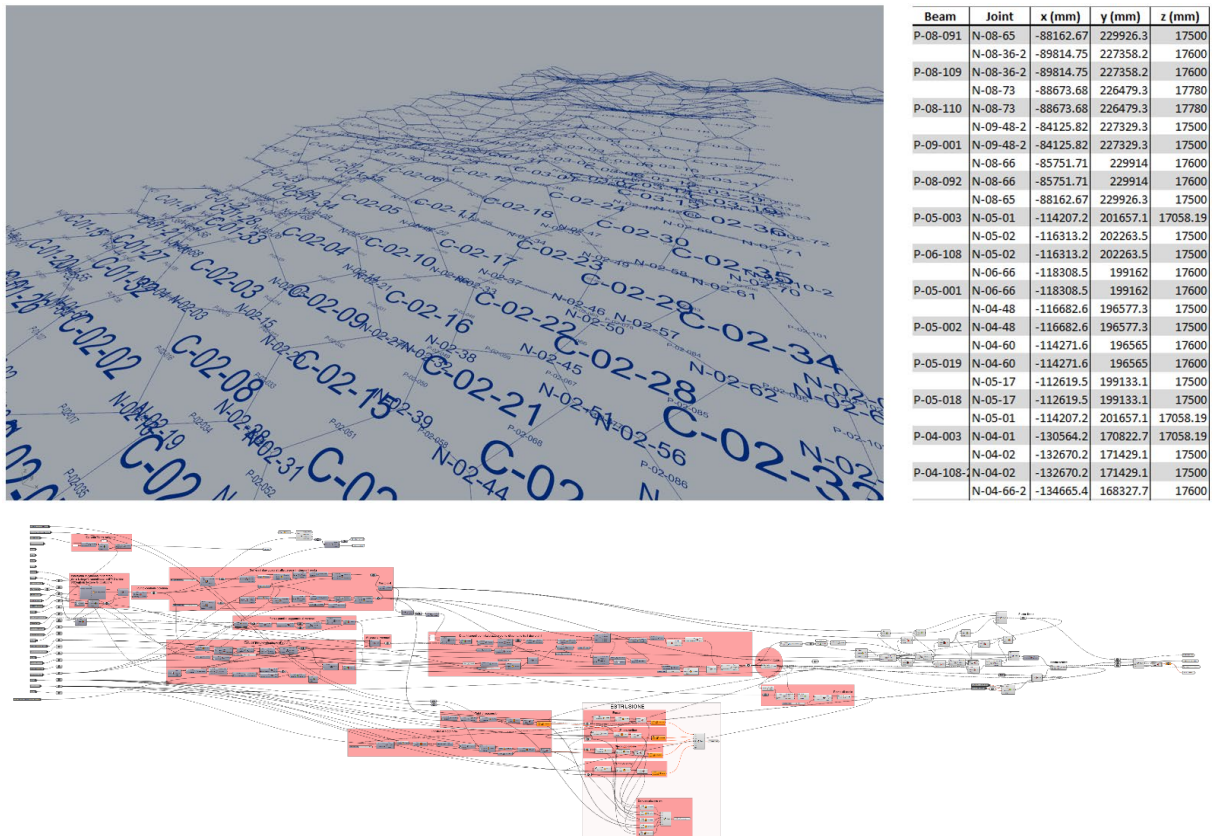


Figure 5: The use of parametric allows all geometric values of the project to be under control.

3. Google Sidewalk Project

The google sidewalk building ‘Raincoat’ prototype was a modular structure that acted as a secondary façade element, providing shelter from wind, rain and snow, improve outdoor comfort for pedestrians. This modular unit was intended to be deployed along the building façades of the planned google sidewalk development located by Toronto waterfront.

Membrane architecture: the seventh established building material. Designing reliable and sustainable structures for the urban environment.

The intent of having a modular system was to be able to deploy the Raincoat system to multiple cities around the world. The frame was designed to be able to be dismantled and reassembled. Having this versatility would enable the frames to be manufactured from several locations globally and assembled on site as a kit of parts (see fig. 6).

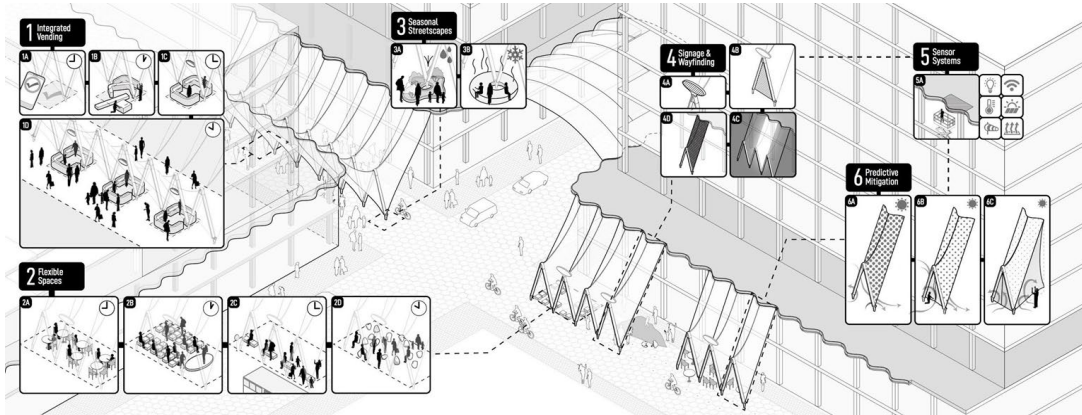


Figure 6: Architectural Rendering of modular system

3.1. Design process

The geometry of the Raincoat was studied through an iteration of fluid dynamic studies. These studies aimed to determine a geometry that would break up the wind and reduce strong gusts of wind to much lighter force. The geometry that was eventually decided on was a sawtooth geometry that would distort wind patterns that otherwise would have flowed quickly past the façade (see fig.7). This sawtooth geometry was further refined to allow for one long curved edge, one long straight side edge and a top and bottom edge that were not parallel; basically, the geometry for the cushion is a type of twisted rectangle with a curve on one side.

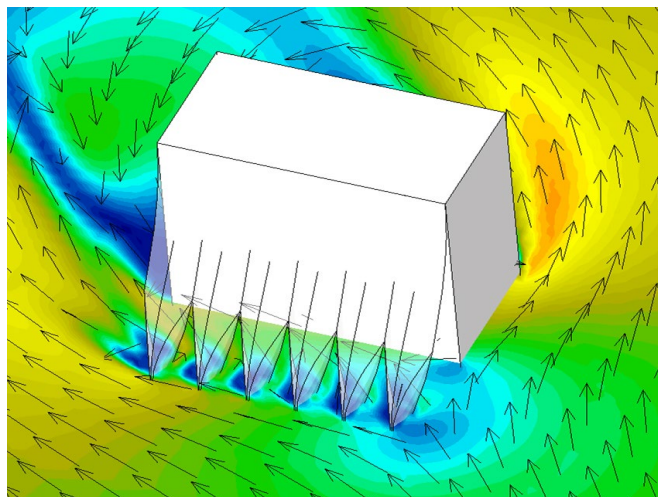


Figure 7: Wind Study and cushion geometry

The innovation of using the geometry of an ETFE cushion to create a more comfortable environment was achieved and confirmed with over a year of weather testing, that was carried out on prototype. The weather testing confirming the geometry consistently broke up the wind during windy days.

Membrane architecture: the seventh established building material. Designing reliable and sustainable structures for the urban environment.

Along with breaking up the wind to improve human comfort, the Raincoat also needed to control the light. This was achieved by having an operational 4 layer cushion with a special 2 air pressure unit. The geometry was difficult to work with since the middle layer(s) needed to move up and down to act as a variable aperture that would allow more or less light through. The cushion had two middle layers sandwich together in the middle or separate and press against the outer layers, depending on the internal pressure of the two chambers in the cushion (see fig. 8).

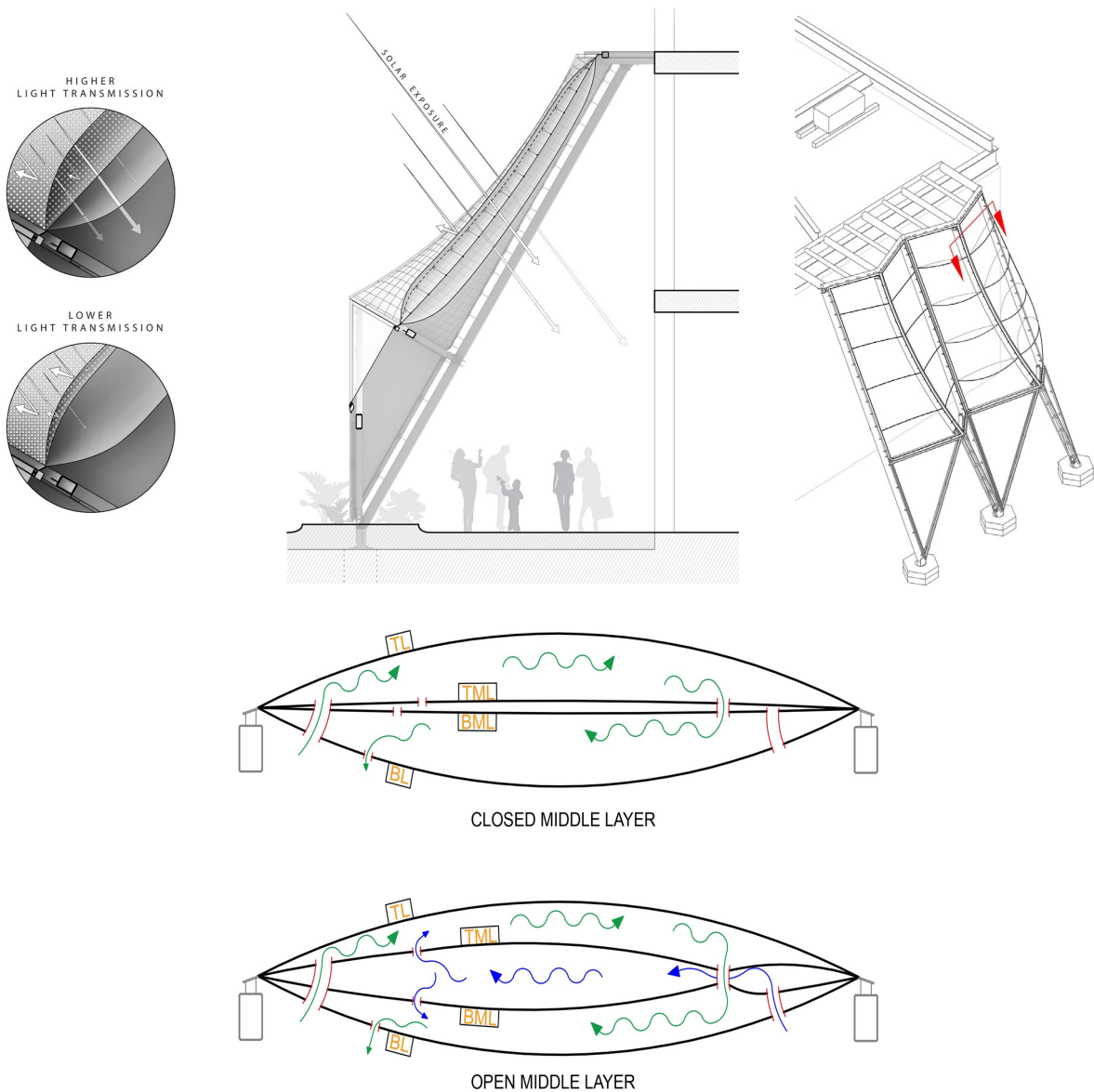


Figure 8: Operable Cushion

The ETFE cushions were custom printed with lines on the outer and inner layer that depending on the state of the middle layers would line side by side achieving an opaque surface or separating away from each other creating a transparent surface. This innovation in achieving an operable cushion with a geometry that was designed to break up the wind was a challenge, but during the prototype testing proved to be effective. A weather sensor provided inputs to the

Membrane architecture: the seventh established building material. Designing reliable and sustainable structures for the urban environment.

air pressure unit to influence the pressure differential in the cushion to allow varying degrees of light through the cushion based on temperature and sunlight levels during that hour.

The idea to have a lightweight modular façade structure that could influence the behaviour of wind, shield pedestrians from snow and rain, while allowing varying degrees of light pass through the cushion based on weather conditions was feasible only with ETFE.



Figure 9: Site photos

4. Conclusion

Textile architecture has been undergoing a strong evolution in recent years, reaching an ever-increasing level of complexity and providing innovative solutions capable of responding to new requirements for energy performance and people's comfort. This evolution has also been possible thanks to the development of advanced and interconnected design tools facilitating the exploration of new design solutions. Two projects of ETFE structures were then presented: Marble Plaza in Verona and Google Sidewalk in Toronto. Their design process was guided by advanced parametric design tools that allowed to develop complex and innovative solutions, investigating and implementing a large number of design options while respecting project schedules and costs. These projects have also allowed the development of new approaches and technological solutions and are a first step for further developments on a larger scale and in different areas.

Membrane architecture: the seventh established building material. Designing reliable and sustainable structures for the urban environment.

References

- [1] M. Maffei, A. Biasi, F. Ceccato, One Single Model: a New Parametric Approach to Megastructures
- [2] <https://www.dezeen.com/2019/03/11/building-raincoat-prototype-sidewalk-labs-toronto-smart-city/>



tensinantes2023 : TensiNet Symposium 2023 at Nantes Université

Membrane architecture: the seventh established building material. Designing reliable and sustainable structures for the urban environment.

Proceedings of the TensiNet Symposium 2023

TENSINANTES2023 | 7-9 June 2023, Nantes Université, Nantes, France

Jean-Christophe Thomas, Marijke Mollaert, Carol Monticelli, Bernd Stimpfle (Eds.)

Modelling of impacts onto tensile structures

Adam Bown*, Adrian Cabello^a, Dr Artem Holstov^b

*Tensys Ltd, 122 Wells Road, Bath, BA2 3AH, UK, adam.bown@tensys.com

^a Tensys Ltd. adrian.cabello@tensys.com

^b Tensys Ltd. artem.holstov@tensys.com

Abstract

This paper describes the ongoing investigations by Tensys into the modelling of impacts onto pre-tensioned tensile structures. It commences with an assessment of inaccuracies of the current code-based approaches to determining a design impact force. These approaches are calibrated for impacts of rigid, linear elastic materials, making the recommended impact duration unsuitable for tensile structures.

The paper then describes the ‘conservation of energy’ method, often employed by Tensys to represent dynamic events, and the drawbacks associated with this. This is an iterative process underpinned by the assumption that all of the initial kinetic energy is dissipated into the tensile structure via strain energy.

The final section describes how Tensys have extended their dynamic-relaxation-based, static analysis solver, to permit dynamic analysis simulations by removing the kinetic damping.

Keywords: Tensile structure, static analysis, dynamic analysis, impact, dynamic relaxation, kinetic damping

1. Introduction

For over thirty years Tensys have been undertaking the design and analysis of tensile structures, using in-house finite element analysis (FEA) software inTENS⁽ⁱ⁾. The design of a typical fabric structure usually only involves *static* analyses. However, on occasion, the assessment of *dynamic* loading conditions is required, for example, when the function of the structure is to arrest *impact* forces in a controlled manner.

Whilst there has been previous interest in modelling of dynamic impact events at Tensys, recent design development work on Flex-Gate[®] ⁽ⁱⁱ⁾ has provided the motivation for a more rigorous understanding of dynamic impacts onto tensile structures and for the expansion of the dynamic capabilities of inTENS.

Flex-Gate[®] - a proprietary product of ILC Dover. De. USA - is a temporary, deployable, flexible composite structure used as a flood barrier – essentially, a soft dam. The construction consists of interwoven horizontal Kevlar belts, and vertical Polyester belts stitched together at their intersections. Inside the belts is a loose bladder of PVC to provide a watertight barrier.

Membrane architecture: the seventh established building material. Designing reliable and sustainable structures for the urban environment.

The barriers are typically installed at the entrances to key buildings or infrastructure, such as subway entrances, during flood conditions. They are deployed sideways along an upper suspension cable like a curtain and secured along the bottom and the two vertical sides to provide a watertight barrier.

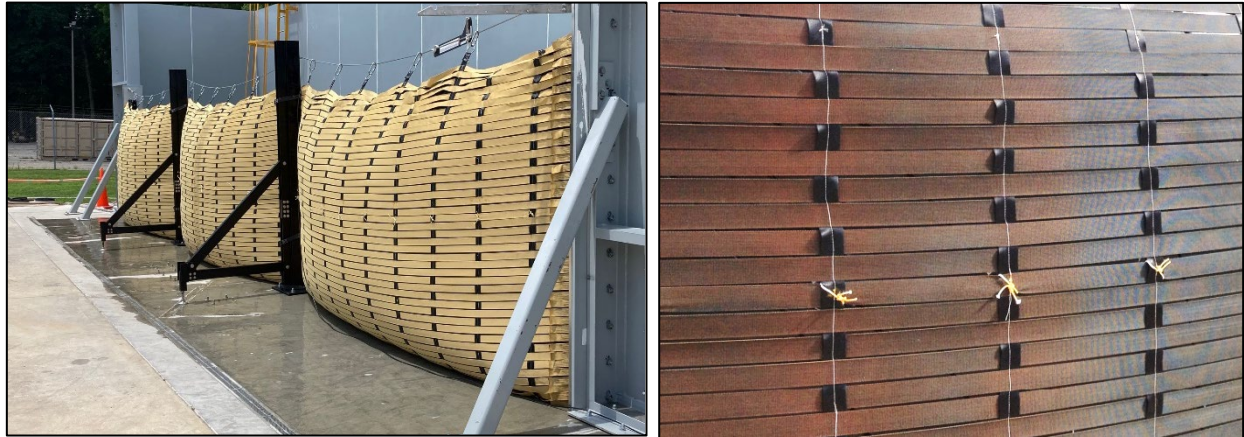


Figure 1: Format and construction of ILC Dover Flex-Gate system.

These structures are typically loaded with, and hence analysed for, hydrostatic and hydrodynamic forces (water surge) and impacts from floating debris, the latter of which is the focus of this paper.

The challenge of modelling impacts using static simulations reduces to the determination of a single dynamically amplified impact force. From Newton's second law, the required force is a function of the deceleration rate and, hence impact duration. However, this presents a dilemma since the calculation of the impact duration requires a *prior* knowledge of the expected deflection distance.

During the first analyses it became clear that the impact cases were dominant from the loading perspective, compared to the hydrostatic and hydrodynamic, and were thus driving material demands. It was felt that material weight savings could be achieved if the dynamic forces could be defined more accurately.

2. Code based approach

Initial attempts at defining the magnitude of the impact force referenced the United States design code, ASCE/SEI 7-10 Chapter 5⁽ⁱⁱⁱ⁾ on flood loads, providing equation 1.

$$F = \frac{\pi \cdot W \cdot V_b \cdot C_i \cdot C_o \cdot C_D \cdot C_B \cdot R_{max}}{2 \cdot g \cdot \Delta t} \quad (1)$$

Where

- F = impact force
- W = debris weight
- V_b = Velocity of object
- g = gravitational acceleration
- Δt = impact duration
- C_i = importance coefficient

Membrane architecture: the seventh established building material. Designing reliable and sustainable structures for the urban environment.

C_o = orientation coefficient
 C_D = depth coefficient
 C_B = blockage coefficient
 R_{max} = maximum response ratio

The underlying basis of this equation is the impulse-momentum approach described by Haehnel and Daly^(iv) (referred to as H&D from here on).

$$F_{ave} = \frac{W \cdot V_b}{g \cdot \Delta t} \quad (2)$$

The H&D research was undertaken and validated on a very specific situation, that is, the impact of a floating wooden object onto hard structures of concrete, steel or timber.

A limitation of this approach is that it provides a time-averaged force, rather than a peak design force. If a linear variation of force v's time is considered, the maximum force would simply be twice the average force. However, H&D assume the impact yields an elastic response, meaning the force v time relationship will follow a sinusoidal distribution. The factor required to convert the average force to maximum forces is therefore $\pi/2$, as illustrated in (3) and figure 2.

$$F_{max} = \frac{\pi \cdot F_{ave}}{2} \quad (3)$$

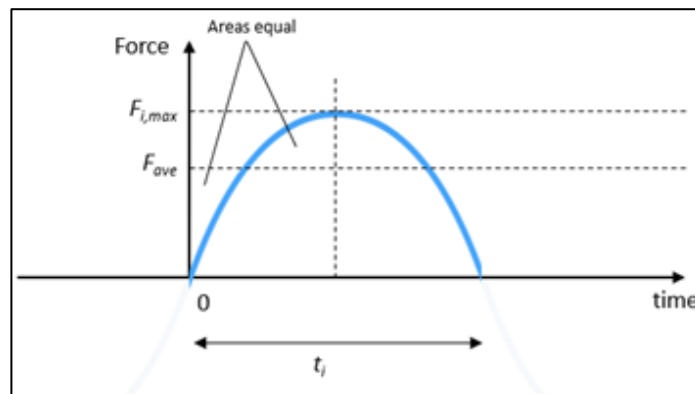


Figure 2: Derivation of peak force F_{max} , from $F_{average}$, assuming a sinusoidal distribution of force v time

The final ASCE equation (1) includes several additional factors compared to the underlying H & D formulation. The most notable of these factors is the response ratio, R_{max} . R_{max} is a multiplier which adjusts the value of the impact force depending on the ratio of impact time to the natural period of the structure. In qualitative terms, R_{max} increases the value of force for impacts close to the natural period of the impacted structure, and, conversely, decreases the force when the impact duration is far from the natural period.

The ASCE recommended impact duration time (Δt) is obtained from a literature review on the subject undertaken by Kriebel et al.^(v) in 2005. Based on this review, impact times were shown to vary from 0.01 to 0.05 seconds. The code ultimately recommends the use of an average value of 0.03 seconds. This value is unrepresentatively low for flexible structures, which was causing early code-based impact force calculations to be extremely conservative.

Membrane architecture: the seventh established building material. Designing reliable and sustainable structures for the urban environment.

Whilst the code-based approach provides a conservative starting basis for calculation of peak impact force, later sections will illustrate that the assumption of an elastic response is far from accurate for the application in question and was yielding discrepancies as the same order as the choice of impact time.

3. Conservation of energy

Tensys first considered a ‘conservation of energy’ approach (CoE) in the Hybrid Air Vehicles LEMV project^(vi) with the aim of determining a static solution to the time dependant landing case. The underlying assumption of the CoE approach is that there is a single static state where the impacting object is momentarily at rest. It is assumed that at this moment all the initial kinetic energy of the impact has been transformed to changes in the potential, mechanical strain and volumetric strain energies (equation 4, PE, SE and VE respectively). Hence, this state represents the maximum deflections, mechanical stresses and strains in the system as a result of the impact.

$$KE_{start} = \sum(\Delta PE + \Delta SE + \Delta VE) \quad (4)$$

In practical terms, finding this state requires an iterative process of outputting the sum of strain and potential energy variations from a series of static solutions modelled in inTENS with incrementally increasing impact force or imposed deflection. The total energy changes can be plotted against the chosen varying parameter. The solution at which these energy changes match the starting kinetic energy of the impacting object can be found from the plot, providing an estimate of the maximum impact force or distance (see figure 4). A final static analysis is then run for this equilibrium state, which is used to assess the maximum stresses and strains in the system resulting from the impact. In contrast to the code-based approach, the CoE method does not require approximation of the impact time, however, this value can be back calculated based on the starting velocity and impact distance.

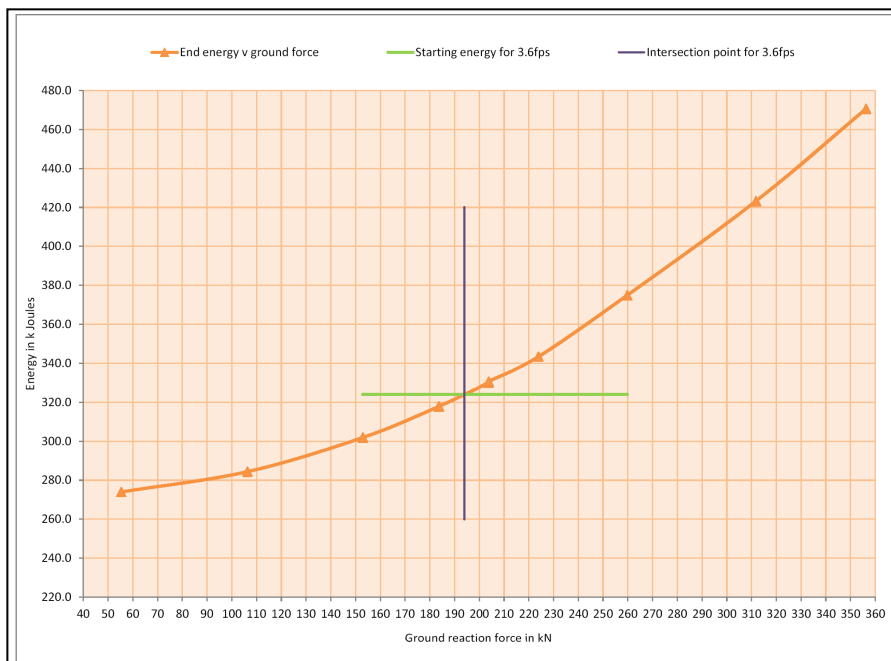


Figure 3: Graphical approach based on conservation of energy principles, to find a design landing force for Hybrid Air Vehicles, LEMV craft.

Membrane architecture: the seventh established building material. Designing reliable and sustainable structures for the urban environment.

The CoE approach was attempted for the Flex-gate. Whilst it gave more realistic predictions of the amplified dynamic impact force than the code-based approach, there remain a number of drawbacks and uncertainties to this method:

- The iterative process is slow. For every impact case considered (of which there may be many, e.g. different impact locations), a number of static cases are required to derive the governing relationship between impact force and the dissipated energy.
- The assumption of an instantaneous equilibrium state where the structure is perfectly static results in overly conservative predictions for multi-dimensional complex systems since there is likely to be some residual kinetic energy left in the system at the state with maximum deflection. As shown in the later studies using the inTENS explicit dynamic solver (chapter 5), the various energies can fluctuate during an impact onto a complex system (wave-like propagation of impact), and the problem is concerned with finding the force associated with the first KE minimum (figure 5).

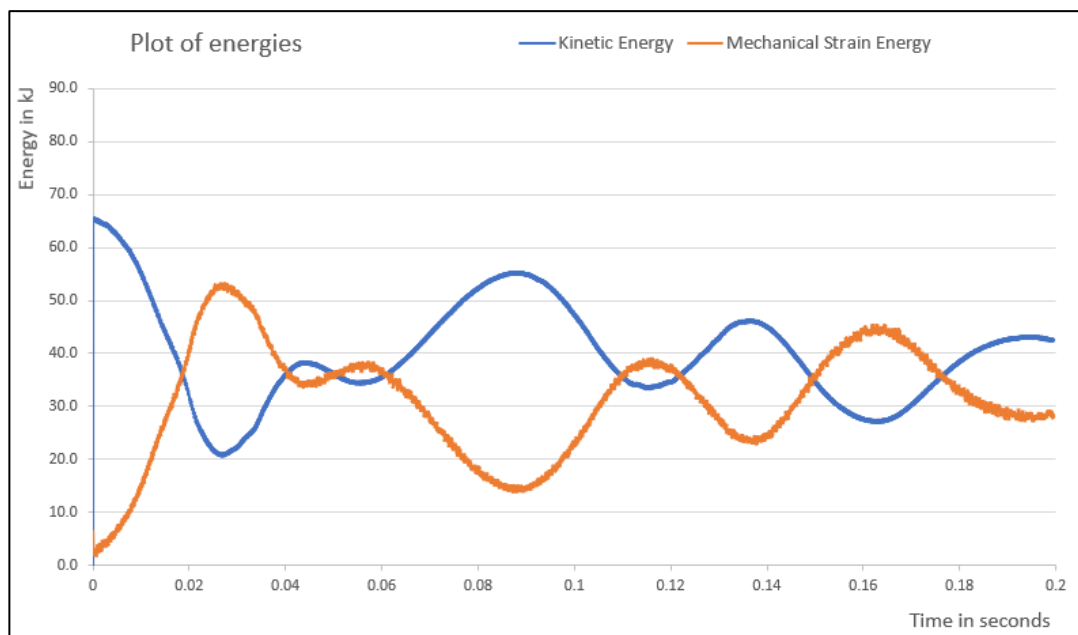


Figure 4: Variation in kinetic and mechanical strain energy changes for impact onto complex fall arrest net. Note that rather than a full transfer of KE to strain energy, the maximum strain energy occurs at the first KE minimum.

- Impact location. Analyses of the dam system require impacts onto various locations of the dam surface. For central impacts, a significant proportion of the structure is mobilized and the mechanical strain energy is well distributed around the belts. However, for impacts close to a vertical edge, the use of the CoE method was found to be overly conservative. In these cases in reality a large proportion of initial energy would be dissipated into the vertical support structure. Since these elements were not modelled in the FEA, this energy dissipating route was not accounted for, resulting disproportionately higher strain energy requirements for the belts.

Membrane architecture: the seventh established building material. Designing reliable and sustainable structures for the urban environment.

- Energy losses through heat dissipation are not considered, although these are assumed to be small.
- The current approach makes no allowance for the energy dissipated, via the structure, into the water. Unlike heat losses, this action is expected to absorb a significant proportion of the starting energy.

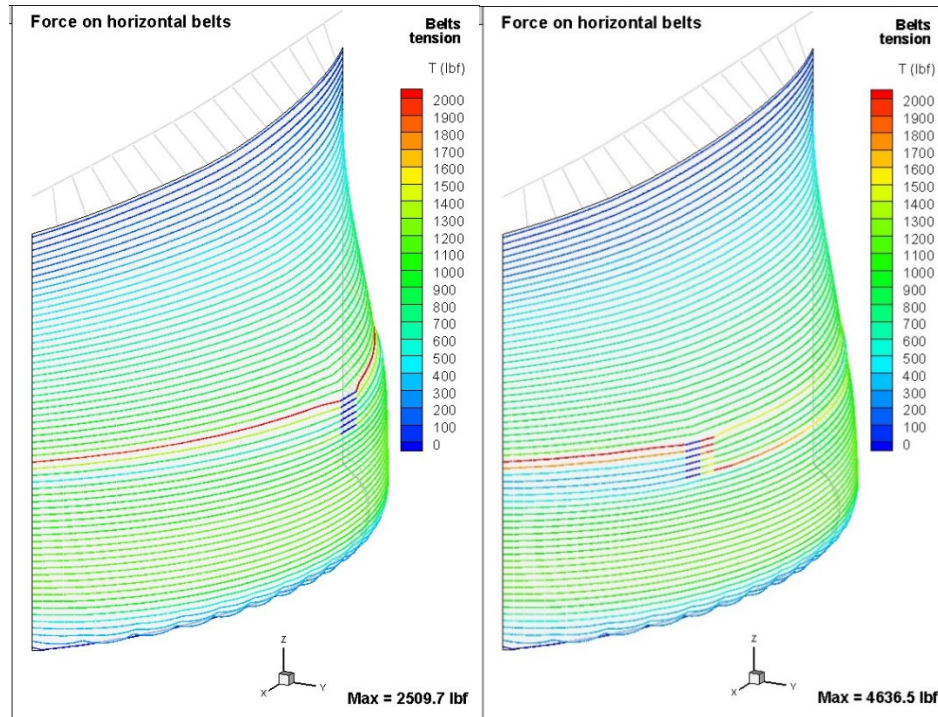


Figure 5: Comparison of belt tensions in the structure resulting from central (left) and side (right) impacts.

4. Physical tests

In an attempt to improve their understanding of the impact events, ILC Dover undertook a program of physical tests. The tests (set up shown in figure 6) involved dropping weights onto horizontal tensioned webbing belts in a controlled manner with the impact velocity, arrest distance and belt tensions recorded. A large number of tests were undertaken, with the varying parameters being belt type (Polyester and Kevlar), drop height, drop location and the mass of the falling object.

The objectives of the tests were to

- compare the resultant impact forces with existing code approaches,
- quantify the typical impact durations,
- attempt to derive a single equivalent contact stiffness value,
- validate and verify the Tensys analytical approaches.

Membrane architecture: the seventh established building material. Designing reliable and sustainable structures for the urban environment.

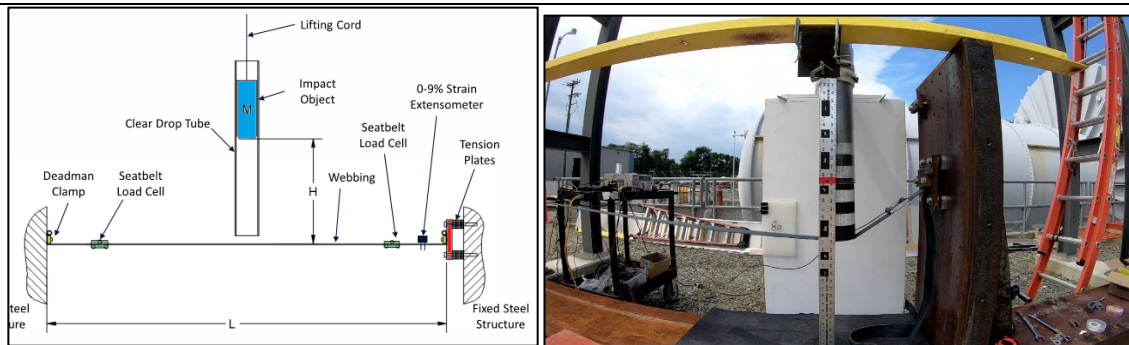


Figure 6: Schematic diagram (left) and a photo (right) of set up for the physical tests, used to find an empirical relationship between impact energy and resultant belt tensions

The choice of the initial pre-tension was commensurate with the current design of the flex-gate system. The initial fall velocity, impact times and maximum deflections were measured using high precision video recording equipment and the webbing belt tensions were recorded with in-line load cells. Interrogation of the results showed that impact times were 2-3 times higher than the code-based recommendation of 0.03s, introduced in section 2.

Tensys simulated a large number of the physical tests results using their CoE approach. Owing to the time penalty of the CoE approach defined earlier, for these simulations Tensys used a combination of inTENS FEA models, coupled with simplified time-stepping transient analyses undertaken in Microsoft Excel.

The latter method commences with the definition of the initial state of the belt in terms of span, stiffness and pre-tension. A starting velocity, mass and impact location is chosen for the impacting object. A suitable time increment is selected and the following parameters are updated in turn; deflection distance, belt geometry, belt strain, belt tension, resisting force and finally updated acceleration. Values of delta strain and potential energy are also updated. This sequence can be extended indefinitely to define the motion of the object and track the energy changes.

The belt forces were recorded and compared to estimates derived using the following:

- i. Momentum change equation, $F = ma$. (yields average force, rather than peak)
- ii. ASCE equation (peak force)
- iii. H&D (peak force)
- iv. Tensys' CoE approach

Figure 7 below provides a comparison between the measured and theoretically calculated impact forces.

Membrane architecture: the seventh established building material. Designing reliable and sustainable structures for the urban environment.

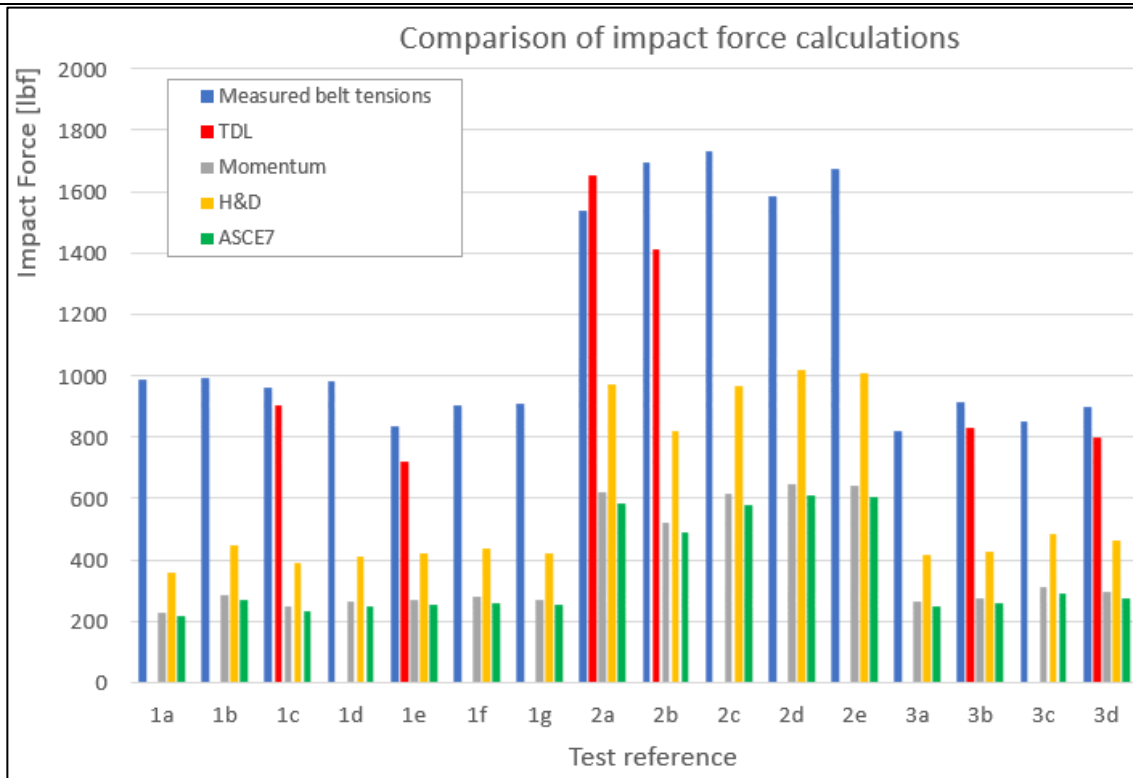


Figure 7: Comparison of the measured and theoretically calculated impact force values

As expected, the momentum equation (grey) provides a low value for impact force, since this approach returns an average value rather than the peak force. Interestingly, the ASCE code values (green) are also low. In this plot, this finding is related to an inaccurate choice in the value of R_{max} (0.6). Since this value is unlikely to be known, this illustrates another drawback of the ASCE approach. In the case of uncertainty this value should be set as unity.

In fact, when all the additional factors are set to unity the output from the ASCE method simplifies to that of the H&D equation.

It is expected that, due to an unrealistically low recommended value for impact duration (i.e. 0.03 seconds), the H&D equation should provide a conservative estimate of the impact force. But even when the *correct* impact duration from the tests are entered into the equation, the calculated impact forces (yellow) are actually *below* the measured values.

The reason lies in the factor used to convert the average force to peak force, $\pi/2$. Recall from section 2 that this factor is derived from the assumption that the force v time profile is sinusoidal with a period of π . The validity of this assumption can be assessed by plotting out some sample force v time responses for a horizontal belt subjected to a central impact, from the time-stepping calculations introduced earlier. See figure 8. The force distribution has been plotted for two choice of belt stiffness, elastic and non linear. A normalised sine wave has also been included for comparison.

Membrane architecture: the seventh established building material. Designing reliable and sustainable structures for the urban environment.

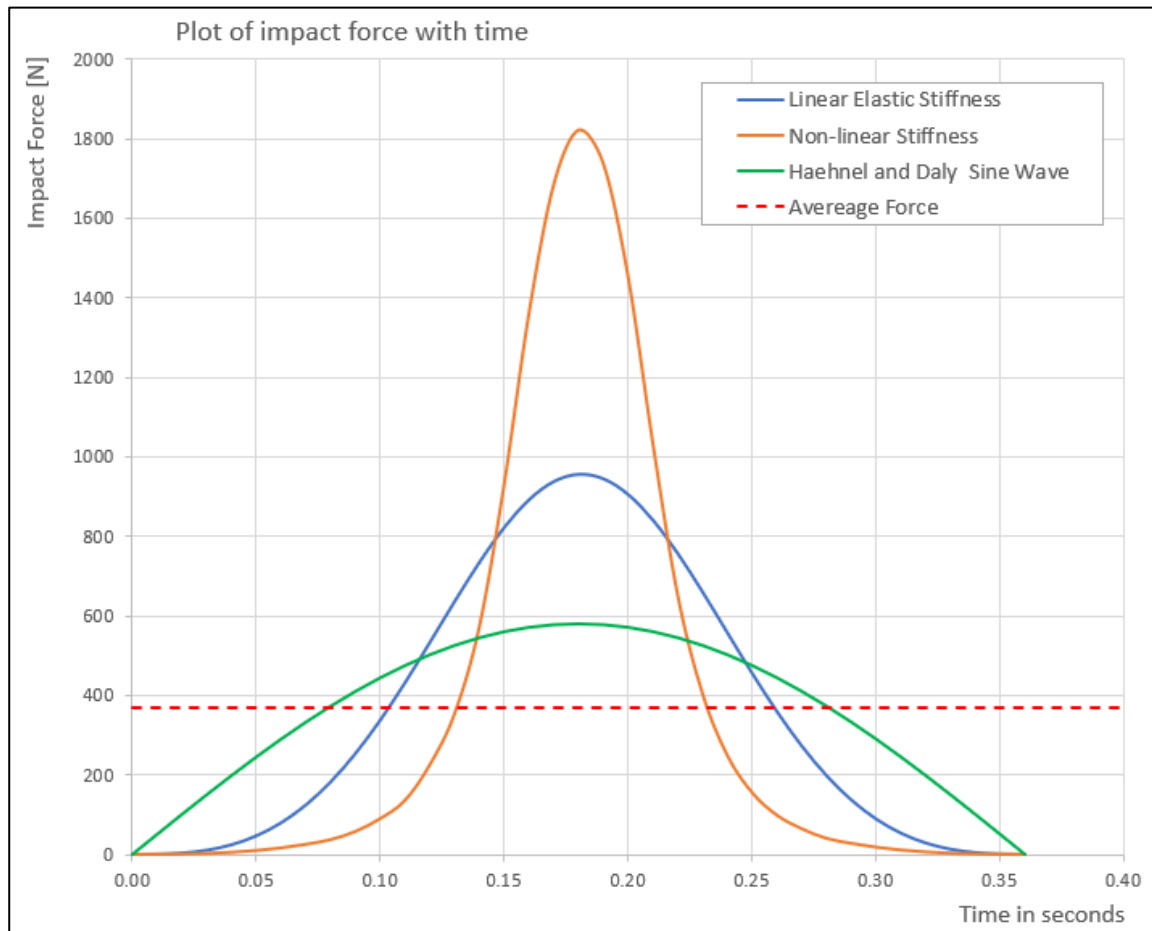


Figure 8: Variation of force v. time for loaded horizontal belts

The areas under each graph, i.e. the work done, are the same. Hence, the *average* force (red dashed line) is also equal for all three graphs. The plot shows that the peak impact force onto a linear elastic belt (top of the blue graph) exceeds the calculated H&D peak value (green) by ~45%. Furthermore, the assignment of non-linear belt properties results in the peak impact force doubled compared to the linear elastic belt.

Unlike a stiff rigid body, which develops resistance force that is proportional to its deformation immediately after the start of an impact, the initial deformation of a tensioned belt requires very little force as it lacks (geometric) stiffness in the direction of the impact when straight. This delayed response results in a relatively flat section at the start of the force-time graph and a sharper increase in the force carried by the belts as their stiffness is mobilized more efficiently at higher deflections.

The combination of *geometrically non-linear response* of the system and *non-linear material* behaviour seen in both the Polyester and Kevlar belts means that the sinusoidal distribution of force v time is not applicable. The *exact* force extension response of belts is also known to vary with initial pre-stress, number of loaded cycles and time held at pre-tension (figure 9).

The initial findings from the physical tests ultimately prompted a new follow-up study relating to the correct choice of stress-strain curve to adopt for the FEA simulations. However, that work is outside the scope of this paper.

Membrane architecture: the seventh established building material. Designing reliable and sustainable structures for the urban environment.

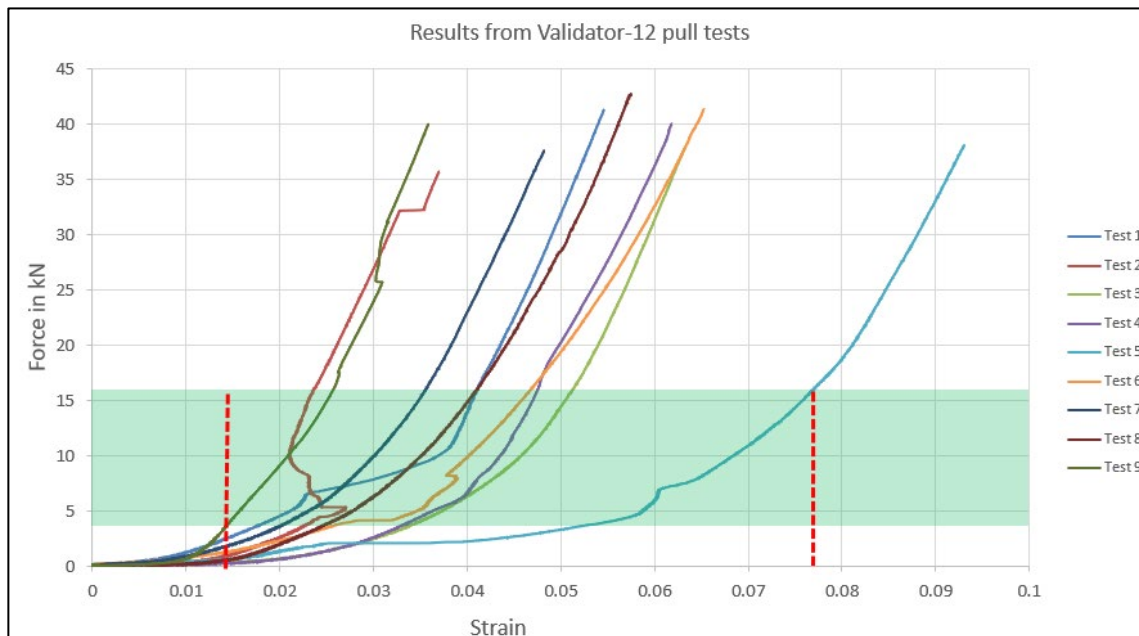


Figure 9: An example of the variation in force v. extension for typical woven Kevlar belts, belt to belt and cycle to cycle

Provided a representative force-extension response was chosen, the Tensys' CoE approach, provided close predictions of the impact force and deflections.

Overall, the testing program has advanced the knowledge about the behaviour of flexible impact arresting systems and confirmed that the code-based approach to defining impact forces is not suitable for soft dams. Owing to the complex time and loading dependent response of the woven belts, it proved challenging to find a single value for contact stiffness which could be considered universally applicable for these systems.

5. Dynamic analyses

In parallel to the Flex-Gate project, Tensys were actively working on a number of other projects involving impacts onto tensile systems, such as safety nets. In order to enhance Tensys' capabilities for modelling of these types of structures, the logical next step was taken to extend the static solver of inTENS to allow explicit dynamic simulations.

inTENS utilizes an explicit dynamic relaxation solver. Kinetic damping^(vii) is used to facilitate convergence of the models to a single equilibrium solution for a particular set of boundary conditions and imposed stresses. Kinetic damping works by tracking the total sum of all nodal energies (using fictitious values for nodal lumped mass) and resetting all velocities to zero once a peak value of KE is found (i.e. approaching the equilibrium geometric state). In this way, the entire kinetic energy of the deflected system is gradually damped out and a stable, equilibrated static state is found.

Membrane architecture: the seventh established building material. Designing reliable and sustainable structures for the urban environment.

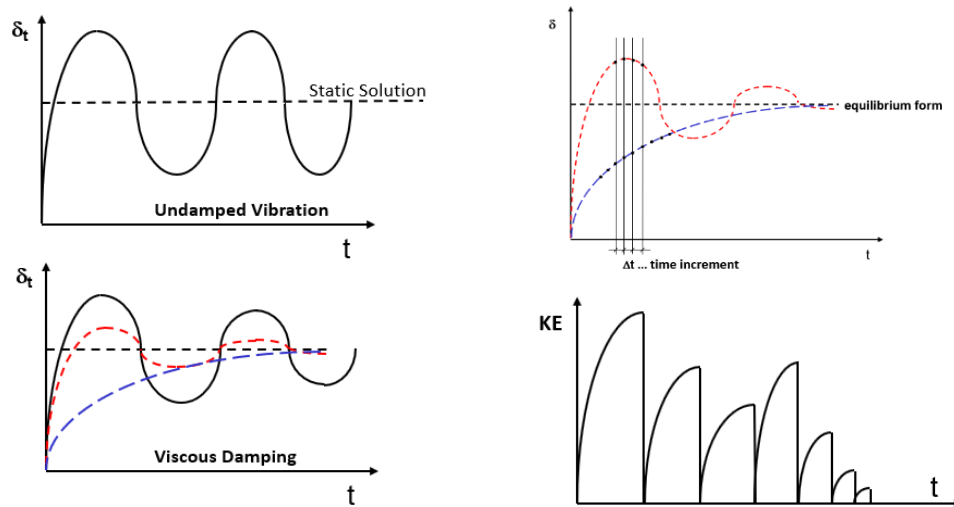


Figure 10: Kinetic damping is a convenient technique for damping an oscillating system to find the single static equilibrium solution. The total KE of the oscillating system is tracked, and when a maximum value is found, the nodal geometry are reset to zero. In this way, the kinetic energy of complex systems can be gradually reduced until the equilibrated static state is found.

The switch to permit explicit dynamic sequences was instigated by the *removal the kinetic damping*. The additional amendments required for inTENS Explicit were

- The change from artificially assigned values for lumped masses and time step increment to real masses representative for the analysed system and true time.
- Introduction of time dependent loading, or initial velocities,
- Introduction of a range of run controls such as geometric and viscous damping, time step control and frequency of updating the applied loads.

The code was initially validated for a number of examples of simple harmonic motion with existing closed form solutions, such as vertical and horizontal tensioned springs. The output from the explicit dynamic solver was also validated against the CoE and transient time-stepping simulations of the tensioned horizontal belt models defined in section 4. Ultimately, the new code was extended to modelling of impacts onto full complex impact nets. Further development of the inTENS explicit algorithm will involve the added consideration of the dampening effect of water, required to accurately represent the behaviour of a soft dam under an impact of floating debris.

6. Conclusion

This paper describes the refinements undertaken by Tensys, in the way modelling of impact events onto tensioned structures is carried out.

The code-based approach was deemed unsuitable, since the recommended equations and parameters were calibrated for impacts onto ‘hard’ structures, exhibiting elastic response. As such, they are not applicable for impact arresting systems exhibiting non-linear geometric and material behaviours.

Membrane architecture: the seventh established building material. Designing reliable and sustainable structures for the urban environment.

The use of a ‘conservation of energy’ approach was introduced and proven to provide an effective method for calculating impact forces, based on a comparison with the results of physical drop tests on tensioned horizontal belts undertaken by ILC Dover. However, the accuracy of the predicted response relies heavily on the ‘correct’ choice of force-extension response for the woven belts.

Finally, the paper introduces the evolution of the Tensys’ inTENS code from a static-based solver to one with a dynamic simulation capability. This solver has been proven a useful tool for modelling impacts onto tensioned arrest nets. However, use of inTENS Explicit on the Flex-gates products is still limited due to the uncertainties about the dampening effect of the water mass behind the dam.

Acknowledgements

The authors would like to thank ILC Dover for the opportunity to work on the design of the Flex-Gate[®] system.

References

- i) Wakefield, DS., (1999), ‘Engineering Analysis of Tension Structures : Theory and Practice ‘, *Engineering Structures*, 21, 680-690
- ii) <https://www.ilcdover.com/products/flex-gate-portal/>
- iii) ASCE/SEI 7-10 Minimum Design Loads for Buildings and Other Structures (2010)
- iv) Haehnel, R., and Daly, S. (2002), Maximum Impact Force of Woody Debris on Floodplain Structures: *US Army Corps of Engineers*.
- v) Kriebel, D. L., Buss, L. and Rogers, S. (2000), Impact loads from flood-borne debris. *American Society of Engineers*.
- vi) <https://www.hybridairvehicles.com>
- vii) Barnes MR, Wakefield DS (1998). Form-finding, analysis and patterning of surface stressed structures. *First Oleg Kerensky Memorial Conference, London*,



tensinantes2023 : TensiNet Symposium 2023 at Nantes Université

Membrane architecture: the seventh established building material. Designing reliable and sustainable structures for the urban environment.

Proceedings of the Tensinet Symposium 2023

TENSINANTES2023 | 7-9 June 2023, Nantes Université, Nantes, France

Jean-Christophe Thomas, Marijke Mollaert, Carol Monticelli, Bernd Stimpfle (Eds.)

Porto Pi shopping center's floating pergolas

Juan García-Lastra Zorrilla¹, Juan Rey-Rey², Alejandro Mínguez³

¹ LASTRA&ZORRILLA, juanlastra@arquitextil.net

² MECANISMO INGENIERÍA, juan.rey@mecanismo.es

³ EOS Arquitectura e Ingeniería, alejandro.minguez@eos.com.es

Abstract

The Porto Pi shopping center in Palma de Mallorca was renovated between 2020 and 2021, at a time of great uncertainty and blurred horizons due to the COVID-19 crisis. The goal was to give a facelift to a shopping center with great potential to become a new oasis where customers could spend time outdoors enjoying the weather of the Balearic archipelago.

For this purpose, the hereby presented textile elements were designed with the function of providing shade while at the same time being an aesthetic statement. These elements had to rise above the level of the pedestrians and the interior streets of the shopping center.

The floating pergolas are comprised of conoids couples that make up textile volumes anchored to steel frames, installed on the existing structure of the shopping center. Depending on the location of these groups of pergolas, the conoids have different complexities and requirements that were taken into account in the design phase.

This paper deals with the different processes that were carried out in order to make these pergolas. From the design standpoint, in which the members of the team made up of architects, engineers and textile manufacturers had to collaborate hand-in-hand; from membrane and steel structure manufacture, which make up the pergolas, to the fabrication and assembly process, which had its complexities, given the case of being a running shopping center during the summer in one of the most touristic cities in the Mediterranean.

It will also delve in detail regarding the membrane and steel element engineering process, which was focused on facilitating maintenance and easy assembly/disassembly of these elements, presenting its own challenges.

Keywords: Collaborative design, single layer membrane structure, membrane assembly, membrane maintenance, conoid, membrane shade, tensile structure analysis, membrane detailing

Membrane architecture: the seventh established building material. Designing reliable and sustainable structures for the urban environment.

1. Introduction

The Porto Pi shopping center is open to the city, with outdoor malls that previously lacked a visual reference to indicate the main access points. In addition, the high temperatures in these open spaces and the exposure to solar radiation made it necessary to install light shading elements.

The design of these elements is based on the concept of tree cover, whose superimposition of multiple layers of branches and leaves generates shadows, reducing the temperature and generating ventilation and air flow through the permeability of these layers.

Thus, the overlapping floating pergolas produce the desired climate control effect by generating a dense shade, while allowing a continuous flow of air between all its elements and layers.

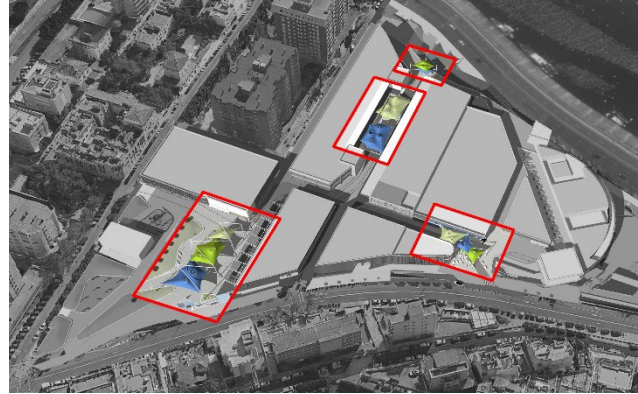


Figure 1 Location of the pergolas throughout the mall

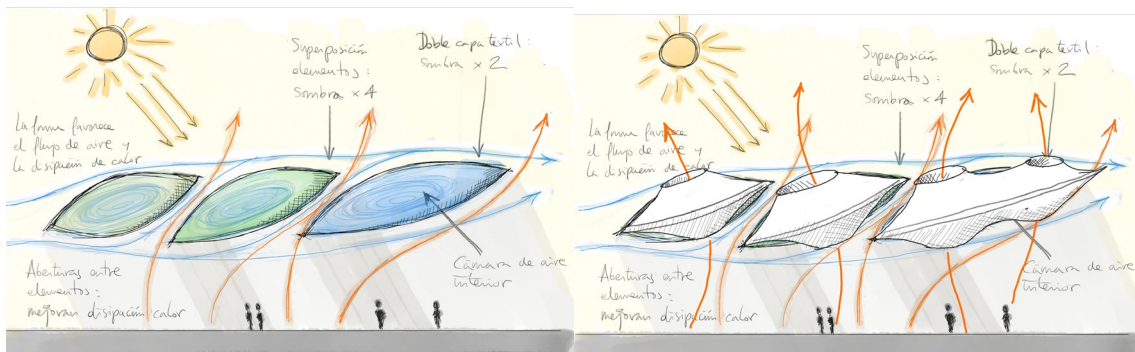


Figure 2 Concept sketches showing the climatic service of the pergolas

The final design, consisting of large clouds composed of micro-perforated fabric, adapts their number, shape and support system to the different locations within the center, as well and the structural conditions of each area of the existing building.



Figure 3 Computer generated images of some of the pergolas before starting the project

Membrane architecture: the seventh established building material. Designing reliable and sustainable structures for the urban environment.



Figure 4 Main square's pergolas in reality



Figure 5 Porto Pi drive through entrance's pergolas

2. Team's workflow

The detailing level of the project had to be maximum, in order to be able to manufacture both the steel and tensile structures and fitting the new structure inside the existing mall without any interference.

The team responsible for carrying out this project was made up of architects (EOS Arquitectos), engineers (MECANISMO INGENIERÍA) and tensile structure manufacturers (LASTRA&ZORRILLA). The client was MERLIN Properties.

Membrane architecture: the seventh established building material. Designing reliable and sustainable structures for the urban environment.

In a project of this kind, in which a new structure is added to an existing building, design constraints and interferences arise as the new structure takes shape.

The design procedure consisted of a cyclical process of proposal development with changes that approached through successive iterations a final outcome that could simultaneously satisfy the requirements imposed by external and spatial, mechanical, structural, constructive, aesthetic and assembly constraints. On numerous occasions steps back had to be taken in the design process in order to correct aspects that would satisfy all the requirements.

This coordinated work between the team members is one of the most significant aspects of the project (Figure 1).

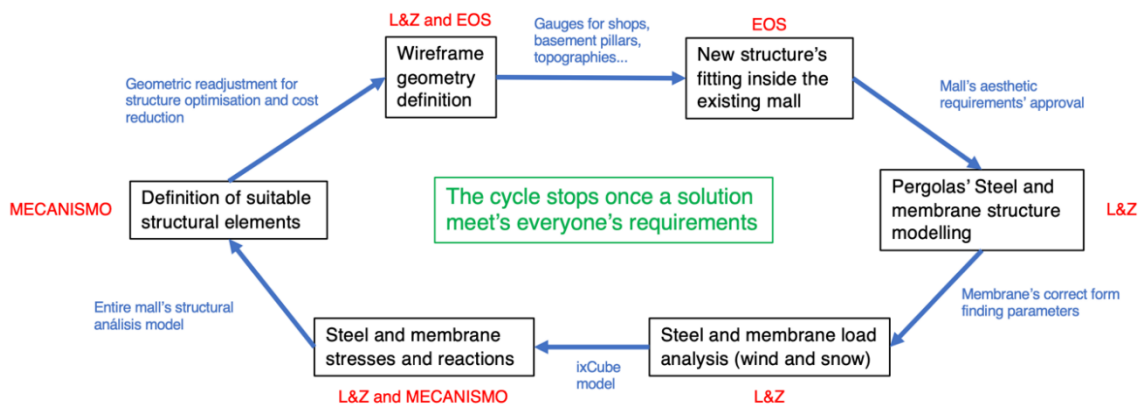


Figure 6 Design team's workflow during the project

3. Structure design

3.1. Introduction

This section presents the calculation procedure followed to check the structural validity of the floating masts that give shape to the textile conoids, together with the main steel structures of the beams and vertical masts, as described in the previous chapters.

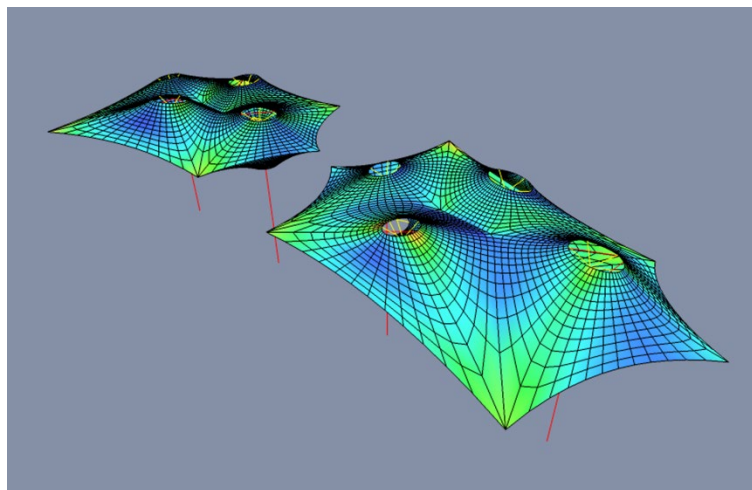


Figure 7: Enveloped stresses in ULS of two of the mall's pergolas under analysis loads

Membrane architecture: the seventh established building material. Designing reliable and sustainable structures for the urban environment.

3.2. Structural analysis and dimensioning

For the design and dimensioning of the structure, different kinds of models were prepared: complete 3D calculation models of each of the structures, as well as partial calculation models for the analysis of specific elements.

Thus, the forces in the different bars that compose the floating masts have been obtained after the elaboration of calculation models that integrate the textile structure, the internal structures (compression bars, floating masts) and the external structure (external frame that supports the fabrics and provides lateral stiffness to the assembly).

Some relevant considerations in the development of these models were:

- Consideration of the real stiffness of all elements of the assembly (floating masts, compression beams, supports, etc.).
- Consideration of the interaction between conoids.
- Boundary conditions adjusted to the construction reality.

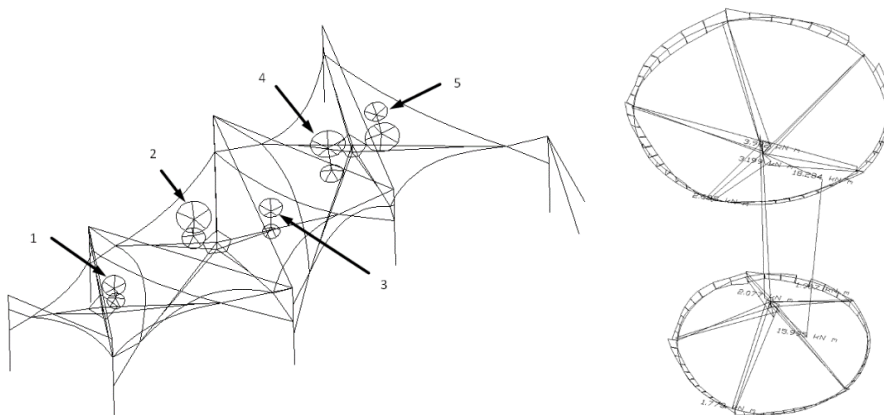


Figure 8: One of the biggest pergola groups floating masts and bending moment envelope on floating mast 1

The rings are dimensioned in flexural tension, while diagonals and shafts are dimensioned in flexural compression considering buckling.

A comparative analysis of the elements of a floating mast in both steel and aluminum was carried out to assess the implications of using one or the other material, finally opting for the steel option due to the large difference in the size of the sections obtained.

Membrane architecture: the seventh established building material. Designing reliable and sustainable structures for the urban environment.

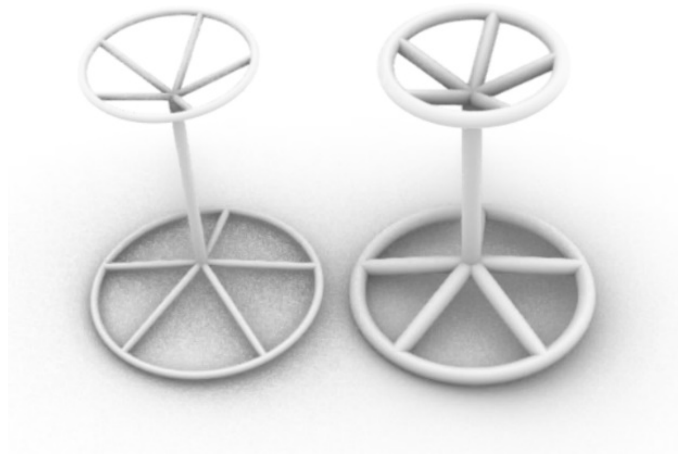


Figure 9 Comparative design of the floating mast structure in steel (left) and aluminum (right).

3.3. Connection to the existing structure

A remarkable aspect to highlight from the structural design standpoint is the design of the masts. Due to the structural configuration of the assembly, it was necessary to support very significant bending moments at the base of the masts. Given the impossibility of implementing tie rods for architectural reasons, it was necessary to embed the masts in the base. The challenge in this case derived from the existence of several parking levels below the street level, which resulted in the need to extend the masts at least one floor down to transfer the bending moment to the floor slabs of the ground floor and basement floor -1 as a pair of forces.

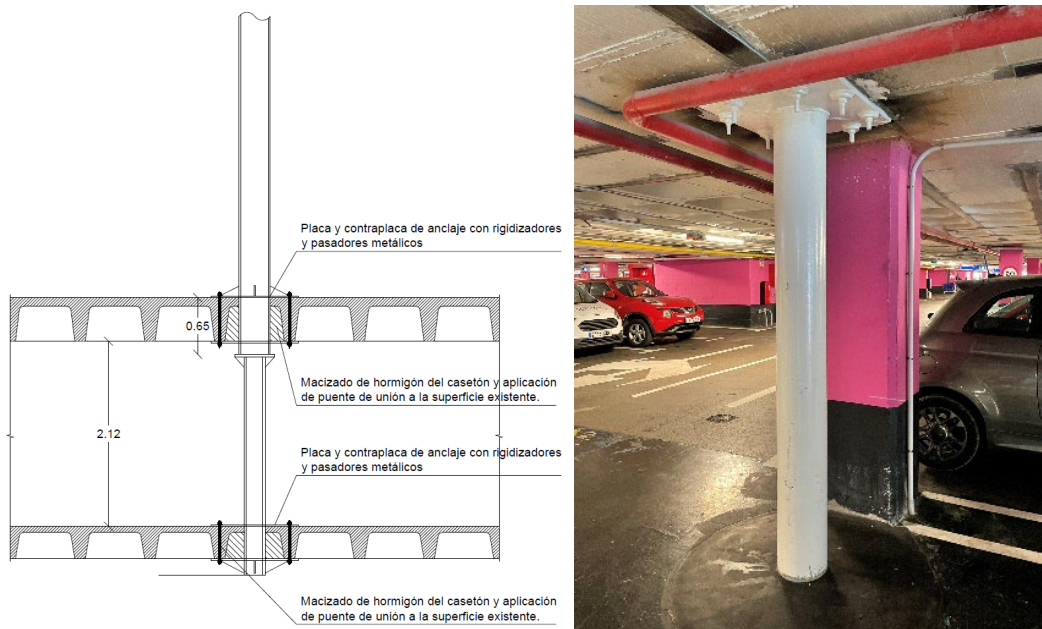


Figure 10 Connection of the masts to the existing structure. On the left detail in section, on the right photo of the connection executed for the embedding in the floor slabs of the existing parking

Membrane architecture: the seventh established building material. Designing reliable and sustainable structures for the urban environment.

3.4. Steel and membrane connection detailing

The textile elements had to adapt to numerous design conditions. These determining factors would appear during all the stages of its life cycle: design, manufacturing, transport, assembly and subsequent useful life and maintenance.

Some of these conditions will be featured and summarized below, as well as their nature and the solution provided.

Table 1 Description of some constraints that appeared through the project's definition and brief description of the developed solution

Element	Constraint nature	Constraint	Solution	Reference
Corners	3D design, ease of execution and cost reduction	Each of the of the conoid corners had a different angle. Manufacturing each corner would have been very expensive and time consuming. In addition, it would've required that each plate would've been unique, which could be a serious problem if it were lost on site.	Each corner is solved with 2 toggles, with room to adapt to each angle. The curved sheet will be uniform for all. Each perimeter cable is fixed with a toggle that will hold the threaded rod of the cable and on which it can be tightened.	Figure 6
Floating mast	Installation and form finding	In membrane conoids, radial tension is applied at the corners, edges and central ring. During assembly, all possible means must be available to stretch or to let the membrane loose.	A telescopic system is used in the rim connections with the floating masts in order to be able to stretch the cones globally in the radial direction. In addition, the membrane corners and perimeter cables will have adjustment systems for tensioning.	Figure 7
Floating mast	Installation	When fixing the membrane conoids to their rings, one must be very precise so that they are not misaligned in plan. It's very easy to end up with a torsion on the membrane.	Rotating system in the Z axis made up of a male and a female part.	Figure 8
Floating mast	Structural safety and installation ease	The conoids had to hover, without being attached to the structure. There is always the risk of falling on the pedestrians.	The hanging masts will be fixed to the main structures by steel cables. These steel cables will facilitate the assembly by allowing each pergola to be hanged on a first stage of installation and finished on a second stage.	Figure 9
Steel structure	Fabrication	It was requested that each steel element of each conoid (rims, floating masts) had different dimensions. That involved a lot of design and manufacturing time, as well as cost.	Manufacturing was homogenized as much as possible: 3 rim sizes, 3 structural profiles. Steel plate thicknesses were unified as much as possible, similar details for all the corners...	Figure 10

Membrane architecture: the seventh established building material. Designing reliable and sustainable structures for the urban environment.

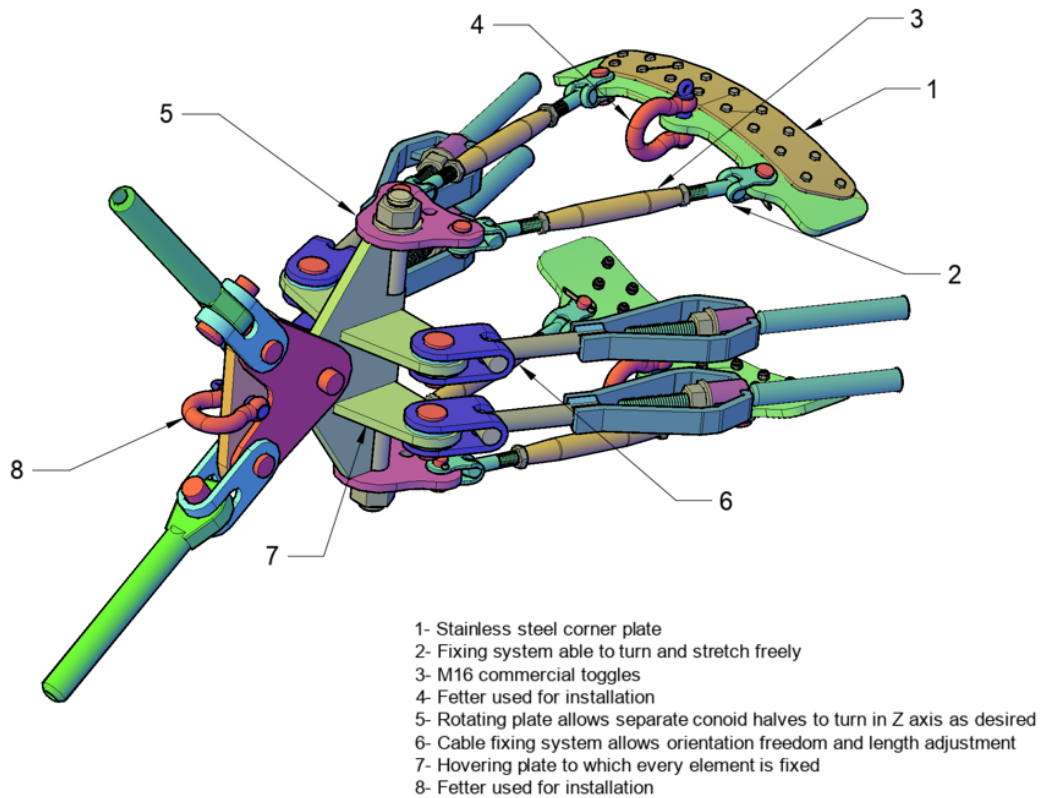


Figure 11 Elements that make up one of the corners

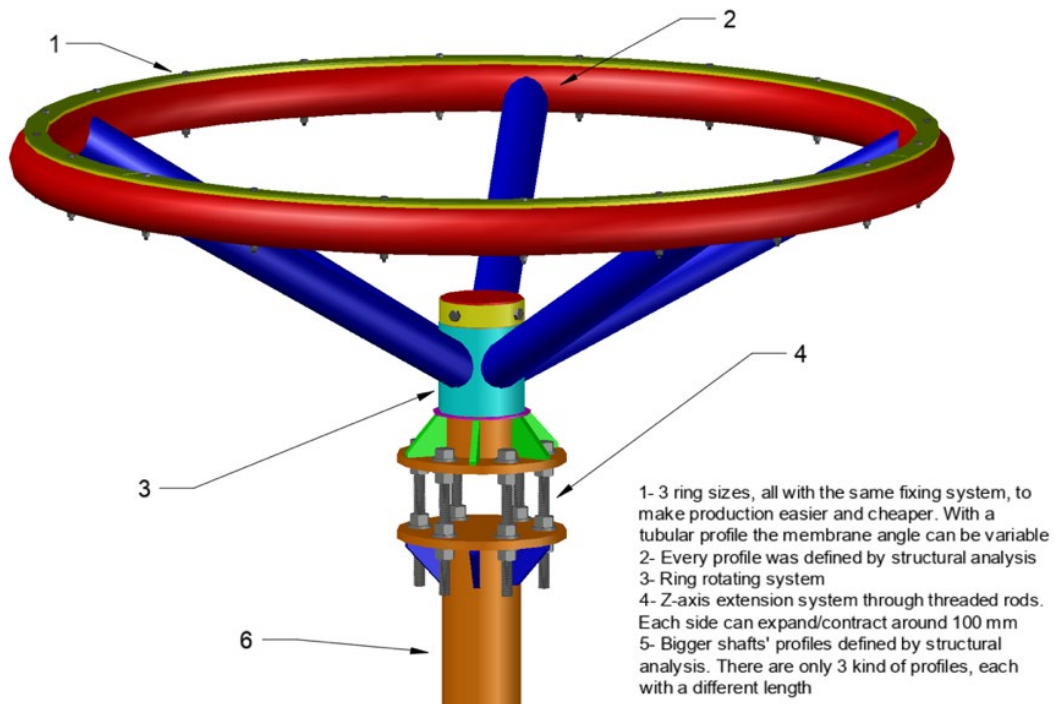


Figure 12 Detail of one of the floating mast rings with its extension system

Membrane architecture: the seventh established building material. Designing reliable and sustainable structures for the urban environment.

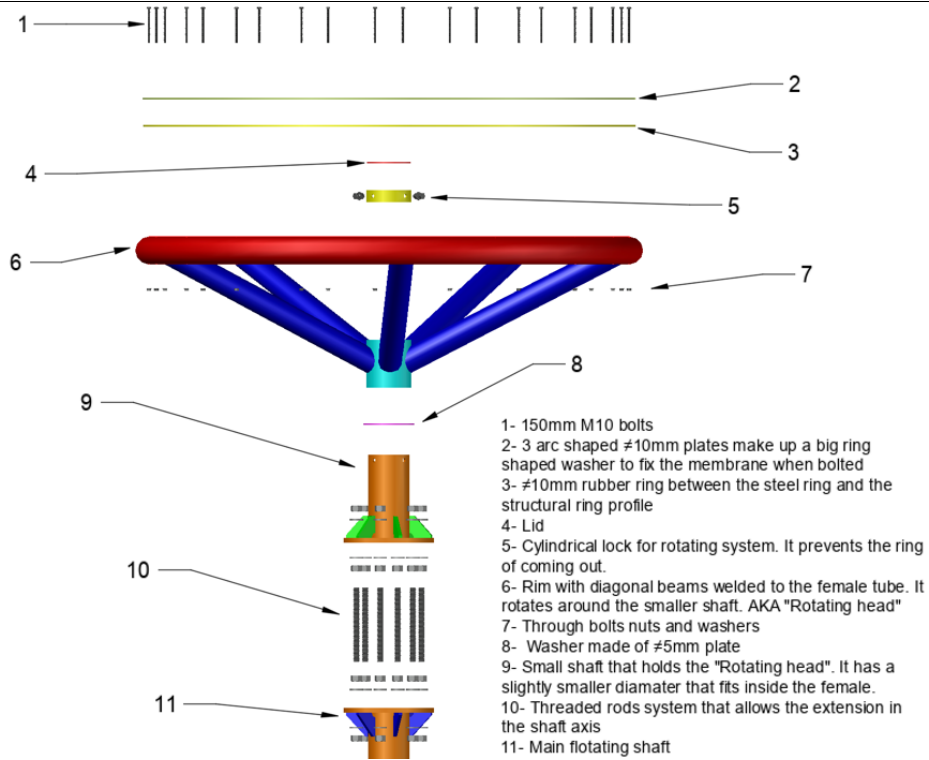


Figure 13 Elements that make up the floating mast rings

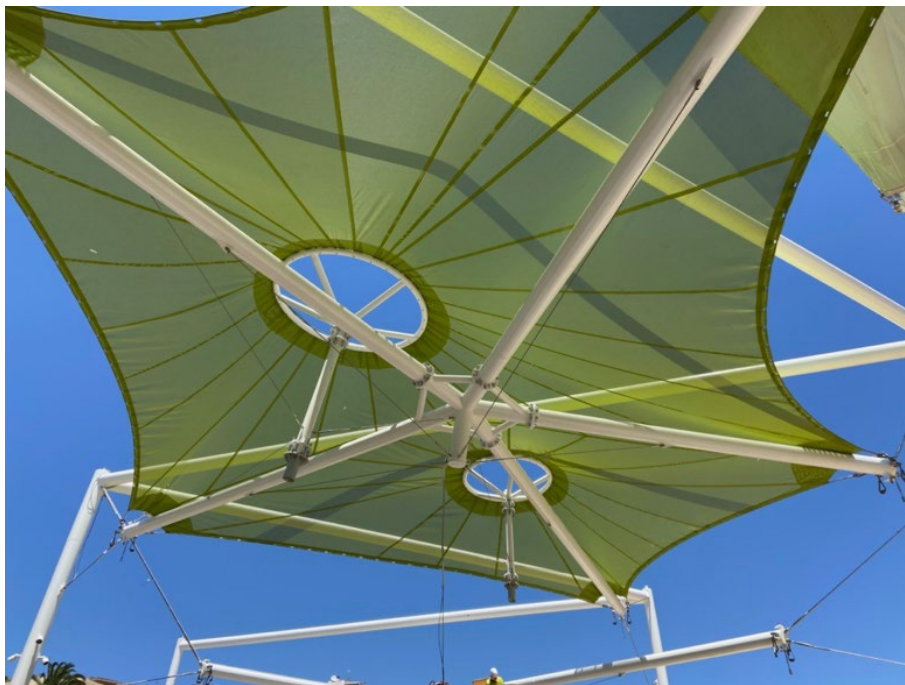


Figure 14 Top half of one pergola hanging thanks to the safety cables

Membrane architecture: the seventh established building material. Designing reliable and sustainable structures for the urban environment.



Figure 15 Steel floating masts elements sitting in the paint shop. The joints between shafts are all the same, but on different sizes.

4. Membrane fabrication

The 3D models used for each element's fabrication were created from previous 3D wireframe models of the structural models, so that the generated mesh and therefore its pattern would adapt as much as possible to those geometries.

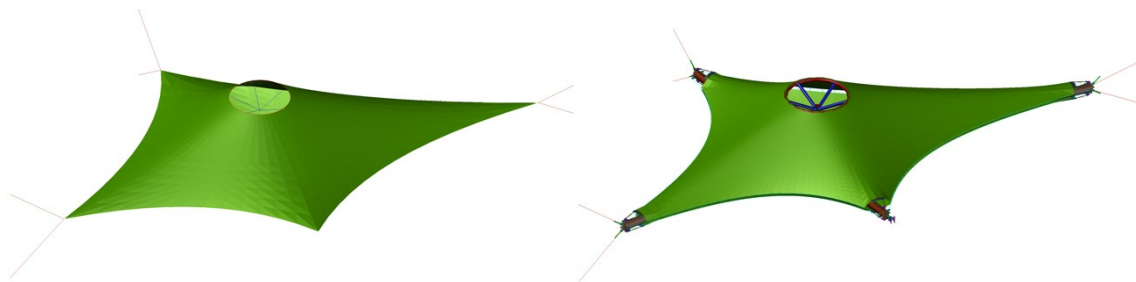


Figure 16 Definition comparison between the membrane and structure analysis model (left) and the membrane and steel structure fabrication model (right)

They were much more complex and heavier models than those used for the structural calculation.

Each conoid was broken down to between 16 and 36 radial panels that, welded together, made up the figure obtained from the 3D designs.

Membrane architecture: the seventh established building material. Designing reliable and sustainable structures for the urban environment.

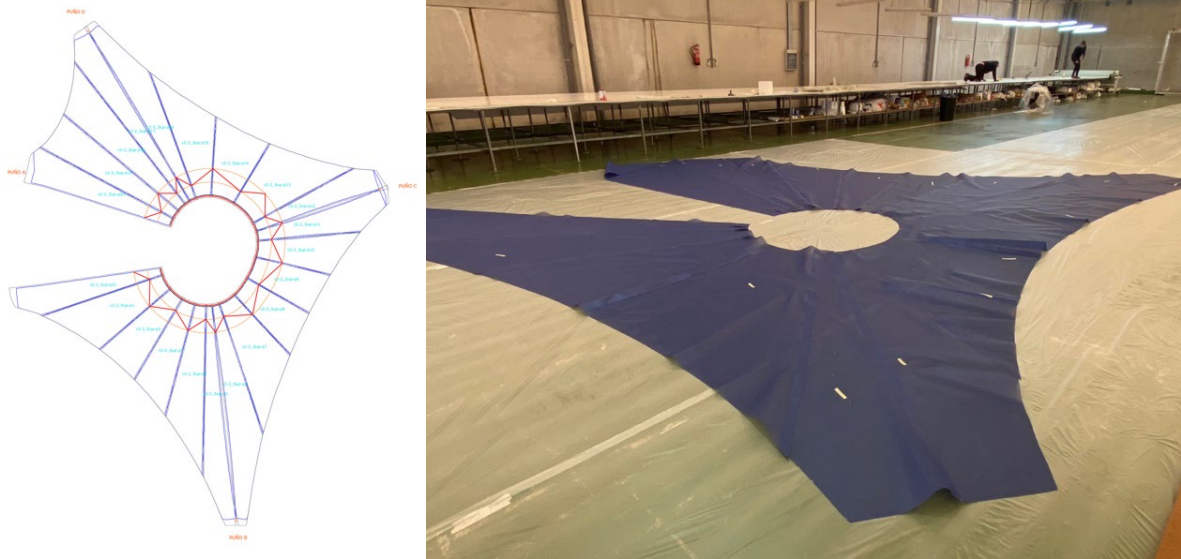


Figure 17 One of the conoid's patterning layout and its execution on the workshop

The pergolas that were made up of more than one conoid were made by individual conoids to later weld those parts together, matching with the radial seams.

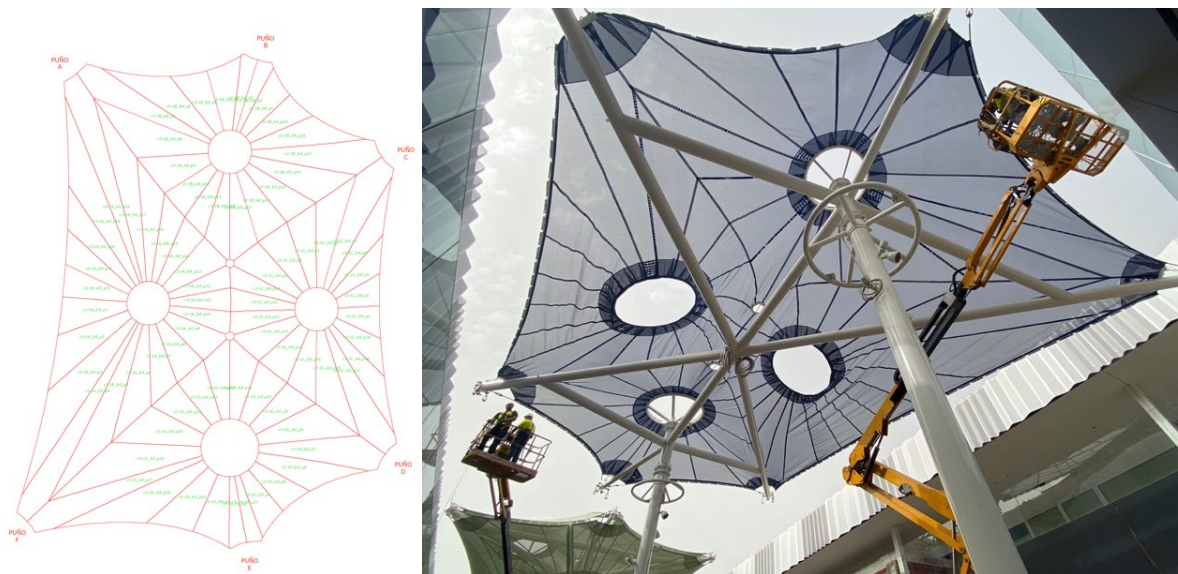


Figure 18 Patterning layout of one of the biggest PVC membranes made up of 4 conoids and its execution on site

5. Assembly

The mall administration imposed very strict conditions regarding working hours. Many of the pergolas could only be worked on for only half a working day.

Membrane architecture: the seventh established building material. Designing reliable and sustainable structures for the urban environment.

Since these membrane and steel elements had a high degree of prefabrication, their assembly was quite fast, despite the mall conditions. Small cranes had to be used to lift the floating steel structure.



Figure 19 Assembly of one of the conoids using small cranes and cherry pickers

6. Conclusions

The open spaces of the Porto Pi shopping center required a cover from the sun as well as a symbol of the modern renovation that was taking place.

Some striking, complex and innovative elements were devised for this purpose.

The development of these elements required the joint work of a multidisciplinary team, with a careful and attentive design, taking into account key aspects of the different phases of a tensile structure project, as well as the challenges posed by the proposed typology.

References

Schlaich J., Bergermann W. and Sobek W. (1989), Tensile membrane structures. Invited Lecture in the IASS Congress in Madrid.

Weller F. (2017), Common problems in the design and construction of membrane structures. VIII International Conference on Textile Composites and Inflatable Structures.

Philipp B., Wüchner R. and Bletzinger K-U (2013), Conception and design of membrane structures considering their non-linear behaviour, Proceedings of the STRUCTURAL MEMBRANES.



tensinantes2023 : TensiNet Symposium 2023 at Nantes Université

Membrane architecture: the seventh established building material. Designing reliable and sustainable structures for the urban environment.

Proceedings of the Tensinet Symposium 2023

TENSINANTES2023 | 7-9 June 2023, Nantes Université, Nantes, France

Jean-Christophe Thomas, Marijke Mollaert, Carol Monticelli, Bernd Stimpfle (Eds.)

PumpItUp, gite mobile for the European cultural capital Esch-sur-Alzette 2022

Bernd STIMPFLE*

*formTL ingenieure für tragwerk und leichtbau gmbh

Güttinger Str. 37, 78315 Radolfzell, Germany

bernd.stimpfle@form-tl.de

Abstract

Esch-sur-Alzette in Luxembourg is Capital of Culture 2022, together with Novi Sad in Serbia and Kaunas in Lithuania. Under the motto "Remix Culture", the city wants to present the cultural mix of the region and also combine the old industrial culture with the new. One of the projects for Esch 2022 is the Minette Trail, an approximately 90 km long hiking trail through a former industrial region in the south of Luxembourg. As overnight accommodation, 11 "Kabaisercher" have been planned by various teams of architects. One of these hostels is PumpItUp, a pneumatic mobile shelter. The pneumatic shell is on a trailer with two foldable wings. The shelter is set up and dismantled several times, at different locations. The pneumatic envelope forms a spherical shape from two layers of membrane, coupled at many nodes with synthetic fibre ropes. This paper presents the project from the design to the fabrication and installation.

Keywords: membrane, polyester-ropes, pneumatic structure, temporary structure

1 Design

Based on the architects' competition design, a pneumatic shape was developed. The internal pressure and the prestress in the membranes balance the system. The prestress creates bending stiffness in the two-layer envelope to resist against external loads.

In order to achieve the required stiffness, a significantly thicker wall was created compared to the competition design. The wall thickness of 0.3 m was increased to approximately 1 m. Due to the steep walls inside, this does not restrict the use.

Two approaches were examined to determine the connection points. In the first approach, the two parts of the envelope are coupled in radial sections, with the disadvantage that the density of the ropes increases towards the zenith. Therefore, the principle of the geodesic dome was

Membrane architecture: the seventh established building material. Designing reliable and sustainable structures for the urban environment.

applied as a second variant. The dome is divided into bigger triangular panels, each then subdivided into 36 smaller triangles. The rope connections are attached to the corners of the small triangles. This creates a harmonious shape with an even distribution of the connection points.

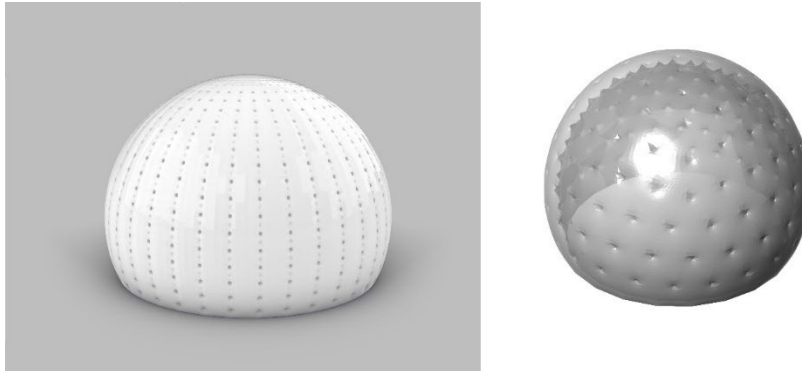


Figure 1: Radial connections and Geodesic dome

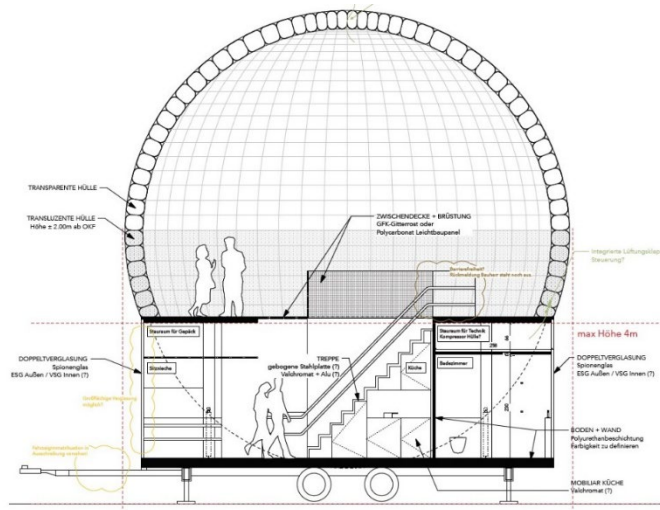


Figure 2: Section through the competition design (source: 2001)

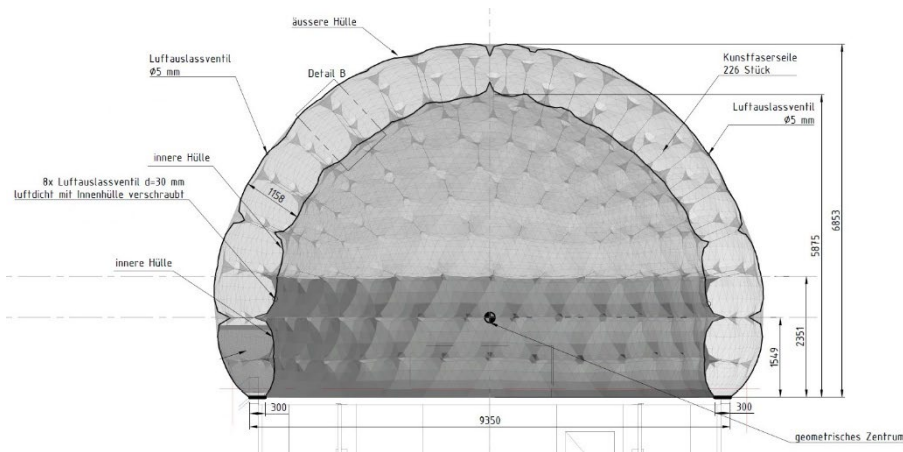


Figure 3: Section through the formfinding shape

Membrane architecture: the seventh established building material. Designing reliable and sustainable structures for the urban environment.

2 Project description

The pneumatic envelope forms a sphere made from two layers of membrane. Both layers are made of high translucent PVC coated polyester membrane. Ten transparent bulls' eyes allow the view to the sky.

The outer and inner membranes are coupled at the nodes with synthetic fibre ropes. The connection to the platform is made with zips and aluminium clamping strips along the perimeter.

In order to allow natural ventilation, two ventilations tunnels connect inner and outer membrane, closed with an open mesh on the outside, and a removable cover on the inside.

3 Analysis

Professor Mike Barnes' software was used for the analysis. TLform for formfinding and TLload for the load analysis. The software uses the method of dynamic relaxation and takes into account the special features of membrane, foil and rope structures. These are, to name some examples, formfinding, orthotropic material behaviour (longitudinal and transversal direction) and large deformations.

The numerical model is discretised by cable elements, as well as triangular membrane elements. It is analysed with geometric non-linearity, taking into account the change in length of the elements as well as the deformation of the entire structure. The equilibrium is determined in the deformed states.



Figure 4: Isometric view numerical model

The mobile hut (gite mobile) is a temporary structure according to EN 13782. According to the Luxembourg national application document for Eurocode 1 part 1-4, the reference wind speed is 24 m/s, thus the wind load table from EN 13782 can be applied. Snow load was not taken into account as the use in winter is not foreseen.

The wind load is distributed according to EN 1994-1-4 for a hemisphere.

Membrane architecture: the seventh established building material. Designing reliable and sustainable structures for the urban environment.

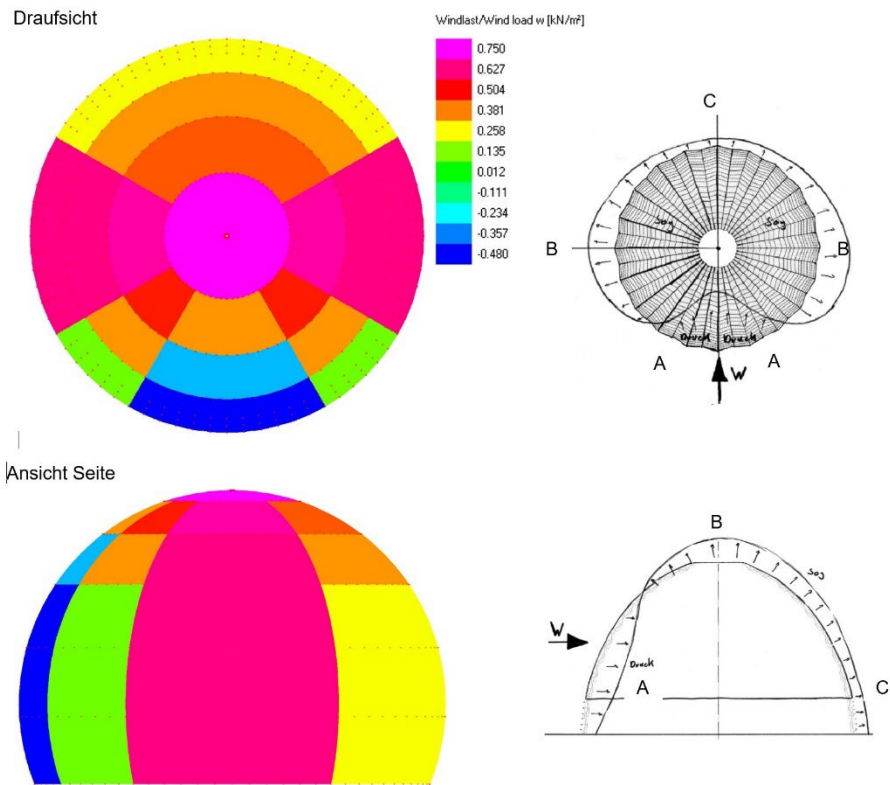


Figure 5: Applied wind load distribution

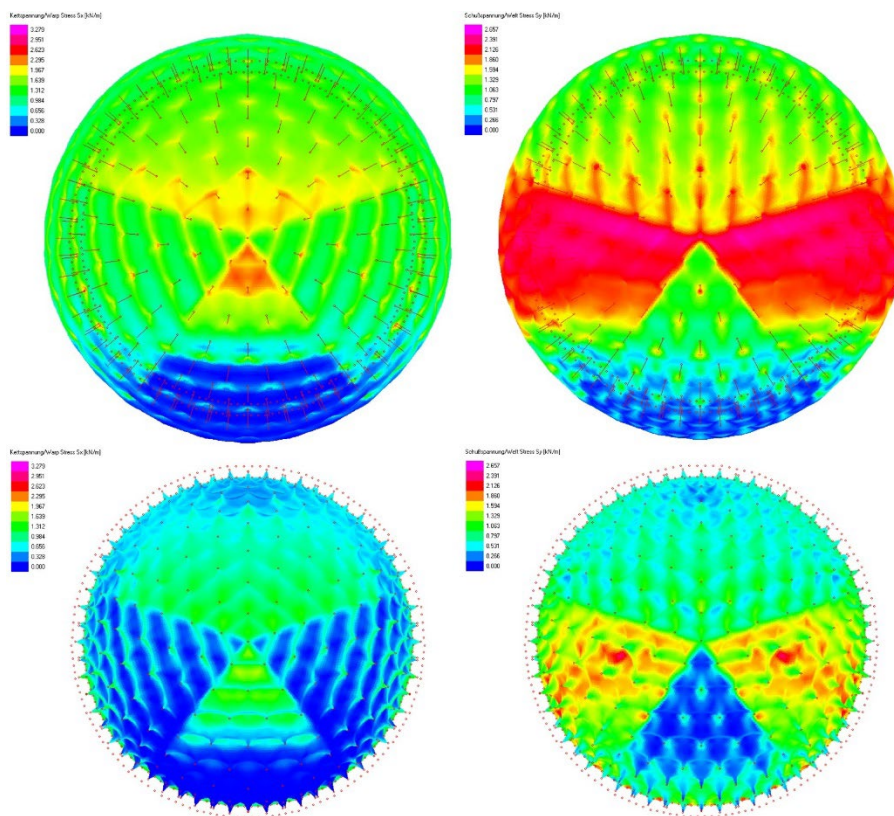


Figure 6: Stress in the outer and inner envelope under full wind load

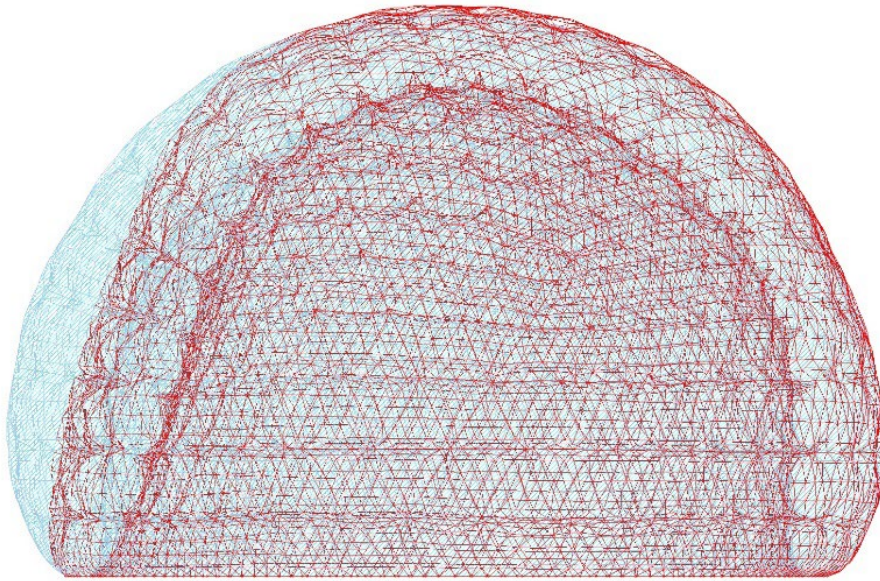


Figure 7: Deformation under maximum wind

Since the bending stiffness of the envelope is not very high, it reacts to wind pressure with a significant inward deformation. However, the stability under design wind conditions is not limited.

4 Air supply

A support air unit provides an internal pressure of 1000 Pa in order to provide the pneumatic prestress. The unit is fabricated as a special design. The blower and the dryer are housed in two separate cases, installed in the chassis of the trailer.

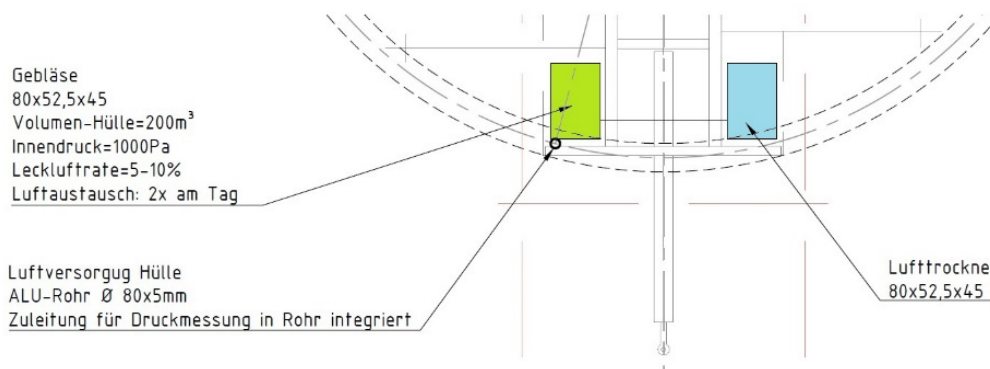


Figure 8: Integration of the blower unit in the chassis

In order to minimise the permanent stress in the foil, the inner pressure was reduced from initially 1500 Pa to 1000 Pa, as the analysis showed sufficient stability even at lower pressure.

Membrane architecture: the seventh established building material. Designing reliable and sustainable structures for the urban environment.

5 Detailing

The two layers of membrane are connected by polyester ropes. Polycarbonate discs with carriage bolts and eye nuts are welded into the membrane. The ropes are connected with small carabiners.

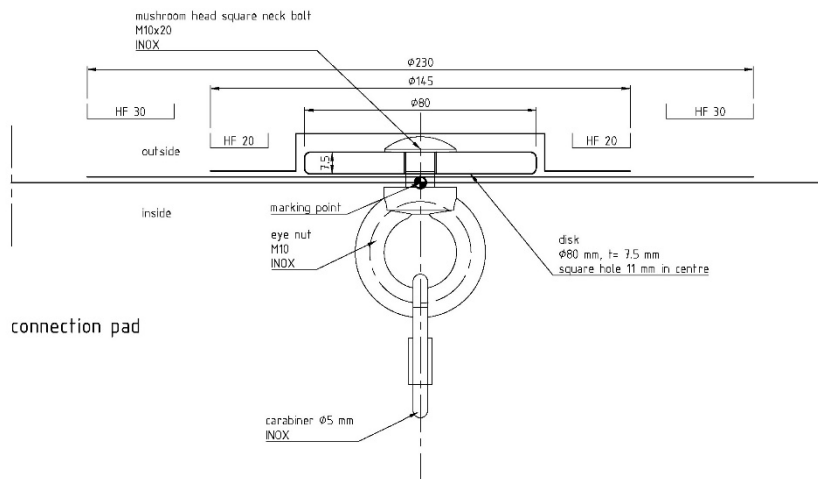


Figure 9: Connection for the ropes

This node detail was checked in a load test for the initially foreseen PVC foil. At 1.5 kN load, which corresponds to the maximum load in the project, a shape was achieved that fits well to the shape analysed. Up to a force of 8 kN the detail resisted against failure, but with significant plasticisation



Figure 10: Nodal test in the load steps 1.5 kN and 4.5 kN

The connection to the platform is made with clamping plates along the perimeter of the platform. Keder strips with zips allow quick assembly and disassembly. The pneumatic structure is welded airtight, and the zips are applied on the outside to the pneumatic system, so that no airtightness is required for this detail.

Membrane architecture: the seventh established building material. Designing reliable and sustainable structures for the urban environment.

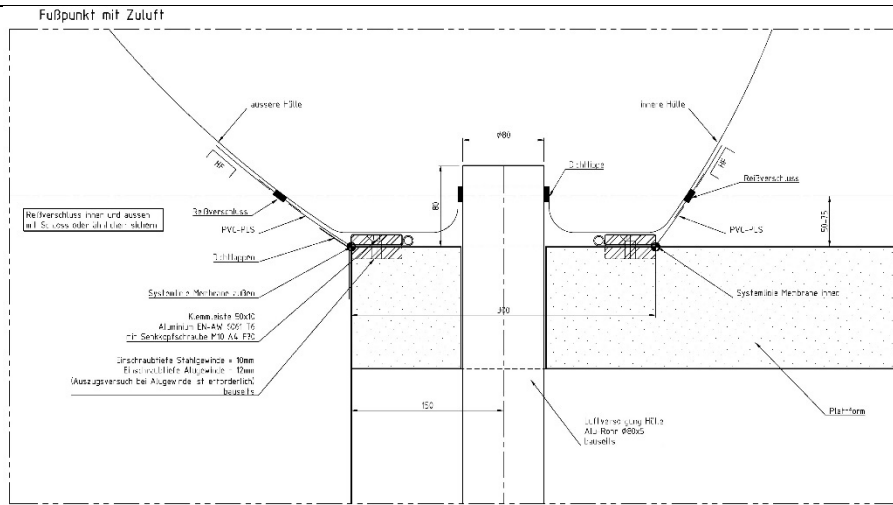


Figure 11: Connection to the platform

In one corner of the trailer, the 80 mm air supply pipe ends between the two clamping lines above platform level. The membrane has a slightly smaller opening, which is placed over the pipe.

6 Cutting pattern and fabrication

The shape of the structure is locally heavy curved, which would require a very high effort for the fabrication. For an optimal manufacturing process, the patterning model was generated as an averaged rotational surface, with an almost identical overall surface.

A comparing analysis with this model under inner pressure led back to the original membrane geometry, which confirmed the feasibility of this cutting method.

This cutting model was separated at the main lines of the geodesic dome and then cut horizontally. The cutting patterns also contain the location of the connection points for the cables, the bull's eyes and the ventilation tunnels.

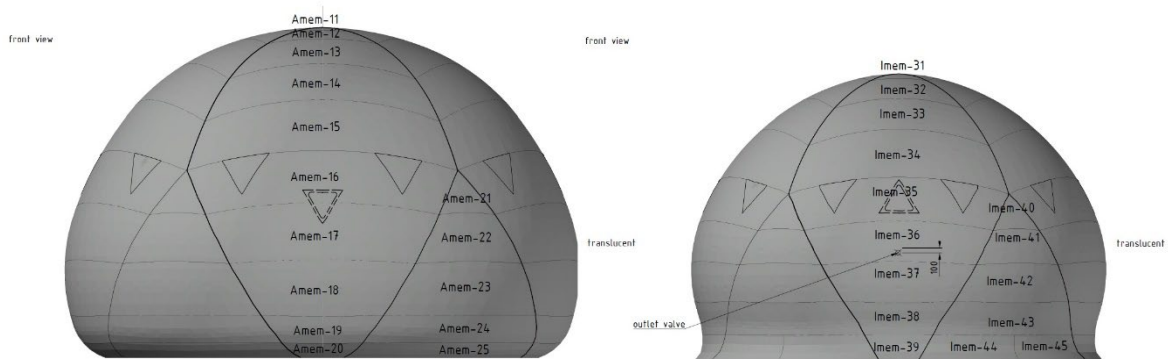


Figure 12: Smooth patterning model Outside and Inside

Membrane architecture: the seventh established building material. Designing reliable and sustainable structures for the urban environment.

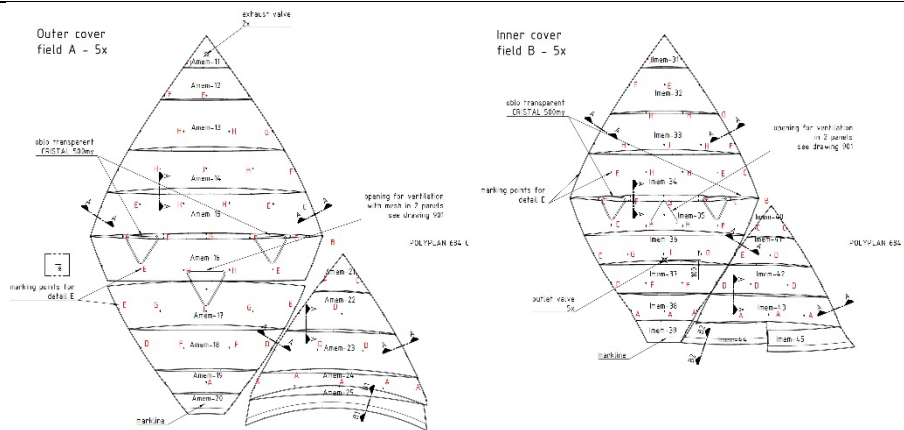


Figure 13: Membrane and Foil pattern

The compensation was determined on the basis of biaxial tests. The biaxial tests and their evaluation were carried out in accordance with EN 17117-2, based on the project-specific stress level.

The single pattern are joined with HF weld seams. In a first step, the sub-panels are manufactured and then the sub-panels are assembled. Special round electrodes were fabricated for the nodal supports.

7 Installation

At the end of December 2021, directly after completion of the envelope, a test assembly was carried out to test the inflation and folding of the membrane.

With the increase of the internal pressure, the envelope is lifted up. The outer membrane pulls the inner membrane via the connecting ropes.

Shortly before the pressure of 1000 Pa was reached, the zenith was also completely up and the planned shape was achieved. If you lean against the wall from the inside, the construction only reacts slightly. People inside the envelope can only be perceived when they lean against the envelope wall.



Figure 14: Test inflation of the finalised translucent envelope (source: Canobbio)

Membrane architecture: the seventh established building material. Designing reliable and sustainable structures for the urban environment.

The assembly of the PumpITup project on the trailer took place in an old industrial hall in Schiffflange. The chassis comes from Belgium, the body from France and the membrane envelope from Italy.

The circumferential keder strips with the corresponding zip half were attached along the perimeter of the platform with clamping plates.

Then the pneumatic cover was placed in the centre of the platform with a crane. The cover was spread out and the zips were connected all around. After all the connecting lines were connected, the blowers could pressurise the envelope. As already seen in the test set-up in Italy, the hull slowly lifted.

As the internal pressure increases, the theoretical shape sets in and the gite mobile becomes walkable and tangible.



Figure 15: Final installation

The first outside installation was then realised in the natural reserve Ellergronn. As it is a mobile hut, shortly after this installation, it has been taken to Luxemburg-Kirchberg, and has been presented at the fair Home Expo, before coming back to the city of Esch sur Alzette.

Membrane architecture: the seventh established building material. Designing reliable and sustainable structures for the urban environment.



Figure 16: Inner view



Figure 17: Bulls eye

Membrane architecture: the seventh established building material. Designing reliable and sustainable structures for the urban environment.



Figure 18: Evening hours (source: Ludmilla Cerveny)



Figure 19: Final project at night (source: 2001)

Membrane architecture: the seventh established building material. Designing reliable and sustainable structures for the urban environment.

8 Conclusion

The mobile hut was created in an interdisciplinary collaboration. It is both a vehicle and a full accommodation. The transparent envelope covers the sleeping place for hikers. During the day the translucent envelope provides a clear and bright space inside, and at night, it appears like a glowing bulb, and through the bulls eyes the guests can see the sky. The overnight stay becomes a special and unforgettable experience.

9 Project data

Surface area outer membrane: 251 m²

Surface area inner membrane: 168 m²

Covered area: 93 m²

Membrane material: Sattler Polyplan 684 C

Foil material bulls eye: Cristal Plus 500 µm

10 Acknowledgements

Client: Ville d'Esch-sur-Alzette

Architecture: 2001 territories, buildings, spaces & ideas, Esch-sur-Alzette, Luxembourg

Interior design: NJOY_architecture inside, Luxembourg

Structural design pneumatic envelop: formTL ingenieure für tragwerk und leichtbau gmbh, Radolfzell, Germany

Execution pneumatic envelop: Canobbio Textile Engineering srl, Castelnuovo-Scrvia, Italy

Air supply: Elnic, Rosenheim, Germany

11 References

Barnes, M. R. (1999). Form finding and analysis of tension structures by dynamic relaxation. *International Journal of Space Structures*, 14(2), 89-104. <https://doi.org/10.1260/0266351991494722>.

EN 13782:2015 Temporary structure - Tents - Safety

ILNAS-EN 1991-1-4:2005+A1:2010 - AN-LU:2020, Eurocode 1: Actions sur les structures - Partie 1-4: Actions générales - Actions du vent - Annexe Nationale Luxembourgeoise

EN 1991-1-4:2005 + A1:2010 + AC:2010: Eurocode 1: Actions on structures - Part 1-4: General actions - Wind actions

EN 17117-2:2021: Rubber- or plastics-coated fabrics - Mechanical test methods under biaxial stress states - Part 2: Determination of the pattern compensation values

B. Stimpfle, "PumpItUp – gite mobile für die Kulturhauptstadt Esch-sur-Alzette 2022". *Stahlbau* 8/2022.



tensinantes2023 : TensiNet Symposium 2023 at Nantes Université

Membrane architecture: the seventh established building material.
Designing reliable and sustainable structures for the urban environment.

Proceedings of the Tensinet Symposium 2023

TENSINANTES2023 | 7-9 June 2023, Nantes Université, Nantes, France

Jean-Christophe Thomas, Marijke Mollaert, Carol Monticelli, Bernd Stimpfle (Eds.)

The integration of CAD and FEA for lightweight design and analysis

Ann-Kathrin Goldbach*, Kai-Uwe Bletzinger^a

*^aLehrstuhl für Statik, Technische Universität München

Arcisstr. 21, 80333 München

ann-kathrin.goldbach@tum.de

Abstract

The design cycle of membrane and lightweight structures, consisting of the highly non-linear analysis steps of formfinding, structural analysis, cutting pattern generation and construction staging, is well established. Computer Aided Design (CAD)-integrated analysis not only keeps the smoothness of the typically double-curved surfaces of structural membranes intact and available for analysis, but also maps the connections and dependencies of the mentioned analysis steps. Therefore, it captures the interaction of form and force as well as the iterative nature of the design process, see e.g. Goldbach (2021). Design decisions can therefore be made under consideration of the whole design cycle, which is analyzed within one software environment. This leads to unifying the design and analysis model and thus the computational tools of architects and engineers. Furthermore, a parametric environment allows for very flexible modeling with respect to geometrical as well as mechanical properties of the structure. Optimization loops can easily be added to any parameter to ensure the ideal utilization of the design space, also with respect to the verification of the ultimate and serviceability limit states. The basis for CAD-integrated design and analysis, namely Isogeometric B-Rep Analysis (IBRA) is a Finite Element Method based on the mathematical description of the CAD model (as introduced in Breitenberger et al. 2015). In line with the creation of a (structural) digital twin, the CAD model is enhanced by additional information, in this case the mechanical properties to build a FE model.

This contribution will show the advantages of the integration of CAD and Finite Element Analysis (FEA) and introduce the idea of a structural digital twin, that is capable of depicting the design and construction process of lightweight structures. In addition, advances will be presented and illustrated with an exemplary model of a lightweight structure. For this, the freeware Kiwi!3D of str.ucture and TUM will be used as a plugin to a parametric CAD software.

Keywords: Design Cycle, Digital Twin, FEM, Formfinding, IBRA, IGA, CAD-integration, Lightweight Design, Parametric Design, Structural Membranes

Membrane architecture: the seventh established building material. Designing reliable and sustainable structures for the urban environment.

1. Introduction

Membrane structures fulfill the requirements of lightweight design by their ability to cover large spans with a minimal material input and neglectable self-weight. Depending on the material and constructive design, they can fulfill a multitude of purposes in the built environment, ranging from flexible modular shelters to stadium roofs and hangars. However, regardless of the dimension, the principle that allows pliable technical textiles to be built into structures that can withstand external loading is the combination of curvature and (pre-)stresses, i.e. form and forces. Structural membranes need to be designed at the interface of architecture and engineering, as the shape and the stress state are inseparable.

The integration of Computer Aided Design (CAD) and Finite Element Analysis (FEA) with Isogeometric B-Rep Analysis (IBRA) leads to an environment that provides this interface. By utilizing the design (CAD-) model for analysis purposes and keeping its description intact throughout consecutive analysis steps, one model serves as the basis for collaboration. This unified approach and its components with respect to geometry description and FE methodology will be shown in Section 2. A detailed description of the method and possible applications can be found in e.g. Goldbach (2021).

In light of the ongoing discussion and demand of digital twins for the lifecycles of buildings (e.g. DBZ (2020)), the integration of CAD and FEA provides an eligible solution for creating a structural twin with a number of advantages for lightweight design and analysis. It will be explained, how a parametric CAD-integrated analysis environment can be set up to depict the dependencies of formfinding, structural analysis and cutting pattern generation (i.e. the design cycle of structural membranes). The structural digital twin can also be used to simulate construction processes with mounting analyses. With respect to a building's lifecycle, the possibility to adapt geometrical and mechanical properties of the model is beneficial once again, as it allows for the inclusion of monitoring observations and their effect on the structural behavior.

2. Integration of CAD and FEA

With the introduction of Isogeometric Analysis (IGA) by Hughes et al. (2005), the first step towards bridging the gap between the Computer Aided Design (CAD) and Finite Element Analysis (FEA) environments was made and a number of numerical techniques for CAD-integrated analysis were developed based on this research. The main idea of IGA is the direct utilization of the CAD-model as the FE Analysis model, see e.g. Cottrell (2009).

The branch of Isogeometric B-Rep Analysis (IBRA) by Breitenberger et al. (2015) focuses on using the full description of a CAD-model – i.e. a B-Rep model based on Non-Uniform Rational B-Splines (NURBS), so that important features of modern CAD programs like trimming can be applied while designing a geometry without compromising the analysis model.

Another advantage of CAD-integrated analysis is the possibility to build fully parametrized models with respect to geometric as well as structural properties. This leads to very flexible simulation models that can be used to explore numerous variants within the design space. Especially for membrane structures, where both geometrical and mechanical properties can result in significant changes of the structural behavior, the possibility of performing efficient parameter studies and can have major advantages for the whole design process.

2.1. NURBS, B-Rep and CAD-integrated analysis

Typical CAD models are built as B-Reps, following the simple principle that all geometrical entities are defined by their boundaries, e.g. edges through vertices and surfaces through edges. B-Reps can have various boundaries, that means that parts of a geometry can be “cut out” or “off” by trimming operations.

Non-Uniform Rational B-Splines (NURBS) are one of the standard geometry descriptions used in CAD for curves and surfaces, that consist of so-called control-point polygons, NURBS shape functions and weights at the control points, see Figure 1. NURBS are explained in detail in e.g. Piegl (1997).

In order to perform CAD-integrated analysis with IBRA, the NURBS-based B-Rep geometry description is used to define Finite Elements, e.g. turning surfaces into membrane elements. Following the isoparametric concept, the NURBS curves that are used for geometry description simultaneously provide the shape functions for FEA. The degrees of freedom lie at the control points and thus no longer have to be on the surface or curve – which is the most prominent difference to classical FEM with faceted meshes. A beneficial property of NURBS representation is, that refinement of the discretization can be performed without changing the shapes. Figure 1 summarizes the basics of IBRA with B-Rep geometry definition, a very simple example of isogeometric elements on a doubly curved surface, as well as a NURBS curve with its control point polygon and basis functions. In Bauer (2020), the IBRA element definitions that are most relevant for lightweight design are explained in detail.

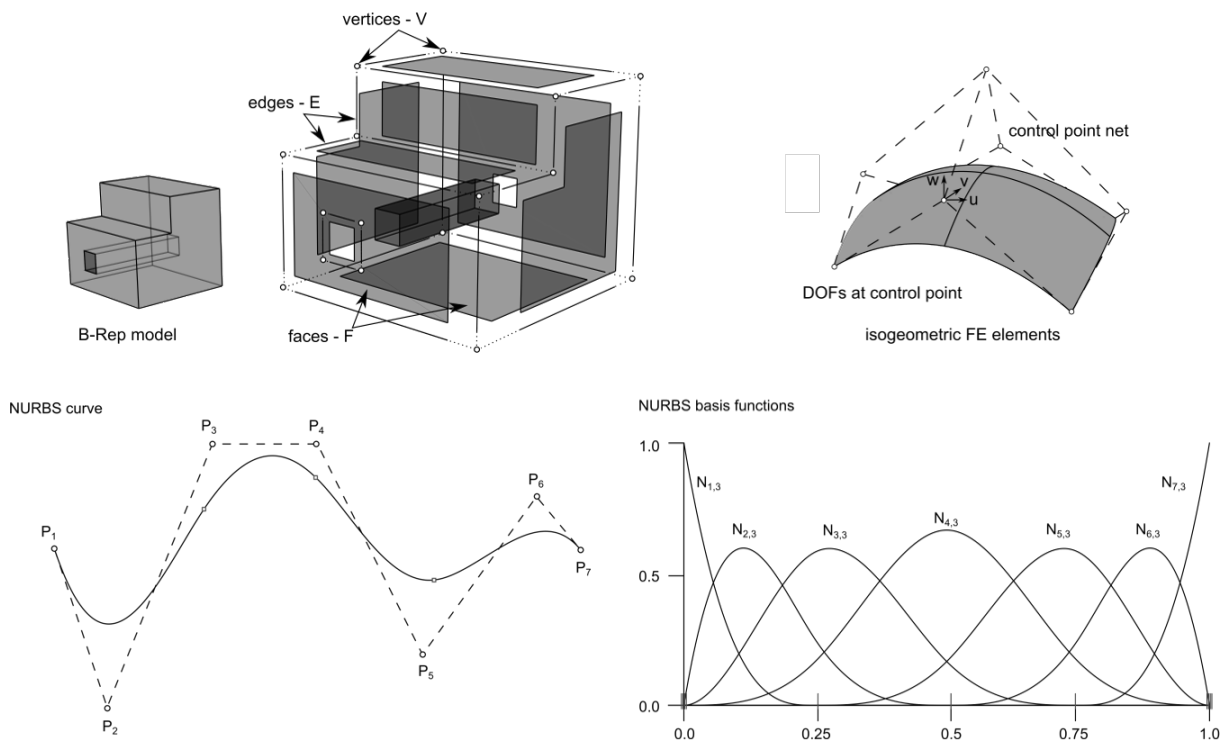


Figure 1: Geometry representation in CAD and IBRA. Top left: B-Rep model. Top right: control point polygon and DOFs of IBRA model Bottom: NURBS curve with its shape functions. Adapted from Goldbach (2021).

Membrane architecture: the seventh established building material. Designing reliable and sustainable structures for the urban environment.

2.2. Unified Workflow

Through CAD-integrated analysis, the design and analysis model become one and the unified workflow (as shown in Figure 2) emerges. The highly time-consuming tasks of meshing and transferring data back and forth between different software is omitted, facilitating the interaction between architects and engineers. Not only can all steps from Pre- to Postprocessing be performed within a CAD-program, but the B-Rep model is kept intact throughout the analysis process. Therefore, linking consecutive analyses is straight-forward, which is a significant advantage for the design cycle of structural membranes, where the analysis results of formfinding, structural analysis and cutting pattern generation strongly depend on each other and thus need to be calibrated iteratively.

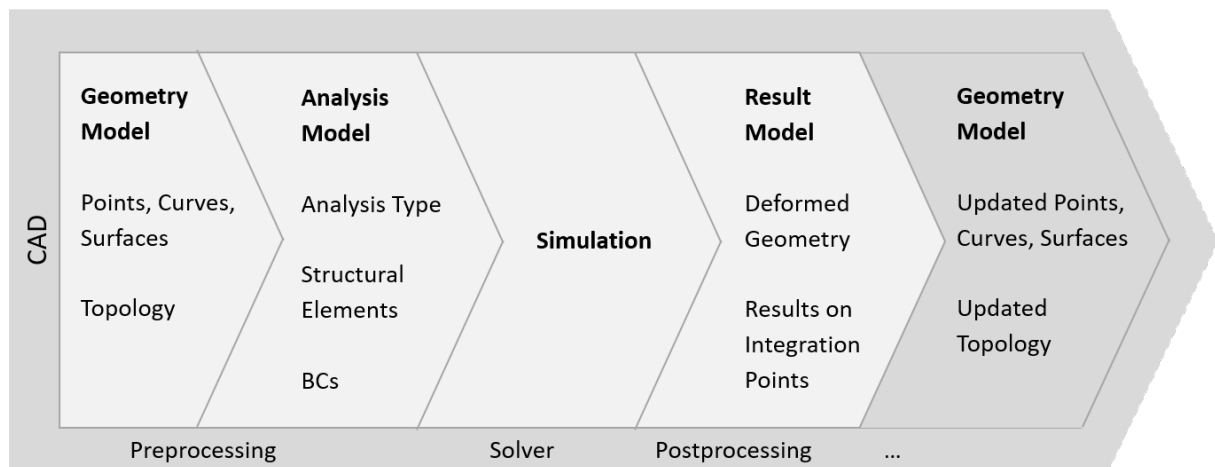


Figure 2: The unified workflow: from Pre- to Postprocessing and consecutive analyses within the CAD software environment. Adapted from Goldbach (2021).

2.3. Parametric Design and Analysis: towards a structural digital twin

During the design phase, changes in a number of parameters that are decisive for a structure's load bearing behavior are to be expected – especially for lightweight structures. Parametric models meet the iterative nature of design by providing flexible input parameters, see e.g. Brown (2019). In the CAD-integrated approach, both geometrical and structural parameters can easily be calibrated towards an optimal solution in every design step. For membrane structures, the updated parameters need to be applied to formfinding, structural analysis with verification as well as cutting pattern generation. Within the unified workflow (briefly explained in the previous section), these analysis steps can be linked and therefore, all parameter updates can automatically be considered for the whole design cycle. Additional optimization loops that are connected to the parametric model can be useful in some cases, as shown in Goldbach et al. (2021).

As design and analysis model are one, a performance based design can efficiently be reached whilst this model can serve as the basis of communication between the participating parties. Figure 3 shows the unified workflow for the parametric design cycle of structural membranes with the steps of formfinding, structural analysis, cutting pattern generation and mounting and some input parameters. In the sense of a structural digital twin, this setup not only allows for case studies in preliminary design, but can also be used to include monitoring data during the structure's life cycle or for the planning of (geometrical or structural) alterations.

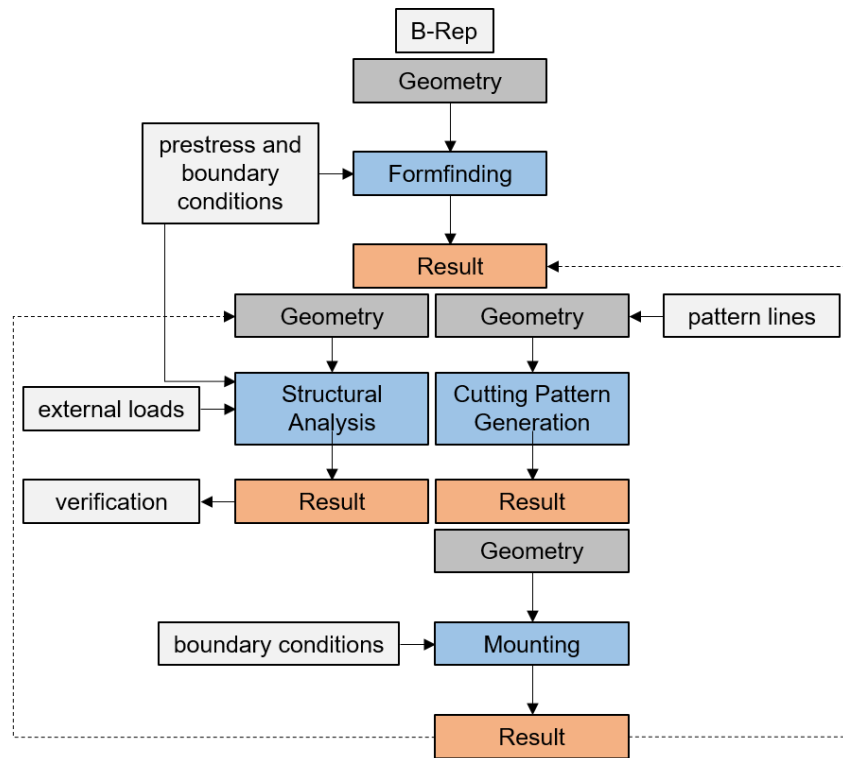


Figure 3: Dependencies and links in the parametric model set-up for the design cycle of structural membranes. Adapted from Goldbach (2021).

3. Design and analysis of an exemplary hybrid lightweight structure

During the summer term, the “Membrane Workshop” at Technical University of Munich is held for postgraduate students of civil engineering, architecture and computational mechanics. Besides gaining theoretical knowledge on the design cycle of membrane structures, the students build interdisciplinary teams and develop design projects for a given topic. They use Kiwi!3d with Rhino and Grasshopper throughout the conception phase and perform first analyses to do a preliminary assessment of their designs’ structural behavior. The CAD-integrated design and analysis environment has proven to have a very positive effect on these design projects with respect to originality, level of completion as well as the interaction and communication within the groups.

In 2022, the 50th anniversary of the Olympic roofs in Munich lead to the design task of creating new lightweight covers and spaces around the Olympic lake. The example shown here was developed as a “pathway” along the lake, leading to a stage that was also covered by a membrane structure within this student project work.

Membrane architecture: the seventh established building material. Designing reliable and sustainable structures for the urban environment.

The student group's design steps with Kiwi!3d were as follows:

- definition of dimensions (path width, length and height)
- parametric modeling of surfaces
- parametric modeling of cable and membrane elements and supports
- formfinding analysis with rigid arches
- structural analysis under typical load scenarios for rough dimensioning of membrane, cables and (now elastic) arches based on the previously formfound model

Figure 4 shows the resulting design solution for the pathway and its development in the parametric CAD-environment from the first geometry model for formfinding up to a final rendering for presentation. Apart from testing geometry variations through the parametric setup, mechanical parameters such as the prestress in the membrane and cables of the structure were adapted iteratively to ensure the structural integrity for estimated simplified load cases.

4. Conclusion and Outlook

It was shown how a parametric CAD-integrated design and analysis framework holds a number of advantages for lightweight design and analysis. The integration of CAD and FEA not only leads to significant potential for the collaboration of architects and engineers, but also provides the possibility of the assessment of the structural behaviour throughout a building's lifecycle. The requirements for a structural digital twin – using predictive analysis to simulate the structural response of a building to certain environmental influences - are thus met by the unified workflow with Isogeometric B-Rep Analysis presented in this paper.

One of the remaining challenges for lightweight and membrane structures that was not addressed in this paper, lies within these mentioned environmental impacts. Due to their complex shapes and often high flexibility (or large deformations), the determination of pressure coefficients due to wind loading is yet to be investigated. A wind engineering study for the Olympic roofs in Munich has yielded a concept to compute the wind loads in a numerical wind tunnel, that should be mentioned in this context (see Péntek et al. (2022)). Apart from the simulation of the turbulent flow, the topic of creating a structural digital twin that is carefully calibrated to model the existing structure, was addressed in detail and revealed further aspects related to the monitoring of lightweight structures for future exploration. Future work thus not only needs to focus on the development of numerical methods that can simulate special load cases like ponding and wind, but also needs to define appropriate interfaces for the incorporation of monitoring data into structural models in order to be turned into accessible structural digital twins.

Acknowledgements

The collaboration with Prof. Dr.-Ing. Lars Schiemann in teaching the “Membrane Workshop” at TUM is gratefully acknowledged, as well as the design project contribution by the architecture and engineering students.

Membrane architecture: the seventh established building material. Designing reliable and sustainable structures for the urban environment.

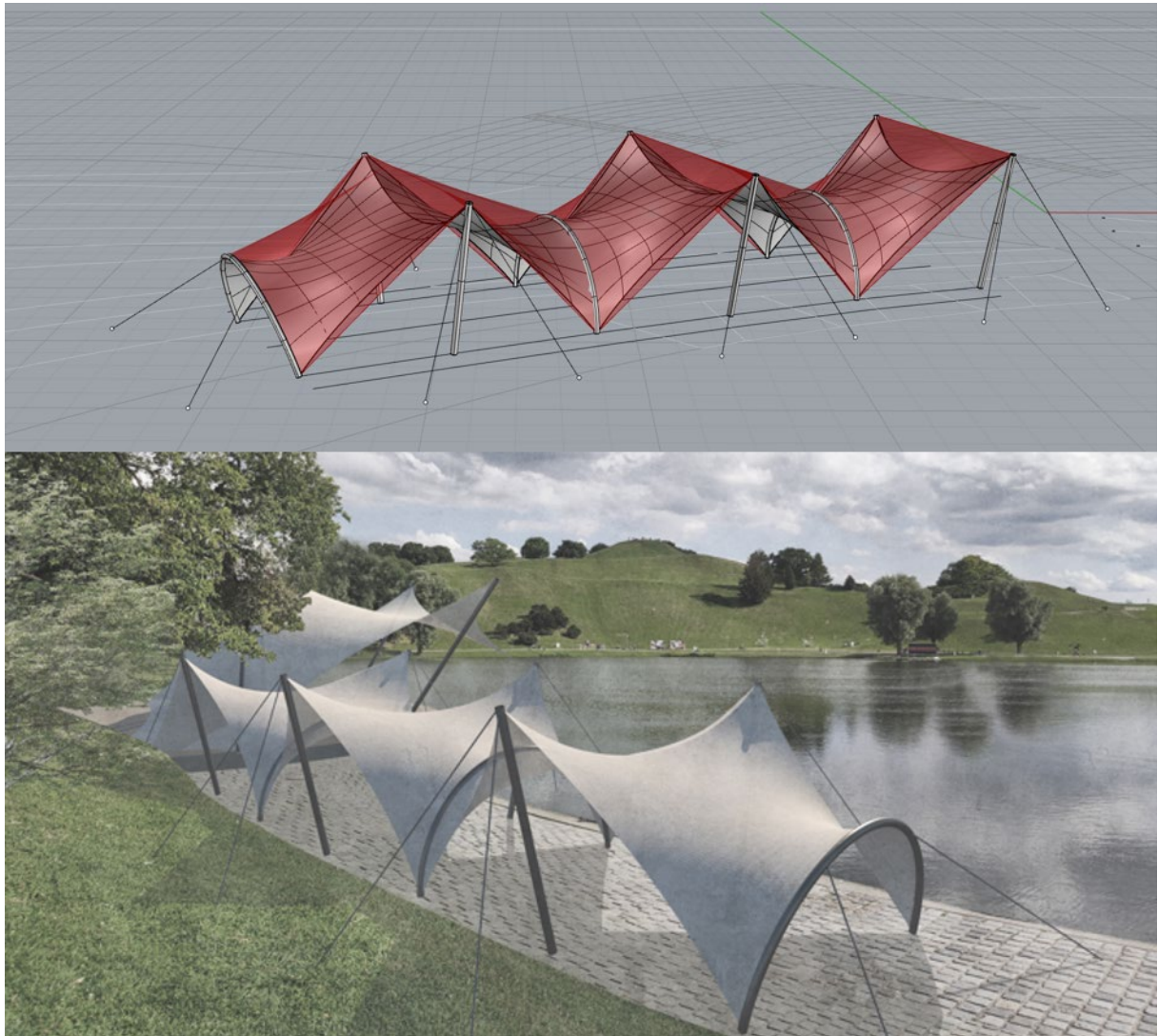


Figure 4: Hybrid structure designed with Kiwi!3d for Grasshopper and Rhino, by architecture students D. Agostini and D. Binci and engineering students A. Ciolek and J. Suchowerchov during the “Membrane Workshop” at TUM, summer term 2022. Top: Parametric CAD- and analysis model – initial geometry (red) and formfound equilibrium surfaces (grey). Bottom: rendering of final design solution set in the Olympic parc in Munich.

Membrane architecture: the seventh established building material. Designing reliable and sustainable structures for the urban environment.

References

- Bauer, A. (2020), CAD-integrated isogeometric analysis and design of lightweight structures, Dissertation, Technical University of Munich.
- Breitenberger M. et al. (2015), Analysis in computer aided design: Nonlinear isogeometric B-Rep analysis of shell structures. In: *Comp. Methods Appl. Mech. Eng.* 284 (pp. 401-457).
- Brown N.C., Mueller C.T. (2019). Design variable analysis and generation for performance-based parametric modeling in architecture. In: *International Journal of Architectural Computing*. 17(1):36-52. DOI:10.1177/1478077118799491
- Cottrell, J.A. et al. (2009) *Isogeometric Analysis: Toward Integration of CAD and FEA*. Chichester: John Wiley and Sons Ltd., ISBN: 0470748737. DOI: 10.1002/9780470749081.
- DBZ (2020), Die nächste Evolutionsstufe der BIM-Methode: Der digitale Zwilling, In: *Deutsche Bauzeitschrift* 01/2020, https://www.dbz.de/artikel/dbz_Der_digitale_Zwilling_3472174.html
- Goldbach A. (2021), The CAD-integrated design cycle of membrane structures, Dissertation, Technical University of Munich.
- Goldbach A. et al. (2021), Advantages of Isogeometric B-Rep Analysis for the parametric design of lightweight structures. In: *Proceedings of the IASS Annual Symposium 2020/21*.
- Hughes, T. et al. (2005), Isogeometric analysis: CAD, finite elements, NURBS, exact geometry and mesh refinement. In: *Comp. Methods Appl. Mech. Eng.* 194 (pp. 4135–4195). DOI: 10.1016/j.cma.2004.10.008.
- Kiwi!3D, <https://www.kiwi3d.com/> accessed on June 13, 2022.
- Péntek M. et al. (2022), Numerical modeling and simulation of lightweight structures - using the example of the Olympic Stadium in Munich on its 50th anniversary. In: *33. Forum Bauinformatik*.
- Piegl, L. and Tiller, W. (1997) *The NURBS Book*. Second Edition. Monographs in Visual Communication. Berlin and Heidelberg: Springer, ISBN: 978-3-642-59223-2. DOI: 10.1007/978-3-642-59223-2.

Proceedings of the Tensinet Symposium 2023

TENSINANTES2023 | 7-9 June 2023, Nantes Université, Nantes, France

Jean-Christophe Thomas, Marijke Mollaert, Carol Monticelli, Bernd Stimpfle (Eds.)

Swatch Omega Headquarters - Multifunctional ETFE-Modules in Building Envelope

Karsten Moritz*, Koffi Alate *

* Taiyo Europe GmbH, 82054 Sauerlach, Mühlweg 2, Germany

info@taiyo-europe.com, www.taiyo-europe.com

Abstract

Contemporary membranes, i.e., very thin, flexible components made of high-performance fabrics, were developed since the end of the 1950th, 20 years later also made of foils. At first, they were only seen as pre-tensioned sails over exposed open spaces, later also, for example above grandstands of stadiums and arenas. Today they belong in the well-known canon of innovative materials and construction methods. Membrane construction is already taught at universities as part of the study to become an architect or structural engineer. Today, the interested observer will discover membranes also as part of building envelopes in many cities around the world. This is thanks to the evolution of the sophisticated materials and construction methods, from sail to multifunctional and transparent or translucent multilayer-modules. The Swatch Omega Headquarters in Biel, Switzerland, completed in 2019, shows the possibilities like no other building, but also some challenges when using modular elements clad with membrane materials used in the building envelope - in this case ETFE-foils.

Keywords: Membrane structure, ETFE-foil cushion, building envelope, lightweight construction, multifunctionality, modularity, pre-fabrication, serial production



Figure 1: Bird's eye view, ©Swatch Omega AG

1. Introduction

The s-shaped Swatch-building with an enveloping surface of 11,000m² and a height of 27m measures in plan-view 240m in length and 35m in width. It is an eye-catching and exciting building, but its shape blends harmoniously into the urban environment. The impressive building has been designed by the Japanese architect and Pritzker Prizewinner Shigeru Ban. [1] – [6], (Fig.1).

The spatial structure consists of a barrel-shaped lattice shell made of high-strength glue laminated timber (GL 24h to GL 32h). The wood used, mainly spruce (1,997 m³), comes from Switzerland (1,997 m³) [4]. The lattice structure forms 2,800 honeycombs of very different geometries. In addition, nine balconies (each 10-20m² in size) penetrate the building shell [4]. The honeycombs formed in this way were fitted with precisely produced double curved modular frames also made of glued laminated timber.

Depending on the requirements of the respective interior, the module frames were fitted with different fillings. In addition to many modules with glass panels, some with integrated sun protection, there are 898 modules, some of which are clad with transparent and some with translucent white ETFE foils, clamped by aluminum profiles making them durable, weatherproof and airtight.

The company Roschmann, located in Gersthofen, Germany, as general contractor was responsible for the planning, manufacturing and assembly of the building envelope's cladding made of hundreds sophisticated wooden modules, equipped with compositions of glass, ETFE-foils, polycarbonate plates and other materials. Taiyo Europe GmbH located close to Munich, specialized on membrane structures, also ETFE-foils, was commissioned by Roschmann with the planning, manufacturing and assembly of the ETFE foil modules, but also with the air supply for all modules, also the ones with glass. Some of the challenges in this construction task are described below.



Figure 2: Exterior view from a balcony, ©Swatch Omega AG

2. Air-flushed CCF building-envelope

The air flow through the ETFE foil modules ensures a low nominal overpressure of 250 Pascal. As a result, the ETFE foils are doubly curved, i.e., synclastic and prestressed. In this way, they can absorb loads from wind and snow via tensile forces and transfer them to the module frame, from there to the grid shell primary structure. In addition, the pretension causes the foils to tighten and, therefore, to prevent wrinkles.

The blown-in air flow is cleaned and pre-dried using air filters and adsorption dryers in order to avoid the accumulation of dust and the formation of condensate in the intermediate space. The modules fitted with glass also have this air flow. This type of façade-construction, used here for glass and membrane structures is called “closed cavity façade” (CCF). This technology has been used in ETFE-foil constructions since the early 1980’s. It has proven itself, therefore, for many years in building construction. In this way, also components integrated, such as sun protection slats and retractable curtains, remain permanently dust-free.

In total 898 of the spatially curved glued laminated timber modules are equipped with two layers of ETFE-foils. Thereof 721 modules (2,726m²) are additionally equipped with double-web polycarbonate-plates bended around both axes in the space between two separate foils (type I). These modules are located in areas with high thermal insulation requirements. They deliver the best possible protection, with a simulated thermal transmittance (U-value) around 0.6 W/(m²K) depending on the module’s composition and geometry. 170 modules (170m²) have been realized as conventional double-layer ETFE-foil-cushions above open spaces (type 2). 74 modules (309m²) are openable to naturally ventilate the interior (type 3, see Fig. 4). More than 3,500 m² of the envelope’s surface (in total 11,000m²) are showing modules equipped with ETFE-foils. Figure 3 shows number and location of the module-types used.

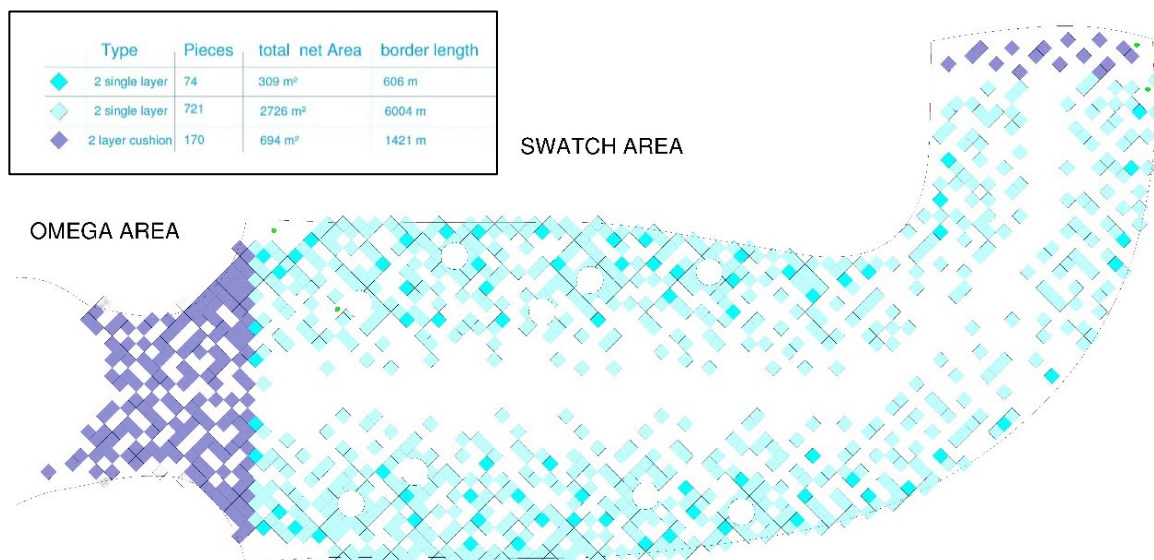


Figure 3: Ground plan view of the Swatch building – 3 ETFE-module types, ©Taiyo Europe

Membrane architecture: the seventh established building material. Designing reliable and sustainable structures for the urban environment.

The architects also attached great importance to good room acoustics. For this purpose, a large number of cross-shaped soft surface elements were attached to the inside of the roof skin. The ETFE foils also contribute to good room acoustics, as they are soft and therefore sound-absorbing. They reduce the time of reverberation compared to hard materials.

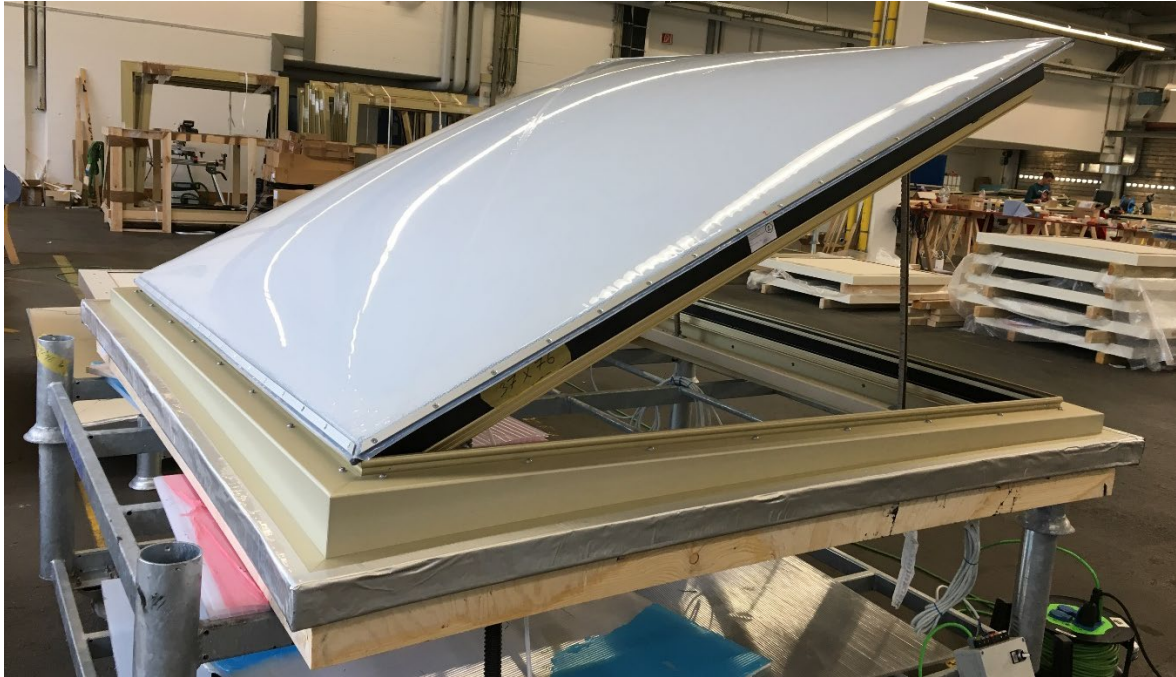


Figure 4: Dry run of an openable module (type 3), Roschmann workshop, ©Taiyo Europe

3. Prefabrication

Each honeycomb has its own double-curved geometry. Therefore, cutting pattern generation, foil-cutting and welding of the ETFE-element's boundary (keder-pocket) were time-consuming. Additionally, the uneven barrel-shaped lattice shell geometry led, in some cases, to very small modules and to extremely sharp corners of the ETFE-elements (Fig. 5 and 7).



Figure 5: 1:1 test sample of a sharp ETFE-foil-corner produced by Diaferia, ©Taiyo Europe

Membrane architecture: the seventh established building material. Designing reliable and sustainable structures for the urban environment.

All ETFE-foil elements were precisely welded together in the factory according to the cutting planning and the static analysis, taking into account the materials and systems rigidity. The edges of each element were formed by a circumferential welt pocket, also made of ETFE foils. A so-called “keder”, i.e., a round cord, for example made of EPDM and with a diameter of 4.5mm, was then drawn into this pocket (Figures 5 and 6). Then the prepared clamping profiles, were pushed onto the welt pockets in order to fasten the entire element to the inside of the wooden frame with a precise fit. Prepared means in this case: cut to length, pre-bent, pre-twisted, drilled, deburred, anodized, stamped with an individual number and cleaned. Due to the three different module types, there were a number of different profile-types. At the request of the architects, all visible profiles were anodised in a gold tone (Fig. 8-11).

So that the foil-element is wrinkle-free under overpressure at the end, the foils are cut smaller along the element’s boundary than the boundary-lengths are occupies when installed. This means that you have to pull the respective profiles together with the ETFE-element to the wooden frame so that you can connect the assembly with the prepared wood screws. With the partially doubly curved and axially twisted wooden frames, this work step was like a game of patience, especially in the sharp corners (Fig. 5 and 7). To make matters worse, the seal previously glued between the clamping profile and the wooden frame must not be damaged. After installing the foil elements (and in Type 1 also the polycarbonate sheet between the two individual layers), the entire module was subjected to an airtightness test lasting half an hour (Fig. 8 and 9). If the overpressure applied in a defined manner and measured with a calibrated manometer was not constant during this time, the element was opened again, the leak searched with the help of a foam-forming liquid and sealed. The element was then re-assembled and the leak test repeated. No module left the production hall without the proof of airtightness.

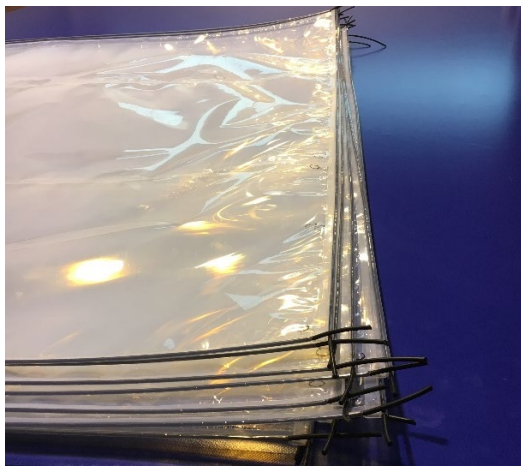


Figure 6: Welded transparent ETFE-foil elements, produced by Diaferia, ©Taiyo Europe



Figure 7: White ETFE-foil element mounted on a timber frame and tested with an internal overpressure, ©Taiyo Europe

The factory assembly of the prefabricated wooden frame modules with an average of 40 component categories (clamping profiles, fasteners, ETFE foils, polycarbonate plates, seals, gaskets, inlet and outlet valves, pressure sensors, bushings for sensor cables, ...) was carried out with meticulously pre-planned work processes, i.e., serially to a certain extent. The prefabrication took place in a workshop in Gersthofen, which was provided by Roschmann especially for this project. However, since there were no identical modules among the 898 modules, the relatively light wooden frames were turned manually so that they could be

Membrane architecture: the seventh established building material. Designing reliable and sustainable structures for the urban environment.

processed and fitted from both sides (Fig. 7 – 17). In hindsight, this decision also proved to be the right one, as leaks could be identified, and the process could be optimized quickly. Ultimately, however, the construction industry must also admit that other economic sectors are significantly more advanced in terms of serial and automated production methods.



Figure 8: Clamping profiles anodized in a golden tone, straight, pre-bended and pre-twisted, ©Taiyo Europe



Figure 9: Fixation test of a clamping profile with inserted keder-pocket, ©Taiyo Europe



Figure 10: Each profile was given an individual stamped number for correct placement on the component, ©Taiyo Europe

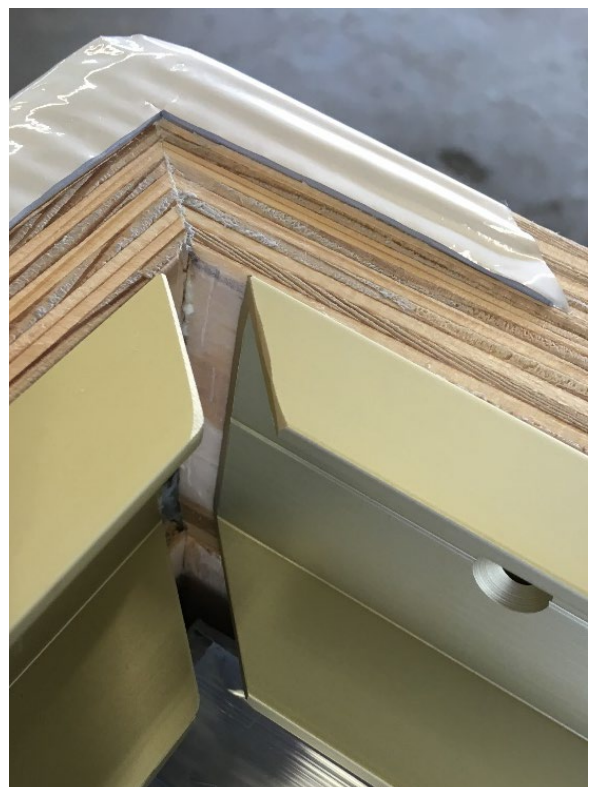


Figure 11: Corner assembly of the cut-to-length, pre-drilled, deburred and polished profile, ©Taiyo Europe

Membrane architecture: the seventh established building material. Designing reliable and sustainable structures for the urban environment.



Figure 12: White ETFE-foil element mounted on a curved timber frame (balcony area), ©Taiyo Europe

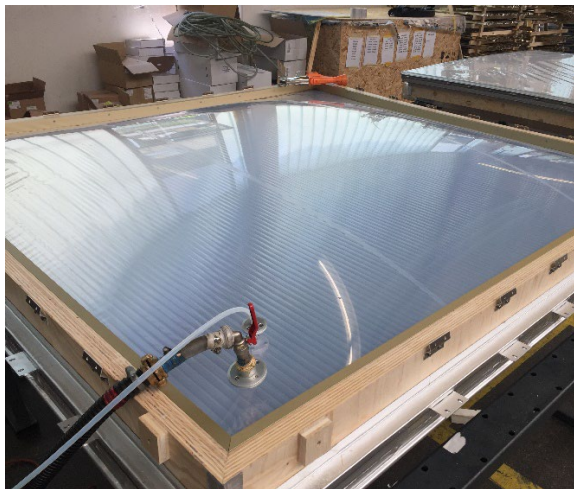


Figure 13: Rectangular ETFE-element with integrated bended double-web polycarbonate-plate, air-leak-test with overpressure, ©Taiyo Europe

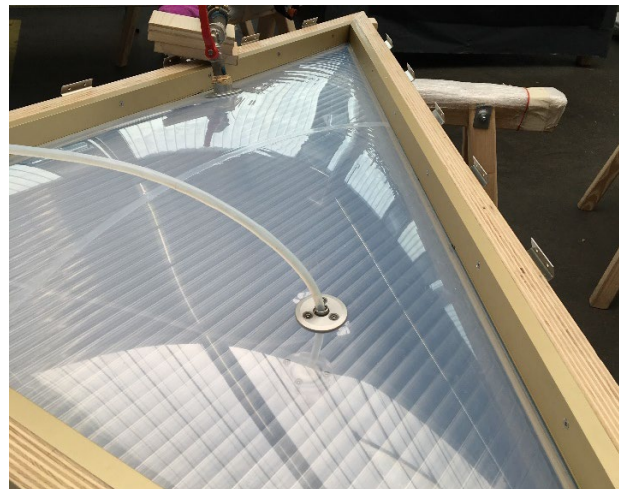


Figure 14: Triangular ETFE-element with integrated bended double-web polycarbonate-plate, air-leak-test with overpressure, ©Taiyo Europe

Membrane architecture: the seventh established building material. Designing reliable and sustainable structures for the urban environment.

To ensure that no moisture gets between the foils before installation, Roschmann supplied all elements with filtered and dried air during transport (Fig. 16 - 17). The mobile blower stations drove to the construction site with the elements on the loading areas of the trucks.



Figure 15: ETFE-modules completed and released, ©Taiyo Europe



Figure 16: ETFE-modules on transport racks, ©Taiyo Europe



Figure 17: ETFE-modules with temporary air supply for their transportation, ©Taiyo Europe

4. Air Supply Duct System

A total of about 8 km of air ducts were laid in the building envelope, risers, mains and stubs (Fig. 18). They supply all CCF modules, those made of glass and those of ETFE foils, with a standard overpressure of 250 pascals (Fig. 19). The fans are able to generate a higher overpressure of 600-1000 Pa in the modules, which can be increased automatically (sensor-controlled) or manually in the roof area when the snow load rises. The pressure measurement and the pressure control of the fans are carried out using pressure sensors, integrated into the modules at defined points. They deliver their data via sensor cables to the 5 blower stations, which are placed at three locations (in the basement and in the roof area).

Risers, mains and stubs are invisible because they were laid in the double floors or in recesses in the wooden structure and covered with wooden cover profiles. The covers can be removed easily to allow maintenance of the lines. Only the flexible, translucent hoses that connect the

Membrane architecture: the seventh established building material. Designing reliable and sustainable structures for the urban environment.

modules at the end, are partially visible along the timber construction. They are protected from damage by decorative perforated panels made of anodised aluminium (Fig. 20).

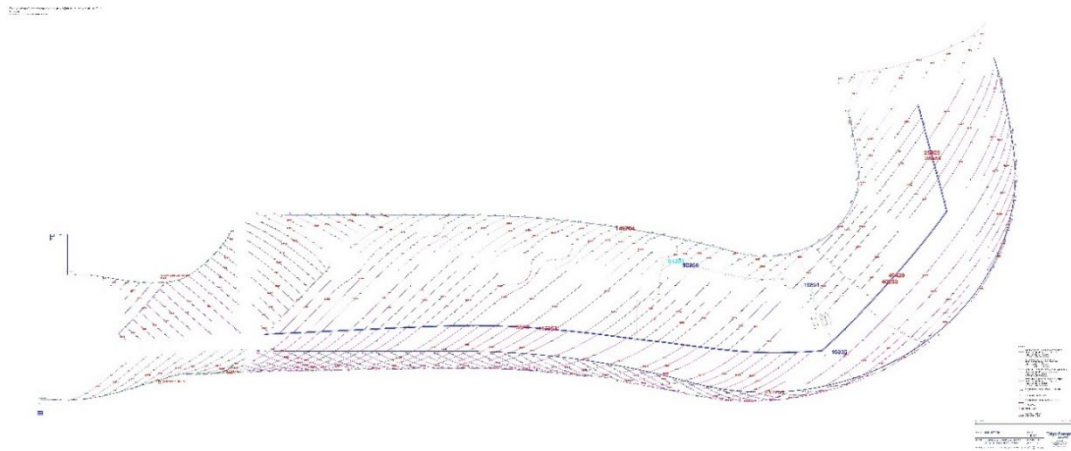


Figure 18: Air supply duct system for air-distribution (risers, mains and stubs), ©Taiyo Europe

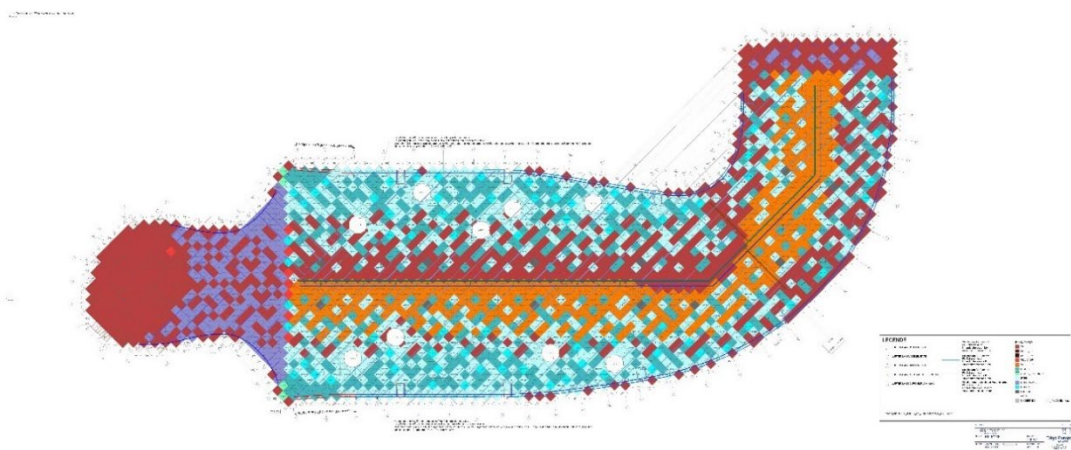


Figure 19: Different modules that are supplied with filtered and pre-dried air, ©Taiyo Europe

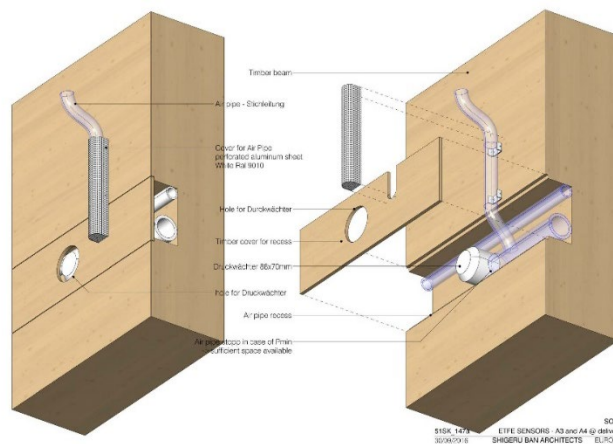


Figure 20: Hidden routing of the air supply ducts in the timber structure and along, ©Taiyo Europe

Membrane architecture: the seventh established building material. Designing reliable and sustainable structures for the urban environment.

5. External Quality Control of ETFE-element's production

Due to the large number of small ETFE foil elements difficult to be weld on one hand and due to the tight project schedule on the other hand, Taiyo Europe commissioned two manufacturing companies with the foil assembly: Novum Membranes GmbH in Edersleben, Germany, and Diaferia S.R.L. in Bari, Italy. Both delivered excellent weld seam qualities. The external quality control of the two production facilities and the quality of the weld seams was commissioned in consultation with the project partners and the customer to the accredited membrane testing laboratory Textiles Hub of the Polytecnico Milano (Fig. 21).

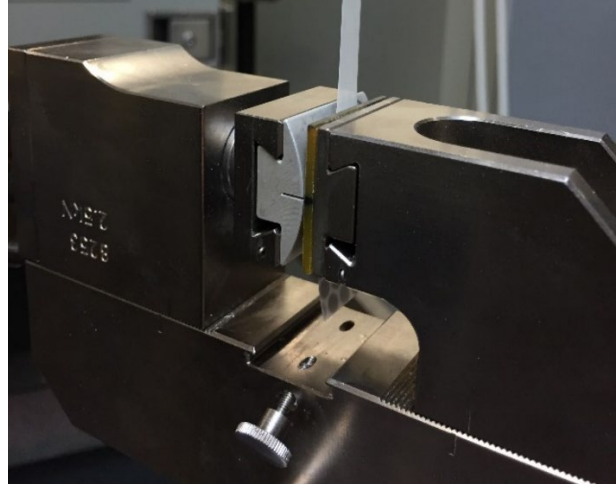


Figure 21: Uniaxial tensile tests on strip-specimens in accordance with DIN EN ISO 527-1, DIN EN ISO 527-3, ©Taiyo Europe

6. Outlook

The Swatch Omega Headquarters in Biel, Switzerland impressively shows that modular construction in the field of membrane structures is on the rise. The membrane world will therefore increasingly deal with the question of how to convert the associated processes into an automatic or serial production. In view of the spatial geometries and the diversity of the elements, however, this task is by no means trivial.

7. Project Participants

Table 1: Project Participants (Building Envelope)

Building owner	Swatch AG, Biel, Schweiz	www.swatchgroup.com
Architects	Shigeru Ban Architects Europe, Paris, France	www.shigerubanarchitects.com
Architects (overall and planning management, submission and implementation planning, construction management)	Itten+Brechbühl AG, Basel, Switzerland	www.ittenbrechbuehl.ch
Projekt Management	Hayek Engineering AG, Zürich, Switzerland	www.hayek-group.com
Timber structure building envelope	Blumer-Lehmann AG, Gossau, Switzerland	www.blumer-lehmann.ch

Membrane architecture: the seventh established building material. Designing reliable and sustainable structures for the urban environment.

Wooden frame modules	Georg Ackermann GmbH, Wiesenbronn, Germany	www.ackermanngmbh.de
Structural Engineering of timber construction	SJB Kempter Fitze AG, Herisau, Switzerland	www.jsjb.ch
Façade planning	Leicht, Rosenheim, Germany	www.leichtonline.com
Building physics calculations	Leicht Physics GmbH, Bad Aibling, Germany	www.leichtphysics.com
Building climatic and building physics investigations	Transsolar Energietechnik GmbH, Stuttgart/Munich, Germany	www.transsolar.com/de
Façade/building envelope (planning and execution)	Roschmann-Group, Gersthofen, Germany	www.roschmann-group.de
ETFE foil elements and air supply (planning and execution) commissioned by Roschmann Group	Taiyo Europe GmbH, Sauerlach, Germany	www.taiyo-europe.com
ETFE foil assembly commissioned by Taiyo Europe	NOVUM MEMBRANES GmbH, Edersleben, Germany und DIAFERIA S.R.L., Bari, Italy	www.membranes.novumstructures.com ; www.diaferia.it
External quality control of the ETFE-foil element's manufacturing commissioned by Taiyo Europe	Politecnico di Milano, Textiles Hub, Mailand, Italy	www.textilearchitecture.polimi.it
Sanitary, heating, ventilation and air conditioning technology planning	Gruner Gruneko AG, Basel, Schweiz & ISP und Partner AG, Sursee, Switzerland	www.gruner.ch , www.isppartner.ch
Electrical engineering planning	HKG Engineering AG, Aarau, Switzerland	www.hkg.ch
3D implementation planning	Design to Production, Erlenbach, Switzerland	www.designtoproduction.com

8. Referencing literature

- [1] Swatch inaugurates its Headquarters in Biel, Swatch Group, Press Release, 03.10.2019, <https://www.swatchgroup.com/en/services/archive/2019/swatch-inaugurates-its-headquarters-biel>, download: 04.02.2023
- [2] The new Swatch Headquarters, <https://www.swatch.com/de-de/swatchhq.html>, Swatch Group, download: 04.02.2023
- [3] Swatch and Omega Campus / Shigeru Ban Architects, ArchDaily, [Swatch and Omega Campus / Shigeru Ban Architects | ArchDaily](#), download: 26.03.2023
- [4] Der neue Hauptsitz von Swatch, Text: Charles von Büren, in: AIV issue 6/2019
- [5] Swatch Group Hauptsitz, Biel, Leicht, <https://www.leichtonline.com/projekte/swatch/>, download: 26.03.2023

Membrane architecture: the seventh established building material. Designing reliable and sustainable structures for the urban environment.

[6] Swatch Omega Headquarters, Bienne, Switzerland, Transsolar Energietechnik GmbH, Swatch <https://transsolar.com/projects/biel-swatch-omega-hauptquartier>, download: 26.03.2023



tensinantes2023 : TensiNet Symposium 2023 at Nantes Université

Membrane architecture: the seventh established building material. Designing reliable and sustainable structures for the urban environment.

Proceedings of the Tensinet Symposium 2023

TENSINANTES2023 | 7-9 June 2023, Nantes Université, Nantes, France

Jean-Christophe Thomas, Marijke Mollaert, Carol Monticelli, Bernd Stimpfle (Eds.)

Temporary structure Grand Palais Éphémère

Patrick Vaillant*, Beatriz Arnaiz^a, Feike Reitsma^b

IASO S.L., Av de l'Exèrcit 35-37, 25194 Lleida, Spain, www.iasoglobal.com

* patrick.vaillant@iasoglobal.com

^a beatriz.arnaiz@iasoglobal.com ^b feike.reitsma@iasoglobal.com

Abstract

Designed by the architectural firm Wilmotte & associés, this temporary building fits elegantly into the Parisian landscape of the Champ-de-Mars. Between the Eiffel Tower and the military school, 44 wooden arches rise to a height of 20m. The cross-shaped building covers some 10,000m², with dimensions of 146.5mx52.5m in the east-west wing and 139.3mx34.3m in the north-south wing.

The objective of optimising the materials used -which is of paramount importance in terms of sustainability- is achieved in the second membrane skin thanks to the very nature of the application of tensioned membranes. The building's skin is made of PVC membrane (Sattler) in the upper area and transparent ETFE sheeting (Nowofol) on the sides, enclosing vertical facades with the new Flexlight STFE 50 material and the Frontside View 381 (Serge Ferrari). These membranes are 100% recyclable, as are the aluminium and steel used to frame and anchor them to the wooden structure.

Keywords: membrane architecture, tensostructure, sustainability, future architecture, ephemeral pavilion, record time, ETFE, PVC, Flexlight STFE 50.

1. Introduction

The Grand Palais Éphémère is a temporary 10,000 sqm building designed by Wilmotte & Associés and constructed on the Champ-de-Mars in Paris, in front of the Ecole Militaire on the axis of the Eiffel Tower.

During the time the emblematic Grand Palais is closed for major restoration work, this ephemeral building is intended to house the major art, fashion, and sporting events, such as the FIAC, Saut Hermès and Chanel fashion shows.

Membrane architecture: the seventh established building material. Designing reliable and sustainable structures for the urban environment.

In summer 2024, the Grand Palais Éphémère will host the judo and wrestling competitions of the Paris Olympics. The building - overseen by the Réunion des musées nationaux – Grand Palais and Paris 2024 and produced by GL Events – is able to accommodate 9.000 people.

Located on the Champ-de-Mars, the Grand Palais Éphémère has a strong connection with the history of the Universal Exhibitions. The urban and aesthetic integration of the structure represented a major challenge and the architectural ambition. The slightly curved design follows the curves of the feet of the Eiffel Tower viewed from its perspective. The height has been strictly limited to the needs of future use and therefore leaves the dome of the Military School sixteen metres higher, so as not to hide it. The curvature of the ensemble does not show any break in the lines between the roof, which has no acroterion.

The wooden structure of the building is not only designed to be modular and quick to assemble, but also to be reused in multiple configurations when it is dismantled after the 2024 Olympic and Paralympic Games. It required 1.500 m³ of European spruce assembled in glued laminated timbers, sized for efficient road or river transport to reduce assembly time on site. At the end of four years of use, the building will be completely dismantled and reused. Stored by its builder-owner (GL Events), the four naves can be used separately to adapt to the size of different projects.

The Grand Palais Éphémère is a flexible, agile, circular bio-sourced construction, designed in wood, a renewable resource, from a sustainably managed forest (PEFC). In addition, the profile of the structural arches working in compression helps to minimise the mass of wood used. The resulting geometry of the framework arches provides a useful volume covered by a reduced roof area and the dual skin has significant acoustic, thermal and ventilating properties, thereby using less energy.



Figure 1: Global view towards the Eiffel tower

Membrane architecture: the seventh established building material. Designing reliable and sustainable structures for the urban environment.

2. The start of the project

The initial project was designed with a mixed roof: steel sheets on the upper part and polycarbonate on the lower parts, but the installation time for the metal part was apparently not compatible with the construction schedule. GL EVENTS therefore consulted in the pre-project phase to find out whether it was viable to replace the metal part with a PVC membrane.

During those discussions, the question arose to study the replacement of the polycarbonate with ETFE films to keep the aesthetic concept developed by Wilmotte. It was important for GL EVENTS to confirm that the textile roofing solution was not only technically feasible, but would also fit within the timeframe of the site planning.

After demonstrating to GL EVENTS that the textile membrane alternative was technically viable and that everything could be installed within the construction schedule, the roofing initially planned with metal sheets + polycarbonate was finally validated in textile membranes and ETFE films by GL EVENTS and WILMOTTE.

Following this, the tender for the textile roofing included:

- A light grey PVC textile membrane on the upper part of the building
- A transparent ETFE film on the vertical parts (facades) of the building.

Later the mesh membranes at the lateral sides were added together with additional transparent membranes on the top lateral sides.



Figure 2: Start on site

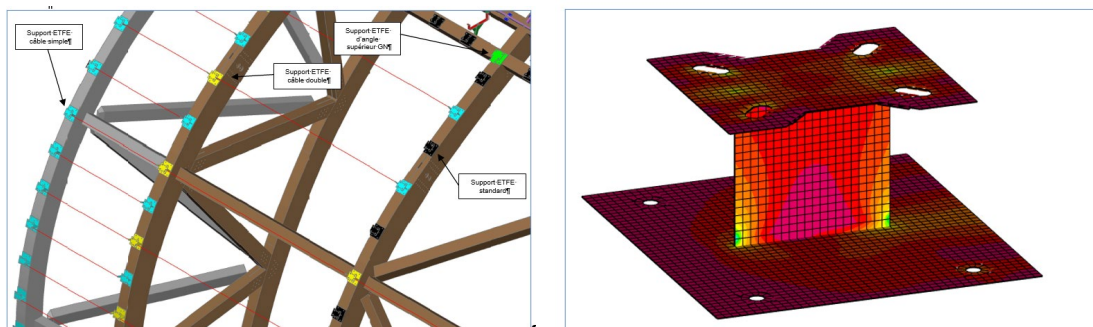


Figure 3: preinstalled and calculated brackets

Membrane architecture: the seventh established building material. Designing reliable and sustainable structures for the urban environment.

3. Restrictions, Obligations and Covid

In general membrane projects must follow the construction codes in each country and can be followed by the well-known Tensinet guide (which is under development) and of course applying the Eurocodes were applicable.

The project's membranes must comply with a reference guide in France: "Recommendations for the design of permanent textile roofing structures". However, the PVC membranes used in the project did not comply with certain criteria of the recommendations and the system had to be validated by the CSTB (Centre Scientifique et Technique du Bâtiment) by obtaining an ATEX (Appréciation Technique Expérimentale).

These certifications are generally issued by safety commissions that examine the admissibility of non-conventional systems to obtain a ten-year guarantee.

Similarly, ETFE is not recognised as a conventional material and was also included in an ATEX to validate its application on the GPE.

The two ATEX applications were emitted to the Scientific and Technical Building Centre (CSTB): one for the roof of the building (PVC and ETFE), the other for the two side façades of the building parallel to the Military School (woven PVC, etc.). Thanks to the responsiveness of the approval committees and the Socotec inspection office, which was the rapporteur for these two dossiers, the approvals were obtained in a single quarter: the race against time was clearly understood by all those involved in the project.

But then the Covid 19 lock-in came to a standstill in this tight schedule. A week after GL Events and IASO signed their contract, all teams were forced to work by videoconference.... This additional constraint had no impact on the design phase: it simply intensified the exchanges between the project management, the contracting authority, and the technical design offices to validate the textile envelope drawings. The slightest error in the calculations would have delayed the work, while compromising the estimation of the PVC and ETFE surfaces ordered beforehand.



Figure 4: Covid restrictions

Membrane architecture: the seventh established building material. Designing reliable and sustainable structures for the urban environment.

4. Project data

The building will have a lifespan of approximately 3.5 years (from the beginning of 2021 until the end of the Paralympic Games in summer/autumn 2024). The aim is to be able to reinstall it elsewhere in France or abroad for a long period, either completely or partially.

The “Grandes Nefs” are 52m wide between supports for a total length of approximately 140m and the “Petites Nefs” are 34m wide between supports for a total length of approximately 130m.

The whole building is made of wood, except for the posts which are made of steel.

The type of wood used is of class 2 for the whole structure, except for the canopy which is class 3.

Under the roof of the building, there is a second rigid waterproof envelope to improve acoustic comfort (not included in the lot).

There are 34 fire safety vents on the roof and the membrane quantities of the building are:

PVC roof area:	10200 m ²
ETFE roof area:	5230 m ²
Area of the 2 PVC facades:	1160 m ²
STFE 50 lattice girder closure:	600 m ²

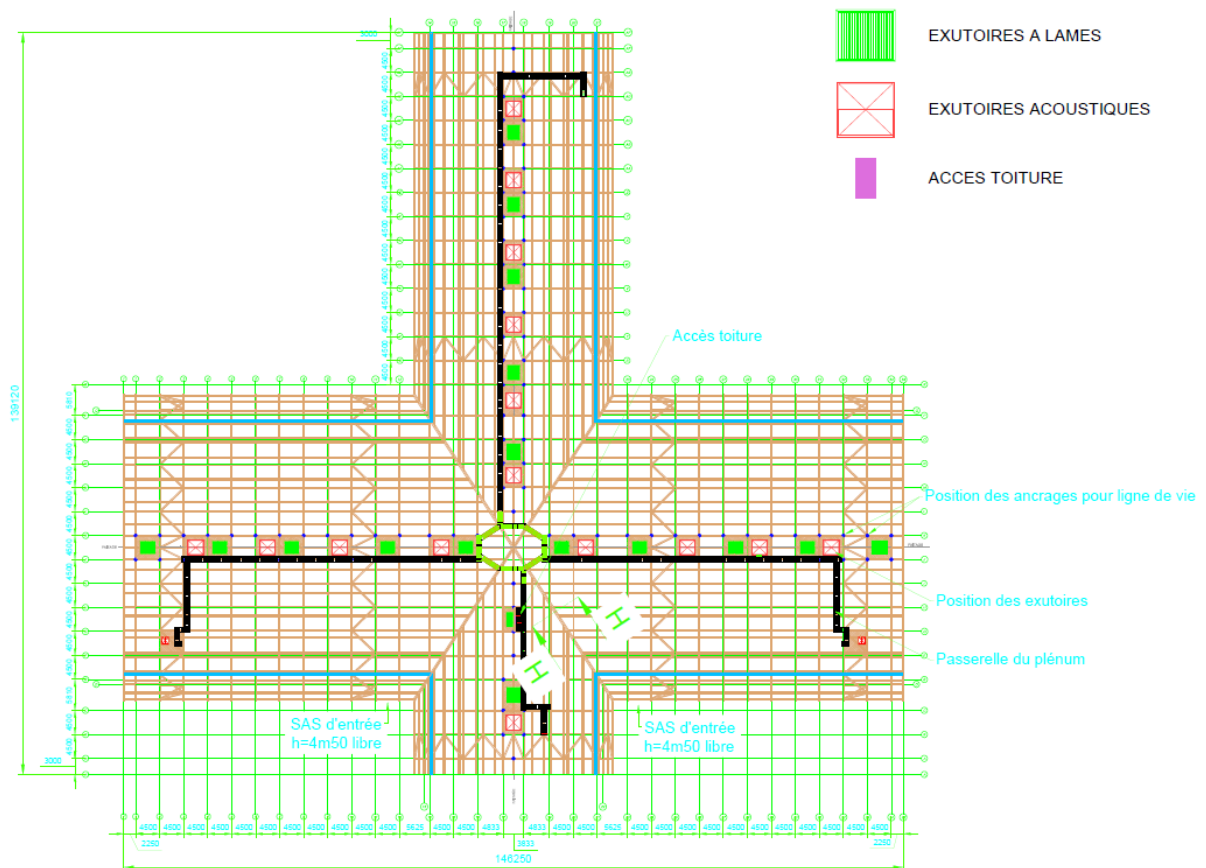


Figure 5: A plan overview

Membrane architecture: the seventh established building material. Designing reliable and sustainable structures for the urban environment.

From the 3D model of the framework provided by MATHIS, a 3D model was made of the membranes in order to carry out all the dimensioning calculations, and then to define all the manufacturing plans.

For the roof, this consisted in:

94 independent PVC membranes.

34 fire protection vents.

92 independent ETFE membranes.

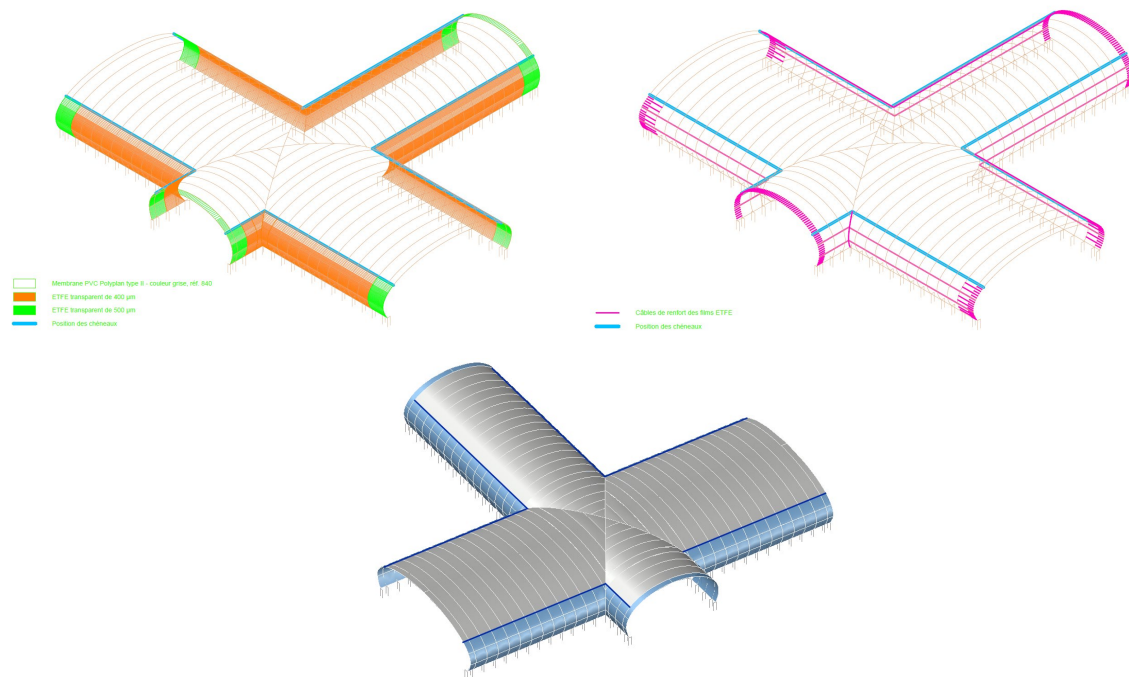


Figure 6: PVC roof and ETFE façade and the cable distribution

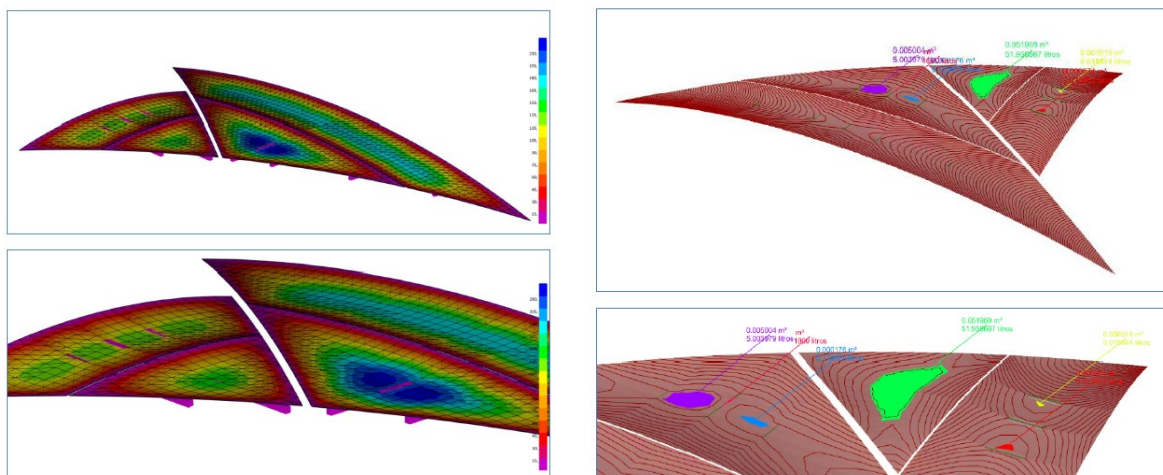


Figure 7: Snow calculation and waterponding control

Membrane architecture: the seventh established building material. Designing reliable and sustainable structures for the urban environment.



Figure 8: night view seen from the Military School

6. Conclusion

A remarkable feature of this project is its rapid resolution of engineering, certification, manufacturing, and assembly: it took only 6 months from contract award to installation. This was made possible by the good coordination of all parties involved in the work and very well managed logistics. It is worth noting that during this tight deadline, the pandemic caused by Covid arose, which did not prevent the timeline from being met. It was a success to develop the project without any errors, which would have prevented the deadlines from being met. The project was developed and completed very satisfactorily, overcoming all the conditioning factors that arose.

The result is an iconic example of textile architecture which, through its use to house the tatamis for the 2024 Olympic Games, and through the visibility of its location, results in the wide dissemination of a good example of the use of textile materials in architecture. The insertion of these materials into the building landscape has an important impact on the evolution of architecture with respect to the paradigm shifts and environmental challenges being imposed by climate change.



tensinantes2023 : TensiNet Symposium 2023 at
Nantes Université

Membrane architecture: the seventh established building material.
Designing reliable and sustainable structures for the urban
environment.

Proceedings of the Tensinet Symposium 2023

TENSINANTES2023 | 7-9 June 2023, Nantes Université, Nantes, France

Jean-Christophe Thomas, Marijke Mollaert, Carol Monticelli, Bernd Stimpfle (Eds.)

Affine minimal surfaces: an intuitive family of shapes for textile architecture

Rémi BELLOC^{a,b}, Cyril DOUTHE^{a *}, Ken'ichi KAWAGUCHI^b

^a Laboratoire Navier, 6&8 avenue Blaise Pascal

77420 Champs sur Marne, France

*cyril.douthé@univ-eiffel.fr

^b Kawaguchi Lab, The University of Tokyo, Japan

Abstract

The form-finding of shapes for textile architecture has been a challenge from the very beginning of its modern history. Many methods have been used from physical experiments on soap films to numerical modelling with the force density method (Schek, 1973), the dynamic relaxation method (Barnes, 1999) or, more recently, the update reference strategy (Bletzinger, Bauer, & Wüchner, 2017). In all these numerical methods, designers work on the tuning of some parameters which constraint the local ratio of tensions in order to bring the surface to its desired shape. The link between these parameters and the final shape is unfortunately rarely intuitive. Thus, the proposed paper aims at presenting a family of surfaces with 6 parameters called Affine Minimal Surfaces which enlarges the traditional framework of Minimal Surfaces keeping their simplicity. These parameters are linked to 6 affine transformations of the surface boundaries and are therefore easy to handle by non-experts. Some basic geometrical aspects of affine minimal surfaces and the proposed design methodology are first presented. Then, the prestress state of these surfaces is described from the local equilibrium. Their mechanical behaviours under external loads is investigated through a mechanical model based on a cable net/membrane analogy. Finally, case studies highlights their advantages and limitations through the modification of their curvatures.

Keywords: membrane, form-finding, structural mechanics, conceptual design, lightweight structures.

1. Introduction

A typical challenge in the design of a tensioned membrane is the form finding process, which is the generation of a pre-tensioned geometry in equilibrium for a given set of boundaries.

Membrane architecture: the seventh established building material. Designing reliable and sustainable structures for the urban environment.

Meanwhile, the pre-tension field ensures the stability of the form and its good mechanical behaviour under external loads by preventing any slackening. Thus, such geometries have a close form-force relationship.

The first experiments in form finding were carried out on models or soap films. But the emergence of computer science led to the development of numerical methods such as the force density method (which was historically the first one) (Schek, 1973), the dynamic relaxation (Barnes, 1999) or the update reference strategy (Bletzinger, Bauer, & Wüchner, 2017).

In the form-finding process, the engineer, for a given set of boundaries, operates on the tension field to design the final geometry. However, the correlation between the tension field and the shape is rarely intuitive. The final geometry is thus usually dictated by a uniform (or constant in both principal directions) tension field. With the idea of designing membranes in collaboration with architects, a geometry-oriented approach would be more relevant. The associated tension field becomes a consequence of the shape.

In this paper, we study how, using affine minimal surfaces, the generation of alternative tensioned membranes can become intuitive and flexible. Mathematically affine minimal surfaces described minimal surfaces transformed by affine operations. The transformations are straightforward and offer intuitive control over the surface. For a given minimal surface, the user has a set of 6 parameters to alter the geometry while keeping the same boundaries. The tension field associated with these transformed surfaces is deduced easily, contributing to their simplicity.

2. Affine minimal surfaces properties

In this section, we briefly recall the notion of minimal surface and affine transformation in \mathbb{R}^3 . Then we consider the properties of affine minimal surfaces, generated from affine transformations of minimal surfaces.

2.1. Minimal surfaces

A minimal surface is a surface which minimizes its area for a given boundary. It is also a surface in equilibrium under a uniform isotropic tension field equal in all points and directions. It acts as a soap film.

2.2. Affine Transformations

An affine transformation in \mathbb{R}^3 is:

$$T_A: \begin{pmatrix} x \\ y \\ z \end{pmatrix} \rightarrow \begin{pmatrix} a_{11} & a_{12} & a_{13} \\ a_{21} & a_{22} & a_{23} \\ a_{31} & a_{32} & a_{33} \end{pmatrix} \begin{pmatrix} x \\ y \\ z \end{pmatrix} + \begin{pmatrix} b_1 \\ b_2 \\ b_3 \end{pmatrix} \forall i, j \in \{1,2,3\}, a_{ij} \in \mathbb{R} \text{ et } \forall i \in \{1,2,3\}, b_i \in \mathbb{R}.$$

Thereafter, the vector \mathbf{b} will be considered null because it implies only a translation of the considered element.

One can decompose an affine transformation into scaling, shearing and rotating operations. Since the rotation operations do not modify the geometry of the surfaces, we will ignore them.

Membrane architecture: the seventh established building material. Designing reliable and sustainable structures for the urban environment.

This provide us a set of transformations of 6 parameters (shown in figure 1): 3 scalings (along X, Y and Z) and 3 shearings (along XY, YZ and XZ).

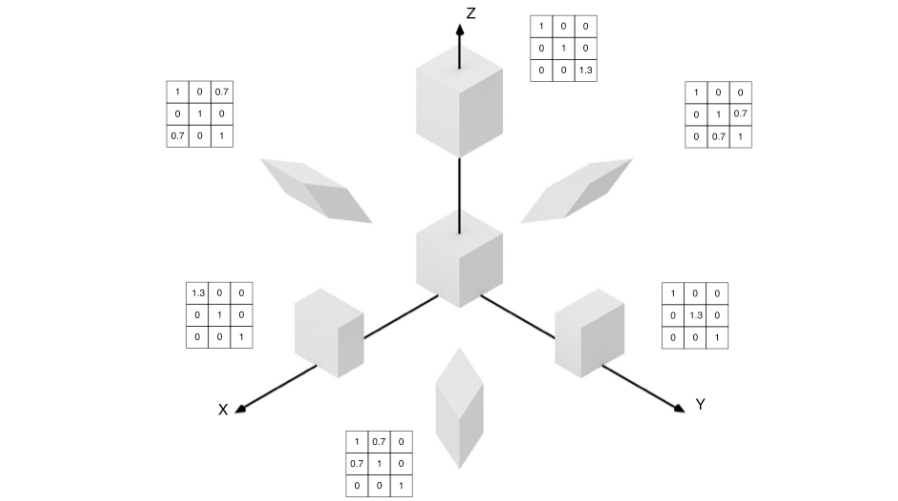


Figure 1 - Affine transformations of a cube (excluding rigid body motions).

2.3. Transformation process

At this point, the relevance of performing an affine transformation is very limited since it modifies the boundaries of the surface. In reality, the process studied here and illustrated in figure 2, can be described as a "back-and-forth" transformation and is composed of two affine transformations. Starting from the Surface (1) based on a set of boundaries (two circles and a cylinder for the catenoid), we first perform an affine transformation to get a second Surface (2). Then, Surface (2) is minimized to get Minimal Surface (2). Finally, the reverse affine transformation leads to an Affine Minimal Surface (1) based on the initial set of boundaries.

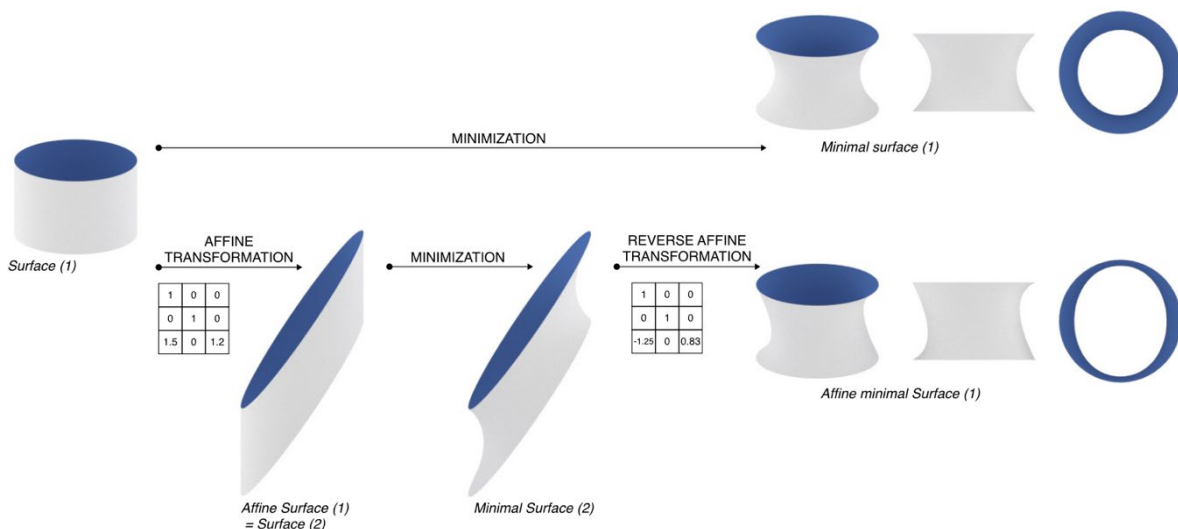


Figure 2 - Back-and-Forth transformation process

The admissible affine transformations are the invertible ones. Moreover, it is necessary to ensure that the initial transformation will result in a minimal non degenerated surface (for

Membrane architecture: the seventh established building material. Designing reliable and sustainable structures for the urban environment.

example, the initial affine transformation of a catenoid cannot separate the two circles beyond $d/D=0.66$).

This process gives control over the final geometry. For a given set of boundaries, the minimization only provides one solution, but thanks to the affine transformations one can affect the final shape. This widens the range of solutions given for this set of boundaries while keeping the simplicity of modeling minimal surfaces. With these transformations, one can increase or reduce the curvature of a surface, create asymmetries, or stabilize a previously degenerate solution (in Figure 3, the stabilization of a catenoid whose boundaries are distant beyond $d/D = 0.66$).

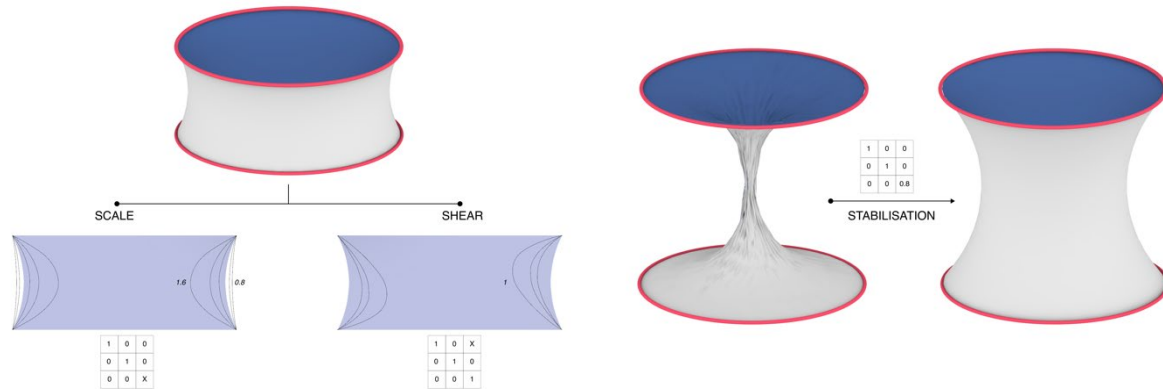


Figure 3 - Curvature modifications and stabilization of surface by affine transformations

2.4. Fundamental mechanical properties

Up to now, we have considered the impact of the transformations on the geometry of these surfaces. However, the objective of our work is to study tensioned membranes, which have a physical reality. This is why, in addition to the geometry, we are interested in the modification of the mechanical behaviour of these surfaces. First of all, we must ensure that affine minimal surfaces can be equilibrated by a pre tension field. This is actually the case, as it can be shown that, if a surface is in equilibrium under a given self-stress state, then its affine transformation is in equilibrium under the affine transformation of the inner stresses weighted by some metric changes.

The demonstration is not shown here for conciseness reasons but only the results. It derives straight forward from the affine transformation of Pucher equations (Gmür, 1958). Indeed, in Pucher formalism, membrane equilibrium equations are written in the global frame $(\underline{e}_x, \underline{e}_y, \underline{e}_z)$ which is suited for an easy definition of the affine transformation, as simple matrix $\underline{\underline{A}}$ applied to the coordinates of the minimal surface Σ as shown in section 2.2.

Let us hence define the surface reference frame $(\underline{e}_x, \underline{e}_y)$ aligned with the global axes $(\underline{e}_x, \underline{e}_y)$ but projected vertically on the surface tangent plane. This frame is neither orthogonal, nor unitary with $\|\underline{e}_x\| = dx/dX$ and $\|\underline{e}_y\| = dy/dY$. In this local frame, we note N_{xx}, N_{yy}, N_{xy} the internal forces due to prestress in the minimal surface which, by definition, are in equilibrium.

When applying the affine transformation $\underline{\underline{A}}$, the reference frame is changed into $\bar{\underline{e}}_x = \underline{\underline{A}} * \underline{e}_x$ and $\bar{\underline{e}}_y = \underline{\underline{A}} * \underline{e}_y$ with $\|\bar{\underline{e}}_x\| = \overline{dx}/dX$ and $\|\bar{\underline{e}}_y\| = \overline{dy}/dY$. One can show that, within this reference frame of the affine minimal surface, the following internal forces are in equilibrium:

Membrane architecture: the seventh established building material. Designing reliable and sustainable structures for the urban environment.

$$\bar{N}_{xx} = N_{xx} \frac{dy}{dx} \frac{d\bar{x}}{dx}, \bar{N}_{yy} = N_{yy} \frac{dx}{dy} \frac{d\bar{y}}{dy} \text{ and } \bar{N}_{xy} = \bar{N}_{yx} = N_{xy} = N_{yx}$$

The self-stress tensor $\bar{N}_{xx}, \bar{N}_{yy}, \bar{N}_{xy}$ is found in a skew basis (\bar{e}_x, \bar{e}_y) so that its principal direction and values can only be found numerically. Its local expression is however sufficient for practical implementation in a finite element software.

3. Numerical mechanical modelling

3.1. Modelling process

The mechanical modelling of affine minimal surfaces is complex as it is necessary to introduce a non-uniform prestress field and the resulting geometric stiffness into the calculations. Traditional finite element software used for membrane calculation do not allow this easily. We have thus chosen to adapt our problem of a non-uniform pre-stressed membrane into a problem of non-uniform prestress into an equivalent bar network so that it can be solved with a standard finite element software, like Grasshopper/Karamba.

The diagram in Figure 4 describes the main steps of the modelling. This process is divided into three parts: the geometrical modelling known as "The back and forth transformation", the finite element study and the post processing.

- *The back and forth transformation:* takes as input the initial rough geometry supported by the boundaries and an affine transformation. It returns the mesh of the affine minimal surface to be studied.
- *The finite element study:* starts with the transformation of the mesh into an equivalent cable network according to the input mechanical parameters (Barnes, 1999) (Gosling & Zhang, 2011). Next, a standard finite element calculation of the pretensioned cable network with or without external loadings is performed in Karamba. It finally returns the displacements at the nodes and the final tensions in the cables.
- *The post-processing:* consists on one hand in the reconstruction of a stress field based on the tensions returned after the finite element analysis (Nicot, 2013), and on the other hand in the construction of the geometrical properties of the mesh (Douros & Buxton, 2002). It returns the values and directions of the principal stresses, values and directions, and the mean and Gaussian curvatures.

Membrane architecture: the seventh established building material. Designing reliable and sustainable structures for the urban environment.

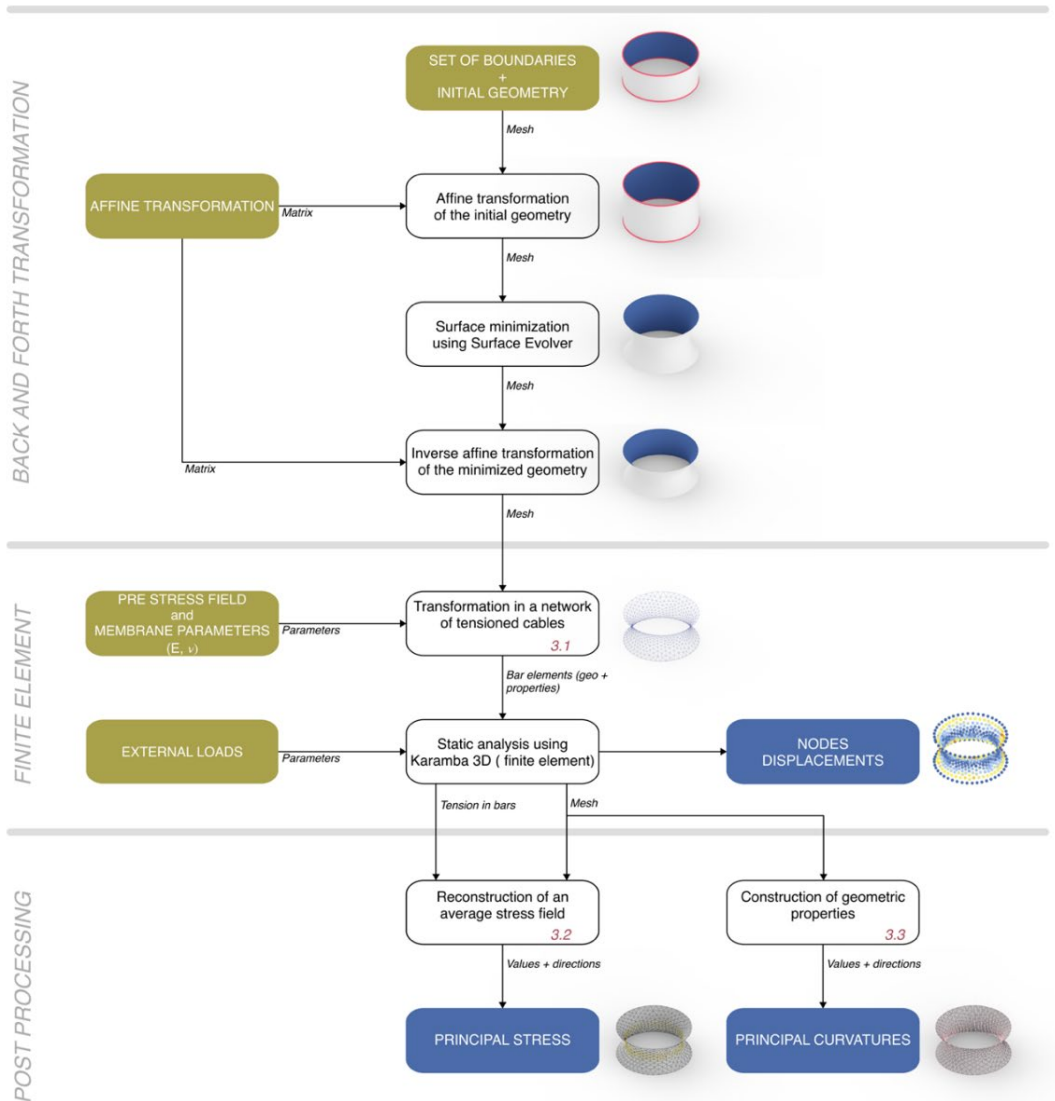


Figure 4 - Steps of the modelling process

The modelling is described in the Master Thesis of (Belloc, 2022), in particular the cable network modelling, the reconstruction of the stress field and the construction of the geometrical properties of the mesh.

3.2. Model validation and calibration

To validate the model, we studied the consistency of the displacements of our bar network resulting from the finite element calculation. Then, we discussed the accuracy of both the stress field reconstruction and the geometrical properties. Finally, we perform a comparative study with the KIWI 3D software (Bletzinger, Bauer, & Wüchner, 2017), in order to quantify the differences between our model and another membrane calculation software. Figure 5 illustrates the results of this comparison on a hat like membrane loaded by a snow load. One verifies that there is a very good agreement for displacements, and principal stress direction as well as amplitude.

Membrane architecture: the seventh established building material. Designing reliable and sustainable structures for the urban environment.

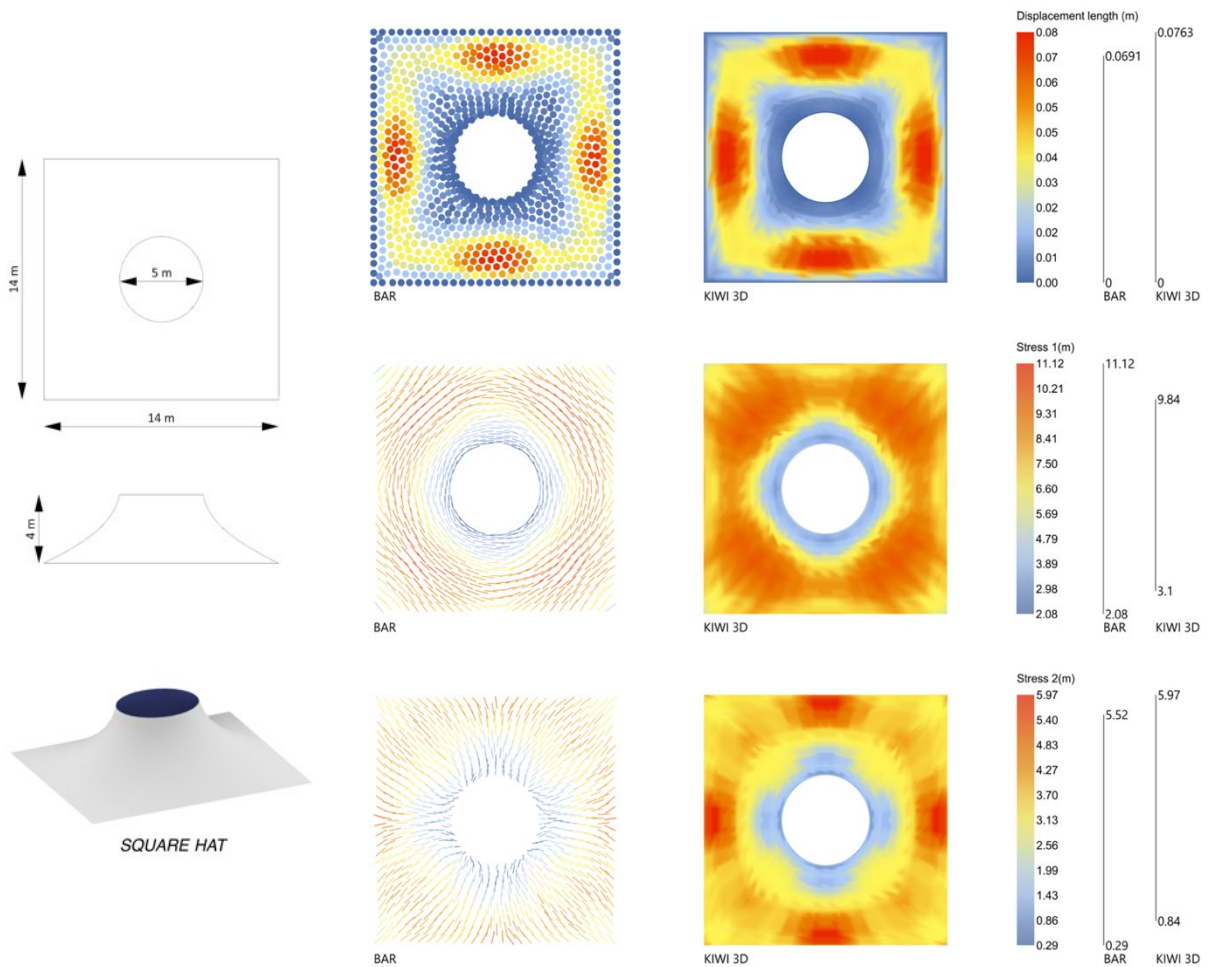


Figure 5 - Visual comparison between the models (left : bar network; right: Kiwi 3D)

4. Case study

4.1 Surface fitting with affine minimal surfaces

We focus here on a structure called Lilas by Zaha Hadid architects. Lilas is a set of three membrane structures created for "The Summer Party" at the Serpentine Gallery in London in 2007 (see Figure 6 left). Each membrane is independent and is supported at the top and bottom by diamonds shape boundaries.

We try to reproduce one of these structures. The distance and size difference between the top and bottom boundaries are too large to support a non-degenerate minimal surface. It is therefore necessary to find an affine transformation to approach the final geometry.

First, we want to generate a stable surface with roughly the same shape. To this end we perform a series of scaling according to Z (see Figure 7). Then we focus on the asymmetric nature of the target surface. To do this, we shear our geometry in the YZ plane. The resulting surface does not correspond perfectly to that of Zaha Hadid but it does approximate it closely (see Figure 6 right). It is thus possible for us to approximate these complex membranes through quick manipulations. For this type of project, the use of minimal affine surfaces can be a very powerful predesign tool. Moreover, the resulting prestress field is immediately accessible (see Figure 8).

Membrane architecture: the seventh established building material. Designing reliable and sustainable structures for the urban environment.

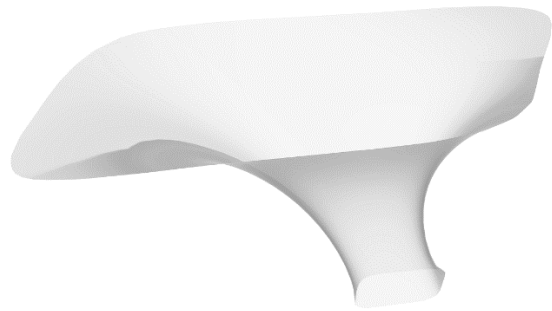


Figure 6: Surface fitting with affine minimal surfaces. (Left): target surface by Zaha Hadid, Right: best fit results

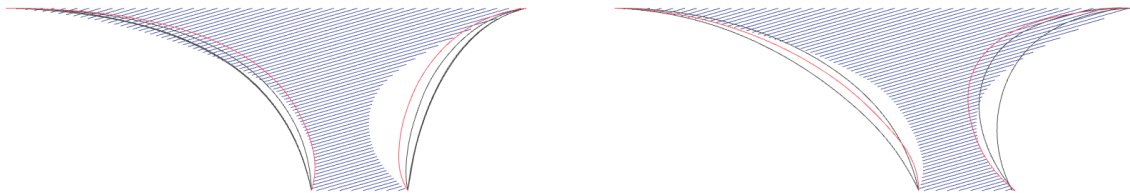


Figure 7: Effect of affine transformation on the shape: Scaling in Z direction (left) and shearing in the YZ plane (right)

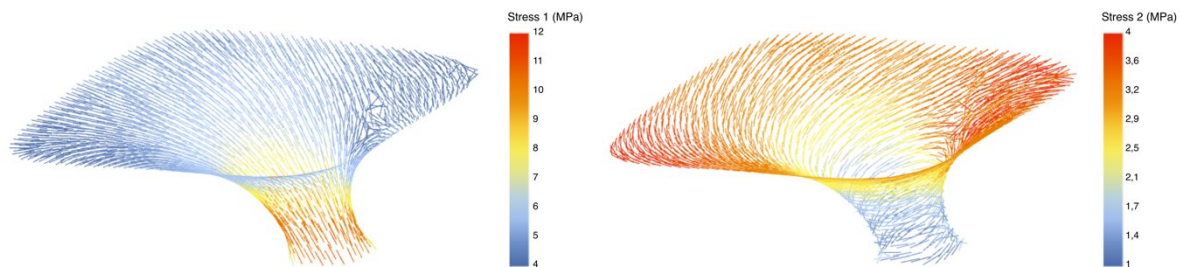


Figure 8 Stress field in the best fit surface.

4.2 Discussion

During this first study, the affine transformation operations we have implemented were applied in the global frame. Although allowing a straightforward description of the transformation, the manipulation of a matrix in this frame can quickly become tedious when one wishes to target the transformation of a particular area.

In order to simplify the process, we define “oriented” affine transformations, described in a user's frame of reference before being re-expressed in the global one. For this purpose, the user defines a plane oriented in the direction of the target area, describing the new frame of reference of the affine transformation. It is then sufficient to perform "elementary" affine transformations (such as scaling along the first direction, or shearing of the plane) to access a wide variety of modifications. Figure 9 illustrates how this method can intuitively be used to modify the shape of the membrane. In a further work, this could also be automated in order to find the best possible set of affine transformations to fit a desired surface.

Membrane architecture: the seventh established building material. Designing reliable and sustainable structures for the urban environment.

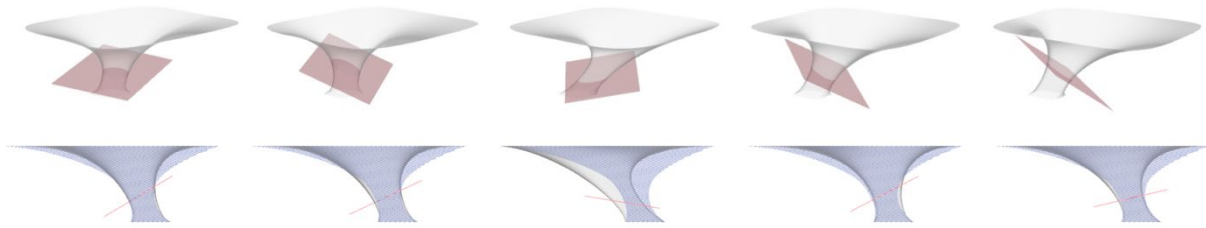


Figure 9 Oriented affine transformation and resulting affine minimal surfaces

5. Conclusions

In this paper, we introduced affine minimal surfaces as an intuitive family of shapes for textile architecture. We explained how they can be generated from a given boundary and validated numerically our form-finding method. We also show how these shapes can be deformed for surface fitting.

Beside their aesthetical interest and the six additional degrees of freedom that these surfaces gives to the designer, it would be interesting to study their mechanical properties. Investigations in this sense are presently under progress and should demonstrate whether or not these transformations have an influence on the structural behaviour of the membrane under external load. The results should be published in a coming paper.

References

- Barnes, M. R. (1999). Form Finding and Analysis of Tension Structures by Dynamic Relaxation. *International Journal of Space Structures*, 14(2), 89-104.
- Belloc, R. (2022). *Affine minimal surfaces*. Champs sur Marne: Ecole des Ponts ParisTech.
- Bletzinger, K. U., Bauer, A. M., & Wüchner, R. (2017). Isogeometric analysis for staged construction within lightweight design. *VIII International Conference on Textile Composites and Inflatable Structures*.
- Breitenberger, B., & Philipp, B. (2016). Integrated design and analysis of structural membranes using isogeometric b-rep analysis. *Computer Methods in Applied Mechanics and Engineering*, 312-340.
- Douros, I., & Buxton, B. (2002). Three-dimensional surface curvature estimation using quadric surface patches. *Scanning*.
- Gmür, O. (1958). Berechnung von doppelt gekrümmten schalen und versuche an solchen aus tonhohlsteinen. *Schweizerische Bauzeitung*.
- Gosling, P. D., & Zhang, L. (2011). A high-fidelity cable-analogy continuum triangular element for the large strain, large deformation, analysis of membranes structures. *CMES*, 203-251.
- Nicot, F. (2013). On the definition of the stress tensor in granular media. *Int.J. Solids Struct.*
- Schek, H. J. (1973). The force density method for form finding and computation of general networks. *Computer Methods in Applied Mechanics and Engineering*, 115-134.



tensinantes2023 : TensiNet Symposium 2023 at Nantes Université

Membrane architecture: the seventh established building material. Designing reliable and sustainable structures for the urban environment.

Proceedings of the Tensinet Symposium 2023

TENSINANTES2023 | 7-9 June 2023, Nantes Université, Nantes, France

Jean-Christophe Thomas, Marijke Mollaert, Carol Monticelli, Bernd Stimpfle (Eds.)

Value enhancement of the roof of the CC Le Polygone Montpellier

Fabián ASCASO*, Beatriz ARNAIZ^a, Ramon JULIÁN^b

IASO S.L.

Av de l'Exèrcit 35-37, 25194 Lleida, Spain, www.iasoglobal.com

* fabian.ascaso@iasoglobal.com

^a beatriz.arnaiz@iasoglobal.com

^b ramon.julian@iasoglobal.com

Abstract

The renovation of the Le Polygone Montpellier shopping centre includes a complete replacement of the roof to bring natural light into the complex while ensuring the necessary protection from inclement weather. The solution consists of an extremely light metal structure with variable cable-stayed arches, covered with 106 ETFE cushions, all different from each other, incorporating an IR-CUT treatment combined with different types of screen printing to block the passage of infrared rays and filter the passage of light. The lightness of the metal structure translates into high deformability, which must be integrated into the design of the ETFE cushions and the assembly methodology of the aluminium frames that fix them to the structure. The bracing of the structure implies a decoupling of the aluminium frames from each of the cushions, requiring the development of specific solutions for the drainage of the insulated aluminium frames down to the perimeter channels. These particularities are solved thanks to the adaptability of the ETFE inflatable cushion system, a material compatible with unconventional geometries compared to more traditional roofing materials.

Keywords: structural lightness, assembly methodology, structural deformation, parametric design, parametric manufacturing, drainage, luminosity, screen printing, IR-CUT, ETFE.

1. Introduction

The Polygone shopping centre, located in the heart of Montpellier, has undergone a complete refurbishment entrusted to Jean-Paul Viguier, architect of the similarly designed Confluences leisure and shopping centre in Lyon.

The Polygone shopping centre, which opened in 1975, is the locomotive of Montpellier's city centre and brings together 110 brands in a 45,000 m² shopping area visited by almost 11 million

Membrane architecture: the seventh established building material. Designing reliable and sustainable structures for the urban environment.

visitors a year. The renovation project, which will be followed by a subsequent extension, aims to reinforce the attractiveness of the shopping centre in the face of competition from the Odysseum leisure and shopping centre, created to the east of the city. "It will be a new building," said architect Jean-Paul Viguier, responsible for the design of the project, who explained that "Le Polygone was built at a time when we were fascinated by American shopping centres, energy-intensive facilities that created artificial environments, isolated from the city. The renovation aims precisely the opposite: "to open up the building to the city".

The main element of this intention is the complete replacement of the roof with a 150 metre long ETFE "skylight street", varying in width from 16 to 24 metres, which allows natural light to penetrate the three levels of the shopping centre.

The new roof is based on an extremely light metal lattice and cable-stayed structure, which supports a total of 106 3-layer ETFE cushions in triangular and rhomboidal shapes. In cross-section, the cushions are arranged on arcs of varying radii, while in longitudinal section, the structure describes various undulations that are reproduced by the cushions. This configuration is broken down into 5 blocks separated by expansion joints, covering an area of more than 3000m².

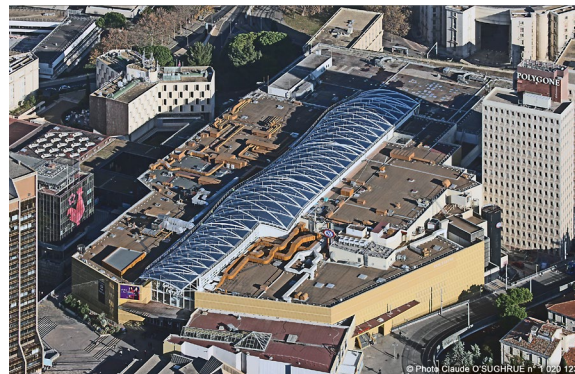
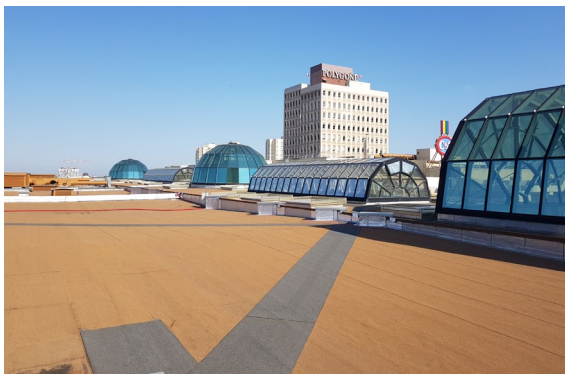


Figure 1: On the left, what the roof looked like before the renovation; on the right, the new ETFE cushion roof completed.



Figure 2: On the left, increased natural light through the new ETFE cushion cover; on the right, external appearance of the constantly variable roof geometry.

Membrane architecture: the seventh established building material. Designing reliable and sustainable structures for the urban environment.

2. General methodology for the installation of the new roof

Two major challenges condition the general methodology for the installation of the new shopping centre roof.

Firstly, the shopping centre must remain open to the public for the entire duration of the renovation work, ensuring that the building is watertight at all times. To meet this requirement, the new roof has to be built on top of the existing roof, which can only be demolished at the end.



Figure 3: On the left, the shopping centre remains open during the renovation work; on the right, the ETFE cushion roof is being installed over the existing roof.

Secondly, due to the need to maintain the existing roof until the new roof is completed, very restrictive conditions for the use of lifting aids are imposed due to the limited permissible load of the existing roof.

This second conditioning factor determines in a transcendental way the assembly methodology of the metallic structure developed by the structural engineer. In an area of the existing roof, adjacent to the roof to be renovated, with a slightly higher admissible load and within reach of the only tower crane foreseen in the project, a working platform was built for the assembly of the metal structure of the new roof. On this platform, the metal structure of each of the 5 blocks is assembled using scaffolding. When a block is completely assembled, it is unpropped and moved by means of a system of tractors and guides to its final position on the existing roof, thus freeing up the working platform for the assembly of the next block.



Figure 4: Assembly of the metal structure on the adjacent working platform.

Membrane architecture: the seventh established building material. Designing reliable and sustainable structures for the urban environment.



Figure 5: Blocks n°1 and n°2 already moved to their final position, and block n°3 being assembled on the working platform.

3. Influence of the metal structure and its assembly methodology on the performance of the IASO inflatable cushion system.

The metal structure of the new roof is characterised by its extreme lightness and slenderness which, despite its upper and lower bracing system, leads to large deformations under its own weight. This characteristic, together with the general assembly methodology described above, has a direct influence on the execution of the IASO ETFE cushion system, both in the aluminium base frames to which the cushions are fixed and in the ETFE cushions themselves.

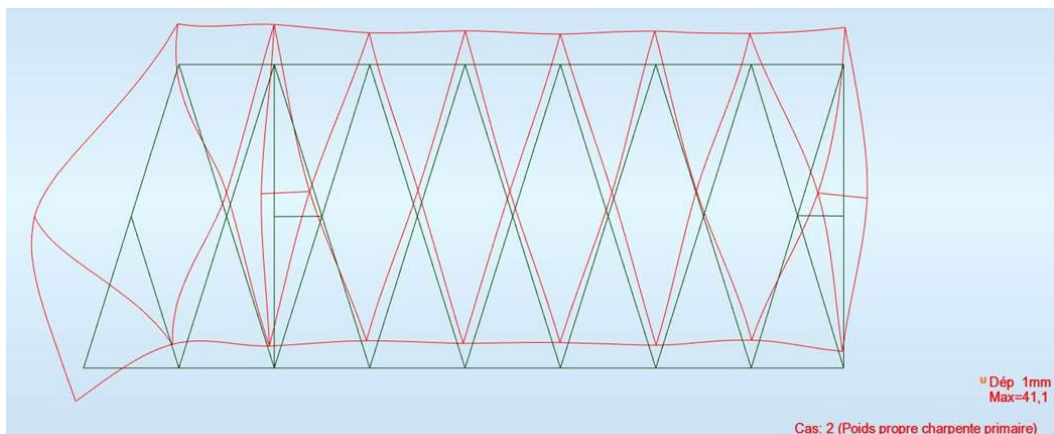


Figure 6: Example of theoretical deformation of the steel structure of block no. 1 under its own weight provided by the Robot calculation software.

Membrane architecture: the seventh established building material. Designing reliable and sustainable structures for the urban environment.

3.1. Influence on aluminium frames

The irregular geometry of the metal structure as it deforms under its own weight, as shown in Figure 6, makes it impossible to design and manufacture the aluminium frames for attaching the ETFE cushions to the structure, which the aluminium extruder supplies in straight sections, according to this deformed geometry. However, it is essential that, within the admissible installation tolerances, the aluminium frames correspond to the geometry of the metal structure, and in turn to the geometry of the ETFE cushions.

To solve this difficulty, it was decided to take advantage of the elasticity of the aluminium from which the frames are made, as well as the assembly methodology of the metallic structure, installing the aluminium frames during the phase in which the metallic structure is propped up on the working platform, without having yet been deformed by its own weight. In this way, when the structure is unpropped and acquires the relevant deformation, the aluminium correctly fixed to it deforms consequently thanks to its elasticity, reproducing the definitive geometry of the structure under its own weight.



Figure 7: Assembly of aluminium frames on a propped metal structure before deformation under its own weight.

3.2. Influence on the ETFE cushions

Once the aluminium has been made to adopt the geometry of the deformed structure, the challenge is to design and manufacture the ETFE cushions according to this new irregular geometry.

To do this, the starting point is the theoretical deformation data of each of the nodes of the metal structure provided by the Robot calculation programme of the structural engineer. Next, the IASO engineering team carries out a parameterised extrapolation of this data, point by point, to deform the theoretical contours of the cushions and make them correspond to the aluminium frames that are deformed on site when the steel structure is unpropped. These new contours are the ones finally used in the development of the pattern engineering for the manufacture of the ETFE cushions.

Membrane architecture: the seventh established building material. Designing reliable and sustainable structures for the urban environment.

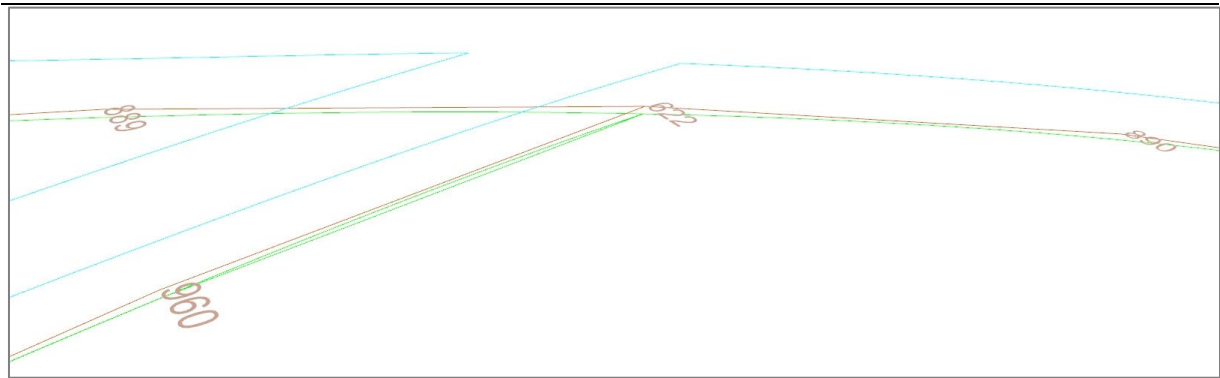


Figure 8: In brown, theoretical geometry of the structure; in green, deformed geometry of the structure; in blue, new cushion outline generated from the deformed geometry.

4. Execution details.

Some details that further characterise the execution of this unique project are described below.

4.1. Parameterisation of manufacturing engineering

4.1.1. Aluminium profiles

Because each of the metal frame arches that make up the cross-section of the roof has a different radius and the longitudinal edges of the structure also vary in altimetry, it follows that each of the corners of the aluminium sections corresponding to the different nodes of the structure has a unique, non-standardised geometry.

This particularity prompted the IASO engineering team to implement the parameterisation of the design and generation of the manufacturing drawings of the aluminium profiles, which until now had only been developed and checked theoretically in previous projects. Thus, the CC Le Polygone Montpellier is the first project in which IASO has manufactured all of its aluminium profiles by fully automating the design and production of manufacturing drawings using parametric software. The result is more than satisfactory, with no incidents recorded during either the manufacturing process or the installation process.

4.1.2. ETFE cushions

The parameterisation in obtaining the pattern of the ETFE cushions and subsequent production of the manufacturing drawings that IASO has been carrying out for years takes on greater significance in this project, in which the patterns are obtained from totally irregular contours deformed in accordance with the deformation due to the structure's own weight, as explained above.

4.2. Sealing and drainage system between aluminium frames

The upper bracing of the metal structure leads to an unusual configuration in the inflatable cushion system: the aluminium frames cannot be common to two adjacent cushions, but have to be dissociated to allow free passage between the cushions of the posts and the bracing lugs of the structure.

Membrane architecture: the seventh established building material. Designing reliable and sustainable structures for the urban environment.

This problem means that each cushion must have an independent aluminium frame, and it is necessary to create a watertight package that closes the gaps between frames while allowing the passage of posts and lugs, as well as to develop a drainage system that connects the insulated aluminium frames to each other in order to drain the water that is recovered to the perimeter gutters.

To solve the sealing package between aluminium frames, a new aluminium profile is designed specifically for the project, which allows the clipping of the ETFE cushion on one side and the support of the sealing package on the other. The intersections of the sealing package with the posts and lugs are treated with special devices, as illustrated in Figure 10. The new aluminium profile in turn allows the incorporation of threaded holes in one of its walls, into which are threaded the sealing terminals of a probe system that drains the water between the profiles of different frames to the lower perimeters arranged as gutters.

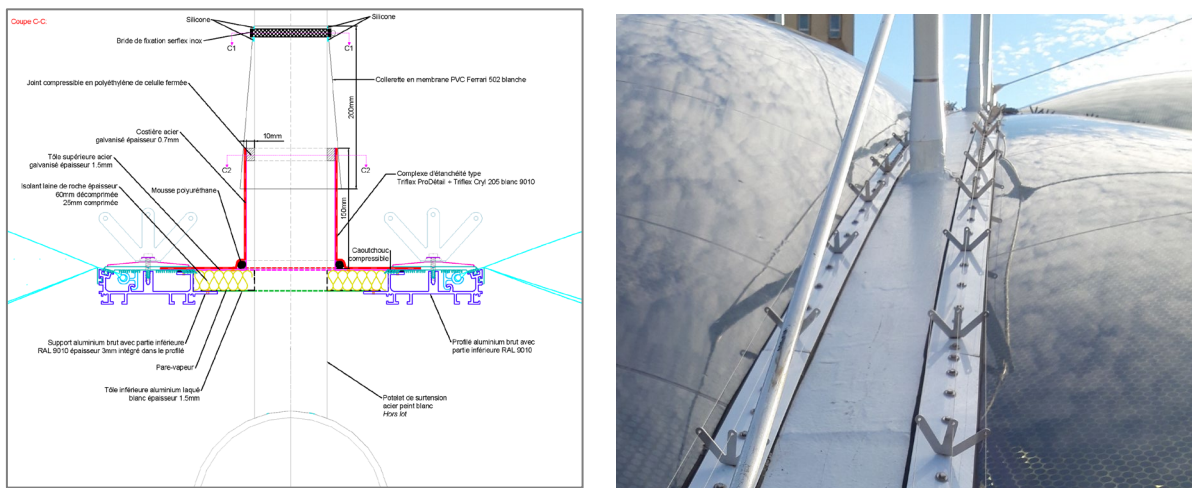


Figure 9: Sealing package between aluminium frames, with special device for the treatment of the intersection with the posts of the top bracing of the metal structure.

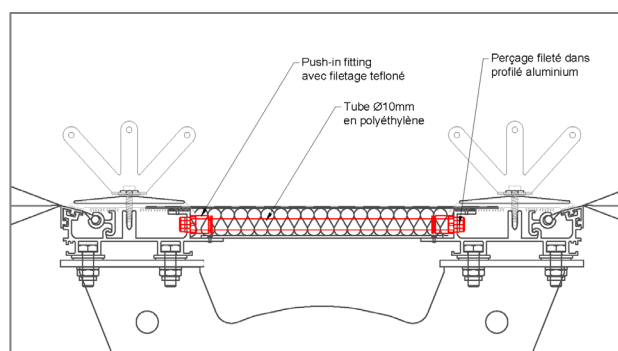


Figure 10: Drainage system between insulated aluminium frames.

4.3. Light treatment by the ETFE cushions

Another special feature of the construction of the ETFE cushion roof of the CC Le Polygone Montpellier is its treatment with regard to the passage of light.

The 3-layer ETFE cushions incorporate in their top layer an IR-CUT treatment applied in the mass of the material itself, which prevents the passage of infrared rays to limit the thermal

Membrane architecture: the seventh established building material. Designing reliable and sustainable structures for the urban environment.

contribution of sunlight in the shopping centre. Likewise, the top layer consists of a silk-screen printing with 16mm diameter moles with a density varying between 0% / 20% / 50% / 70% to filter the passage of light depending on the spatial orientation of the complex. The dynamic night lighting system incorporated in the project further enhances the translucent-transparent character of the ETFE cushions in the shopping centre.



Figure 11: The bluish appearance of the IR-CUT treatment when viewed from the outside, together with the variable surface density screen-printed dots.

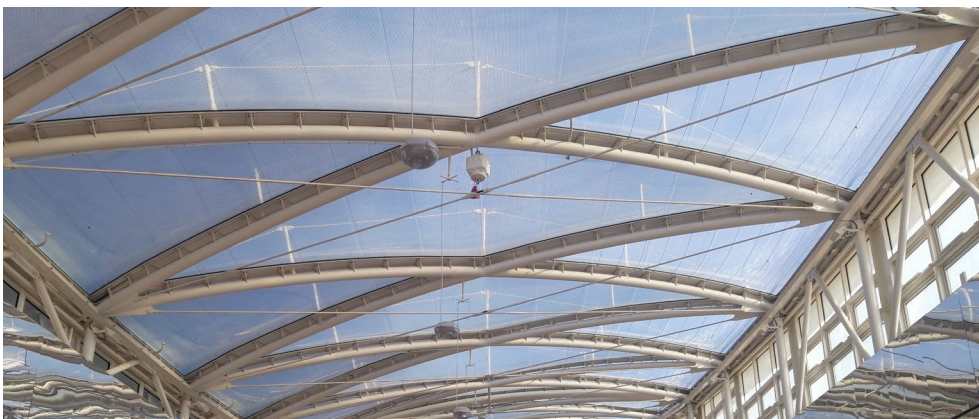


Figure 12: Variable surface density of the silkscreen as seen from the inside, with higher density on the left of the image and lower density on the right.

Membrane architecture: the seventh established building material. Designing reliable and sustainable structures for the urban environment.



Figure 13: Lighting system on the roof of the shopping centre as seen from the inside.



Figure 14: Lighting system on the roof of the shopping centre as seen from the outside.

5. Conclusion

The remodelling of the roof of the Le Polygone Montpellier shopping centre is characterised by multiple particularities, mainly associated with the geometry, deformability and assembly methodology of the metal structure, which are of great importance in the execution of the inflatable cushion system that covers it. This aspect not only translates into the need to develop specific solutions for each particular project, which are unequivocally associated with the parameterisation and automation of increasingly important engineering processes, but above all highlights the great coordination required between the teams in charge of the metal structure and those in charge of the textile enclosures of roofs or façades, in order to achieve an optimum result in the execution of this type of project.



tensinantes2023 : TensiNet Symposium 2023 at Nantes Université

Membrane architecture: the seventh established building material.
Designing reliable and sustainable structures for the urban environment.

Proceedings of the Tensinet Symposium 2023

TENSINANTES2023 | 7-9 June 2023, Nantes Université, Nantes, France

Jean-Christophe Thomas, Marijke Mollaert, Carol Monticelli, Bernd Stimpfle (Eds.)

Optimization of tensegrity systems with tensioned fabrics

Dr. Fevzi DANSIK*, Dr. Meltem SAHIN^a, Necati C. SAMAT^b

* Managing Partner at AG, Istanbul, Turkey, fevzidansik@asma-germe.com

Cihangir Mh. Şehit Yavuz Bahar Sok. No= 4-2, 34310 Avcılar, İSTANBUL / TÜRKİYE

fevzidansik@asma-germe.com

^a Assistant Professor at Mimar Sinan Fina Art University, Istanbul, Turkey

^b Chief Engineer at AG, Istanbul, Turkey

Abstract

There are many different types of tensegrity systems depending on the arrangement of the tensioning and compression elements. All these systems are stable by equilibrating the pre-tension and pre-compression forces that constitute the system. This is known as tensional integrity or can be referred to as self-equilibrium. Nowadays, tensegrity systems with tensioned fabrics are widely used as a combined load bearing system. Their lightweight solutions and elegant arrangement of the cables, struts and tensioned fabrics attract many designers. In this paper, the design and optimization tools developed for tensegrity and tensioned systems are introduced by implementing them on the project as a case study.

Keywords: formex algebra, conceptual design, form finding, optimization, tensegrity systems, membrane structures, cable structure, tensioned fabric structures, geometrical non-linearity

1. Introduction

The tensile structures including the tensegrity systems have geometrically non-linear behavior. Hence, their structural behavior depends on their form under given pre-tension and pre-compression forces. This form is known as the equilibrium form. The relative stiffness between the tension elements, compression elements and fabric elements affect this form directly. Therefore, the effectiveness of the structure and even the structural stability depend on the initial values of its form and configuration. If not properly selected, the geometrical non-linear analysis may not converge, even if it does, the structural elements may be under higher tensile and/or compressive stress resulting higher cost for the structure. Especially, the cables, their end fittings and connection plates have a significant effect on the cost of these systems. Consequently, it is crucial to select an optimum system when starting with the statical analysis. In this paper, the design and optimization tools developed by Dansik (1999) for tensegrity and

Membrane architecture: the seventh established building material. Designing reliable and sustainable structures for the urban environment.

tensioned systems are introduced to emphasize the importance of the initial geometry on the structural performance for geometrical non-linear structures. To do so, the algorithm is implemented on the project as a case study (Figure 1 & 2).

The optimization tool developed by Dansik (1999) aims to regularize the stress differences among the set of elements under pre-tension or pre-compression. The process uses an iterative algorithm based on the force density method developed by Schek (1917) to find the equilibrium forms. The aim of the algorithm is to minimize the stress differences by changing the initial element forces. These processes have been used for the optimization of the cable forces of the tensegrity system with tensioned fabric. The Amphitheatre Cover in Youth Centre in Istanbul – TURKIYE was chosen as the case study (Figure 1 & 2). After determining the optimum solutions, the structural analysis was carried out by using RFEM software.



Figure 1: The Amphitheatre Cover in Youth Centre in Istanbul

It should be noted that the presented algorithm is not a method for form finding process.

The aim of this study to emphasize the importance of the initial geometry on geometrically non-linear structural system.

2. Tensegrity Systems

There are many different definitions for the term ‘Tensegrity’. In this study, A ‘tensegrity system’ is considered as a configuration where only tensioning elements, to be referred to as ‘cable’ and only compression elements, to be referred as ‘struts’ are used together. Many types

Membrane architecture: the seventh established building material. Designing reliable and sustainable structures for the urban environment.

of tensegrity systems may be designed arranging of the cables and struts. All these systems are in a stable state by equilibrating the pre-tension and pre-compression forces that constitute the system. This is known as tensional integrity or can be referred to as self-equilibrium. Nowadays, tensegrity systems with tensioned fabrics are widely used as a combined load bearing system. Their lightweight solutions and elegant arrangement of the cables, struts and tensioned fabrics attract many designers. This was instrumental in choosing a tensegrity system including tensioned fabric as a case study.



Figure 2: The Amphitheatre Cover in Youth Centre in Istanbul

3. Form Finding Process for Tensegrity Systems

Cable nets and fabric systems are categorized together as ‘tensile’ structures. Tensile structures are made of material which has negligible weight and no flexural rigidity such as high strength cables and/or fabric. Therefore, tensile structures must always be stretched. In other words they must either pneumatically or mechanically be prestressed to stand up. This means that their initial geometry is not known, and they are geometrically non-linear. Hence, the form and the configuration of a tensile structure cannot be obtained only using geometric concepts alone because its form must satisfy the equilibrium conditions due the initial pretension forces. The process of finding this initial form and configuration is known as the ‘form finding process’. The tensioning is introduced mechanically by struts in the tensegrity systems. Hence, the form and the configuration of a tensegrity system is also subjected to the form finding process.

There are many numerical methods for form finding process. The force density method is used in this study. After finding the equilibrium form, the statical analysis of the tensioned structure

Membrane architecture: the seventh established building material. Designing reliable and sustainable structures for the urban environment.

including the tensegrity system can be done by using any software that can perform the geometrically nonlinear analysis.

The force density method has been developed by Schek (1917) to find the non-linearly equilibrium state of the network of elements having no flexural rigidity and having pin connections. This is achieved by solving the linear set of equilibrium equations which are constituted by defining a ratio between the force and the length for each element of the network. Hence, it is possible to obtain a different equilibrium form for each different set of element force density for the same network. This may be considered as a good aspect of the method since there are endless possibilities. On the other hand, to select the most suitable solution among the endless possibilities is the main challenge since it depends on many different engineering and architectural demands. In order to tackle this task, two new iterative algorithms are developed to minimize the stress and length variation of elements among the given set of configurations by Dansik (1999).

4. Optimization Algorithm

The equilibrium forms for the given set of boundary conditions are directly affected by the relative stiffness among the cables, struts, and fabric elements. Therefore, the effectiveness of the structure and more importantly the structural stability depend on the initial values of the form and its configuration. If not properly selected, the geometrically non-linear analysis may not converge, even if it does, the structural elements may be under higher tensile and/or compressive stress resulting higher cost for the structure. Hence, it is very important to seek an optimum solution as the initial geometry and pre-stressing level.

It should be noted that the presented algorithm is not a tool for form finding process. It is an optimization tool developed by Dansik (1999) aims to regularize the stress differences among the set of elements under pre-tension or pre-compression. This algorithm uses the form finding method developed by Schek (1917), known as the force density method, to find the equilibrium forms. The aim of the algorithm is to minimize the stress differences by changing the initial element forces. Afterwards, the results can be exported to commercially available software for further analysis and design process which may have different methods. In this study, RFEM is used.

The optimization developed by Dansik (1999) is basically started with the initial equilibrium form obtained by the set of the force densities defined with respective relative axial stiffness for each group of elements of the configuration, that is, cables and strut elements with different section and material aspects.

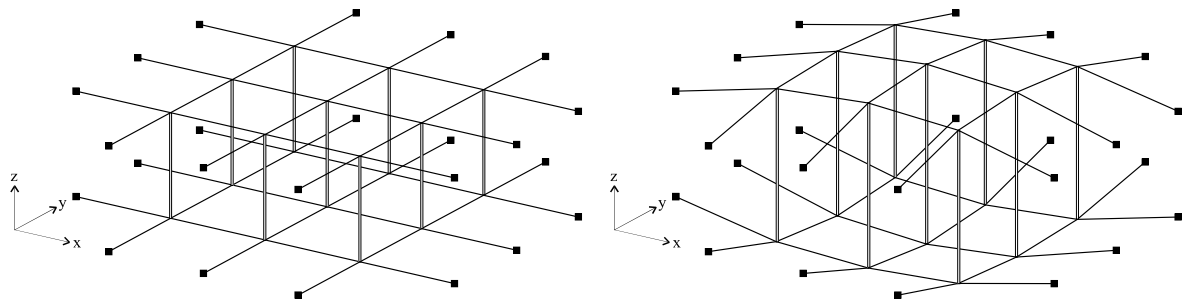
Then, the ratio between the minimum and maximum stresses of the elements is calculated for each group of the elements. If this ratio is one, which is the limit, there will be no stress variation over the considered group of elements. This can be considered as the minimum surface. Although it is possible to reach the limit with the proper boundary conditions, the aim of the algorithm is not to seek a minimum surface but to minimize the stress variation over an equilibrium form for the considered group of the elements. Hence, the relative difference between two consecutive steps is considered as the termination criteria of the algorithm. If this relative difference is not changing between two consecutive steps than the algorithm stops. If not, the element force densities for the next step are calculated by using the average stress and the lengths of the considered elements in equilibrium form in the current step.

Membrane architecture: the seventh established building material. Designing reliable and sustainable structures for the urban environment.

In order to elaborate consider, the configuration of the double layer tensegrity system is shown in Figure 3(a). The top and the bottom layers are cables which are indicated by single line while the vertical web elements are struts which are indicated by double lines. Let the axial stiffness of the struts be chosen as 5 times more that of cables. Hence, the force density of the cables is defined as 1 and the force density of the struts is 5 to impose the relative difference between the different groups of the elements. The optimized equilibrium form is given in Figure 3(b).

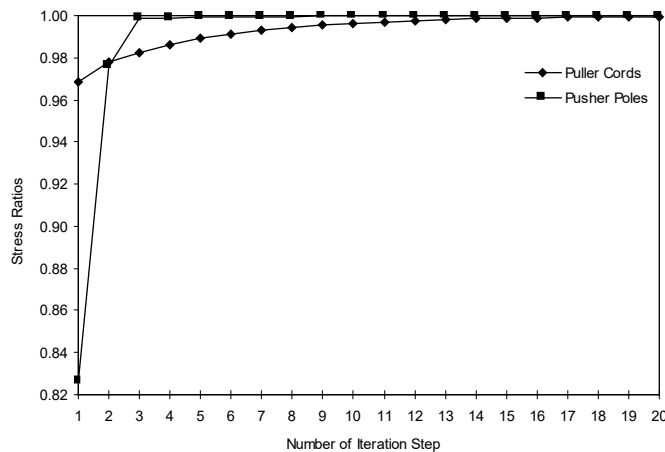
The variation of the stress ratios is given graphically in Figure 3(c). It is shown that the stress ratio for the struts converges to 1 relatively faster than that of the cables at the 6th of the iteration process. However, the iteration process continues until the ratio for the cables reaches 1 at the 20th iteration.

The same approach has also been implemented to minimize variation of the lengths of the elements among the given set of configurations using Dansik (1999).



(a) Initial Configuration

(b) Optimized Equilibrium Form



(c) Iteration History

Figure 3: Steps of Optimization Algorithm

5. Case Study

The optimization algorithm described briefly in Section 4 without any alteration has been used for the optimization of the cable forces of the tensegrity system with tensioned fabric in Amphitheatre Cover in Youth Centre in Istanbul – TURKIYE (Figure 1, 2, 4 & 5). The cover

Membrane architecture: the seventh established building material. Designing reliable and sustainable structures for the urban environment.

is spanning approximately 39 m by 22 m and the cables are connected to the reinforced concrete beam with 40 cm height along the perimeter. The original design was given by the architect as shown in Figures 4 & 5. The main request was to keep the depth of the cable net under 2 m.

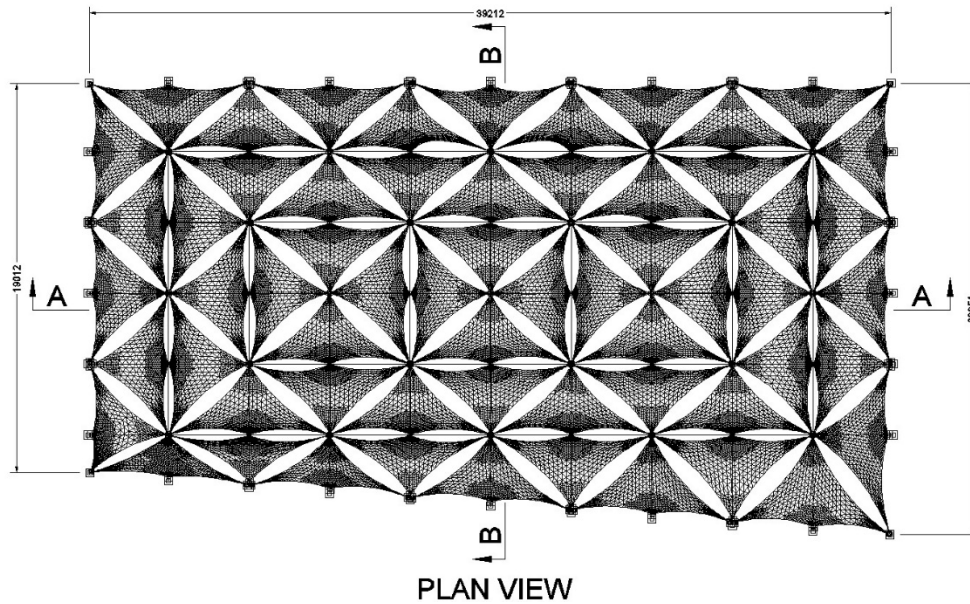


Figure 4: Original Design

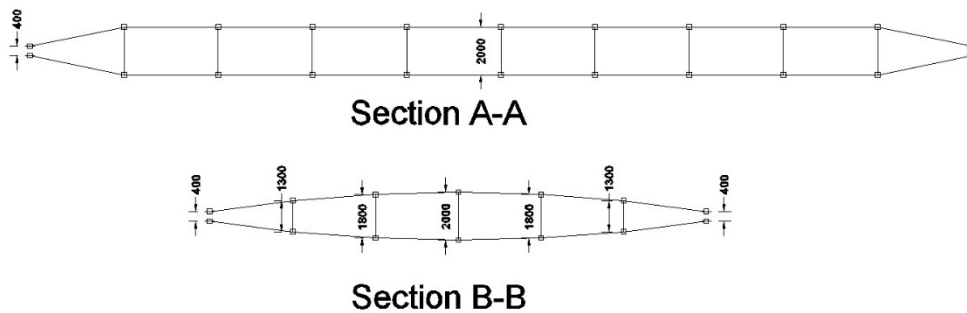


Figure 5: Requested Geometrical Cross Sections

The structure was built from the results of the study introduced in this paper by using the design aspects as defined in sequel.

The fundamental wind velocity is 33.33 m/sec (120 kph) for the location of the structure. The wind loads are calculated according to EN1991-1-4 chapter 7.3. The surface is loaded with fully with suction and compression loads as 1.63 kN/m^2 and -1.20 kN/m^2 respectively.

The snow load, 0.60 kN/m^2 is not considered since it is less than the wind pressure value.

The composition of the cables is considered as OSS. S235 steel is used for the struts. PVC-PES open mesh is chosen for the fabric, and its typical mechanical properties are considered for the analysis. It should be mentioned that the tensioned fabric is not included during the optimization process. It is ended using the form finding and statical analysis by RFEM.

The tensioned fabrics are not shown in the graphics to have a clear view of the cable forces.

6. Analysis of the Original Design

The statical analysis is carried out with RFEM software. As the first step, the form finding process is done by keeping the original geometry. The cross sections of the result are given in Figure 6. It shows that the cable lines in section B-B are catenary due to the tensioned fabric.

The convergence problems occurred during the analysis which meant that there is stability problem since some tension elements work in the compression. Hence, the prestressing values of these cables are increased many times. The cable forces for form finding, wind suction and pressure loads are given in Figure 7, 8 and 9. It is shown that there are still very small compression and yet it is possible to find a solution. However, this process has yielded to the high level of cable forces. Consequently, the reaction forces are increased in the level that cannot be carried out by the existing reinforced concrete beam. The last but not the least, the cable sizes are reached to 36 mm which throws the limit over project's budget.

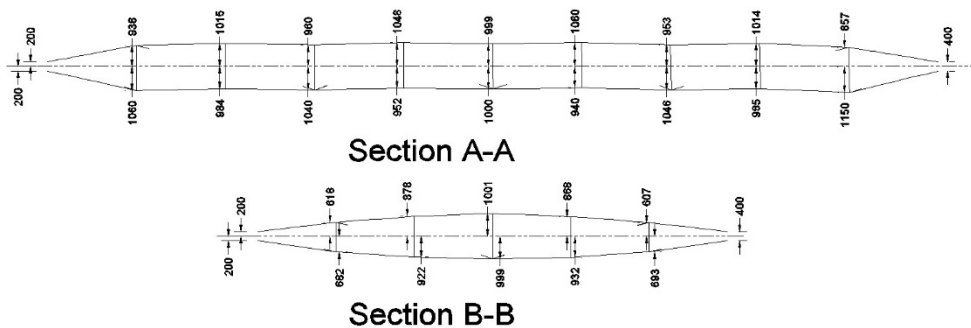


Figure 6: Cross Section After Form Finding by using RFEM

7. Optimisation of the Original Design

The force density method, which is used in this optimization algorithm, gives the equilibrium state of a net system for the given element force to length ratio and the boundary conditions by converting the non-linear equation solution to a simple linear one. There is always a solution with any set of ratios which is called the force density. Hence, the main question with this method is which set of force densities are used. To tackle this problem, the relative stiffness between the structural elements is considered to define the force densities. For this case study, the cable in the long span is defined as 1.33 times stiffer than that of in the short span since it is foreseen that the cable diameter is 28 mm and 24 respectively.

The catenary form of the system is to be defined by the struts, compression element. Therefore, the relative stiffness ratio is defined to reach 2 m depth as requested by the architect. To do so, a few iterations are done by changing the force density of the struts and keeping the same 1,33 and 1,00 values the same until reaching the required depth as shown in Figure 11. The obtained force density ration is -0,16. Then the optimization algorithm is run by defining force densities for the cables in the long direction, short direction, and struts as 1.33, 1.00 and -0.16 respectively.

The iteration step shows the iteration steps is given Figure 10. The changes of the ratio between the minimum to max stress for tension and compression can be seen from Figure 10. These ratios reach nearly to one after 8 iteration steps only. The resulting geometry is exported to RFEM directly. Then, the form finding is done by RFEM in order to obtain the pre-tensioning forces while keeping the geometry the same. Afterwards, the statical analysis is done by RFEM.

Membrane architecture: the seventh established building material. Designing reliable and sustainable structures for the urban environment.

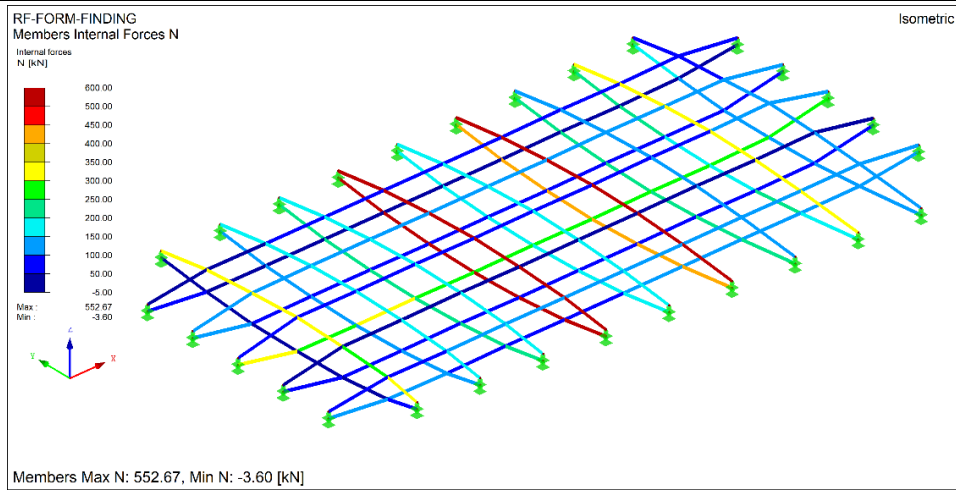


Figure 7: Cable Forces for the Original Design for the Form Finding State

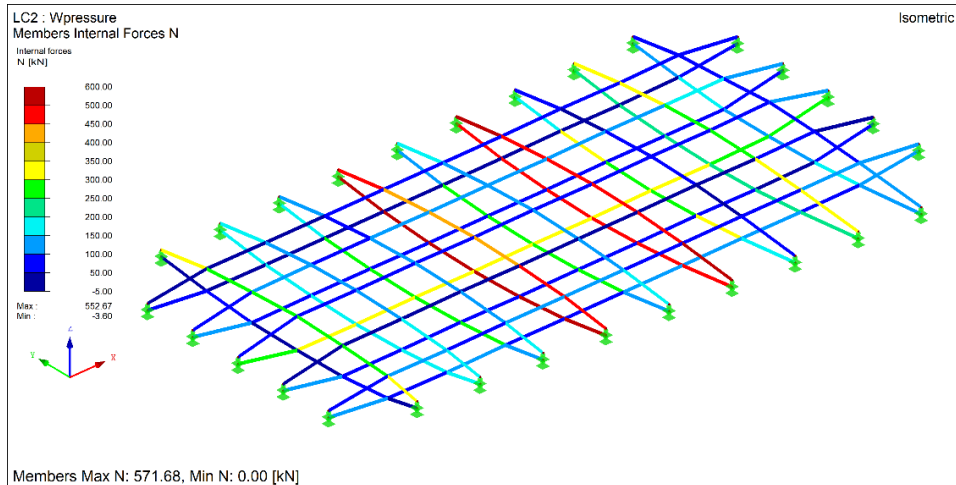


Figure 8: Cable Forces for the Original Design for the Wind Pressure

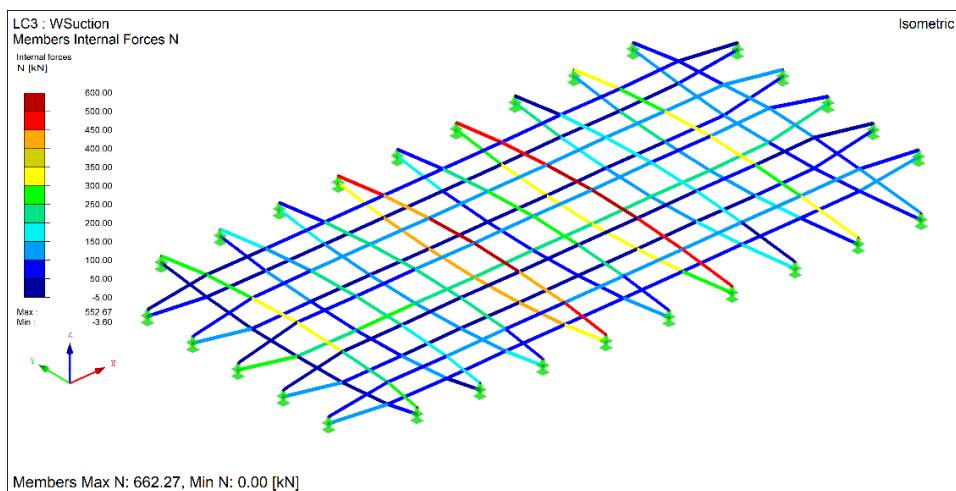


Figure 9: Cable Forces for the Original Design for the Wind Suction

Membrane architecture: the seventh established building material. Designing reliable and sustainable structures for the urban environment.

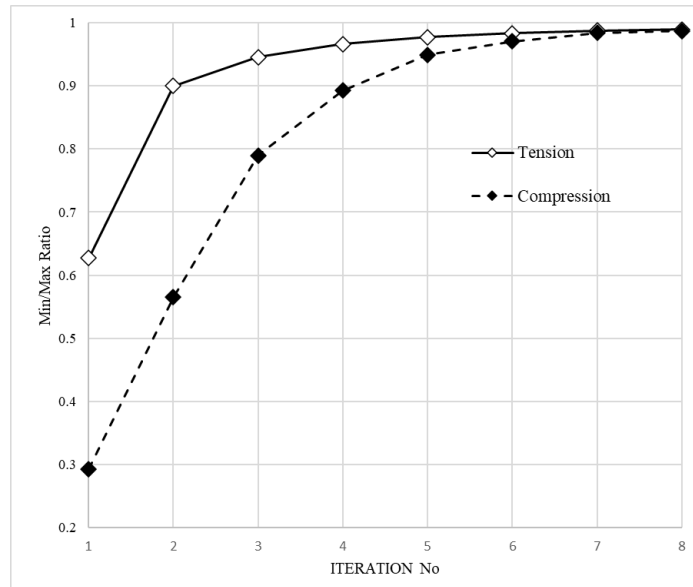


Figure 10: The Iteration Steps for the Case Study

The form finding process is done by using RFEM and the process is done again. The resulting geometry is directly used in the statical analysis and design of the structure.

8. Analysis of the Optimized System

After importing the optimized geometry to RFEM, the statical analysis is carried out. The statical model in this case is more stable and hence it has been possible to converge to the solution easier. The cable forces for form finding, wind suction and compression are given in Figure 12, 13 and 14.

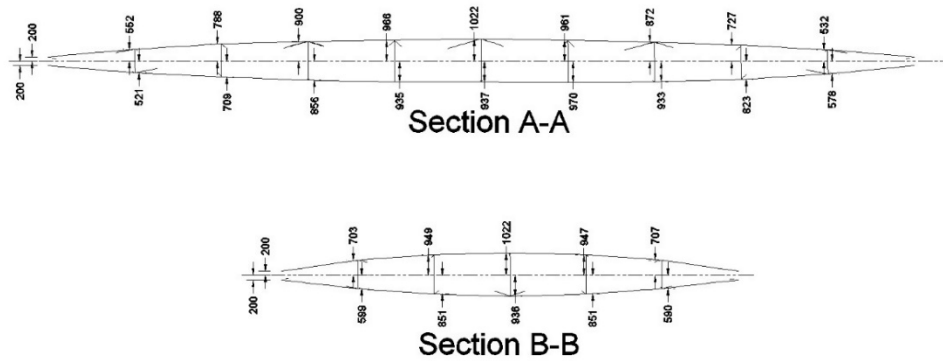


Figure 11: Cross Sicitons of the Optimized System

Membrane architecture: the seventh established building material. Designing reliable and sustainable structures for the urban environment.

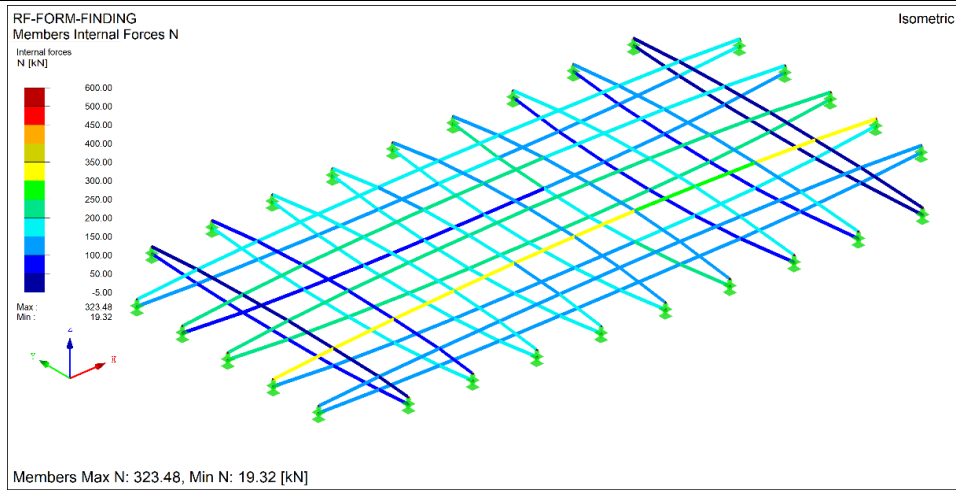


Figure 12: Internal Forces under Prestress (Form Finding State)

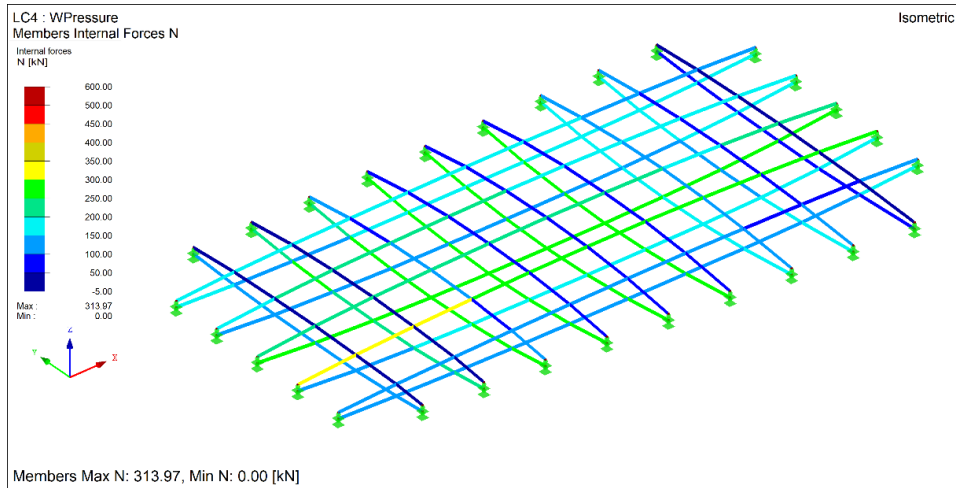


Figure 13: Internal Forces under Wind Pressure

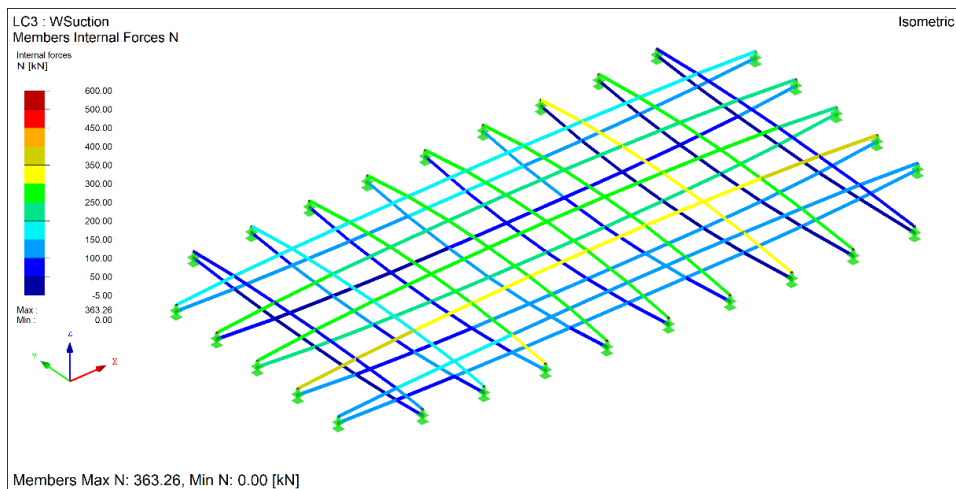


Figure 14: Optimized Cable Forces Wind Pressure

9. Conclusion

The comparison graphics are given in Figures 15, 16 and 17.

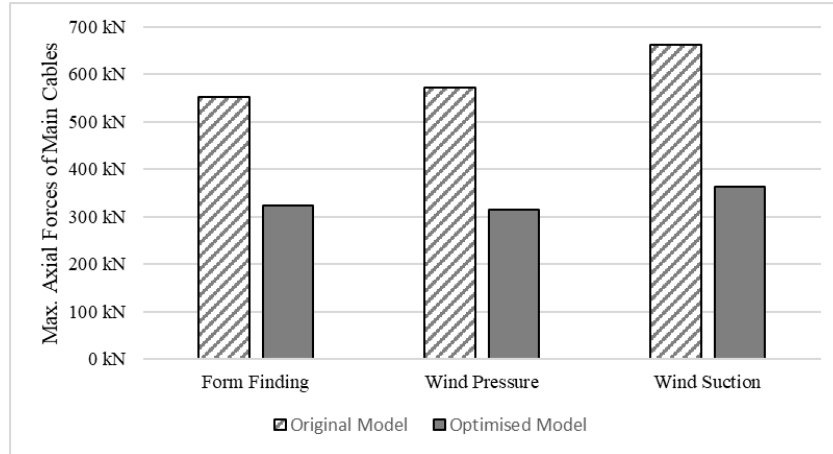


Figure 15: Maximum Axial Forces of Main Cables

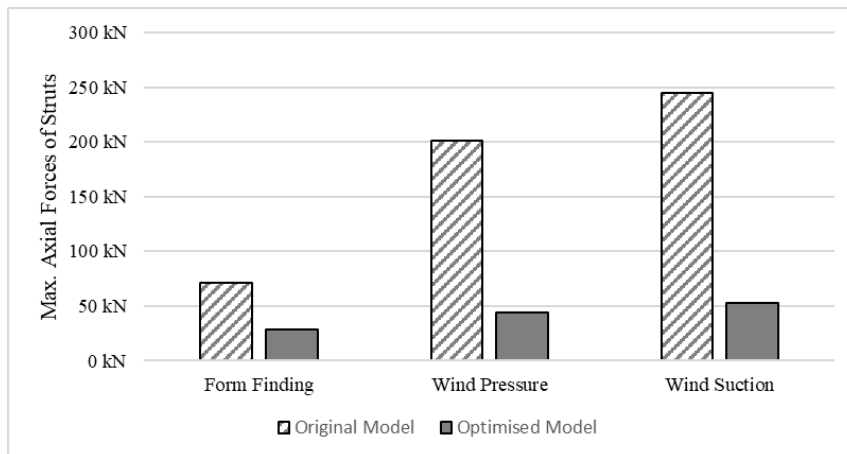


Figure 16: Maximum Axial Forces of Struts

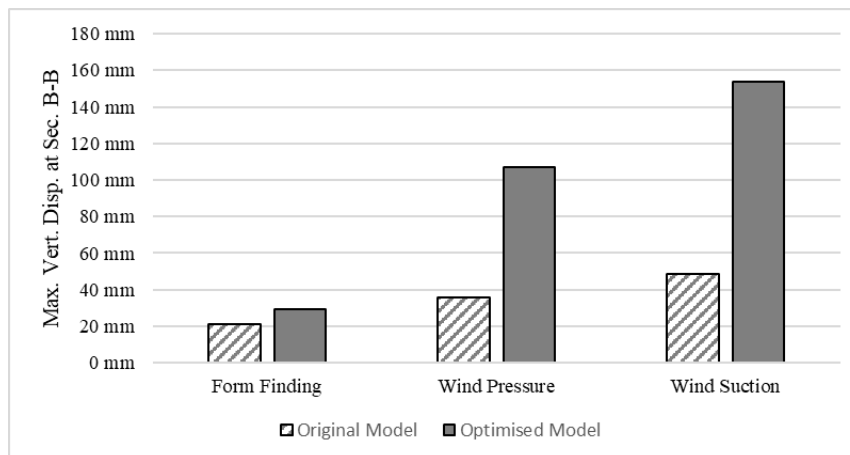


Figure 17: Maximum Vertical Displacements

Membrane architecture: the seventh established building material. Designing reliable and sustainable structures for the urban environment.

The findings can be outlined as follows:

- The cable forces are decreased nearly up to 45%.
- The strut forces are decreased nearly up to 80%.
- The only increase in the deformation since the significant reduction in the prestressing.
- It has been possible to reduce the cable diameters 36 mm to 28 mm and 24 mm.

The impact of these reductions on the cost of the cable and its fitting is nearly 40%.

This study emphasizes the importance of the initial geometry on geometrically non-linear structural system.

The introduced algorithm has been used on some other tensile structures that the authors worked on. The results have been similar.

References

- H. J. Schek (1974), The force density method for form finding and computation of general network, *Computer Method in Applied Mechanics and Engineering*, vol 4, pp. 115-134, 1974.
- F. Dansik (1999), *Configuration Processing and Force Density Method*, PhD Thesis, The Space Structure Research Center, University of Surrey, 1999.



tensinantes2023 : TensiNet Symposium 2023 at Nantes Université

Membrane architecture: the seventh established building material. Designing reliable and sustainable structures for the urban environment.

Proceedings of the Tensinet Symposium 2023

TENSINANTES2023 | 7-9 June 2023, Nantes Université, Nantes, France

Jean-Christophe Thomas, Marijke Mollaert, Carol Monticelli, Bernd Stimpfle (Eds.)

Retractable membrane roofs as urban shading device

Dongyuan Liu*, Gregor Grünkorn^a, Julian Lienhard^a, Ata Chokhachian^b, Thomas Auer^b

*Tragwerksentwurf (TWE)

Universitätsplatz 9, 34127 Kassel, Germany

liu@uni-kassel.de

^b Chair of Building Technology and Climate Responsive Design, School of Engineering and Design, Technical University of Munich, Germany

Abstract

Heat islands in urban environments are formed due to the lack of vegetation, densification of buildings, and the large amount of thermal mass. As urbanization and climate change soar, increasing challenges on sustainable and comfortable living are posted. While active cooling systems are energy demanding, passive measures like growing trees or roof-top vegetation are restricted to conditions, such as limiting space, growing time, and water sources. It's safe to say that there is no one-fit-all solution in the mitigation of urban heat islands.

In this paper, the application of retractable membrane roofs for urban shading is briefly reviewed, and a workflow utilizing the concept of anchoring force polygon for typical site geometries, namely linear street canyons and polygonal courtyards, is proposed for the conceptual design of such roofs.

The proposed workflow starts from considering planar equilibrium conditions. The results then inform the membrane form-finding with a finite element based program; shading performance was examined by radiation analysis. The effectiveness of the proposed design workflow was showcased by a design example, where the retractable membrane roof is deployed upon a non-parallel street canyon.

Keywords: retractable membrane roof, parallel bunching, conceptual design, form finding, shading, urban heat island

1. Introduction

This section reviewed some applications of retractable membrane roof in urban context and determines the scope of this paper, in climate, urban and the roof design aspects. Section 2 considers the methods and metrics in quantifying of outdoor thermal comfort, highlighting the importance of urban shading; a radiation study considering both the existing building and the deployed membrane roof is summarized. Section 3 introduces the concept of anchoring force

Membrane architecture: the seventh established building material. Designing reliable and sustainable structures for the urban environment.

polygon and the following form finding workflow with FE-based program Kiwi!3D. Finally, section 4 showcases the conceptual design method via a roof on an unparallel street canyon.

1.1 Urban heat islands and outdoor thermal comfort

Over the last years, we have witnessed an increasing public awareness about the effects of the natural and built environment on microclimate in cities. Despite being an encouraging sign, good evidence and objective measures remain lacking for how environmental aspects impact individual behaviour of people in urban contexts. Driven by climate emergency and its effect on outdoor spaces - which accommodate various activities and improve the livability of the cities - there is an urgent need to better understand current and future characteristics of urban microclimate and environmental qualities in anthroposphere scale (Chen and Ng 2012). One of the key parameters to assess and quantify environmental measures in cities is people's exposure to extreme conditions and its acceptable thresholds. This is closely linked to both climate change and urban morphology meaning that any effort to mitigate the former may further improve the latter. Successful implementation of outdoor comfort and heat exposure measures demands innovative tools and reliable methods addressing dynamic and transient nature of urban environments (Chokhachian 2022).

One of the effective strategies to promote walkability and having a positive impact on health and wellbeing of citizens is to give them comfort opportunities with trees or manmade canopies and structures (Zhao, Sailor, and Wentz 2018). There is no doubt that urban trees and living structures are optimal solution for urban heat mitigation, but they also come with their own limitations in terms of water requirements, space, and the time they need to develop reasonable leaf area to have a significant impact.

In this context both simulations and experimental studies have demonstrated that one of the most effective strategies to avoid surface overheating is shading. Textile shading devices are an attractive option when the use of vegetation is restricted, removable solar protections are advisable, or a flexible geometrical design is needed, for the varying requirements through different seasons. (Hwang, Lin, and Matzarakis 2011)

Mediterranean cities, typically facing these constraints, provide a traditional example of the use of textile solar protections. These devices usually consist of a set of sun sails placed as a canopy at different heights within the street canyon. The most evident effect of sun sails is a reduction in the solar radiation penetrating the urban canyon. However, the installation of these devices modifies the street microclimate in other ways, involving changes not only in the radiative fluxes but also in the air temperature and wind flow within the canyon. All these processes affect the energy balance of urban surfaces, and thus their temperature.

1.2. Canyons and courtyards

Street canyons and courtyards are among the most common and representative building blocks in the cities. They can be formed by individual buildings, or by the construction of terraced houses, leaving openings or being entirely closed off.

Despite the diversity in geometry, their linear and polygonal abstracted forms can be used as the basic boundary conditions in the designing of shading roofs.

Membrane architecture: the seventh established building material. Designing reliable and sustainable structures for the urban environment.



Figure 1: Street canyons and courtyards identified in city Kassel, Germany

1.3. Parallel and central bunching roofs

Back in 1970s, Frei Otto and his team published IL5 (Otto and al. 1971) where extensive studies on retractable membrane roofs were reported. Here, we focus on the parallel bunching and central bunching constructions for linear and polygonal site conditions respectively.

MEMBRANEN, TRAGKONSTRUKTION FESTSTEHEND/ MEMBRANES, SUPPORTING STRUCTURE STATIONARY	RAFFEN/ BUNCHING				
	ROLLEN/ ROLLING				
MEMBRANEN, TRAGKONSTRUKTION BEWEGLICH/ MEMBRANES, SUPPORTING STRUCTURE MOVABLE	SCHIEBEN/ SLIDING				
	KLAPPEN/ FOLDING				
	DREHEN/ ROTATING				

Figure 2: Parallel and central bunching roofs (Otto and al. 1971)

Two reference projects from practice are drawn. First one is the roof over the courtyard of Vienna city hall designed by sbp (Bergermann, Gugeler, & Keck, 2004), and the second one being the roof in area Metzgergasse of city Buchs, Switzerland, over a commercial street designed by str.ucture.

Table 1: Comparison of two reference projects

Project	Vienna city hall roof	Metzgergasse roof in Buchs
Span: cross x longitudinal (retractable) directions	34 x 32	11 x 50
[m]		

Membrane architecture: the seventh established building material. Designing reliable and sustainable structures for the urban environment.

Membrane material	PVC coated Polyester	PTFE fabric
Ridge-to-ridge span [m]	3.58	4.2
Ridge-to-valley anchor span [m]	3	4.95
Ridge cable	stranded rope $\phi 12$	Polyester belt
Valley cable	two steel tubes kinked at middle	Polyester belt
Edge cable	-	Polyester belt
Driving mechanism	rotational motor on teeth rail	cable loop and sliding anchor

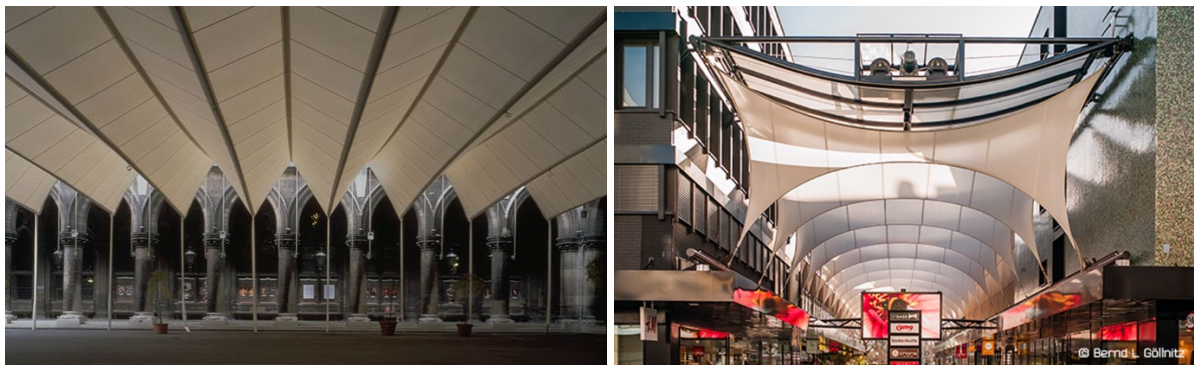


Figure 3: Roof over Vienna city hall (left) ©Monika Nikolic. Roof in Metzgergasse, Buchs ©Bernd L Göllnitz.

Despite similarities in function, site geometry and structure typology, the realization of these two projects show significant difference. The most noticeable is arguably the valley lines. Segmented steel tubes as ballast for uplift wind were used in Vienna roof, which is three times larger in span. Whilst the Buchs roof used flexible elements for both ridge and valley lines. The second notice is the different role played by the short edge cables. There is no evidence to the authors' knowledge that the Vienna roof embedded prestressed edge cables intentionally; the membrane is mainly stressed in warp direction by valley line ballast. In the case of Buchs roof, the membrane is stretched almost evenly in both directions. Curvature in edge cables is significant. Last but not the least, anchoring and actuation mechanism differ significantly. The Vienna roof employed several motors along its rails, meaning these moving anchors are potentially capable of providing reaction forces parallel to rail when motors are locked. On the contrary, Buchs roof has only one motor, tensioning the roof horizontally only at both ends. The sliding anchors in between provide only reactions that are perpendicular to rail.

A comparison of external load bearing capacity of the two is beyond the scope of this paper. Nevertheless, the simpler construction of Buchs roof is considered more suitable for moderate span urban shading applications herein, given properly defined operational wind speed among other load parameters.

2. Site conditions: geometry variation and shading requirements

Designing retractable membrane roofs in built-up urban areas for shading has two obvious challenges, namely the complexity of site geometry and the varying shading requirements, due to shadows cast by surrounding buildings. In the case of a parallel bunching roof (Buchs'

Membrane architecture: the seventh established building material. Designing reliable and sustainable structures for the urban environment.

typology with sliding anchors), this means alignment of anchoring forces perpendicular to rails and arranging membrane patches to shade efficiently.

2.1 Urban Thermal Comfort

Methodologically, there are two main approaches to evaluate and predict thermal comfort conditions in cities: simulation-based approach and experimental (sensing) method. Nowadays, supported by powerful computational systems and cloud computing resources, running complex and multi-scale models has become increasingly possible (Nazarian, Acero and al. 2019). The current efforts to simulate perceived pedestrian thermal comfort in urban settings is enormous, since the environmental conditions are highly localized and involve phenomena that are time and calculation-intensive to simulate. These models also require substantial urban and meteorological data inputs.

The current efforts to model outdoor comfort including all the effective measures of the physical domain are complex since environmental conditions are highly localized and involve phenomena that are time-intensive and computationally expensive to simulate. To fully describe the thermal sensation of a person on an urban plaza or walking under a tree on a sunny day with moderate wind, requires a series of interrelated models.

2.2 Shading evaluation

The shading efficiency of a membrane roof can be evaluated by counting shading events on a given site. An hour of year, which corresponds to a specific sun angle, accounts for one event. Shadows cast by the existing building and the membrane are both considered, the former as a shading event of 1.0 and the latter depending on the transmittance of material, as it affects the shading quality (Garcia-Nevado, Beckers, and Coch, 2020). In the case of PTFE fabric, this value is about 0.5 (Knippers, Cremers, Gabler, and Lienhard, 2011). Fig. 4 shows the proposed counting method of a non-parallel street canyon given a specific location and hour of year.

A period in summer can then be chosen and the accumulation of shading events be calculated, as Fig. 5 shows for the hot period in year between June to September, 10:00 to 14:00 during a day. The membrane shading figure is produced according to form found geometry in Section 4.

3.1. 2D Equilibrium at the Anchors

This section introduces the anchoring force polygon, which is the reciprocal of anchoring elements' 2D projection.

3.1.1. Edge cables and ridge/valley cables

Reciprocal figure is a useful tool in finding 2D equilibrium for its clear presentation of form and force when applied in the field of graphic statics. The construction of the figures can be either orthogonal or parallel and in fact to any angles (Maxwell 1864). The authors find it convenient to use orthogonal construction, for that this maintains the relative location of the reciprocal edges in two figures.

Typical membrane patches in parallel bunching roofs feature edge cables for their benefits in reinforcing and anchoring. The ridge/valley cables (welded belts in the case of Buchs' roof) can be used to control the vertical height of the roof. Finding their prestress is an important first step in the conceptual design phase.

Considering the 2D projection of a membrane patch whose corner is connected to a pair of edge cables of various radii r_1 and r_2 in the absence of ridge/valley cables. Given the prestress of membrane p , the cable forces are $p \cdot r_1$ and $p \cdot r_2$ respectively. The sum of both edge cable forces needs to be balanced by an anchoring force, whose direction can be determined graphically as indicated in the following diagram (Otto and al. 1971), by their shared chord.

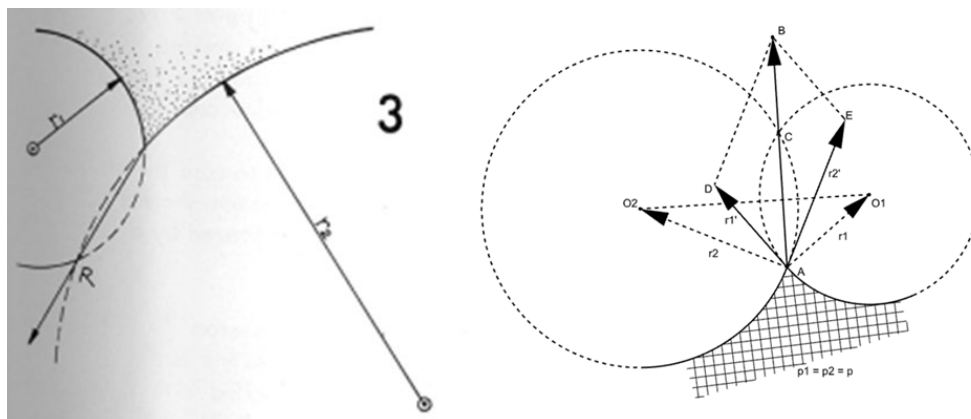


Figure 6: Determination of anchoring force direction given a pair of edge cables (left, Otto and al. 1971) and the anchoring force construction of an edge cable pair (right)

In addition to its directional determination described in IL5, a graphical method to determine the amplitude of the anchoring forces is introduced.

In Fig 6., considering the membrane prestress is unity i.e., $p = 1$, the magnitudes of the edge cable forces are given by their radii. The non-unity prestress can be considered by scaling the force diagram afterwards. In the following diagram, the anchoring force direction is in \overrightarrow{AC} , and furthermore its amplitude is the distance of the two centers O_1 and O_2 .

This can be done by proving the congruence of $\triangle AO_1O_2$ and $\triangle DBA$ as the following.

The anchoring force is in equilibrium with the edge cable force pair, thus (1). And for the tangential condition of the edge cable forces and the above-described unity membrane prestress, we have (2) and (3).

Membrane architecture: the seventh established building material. Designing reliable and sustainable structures for the urban environment.

$$\overrightarrow{AB} = \overrightarrow{r_1'} + \overrightarrow{r_2'} \quad (1)$$

$$\overrightarrow{r_1'} \cdot \overrightarrow{r_1'} = 0, |\overrightarrow{r_1'}| = |\overrightarrow{r_1'}| \quad (2)$$

$$\overrightarrow{r_2'} \cdot \overrightarrow{r_2'} = 0, |\overrightarrow{r_2'}| = |\overrightarrow{r_2'}| \quad (3)$$

In $\triangle O_1O_2A$, we have (4).

$$\overrightarrow{O_1O_2} = \overrightarrow{r_2} - \overrightarrow{r_1} \quad (4)$$

Since:

$$\begin{aligned} \overrightarrow{AB} \cdot \overrightarrow{O_1O_2} &= \overrightarrow{r_1'} \cdot \overrightarrow{r_2} - \overrightarrow{r_1'} \cdot \overrightarrow{r_1} + \overrightarrow{r_2'} \cdot \overrightarrow{r_2} - \overrightarrow{r_2'} \cdot \overrightarrow{r_1} \\ &= \overrightarrow{r_1'} \cdot \overrightarrow{r_2} - \overrightarrow{r_2'} \cdot \overrightarrow{r_1} \\ &= |\overrightarrow{r_1'}| |\overrightarrow{r_2}| \cdot [\cos(\langle \overrightarrow{r_1'}, \overrightarrow{r_2} \rangle) - \cos(\langle \overrightarrow{r_2'}, \overrightarrow{r_1} \rangle)] = 0, \end{aligned}$$

we have proven the orthogonality of \overrightarrow{AB} and $\overrightarrow{O_1O_2}$, meaning anchoring force \overrightarrow{AB} is indeed in the direction of the shared chord \overline{AC} . With this orthogonal condition, we have:

$$\angle DAB = \frac{\pi}{2} - \angle BAO_1 = \angle O_2O_1A$$

$$\angle DBA = \angle BAE = \frac{\pi}{2} - \angle O_2AB = \angle O_1O_2A$$

Thus $\triangle AO_1O_2$ and $\triangle DBA$ are congruent, so that we have the equivalence of $\overline{O_1O_2}$ and \overline{AB} .

This means, the anchoring force vector \overrightarrow{AB} can be determined, directionally by the shared chord of the anchoring force circle pair, and amplitude wise by the distance of two centers.

3.1.2. Anchoring force polygon

With such, an anchoring force polygon can be introduced by simply connecting the centers of an array of circles. These circles then give a 2D representation of a tensile membrane patch. Here every adjacent pair of circles share two intersections.

The force polygon is the orthogonally constructed force diagram of the form of anchoring elements such as the short anchoring cables that connect the roof to the rail. The closed polygon denotes the equilibrium condition of anchoring forces, which has to be always fulfilled.

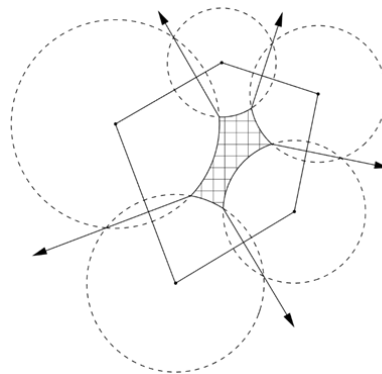


Figure 7: Anchoring force polygon for an arbitrary patch

3.1.3. Ridge/valley cables

In cases where ridge/valley cables are present at an anchor apart from a pair of edge cables, the total anchoring force points not any more in direction of the shared chord. A decomposition of the anchoring force vector is thus necessary. This is shown in the case study.

3.2. Informed form-finding in 3D

Using the cable pretension forces found in 2D equilibrium directly in Kiwi!3D was tested. Larger the slope of the intended edge cable in 3D, the more shrinks the edge cable towards the membrane. They should be factorized according to the intended slope. Although the observed deviation is arguably small, this remains an ongoing research question to the authors.

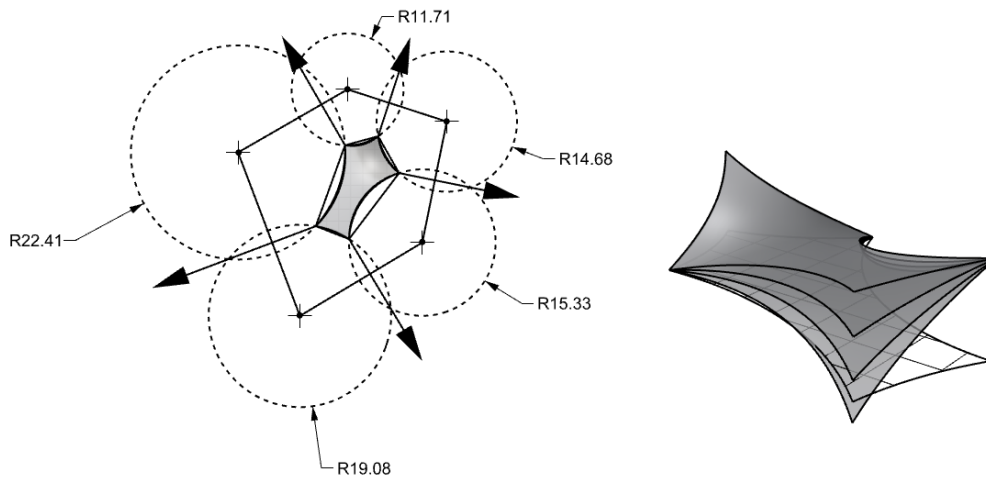


Figure 8: 2D equilibrium (left) and informed 3D form finding results of various edge cable slopes (right)

4. A Case Study: an unparallel street canyon

4.1. 2D Equilibrium at the Anchors

This chapter features a case study of a retractable membrane roof in the context of an unparallel street canyon using the introduced design workflow. The East West oriented non-parallel canyon is about 11 m at its widest, and 60 m in length. The parallelism measures 6.4° .

In the case that the ridge and valley lines are absent, the anchoring force polygon is straight forward as the following Fig. 9. Graphically, a 2D equilibrium is found. Due to the direct control on the anchoring force directions of the sliding anchors, it's trivial to make sure they are perpendicular to rail. In fact, due to the fact that the opposing anchor points share the same span in longitudinal direction, if their edge cable pair has the same rise, the ratio of their forces and thus the anchoring forces is the cosine of the angular offset of the unparallel boundaries. In other words, they share similarity.

Membrane architecture: the seventh established building material. Designing reliable and sustainable structures for the urban environment.

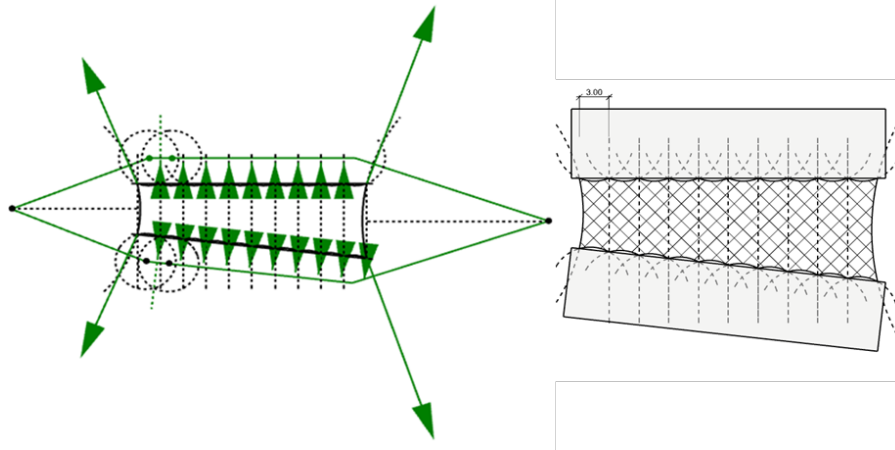


Figure 9: Anchoring force polygon for design without ridge/valley lines

In most cases though, the presence of ridge/valley lines is essential. It's crucial to take them into consideration, while maintain the control of anchoring forces, especially their directions. This can be done by decomposing the total anchoring forces into two, one for the sum of edge cable pair, the other for ridge/valley cables. The following is one possible decomposition (Fig. 10) at one anchor, followed by the resulted 2D geometry (Fig. 11).

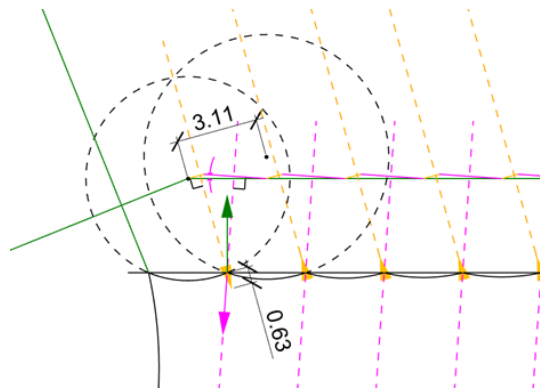


Figure 10: Decomposition of total anchoring force (green) into edge cable force (gold) and ridge / valley lines (magenta)

In Fig 10., the magenta colored edge indicates the direction of ridge/valley cable, and the edge in gold denotes the direction of summation of edge cable pair, following the orthogonal construction. And since they are decomposed from the previous green edge, the total anchoring force is still in the perpendicular direction to rail. However, the magnitude of edge cable pair sum does not match with their center distance anymore (about to the factor of 5). This simply means the force polygon inherited from last analysis (without ridge/valley lines) need to be scaled. Only the directional information is relevant in its current presentation. Another interesting fact is that the edge cable forces vary linearly in this construction (Fig 11.).

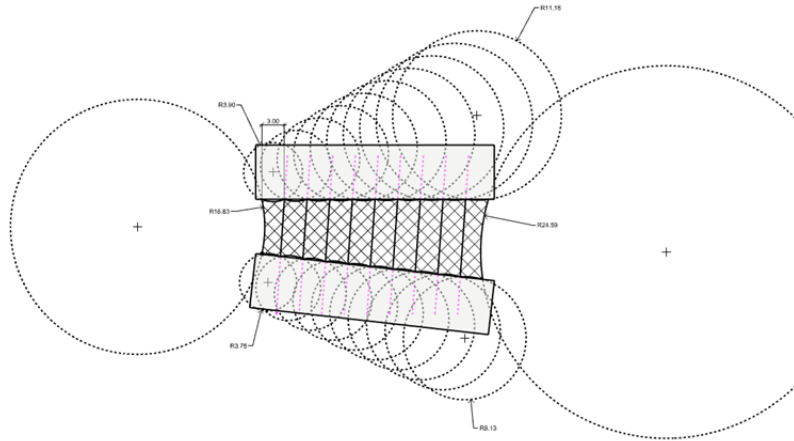


Figure 11: Resulted geometry of the decomposition.

4.2. Informed form-finding in 3D

FE based program Kiwi!3D is used to form find in 3D as the following. In this case the membrane can be stowed on both ends of the center widening canyon, and while being driven from both ends to the center, prestressed state in equilibrium is reached.

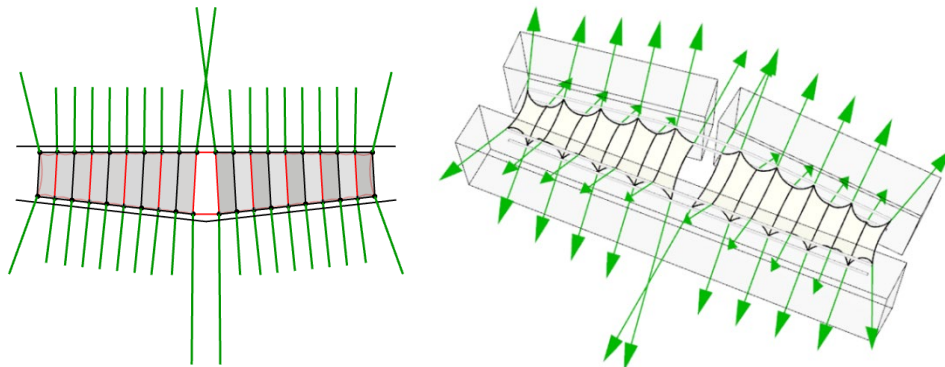


Figure 12: Top view (left) and perspective view (right) of anchoring forces

Due to the fact that the south part of this East-West oriented (EW) canyon herein is self-shaded i.e., shaded by existing buildings (Fig. 5), the membrane can be designed to leave the south side open, saving material and potentially encouraging air exchange. Fig. 13 shows such a version with the same form finding method stated above.

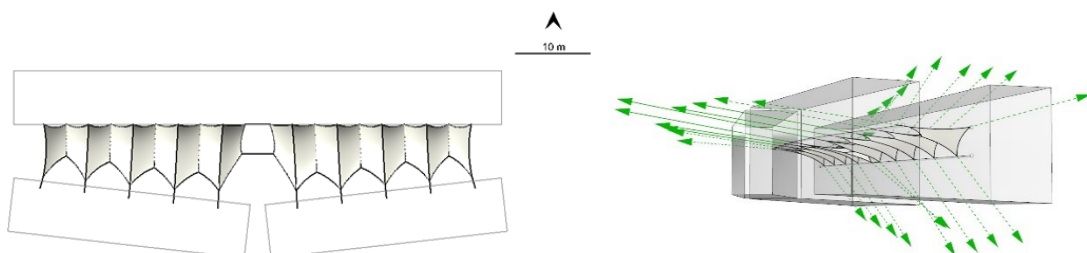


Figure 13: Top view (left) and perspective view (right) of south retrieved roof on an EW canyon

5. Conclusion and further studies

The introduced method of construction of anchoring force polygon is useful in the conceptual design phase of retractable membrane roofs in complex urban context. Further research topics include better control of 2D equilibrium construction such as scaling of the force polygon, varying cables curvatures and the factoring of planar equilibrium into 3D.

The proposed shading counting method accounts for the transmittance of the membrane material, thus is suitable for multiple layer shading construction, which could be an interesting topic in future research. Shading on façade is not part of the scope of this paper but in the case of low albedo façade, this could be influential.

Acknowledgements

This research is supported by an ongoing Zukunft Bau project “C³: City Climate Canopies”, with reference number: SWD-10.08.18.7-21.55.

References

- Chen, L., & Ng, E. (2012). Outdoor thermal comfort and outdoor activities: A review of research in the past decade. *Cities*, 29(2), 118–125.
- Chokhachian, A. (2022). Experimental and simulation-based analysis of outdoor thermal comfort conditions in urban environments [Thesis for: Doctor of Engineering, Technische Universität München].
- Zhao, Q., Sailor, D. J., & Wentz, E. A. (2018). Impact of tree locations and arrangements on outdoor microclimates and human thermal comfort in an urban residential environment. *Urban Forestry & Urban Greening*, 32, 81–91.
- Hwang, R.-L., Lin, T.-P., & Matzarakis, A. (2011). Seasonal effects of urban street shading on long-term outdoor thermal comfort. *Building and Environment*, 46(4), 863–870.
- Reicher, C. (2017). *Städtebauliches Entwerfen. Lehrbuch (5. Auflage.)*. Wiesbaden [Heidelberg]: Springer Vieweg.
- Maxwell, J. C. (1864). XLV. On reciprocal figures and diagrams of forces. *The London, Edinburgh, and Dublin Philosophical Magazine and Journal of Science*, 27(182), 250–261. Taylor & Francis.
- Institut für leichte Flächentragwerke. (1971). *IL5 Wandelbare Dächer Convertible Roofs*.
- Bergermann, R., Gugeler, J., & Keck, T. (2004). Wandelbares Membrandach im Innenhof des Wiener Rathauses. *Stahlbau*, 73(6), 373–380.

Membrane architecture: the seventh established building material. Designing reliable and sustainable structures for the urban environment.

Manoli, G., Fatichi, S., Schläpfer, M., Yu, K., Crowther, T. W., Meili, N., Burlando, P., et al. (2019). Magnitude of urban heat islands largely explained by climate and population. *Nature*, 573(7772), 55–60. Nature Publishing Group.

Garcia-Nevado, E., Beckers, B., & Coch, H. (2020). ASSESSING THE COOLING EFFECT OF URBAN TEXTILE SHADING DEVICES THROUGH TIME-LAPSE THERMOGRAPHY. *Sustainable Cities and Society*, 63, 102458.

Knippers, J., Cremers, J., Gabler, M., & Lienhard, J. (Eds.). (2011). *Construction manual for polymers + membranes: Materials, semi-finished products, form-finding, design*. Edition Detail. Basel: Birkhäuser.



tensinantes2023 : TensiNet Symposium 2023 at
Nantes Université

Membrane architecture: the seventh established building material.
Designing reliable and sustainable structures for the urban
environment.

Proceedings of the Tensinet Symposium 2023

TENSINANTES2023 | 7-9 June 2023, Nantes Université, Nantes, France

Jean-Christophe Thomas, Marijke Mollaert, Carol Monticelli, Bernd Stimpfle (Eds.)

Use of Parametric Design in Design to Production Process of a Membrane Facade

Roberto Canobbio* and Milan Dragoljevic^a

* Canobbio Textile Architecture,

15053, Castelnuovo Scivvia (AL), Italy,

roberto.canobbio@canobbiotextile.com

^a PhD Candidate at Politecnico di Milano, Milan, Italy

Abstract

Design and use of the textile elements require the utilization of a special process. The form-finding optimizes the double-curved form (Berger 1999) and during the next step leads to obtaining the cutting pattern. Both of these stages require specialized software and a big amount of time in order to set up and perform the procedures correctly. This ensures a high level of precision in the production stage. However, in special cases when the shapes are designed as simpler forms, these rigorous operations can slow down the entire process. That is why, in the case presented in this paper, a new approach is proposed: by using parametric design software, it is examined the possibility to generate cutting patterns for non-complex elements without double curvature. Thanks to the algorithms, a direct connection is created between the 3D elements (uncurved or minimally curved surfaces) positioned on the structure and 2D cutting pattern. The parametric approach allows control of the element shapes and cutting/seam lines on the facade while respecting the limitations imposed by production capacities: above all, the dimension limits of the parts. In order to check the precision of the new approach, a certain number of elements is generated using the more precise and slower approach and the results are compared. As the final finding, the parametric approach demonstrates a high level of precision and an acceptable level of correspondence with the other procedure. The advantage of the parametric method and its time-saving potential is fully utilized in the case of external border updates using metal carriers as the input. In the final stage, the elements are installed with a high level of accuracy considering the connection with other parts and also their own 3D shape and seam lines.

Keywords: Lightweight structure, design to production, digital fabrication, textile façade

Membrane architecture: the seventh established building material. Designing reliable and sustainable structures for the urban environment.

1. Introduction

1.1. Design of textile elements

Textile in architecture requires a special way of use. As a material, it has an insignificant resistance to compression and bending. This means that it has to be brought to a special shape in order to be able to act as the structural element and resist the loads. This shape is anticlastic curvature and in simpler terms, it means that the fabric is double-curved and prestressed. The shape of the fabric canopy is vital to its ability to resist all applied loads in tension [Bridges, Gosling, Birchall]. Boundary conditions determine the fabric shape and stress distribution; ideally a uniform prestress is applied to the fabric. To achieve a uniform prestress the fabric must take the form of a minimal surface (Bletzinger, Ramm 2001). However, a true minimal surface cannot be formed for all boundary conditions and a pseudo-minimal surface should be utilized instead. This type of surface is accepting increased stresses in the region where the soap bubble would have failed (Bridgens and all 2004).



Figure 1: Membrane cover for archaeological site Hagar Qim, Canobbio Textile



Figure 2: Tensostruttura Università Maria Santissima Assunta LUMSA, Canobbio Textile

Membrane architecture: the seventh established building material. Designing reliable and sustainable structures for the urban environment.

Textile is classified as a high-performance material due to its high ratio of structural strength compared to the dead load. However, its use depends on bringing it to a state of pure tension. The earliest examples also strictly followed the rules about the shape – having structures with double curvature. However, in the past decades, there is a growing use of uncurved or minimally curved surfaces. The best example of this new approach can be found in London, where O2 Arena envelope is created as a synclastic surface being generated by a cable net clad in almost flat fabric panels (Bridgens, Birchall 2012). Although without curvature as the leading design criteria, in this case, the ability of the membrane to resist loads and spanning capability are the important properties of the design. Because of this, the membrane is not just a replacement for flat cladding but still contributes to the design by its own criteria.

2. Design Process

Due to the fact that the textiles as materials have high resistance along the weave directions and can handle very low bending and compression conditions, the form of the structure has to be calculated and modelled in a such way that the positive properties are used the most, while the negative ones do not have importance. This is obtained by forming anticlastic textile forms. As the two main performance criteria, stress and deflection are used. As already noted, the main stress directions are weave ones – warp and fill. Stresses in warp and fill directions for each load case are compared to the fabric strip's ultimate tensile strength (BSi. BS EN ISO 1421 1998). Considering the deflection limits, there are not strictly defined like for the rigid building structures. However, in the case of fabric structures, there are always possibilities of water collection (so called ponding) and clash of the membrane with other parts of the structure. These two criteria are always checked during calculations.

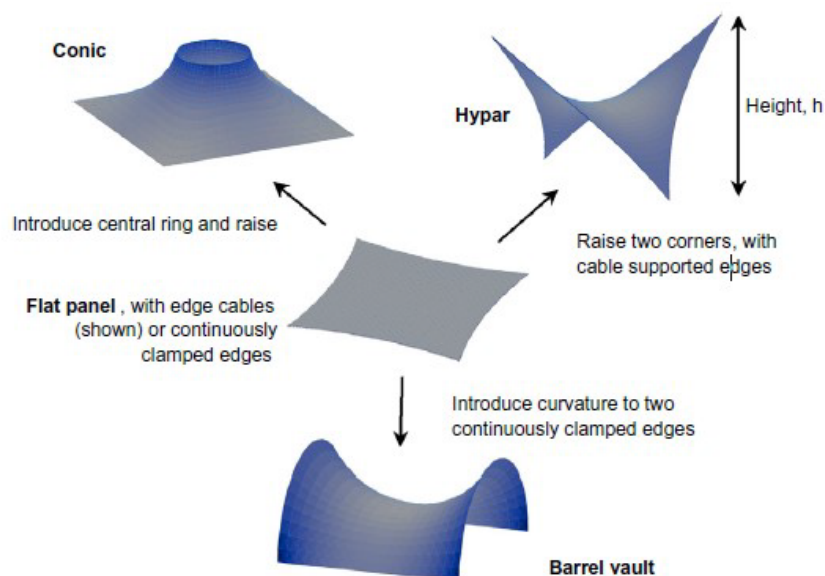


Figure 3: Manipulation of boundary conditions within a square plan and subsequent form finding enables three fundamental tensile forms to be developed (Bridgens, Birchall 2012)

Membrane architecture: the seventh established building material. Designing reliable and sustainable structures for the urban environment.

Membrane structure modelling is a process executed in two stages – the first one is a form finding and the second is a load analysis. For the first stage, boundary conditions (support geometry, fixed or cable edges) and form-finding properties (fabric and edge cable prestress forces) are defined (Bridgens, Birchall 2012). This is done by changing the boundary conditions of the structure. Image N shows different forms developed by the change of boundary conditions. After this, the loads (wind, snow and prestress) are applied to the structure in order to examine its behaviour.

The next phase in the design process is defining the cutting pattern. Since the membrane structures are assembled by welding or stitching the parts, the cutting lines should be defined on the whole structure. Later are also added other elements which support the tensile structure, such as edge cables, membrane plates, clamps etc. The final seam layout is a function of the curvatures within the surface, the roll width in which the fabric is supplied and any architectural requirements (Gibson 2015). Roll width depends on the used machine and can vary from 1.8 to 2.6 m. The other important factor when creating a cutting pattern is following the warp and fill directions. This is fundamental for following the structural calculations – if the warp/fill directions are changed, the calculations are not correct anymore and should be repeated.

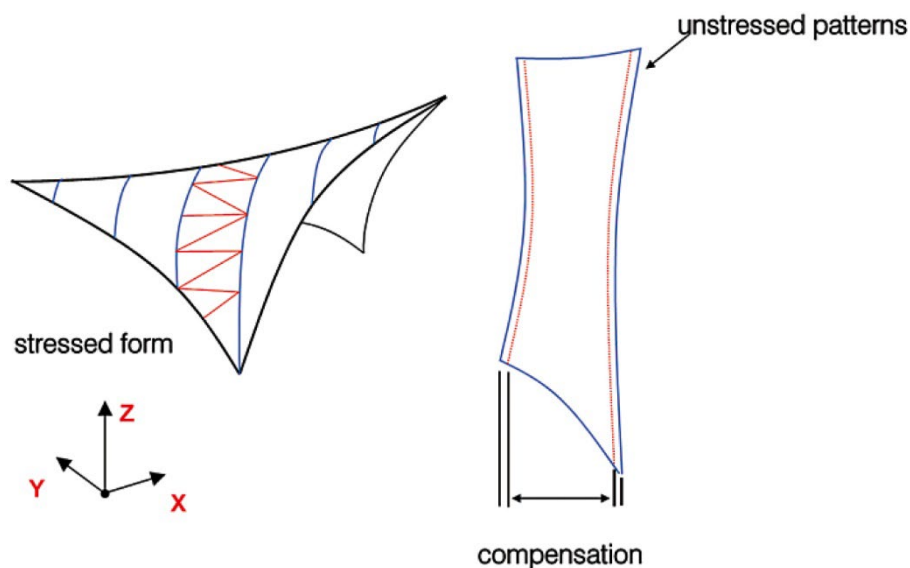


Figure 4: Cutting pattern and compensated template (Gibson 2015)

The final stage in the design process is compensation. The templates extracted from the 3D surface need to be shrunk so that, once installed, the induced strains generated during the installation process will generate the required prestress within the surface (Gibson 2015). This prestress provides load resistance and also stops wrinkles from occurring. Compensation, or more precisely, prestress values are not uniform for the whole surface but depend on the load zones.

Membrane architecture: the seventh established building material. Designing reliable and sustainable structures for the urban environment.

2.1. Uncurved membrane structures

Although less efficient considering the load resistance, uncurved or minimally curved surfaces found their field of application. The opportunity for their use emerges from architectural, economic and certain practical reasons. However, in these cases, special attention is dedicated to the problems of high membrane stress which is caused by low load resistance, high deflections and ponding issues.

As already noted, the most efficient way of using membrane structures is anticlastic shape. In this case, the load within the structure is opposed by the tension in the fabric. A good approximation of the actual force in a minimally curved cable is defined by the formula:

$$F = wl^2/8h$$

Where “w” is the load per unit length “l” and “h” is the sag in the tension element [Huntington]. It is noticeable that h and F are in the inverse linear relationship, so as h converges to 0, the force in the cable approaches infinity. This means that the force in the fabric directly depends on the curvature.

Issues with the use of uncurved or minimally curved membranes come from two properties of these structures. The first one is connected to its load-carrying mechanism. For this type of membrane, the sag is minimal and as noted in the equation above, membrane stress, therefore, tends to be high relative to span and loading (Huntington 2008). As a consequence of this, the membrane has to have higher tensile strength. This further impacts also all the structural elements connected to the membrane: increasing their size, price and potentially negative visual impact. In the end, all of these increased loads are traced back down to the foundations which should also be adjusted. In conclusion, the inefficient load resistance of flat or minimally curved membranes can lead to expensive and oversized structures.

The second type of issues comes from the large deflections occurring in these structures. This causes problems with the drainage of the water or snow. So called ponding has to be avoided in the design stage by creating a shape that will not cause an accumulation of water in the case of large deformation. Other than this, large deformations can cause unpleasant noises or concerns for the building users.

2.2. Membrane facades

Textile as the material for the facades has several benefits: low self-weight, translucency, cost efficiency, fast and easy installation and maintenance, etc. Membrane facades can act as a single-layer envelope or as a second skin to an already existing facade (usually a glass one). In the first case, the main requirements are high dimensional stability in relation to the temperature differences during the day and the seasons, good mechanical strength and lasting time (Monticelli 2015). With the recent development of textile materials, these requirements are addressed and achieved with positive results. As the second skin, the membranes should behave more as protection from rain, wind and snow. In this case, the application is more discrete and these cladding systems are manufactured with open mesh PES/PVC fabrics in order to ensure an efficient sunscreen without compromising the brightness and visibility of the outside environment, avoiding glare effects (Monticelli 2015).

Membrane architecture: the seventh established building material. Designing reliable and sustainable structures for the urban environment.

3. Case study of the Cairo Handball Arena

The case study for the application of the parametric design is a facade of the Handball Arena in Cairo. The facade is designed as a continuous set of 40 pyramid-shaped panels. Every panel has unique dimensions and is slightly different from the others. Although this architectural property improves the aesthetic value of the object, it causes a need for 40 different membrane calculations and cutting patterns. Following the process described in the initial chapters of this paper, it is needed a significant amount of time to repeat it 40 times.



Figure 5: Handball Stadium Cairo, Canobbio Textile

3.1. Methodology

When considering the introduced properties and the potential issues of the membranes and confronting them with the selected case study, important conclusions come out:

- 1) Since the panels are oriented vertically and the building is located in a climate with minimal precipitation, there is a very low risk of ponding and large deformations caused by external vertical loads.
- 2) The function of the facade is sun protection and shading.
- 3) The form of the panels classifies the facade as a flat membrane.

Using these conclusions as the guidelines, the form-finding part of the process could be simplified and performed without the need for extensive calculations. However, the second part of the membrane design process, load analysis (with wind load above others) still needs to be completed. When this analysis confirmed the form and the reliability of the used material, the process was continued with the cutting pattern definition.

Membrane architecture: the seventh established building material. Designing reliable and sustainable structures for the urban environment.

Based on the previous examinations, it is decided that the design to fabrication could be carried out through the use of a parametric design, specifically the software Rhino + Grasshopper. The algorithms incorporated both form definition and transfer to cutting pattern. Thanks to the algorithms that are written and applied, the real-time connection between the 3D model and the cutting pattern is created. This connection provides a very high level of precision and the possibility of a fast update. Other than the membrane cutting pattern, one of the big challenges in current work with the membrane structures is the design of the secondary structure (used for connecting the fabric and the primary load-bearing elements). Considering the budget and the technology required, this part of the project is significantly less important, but the engineering phase requires a disproportional amount of time and effort. The parametric approach presented here brings important improvement to the control of the whole project in the engineering phase.

The utilized material for this project is innovative and state-of-the-art permeable textile by Serge Ferrari: FT 381. The material is perforated which allows the building to breathe and the facade to act transparently. Also, in the case of an emergency, such as a fire, it expels smoke.

In addition to the material selection, which guarantees the longevity of the elements themselves, the structure functioning is ensured by engineering decisions considering the secondary structure and anchoring details. The planned system allows additional tensioning of the facade, which keeps its resistance on the requested level during the whole period of use.



Figure 6: Facade tensioning system which ensures the long-term functioning of the facade system

Membrane architecture: the seventh established building material. Designing reliable and sustainable structures for the urban environment.

3.2. Results and drawings

Before the panelization process, the structural calculations for the project are performed. In this case, the software Straus 7 is used for generating stresses and deformations with non-linear static analysis.

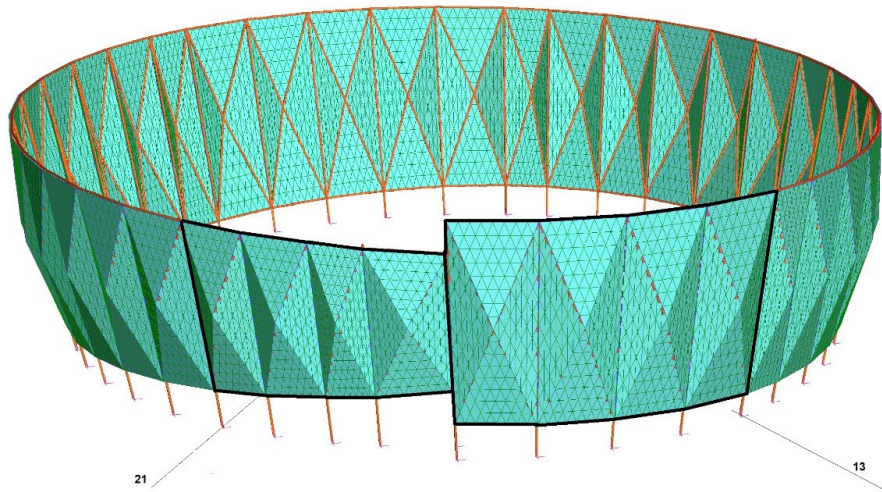


Figure 7 – Structural calculations model

3.2.1 Utilized Standards

The applied loads are following the standards:

European Norm UNI-EN 13782/15 - “Temporary structures - Tents - Safety”

Eurocode 1 – Basi di calcolo ed azioni sulle strutture UNI ENV 1991-1-4

European Design Guide for Tensile Surface Structures JRC100166 – 2016

3.2.2 Utilized Materials

The materials are defined as following:

- Membrane

polyester fabric coated PVC - Ferrari Frontside Mesh 381 - (weight = 550 g/sqm)

tensile strength w/w (daN/5 cm): 330/330 (EN ISO 1421) = 66 / 66 kN/m

Young's modulus along warp direction = $E_1 = 700 \text{ daN/cm} = 700 \text{ kN/m}$

Young's modulus along weft direction = $E_2 = 700 \text{ daN/cm} = 700 \text{ kN/m}$

Poisson's ratio $\nu_{21} = 0,5$

Shear Moduli = $G_{12} = 40 \text{ daN/cm} = 40 \text{ kN/m}$

- Steelwork

Generally steel pipes and plates in steel minimum quality S235

· Yield strength: $f_{yk} = 235 \text{ MPa}$;

· Breaking strength: $f_{tk} = 360 \text{ MPa}$;

Where specified, the steel grade has to be S355 quality

· Yield strength: $f_{yk} = 355 \text{ MPa}$;

· Breaking strength: $f_{tk} = 510 \text{ MPa}$;

3.2.3 Applied Loads

Referring to the applied standards, here are the design loads values adopted in the calculations.

Membrane architecture: the seventh established building material. Designing reliable and sustainable structures for the urban environment.

Dead load:

$$G_k = 7800 \text{ daN/m}^3.$$

Prestress:

Pk,WARP @ 3.0 kN/m

Pk,FILL @ 3.0 kN/m

Wind load:

Wind load pressure at specified height Z is calculated using the following equation:

$$q_z = 0.613 \cdot K_z \cdot K_{zt} \cdot K_d \cdot V^2 \cdot I$$
$$q_z = 0.613 \cdot 1.31 \cdot 1 \cdot 0.85 \cdot 33^2 \cdot 1 = 74.1 \text{ kg/m}^2$$

Where:

- K_z is the velocity pressure exposure coefficient evaluated at height z
- K_{zt} is the topographic factor
- K_d is the wind directionality factor
- V is the basic wind speed obtained from the Egyptian code ($V=33 \text{ m/s}$)
- I is the importance factor

The wind load is applied perpendicular to the surface.

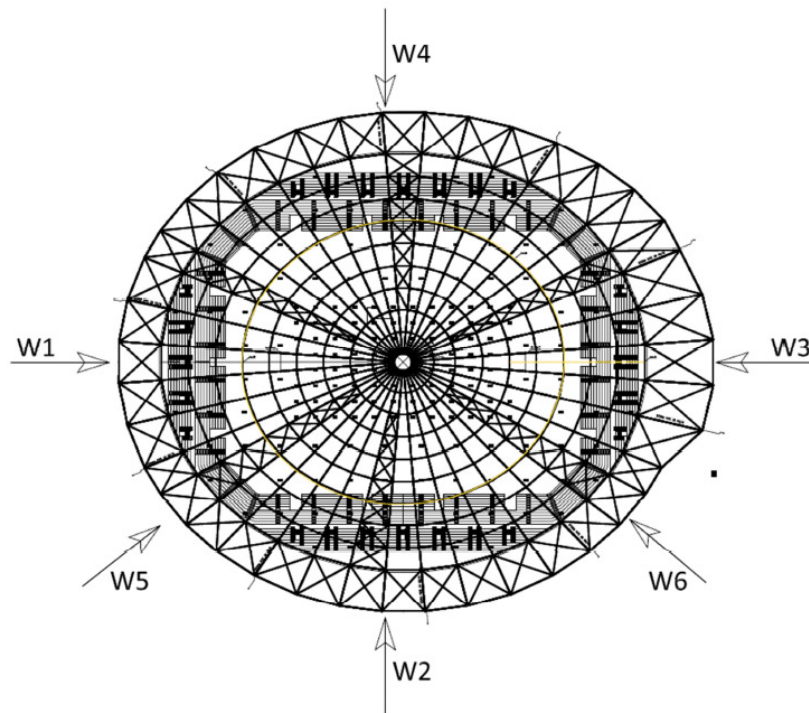


Figure 8 – Applied wind load directions

The analysis is performed for all 40 panels. The calculations show that the membrane Ferrari Frontside View 381 (or equivalent) is suitable in terms of bearing capacity for the purpose of the project, with given input loads. The calculations show that the fixing detail proposed is suitable in terms of bearing capacity.

Membrane architecture: the seventh established building material. Designing reliable and sustainable structures for the urban environment.

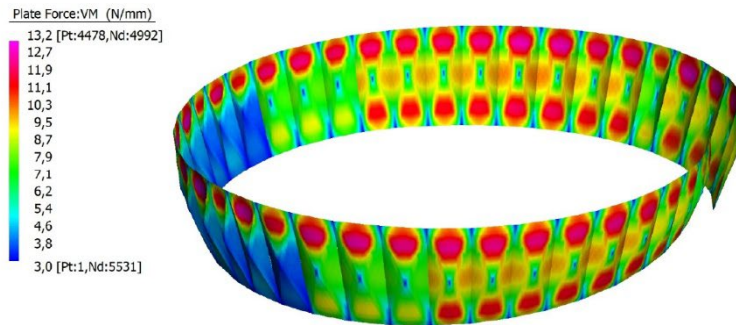


Figure 9 – Von Mises Stress – Load combination LC-W1-1

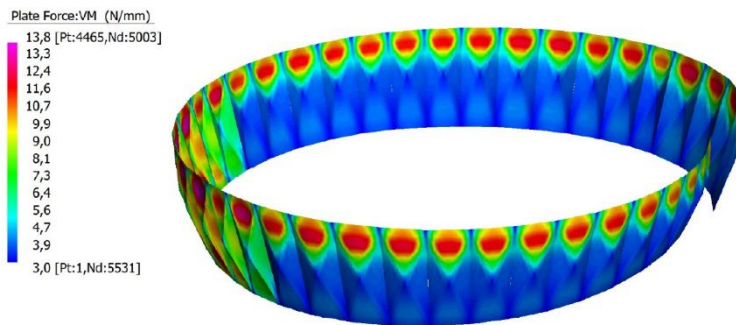


Figure 10 – Von Mises Stress – Load combination LC-W1-2

In the following part of the project, the algorithms automatize the division process of the panels. Since the dimensions are multiple times larger than the width of the cutting machine and the used material, it is necessary to split them and design seam lines. A special request, in this case, is to set up seam lines intersecting each other exactly at the edge of the pyramid. Through the algorithm, both of these rules are incorporated into the design process.

Membrane architecture: the seventh established building material. Designing reliable and sustainable structures for the urban environment.

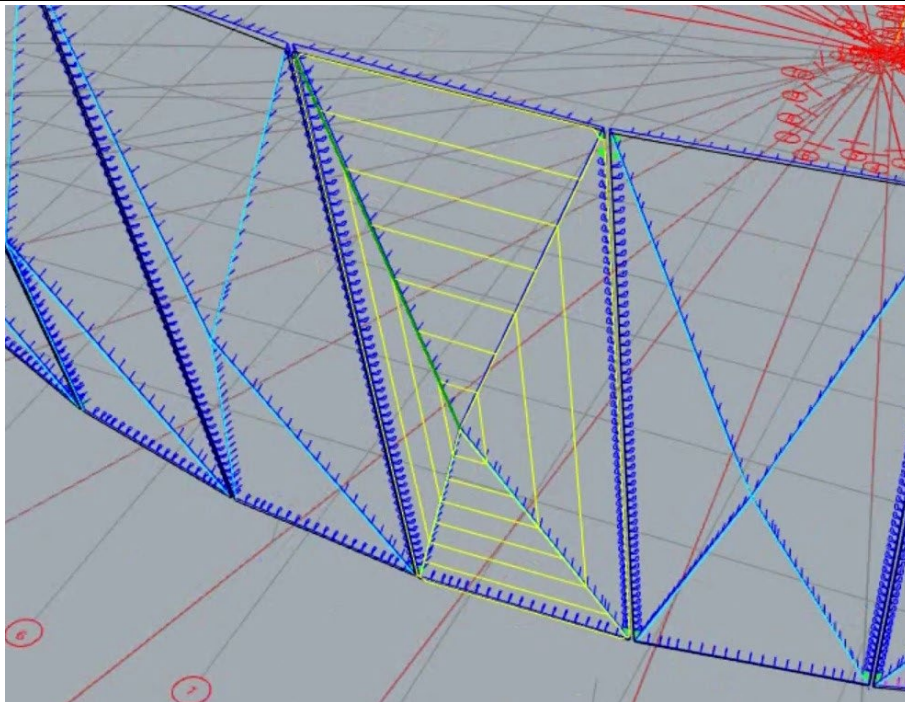


Figure 11: Seam lines intersecting each other at the edge of the pyramid

As the final outcome of the work process, the parts for cutting are produced. Also, all of the marks which are important for assembly were automatically applied, making the design to production process direct and instant. This significantly helps the work process, especially in the case of project updates, which are inevitable when multiple actors are included in the process.

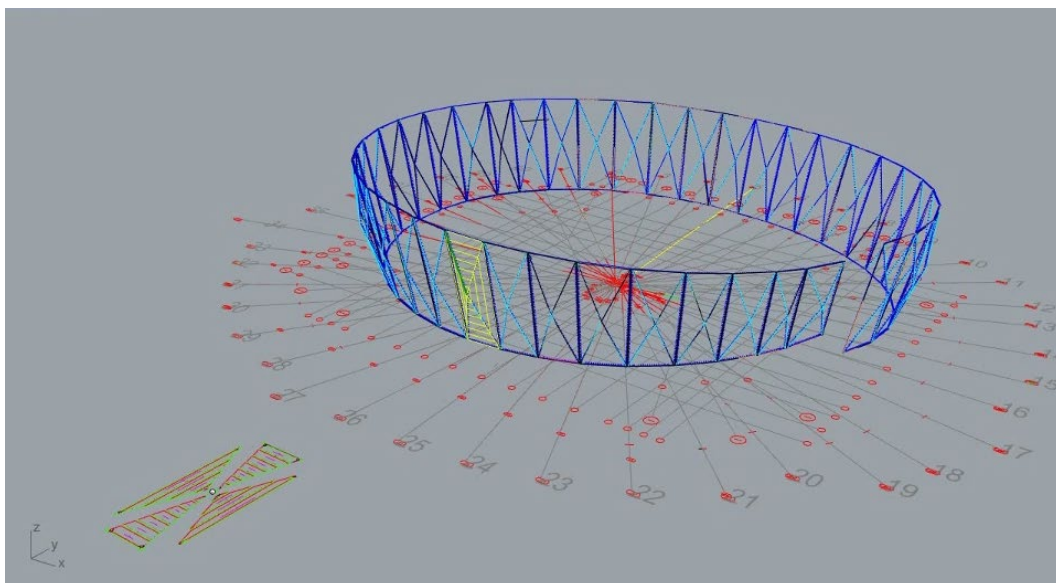


Figure 12: 3D panel division and the produced cutting pattern

Membrane architecture: the seventh established building material. Designing reliable and sustainable structures for the urban environment.

In addition to the cutting pattern, the generated geometrical and quantity data is reutilized for the creation of the secondary structure and anchoring details. With the parametrization of the process, these time-consuming engineering activities are automatized and reduced.

3.3. Discussion

As part of the control of the process, the proposed approach is confronted with longer and already examined processes of work. It is done by selecting a representative sample of the 40 panels. The cutting patterns and final forms are corresponding in a very high percentage, which allows the further utilization of the new process.



Figure 13: Seam lines intersecting each other at the edge of the pyramid

Membrane architecture: the seventh established building material. Designing reliable and sustainable structures for the urban environment.



Figure 14: The final look of the facade with the perforated fabric and the visible structure behind

4. Conclusion

In conclusion, since the process of design and production of membrane structures is complex and requires a lot of time, the presented procedure improves it for this special case of the structures. Because of the use of a flat membrane, the form-finding part of the process can be directly connected with the cutting pattern and make an instant connection. This allows better control of the parts and their assembly.

Membrane architecture: the seventh established building material. Designing reliable and sustainable structures for the urban environment.

References

- H. Berger, “Form and function of tensile structures for permanent buildings”, *Engineering Structures*, vol 21, 1999, pp 669–679.
- Bletzinger K-U, Ramm E. Structural optimization and form finding of light weight structures. *Comput Struct* 2001;79:2053–62.
- Bridgens BN, Gosling PD, Birchall MJS. Tensile fabric structures: concepts, practice & developments. *Struct Eng: J Inst Struct Eng* 2004;82:21–7.
- Bridgens BN, Birchall MJS. Form and function: The significance of material properties in the design of tensile fabric structures. *Engineering Structures Volume 44*, 2012, Pages 1-12.
- BSi. BS EN ISO 1421. Rubber-or plastics-coated fabrics. Determination of tensile strength and elongation at break. British Standards Institute; 1998.
- Gibson, N.D. How to get a membrane structure off the drawing board. *Steel Construction*, 2015. 8: 244-250.
- Huntington CG. Structures using uncurved or minimally curved tensioned fabric membranes. 2008 Structures congress – crossing borders. Vancouver, Canada: American Society of Civil Engineers; 2008.
- Monticelli C. Membrane claddings in Architecture. *Fabric Structures - J Llorens*. 2015.
- European Norm UNI-EN 13782/15 - “Temporary structures - Tents - Safety”
- Eurocode 1 – Basi di calcolo ed azioni sulle strutture UNI ENV 1991-1-4
- European Design Guide for Tensile Surface Structures JRC100166 – 2016



tensinantes2023 : TensiNet Symposium 2023 at Nantes Université

Membrane architecture: the seventh established building material. Designing reliable and sustainable structures for the urban environment.

Proceedings of the Tensinet Symposium 2023

TENSINANTES2023 | 7-9 June 2023, Nantes Université, Nantes, France

Jean-Christophe Thomas, Marijke Mollaert, Carol Monticelli, Bernd Stimpfle (Eds.)

Corolla, the soft-robotic coworking pod

Paolo BECCARELLI*, Ofir ALBAG^a, Martin HUBA^a, Roberto MAFFEI^b

* The University of Nottingham

University Park, Nottingham NG7 2RD, UK

paolo.beccarelli@nottingham.ac.uk

^a Studio albaghuba, Milan, Italy

^b Maco Technology srl, Provaglio d'Iseo (BS), Italy

Abstract

This paper presents the design, manufacturing and installation of the soft-robotic coworking pod “Corolla”, one of the winning entries of the ‘Design Competition Expo Dubai 2020’, an initiative promoted by Regione Lombardia and Camera di Commercio di Milano Monza Brianza Lodi in collaboration with Politecnico di Milano, under the theme “Connecting Spaces”. The winning projects were exhibited at the HOMI Outdoors Fair in Rho Fiera Milano and will be showcased in several public events in 2021, including Milano Design Week and Expo Dubai 2020 [1] [2].

This prototype is the outcome of a research project into soft-robotic responsive envelope systems, aimed to create a new, lightweight, adaptive envelope typology to provide increased comfort and an energetically efficient solution for outdoor living. Soft robotics is an emerging field in robotics that takes inspiration from invertebrates which are able to move without any rigid body parts. Emulating those biological mechanisms provides significant advantages over traditional rigid robotics, such as reduced weight, cost and increased robustness and flexibility.

The 1:1 scale prototype investigated the potential of the use of automation in architecture and provided a better understanding of cost-effective pneumatic actuators made of coated fabrics with the final goal of exploring the possibility of applying soft robotic technologies and principles to architectural projects.

Keywords: pneumatic structures, Expo Dubai 2020, lightweight structures, structural membrane, adaptive, mock-up, manufacturing, soft-robotic, optimization, responsiveness, robotics.

Membrane architecture: the seventh established building material. Designing reliable and sustainable structures for the urban environment.

1. Introduction

The Corolla pavilion is the outcome of a research project into soft-robotic responsive envelope systems, carried out by Ofir Albag and aimed to create a new, lightweight, adaptive envelope typology to provide increased comfort and an energetically efficient solution for outdoor living. Soft robotics is an emerging field in robotics that takes inspiration from invertebrates which are able to move without any rigid body parts. Emulating those biological mechanisms provides significant advantages over traditional rigid robotics, such as reduced weight, cost and increased robustness and flexibility.

Albag's research activity underpinned the design of a co-working pod designed by Studio albaghuba and submitted by Maco Technology srl to a design competition organized to support the further development and construction of a 1:1 scale prototype of the product (www.albaghuba.com, 2023).

Corolla is one of the winning entries of the 'Design Competition Expo Dubai 2020', an initiative promoted by Regione Lombardia and Camera di Commercio di Milano Monza Brianza Lodi in collaboration with Politecnico di Milano, under the theme "Connecting Spaces". The winning projects were exhibited at the HOMI Outdoors Fair in Rho Fiera Milano and it has been presented at several public events including Expo Dubai 2021 (www.designboom.com, 2023).



Figure 1: Two architectural impressions of the winning entry for the "Design Competition Expo Dubai 2020".

The Corolla co-working pod was recognized with the **2021 International Achievement Award (IAA) - Air Structures category** for design excellence in specialty fabrics applications. The International Achievement Awards competition is sponsored by IFAI which received 223 entries from 14 countries and selected the winners according to the complexity, design, workmanship, uniqueness and function of the project.

2. Towards a Definition of Soft Architecture

Since the beginning of time architecture was conceived as an entity opposite to the organic, an immutable object that withstands the effects of time. For centuries the keyword associated the most with the construction of buildings was stability, the tendency to stay firm and preserve the same characteristics over a long period of time. This is what people traditionally aspired for in their buildings, leading thus to a certain degree of stagnant predictability.

Membrane architecture: the seventh established building material. Designing reliable and sustainable structures for the urban environment.

Architects have been and still primarily deal with the classical building materials that help them achieve their goal of defining and enclosing space, which are usually concrete, steel, glass or wood. These traditional materials are familiar and easy to use in construction, designers could work with empirical and experimental data already gained from decades of experience and use advanced methods that provide complex calculations allowing the use of these materials without major risks. All of these available methods using well-known building materials are creating a design leading to more or less foreseeable outcomes.

Nowadays, new ideologies and technologies are being gradually introduced into architecture making a new paradigm prevail for the built environment, in which the guiding keyword is adaptability, the ability to change, transform and react according to the changing needs and environmental conditions (Andresen, 2005). There seems to be an increasing interest in the less known crossroad of fields where architecture meets automation, the point at which architecture becomes a machine. This automation process is aimed to improve our desirable results - the performance of our built spaces. Keywords like optimization, responsiveness and robotics are prominently more present and affecting our lives.

Recent decades have experienced several small movements in architecture deriving from High-tech architecture, also known as Structural Expressionism. These are showing a shift from fashionable attitudes towards the scientifically supported design of the form. The constant change in lifestyle and rising awareness of the problem of global warming and sustainability are forcing architects to search for new solutions. Some of these involve familiar materials in new unconventional uses and some exploit the breakthrough in the chemical industry by introducing innovative responsive materials with embedded active properties.

The emergence of the field of biomimicry in design and engineering is providing new solutions and technologies with the conception of bio-inspired ideas, using the principles of biology - decentralization, bottom-up control, evolutionary advances, and taking inspiration from biological systems and mechanisms existing in nature. These two latter fields had given birth in recent years to an exciting new field in automation and robotics: soft robotics (Trivedi et al., 2008). Its original concept is to make all of the components in a robot soft and flexible in order to move and manipulate in very limited spaces and change gaits fairly easily. Using innovative elastic materials to emulate biological structures and mechanisms, inspired by animals such as octopus or starfish, allows for unprecedented advantages over traditional "hard robotics". Unlike hard robots, which are fabricated from metals and often heavy and expensive to make, flexible robots are relatively cheap and easy to produce, they require simplistic designs and controls to generate a wide range of mobility, and, in some areas, they could be more resistant than their hard-bodied counterparts to damage from common dangers (Whitesides, 2011).

Architectural design tends to be rather inflexible in its nature, with changes and innovations being introduced over the course of decades, it is extremely challenging to involve new technologies and materials in new construction. This work aims to contribute to establishing the theoretical background, tools and methods that will push forward the evolution of architecture shaping a new generation of constructions based on new materials.

Membrane architecture: the seventh established building material. Designing reliable and sustainable structures for the urban environment.

3. Robotics in Architecture

During the 20th century, it has been possible to see the progressive use of automation in the construction sector. The concept of kinetic architecture describes buildings designed to allow parts of the structure or envelope to move, without compromising overall structural integrity. A building's capability for motion can be used to enhance its aesthetic value, respond to environmental conditions, and perform functions that require an easily adjustable, alternating solution, which would be impossible for a static. The possibilities for practical implementations of kinetic architecture, or rather, the automatized mobilization of larger, more significant building components, increased rapidly in the late 20th century due to technological advances in mechanics, electronics, and robotics (Zuk, 1970). In his 1970 book "Kinetic Architecture", William Zuk inspired a new generation of architects to experiment and design a broad variety of functioning kinetic buildings. Since the 1980s, thanks to the introduction of new construction concepts and the commercial widespread of robotic systems, kinetic buildings have become increasingly common internationally and in daily use (Salter, 2011). Examples of such kinetic systems implemented in constructions vary from movable structural elements (such as movable bridges) to adaptive envelopes, such as retractable roofs or movable shading devices.

Despite the introduction of the "intelligent buildings" concept in 1982 (Graham and Marvin, 1996), only in recent years it has been possible to see the development of kinetic architecture into more advanced projects which go beyond mere automation, embracing complex cybernetic processes (the science of control and communication in animals, men and machines) and the integration of artificial intelligence under the definition of smart architecture (Senagala, 2005) where the term smart describes all the advanced technological solutions coming from kinetic architecture and now including responsive, performative, interactive or adaptive architecture.

Over the last century robots, or automated machines, entered into everyday life at an increasing rate, bringing with them significant transformations into our industries and lifestyle saving labor, energy and materials and performing with better quality, accuracy and precision (Aramburo and Trevino, 2008). In his book "e-topia" Mitchell claims that in the near future our buildings will become robots for living (Mitchell 2000). Most efforts have concentrated on either adding sensory / computational elements to existing buildings - smart architecture (Johanson, Fox, Winograd, 2002), or introducing self-contained robots into existing spaces (Siciliano, Khatib, 2008). Recent advances in soft and smart materials, compliant mechanisms and nonlinear modelling, paved the way to a more popular use of soft materials in robotics worldwide. Soft robotics can be defined as a morphological class of bio-inspired robotics which greatly draws its inspiration from nature and animals such as octopuses or starfishes, the same concepts which inspired the Corolla pavilion.

4. The design of the pneumatic actuators of the Corolla Pavilion

For the design of the Corolla pavilion, the authors decided to explore the possibilities offered by soft robotics, a new research area in the field of developmental robotics where the actuators are made of flexible soft components. The current more promising technologies are PneuNets

Membrane architecture: the seventh established building material. Designing reliable and sustainable structures for the urban environment.

bending actuators, fibre-reinforced actuators, pneumatic artificial muscle, dielectric elastomer actuators and multi-module manipulators (De Falco et al. 2014) which, when required, can be integrated with elastomer-embedded 3d-printed sensors (Muth et al. 2014) and microfluidics to change colour or opacity of the actuator.

After an accurate review of the current state of the art, pneumatic artificial muscles have been identified as the most suitable typologies for architectural applications due to the inflatable technology, already tested in the building sector, and the loadbearing capacity achievable with pneumatic structural elements. Inflatable architecture has been widely used in the second half of the 20th century with ETFE envelopes and Tensairity beams successfully used in the building sector. The challenge for the corolla Pavilion was to control the movement of the inflatable structural envelope according to the input received from a set of sensors and the commands given by a controller making the structure responsive to the environmental conditions.

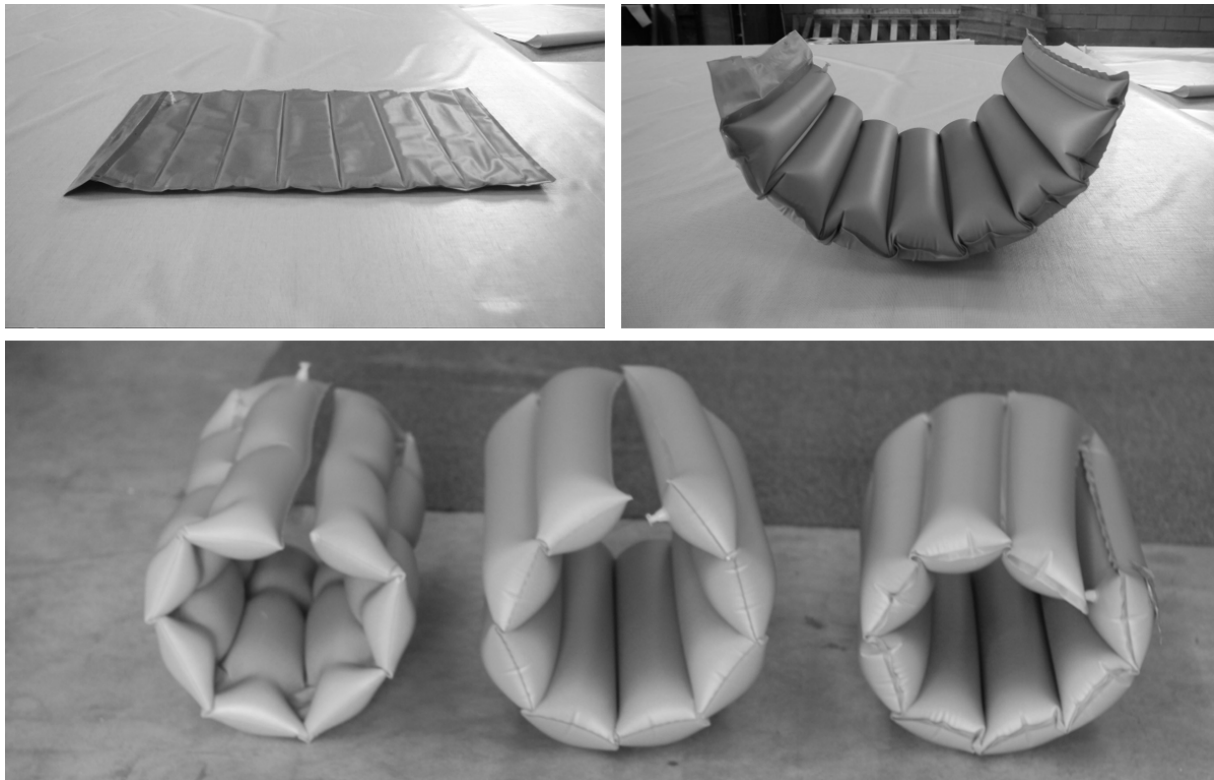


Figure 2: The initial prototypes developed to assess the viability of the concept and select the most appropriate welding pattern.

A three-layer pneumatic mattress was selected as the most appropriate structural concept and lab tests on 1:5 scale prototypes provided the initial insight into the feasibility of the project and the key parameters to be investigated. The development of the pneumatic actuators was further developed with FEM computer simulation and 1:1 scale mock-ups which correlated the geometry, the movement and the loadbearing capacity of the actuators with the geometry of the welding pattern and the level of pressure in the two internal air chambers (Figs. 2, 3).

Membrane architecture: the seventh established building material. Designing reliable and sustainable structures for the urban environment.

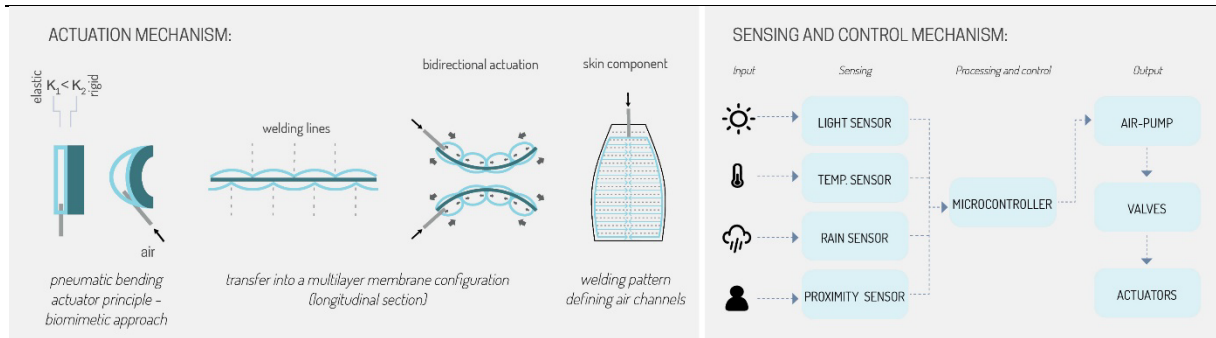


Figure 3: Schematic explanation of the actuation and controlling mechanisms.

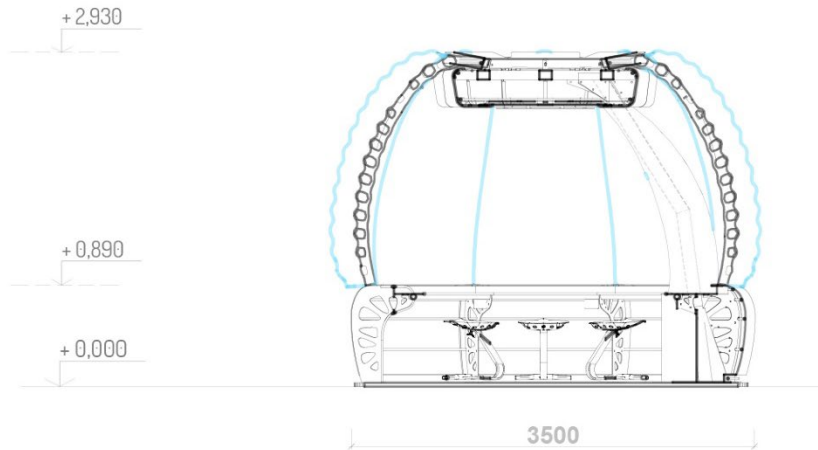
5. The Corolla co-working pod

After the successful development of the pneumatic actuator's prototype, the team of designers focused on the challenging task of the design of the full pavilion. Examples in literature describe the problems associated with the design and control of soft-robotic systems which requires knowledge from many areas including biomechanics, compliant control, smart materials and flexible robots (Sanan, 2013).

The co-working pod is designed as a modular steel structure enclosed by a soft-robotic skin system made of eight pneumatic actuators manufactured with TPU coated Nylon fabric, 349 cm long and 64 cm and 144.5 cm wide at their ends when deflated. (Figs. 4, 5) Each of these 'petals' is made of two internal air chamber networks, stamped with a special welding pattern, consisting of a series of horizontal welding lines. The distance between the lines has been designed according to the geometry and resistance required, and it is directly related to the maximum curling angle and overall ability to resist gravity and external forces such as wind. Adequate spaces are kept from the edges allowing the circulation of the air in between the chambers. This specific pattern is designed to make the petal curl up or down when the chambers are inflated (Figs. 2, 3) at different pressures.

The actuators are fixed to the structure using eight folded steel supports which are radially fixed with hinges to the top octagonal frame of the pod, supported by a curved beam cantilevered from the steel basement. A pneumatic system connects two air pumps located in the base with each side of the eight actuators, enabling the control of the two air chambers of the actuators. The column base is strategically positioned on the perimeter of the space, freeing up internal space for collaborative interactions between the users. The pavilion is also equipped with an electric circuit which provides the power distribution to the LED lights and the connection between the sensors the data logger and the controlling system. A tensioned TPU coated Nylon fabric cover gives the column and tables their curvy look (Fig. 7).

Membrane architecture: the seventh established building material. Designing reliable and sustainable structures for the urban environment.



Section A-A'

TPU coated Nylon fabric actuators, closed configuration

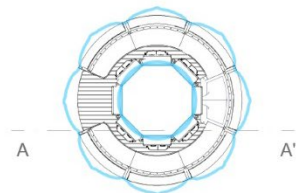
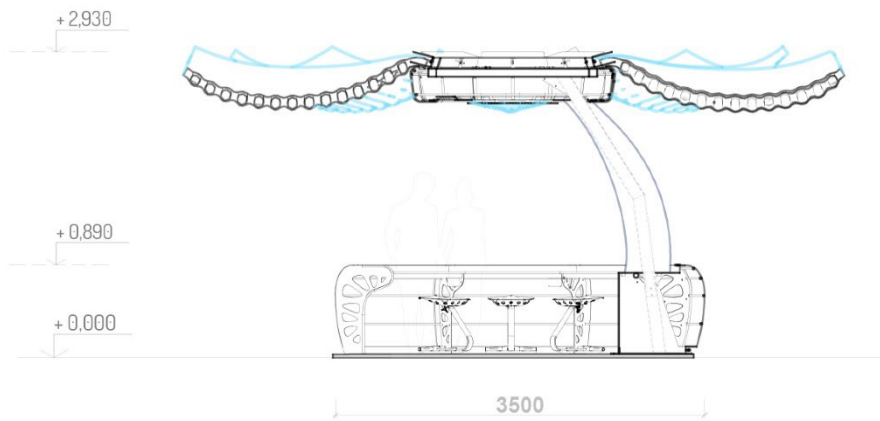


Figure 4: Cross section A-A' of the Corolla co-working pod in closed configuration.



Section B-B'

TPU coated Nylon fabric actuators, open configuration

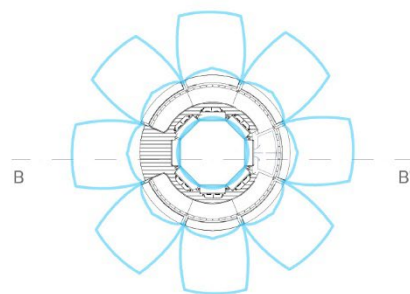


Figure 5a: Cross section B-B' of the Corolla co-working pod in the open configuration.

Membrane architecture: the seventh established building material. Designing reliable and sustainable structures for the urban environment.

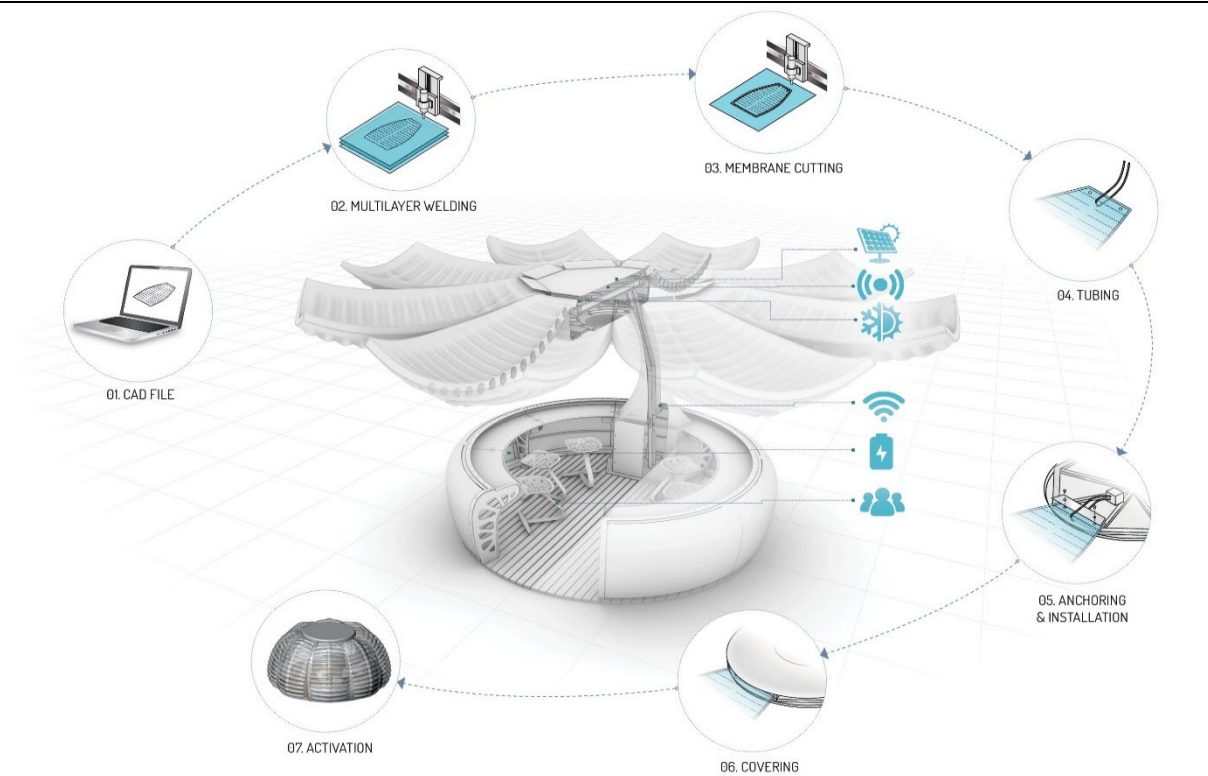


Figure 5b: Scheme of the components integrated in the Corolla co-working pod

According to the concept, the system is fully automated and its response is controlled by a microcontroller connected to the weather sensors, valves and air-pumps. In this way, on a nice sunny day, the petals are left open to enjoy the natural airflow while providing shade from the sun. In case of a rainy, cold or extremely hot day, the skin system closes to protect users from the elements providing a thermally insulated space which can be climatically controlled for optimal comfort of the users (Figs. 5a-b). The pod is also designed to be equipped with a compact HVAC system for heating and cooling, Wi-Fi, charging spots and a PV solar panel to reduce energy grid dependency (Fig. 5b).

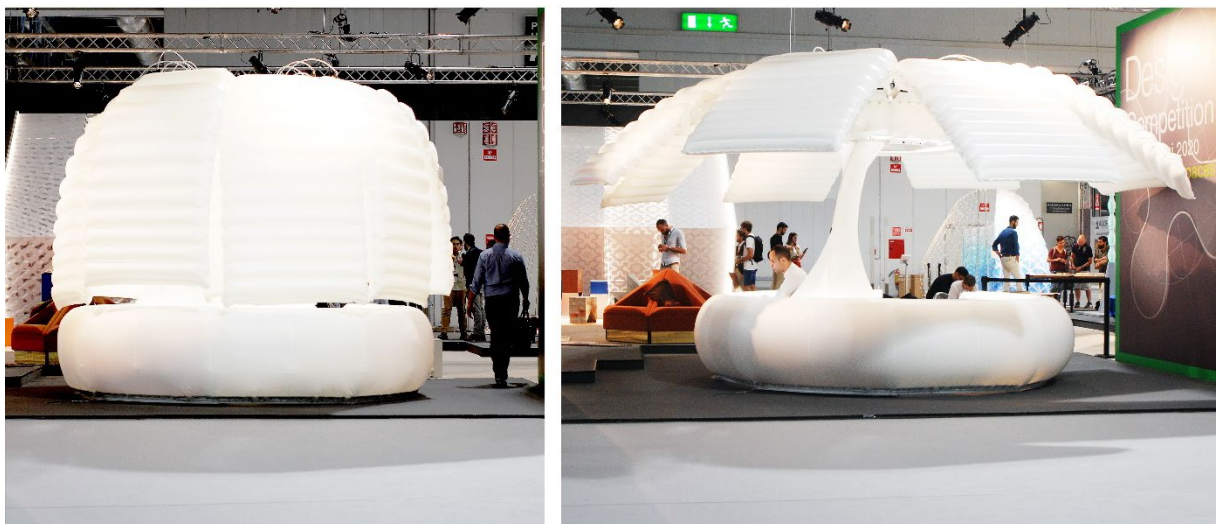


Figure 6: The 1:1 scale prototype of the corolla co-working pod in closed and open configuration.

4. Conclusion

This innovative prototype offered the opportunity to investigate the potential of the use of automation in architecture and provided a better understanding of cost-effective pneumatic actuators made of coated fabrics. Such lightweight kinetic systems that use no rigid parts and are activated by air alone are demonstrated to be feasible by this project on a larger scale than previously attempted. By exploiting the flexible, shape-shifting attributes of soft-robotic actuators it was possible to obtain highly versatile envelope systems that can accommodate different needs or conditions, such as the shift from an open cover to an enclosed space in Corolla. This ability together with weather sensors provides the opportunity to fully automate this adaptive process in an effective and resource-efficient way, much like a living organism.



Figure 7: The corolla co-working pod.

Acknowledgements

The construction of the prototype was made possible by the support provided by Regione Lombardia and Camera di Commercio di Milano Monza Brianza Lodi in collaboration with Politecnico di Milano with the prize for the winning entry of the competition “Design Competition Expo Dubai 2020”, “Connecting Spaces” theme.

References

<http://albaghuba.com/>, 2023.

<https://www.designboom.com/architecture/studio-albaghuba-corolla-responsive-coworking-pod-11-21-2020/>, 2023.

Membrane architecture: the seventh established building material. Designing reliable and sustainable structures for the urban environment.

-
- Andresen K, Gronau N (2005), An approach to increase adaptability in ERP systems. In *Managing modern organizations with information technology: proceedings of the 2005 Information Resources Management Association international conference*, San Diego, Idea Group Publishing, Hershey (pp. 15-16).
- Trivedi D, Rahn C, Kier W (2008), Soft robotics: Biological inspiration, state of the art, and future research, *Applied Bionics and Biomechanics*, 5(3), 99-117.
- Whitesides G, Shepherda R, Ilievskia F, Choia W, Morina S, Stokesa A, Mazzoa A, Chena X, Wang M (2011), Multigait soft robot, Department of Chemistry and Chemical Biology, Harvard University.
- Zuk, W., & Clark, R. H. (1970), *Kinetic architecture*. Van Nostrand Reinhold.
- Salter C (2011), *Entangled: Technology and the Transformation of Performance*, MIT Press, pp. 81–112.
- Graham S, Marvin S (1996), *Telecommunications and the City. Electronic Spaces, Urban Places*. London, Routledge.
- Senagala, M. (2005), Kinetic, Responsive and Adaptive: A Complex-Adaptive Approach to Smart Architecture. In *Presented and Published in the Proceedings of SIGRADI 2005 International Conference, Lima, Peru*.
- Aramburo J, Trevino A (2008), *Advancements in Robotics, Automation and Control*, InTech.
- Mitchell W (2000), *E-topia*, MIT Press.
- Johnson B, Fox A, Winograd, T (2002) Inventing wellness systems for aging in place, *IEEE Pervasive Computing*, vol. 1, no. 2, pp. 67–74
- Siciliano B, Khatib O (2008), *Springer Handbook of Robotics*, Chapter 55: Robots for Education, pp. 1283–1301.
- Falco I, Cianchetti M, Menciassi A (2014), A Soft and Controllable Stiffness Manipulator for Minimally Invasive Surgery: Preliminary characterization of the modular design, *IEEE Engineering in Medicine and Biology Society*.
- Muth J, Vogt D, Truby R, Menguc Y, Kolesky D (2014), Embedded 3D Printing of Strain Sensors within Highly Stretchable Elastomers, *Advanced Materials*, Volume 26, Issue 36, September 24, 2014, Pages 6307–6312.
- Sanan, S. (2013), *Soft inflatable robots for safe physical human interaction* (Doctoral dissertation, Carnegie Mellon University).



tensinantes2023 : TensiNet Symposium 2023 at Nantes Université

Membrane architecture: the seventh established building material.
Designing reliable and sustainable structures for the urban environment.

Proceedings of the Tensinet Symposium 2023

TENSINANTES2023 | 7-9 June 2023, Nantes Université, Nantes, France

Jean-Christophe Thomas, Marijke Mollaert, Carol Monticelli, Bernd Stimpfle (Eds.)

The Wave Pavilion from 2014 to 2023: origins, realization and reuse

Mathieu LEMUNIER*, Rogier Houtman

*HIGH POINT, 6, rue de la Désirée – 1700 LA ROCHELLE - FRANCE

m.lemunier@highpoint-structures.com

^a TENTECH BV Rotsoord 9A - NL-3523 CL UTRECHT – THE NETHERLANDS

Rogier@tentech.nl

Abstract

In 2014-2015, on behalf of BNP, High Point developed and realized an iconic nomadic structure designed by Sylvain Dubuisson named Wave pavilion. In 2023, High Point plans to reinstall this pavilion at La Rochelle to welcome its new company offices. High Point offices would be then looking like a totem of the tensioned membrane construction field. Furthermore, reuse of that already built structure will allow raw materials extreme minimization. Thus that project should be considered in the context of a strong environmental approach with a negative carbon footprint.

Keywords: Exhibition pavilion, hybrid roof, Tensairity ring, tensioned membrane, environmental optimization, iconic design, inflatable roof

1. High Point: short presentation of the company

High Point is a company specialized in lightweight structures and flexible solutions. It is based in La Rochelle – France and was created in 2011 by Mathieu Lemunier. Today High Point is managed by Mathieu Lemunier and Jonas Franken Roche. Since 2020, High Point together with Tentech are involved into the 60 tons large capacity Airship project Flying Whales. Flying Whales' rigid airships are 200 meters long and 50 meters high. High Point and Tentech, as technical partners of that project, are developing the tensioned envelope panels work package.

Membrane architecture: the seventh established building material. Designing reliable and sustainable structures for the urban environment.



Figure 1: Flying Whales Airship, High Point and Tentech engineer the envelope panels - picture: @FlyingWhales

2. Wave pavilion

2.1. Conception and adaptations

At first approach, Sylvain Dubuisson had imagined a circular roof completely inflatable, with an evolving thickness volume, and a relatively flat top surface. However, our conclusions after a first look on the roof project were that the intended inflatable roof could only be done 100% inflatable by linking top and bottom membranes together to keep a relatively flat section. This could be done by use of cables acting like inner tufting, or internal partitioning done by membrane pieces. But both those solutions had some esthetic drawbacks, and anyway the too flat section remained an issue.

To address this project, High Point proposed a hybrid technical solution mixing inflatable structure and elements under tension:

- an inflatable ring of 22 meters in diameter, whose section would have an evolving section from 1.2 meters to 2.4 meters, working under the Tensairity concept,
- a translucent double curved tensioned membrane tensioned inside the ring,
- a high point elevating the center of the tensioned membrane, created by an inflatable sphere of 4.5 meters in diameter.

At first, High Point contracted the roof part of the project. The supported structure was planned to be made in work in a progress look, by rental aluminum truss structures. But regarding close interactions in between the inflatable elements, especially the outer ring, and the supporting structure, decision had been taken to make High Point designing and producing almost the whole pavilion, including supporting steel structure and structural plating. The design process had been made in close collaboration with Sylvain Dubuisson.

Membrane architecture: the seventh established building material. Designing reliable and sustainable structures for the urban environment.

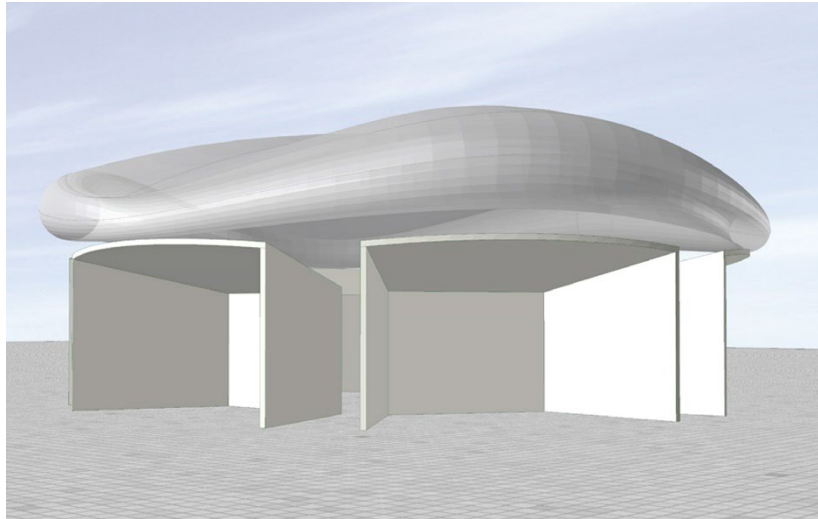


Figure 2: Initial 3D drawing by Agence Sylvain Dubuisson

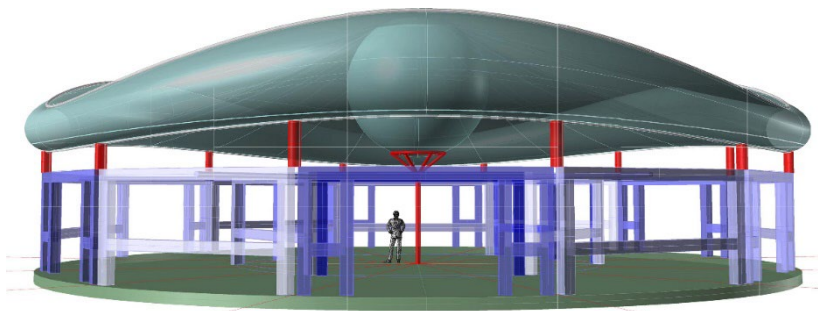


Figure 3: 3D Visualization of the hybrid inflatable / tensioned roof by Tentech

2.2. Engineering

Tentech took over the complete engineering of the Wave Pavilion. Beginning the engineering process, the design was rationalized using Rhino's Grasshopper and slightly twitched to create a more stable and feasible shape. The initially arbitrary shape became a clearly defined geometry described with few parameters. During the further process, the Grasshopper model could be altered to create structural data, patterning data and workshop drawings.

Membrane architecture: the seventh established building material. Designing reliable and sustainable structures for the urban environment.



Figure 4: Interior Wave Pavilion

The structure of the roof works as a tensile compression ring; the torus works as the compression ring for the membrane. Tensairity appeared convenient to increase the buckling resistance of the torus.

Tensairity is a term noted by Pedretti and Luchsinger (Luchsinger et al 2004). The term is a combination of tension, air and integrity and reflects the relationship with tensegrity. It's a method to create inflated structural elements, with a relatively low air pressure. A tensairity beam can be considered an underslung cable beam. In an underslung cable beam the horizontal tension and compression elements are separated and pushed apart by vertical pressure elements. In Tensairity, the vertical pressure elements are replaced by air pressure. The horizontal tension and compression elements are maintained. In 2009 Wever and Luchsinger demonstrated the lower horizontal tension element, the underslung cable, could be replaced with a mesh fabric and demonstrated the increased buckling resistance of the concept.

The structural system works as a tensile compression ring. The donuts spread the roof membrane and the central sphere's pressure controls its tension. Both donuts and sphere are supported by columns.

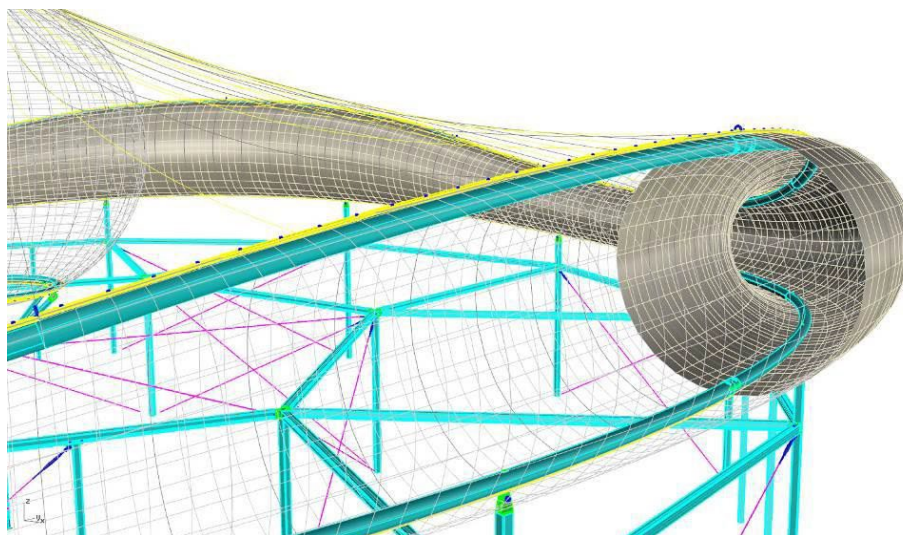


Figure 5: Cross Section inflated tube

Membrane architecture: the seventh established building material. Designing reliable and sustainable structures for the urban environment.

The compression ring is built from the three Tensairity elements, a pressure element in the top, the fabric web and air pressure. The roof membrane is attached to the top of the torus, the horizontal force in this point is transferred to a steel pressure ring which in its turn is stabilized by the pressurized air beam, increasing the buckling resistance of the complete beam.

Inside the air beam, a second steel beam is placed in the bottom. This beam does not have the function to increase the torus' capacity, but to distribute the point loads of twelve supporting columns. The two steel beams are also starting-points during the assembly of the structure. The torus is built from two separate membranes, the inside and outside, and are joined along the upper and lower steel beam. The air tightness is achieved by stacking rubber and PE strips, bolted together.

The statical analysis is performed with the program EASYBEAM combined with the closed volume module EASYVOL (Technet GmbH, Berlin). To analyze the full behaviour of the structure, both the supporting structure and the torus-roof structure were modelled.

To prevent bending moments in the supporting structure caused by the horizontal stabilizing forces, it is chosen to use wind bracings. It was relatively easy to mask the wind bracings within the carpentry sidewalls. Figure 3 shows in blue all the compression elements; in red the wind bracings and supporting cables for the central column are shown.

The central column also functions as an axis. The tension cables attached to the central column can be seen as spokes that transfer by tension the horizontal forces from the one side of the structure to the other side. By doing this, the forces are equally spread over the whole structure. Moreover, it stabilizes the central column in case of emergency.

An equal distribution of the forces inside the structure was necessary because of the way the foundation was made. Since it has to be a demountable and relocatable pavilion, the foundation and floor system is based on weight. The floor itself is build up out of steel profiles and at specific spots, concrete plates (Stelcon plates) of 2 x 2m are inserted in the floor system. They are even shown to the audience since the architect wanted to express a certain 'under construction' atmosphere. And because it is possible to obtain Stelcon plates (or similar) all over the world, it is not necessary to transport the Stelcon plates, but they can be purchased on site.

Proceedings of the Tensinet Symposium 2023

TENSINANTES2023 | 7-9 June 2023, Nantes Université, Nantes, France

Jean-Christophe Thomas, Marijke Mollaert, Carol Monticelli, Bernd Stimpfle (Eds.)

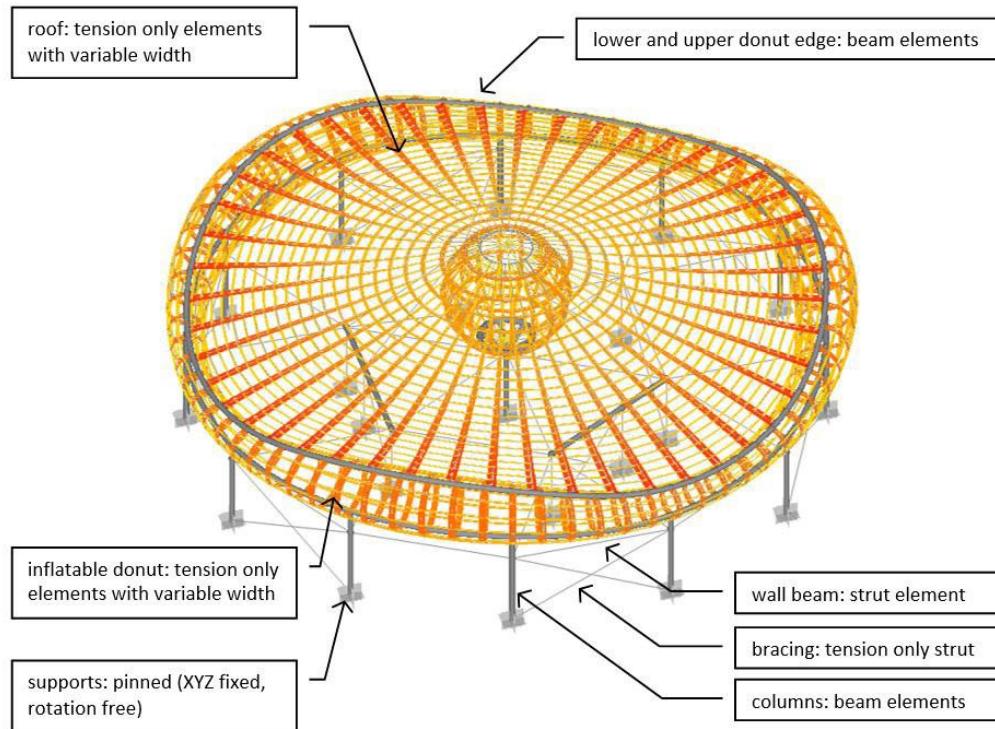


Figure 6: Overview of structure

2.3. Fabrication

Fabrication had been done by Buitink Technology, in their production facility located in Duiven – The Netherlands. A special attention had been paid on the inflatable outer ring membrane treatment: a silver varnish had been applied on the two layers 1002 Preconstraint of Serge Ferrari.

To demonstrate technical constraints and varnished look of the ring, Buitink built a one-to-one mockup of a section part of the ring.

After validation of the design and details, Buitink produced the membrane elements, in high technicity level:

- outer Tensairity inflatable ring in two layers Preconstraint 1002 of Serge Ferrari, with silver varnish treatment
- Tensioned covering membrane in Ferrari 402 extra translucid
- 4,5 meters inflatable sphere in two layers Preconstraint 1002 of Serge Ferrari, with silver varnish treatment

The steel elements, in galvanized steel, built in the work in progress look wished by Sylvain Dubuisson, and the structural floor, mosaic of wood and concrete slabs, had been outsourced to third parties.

Membrane architecture: the seventh established building material. Designing reliable and sustainable structures for the urban environment.



Figure 7: 1:1 mockup of a section part of the Tensairity outer ring

2.4 Installation

2.4.1. Mock installation in the Netherlands

Before the first installation, since the time frame for onsite installation was very tight, a mock installation had been done in the Netherlands. This allowed a final tune up and installation team training. Sylvain Dubuisson, who came in the Netherlands to judge the result, came back in France quite happy of his visit.

2.4.2. On site installation in Paris La Villette

The installation took place in July 2015 on the forecourt of la Cité des Sciences de la Villette. Installation of the roof, the structural floor, the supporting steel structure and the complete roof had been done in a week.

Membrane architecture: the seventh established building material. Designing reliable and sustainable structures for the urban environment.



Figure 8: installation of Wave Pavilion structural floor & roof lifted by a crane for supporting structure installation

Membrane architecture: the seventh established building material. Designing reliable and sustainable structures for the urban environment.

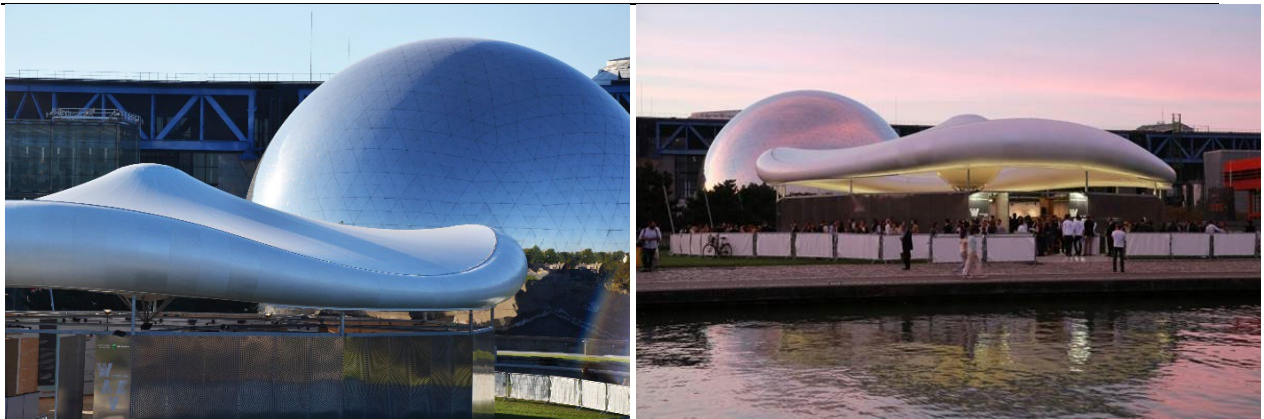


Figure 9 : Wave Pavilion installed at La Villette in 2015

3. 2023: a new life for the Wave Pavilion?

3.1 High Point does not want to send the pavilion to trash and buys back from BNP

After the installation at la Cité des Sciences de la Villette, High Point, and the cancellation of the worldwide tour, High Point, judging the pavilion to be of high architectural value, bought the Wave Pavilion back from BNP. Afterwards, High Point proposed the Wave Pavilion to several costumers to welcome exhibitions or to make temporary restaurants. Even though 3 projects went quite far, none of them came into being and the Wave Pavilion remained un-re-installed. She is still stored in High Point's warehouse, patiently waiting.

3.2 Project of the Wave pavilion for High Point's offices

But in 2023, High Point plans to relocate the Wave Pavilion to the suburbs of La Rochelle in the town of Perigny, and by adapting her, to install its offices inside. In addition to the totem that the Wave Pavilion represents for High Point's business, the reuse of this pavilion for office purposes will allow raw materials extreme minimization, a challenge for our business in the field of lightweight structures and is thus part of a strong environmental approach with a negative carbon footprint. A permit to build had been accepted in 2022, and construction is planned for summer 2023.



Figure 10: 2022 High Point offices permit de build extract

Membrane architecture: the seventh established building material. Designing reliable and sustainable structures for the urban environment.

The new look of the Wave Pavilion intends to be an overview of building tensioned membranes techniques. In addition to the existing inflated elements and covering membrane, the pavilion is planned to be dressed in a mesh textile façade. Below the Tensairity ring, to keep transparency in between the roof and the façade, a transparent single layer of ETFE foil will be installed.

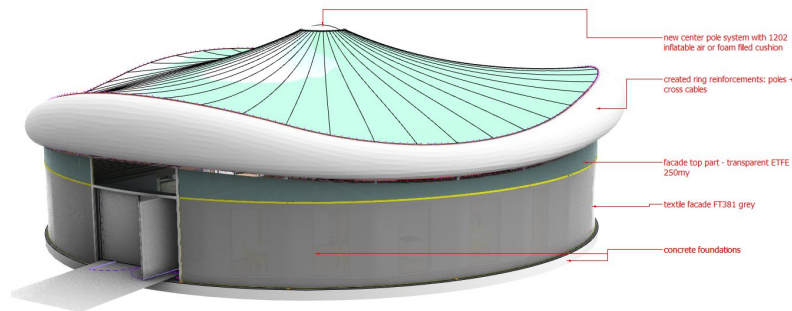


Figure 11: new arrangements of the Wave Pavilion

Inside, offices turning around a central courtyard will be made of wooden structures illuminated by large windows and covered with Stamisol fabric.

4. Conclusion

Tensioned fabric universe is fascinating for some of us. We work in that field not mainly driven by money, but by passion for design and challenges. About the Wave Pavilion, it's too much of a heartbreak to see that such a piece of art could only live for one month, too much of heartbreak to drive her to waste collection site.

However, will this High Point offices building project come to an end? Recent developments of High Point activities are questioning ourselves of the validity of that project. Indeed, our site ground is not that large, and the Wave Pavilion is going to take a lot of it. There is now a strong chance that the Wave Pavilion remained stored for some more years, waiting a new lover to drive her back to life.

References

- Luchsinger et al (2004) "The new structural concept Tensairity: Basic principles", *IASS Proceedings 2004*.
- Van Wijk, J., Houtman, R., (2014). 1400301_RA1_V01_HP_Inno-wav-tion, internal report Tentech BV.



tensinantes2023 : TensiNet Symposium 2023 at Nantes Université

Membrane architecture: the seventh established building material. Designing reliable and sustainable structures for the urban environment.

Proceedings of the Tensinet Symposium 2023

TENSINANTES2023 | 7-9 June 2023, Nantes Université, Nantes, France

Jean-Christophe Thomas, Marijke Mollaert, Carol Monticelli, Bernd Stimpfle (Eds.)

TensyDome : A pavilion combining tensegrity ring and tensile architecture

Nicolas PAULI*

*LIFAM – Laboratoire Innovation Formes Architecture Milieux

School of Architecture of Montpellier (ENSAM), 179 rue de l'Esperou, F-34093 Montpellier Cedex 5, France

nicolas.pauli@montpellier.archi.fr

Abstract

The paper concerns the project of a pavilion called TensyDome of 70 sqm erected in the Villa Cedri garden in Bellinzona (CH) in September 2016. The originality of TensyDome is to combine two expressions of pre-stressed structures: a tensegrity ring for the structural frame and an anticlastic tensile membrane for the envelope. A high attention on details and a structural optimisation underline the “lightweight structure” effect.

The paper describes the keys of the architectural design, the form finding process of (1) the tensegrity structure using dynamic relaxation, and (2) the membrane using force density method, behavior analysis under climatic loads of the global structure (tensegrity and membrane together) using a non-linear finite element method with full Newton Raphson algorithm, the detailing of the nodes and the erection process.

Keywords: tensegrity, tensile membrane, combined tensile structures, tensydome, bending free connection node

1. Introduction

The research for new structural and formal solutions often involves interdisciplinary collaboration. In the case of the design of this project, the architect Filippo Broggin mobilized 2 structural specialists: (1) the laboratory of computer science and mechanics applied to construction (IMAC) of EPFL which developed with prof. Ian Smith, dr.ing. Landolf Rhode-Barbarigos and dr.ing. Nicolas Veuve specific researches on tensegrity systems, and (2) the Laboratory Innovation Formes Architecture Medium (LIFAM) of ENSA Montpellier, one of whose research themes concerns textile architecture.

These cross-scientific skills (topological optimization, form finding, static calculation, etc.) allowed the architect to evaluate the formal and static aspects in "real time" and thus quickly orient the design towards optimal solutions.

Membrane architecture: the seventh established building material. Designing reliable and sustainable structures for the urban environment.

The Architect of the project is arch. EPFL Filippo Brogini; the tensegrity form finding was realized by dr.ing EPFL Nicolas Veuve (see §Acknowledgement). Prof. Nicolas Pauli was involved for technical support of F. Brogini for general design of the pavilion, for the engineering of the membrane envelope, for nonlinear behaviour calculations for frame and membrane, and for detailing (frame and membrane).

2. Architectural design

2.1. Programme et concept

The foundation "Amici Villa Cedri" of Bellinzona has expressed the desire to develop activities in the gardens of Villa Cedri through the construction of a temporary pavilion that can accommodate exhibitions, receptions, events, meetings, not welcomed inside the historic villa.

The pavilion had also to be able, through new architectural forms, to extend its primary function as a venue to a symbolic object in the park. The project focused on the forms generated by an innovative structural device that presents a geometric and conceptual complexity capable of generating beauty.

The idea of combining "Tensegrity system" and membrane was born from this desire (Fig. 1).

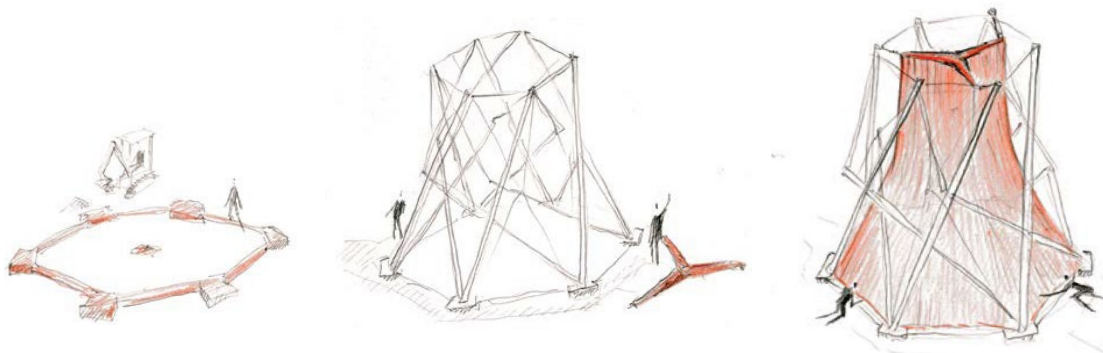


Figure 1: Concept conjugated tensegrity system and tensile membrane (Source F. Brogini)

From this solution, which involves the positioning of the membrane inside the structural frame, was born the idea of maintaining the skeleton throughout the year and positioning the membrane only when necessary and even for short periods; In fact, the membrane remains installed throughout the year.

2.2. Implantation

The exact location of the TensyDome was determined after studying 4 options that were submitted to the Commission and the competent municipal and cantonal offices, with the aim of finding an optimal solution both for the aspects related to landscape integration and for the modality of use desired by the customer.

As a result, the pavilion is installed among the trees of the park and at the back of the fountain. The structure has a splendid decoration with the presence of a bamboo grove (*Phyllostachys aurea*). This implementation made it possible to partially redesign the existing alleys and flower beds, aesthetically rethinking the composition of the existing species. (Fig. 2)

Membrane architecture: the seventh established building material. Designing reliable and sustainable structures for the urban environment.



Figure 2: Pavilion project inside its landscape (Source F. Brogini)

2.3. Formal research of the pavilion structure

Tensegrity structures are prestressed structures composed of elements exclusively loaded in compression (bars) and tension (cables). In their purist definition, the bars are disjoint and are connected only by the stretched elements. They are, by their very nature, particularly efficient and lightweight structures. (fig. 3 et fig. 4)



Figure 3: Simplex (source Wikipedia)

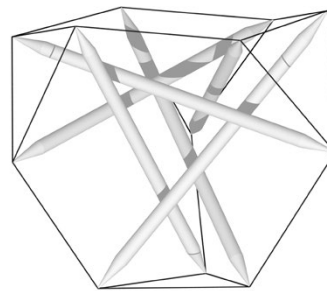


Figure 4: Tetrahedron tensegrity 3 (Source Wikipedia)

In this singular structural family, there are special configurations with continuous bars called "tensegrity ring". These are structures based on the geometry of polygonal based prisms. It is therefore possible to create ring modules with square, pentagonal, hexagonal base. By modifying this prism shape, it is possible to obtain a dome shape. We show in figure 5 a configuration with a pentagonal base and in figure 6 a decagonal base.

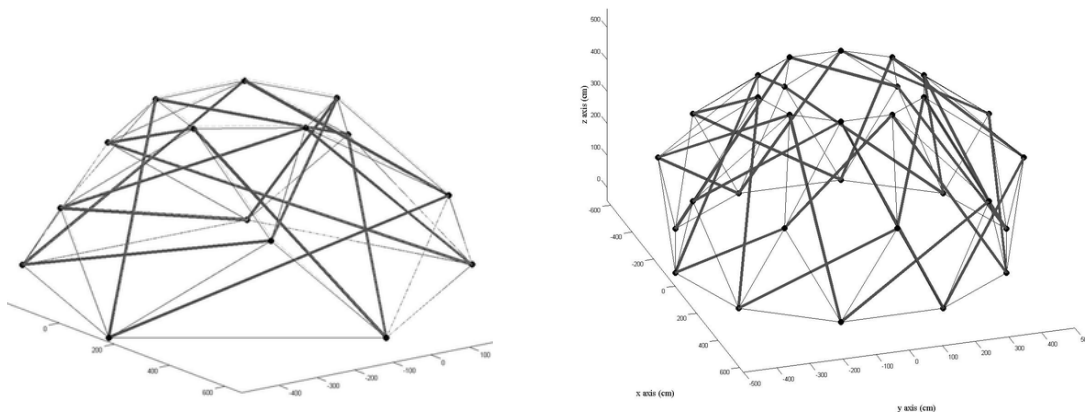


Figure 5 and 6: Tensegrity dome configurations: (a) pentagon (b) décagon (Source N. Veuve / F. Brogini)

Membrane architecture: the seventh established building material. Designing reliable and sustainable structures for the urban environment.

The first geometric analyses helped to exclude certain configurations that were less efficient and unsuitable for the use of the pavilion spaces (internal volume partially occupied by the bars). The configuration that meets the constraints of use, access and positioning of the tensioned membrane is a hexagonal base.

Once the final configuration was chosen, certain geometric parameters such as the height of the intermediate level from the upper level, the radii of the different levels and their relative angle of rotation between them were optimized. We show in figure 7 a configuration with constant intermediate height and in fig. 8 variable intermediate height. This configuration avoid bars touching each other, and the resulting shape was stable. In addition, the orientation of the bars has been adjusted to allow a sufficient height of passage for the entrance to the dome. It is the solution with 2 intermediate heights that was chosen for the project.

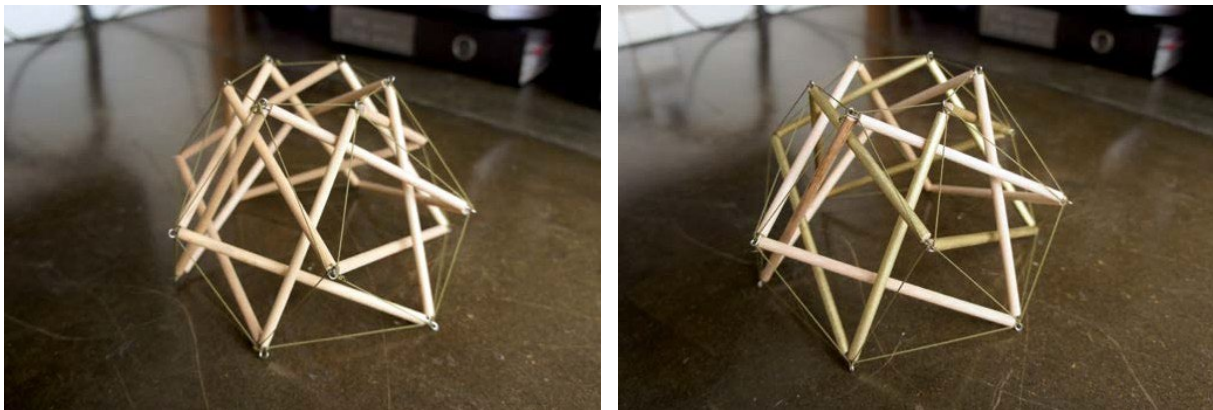


Figure 7 and 8: Hexagonal tensegrity dome: (a) one interm. height (b) two interm. heights (Source F. Brogini)

2.4. Formal optimization for tensioned membrane integration

The finalization of the tensegrity dome shape research consisted in optimizing the diameter of the upper ring in order to set up a tensile membrane that narrows upwards, so as to almost completely eliminate snow accumulation in the upper areas of the pavilion. Finally, the methods of support the upper part of the membrane and the habitability of the space conditioned also the final height of the upper ring as well as its final diameter. (Fig. 9).

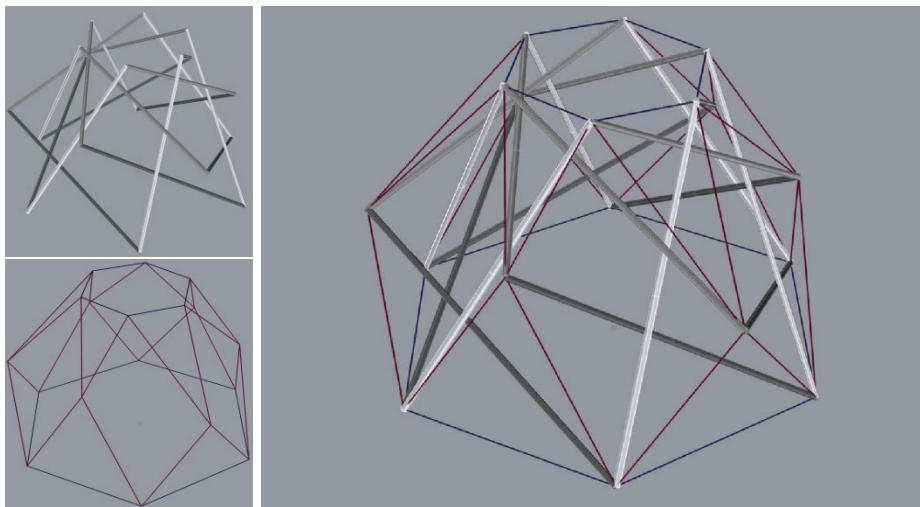


Figure 9: Final design of the tensegrity dome (Source F. Brogini)

Membrane architecture: the seventh established building material. Designing reliable and sustainable structures for the urban environment.

A formal validation by model which includes in particular the membrane and its high support structure with 3 branches is also carried out (Fig. 10)

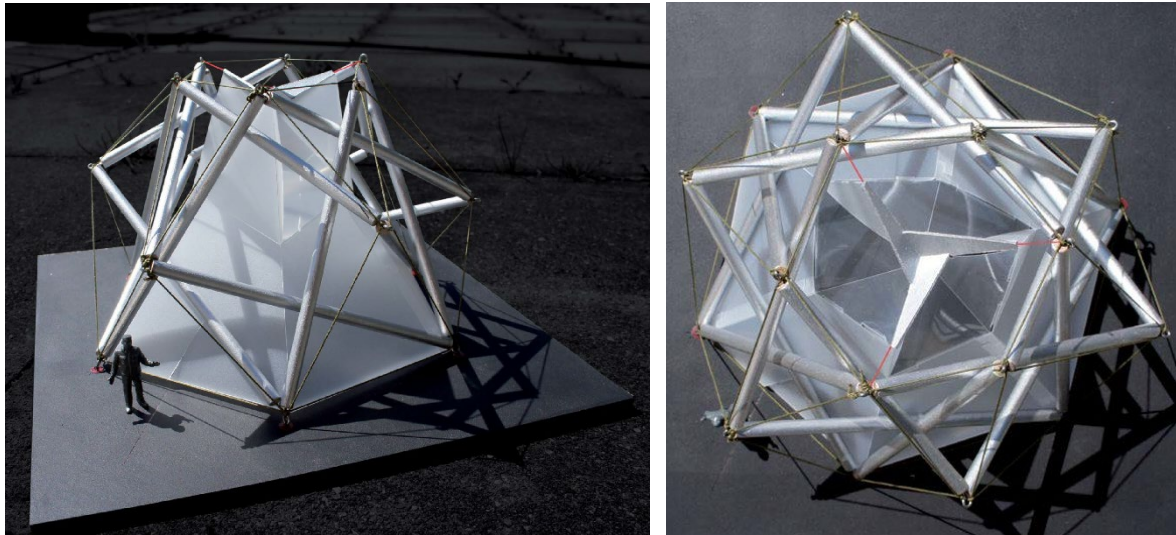


Figure 10: Final mockup of the tensegrity dome (Source F. Brogini)

3. Form finding, behaviour and final geometry

3.1. Form finding of the tensegrity ring

The form finding and justification part of the tensegrity dome was carried out by dr.ing Nicolas Veuve on the basis of his Phd thesis work (Veuve, 2016). The method of static analysis used to study the tensegrity dome is dynamic relaxation (Day, 1965) which has the advantage of simultaneously solving the question of forces and that of the form of final equilibrium.

Various geometric configurations based on prismatic geometries have been studied in order to generate a “dome” enable to house an anticlastic textile envelop with adequate stiffness and to fit with architectural constrains.

The form finding process of the tensegrity dome used optimization algorithms developed as part of the research on the behaviour of deployable tensegrity footbridge, which allow to constrain final positions of the calculated nodes to spatial positions while controlling the internal forces in the elements. In combination, a collision check was also conducted.

Finally, the 2 rows ring (8.20m height) with hexagonal base (13.00m diameter) has been selected for its geometric and static properties.

3.2. Form finding of the membrane envelop

The form finding of the membrane adopts a classical Force Density Method for the formfinding (Schek, 1974). The design of the upper frame as a large three-branch star was governed to enhance the internal volume of the pavilion. The various curvatures have been controlled to fulfil the architectural constrains, such as entrance position and height, general curvature, floor incidence. Figure 11 shows various options of positions on 3-branch upper frame during the designing phase. Figure 12 shows a work on progress (wop) caption during the openings design phase and figure 13 shows the final form designed precisely for the manufacturing phase (cutting pattern).

Membrane architecture: the seventh established building material. Designing reliable and sustainable structures for the urban environment.

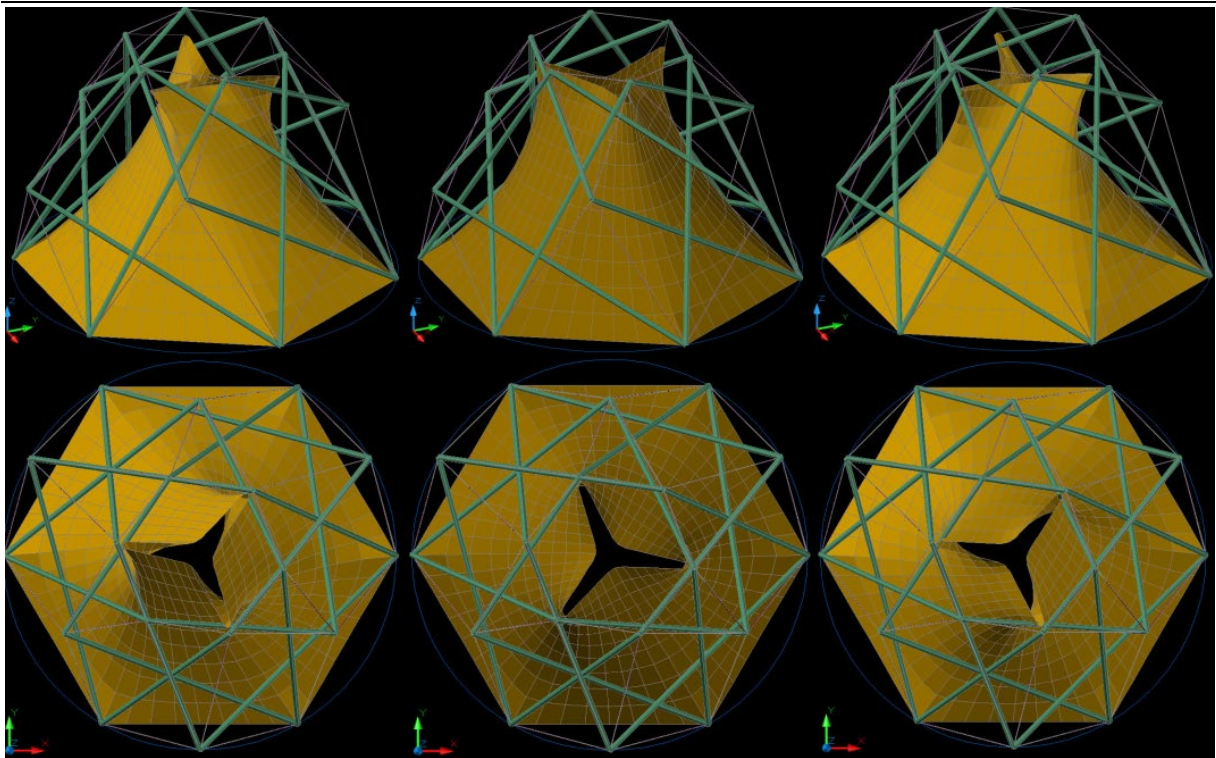


Figure 11: Formfinding options of various rotation of the 3-branch upper frame (Source N. Pauli)

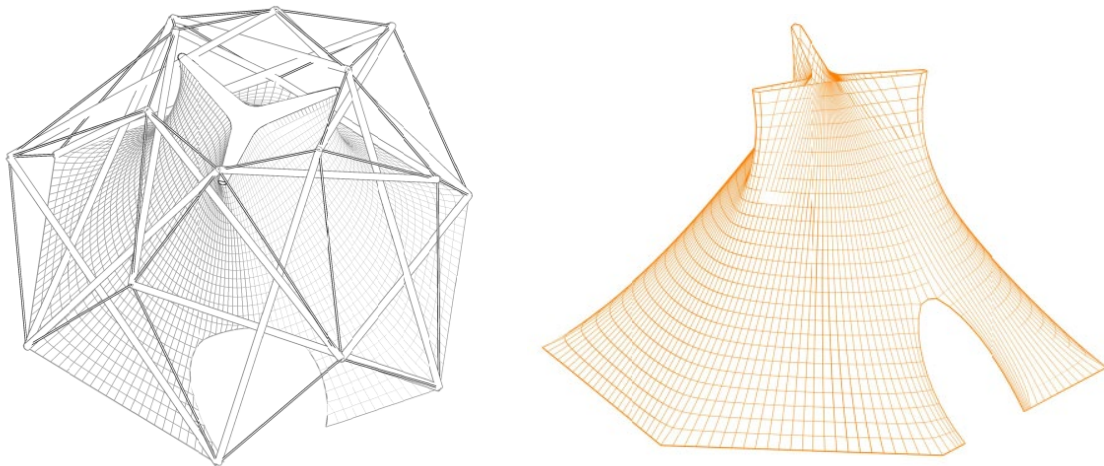


Figure 12 and 13: Formfinding of the membrane with 3-branch upper frame (a) wop (b) final (Source N. Pauli)

3.3. Behaviour under climatic loads

In order to control the whole pavilion behaviour under climatic loads, both model of frame and membrane (modelled as a cable net), has been analysed under RSA (Robot Structural Analysis from AutoDesk) using a full Newton Raphson approach. Furthermore, we demonstrate that the interest of this approach is to identify the strains of the top level of the frame under initial stress and control the final form finding of the membrane and the cutting pattern process to avoid unexpected wrinkles. Moreover the climatic and steel frames standards, additional codes on membranes are referred (Biger et al., 2009) and (Forster & Mollaert, 2004).

Membrane architecture: the seventh established building material. Designing reliable and sustainable structures for the urban environment.

The membrane used is a Ferrari 1002 translucent 3099 series. Pseudo young modulus is extract from biaxial tensile test and raised 90.000 daN/m for stress ratio 2/1. The tensile strength is given at 8.000 daN/m.

3.3.1. Membrane calculation

The principle adopted is based on the discretization of the membrane into a network of cables oriented in the main directions of the fibers of the warp and weft material. The model we establish is purely surface since the resistance of the textile depends only on the Polyester weave included and not on the thickness of PVC coating. Thus, the physical characteristics retained for the cable elements are extrapolated from those of the membrane and related to a fictitious unit thickness: • the cross-section of each cable corresponds to the average width of canvas it represents with a fictitious thickness equal to unity, • the density is the surface mass of the canvas for a fictitious thickness equal to unity, • the modulus of elasticity in both warp and weft directions (resp. E_c and E_t) are expressed in daN/m and by fictitious thickness equal to unity, • the stresses represent the tensions per unit length (width!) for a fictitious thickness equal to unity. In short, the material "canvas" introduced in the RSA program must therefore be read knowing that the dimension "thickness" is eliminated from the calculations.

We have developed for this step special software that allows to calculate at each point (1) the intensity of the loads due to the snow taking into account the horizontal surface associated with each node and the corresponding weighting coefficients or (2) the intensity of the force due to the wind taking into account the membrane surface associated with each node, the facet normal and the corresponding weights. Figure 14 and figure 15 shows resp. wind loads applied on membrane and membrane deflection under wind load.

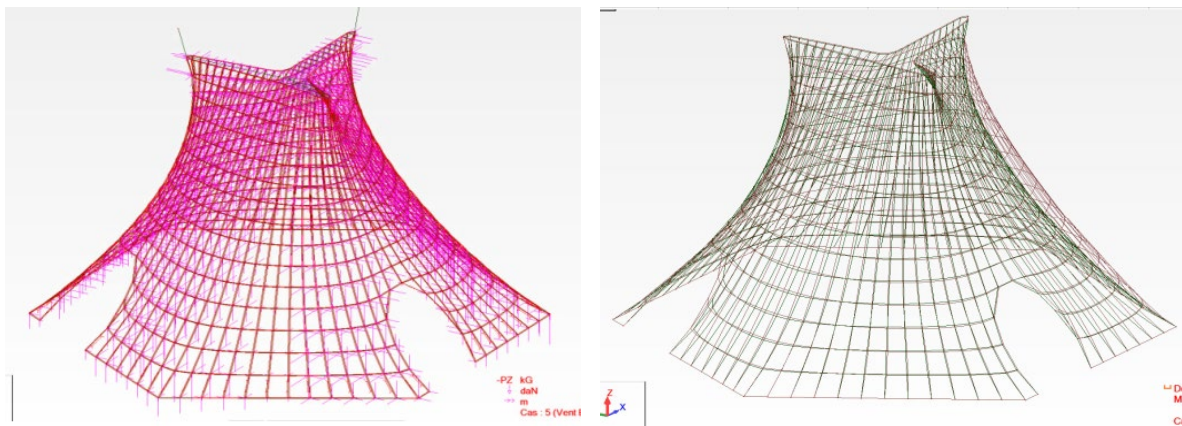


Figure 14 and 15: Wind loads applied on membrane and membrane deflection under wind load (Source N. Pauli)

The stress fields in the membrane under prestress, snow and wind loads are determined. The work rate gives the security ratio, always greater than 4.5 (thanks to the 12m long length of membrane connection upon the 3-branch upper frame).

The loads on support are extracted to dimension ground fittings or main tensegrity frame.

The deflection fields under climatic loads give the angle variation of the membrane on its connexion on ground. The figure 16 shows the initial incidence with the angular variation which have to be taken into account in the design of ground fittings.

Membrane architecture: the seventh established building material. Designing reliable and sustainable structures for the urban environment.

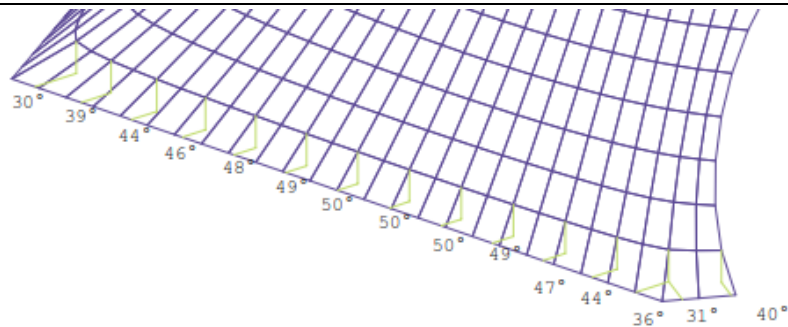


Figure 16: Initial incidence with angular variation under climatic loads on the ground connection (Source N. Pauli)

3.3.2. Tensegrity dome calculation

The Tensegrity dome is basically computed using the same full NR algorithm of RSA, taking into account the initial prestress and the nonlinear behaviour. The loads are given by the membrane calculations. Figure 17 shows tensegrity dome implemented under RSA.

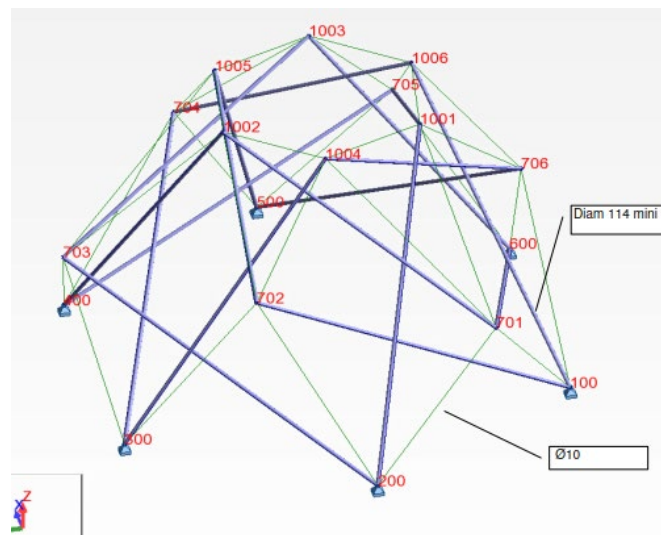


Figure 17: Tensegrity dome implemented under RSA (Source N. Pauli)

The internal forces in struts and cable lead to dimensioning (1) cable to diam 8mm type 16x19 stainless steel and (2) struts to diam 152.4 mm, th. 4,5 mm S 355 steel.

3.4. Final geometry and dimensions

The hexagonal ground geometry consists of sides of 6.50 m. The total diameter on the ground is 13.0m and the diameter of the summit is 5.90m. The total height is 8.20 m and the top of the tensile roof is 7.00 m (height of the PRS profile). The intermediate heights are 3.90 m (diam 13.00 m) and 4.90 m (diam 10.40 m). The floor area, calculated inside the membrane is 78 m², while that calculated at a height of 1.50 m is 45 m². The gauge is 50/60 people. The pavilion has three access exits arranged alternately on the base hexagon and connected directly to the park's footbridges.

Membrane architecture: the seventh established building material. Designing reliable and sustainable structures for the urban environment.

4. Detailing and manufacturing

4.1. Nodes

The structure has a rigid behaviour for a relatively light structure (about 2.5 tons without the foundations). This makes it possible to design simplified joints. Under the effect of horizontal forces due to wind (asymmetrical loading of the structure), the variation in angle of the joint between the bars remains less than 1/10 of a degree. This rotation therefore induces very limited bending forces in the bars. Thus it is not necessary that the joint constitutes a real ball joint between the two bars.

A careful work on the design of the node has been realised in order to avoid the usual roughness of connection between cables and members that tensegrity systems often impose. A compact proposal of the current node has been developed and hides the connection of the cable inside the node using a crimped nut on the continuous cable. A milled mock-up in polyamide has been realised at scale 1:1 (Figs 18 and 19);

This special joint comes in a steel crown that accommodates the structural tubes by welding using a conical reduction. Figure 20 shows the modelling of the milled aluminium knot in its steel crown; Figure 21 shows the realization in the workshop.

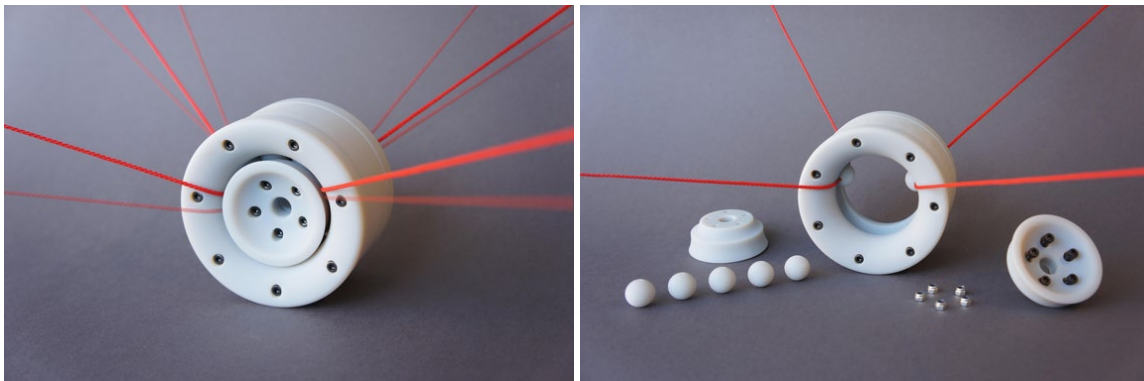


Figure 18 and 19: Polyamide milled mock-up of the node (Source F. Brogini)



Figure 20 and 21: Simulation of the milled aluminium node and its realisation in workshop (Source F. Brogini)

4.2. Foundations and degree of freedom of membrane fitted to the ground

The foundations consist of six reinforced concrete bases connected by a hexagonal peripheral crown. This crown will ensure the lower fixation of the membrane and the drainage of

Membrane architecture: the seventh established building material. Designing reliable and sustainable structures for the urban environment.

rainwater. The foundations are partially buried. Only the pedestals and part of the crown protrude from the ground, but only about 10 cm. A milled stainless steel support screw device allowing rotations is designed to adapt in any circumstance to the initial geometry and movements under load. The rods are adjustable in length to allow the tension of the membrane easily from level 0.00. (Figs 22 and 23)

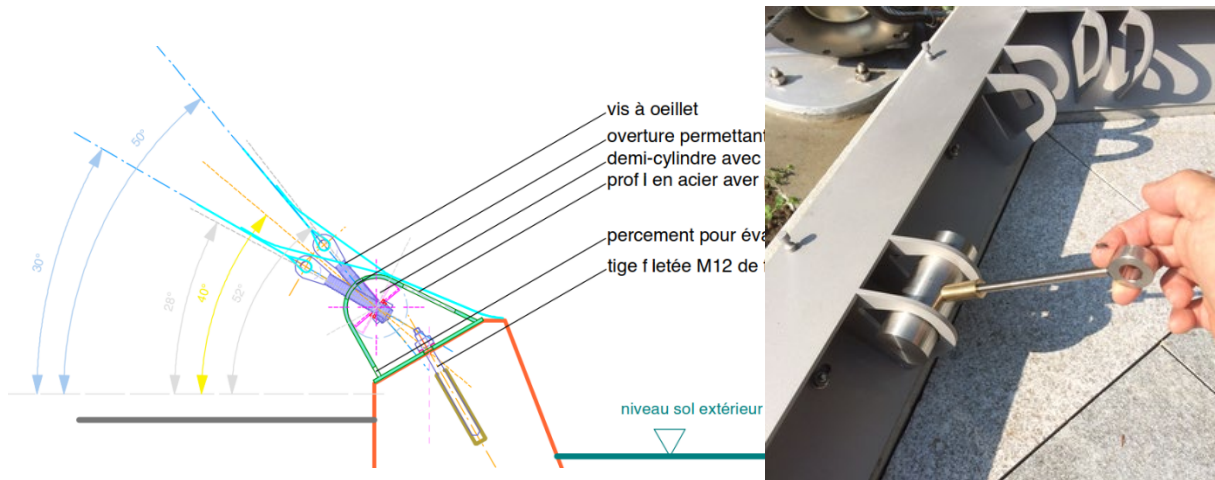


Figure 22 and 23: Cross section of angle free fitting connection and its realisation on site (Source F. Broggin)

4.3. Three Branch upper frame

The upper frame supporting the membrane is realised with a welded girder box (fig. 24). according to the stress calculated, the flange are 6mm thick and the web is 10mm thick. Its height varies from 200 to 300mm and its width from 200 to 510mm. Various suspension eyelet are placed for the installation in position. In order to have as long length of connection with the membrane as possible, a three branch form is given. Here the connection length is more than 12m; as a consequence, no membrane reinforcement are needed in the connection zone (fig. 25).

A specific arrangement is realized for the natural venting of the inner space. 6 ducts of 100mm diameter are placed at the 3 ends of the branches (fig. 26) connected to fish gill like holes on the web of the girder.

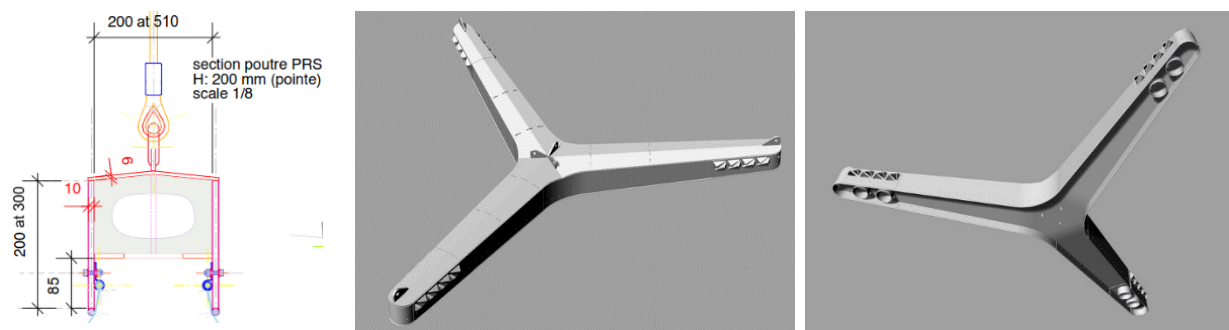


Figure 24, 25 and 26: Cross section + 3D views of the 3branches frame with venting device (seen from bellow) (Source F. Broggin)

The connection of the membrane is realised through the clamping of a aluminium keder profile (fig.27). A specific keder profile is milled for the ends of the branches, because of the high curvature of the zone.

Membrane architecture: the seventh established building material. Designing reliable and sustainable structures for the urban environment.

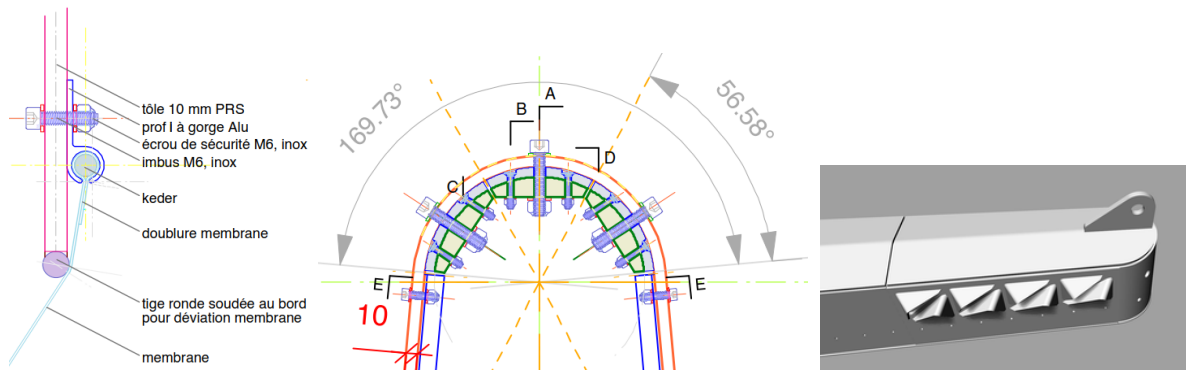


Figure 27, 28 and 29: Standard keder profile + specific milled keder + Fish gill like venting holes (Source F. Brogini)

4.4. Cutting pattern

The cutting pattern process for workshop manufacturing adopts a simple triangulation projection approach with small width panels. An initial compensation is given to anticipate the long term creep of the membrane. Thus, a decompensation is also adopted for the keder zone on the 3 Branches upper frame or on the adjustable fittings in the lower part.

5. Erection process and delivery



Figure 30, 31, 32 and 33: Erection process and final delivered pavilion (Source F. Brogini)

The erection process has been imagined to allow easy handling of various parts of the pavilion. A wooden internal formwork helped for the main frame installation. The membrane was lifted using a small crane. The upper cables suspending the 3 branches frame are constant length. The tension is applied exclusively by the fitting device on the ground. (Figs 30 to 33).

Membrane architecture: the seventh established building material. Designing reliable and sustainable structures for the urban environment.

8. Conclusion

The realization of this pavilion was an opportunity to confront current research on tensegrity with the reality of everyday building. On the other hand, if the membrane engineering was more "classic", it had to be particularly done with high degree of attention. This project allowed to develop an original "bending-free" tensegrity system knot for the connection between bars and cables.

Even if the design team had to work with a lot of seriousness and precision to achieve the beautiful result delivered, this experience proves that university collaborations applied through a contemporary architectural object, can enrich all communities of knowledge and skills.

Acknowledgements

This paper presents the TensyDome project and exploits the discussions with designer Filippo Brogginini* and Tensegrity engineer Nicolas Veuve**

* Arch EPFL Filippo Brogginini is director of Blue Office Architecture, Piazza Governo 3, CH-6500 Bellinzona, Switzerland (e-mail: blueoffice.brogginini@bluewin.ch).

** Nicolas Veuve is project engineer at Emch+Berger SA Lausanne and was formerly in 2016 PhD student under supervision of Prof. Ian Smith in Applied Computing and Mechanics Laboratory (IMAC), School of Architecture, Civil and Environmental Engineering (ENAC), Ecole Polytechnique Fédérale de Lausanne (EPFL) (e-mail: nicolas.veuve@emchberger.ch)

References

- Biger, J. P., Bariteau, P., & Collectifs. (2009). *Recommandations pour la conception, la confection et la mise en oeuvre des ouvrages permanents de couverture textile*. SEBTP.
- Day, A. S. (1965). An introduction to dynamic relaxation. *The Engineer*, 219, 218-221.
- Forster, B., & Mollaert, M. (2004). *European design guide for tensile surface structures*. Tensinet.
- Schek, H.-J. (1974). The force density method for form finding and computation of general networks. *Computer Methods in Applied Mechanics and Engineering*, 3(1), 115-134. [https://doi.org/10.1016/0045-7825\(74\)90045-0](https://doi.org/10.1016/0045-7825(74)90045-0)
- Veuve, N. W. (2016). *Towards biomimetic behavior of an active deployable tensegrity structure* [EPFL]. <https://doi.org/10.5075/epfl-thesis-6866>

Photographic credits

Fig 3: https://commons.wikimedia.org/wiki/File:Tensegrity_3-Prism.png

Fig 4: https://commons.wikimedia.org/wiki/File:Tensegrity_Tetrahedron.png



tensinantes2023 : TensiNet Symposium 2023 at Nantes Université

Membrane architecture: the seventh established building material. Designing reliable and sustainable structures for the urban environment.

Proceedings of the Tensinet Symposium 2023

TENSINANTES2023 | 7-9 June 2023, Nantes Université, Nantes, France

Jean-Christophe Thomas, Marijke Mollaert, Carol Monticelli, Bernd Stimpfle (Eds.)

Beyond bending: tension. Membrane structures 1

Josep Ignasi de LLORENS DURAN

School of Architecture, Barcelona - Universitat Politècnica de Catalunya

Diagonal, 649 - 08028 Barcelona - Spain

URL: <https://futur.upc.edu/JosepIgnasideLlorensDuran> - E-mail: ignasi.llorens@upc.edu

Abstract

It is well known that funicular structures are more efficient because they resort to geometry as well as material capacity. To obtain funicular structures, the load paths may be followed under compression penalized by buckling [Ph.Block et al. 2017] or tension that exploits the full strength of the cross section [O.Popovic & A.Tyas, 2003]. That is why membrane structures are considered more efficient. Nevertheless, their design makes little use of this advantage when it resorts to supporting structures subjected to bending, as too often happens to the point that membrane structures frequently end up being covered conventional steel structures. A comparative case study has been developed to evaluate the impact of different primary structures on the efficiency. Starting from rigid frames, trusses, trussed arches, arches on branched masts, ETFE cushions, cable beams and flying masts have been examined, so that the transition from bending members to predominantly axial force members under tension or compression has been measured by several indicators including weight, surface ratio, wind load exposure, internal force and deformation. Also, different types of masts (with hollow sections, trussed, tapered, subdivided, branched, coupled, clustered, flying and tied) have also been included. In addition, warnings, tips and hints illustrated with selected examples drawn from the own experience and the documentation kindly provided by the authors, including visits to the sites and literature, are presented to improve this situation, together with recommendations for commonly accepted solutions.

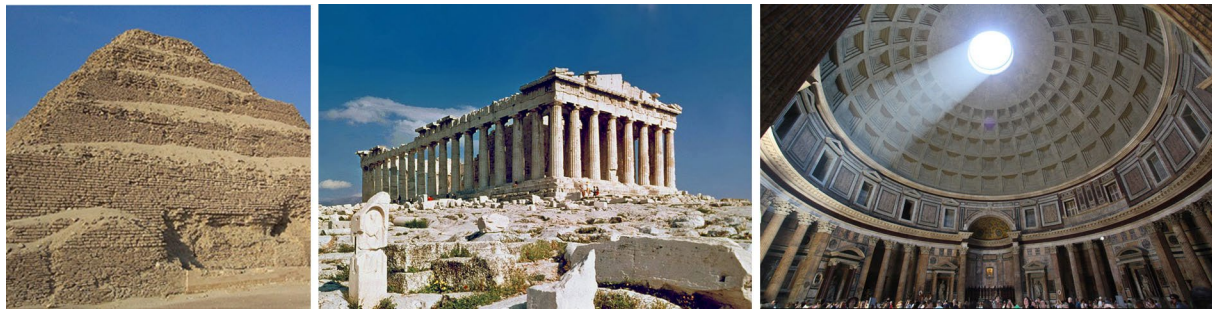
Keywords: structural membranes, textile architecture, structural efficiency, optimization.

1. Introduction

The development of membrane structures has advanced considerably in recent years. They compare favourably with other roofing and cladding materials because their lightness reduces the structural load and their flexibility increases the allowable deformability, so the supporting structure can be considerably reduced in size. But some designs do not take it into

Membrane architecture: the seventh established building material. Designing reliable and sustainable structures for the urban environment.

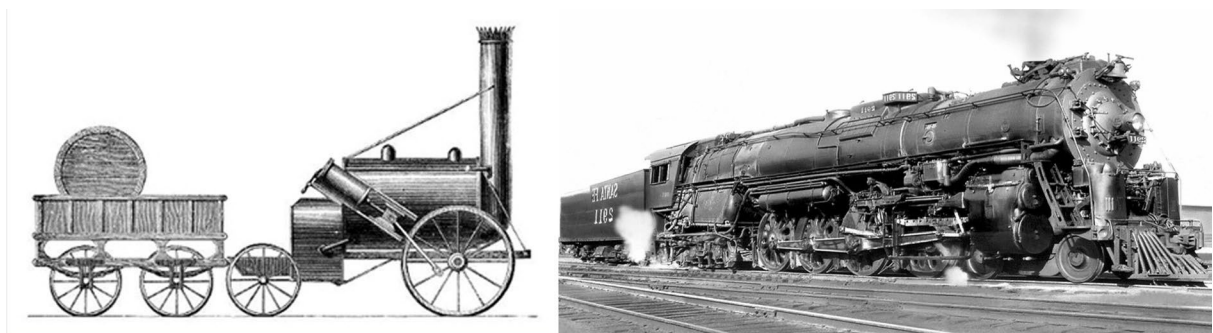
account to the point that membrane structures frequently end up being covered conventional steel structures. It was already mentioned in a previous article [J.Llorens, 2010] that, new technologies begin copying previous models but, at the end, they develop different forms that correspond to their capabilities (Figs 1 to 7).



Figures 1 to 3: Building under compression evolved identifying the path of loads. 1 Stepped pyramid of Djoser at Saqqara (ca.2667 to 2648 BC): loads flow directly from every point to the foundations, Usable space is kept to a minimum. 2 The Parthenon (mid 5th century BC) mimics the forms of wood but stone is not suitable for lintels (bending). 3 Pantheon, Rome (29-19 BC): domes direct the loads across curved surfaces enlarging the usable space. Enormous amounts of material are saved.



Figure 4 Santa Maria del Mar, Barcelona (1329-1383): gothic structures direct loads through lines. Figure 5 Brick-Topia, Fabra i Coats, Barcelona, 2013: a thin only compressed ceramic vault.



Figures 6 and 7: G. Stephenson in 1814 put a steam boiler on wheels. It evolved to the Baldwin's Santa Fe Locomotive, 1944

Membrane architecture: the seventh established building material. Designing reliable and sustainable structures for the urban environment.

From antiquity, membrane structures have not been alien to this phenomenon because they have ranged from being "supported by" to "suspended from", exploiting progressively the advantages of relying mainly on tension, funicularity, curvature, pre-stress, avoiding bending and optimizing compression (Figs 8 to 11).



Figure 8: The yurt is supported by a lattice of wood. Figure 9: the jaima tent is properly a structural membrane. Both illustrate that de dilemma is as old as mankind.



Figure 10: Imagine Clearwater Amphitheater, 2022: the membrane rests on the steel structure. Figure 11: Cardo e Decumano streets, Expo Milano 2015. The membrane hangs from cables. The primary structure is reduced to the lateral masts. Bending is avoided.

2. Comparative study

In order to quantify the impact of considering the structural characteristics of membranes in the design, a comparative study is being carried out. Starting from a case study consisting of arches supported by branched masts, alternative solutions have been examined including commonly used arrangements. So far, I-beams, trusses, arches, cushions, cable beams and flying masts have been analyzed, so that the transition from bending members to predominantly axial force members under tension or compression has been measured by the weight, surfaces ratio, exposure to the wind, internal forces and deformation.

A second part is in progress to complete the most usual repertoire, including cable-stayed, castellated and void beams, tied ETFE cushions, grid shells, cable domes, ridges and valleys, textile halls and pneumatic structures.

Membrane architecture: the seventh established building material. Designing reliable and sustainable structures for the urban environment.

2.1. I beams and arches

A common solution for small and medium size structures is a series of parallel arches supported by multibay frames made of I sections supported by columns. Compared to the other structures presented here, its 12,27 kg/m² reveal that the main I sections are in bending (Figs.12 to 18).

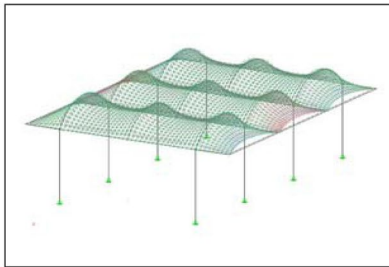


Figure 12: Isometric view.

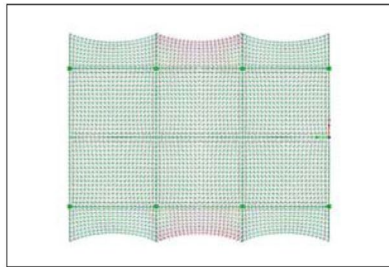


Figure 13: Plan.

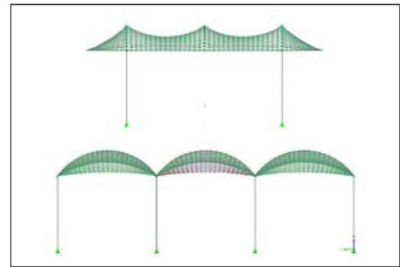


Figure 14: Elevations.

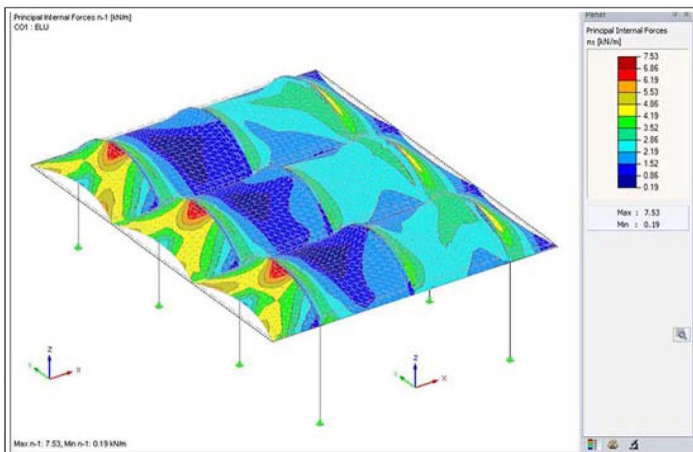


Figure 15: Internal forces

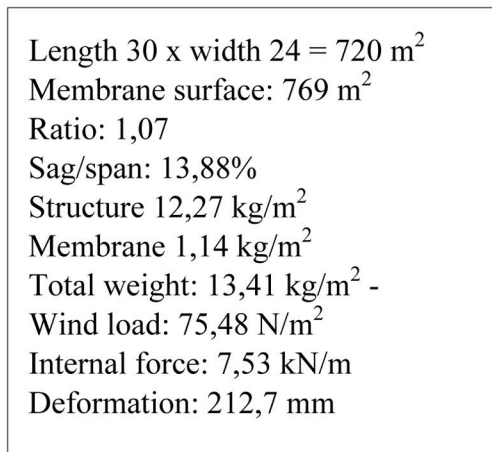


Figure 16: Summary of results



Figures 17 and 18: Examples of application

Membrane architecture: the seventh established building material. Designing reliable and sustainable structures for the urban environment.

2.2. Trusses and arches

A first step to lighten the sections under bending is increasing the depth by trussing, although the number of members and nodes is greatly increased (Figs. 19 to 25).

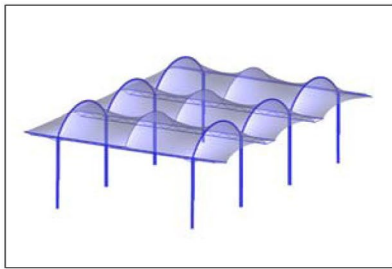


Figure 19: Isometric view.

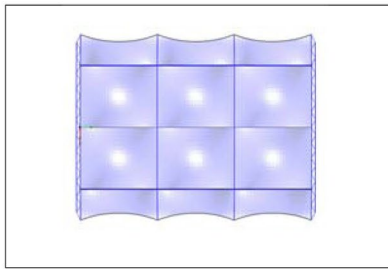


Figure 20: Plan.

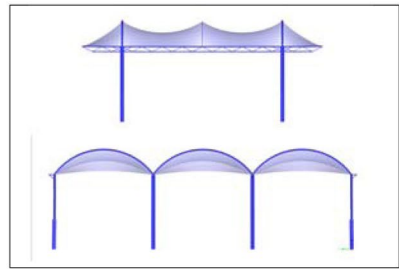


Figure 21 Elevations

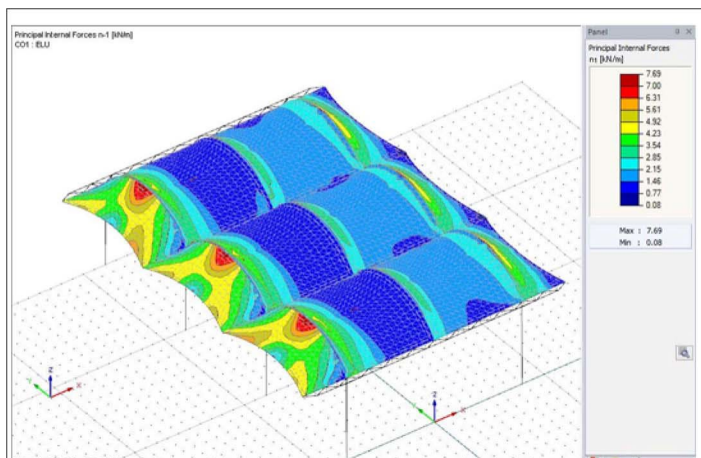
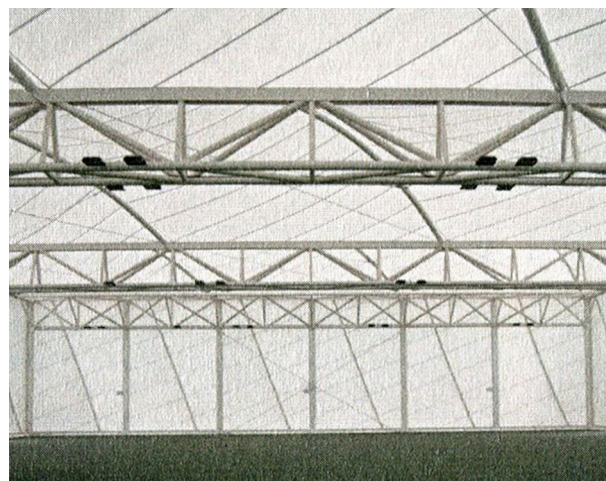
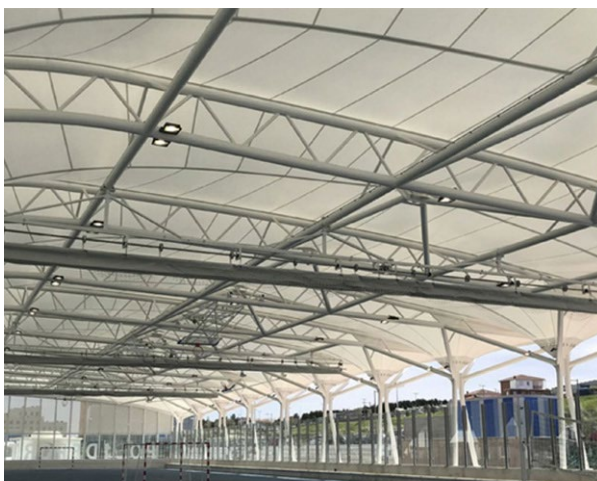


Figure 22: Internal forces

Length 30 x width 24 = 720 m²
Membrane surface: 769 m²
Ratio: 1,07
Sag/span: 13,88%
Structure 9,99 kg/m²
Membrane 1,14 kg/m²
Total weight: 11,13 kg/m² -
Wind load: 75,81 N/m²
Internal force: 7,69 kN/m
Deformation: 126 mm

Figure 23: Summary of results



Figures 24 and 25: Examples of application

Membrane architecture: the seventh established building material. Designing reliable and sustainable structures for the urban environment.

2.3. Trussed arches

A second step to lighten the sections under bending is changing the straight beams into trussed arches (Figs. 26 to 32). In this way, most of the loads are transmitted by compression instead of bending. The effects of buckling are reduced by the short lengths of the bars.

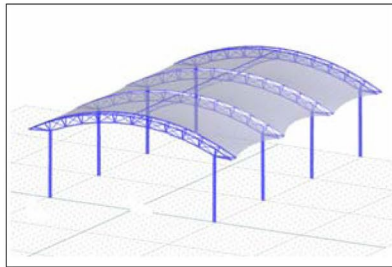


Figure 26: Isometric view.

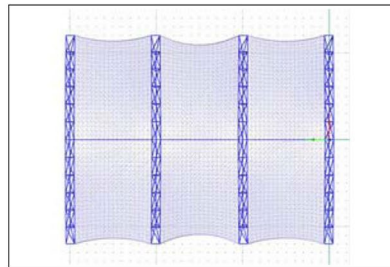


Figure 27: Plan.

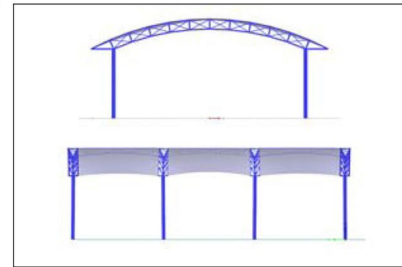


Figure 28 Elevations

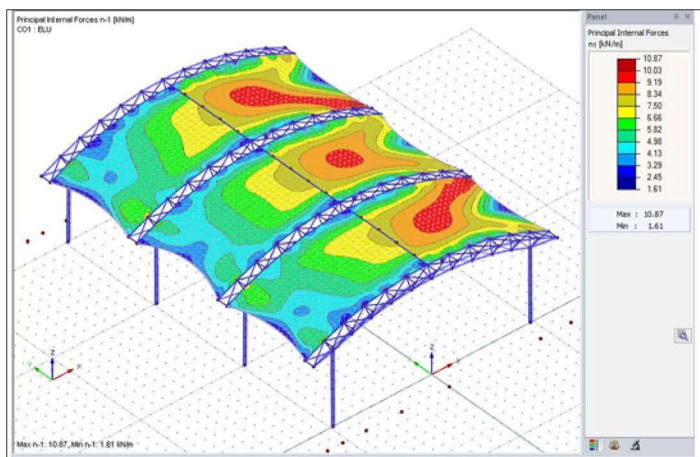
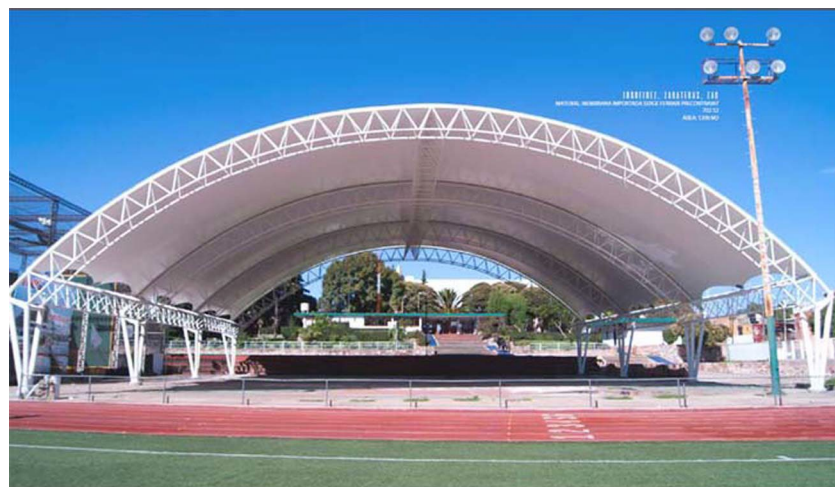


Figure 29: Internal forces

Length 30 x width 24 = 720 m²
 Membrane surface: 606 m²
 Ratio: 0,84
 Sag/span: 2,38%
 Structure 13,24 kg/m²
 Membrane 0,9 kg/m²
 Total weight: 14,14 kg/m² -
 Wind load: 232,51 N/m²
 Internal force: 10,87 kN/m
 Deformation: 100,3 mm

Figure 30: Summary of results



Figures 31 and 32: Examples of application

Membrane architecture: the seventh established building material. Designing reliable and sustainable structures for the urban environment.

2.4. Arches on branched masts

The spans can be reduced by branching the masts. In this way, the buckling lengths are also reduced. Note that in the example presented here the arches consist only of a pair of CHS because the spans are reduced drastically by means of branching the masts as trees in their upper parts (Figs 33 to 37).

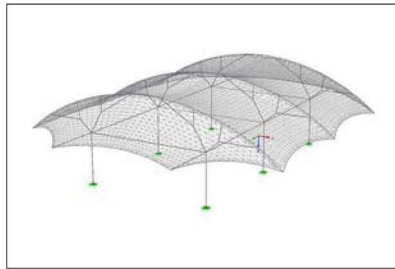


Figure 33: Isometric view.

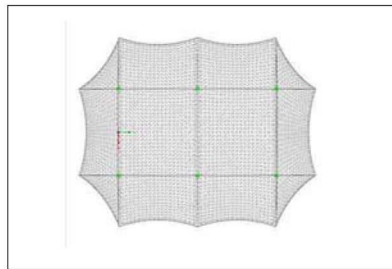


Figure 34: Plan.

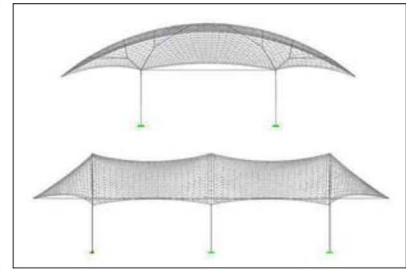


Figure 35 Elevations

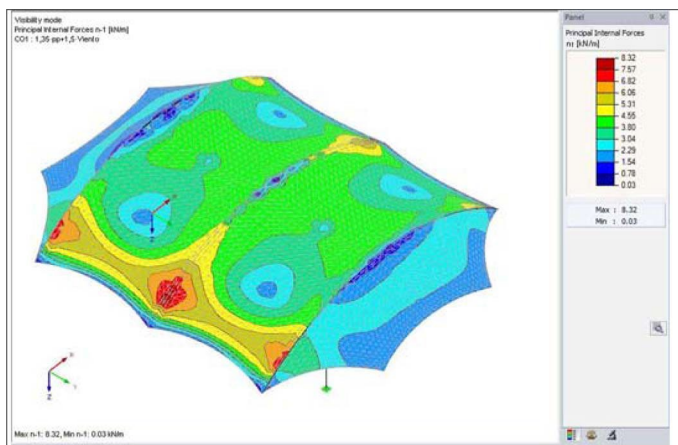


Figure 36: Internal forces

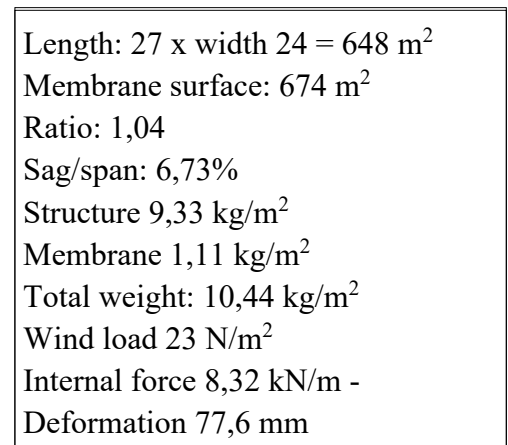
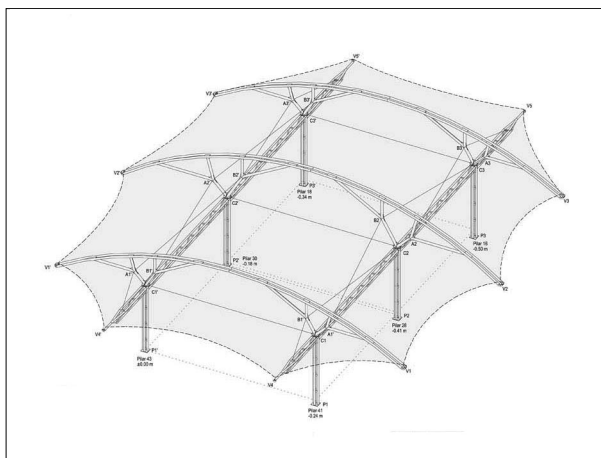


Figure 37: Summary of results



Example of application

Membrane architecture: the seventh established building material. Designing reliable and sustainable structures for the urban environment.

2.5. ETFE cushions

The structural strength of ETFE is lower than that of textile membranes, so it requires more structure. But it compares favourably with glass due to its lightness, transparency and deformability. As a result, its application has developed considerably in recent years, with inflated cushions being the most commonly used forms although they require rigid edges subjected to bending, which is unfavourable for comparative purposes. However, a combination of inflated cushions has been included to assess the differences (Figs. 38 to 45).

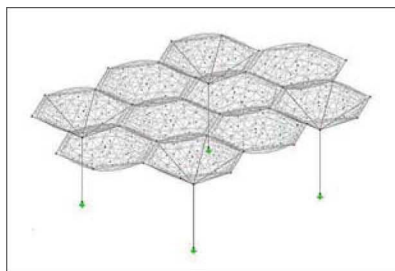


Figure 38: Isometric view.

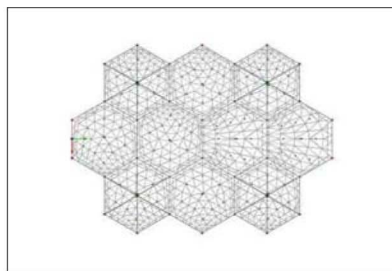


Figure 39: Plan.

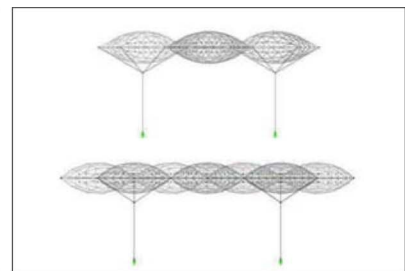
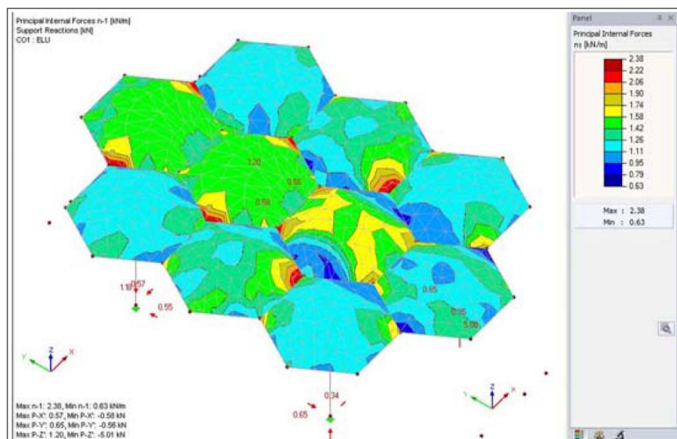


Figure 40: Elevations



Figures 41: Internal forces

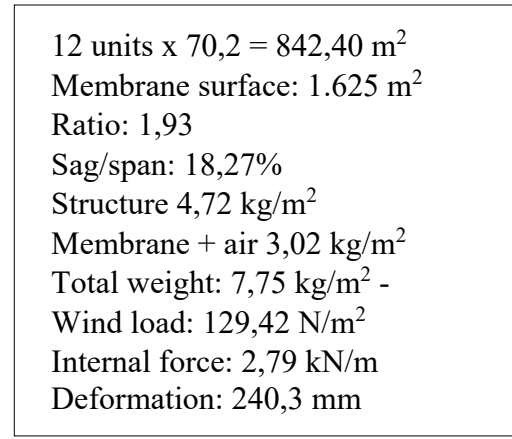
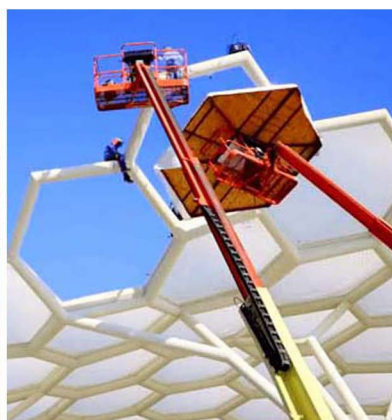


Figure 42: Summary of results



Figures 43 to 45: Examples of application

Membrane architecture: the seventh established building material. Designing reliable and sustainable structures for the urban environment.

2.6. Cable beams

The most effective way to alleviate bending is avoiding it. It can be achieved by cable beams, introduced by David Jawerth in the 1950s [M. Majowiecki, 1971]. Many applications have subsequently been realised that have become part of the tradition of tensile structures (Figs. 46 to 52).

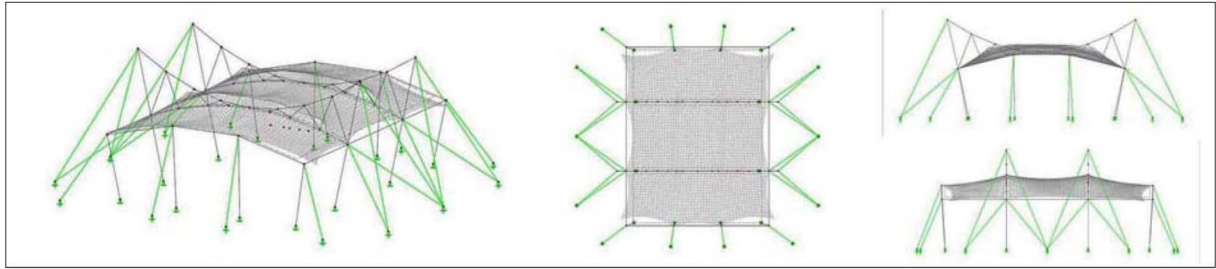


Figure 46: Isometric view.

Figure 47: Plan .

Figure 48: Elevations

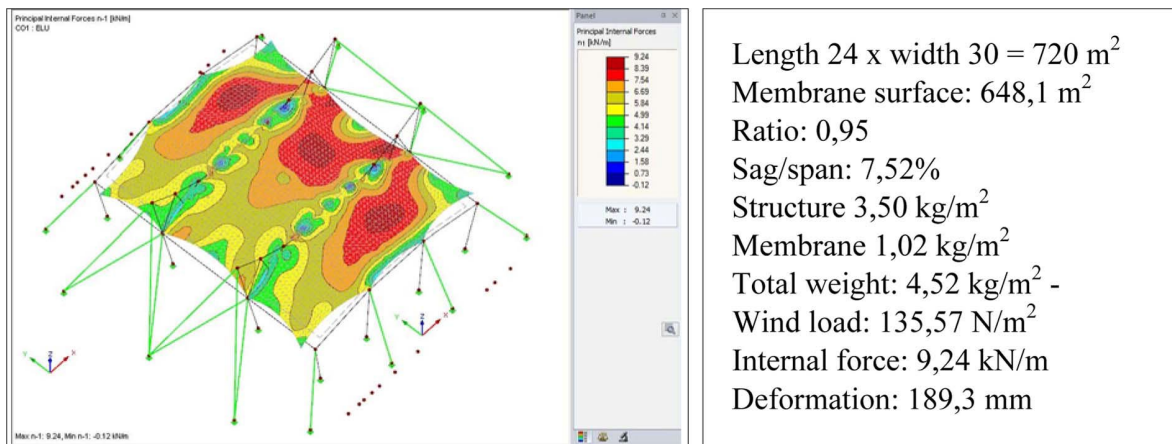


Figure 49: Internal forces

Figure 50: Summary of results



Figures 51 and 52: Examples of application

Membrane architecture: the seventh established building material. Designing reliable and sustainable structures for the urban environment.

2.7. Flying masts

Another way to eradicating bending completely is the use of flying masts. They were introduced by F.Otto and his team at the Olympic Stadium in Munich 1972 (Fig. 58). They reduce dramatically the spans without interfering. External cable-stayed masts are needed that have to be cable-stayed in order to work only under compression.

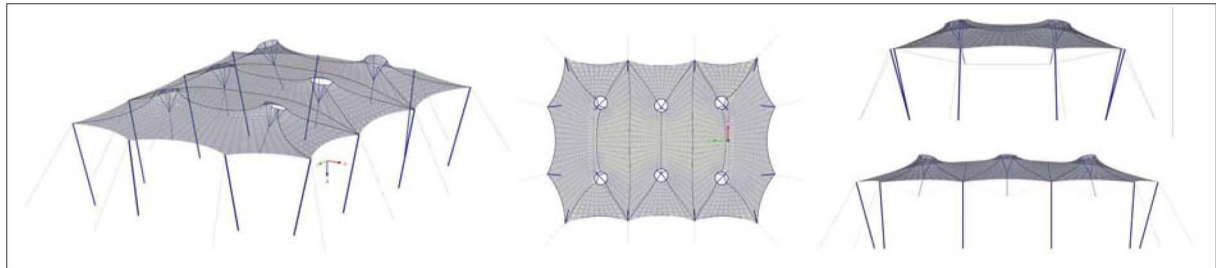


Figure 53: Isometric view.

Figure 54: Plan.

Figure 55 Elevations

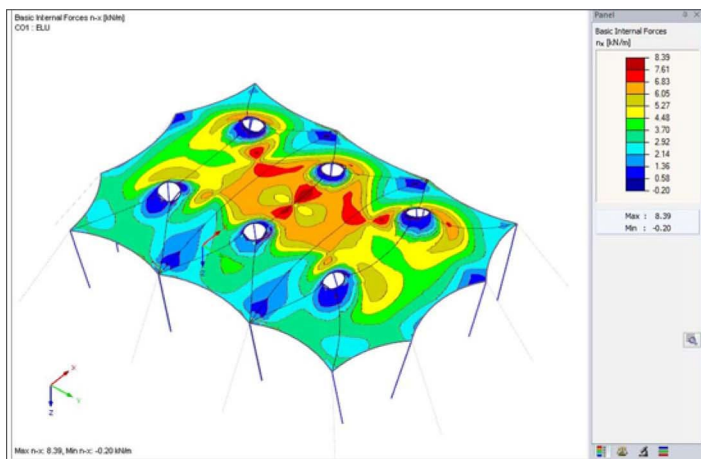


Figure 56: Internal forces

Length 32 x width 22 = 704 m²
 Membrane surface: 746,1 m²
 Ratio: 1,06
 Sag/span: 9,45%
 Structure 2,46 kg/m²
 Membrane 1,13 kg/m²
 Total weight: 3,59 kg/m² -
 Wind load: 144,37 N/m²
 Internal force: 8,39 kN/m
 Deformation: 354 mm

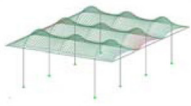
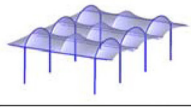
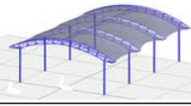

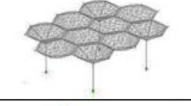
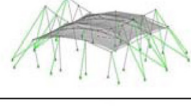
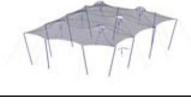
Figure 57: Summary of results



Figures 58 to 60: Examples of application

Membrane architecture: the seventh established building material. Designing reliable and sustainable structures for the urban environment.

3. Conclusions

Case	Description	Areas (m ²)	f/l (%) Weight (kp/m ²) Wind (N/m ²)	Max. internal force and displacement (kN/m and mm)
	I BEAMS	Covered: 720	f/l = 14%	Internal force: 7,53 kN/m
		Membrane: 769	Weight 13,41 kp/m ²	
		Ratio: 1,07	Wind: 75,48 N/m ²	Def. 212,7 mm
	TRUSSES	Covered: 720	f/l = 14%	Internal force: 7,69 kN/m
		Membrane: 769	Weight 11,13 kp/m ²	
		Ratio: 1,07	Wind: 75,81 N/m ²	Def. 126 mm
	TRUSSED ARCHES	Covered: 720	f/l = 2,4%	Internal force: 10,87 kN/m
		Membrane: 606	Weight 14,14 kp/m ²	
		Ratio: 0,84	Wind: 232,51 N/m ²	Def. 100,3 mm
	ARCHES ON BRACED MASTS	Covered: 648	f/l = 7%	Internal force 8,32 kN/m
		Membrane: 674	Weight 10,44 kp/m ²	
		Ratio: 1,04	Wind: 23 N/m ²	Def. 77,6 mm
	ETFE CUSHIONS	Covered: 842	f/l = 18%	Internal force: 2,79 kN/m
		Membrane: 1.625	Weight 7,75 kp/m ²	
		Ratio: 1,93	Wind: 129,42 N/m ²	Def. 240,3 mm
	CABLE BEAMS	Covered: 720	f/l = 7,52%	Internal force: 9,24 kN/m
		Membrane: 648	Weight 4,52 kp/m ²	
		Ratio: 0,95	Wind: 135,57 N/m ²	Def. 189,3 mm
	FLYING MASTS	Covered: 704	f/l = 9,45%	Internal force: 8,39 kN/m
		Membrane: 746	Weight 3,59 kp/m ²	
		Ratio: 1,06	Wind: 144,37 N/m ²	Def. 354 mm

These values show that the lightest structures are those that avoid or reduce bending: FLYING MASTS and CABLE BEAMS. The values obtained by varying the support structure range significantly from 2,46 to 13,24 kp/m². Observe also how the sag/span ratio affects the internal force (Fig. 61). On the other hand, the ratios of surfaces and the weight of the membrane vary little. However, attention has to be paid to deformations: FLYING MASTS, ETFE CUSHIONS and I BEAMS. (Note that generalizations should take into account some particularities of the cases investigated, such as spans and cantilevers).

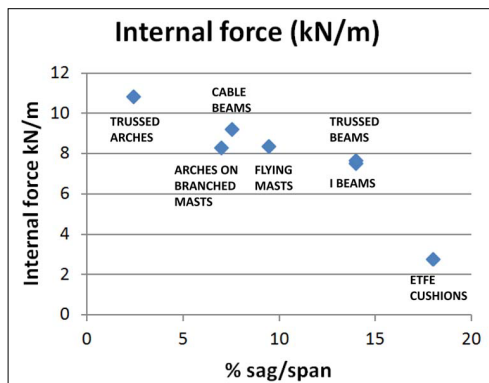


Figure 61: Internal forces are sensitive to sag/span ratio. Increasing f/l reduces the internal forces.

In any case, these considerations concerning the value of the loads and the calculation model are all very well, but in fact, what can really improve the efficiency of the structure is its conceptual approach. In the case of membrane structures, it is a matter of satisfying the basic principles of only tension, funicularity, curvature and pre-tension, avoiding bending and replacing the arches with flying masts, so that the arches, beams and the interior columns disappear in exchange for the interior flying masts and the exterior cable-stayed masts subjected to simple compression.

Membrane architecture: the seventh established building material. Designing reliable and sustainable structures for the urban environment.

Annex. Optimization of masts

As the bending is dispensed with, the masts become the main elements of the primary structure. Different types of masts can be used: hollow sections, trussed, tapered, subdivided, branched, coupled, clustered, flying and tied [J.Llorens, 2019].

Different strategies to cope with over dimensioning imposed by buckling on such long elements include:

- the use of circular hollow steel sections because of their efficiency in compression and torsion, minimal surface area to be protected, minimal wind resistance and availability
- to simplify the transport, the poles may be subdivided and assembled onsite through bolted connections not protruding from the profile of the section.
- tapering is a strategy to prevent from looking oversized compared to the whole structure and the site
- trussed masts are common in travelling circuses to reduce weight, facilitate assembly and lifting from the ground.
- cross-trees and ties lighten the mast by reducing the buckling length. It is a way to save steel and to prevent the mast from looking oversized.
- coupling or clustering the masts make them thinner. Slim tubes look more elegant than a single bulky cylinder.
- branching the masts reduce spans and buckling lengths.

It is also worth remembering that mast sizing must provide sufficient cross-section to resist compressive loading and stiffness enough to prevent buckling. The parameters to be considered are: the load, the height, the constraints, the stiffness, the dimensions and the shape [A.Muttoni, 2006].

Acknowledgements

Structural and CFD analysis have been performed with RFEM and RWIND software available at: <https://www.dlupal.com/en/products/rfem-fea-software/what-is-rfem>
<https://www.dlupal.com/en/products/stand-alone-structural-analysis-software/rwind-simulation>

References

- Ph. Block, T. Van Mele, M. Rippman and N. Paulson (2017): "Beyond bending. Reimagining compression shells". Edition DETAIL, Munich.
- J.Llorens (2010), "Circus and envelats. Two milestones of tensile architecture history". In *TensiNet Symposium 2010*, GSP 1900 Ltd, Sofia.
- J.Llorens (2019): "Detailing masts". In *Structural Membranes 2019, Barcelona*.
- M.Majowiecki (1971): "Tension Structures: Jawerth System". *Acier-Stahl-Steel*, n°4, p.169-177.
- A.Muttoni (2006): "The Art of Structures". EPFL Press, Lausanne.
- O. Popovic and A. Tyas (2003): "Conceptual structural design. Bridging the gap between architects and engineers". Thomas Telford.

TOPIC 2
**Tensioned membrane structures:
the seventh building material**





tensinantes2023 : TensiNet Symposium 2023 at Nantes Université

Membrane architecture: the seventh established building material. Designing reliable and sustainable structures for the urban environment.

Proceedings of the Tensinet Symposium 2023

TENSINANTES2023 | 7-9 June 2023, Nantes Université, Nantes, France

Jean-Christophe Thomas, Marijke Mollaert, Carol Monticelli, Bernd Stimpfle (Eds.)

Computational design workflow for a complex cable network

Jef ROMBOULTS^{a*}, Oriane GUIDET^a, Ludovic REGNAULT^b, Klaas DE RYCKE^{abc}

^aBollinger + Grohmann S.A.R.L

15 rue Eugène Varlin, 75010 Paris

*jrombouts@bollinger-grohmann.fr

^b Ecole nationale supérieure d'architecture Versailles

^c The Bartlett School of Architecture, UCL

Abstract

Cable networks are form-active structures where the overall shape and detailing have a strong impact on both aesthetics and structural behavior. Consequently, a close collaboration is required between designer, structural engineer and contractor. For the structural design of the accessible artwork 'Cloud Cities' by the artist Tomás Saraceno, we have developed a design workflow built around a central 3D model. The artwork is positioned at the top level of the Torre Glories in Barcelona, where an accessible, inner cable net is attached to the existing structure via a surrounding, outer cable net. Wooden panels mark the path through the artwork.

The iterative structural design and analysis of the artwork is subdivided into five parts: 1) form-finding outer net, 2) generating inner net, 3) generating connection cables, 4) optimizing cable lengths, 5) structural analysis. All these steps are performed starting from a central Rhino3D model, assembled and modified using Grasshopper + Kangaroo and the Compas framework developed at ETH Zurich (Van Mele, Liew, Méndez Echenagucia, Rippmann, & others, 2017). Custom Python scripts allow a quick conversion of data from the 3D model to a JavaScript object or spreadsheet and vice-versa. The developed workflow allowed for fast design iterations between all members of the design team, and for an efficient communication with the client and other external parties.

Keywords: design workflow, tensile structures, cable nets, form finding, computational design

1. Introduction

The design of cable networks is complicated by the strong interaction between the network's overall shape and its structural behavior (Kayvani, 2003). Therefore, designer and structural

Membrane architecture: the seventh established building material. Designing reliable and sustainable structures for the urban environment.

engineer should work closely together to achieve the desired result in terms of aesthetics and structural performance. The free-form nature of cable networks often necessitates the development of new and innovative connection details to make the design constructible. These details in turn affect the global behavior of the net. Additionally, the nonlinear structural behavior of the net causes difficulties for many standard finite element packages. Because of these challenges, the design of cable nets is performed iteratively, where most design steps are repeated every iteration to converge to a design that satisfies all stakeholders (De Rycke, et al., 2020). In order to make this workflow practically feasible, it is important that each step can be performed as effortlessly as possible by automating repetitive tasks.

This paper describes the workflow for the design of the accessible artwork ‘Cloud Cities’ by Tomás Saraceno (Figure 3) and summarizes its execution. The artwork is positioned at the top floor of the Torre Glories in Barcelona, where it spans between the existing, curved steel outer shell of the building, and the central concrete circulation core. The artwork consists of an inner cable net formed by an assembly of polyhedron shaped clusters of cables. This inner net is anchored to a so-called transfer net, which surrounds the inner net and transfers the forces to the available anchor points (Figure 1). The cables connecting the inner net to the transfer net are called connection cables in the following. Rigid panels are finally added to mark the path through the artwork and create the impression of floating clouds (Figure 2).

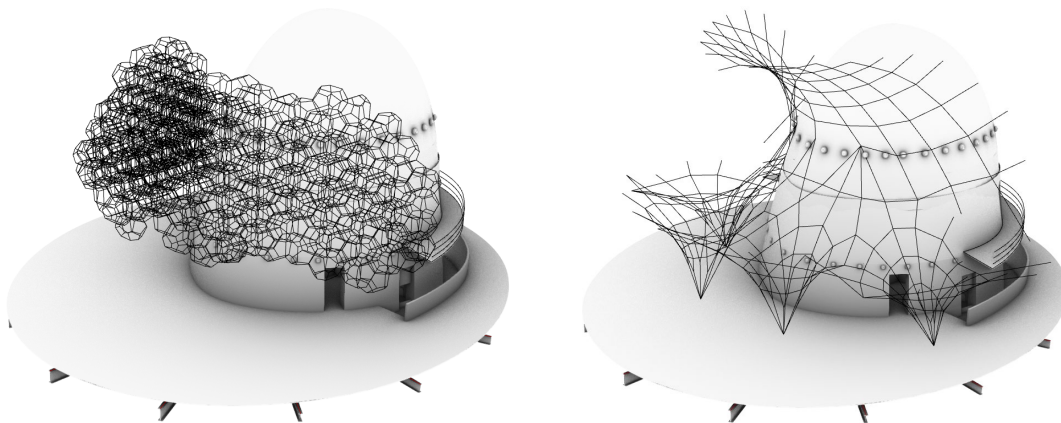


Figure 1: Main cable families. Left: inner net. Right: transfer net.

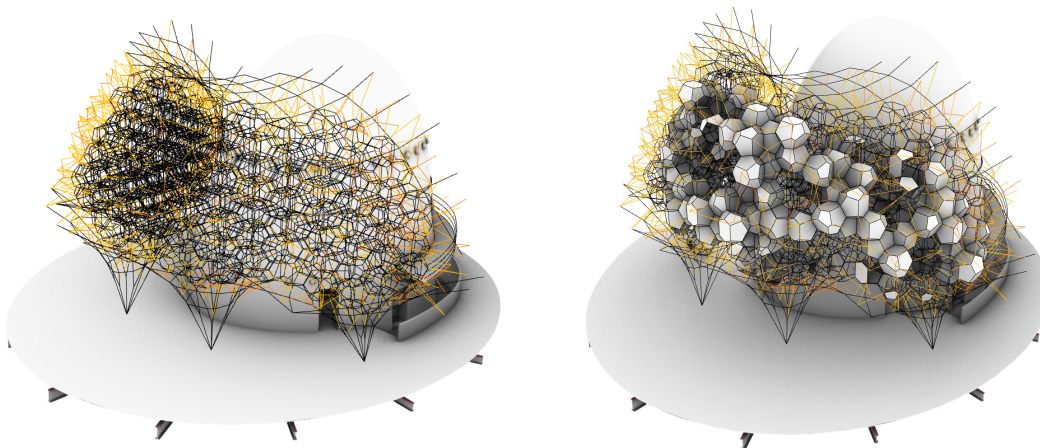


Figure 2: Left: Full cable net with highlighted connection cables. Right: cable net with panels.

Membrane architecture: the seventh established building material. Designing reliable and sustainable structures for the urban environment.

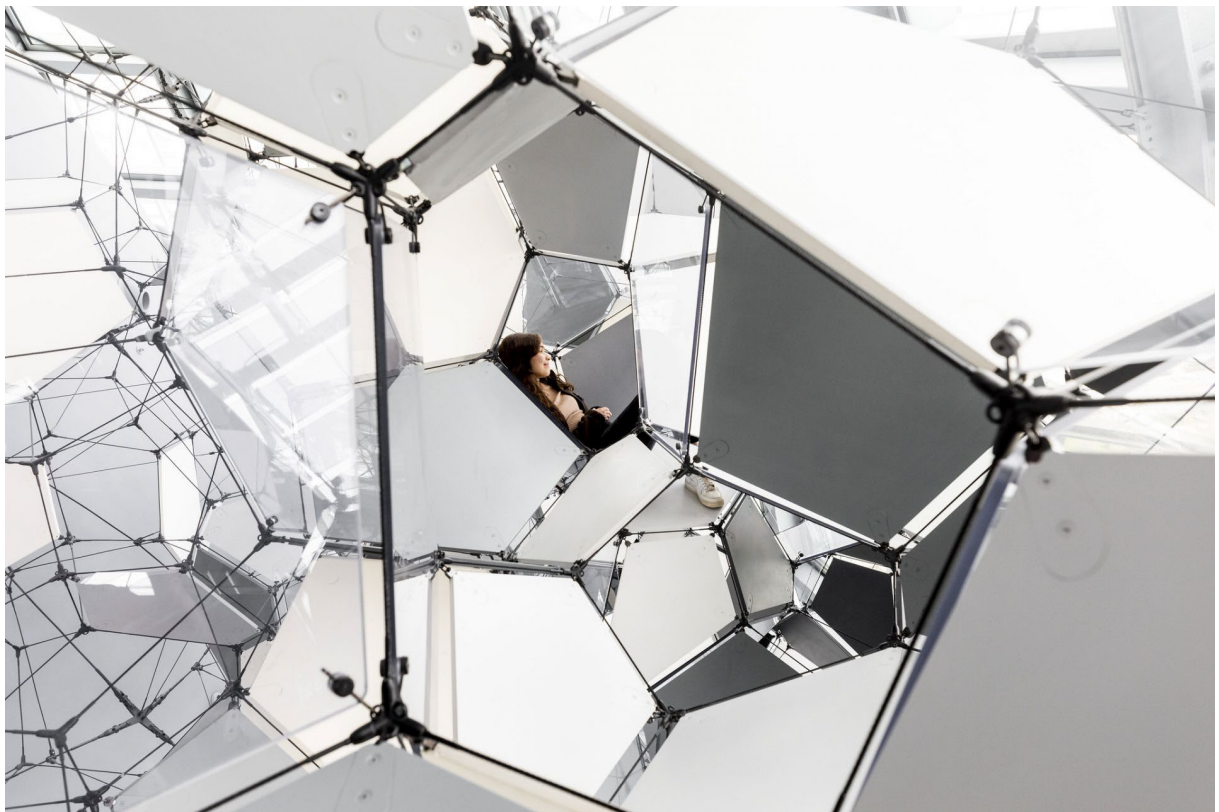
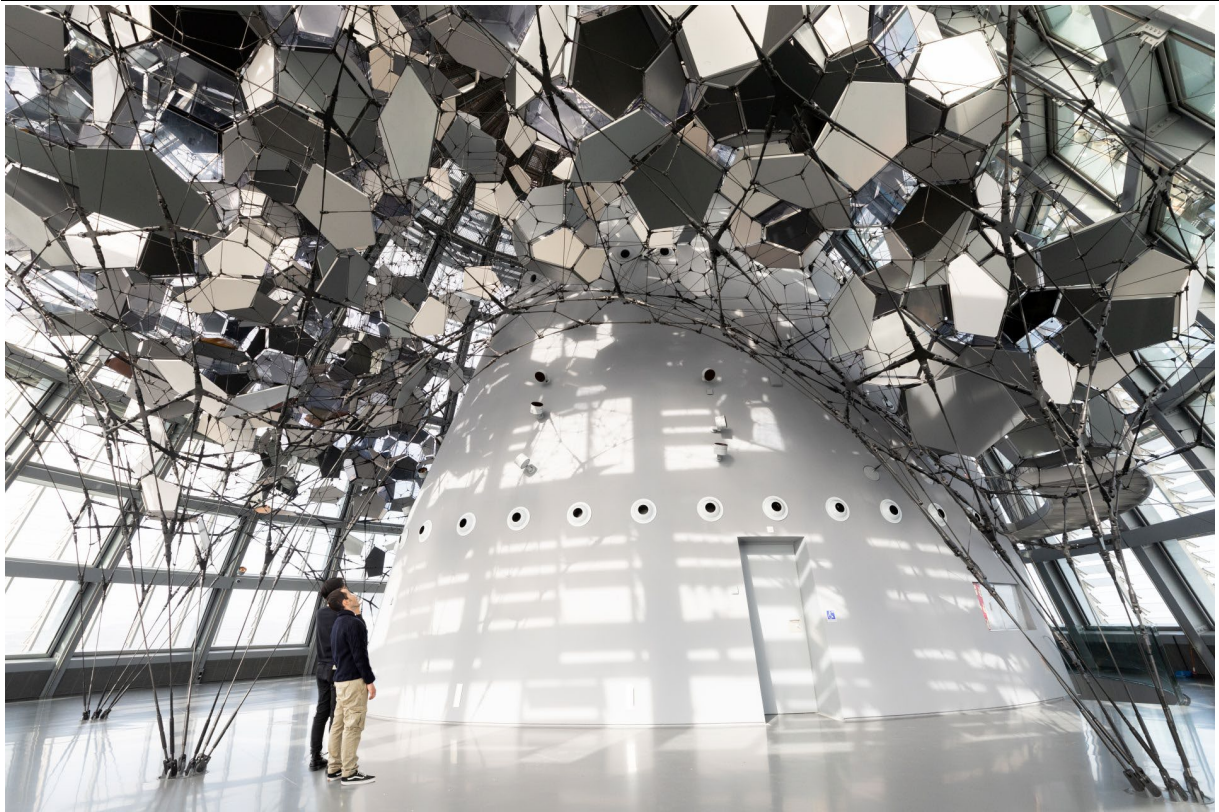


Figure 3: Cloud Cities Barcelona. 2022. © Tomás Saraceno

Membrane architecture: the seventh established building material. Designing reliable and sustainable structures for the urban environment.

The remainder of this paper is organized as follows. Section 2 describes the workflow of the structural design process of the artwork. Next, section 3 summarizes the execution and detailing of the artwork. Finally, section 4 gives a conclusion.

2. Design workflow

We have divided the design of this artwork in the following five consecutive steps: 1) form-finding outer net, 2) generating inner net, 3) generating connection cables, 4) optimizing cable lengths, 5) structural analysis. All data is linked to a main Rhino3D model, where geometrical and structural information is annotated to the geometry to allow it to be used directly for structural analyses, VR visualization and geometrical analyses required for assembly.

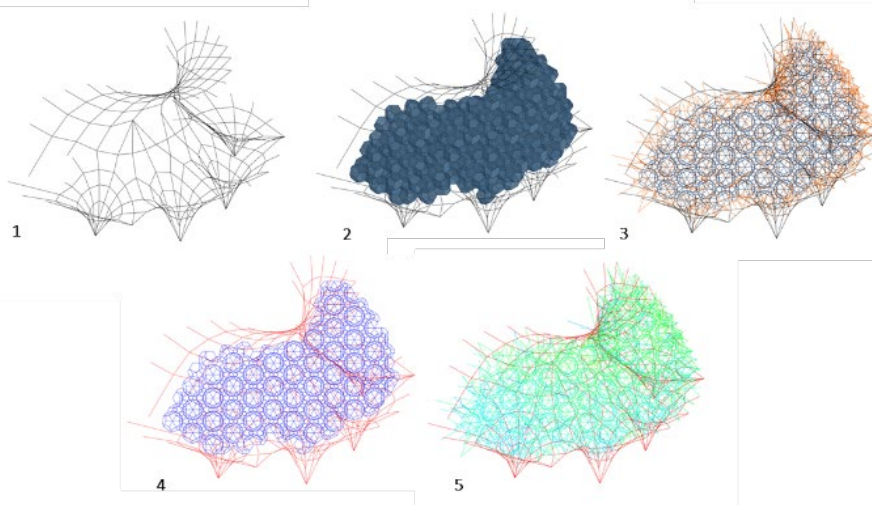


Figure 4: The design is subdivided into five steps: 1) form-finding outer net, 2) generating inner net, 3) generating connection cables, 4) optimizing cable lengths, 5) structural analysis.

The first step in the design is to determine the shape and topology of the transfer net, as this defines the contour of the artwork. The shape of the net is determined in Kangaroo (Piker, n.d.) by adjusting the force densities in the cables. The shape and topology of the net are adjusted iteratively to comply with the constantly evolving artistic view and the constraints given by the client. Figure 5 shows the evolution from the first transfer net to the current transfer net.

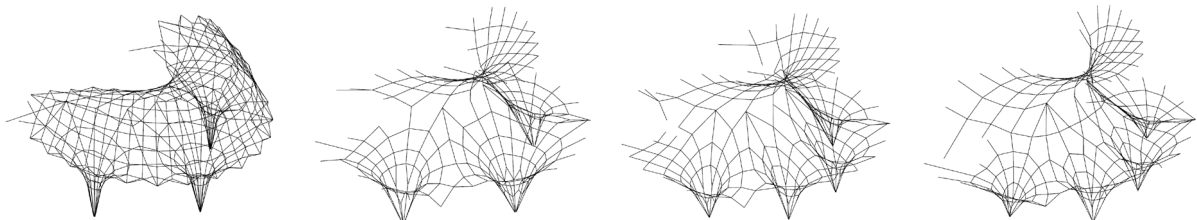


Figure 5: Four snapshots of the iteratively updated transfer nets.

Next, the geometric structure of the inner net is determined by the artist. It consists of tetrakaidecahedrons and dodecahedrons (Figure 6). To generate the cloud of polyhedrons inside the transfer net, a contouring surface is first determined from the formfound transfer net and meridian and ring beams of the outer cupola. A custom grasshopper script fills the contouring surface with the polyhedrons, allowing the user to simply move and scale the polyhedron cloud around in space until a suitable layout is found.

Membrane architecture: the seventh established building material. Designing reliable and sustainable structures for the urban environment.

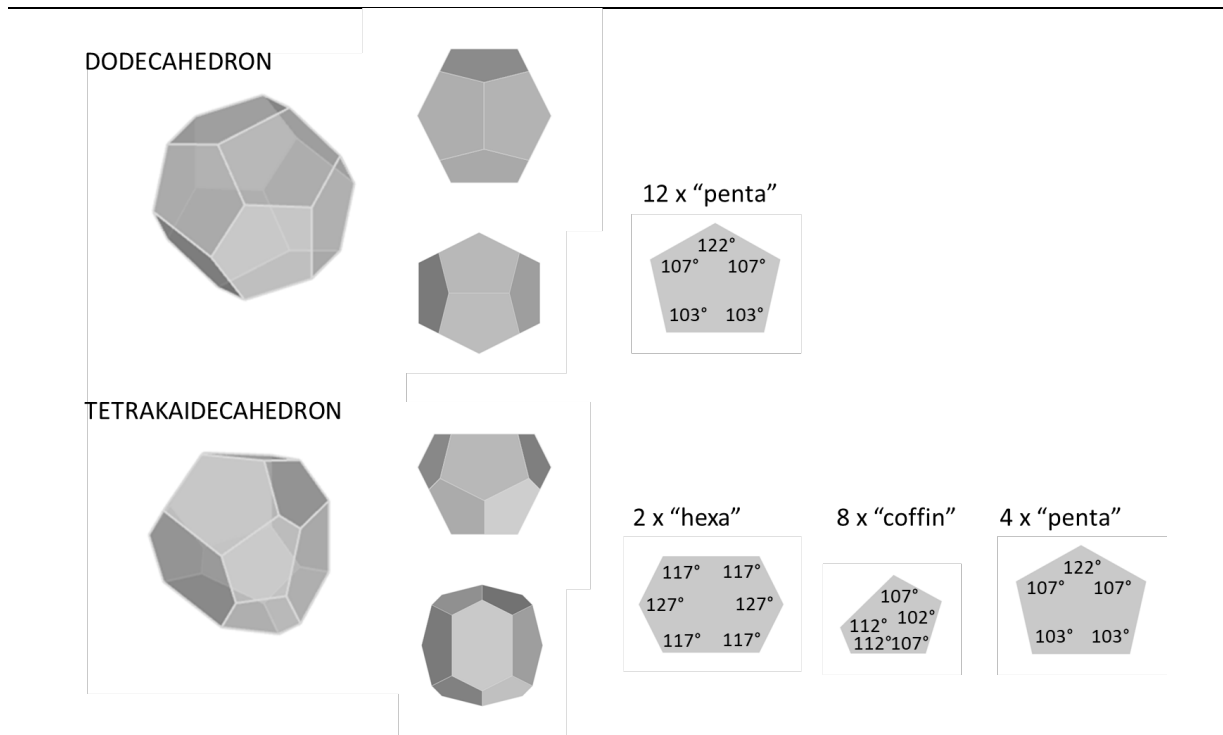


Figure 6: Polyhedrons forming the inner cable net

Next, a grasshopper script automatically generates the connection cables between the inner net and the transfer net. The objective of the script is to select corner points of the inner net and connect them to suitable anchor points. The user can specify a weight factor to prefer a shorter cable or a more optimal cable direction. If no suitable solution is found, the script automatically splits the cable in two, and finds two suitable anchor points.

In order to find a suitable distribution of pretension, an optimization scheme is developed based on (Rombouts, et al., 2021) and described in (Rombouts, Guidet, & De Rycke, 2022), using the undeformed length of a number of cables as the design variables. The distance between specific nodes in the deformed cable net and the designed geometry is minimized, while the tension in each cable is constrained to avoid slack cables on the one hand, and cable failure on the other hand. The sensitivities of this optimization problem have been derived analytically to enable the use of efficient gradient-based optimization solvers. Figure 7 shows the design under self weight, pretension, and the weight of 20 visitors before and after optimization.

Membrane architecture: the seventh established building material. Designing reliable and sustainable structures for the urban environment.

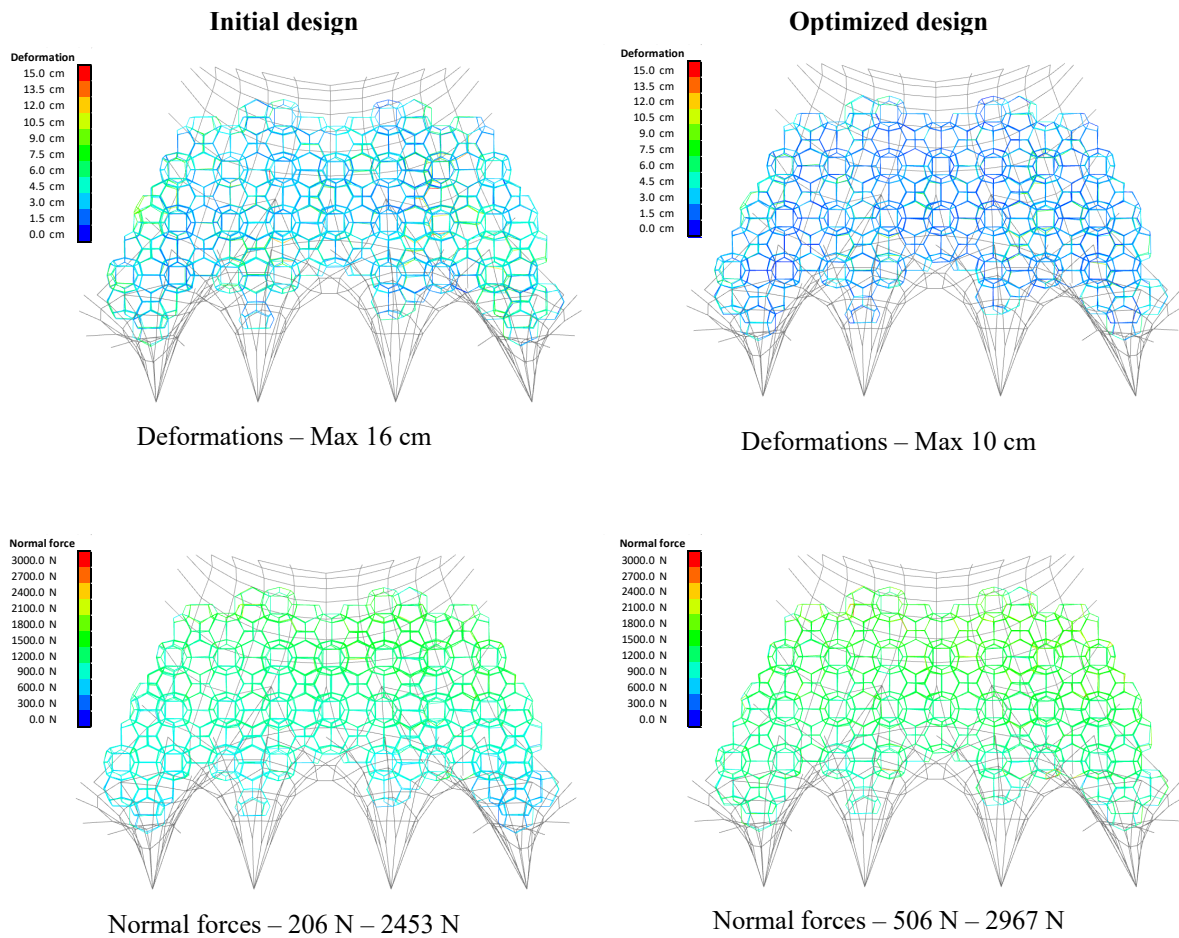


Figure 7: Deformations (top) and normal forces (bottom) for the inner net of the initial design (left) and the inner net of the optimized design (right).

The approach in this paper is built around a central Rhino3D file, which forms a BIM model containing forces, material, element type, loads, connectivity information, etcetera, annotated to the Rhino geometry, and stored as JavaScript Object and Spreadsheet to allow for further analysis, visualization and communication (Figure 8). This workflow proved to be crucial in order to efficiently iterate through the design process between makers, designers and engineers, and to quickly try out new variants. Additionally, it enabled all stakeholders to work in the same environment, reducing time and error related to manually converting the data into other data types (Paschke, Neuhäuser, De rycke, & Gengnagel, 2020).

Membrane architecture: the seventh established building material. Designing reliable and sustainable structures for the urban environment.

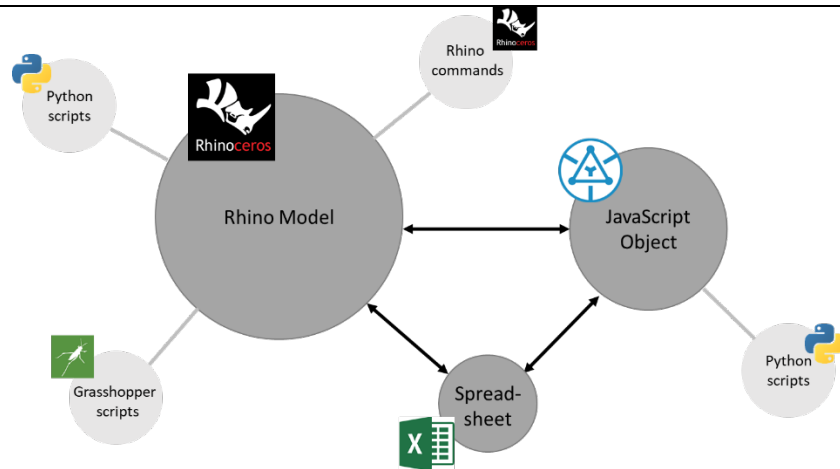


Figure 8: The data structure is built around a central 3D model, where data is extracted/assigned from/to spreadsheets and JavaScript objects.

3. Execution and detailing

Most of the design process followed a design and build process with StageOne as the main contractor. Hence, the connection details and installation strategy were developed in close collaboration between the design team and StageOne. The most important connection details are discussed below, as well as the installation process.

Three different types of nodes were cast for the inner net, each connecting four cables. The node type depends on the position in the inner net. More specifically, it depends on the type of polyhedrons the node connects. For each type, the individual cable connections align with the theoretical direction of the cables. To allow for misalignment due to deformations, a cap screwed on the cast base generates a ball joint for the cable ends allowing around 8° of misalignment. Connection cables attaching to the inner net nodes are given full rotation freedom to accommodate the higher variety in relative directions. Panels are attached directly to the nodes via shackles (Figure 9).

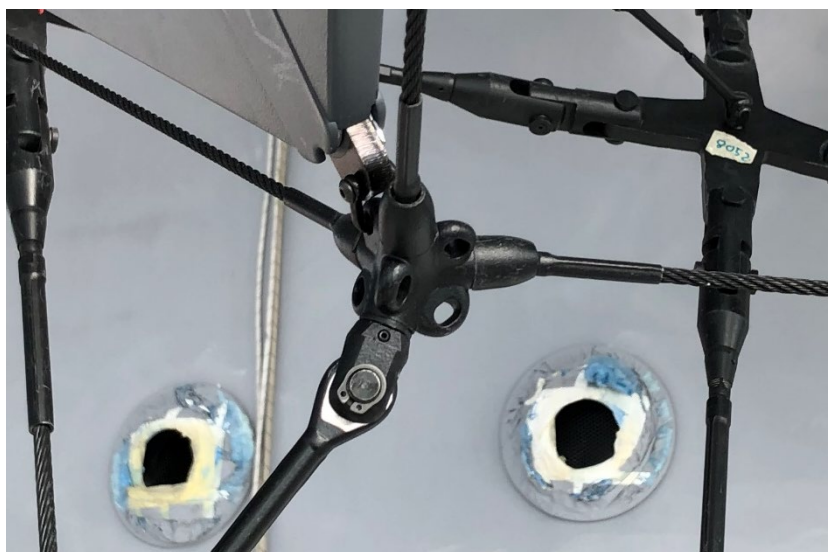


Figure 9: Inner net node connecting three inner net cables (top), one connection cable (bottom), and a plywood panel.

Membrane architecture: the seventh established building material. Designing reliable and sustainable structures for the urban environment.

Although the transfer net was originally foreseen as an assembly of crossing continuous cables, a segmented solution was eventually preferred, as high slipping forces and acute angles would require overly complicated clamping nodes. Instead, custom cut and bend steel plates were used to anchor the individual cable segments, aligning the connection to the theoretical deformed cable orientation. For the design of the nodes, their orientation in space under cable forces needed to be simulated. An approximate analytical expression provided adequate accuracy, as additional hinges were foreseen at the cable ends to account for imperfections and variable displacements under live loads (Figure 10).



Figure 10: Transfer net node connecting four transfer net cable segments.

Once the detailed design was finished, the artwork was installed in the following steps. First, a separate company reinforced the existing structure to accommodate the forces in the cables, and installed the anchor points. Next, the installed anchor points were scanned and the cable lengths were set to the correct length according to the as-built anchor point positions. Now, the top transfer net could be assembled on the ground and installed into position, given a preliminary pretension to define its shape. After this, the inner net, including panels, was gradually assembled from top to bottom, hanging from the top transfer net and anchor points. Finally, the bottom transfer net was assembled and installed.

To tension the artwork, turnbuckles were foreseen at the majority of connections between transfer net cables and anchor points. Simulations showed that the cable net could be brought from fully slack to fully tensioned with only three well-chosen turnbuckles, but more turnbuckles were installed to better control potential imperfections. The tensioning itself was done iteratively, sequentially putting every turnbuckle to the designed tension, and repeating these loops for a handful of times until all measured cables were sufficiently accurately tensioned. The design workflow allowed to easily simulate the full tensioning process considering cable length imperfections.

Membrane architecture: the seventh established building material. Designing reliable and sustainable structures for the urban environment.

Finally, a dozen of connection cables remained slack after tensioning. This was probably caused by the fact that panels were not modeled, and even though their connection allows free movement in theory, this movement is limited in reality. Together with other effects like friction, this generates a certain inaccuracy in the calculation model. However, simulations showed that large imperfections globally have limited impact, as long as the overall tension in the transfer net was well controlled. The slack connection cables were simply replaced by slightly shorter ones.

4. Conclusion

The design of large cable networks is characterized by a constant back and forth between artist, maker and structural engineer, where the understanding of the design problem grows with each iteration. As each design step is performed multiple times, it is important to maximize the efficiency of each step and provide information-rich data for efficient communication between the involved partners.

For the design of the Cloud Cities artwork by Tomás Saraceno, we used a central Rhino3D file, which is developed in five steps to form a BIM model containing forces, material, element type, loads, connectivity information, etcetera, annotated to the Rhino geometry, and stored as JavaScript Object and Spreadsheet to allow for further analysis, visualization and communication. Python and Grasshopper scripts allowed to automate most of the repetitive design steps.

The proposed design workflow proved its use also during execution, where manufacturing information and as-built data could be simply added to the model, and additional simulations could be performed considering on-site measurements.

References

- De Rycke, K., Bergis, L., Vierlinger, R., Regnault, L., Mazzucchi, A., & Bohnenberger, S. (2020). Application of Human-Machine Design Processes to Tensile Structures. *DMSB 2019, Impact: Design With All Senses*, (pp. 32-44). Berlin: Springer.
- Kayvani, K. (2003). Analysis and design of cable supported roof structures. *Advances in Structures* (pp. 57-65). Sydney: Swets & Zitlinger.
- Paschke, M., Neuhäuser, S., De rycke, K., & Gengnagel, C. (2020). Digital Prototyping – Modelling Concepts for a Generative Computer Based-Design of Complex Tensile Structures. *DMSB 2019, Impact: Design With All Senses* (pp. 159-172). Berlin: Springer.
- Piker, D. (n.d.). *Kangaroo Physics*. Retrieved May 11, 2020, from <https://www.food4rhino.com/app/kangaroo-physics>
- Rombouts, J., Guidet, O., & De Rycke, K. (2022). Optimal pretension in cable nets. *Proceedings of the IASS 2022 Symposium*. Beijing.
- Rombouts, J., Liew, A., Lombaert, G., De Laet, L., Block, P., & Schevenels, M. (2021). Designing bending-active gridshells as falsework for concrete shells through numerical optimization. *Engineering Structures*.
- Van Mele, T., Liew, A., Méndez Echenagucia, T., Rippmann, M., & others. (2017). *COMPAS: A framework for computational research in architecture and structures*.



tensinantes2023 : TensiNet Symposium 2023 at Nantes Université

Membrane architecture: the seventh established building material. Designing reliable and sustainable structures for the urban environment.

Proceedings of the Tensinet Symposium 2023

TENSINANTES2023 / 7-9 June 2023, Nantes Université, Nantes, France

Jean-Christophe Thomas, Marijke Mollaert, Carol Monticelli, Bernd Stimpfle (Eds.)

Development and validation of an experimental methodology for the characterization and FEM analysis of fibre-reinforced architectural meshes

Salvatore Viscuso*, Carol Monticelli ^a, Alessandra Zanelli ^b, Alberto Fiorenzi ^c

* Assistant Professor, Politecnico di Milano, DABC, Via Ponzio 31, 20133 Milano, salvatore.viscuso@polimi.it

^a Associate Professor, Politecnico di Milano, DABC, Via Ponzio 31, 20133 Milano

^b Full Professor, Politecnico di Milano, DABC, Via Ponzio 31, 20133 Milano

^c i-Mesh – Sailmaker International Srl, Via Jesina 60, 60022 Castelfidardo (AN)

Abstract

The paper deals with a methodological workflow able to finalize a finite element calculation of fibre-reinforced meshes for architectural functions, e.g. for shading façade panels or canopies. Digital technologies allow to fabricate custom-made weaving, according to the expected function. Raw materials used for the fabrication of meshes have usually excellent flame-retardant properties, high mechanical performances, excellent thermal insulation, and high resistance to attacks of chemical elements. Besides optimizing the CNC fabrication of panels and the correct dimensioning of fibers, the objective of this research is to demonstrate the feasibility and to explore the potentialities as well as the difficulties of using the finite element method for the study of fibre-reinforced meshes, with an ultimate aim to develop a general analytical method in the full range of loadings.

Keywords: lightweight structures, structural membrane, performative design, finite element analysis, optimization, composite material, mechanical testing

1. Introduction

Fibre composite materials are becoming an essential element in many construction technologies. Extensive studies on fibre reinforced materials, such as e-glass, carbon, and basalt (Schmid et al., 2021; Cho, Park, 2021; Ahmad, Sirková, 2018; Zhang et al., 2013) showed the advantages due to the use of these materials in several industrial applications (automotive, packaging, construction, etc.). These materials present many advantages: lightweight, speed of execution, good mechanical properties and good performance at failure. They have also some drawbacks, such as the poor behavior at high temperatures and the relatively high cost of epoxy

Membrane architecture: the seventh established building material. Designing reliable and sustainable structures for the urban environment.

resins; moreover, the replacement of organic matrix with inorganic ones can represent a solution to minimize the carbon footprint of these applications (Azmi et al. 2022).

Due to the orthotropic structure of the meshes with a tailor-made design, it is difficult to fully predict their mechanical characteristics and behavior, especially if they are produced with complicated patterns, as in the case of custom-made woven fabrics. The research work is organized according to the main investigation tasks, which can be summarized in the following list:

- (i) Mechanical characterization of fibers, obtained through uniaxial tests of rovings of diverse materials and TEX, in order to describe the Beam elements for the numerical modeling;
- (ii) Uniaxial and biaxial mechanical tests of cruciform fabric samples (net area: 300x300 mm), in order to describe a strain-displacement graph that associates the feasible geometries of panels to a range of Shell elements in finite element modeling (FEM) stage;
- (iii) Comparison between the data (strain-displacement) acquired from the uniaxial and biaxial cruciform tests and the virtual simulation of the above-described tests achieved with FEM software Karamba for Rhinoceros Grasshopper. Close agreement between numerical results given by this approach and reference solutions is found in all cases;
- (iv) Development of the Karamba script to analyze panels in presence of external loads (snow, wind or temperature loads). The algorithm allows to simultaneously calculate Beam elements (corresponding to the structural layer of the panels) and/or Shell elements (base layer).

Tasks (i), (ii), (iii) are performed at the biaxial testing station of the *Textiles HUB* (Heuristic Understanding in Buildings), an interdepartmental research laboratory that focuses on testing membranes and prototyping lightweight structures, design objects and building component based on textiles and/or polymeric materials.

2. Uniaxial test of material rovings

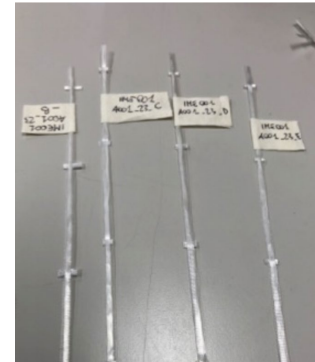
Objective of the first stage is the mechanical characterization of diverse fibre-reinforced rovings (fibreglass, basalt fibre and carbon fibre); the filaments are coated with a transparent polymer resins. The test focuses on the following set of fibre-reinforced materials:

- (i) fibreglass 600 TEX, cross section 3.5x0.4 mm, density 2.5 gr/cm³;
- (ii) fibreglass 1200 TEX, cross section 3.5x0,4 mm, density 2.5 gr/cm³;
- (iii) basalt fibre 1200 TEX, cross section 3.5x0.4 mm, density 2.7 gr/cm³;
- (iv) carbon fibre 800 TEX, cross section 3.5x0.4 mm, density approx. 1.7 gr/cm³.

For each set of fibers, the Table 1 illustrates the average values of maximum load, ultimate strength, yield strength, elongation and strain that are published in literature (Cho, Park, 2021; Ahmad, Sirková, 2018; Zhang et al., 2013).

Table 1: mechanical characterization of fibre-reinforced rovings

Material	Max Load [KN]	Ultimate Strength [KN/mm]	Yield Strength [KN/cm ²]	Elongation [mm]	Strain [%]
Fibreglass 600 TEX	0.3468	0.1066	362.7048	0.0278	2.7818
Fibreglass 1200 TEX	0.8006	0.2398	522.6986	0.0644	6.4402
Basalt fibre 1200 TEX	0.7944	0.2172	595.7352	0.0962	9.6256
Carbon fibre 800 TEX	0.9708	0.2944	735.4544	0.0148	1.4717



These values are then averaged through five tests per material, with specimens of 400 mm \pm 0.5 mm length for glass and basalt rovings and 150 mm \pm 0.5 mm for carbon ones. The test samples are tensioned at a constant length of elongation until breaking for the determination of tensile strength and strain at break, according to Standard UNI ISO EN 1421:2017 (Rubber or plastics coated fabrics - Determination of tensile strength and elongation at break) and ISO 4606:1995 (Textile glass - Woven fabric - Determination of tensile breaking force and elongation at break by the strip method). The selected test speed is 100 mm/min, with an initial strain of 10 N (Besnard et al., 2006).

3. Uniaxial and biaxial tests of cruciform samples

The second step of mechanical test refers to three cruciform samples - type A, B and C - made of 31x31 fibreglass rovings 600 TEX and net area of 300x300 mm (Figure 1). The purpose is to determine the mechanical behavior of a large variety of samples with a given required load profile. Cruciform patterns are studied in order to cover - during the material assignment in FEM software - all possible mesh geometries through the layer stratification of tested patterns.

Uniaxial tests are set in displacement control. Samples are tested with load cycles of 5 mm with a speed of 1mm/min. An initial preload of 0.084 KN is applied to the cruciform mesh (Lecompte et al., 2007). The control system can operate both in force and displacement control, and the curve shows in real time the average values between load and deformation of two of more specimens per each sample type (Figure 2). Subsequently the same geometries are tested on biaxial traction with loading and unloading cycles in displacement control (5 mm per cycle with preload of 0.084 KN). Biaxial tests are performed on cruciform meshes in order to determine the stress and strain curves (Table 2).

Test protocol bases on indications of the Japanese standard MSAJ/M-02-1995 - Testing method for elastic constants of membrane materials. After the execution of three load cycles, samples are carried to failure in order to register the maximum load. Graphs of Figures 3,4 and 5 show stress-strain curves of biaxial test for samples type A and C.

Membrane architecture: the seventh established building material. Designing reliable and sustainable structures for the urban environment.

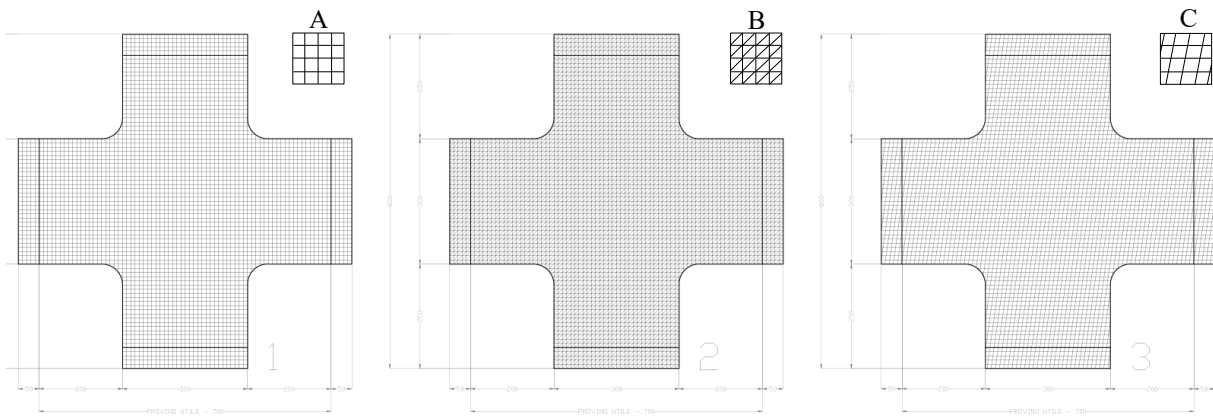


Figure 1: cruciform samples used for uniaxial and biaxial tests: A. quadrilateral mesh with right angle; B. triangular mesh; C. quadrilateral mesh with angle degrees 10

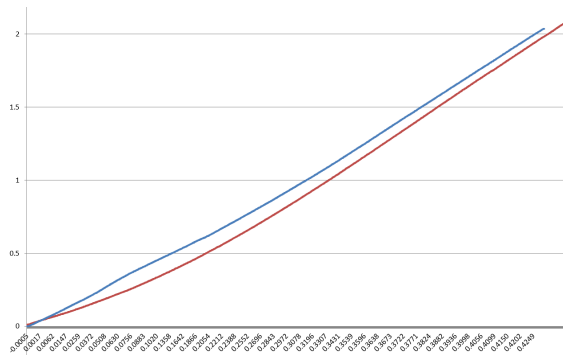


Figure 2: uniaxial test on two specimens type A. Load (y) [KN] - Strain (x) [%] curve of four specimens

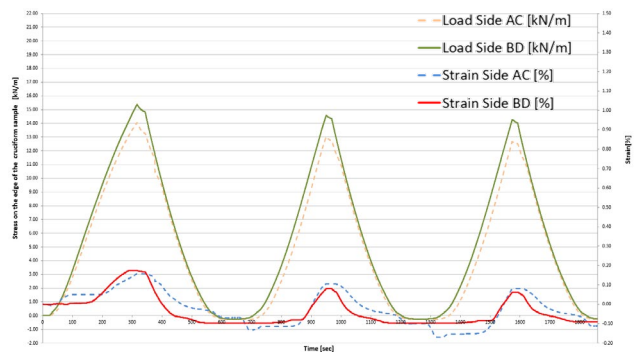


Figure 3: biaxial test on sample type A. Stress - Strain curve of the first specimen denotes the isotropy of the mesh pattern

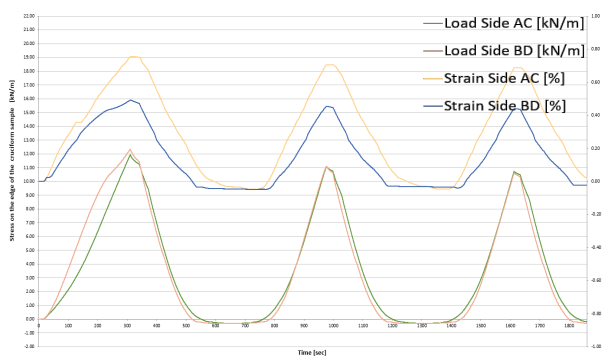


Figure 4: biaxial test on sample type C. Stress - Strain curve show minor deformation in west direction due to geometry of the mesh

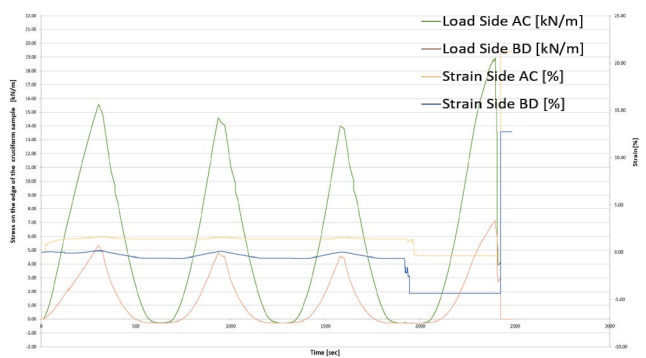


Figure 5: biaxial test on sample type C. Stress - Strain curve make clear different yield and ultimate strengths in warp and weft direction, due to the orthotropic geometry of the mesh.

Membrane architecture: the seventh established building material. Designing reliable and sustainable structures for the urban environment.

Table 2: results of uniaxial and biaxial tests on of cruciform simples

Test sample	Warp max axial load [KN]	Weft max axial load [KN]	Warp max stress [KN/m]	Weft max stress [KN/m]	Warp max strain [%]	Weft max strain [%]
A - uniaxial	2.0368	-	18.86	-	0.429	-
A - biaxial	3.7955	4.27289	14.652	15.243	0.158	0.156
B - biaxial	3.3284	3.25274	12.095	11.105	0.706	0.454
C - biaxial	4.2065	1.3748	14.022	4.583	1.539	0.042

4. Comparison between test data and finite-element analysis

Uniaxial and biaxial mechanical tests allow to compare the obtained displacements with values of FEM simulation. Through the Rhinoceros software, the three cruciform sample types are reconstructed. Once the schematic geometry of each cruciform sample is obtained, it is possible to assign to these the properties of the structural elements (Beams), using data acquired from the mechanical characterization of fiberglass rovings (Table 1). In order to validate the mechanical tests of meshes having both isotropic and orthotropic properties, it was decided to perform the FEM analysis - simulating uniaxial and biaxial tests carried on TEXTILES HUB - for all the three geometries.

In finite-element applications, Beam elements are one-dimensional finite elements, oriented on a tridimensional space. A beam consists of at least two nodes placed at the ends of the element. It is particularly suitable to represent a structural element where one dimension is prevalent on the other two and, for this reason, its geometry corresponds to the barycentric axis of the component.

FEM analysis is performed using the plugin Karamba for Grasshopper (Preisinger, Moritz, 2014). Test data are processed using the components “LineToBeam”, “Support”, “PointLoad”, “MaterialProperties” and “AssembleModel” (Figure 6). The “AssembleModel” output is linked to Analyze, a component that performs the FEM analysis, the maximum displacement and the elastic energy of cruciform meshes. The irrelevant difference between the nodal displacements of Karamba simulations and values obtained from the uniaxial and biaxial tests (Table 3) allows to verify reliability of the software regarding the characterization of fibreglass 600 TEX coated with polymer resin (Table 4).

Table 3: uniaxial test data of simple type A

Time [sec]	Load [kN]	Strain [%]	Displacement [mm]
110.5	0.4272	0.0943	1.1874
225.1	1.1891	0.3535	3.1358
335.1	2.0368	0.4286	4.9910

Membrane architecture: the seventh established building material. Designing reliable and sustainable structures for the urban environment.

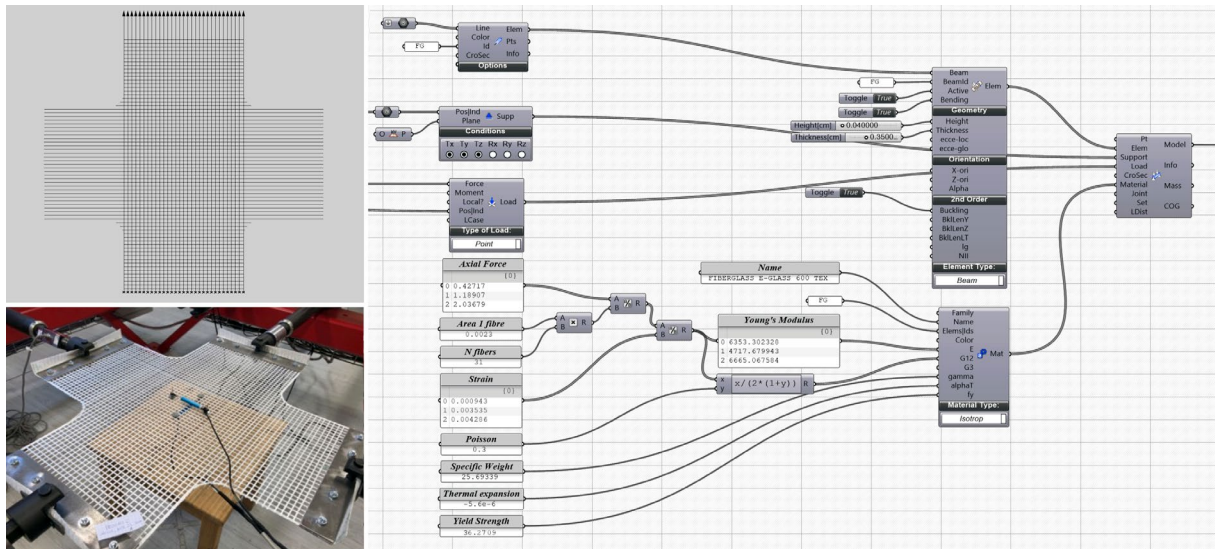


Figure 6: reproduction of uniaxial test on sample type A using FEM software Karamba

Table 4: FEM input-output on simple type A and comparison with uniaxial test data of mechanical test

Input (Mechanical test)		Output (FEM design)	
Load [kN]	Strain [%]	Displacement [mm]	Variance [mm]
0.4272	0.0943	1.2080	+0.0206
1.1891	0.3535	4.5290	+1.3932
2.0368	0.4286	5.4910	+0.4911

5. FEM workflow to analyze panels using Beam and Shell elements

The material characterization allows the definition of standardized procedures (Figure 7), in order to analyze whatever fiber-reinforced mesh panels using one of the following modeling options: (i) designing a tridimensional or planar composition of simplified mesh Beam elements (Workflows 1 and 2); (ii) layering Beams together with one or more Shell elements, in order to approximately rebuild the whole geometry of the fibers into the mesh (Workflow 3).

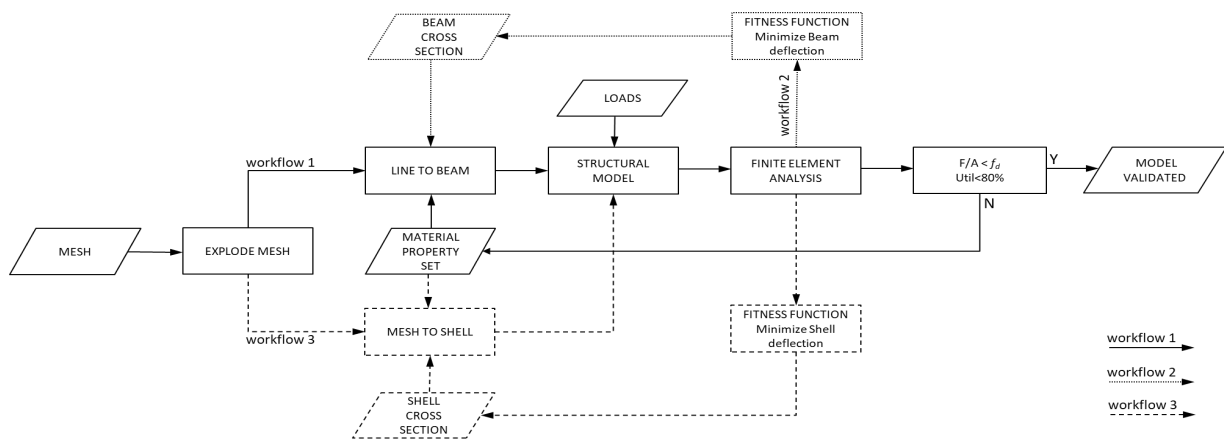


Figure 7: flow chart reproducing workflows 1, 2 and 3 that gradually affine the proposed calculation

Membrane architecture: the seventh established building material. Designing reliable and sustainable structures for the urban environment.

5.1. Workflow 1: Beam analysis using a deterministic algorithm

The file Grasshopper is described below through an application for the structural design of a membrane for a retractable roof. As an example of workflow, the mesh developed for the Dubai Expo Promenade (concept design by Werner Sobek AG; structural design and optimization by the authors), with dimensions of 22x10.5 m, is shown in Figure 8. The canopy is made of coated fiberglass rovings of 1200 TEX; workflow 1 carries out the optimization of BEAM elements only. The roof membrane, fabricated in 11 modules of 2x10.5 m, overlaps two meshes: a structural layer, with Beams of 16÷24 rovings for each one, and a dense base layer. To simplify the calculation, rovings of structural layer are represented in only one Beam element per group (Table 5). However, remaining mesh (base layer) is included in gravity load.

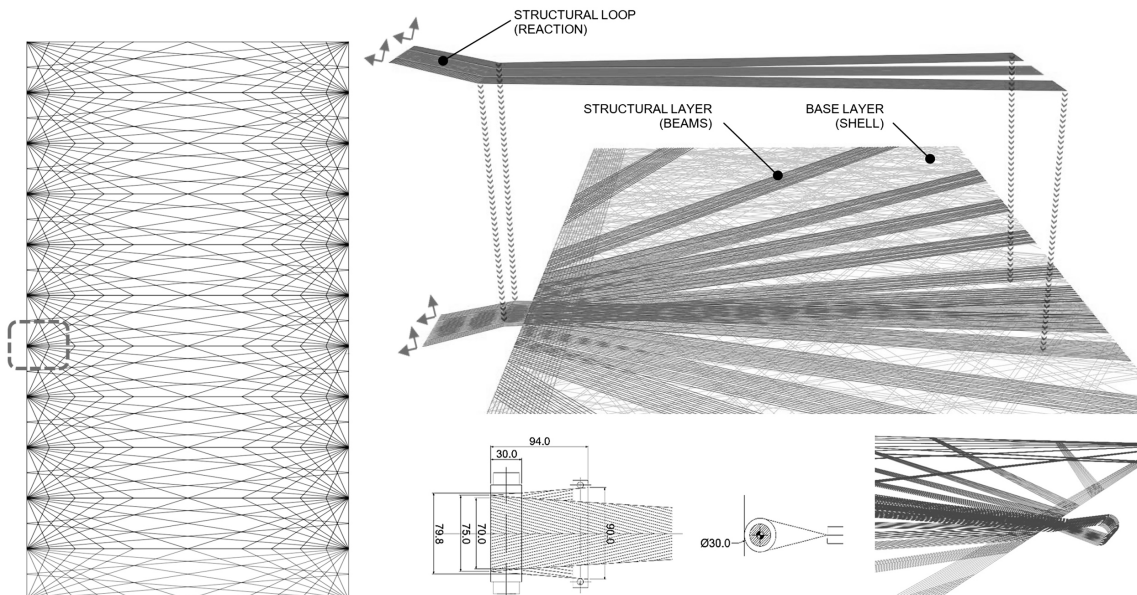


Figure. 8: blueprint of architectural mesh 22x10.5 m and detail on anchor loop

After assigned design variables - material properties, constraints (supports) and loading bearing conditions (selectable from initial strain, point load, mesh load, uniform load, temperature load) - the “AssembleModel” output is linked with the component “LargeDeformationAnalysis”, a tool that allows to manage geometric non-linearity through a load-controlled process in which each interaction scales the external loads of 1/Inc.

Finally, the model is ready to be analyzed. In that specific case, we set the component “Analyze” using the second-order theory. Compared to the first order, in which deformation and tension are constant in the element, second order displacements correspond to linear deformations and tensions. Components “BeamForces” and “ReactionForces” describe data set related respectively to internal forces and reactions of the roof membrane (Table 6). Axial forces make possible the dimensioning of each Beam and the verification that the breaking strength obtained with 24 stipes of 1200 TEX fibers is enough to resist against maximum loadings close to reactions, while internal Beams contain groups of 16 rovings for each one; reaction forces

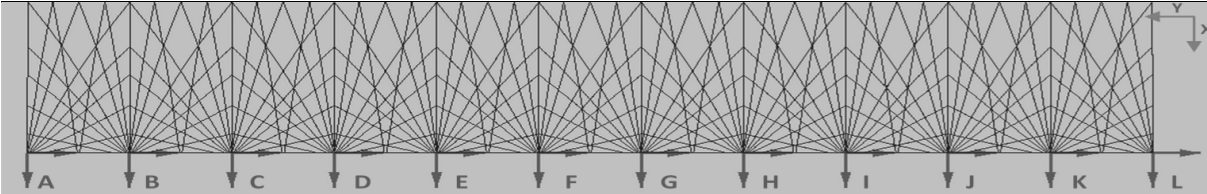
Membrane architecture: the seventh established building material. Designing reliable and sustainable structures for the urban environment.

permit to design and dimension structural nodes through detailed analysis of connection loops between the membrane and steel clamps (Figure 9). Component “Utilization” provides the ratio data list between the load acting on the node and the maximum force that is tolerable by each analyzed section. If the output exceeds the unit, it means that the section used has got over the yield tension. In order to certify an enough level of security, 80% should be considered as the maximum value for a proper utilization of Beams. Focusing on reaction nodes (Figure 10), once fixed in 16 the number of rovings per Beams close to loop, it is possible to localize zones that need reinforces (Util>1), e.g. using rovings of fiberglass 2400 TEX (Table 7).

Table 5: input data in Workflow 1

Dimension		Beam Material	
X	10516 mm	Type	E-GLASS 1200 TEX
Y	22242 mm	Breaking strength	800.60 N
Deflection	7.28 mm	Elongation at break	0.0644
Sag	300 mm	Yield strength	52.26986 KN/cm ²
		Young modulus	7000 KN/cm ²
Cutting Pattern		Coefficient of thermal expansion	-5.60 10 ⁻⁶ /K
X	10538 mm	Specific weight	25.69 KN/m ³
Y	2022 mm	Density	2.5 g/cm ³
		Poisson ratio	0.3
Safety factor (γ)		Load	
5		Suction	0.7x0.133=0.09 KN/m ²
+10% of required TEX		Pressure	0.3x0.133=0.04 KN/m ²

Table 6. extract of output data and Beam dimensioning in Workflow 1



	Id.	Fx [KN] Fy [KN] Fz [KN]	Mx [KN] My [KN] Mz [KN]	Fx [KN]	Required TEX [n] = 1200/0.800 × Fx × γ		Area [mm ²] = Fx/δ × γ	Rovings min [n] = Required TEX+10% 600 or 1200	
					Required TEX	Required TEX +10%		600 TEX	1200 TEX
REACTIONS	A	5.984760 1.826951 0.639492	0.00 0.00 0.00	5.98	47561.01	52317.11	55.49	88	44
	D	9.809230 0.011660 1.098981	0.00 0.00 0.00	9.81	77954.15	85749.56	90.95	144	72
	G	9.806413 0.008597 1.098541	0.00 0.00 0.00	9.81	77931.76	85724.93	90.92	144	72
	INTERNAL BEAMS		MAX Nx	3.17	25226.95	27749.64	29.43	48	24
			AVERAGE Nx	1.66	13182.65	14500.92	15.38	26	13

Membrane architecture: the seventh established building material. Designing reliable and sustainable structures for the urban environment.

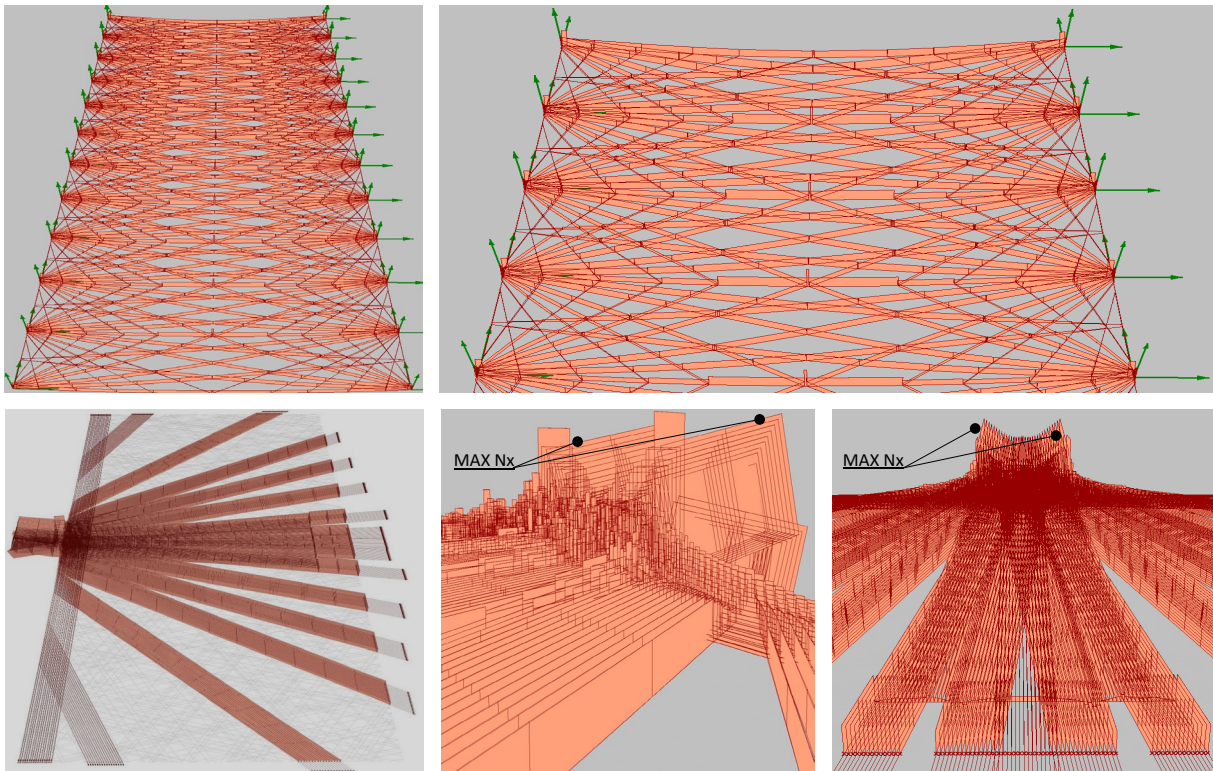
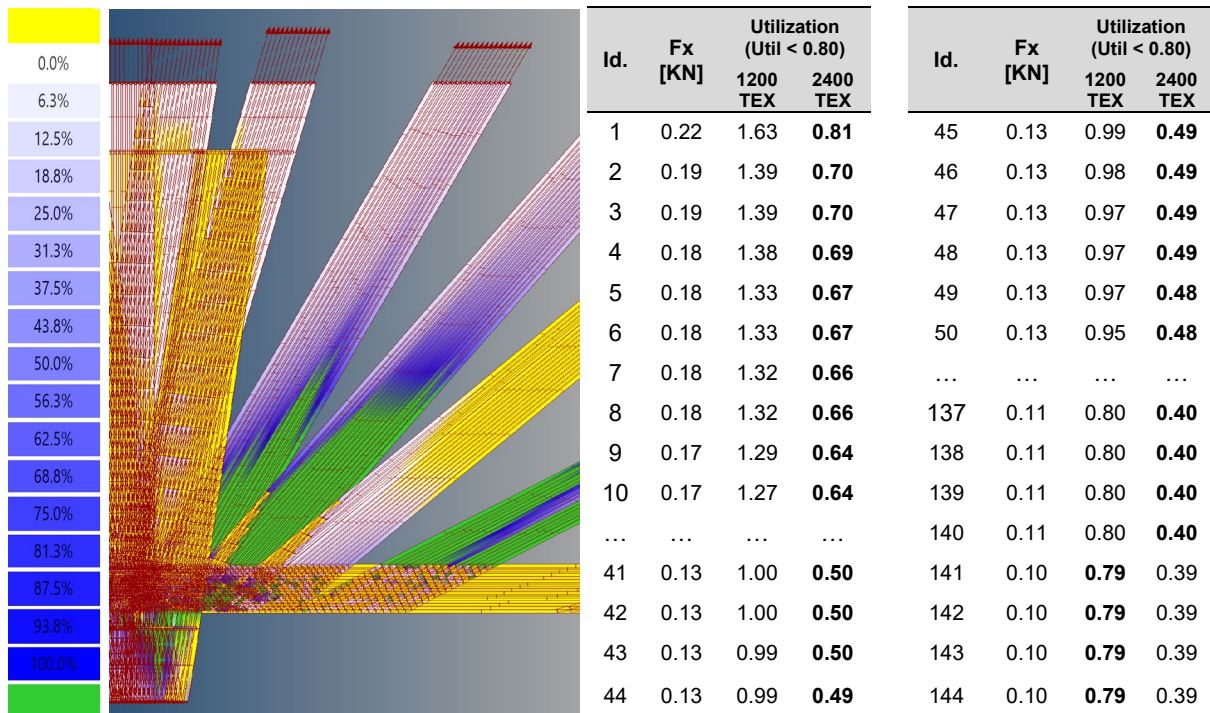


Figure 9: axial force diagram of the membrane and detail on a reaction node

Table 7: detail on the utilization of a reaction node (yellow < 0%, green > 100%) and extract of roving sort list, containing elements with Util>0.80 to be reinforced with fibreglass 2400 TEX (1 Beam = 16 rovings)



5.2. Workflow 2: Beam analysis using an evolutionary algorithm

Through a genetic script, this second stage calculates the optimum the cross-section area for each Beam starting from a possible range of widths and heights. The operation reduces the maximum vertical deflection (from 7.28 to 1.28 mm) and optimizes the area - and consequently the number of rovings - needed for each Beam of the structural layer.

Fitness function is used in genetic programming to guide simulations towards optimal design solutions (Leitão et al., 2017). In particular, each design solution is commonly represented as a string of numbers (referred to as a chromosome). After each round of testing, or simulation, the idea is to delete the n worst design solutions, and to breed new ones from the best design solutions. Each design solution, therefore, needs to be award with a figure of merit, to indicate how close it came to meet the overall specification, and this is generated by applying the fitness function to the test, or simulation, results obtained from that solution.

Variety of the genotype is obtained substantially in two ways: a combinatorial process of the genes, thanks to the different contributions of the parents in the field of sexual reproduction, and by the random gene mutations. For each generation, the so-called pool of genes is constantly changing; since the phenotype variations that make additive contributions to the adaptation type, the continuous improvements take long time, giving rise to major changes. This process is called additive evolution and the consequence of this process is the tendency to generate individuals that are always better adapted to the environment (natural selection). The fitness function must not only correlate closely with the designer's goal, it must also be computed quickly. Execution speed is significant, as a typical genetic algorithm must be iterated many times in order to produce a usable result for a non-trivial problem (Christensen et al., 2015).

The Software Grasshopper offers the possibility to use the genetic solver Galapagos for finding the minimum or maximum of a given fitness function. A fitness function is a particular type of objective function that is used to summarize, as a single figure of merit, how close a given design solution is to achieving the set aims. Figure 10 shows the interaction of the Galapagos component with plugs “FitnessFunction” and “GenePool”. The first one calculates the value of the fitness function, while the second one is a dashboard showing the parameter values. For the structural design of membrane for the retractable roof, once fixed fiberglass type in 1200 TEX, cross sections of Beams are optimized in order to minimize the vertical deflection, through the fitness function described in equation (1) with x = Beam cross section length (genotype), y = Beam cross section height (genotype), z = deflection (fitness), f_d = yield strength; γ = safety factor.

$$xy \frac{600 f_d}{0.35 \gamma} \leq z \leq xy \frac{1200 f_d}{0.80 \gamma} \quad (1)$$

Membrane architecture: the seventh established building material. Designing reliable and sustainable structures for the urban environment.

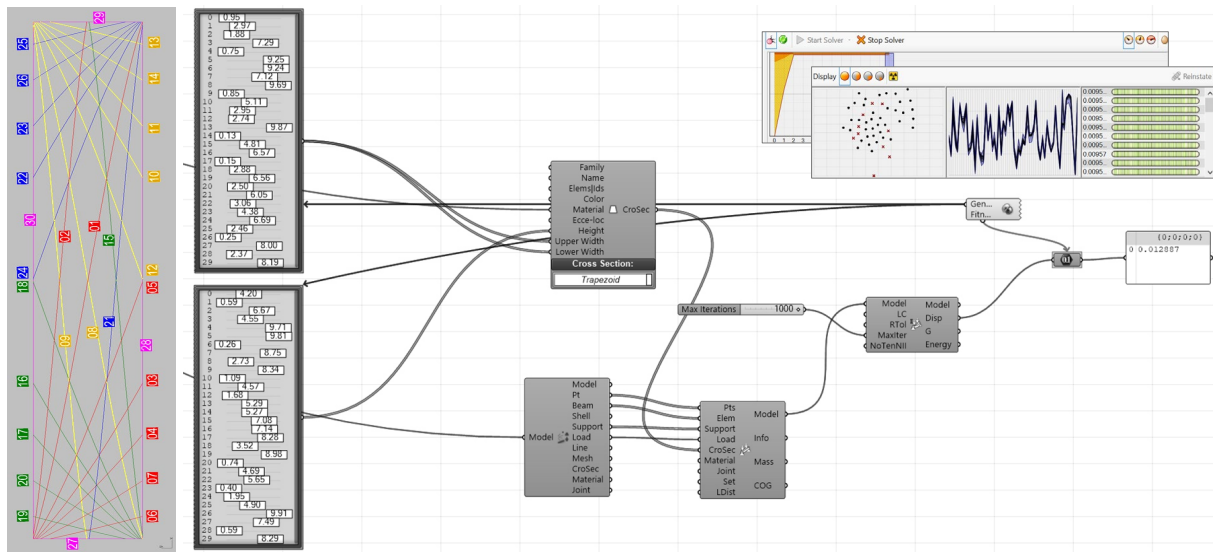


Figure 10: Galapagos setup in Rhinoceros Grasshopper (Workflow 2) for optimizing the rovings' cross sections and minimize the displacement

5.3. Workflow 3: Beam and Shell analysis

Workflows described above can't assign the structural element properties to the whole surface of the membrane, thus represent a limit for taking into account all the boundary conditions, e.g. sail effect of the membrane caused by high gusts. To affine the analysis it is necessary to consider the contribution of Shell elements in order to identify a proper design for the base layer, e.g. defining the number of mesh patterns that need to be layered. Pattern corresponds to geometries of cruciform samples tested on Textiles Hub; the material properties are assigned using data obtained from the mechanical test shown in Table 2.

The design starts from the representation through a surface mesh. A mesh is an approximate representation of a tridimensional surface through a polygonal surface made of adjacent triangles. The mesh obtained with the "MeshBrep" component of Grasshopper is a single entity formed of many triangles that cannot be taken individually. By assigning the shell properties to the triangular elements of the mesh, it would not be possible to optimize the thickness of the individual triangles, but only to consider the thickness of the most stressed element. To obtain greater flexibility and the possibility of assigning thicknesses to each triangular element, it is necessary to operate on each triangle of the mesh, e.g. exploding the mesh in individual triangular faces and, from these ones, rebuilding a new mesh. The resulting mesh is not a single object but is formed by several entities equal to the number of faces; thanks to Karamba component "MeshToShell" it is possible to optimize the numbers of layers for each face using the component "ShellCroSec" linked to a "GenePool".

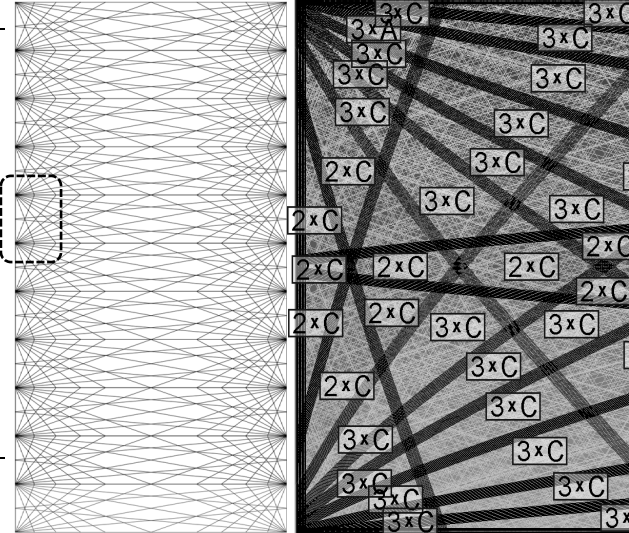
Initially the procedure performs the optimization of only the Beam elements, which form the structural layer, operating on a configuration in which the shell elements are always with a minimum thickness for all the iteration stage. In practice the aim is to optimize the structural

Membrane architecture: the seventh established building material. Designing reliable and sustainable structures for the urban environment.

layer considering the minimal effect of the base layer. Iterations are similar to results described in paragraph 5.2. Through Galapagos, it is possible to optimize the area of the Beam cross sections starting from a possible range of dimensional variables. The operation drastically reduced the maximum vertical displacement, optimizing the area required for each group of rovings. Once cross sections of Beam elements have been determined, they are considered fixed, while the base layer is optimized under suction and pressure loads until the number of layered Shells - obtained by overlapping geometries type C with various orientation - is minimized per each single face that tessellates the mesh. The result is a generative design that performs the permeability of mesh pattern founding on the utilization of the single Shell elements (Table 8).

Table 8. data input of Workflow 3 and output of layered Shell elements (type-C) needed per each face

Shell Material	
Type	TYPE C
Breaking strength 1	420.65 N
Breaking strength 2	127.48 N
Strain 1	1.539 %
Strain 2	0.042 %
Stress 1	14.022 KN/m
Stress 2	4.583 KN/m
Coeff. thermal exp. 1-2	-5.60 10 ⁻⁶ /K
Specific weight	0,88 KN/m ²
Load	
Suction	0.7x0.133=0.09 KN/m ²
Pressure	0.3x0.133=0.04 KN/m ²



6. Conclusions

This paper has introduced an interactive methodology developed to integrate structural analysis in the architectural design environment of mesh structures from the early conceptual design stage. Workflow 1 improves exchange of data between the design environment of Rhino Grasshopper and the FEM analysis in Karamba. Interoperability with file XLS and XML provides intuitive setup and visual aids in order to facilitate the process and enable students and professionals to quickly analyze and evaluate multiple design variations (Wallin, Wasberg, 2016). This encourages them to explore several design alternatives, while considering the structural performance.

Moreover, when architects and students gradually start to manage the software and data input-output of performance analysis, thus learning how to set the design variations they wish to analyze beforehand, they can easily automate the analysis process through the use of

Membrane architecture: the seventh established building material. Designing reliable and sustainable structures for the urban environment.

evolutionary tools (Workflows 2 and 3). Galapagos, in combination with Grasshopper, allows a much easier generic problem/objective specification and solver to operate. Multiple numeric range sliders are generated in permutations to define genomes that gradually affine results towards the optimal design solutions, such as the best orientation of Beams or the curvature of non-planar surfaces. It is possible to use the same approach to generate both a detailed model of a node - e.g., reactions and /or internal joints - or precise representations at architectural scale. Further investigation may examine the mechanical characterization of polymer joints between rovings, in order to upgrade the precision of the analysis and enable this methodology to the calculation of tridimensional tensile meshes and large-span geometries.

References

- Ahmad Z., Sirková B. K. (2018), Tensile behavior of Basalt/Glass single and multilayer-woven fabrics. *The journal of the textile institute*, 109(5), 686-694.
- Azmi A. S., Ahmad Nizal N.A.B., Ismail P.M.A., Ngadiman N. (2022), Study on Mechanical Properties of Organic and Non-Organic Fibre Panel Board, *Multidisciplinary Applied Research and Innovation*, 3(1), pp. 266–281.
- Besnard G., Hild F., Roux S. (2006), Finite-element displacement fields analysis from digital images: application to Portevin - Le Châtelier bands. *Experimental Mechanics* 46, pp. 789-803.
- Cho J., Park J. (2021), Hybrid fiber-reinforced composite with carbon, glass, basalt, and para-aramid fibers for light use applications. *Materials Research Express*, 8(12), 125304.
- Christensen J.T., Parigi D., Kirkegaard P.H. (2015), Interactive tool that empowers structural understanding and enables FEM analysis in a parametric design environment. *Proceedings of IASS IASS 2014 Brasilia Symposium: Shells, Membranes and Spatial Structures: Footprints - Computational Methods*, pp. 1-8(8).
- Lecompte D., Smits A., Sol H., Vantomme J., Van Hemelrijck D. (2007), Mixed numerical–experimental technique for orthotropic parameter identification using biaxial tensile tests on cruciform specimens. *International Journal of Solids and Structures*, n. 44 (5), pp. 1643-1656.
- Leitão, António, Renata Castelo Branco, and Carmo Cardoso (2017), Algorithmic-Based Analysis. Protocols, Flows, and Glitches. *Proceedings of the 22nd Annual Conference of the Association for Computer-Aided Architectural Design Research in Asia*, Suzhou, pp. 137–147.
- Preisinger C., Moritz H. (2014), Karamba - A Toolkit for Parametric Structural Design. *Structural Engineering International*, n. 24 (2), pp. 217–221.
- Schmid, F.C., Haase, W., Sobek, W. (2015), Textile and film based building envelopes–lightweight and adaptive. *Journal of the International Association for Shell and Spatial Structures*, 56(1), 61-74.
- Wallin D., Wasberg M. (2016), *Parametric Design of Building Structures in Cooperation with Architects: Usage and Evaluation of Structural Plug-ins in 3D Visualization Software*. Master's Thesis, KTH Royal Institute of Technology, Stockholm.
- Zhang, Y., Li, Y., Ma, H., & Yu, T. (2013). Tensile and interfacial properties of unidirectional flax/glass fiber reinforced hybrid composites. *Composites Science and Technology*, 88, 172-177.



tensinantes2023 : TensiNet Symposium 2023 at Nantes Université

Membrane architecture: the seventh established building material.
Designing reliable and sustainable structures for the urban environment.

Proceedings of the Tensinet Symposium 2023

TENSINANTES2023 | 7-9 June 2023, Nantes Université, Nantes, France

Jean-Christophe Thomas, Marijke Mollaert, Carol Monticelli, Bernd Stimpfle (Eds.)

Parametric workflow approach in membrane design, from details to construction

Rémi JOURNO*

*formTL ingenieure für tragwerk und leichtbau gmbh

Güttinger Str. 37, 78315 Radolfzell, Germany

remi.journo@form-tl.de

Abstract

Complex geometries using membrane envelopes are often used as illustration for parametric architectural design. The generation of freeform has never been as easy as nowadays, through the democratisation of tools like Grasshopper for Rhinoceros3D for example. Doing so, details are often overlooked, while the focus is kept on the optimisation of the membrane parameters.

The membrane, although resulting in a complex form, actually depends on simple geometric parameters (points, border conditions, cables, bars...). It is the form-finding solver that deals with the complex task of generating the final 3D shape.

But the details are depending on the form-finding geometry itself. They must adapt to it, intersect with it, keep distance to it, or provide water tightness. In designing those envelopes, we need a workflow that adapts to this type of geometry for different situations, for each update of the rerun of the form-finding routine.

How does a good parametric workflow allow to extend the parametric design approach of the form-finding of membranes structures further into the project development?

How can it be applied to the detailed design, the workshop planning, the creation of a BIM model, and the construction?

This paper will present examples of detailed design parametric workflows both for membrane and ETFE envelopes. Using grasshopper for Rhinoceros3D as a core, we are able to both link existing software, and develop custom tools, either project specific, or reusable on other structures. It will explain how using a smart constellation of parametric tools allows for a better planning, communication, and organisation of the production

Keywords: parametric design, workflow, grasshopper, Rhinoceros, details, membrane, ETFE

Membrane architecture: the seventh established building material. Designing reliable and sustainable structures for the urban environment.

1. Introduction

Membrane structures, due to their geometry, always required a computational approach. The early membrane designer could already rely on a software, or at least on a bit of code, to solve the geometric form-finding. The obtained geometry was then used to run stress calculations. It is no different nowadays, except that we also design the rest of the elements on our computer (main and secondary structure, clamps, aluminium profiles, ...). A modern designer has then to work parallelly with different software to model all the components of its construction. Interoperability between those is important, as it allows the membrane design to be better controlled and planned.

The question of work-flow appears. We are able to create connections between the different software we use. It also becomes possible to create a feedback loop to automatically update the geometry. Which key steps of membrane design are we able to integrate into a parametric work-flow?

With Rhinoceros and its plug-in Grasshopper as a core, we propose an integrated parametric design work-flow for membrane structures. First, we will explain how we can parameterise the input files for our form-finding, and automatically generate geometry that adapts to a given context. Then we will give examples of parametric detailing, or how the detail design is automatically processed using the membrane form-found geometry. Finally, once our model is complete, we will show how this model can be directly used to generate post processing information, for example for the workshop planning. We will illustrate our process with a case study project by going through each of our design steps.

2. Project description

The project that we are going to showcase is a disc-shaped cushion roof over Poznan's remodelled Łazarski Market Square, in Poland (Figure 1). It was completed in 2021. Two large ETFE cushions make up this roof. Each cushion is made of two layers (one up, one down). Both layers are 300 μm ETFE. The cushions are reinforced with radial cables, giving the roof its recognisable repetitive geometry. The cushion roof covers an area of about 2400 m^2 . A steel support grid forms a table construction featuring an outer, middle and inner ring. The grid is made up of box profiles aligned at right-angles with rigid connections to the supports. Large-dimensioned cushions attached to the three rings form the pneumatic roof structure. The span of the outer cushion is approximately 13.5 m all around; the inner cushion's maximum span is approximately 17 m, tapering to less than 1 m at both ends. Openings in the foil cushions allow the grid supports to pass through the lower side of the cushion structure at certain points.

Source: B. Stimpfle & D. Emmer, "ETFE-Überdachung des Rynek Łazarski in Posen, Polen". *Bauingenieur* 29/10/2021.

Membrane architecture: the seventh established building material. Designing reliable and sustainable structures for the urban environment.

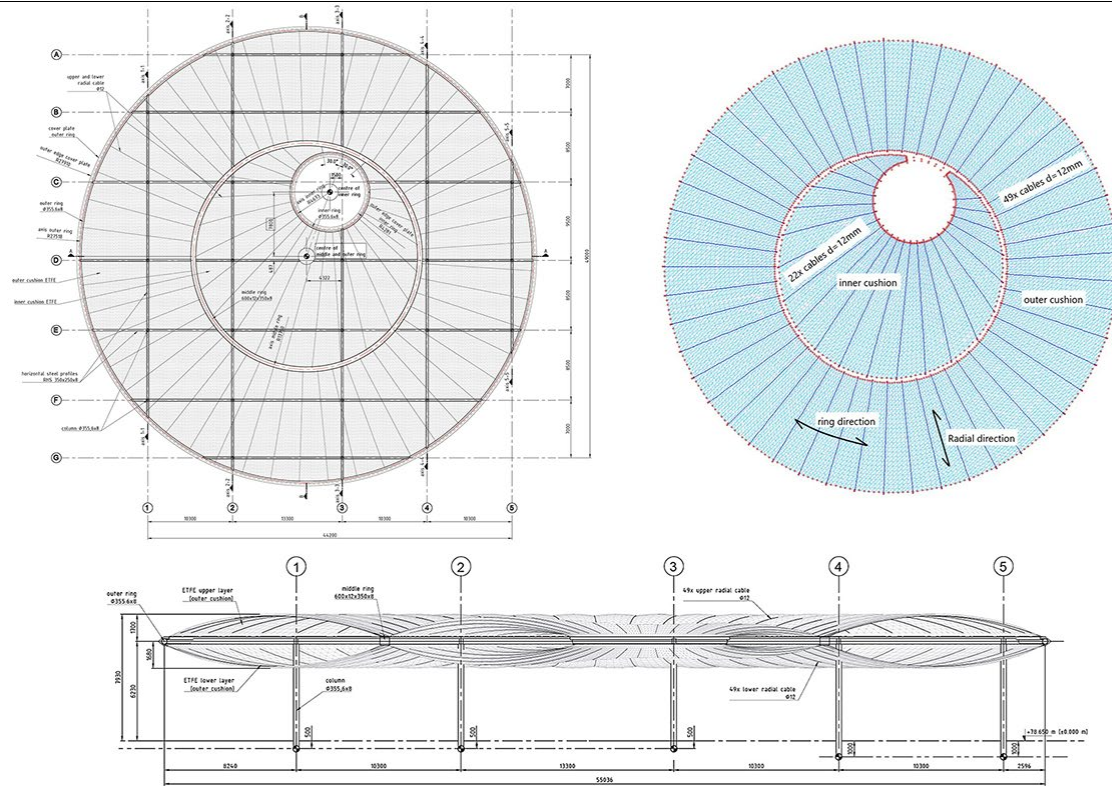


Figure 1: Overview and cross section

3. Parameterize the form-finding inputs

Membrane form-finding and calculation software typically need simple geometrical inputs. They can be directly drawn in the software, but often enough the geometry will be communicated with a text file (Figure 2) containing the coordinates and information about the geometrical objects. Remodelling the geometry or having to type the input file is time consuming, and can lead to mistakes. Furthermore, it slows down the optimisation process between the global model and the solved geometry.

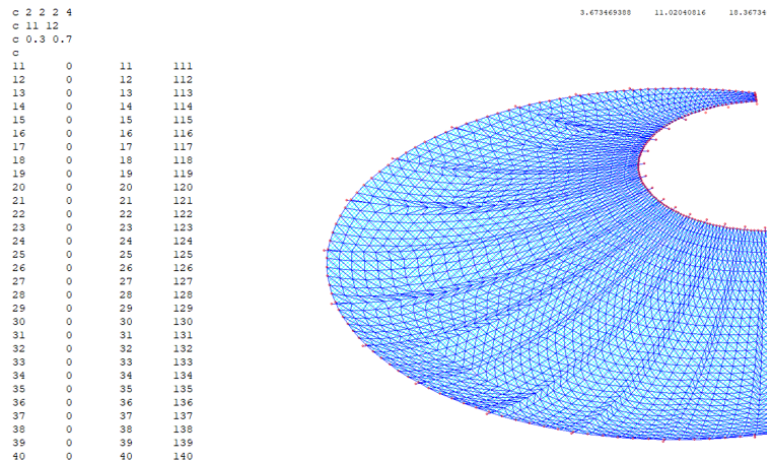


Figure 2: Example of an input file and its solved form-finding

Membrane architecture: the seventh established building material. Designing reliable and sustainable structures for the urban environment.

3.1. Identifying the parameters

Inputs parameters have to be as simple as possible. First the coordinates of each key point. Then the global geometrical shapes such as circles, arch, lines, etc...

In our case study project, we have three circles, each with a centre and a radius (Figure 3). These circles define the border of the membrane. In field, we have radial cables, centred on the same point as the circles, we must only define their amount, and a starting point for the division.

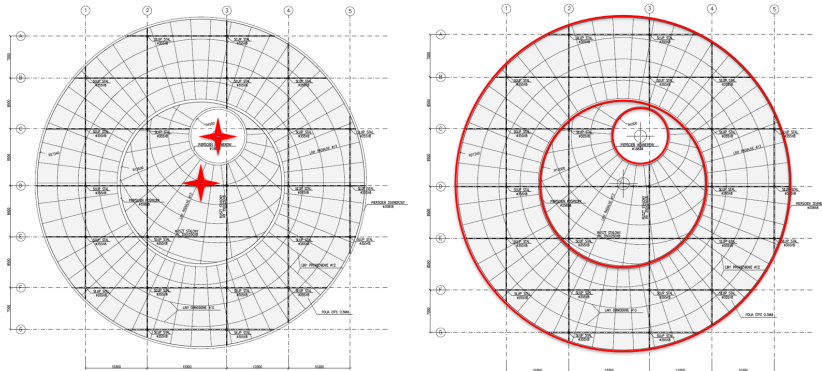


Figure 3: Geometrical parameters

3.2. Automate the input file

With the help of Rhino and Grasshopper, we can link the 3D geometry to the solver. A few lines of code let us export the coordinates and geometry in a .txt file (Figure 4). We can reference the parameters and generate the input file for the solver. This fast automatic export allows us to go back and forth between the input geometry and the solver result. We can adapt the input geometry, or the deformation of the membrane in the form-finding parameters.

We also get to play with an extra layer of parametric possibilities, if we generate part of (or the total of) the geometry with Grasshopper. We can then quickly explore many variations of our project by quickly generating many input files and comparing the results back in our 3D software.

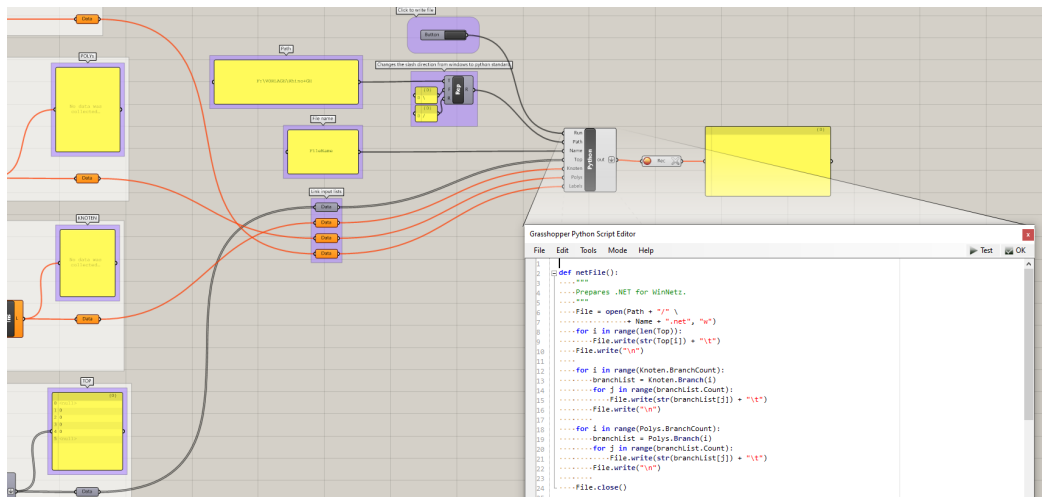


Figure 4: Grasshopper definition to write the input file from Rhino

Membrane architecture: the seventh established building material. Designing reliable and sustainable structures for the urban environment.

4. Parametric detailing

The details are usually modelled after obtaining the membrane geometry out of the form-finding. Indeed, many elements are directly depending on the membrane geometry itself to be placed and/or designed. It can also be, that once the details are created in 3D, a situation occurs where we need to rerun the membrane solver. In that case, having a parametric work-flow allows us to quickly readjust and update our details. We end up creating a feedback loop, where the membrane geometry defines the ground parameters for the details, and where vice-versa, the details will be used to readjust the membrane geometry.

4.1. Detail positioning

The first type of parametric detailing is simply the placement of details. We have a typical detail that comes up several times in our project. But this element is oriented differently each time it is placed, because it has to follow the tangent of the membrane geometry.

In this example, the lower layer of the membrane is penetrated by columns in several grid points (Figure 5). Each of these penetrations is solved with a ring detail that has to be geometrically oriented to fit the best tangent alignment possible to the membrane (Figures 6 & 7). It is important that the tangent follows the membrane geometry as closely as possible, in order to respect the integrity of the membrane calculations.

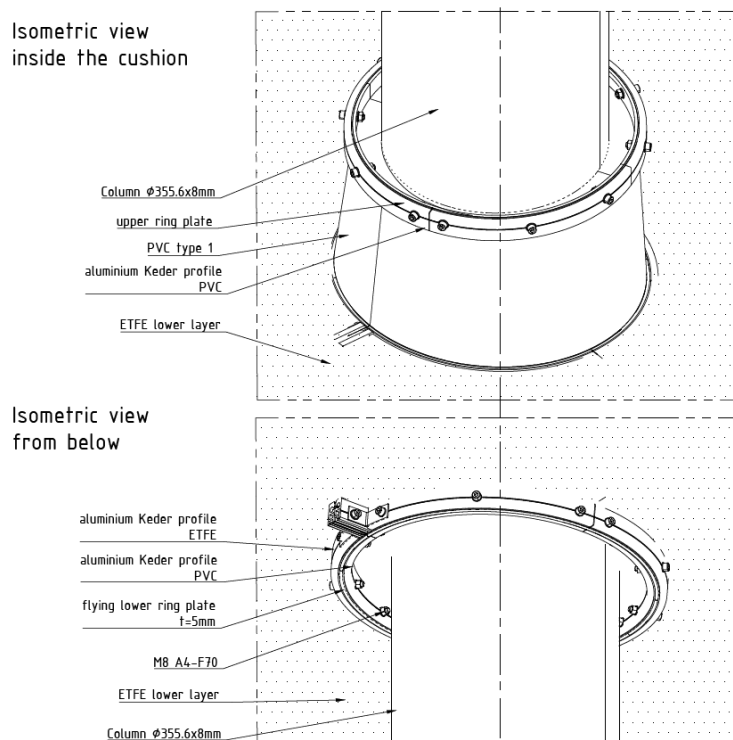


Figure 5: Penetration detail to be placed

Membrane architecture: the seventh established building material. Designing reliable and sustainable structures for the urban environment.

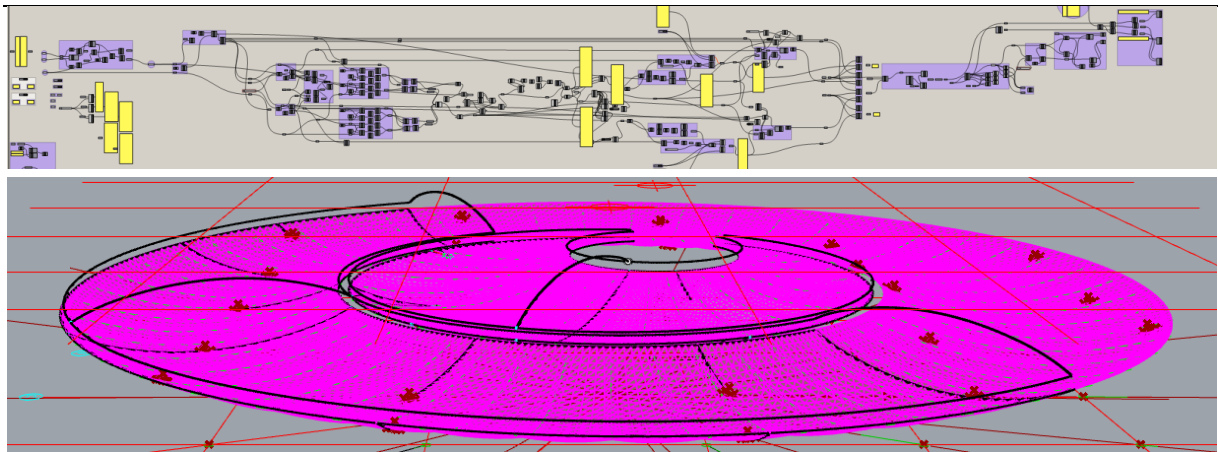


Figure 6: Grasshopper definition for the detail placement

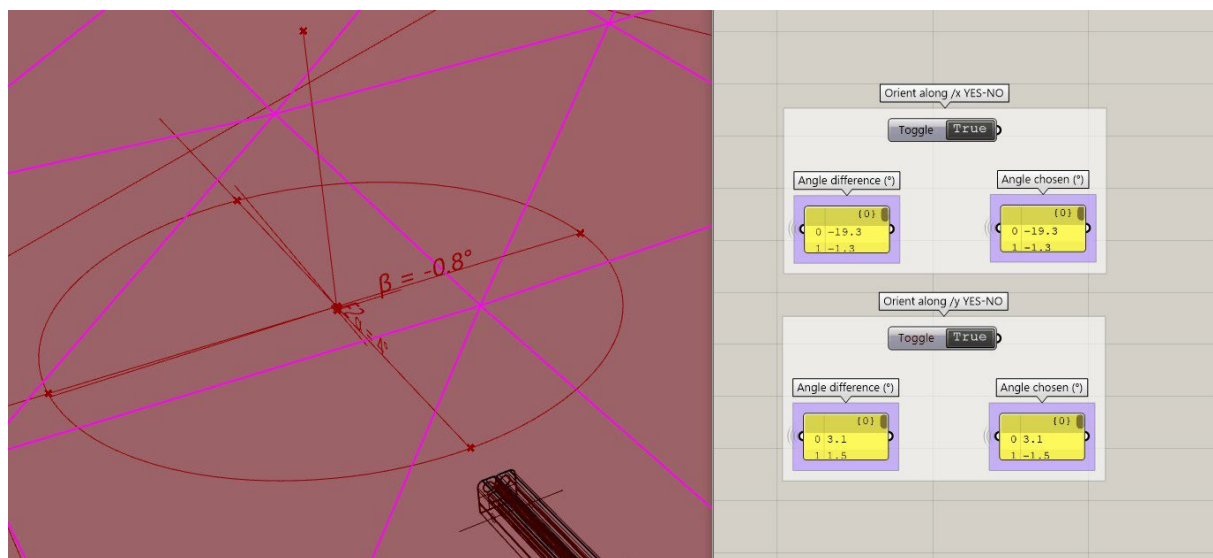


Figure 7: Penetration detail placement with adaptive angles

4.2. Clamping profiles optimization and modelling

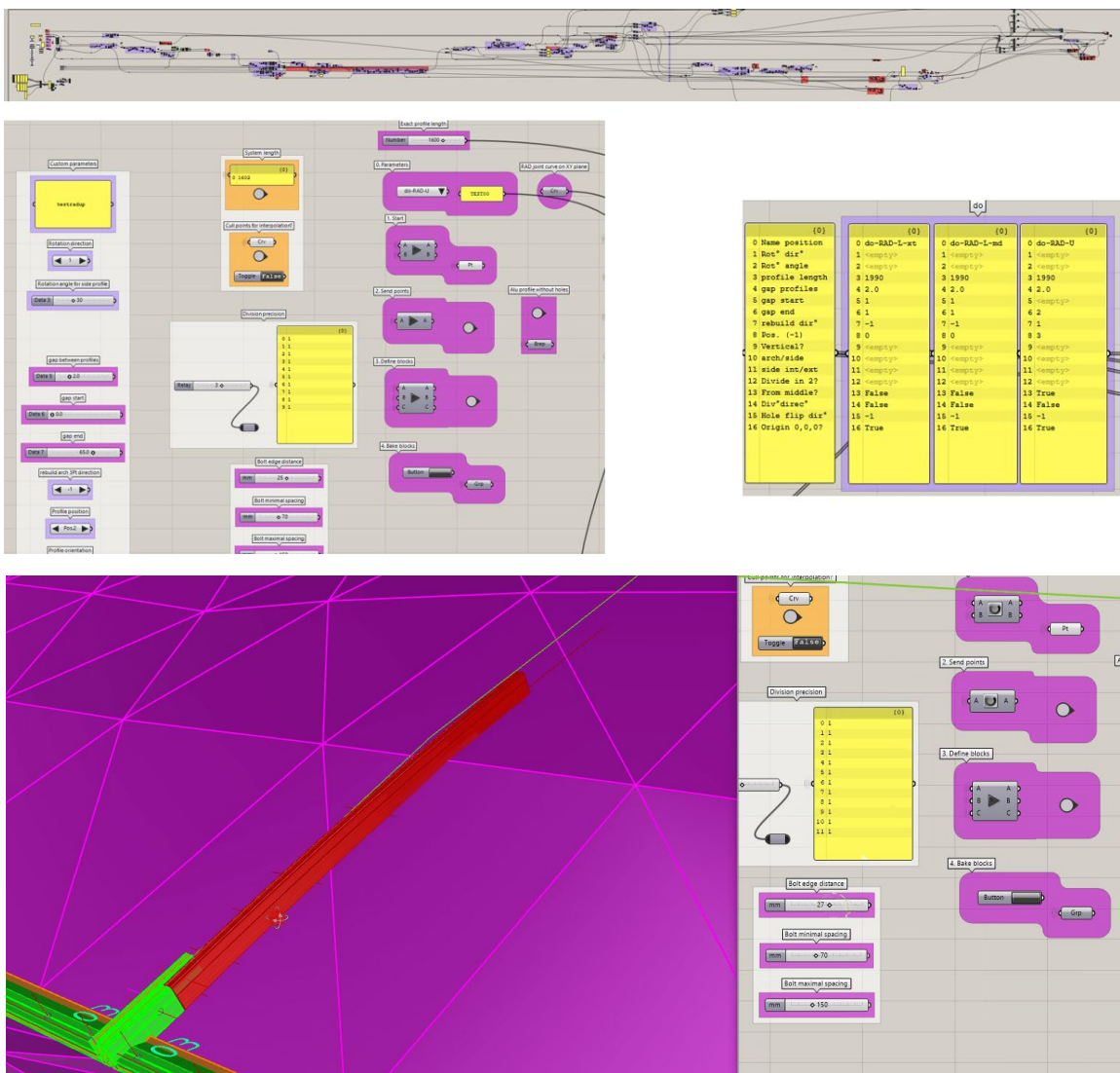
The second type of details are the clamping aluminium profiles. In opposition to the previous ring details, they have to be custom made for each position. That is to say, we cannot simply place a predetermined block, we also have to model the object first.

There are two types of profiles in this project: the radial ones, cutting through the curvature of the ETFE cushion, and the tangent ones, on the free edges of the ETFE, linking it to the primary structure. In both cases, we first try to fit as many similar elements as possible, in order to have standard repetitive parts for the construction. Parameters such as: maximum length, bolt spacing, and minimal residual length are used. For the radial profiles, we not only have to consider the length, but also the radius. Since those follow the cushion's shape, the radius varies along the curve. It means that we have to take in an acceptable tolerance when we discretize the curve into many arches with a fixed radius.

Membrane architecture: the seventh established building material. Designing reliable and sustainable structures for the urban environment.

The Grasshopper definition takes as input both the membrane and some geometric features of the project to know where the radial joints are. It then optimises each zone with as many repetitive elements as possible. Finally, it creates 3D blocks of each single profile type, and places it in the 3D model (Figure 8).

The advantage of such a process, is that if the membrane geometry changes, we can rerun our script, and have the aluminium profiles quickly updated. The other advantage is that we already obtain separate blocks to identify the repetitive parts. This will help us later in the workshop design phase.



Membrane architecture: the seventh established building material. Designing reliable and sustainable structures for the urban environment.

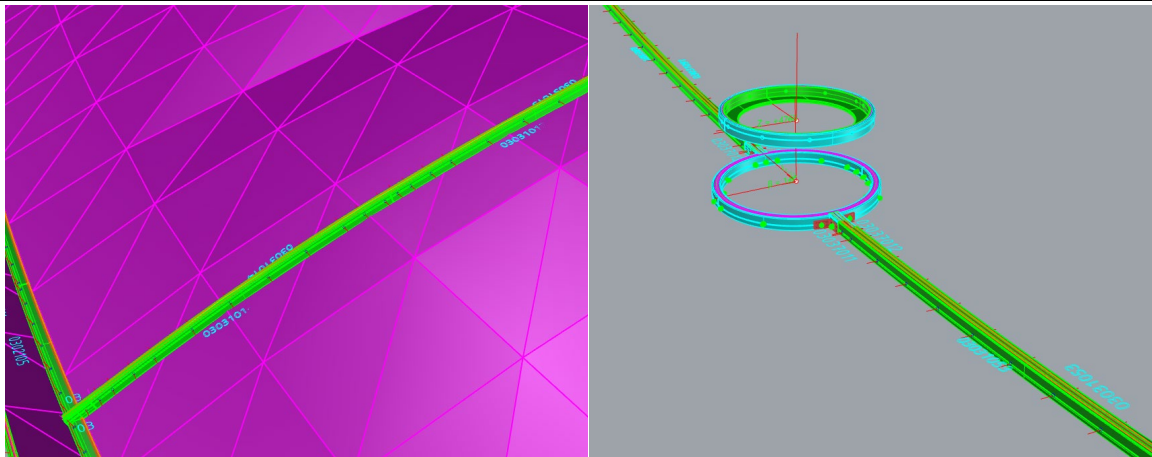


Figure 8: Grasshopper definition for clamping profiles

4.3. Collision optimisation

Finally, details can also be placed using optimisation algorithms, such as the ones given in the Galapagos component of Grasshopper (Figure 9). For the lower tangent profiles, we also had to give as a design parameter some forbidden zones for the fixation bolts. Those were zones where we would have steel plates on the main structure, placed here to attach radial cables. The cables were impossible to move, since they drive the shape of the ETFE, but the aluminium profiles could be adapted to still have a repetitive length, and avoid any collision between the bolts and the steel plates. As a result, we obtain a full model of our details, following exactly the shape of the membrane (Figure 10).

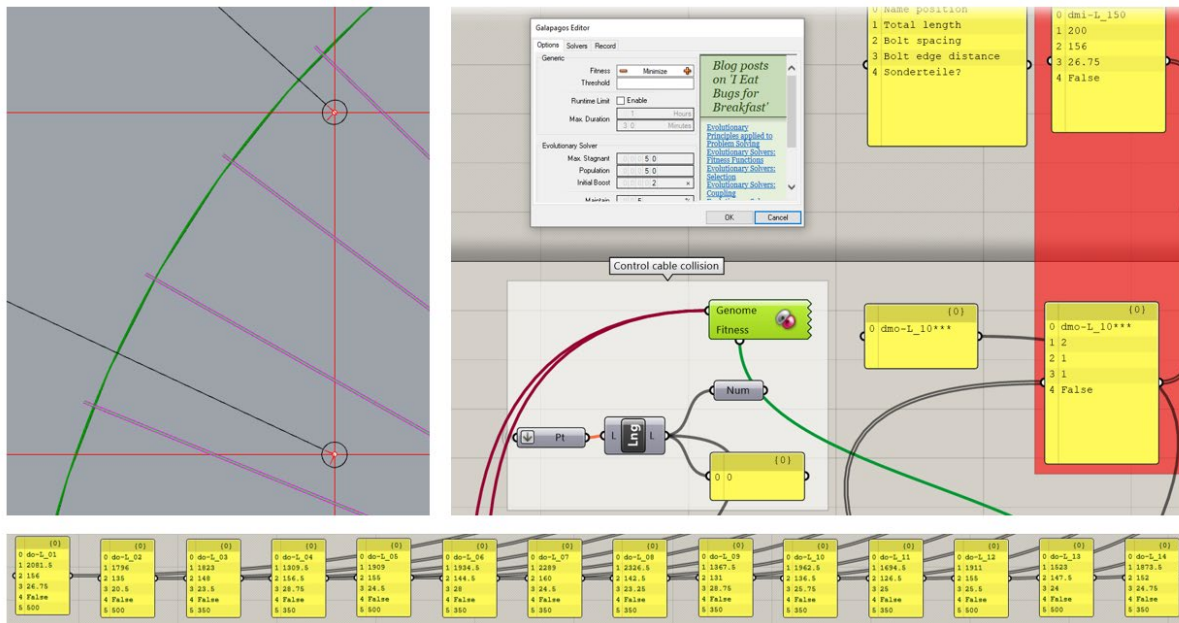


Figure 9: Grasshopper definition for the collision optimisation

Membrane architecture: the seventh established building material. Designing reliable and sustainable structures for the urban environment.

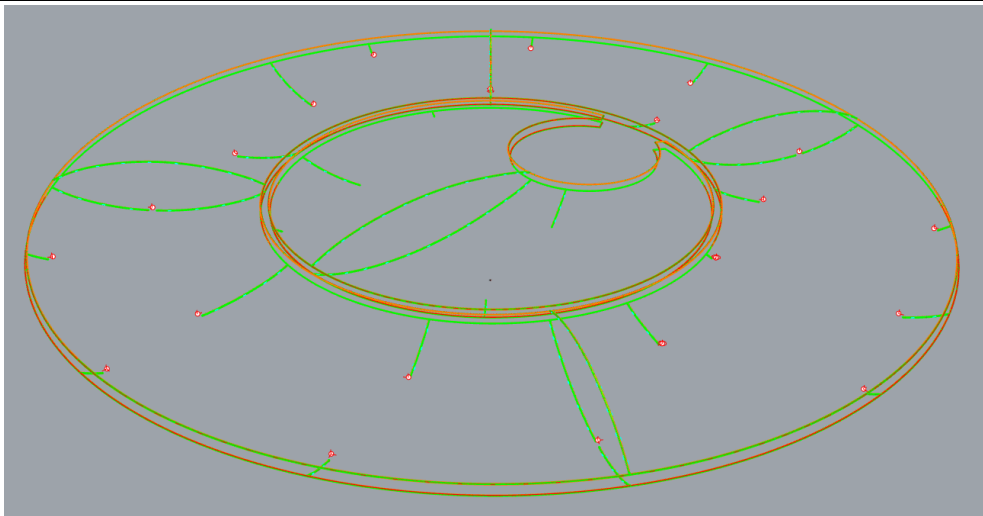


Figure 10: Details model, depending on the membrane geometry

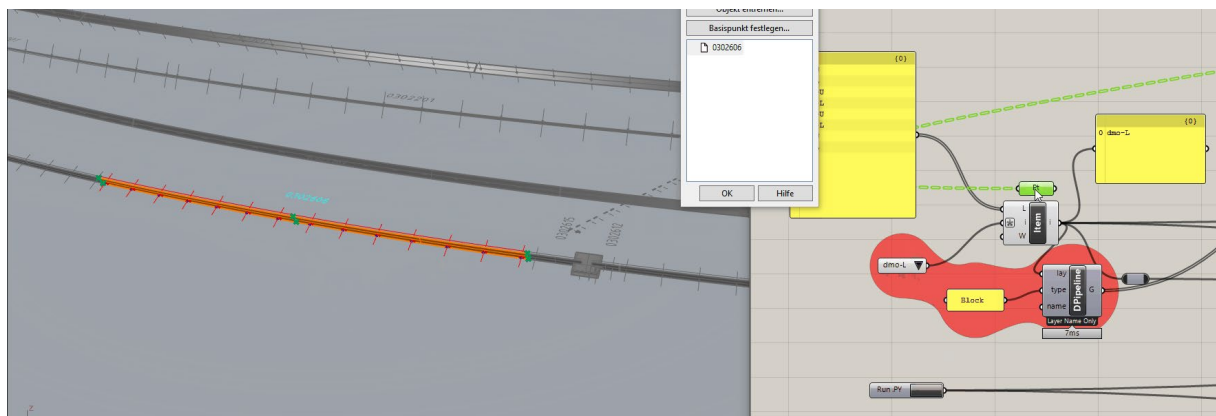
5. Post processing

One of the advantages of having a fully detailed 3D model as a result, is that we can then use it to extrapolate information. These can be for example used to produce the elements, or to feed a shared BIM model.

5.1. Aluminium profiles workshop planning

As we saw before, the aluminium profiles are generated as repetitive blocks in our model, each with their own name. It means, we can use this block with name repetition to generate the drawings to produce them.

Another Grasshopper definition lets us select a profile type and export it as a .txt input file into another software that we use to generate flattened profiles (Figure 11). The flattened profiles are each plotted in separate CAD files, ready to be submitted to the workshop. Information like position, length and quantity can all be extracted from the model.



Membrane architecture: the seventh established building material. Designing reliable and sustainable structures for the urban environment.

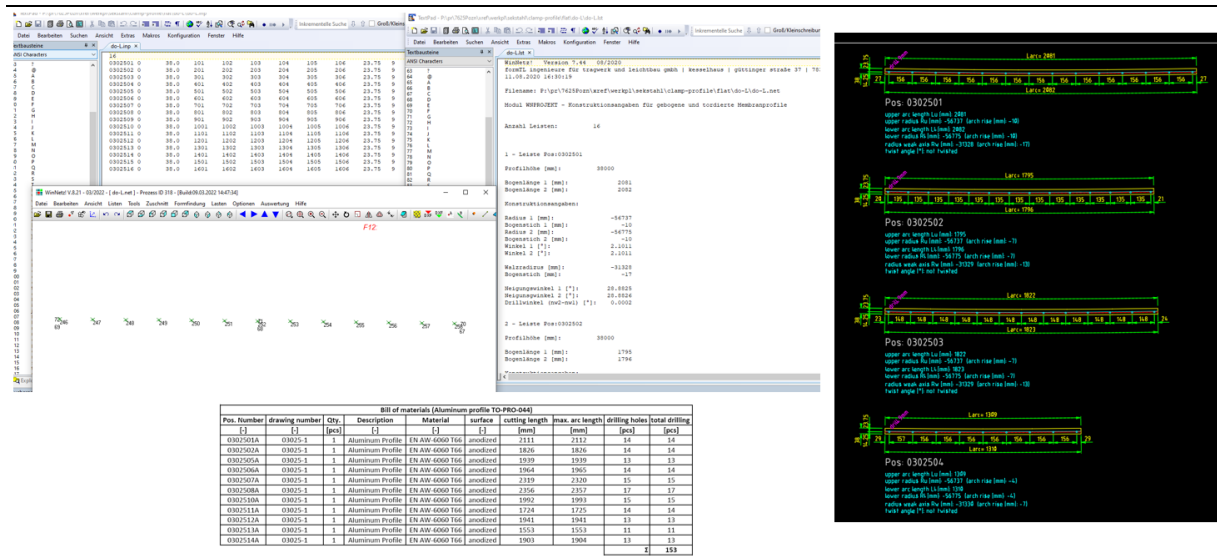
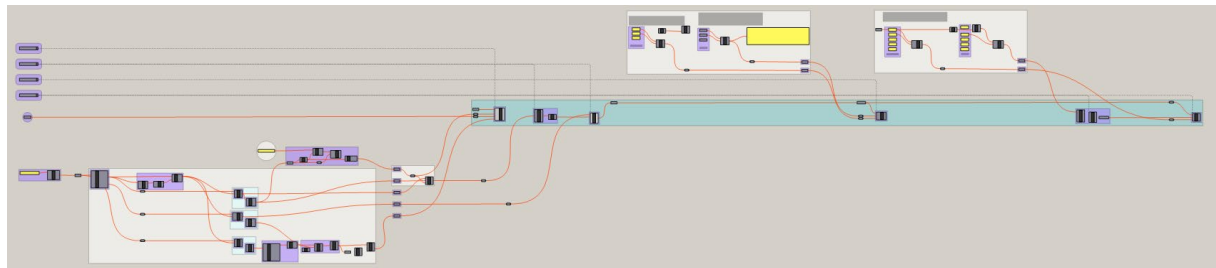


Figure 111: Grasshopper definition for the workshop drawings of the aluminium profiles

4.3. BIM model

In a later development, Rhino and Revit can be linked together with what is called Rhino Inside Revit. Basically, it allows both software to run alongside, and send info to each other using Grasshopper. Having a fully modelled project, we can use this connection to send our geometry with relevant BIM information to Revit. It being, either the membrane, the aluminium details, or anything else. We opted for a solution where we send repetitive elements (our blocks) as Revit families, giving the block name as a family type. Meanwhile the stand-alone 3D elements are sent as Revit geometry, without being part of any family. We can either export the Rhino attributes to Revit, or define specific ones during the export process (Figure 12).



Membrane architecture: the seventh established building material. Designing reliable and sustainable structures for the urban environment.

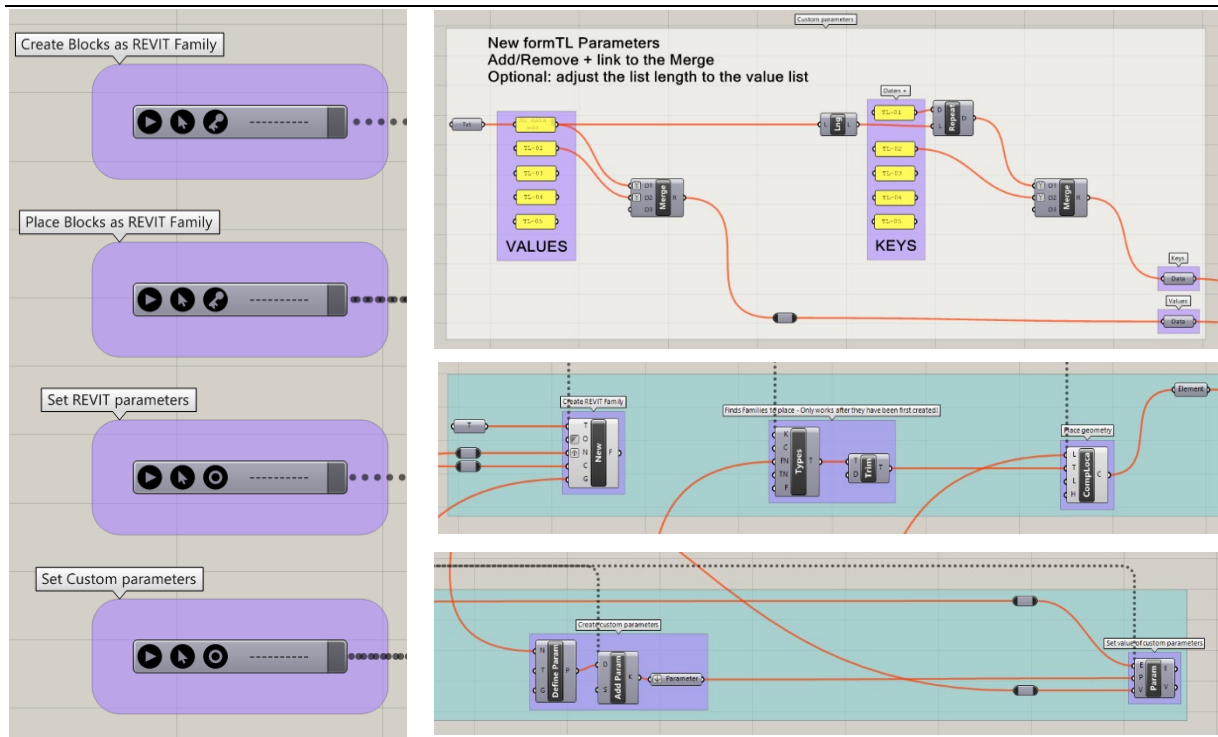


Figure 12: Grasshopper definition for the export to Revit with BIM relevant information

5. Conclusion

Using Rhino-Grasshopper as the core of a parametric workflow allows us to connect all the steps of membrane design together. We are able to give geometrical input to the form-finding solver. We can then use this geometry to develop the details. The modelled details can be sent to production, and the geometry can be used to feed a BIM model.

Meanwhile all of these steps are no longer evolving on a one-way timeline, but retroactively able to influence each other. We can always go back one step with the experience we received from a previous iteration.

Membrane architecture: the seventh established building material. Designing reliable and sustainable structures for the urban environment.



Figure 13: ETFE cushions after installation (source: Temme // Obermeier GmbH)

6. Acknowledgements

Architect: Jacek Bułat, Poznan, Poland

Concept design: Andrzej Kowal, Wrocław, Poland

Execution foil cushions: Temme // Obermeier, Rosenheim, Germany

Structural engineering and workshop design for the cable-suspended cushions as well as interface details: formTL Ingenieure für Tragwerk und Leichtbau GmbH, Radolfzell Germany

7. References

B. Stimpfle & D. Emmer, “ ETFE-Überdachung des Rynek Łazarski in Posen, Polen”.
Bauingenieur 29/10/2021.

P. Debney (2020), Computational engineering

R. Issa (2020), Essential Algorithms and Data Structures for Computational Design in Grasshopper - First Edition



tensinantes2023 : TensiNet Symposium 2023 at
Nantes Université

Membrane architecture: the seventh established building material.
Designing reliable and sustainable structures for the urban
environment.

Proceedings of the Tensinet Symposium 2023

TENSINANTES2023 | 7-9 June 2023, Nantes Université, Nantes, France

Jean-Christophe Thomas, Marijke Mollaert, Carol Monticelli, Bernd Stimpfle (Eds.)

Simulation-based analysis methods for differentiation strategies of CNC-knitted membranes for architectural application

Yuliya SINKE*, Martin TAMKE^a, Mette RAMSGAARD THOMSEN^a

^{*}, ^aCITA - Center for IT and Architecture, Royal Danish Academy

Philip de Langes Alle 10, Copenhagen 1435, Denmark

ybar@kglakademi.dk, martin.tamke@kglakademi.dk, mette.thomsen@kglakademi.dk,

Abstract

Knitting technology through its ability to steer material composition enables the making of architectural functionally graded membranes (AFGMem). During the last decades, the research into knitted textiles for architectural application has gained an increasing interest. There, knit is understood as an innovative material system that enables complex geometry and bespoke composition for a wide range of applications with variegated performances, such as structural membranes, partition screens, casting formworks, actuated structures, and solidified shell-like-canopies. The application, functionality, and performance of the knitted structures directly determine their material differentiation through stitch structure and define the methods for informing its material composition. This paper focuses on further investigation of the simulation-driven approach for material differentiation and presents the recent advancements and the evolution of the method, demonstrated through the material design of three cases of structurally employed membrane structures.

Keywords: computational membrane design, knitted heterogeneous membranes, textile material differentiation, structural analysis, architectural CNC-knitting.

1. Introduction

Knitting membrane through its inherent nature for material grading provides a promising alternative to the traditionally woven homogeneous materials in textile architecture. Membranes, made with knit can stretch to the required 3D shape by using encoded properties of material expansion. Through the strategic placement of various stitch types, numerical programming of knitting offers precise control over the local material variation. As a result, we are able to design and manufacture highly customized textile surfaces that respond to membrane performance demands and are zero waste in nature.

The conventional method of programming knitted textiles resides within the garment design, in which identical items are mass-produced, based on the prior extensive prototyping and manual tuning of the manufacturing files. The architectural field, however, has a greater demand for highly customized non-repetitive bespoke elements, that rely on their three-dimensionality and

Membrane architecture: the seventh established building material. Designing reliable and sustainable structures for the urban environment.

material differentiation for their structural and geometric performance. Therefore, a study of novel methods that would allow large-scale knitted membranes to be designed taking into account their structural requirements is therefore necessary.

2. Informed material variation for knitted membranes

Before the advent of numerically controlled knitting patterns, garment patterning was based on repetitive stamping of small data across the entire textile element. The emergence of computational technologies and simulation engines has made it possible to analyse the human body, leading to the development of high-performance sportswear clothing, protective and medical equipment. There the differentiation of knit patterns is informed by the body's 3D scan input and the required properties of support, compression, stretch and breathability of the designed item (Adidas, 2017; Mikucioniene et al., 2020, p.; Šurc et al., 2020; Tessmer et al., 2022).

In spatial design and architectural research, the inquiry towards the questions of informing the local variation and the development of design criteria, integration of analysis and feedback to the process have led to the identification of the two central approaches for knitted material differentiation, driven by *sensing* and *simulation* (Ramsgaard Thomsen et al., 2016; Ramsgaard Thomsen, Nicholas, et al., 2019).

With the *sensing* approach, the local sense data is collected from the site and then interfaced with the knit fabrication files. This data enables the local transformation of knit pattern structures, resulting in variegated permeability of surface light transmission properties, as seen in Sifter and Derma screens by CITA (Ramsgaard Thomsen et al., 2016) or myThreadPavilion and DataKnit by Sabin Studio (Sabin, 2013, 2021), thereby embedding an additional layer of information to the surface.

With the *simulation* approach, the material performance is digitally simulated to be interfaced with the fabrication files. In this way, the membrane's stretch and expansion behavior can be guided by placing varying stitch types across its surface. This method application is demonstrated through precedents like Isoropia and Zoirotia structures by CITA (Ramsgaard Thomsen, Sinke Baranovskaya, et al., 2019; Sinke, Ramsgaard Thomsen, Tamke, et al., 2022), or Knitted Composite Tower by Tonji University (Liu et al., 2020) and MeiTing Canopy by Southeast University of China (Liu et al., 2022).

In this publication, the authors focus on further investigation of the simulation-driven approach for knit material differentiation and present the recent advancements and the evolution of the method through the pattern design of three cases of structurally employed tensile knitted membrane structures.

Further presented membrane material designs rely on the simulation-based approach for defining their structural shape and providing the material local differentiation guidance based on the presented analysis methods. These methods differ in their evaluation of the performance criteria of each design, which is described in detail in the methods chapter and discussed through the demonstrated design cases of Zoirotia (from 2021 and 2023) and Graded Ceiling Canopy (Figure 1).

Membrane architecture: the seventh established building material. Designing reliable and sustainable structures for the urban environment.

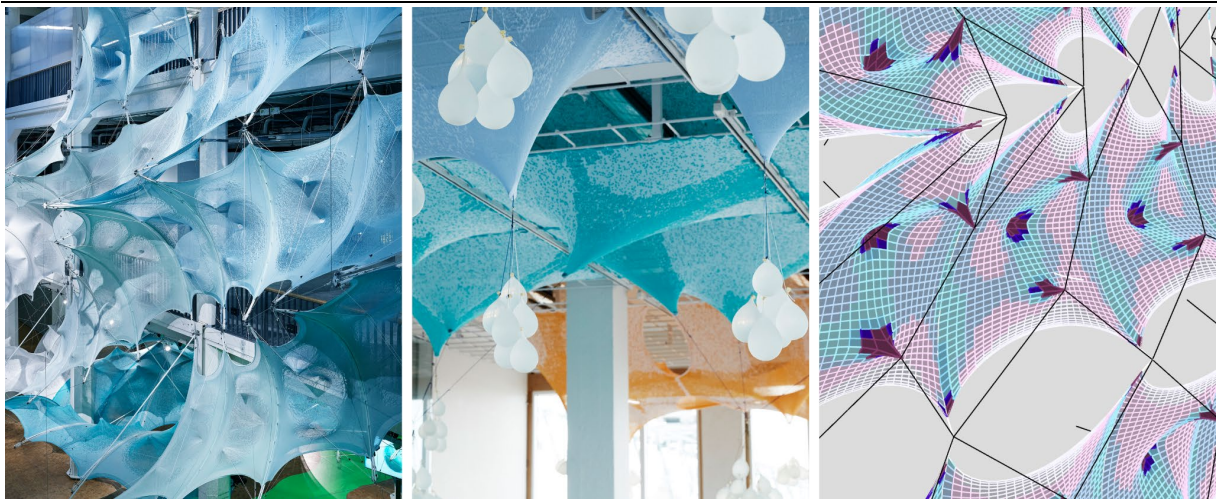


Figure 1: Three design cases, presented in the paper (left to right) - Zoirotia, Graded Ceiling and Zoirotia 2.0

In the first design case - Zoirotia - the distribution of stitches is informed by the form-finding simulation and supported by the geometrical analysis in order to achieve material differentiation allowing the membranes to expand further out from their planes. The second case - Graded Knitted Ceiling, challenges the non-perpendicular tension of the fabric and therefore explores an alternative approach towards material differentiation through the use of simulation-supported structural analysis of surface tensile utilisation. There, identifying the tension concentration on membranes enables the placement of stitches of larger and smaller dimensions to guide membrane expansion. The third case is a digital exploration of reapplying the method of structural analysis for material differentiation back to the first design case of Zoirotia.

3. Method - from form-finding to material programming

In this paper, we discuss *analysis methods* that have been recently developed as part of a comprehensive design-to-production workflow for CNC-knitted membranes, the advancement of which incrementally increased in the work of authors within research activities of CITA - Center for IT and Architecture for the past years (Deleuran et al., 2015; Ramsgaard Thomsen, Sinke Baranovskaya, et al., 2019; Sinke Baranovskaya et al., 2020; Sinke, Ramsgaard Thomsen, Albrechtsen, et al., 2022).

There are several steps in the workflow itself, including the preparation of pre-form-finding geometry (membrane boundaries, anchors, other interfacing elements), followed by the form-finding relaxation to reach the equilibrium shape. Afterward, the form-found membrane is analysed, linking the geometrical form of the membrane design to the surface differentiation of the material. Further, the data from the analysis is translated into pixel-based maps, containing information on stitch selection and the industrial knitting machine actions. These steps are briefly described below, with the primary focus on the analysis part of the workflow.

3.1. Form-finding

Form-finding is widely used for the design of woven-based tensile structures and is crucial in determining the equilibrium shape of tensile membranes, where the forces are set in balance. For designs made up of multiple textile pieces, a well-form-found membrane model informs the cutting pattern of the membrane elements in order to ensure an optimal fiber arrangement and efficient material use. With CNC-knitted membranes, form-finding allows not only to

Membrane architecture: the seventh established building material. Designing reliable and sustainable structures for the urban environment.

resolve the elements cutting pattern, but also to define the stitch-based membrane composition for steering material properties.

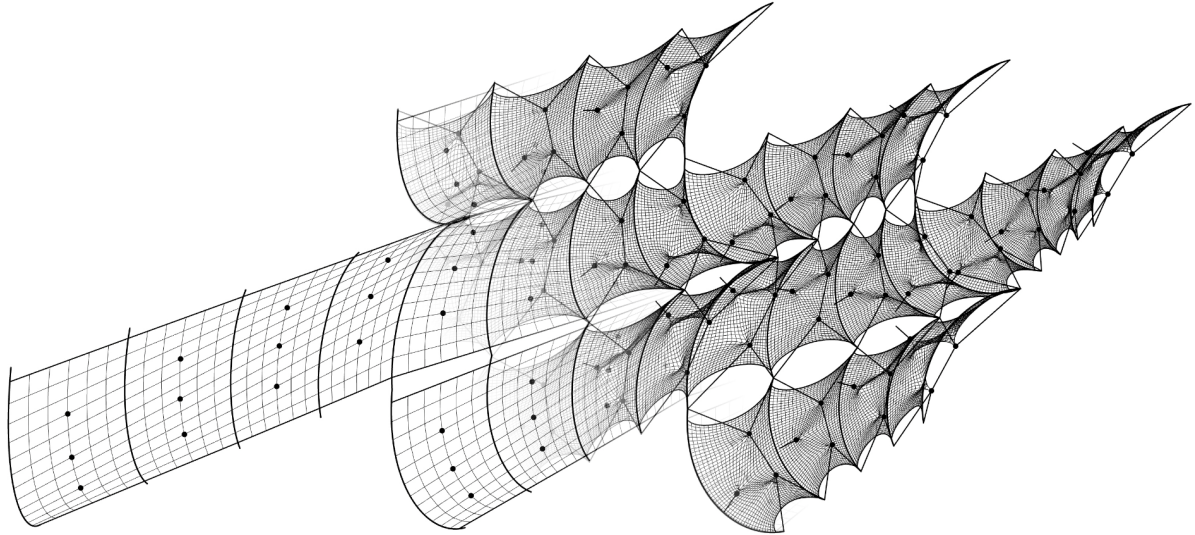


Figure 3: The form-finding set up (left side) and the corresponding equilibrium relation (right)

The form-finding setup and visualization take place within the Grasshopper (David Rutten, 2007) environment for Rhino modelling software (Robert McNeel & Associates, 1980), where the physics simulation engines such as Kangaroo (Piker, 2013) and K2 Engineering (Brandt, 2016) plug-ins can be applied. There is a difference between the two plug-ins in terms of how the mesh properties are assigned in relation to tensile membrane form-finding. Both plug-ins are spring-based and use mesh edges (lines) as a ground for material input. Unlike Kangaroo, which requires the *spring target rest length in mm and abstract strength value as inputs*, K2Engineering operates with structural inputs of spring Young Modulus (MPa), pre-tension (Newtons) and spring cross-section area (m²). This permits the use of the form-finding simulation in conducting further analysis of the design, based on the structure's modifications and performance during the process of form-finding.

3.2. Analysis - geometrical and structural

In further described design examples, the priority for the membrane design is to achieve a controlled expansion of the membrane surface. This is done by the means of strategic distribution of larger and smaller stitch types across the surface for membrane three-dimensionality. For that, the research has developed two methods of surface evaluation - *geometric* and *structural*, where the differences lay in surface evaluation approaches (Figure 4).

The time-based digital form-finding permits the analysis of geometrical performance through the comparison of membrane state *before* and *after* applying the loads. This informs the knitting pattern and leads to an integrated membrane design with a stronger connection between the geometry and material composition, unlike in the knitted material designs, where arbitrary and manually defined surface differentiations are loosely connected to the global geometry and structural performance (Ramsgaard Thomsen, Sinke Baranovskaya, et al., 2019; Sinke Baranovskaya et al., 2020).

Membrane architecture: the seventh established building material. Designing reliable and sustainable structures for the urban environment.

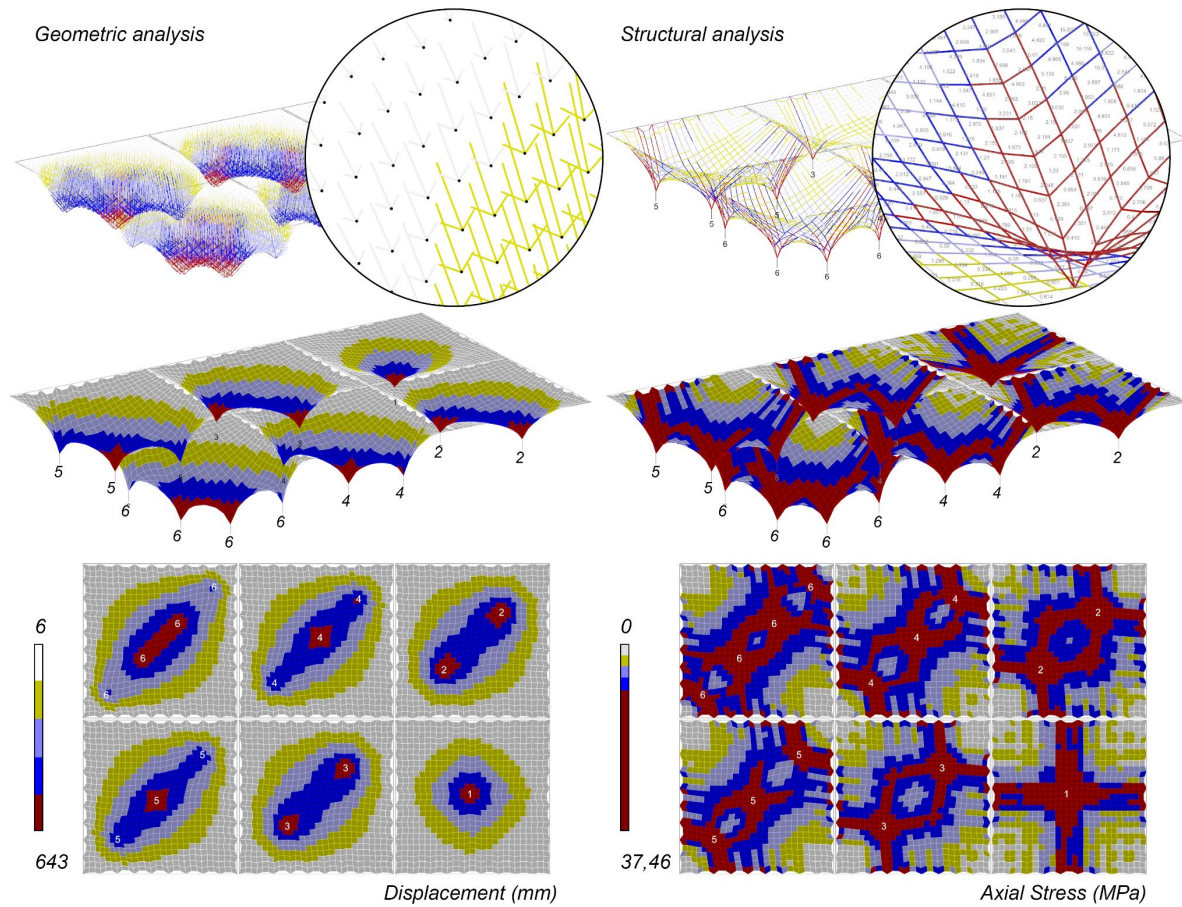


Figure 4: Diagram of geometric analysis (left) vs. structural analysis (right) approach for pattern generation

With the *geometric* analysis approach, the membrane surface is evaluated on the subject of mesh displacement over the process of form-finding. For that, the mesh face center trajectories that occur as result of form-finding are measured. The longest trajectory occurs in the point of an applied load (pull with the weight) and gradually reduces further from this point. This type of calculation can be conducted with both Kangaroo and K2Engineering plug-ins as pure geometric calculation of distance is performed.

The *structural analysis* approach relies on the forces distribution calculation in order to determine the areas of the meshes that undergo the biggest stress when under the applied loads in order to reach the final required pretension. It is crucial to use K2Engineering Solver engine for initial form-finding, as it allows to compare the axial stress (σ) within mesh before and after the loads are applied, where Bar/Cable is the simplest structural element, that transfers forces through the axial action. Here, the BarOutput component of the plug-in calculates the axial stress values F per each mesh edge, following the formula (Equ. 1), where F is the axial force [N], E - Young Modulus [MPa], A is the cross-section area [mm^2], L is the current length [m and x is the extension [m]. The axial stress σ is calculated by dividing force F with the cross section area A (Equ. 2).

$$F = \frac{E \cdot A}{L} \cdot x \quad (1)$$

$$\sigma = \frac{F}{A} \quad (2)$$

Membrane architecture: the seventh established building material. Designing reliable and sustainable structures for the urban environment.

The resulting analysis data package contains a list of numerical values, where for the *geometric* approach it is the *distance*, the mesh has travelled from the initial state to the pre-tensioned state, while for *structural* analysis the values show the *axial stress* per each mesh face in MPa. These values are then used to cluster the mesh into color zones and map the values onto the geometry. Visually these two analysis mappings differ as seen in the diagram above (Figure 4). The geometric approach projects *concentric circles* around areas of applied load, while the structural analysis maps *cross-like* propagation around the areas of membrane loading.

The membrane deformation under the single point load results in a cone-like geometry, therefore when using geometric analysis - it projects concentrically in a circular manner around the points the membrane is pulled as it follows the geometrical changes. The structural analysis shows the forces taking the shortest path from the point of applied load to the edge of membrane clamping. Therefore, the mapping results in a cross-like pattern, are formed by the straight lines of forces distribution from the load point to the edges. With the increase of loading points, the resulting patterns increase in complexity, as the concentric circles and cross-like areas begin to overlap. The emerging pattern corresponds to increased mesh geometrical complexity, while also providing pattern solutions that are not possible to predict manually or analytically.

3.3. Informed differentiation and material programming

The visualisation algorithm of both analysis approaches allows for freedom in tuning the color clustering. This is defined by the number of colors and the percentage threshold of color start and end. The number of cluster colors corresponds to the mesh subdivision density (Figure 5), while the percentage threshold (%) defines the connection between the color mapping and the range of numerical values within the analysed data (Figure 6).

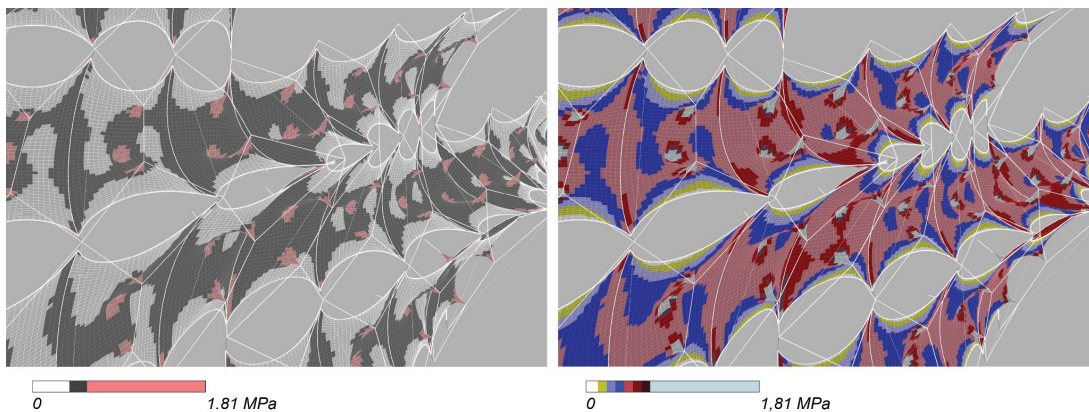


Figure 5: Color threshold diagram: 3 vs 8 colors range, shown using Zoirotia digital design case.

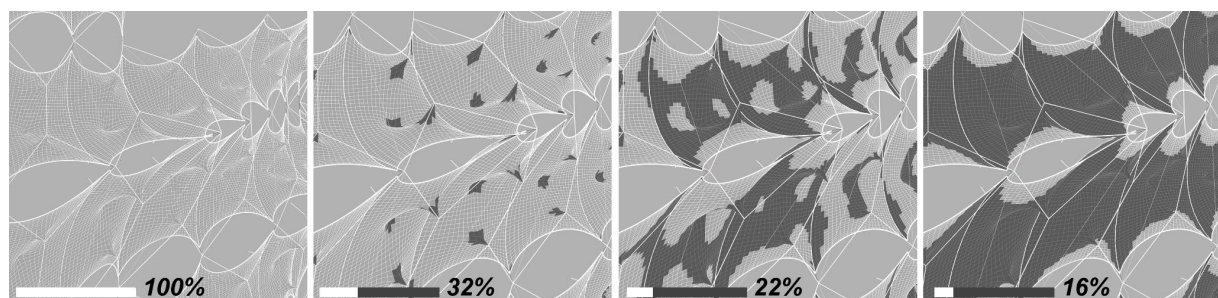


Figure 6: Gradients from 16 to 100% showing that threshold defines the part of the surface axial stress selection (here range from 0-1.56 (up to 1.81 MPa on some membranes)

Membrane architecture: the seventh established building material. Designing reliable and sustainable structures for the urban environment.

The lower threshold percent involves the values at the beginning of data list, while the higher - at the end of the list. The highest (or the lowest) values are in minority within the analysed data, representing the most extreme tension or under-tensioned areas, therefore the visualisation appears very homogeneous when taking these values. The biggest value change occurs at the range from 20-35% (in the given design case), therefore the pattern appears more geometry related and exciting, however this is largely dependent on the design and analysed geometry.

After that, the defined color clusters are used to determine the stitch density, informed by the percentage dithering technique, described in detail in the earlier publication by authors (Sinke, Ramsgaard Thomsen, Tamke, et al., 2022). Each color contains a certain density of larger stitch presence, in order to aid the stretch of the membrane in areas of either higher displacement (geometric approach) or biggest stress (structural approach) to avoid the over-utilization of the fabric and to achieve the desired well-prestressed surface with the high degree of curvature. Dithering patterns encoded in a form of planar point clouds are then translated into the color pixel-based bitmap file, that is later processed by the industrial knitting machine (Figure 7) (Sinke, Ramsgaard Thomsen, Albrechtsen, et al., 2022).

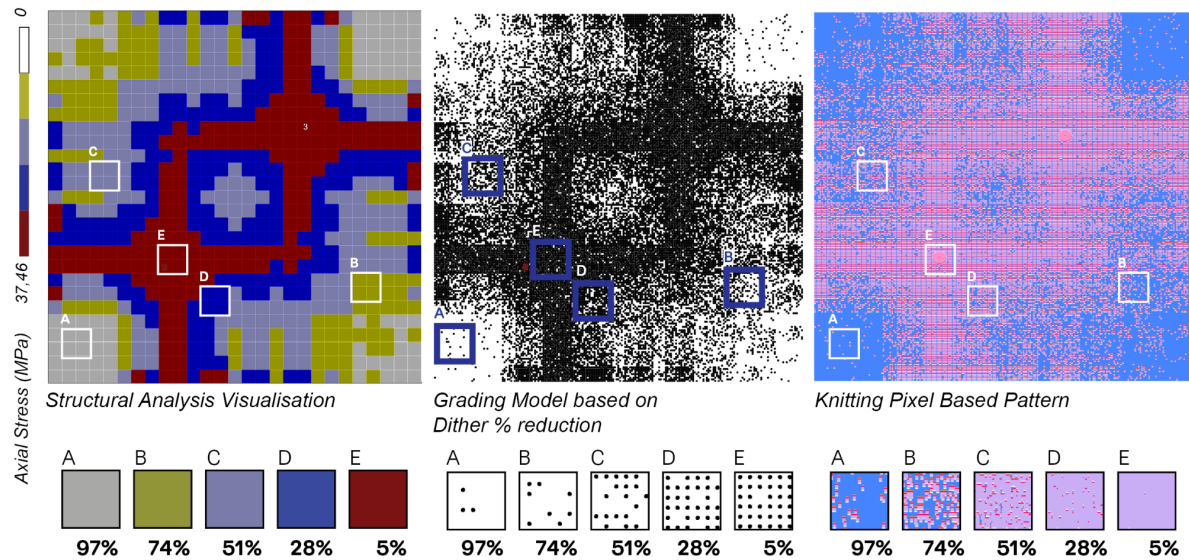


Figure 7: Translation of *structural* analysis data and surface cluster grouping into a knittable pixel-based pattern at the right resolution

4. Differentiated Knitted Membrane Design Cases

The design cases, presented below, demonstrate the application of the above-described methodological tools through differentiation patterns of membrane materials, specific to each case.

4.1 Zoirotia 2021

The first design case - Zoirotia - is a large-scale tensile installation, made of numerous bespoke knitted structural membrane units, where each is highly three-dimensional and pre-tensioned by the cablenet network. The distribution of larger and smaller stitches is informed by the form-finding simulation and supported by *geometrical* analysis, where two simulation stages are compared for the mesh displacement to identify the areas that undergo the biggest geometrical change during the simulation.

Membrane architecture: the seventh established building material. Designing reliable and sustainable structures for the urban environment.

Each membrane is tensioned between the glass fiber rods from the sides and connects to the cablenet, which provides the bending for the rods and the necessary curvature for the textile surface. The cablenet interfaces with the membrane in three points, which results in the formation of cone-like tapered protrusions of the fabric when under tension. The geometric analysis leads to a material differentiation pattern of concentric circles, converged around the points of the cablenet-membrane connection (Figure 8).

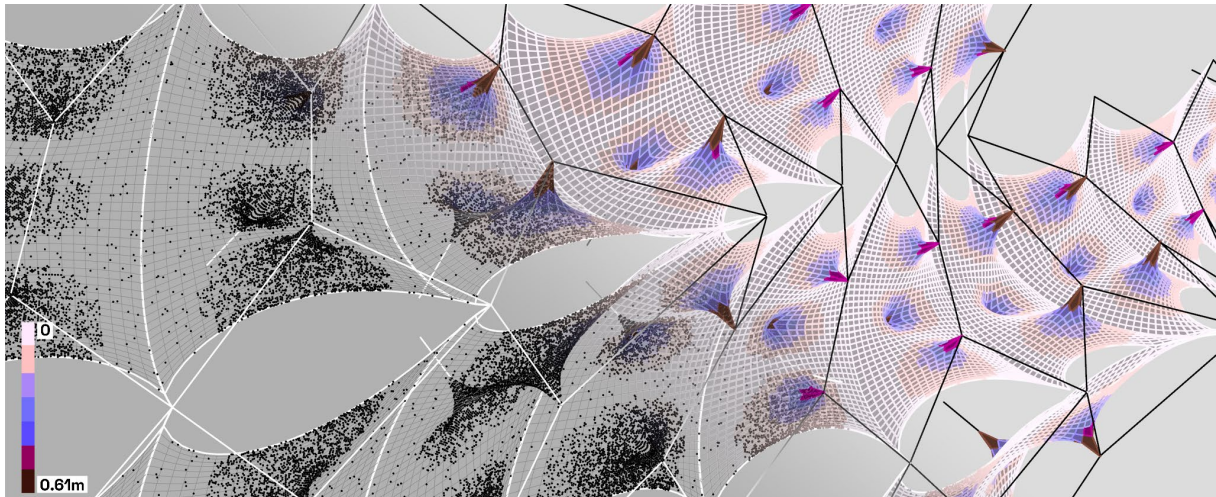


Figure 8: Clustering nature of the membrane surface (right half of image) together with informed material differentiation through dithering (left side of image), 2023.

In the initial workflow set up from the time when the installation was completed in 2021, the data from the geometric analysis was reduced to the cropped boundary of the densest color of the rich-color gradient (256 colors). The propagation of the dither pattern was then done two-dimensionally within the planarised membrane outline, rather than directly being informed by the mesh clustering derived from the analysis. This was a quick technical solution for the material differentiation part of the workflow within the given project timeline. The offset approach led to the loss of data and therefore less precise pattern definition, although close to the right one as compared in Figure 9. As described in the methods earlier, this process was later improved to maintain a more direct correspondence between form-finding and material differentiation of the membrane through the simulation-integrated mesh clustering (Figure 9, right). The zig-zag nature of the zones outlines is explained by the mesh resolution used in the simulation and post-analysis in determining these.

Membrane architecture: the seventh established building material. Designing reliable and sustainable structures for the urban environment.

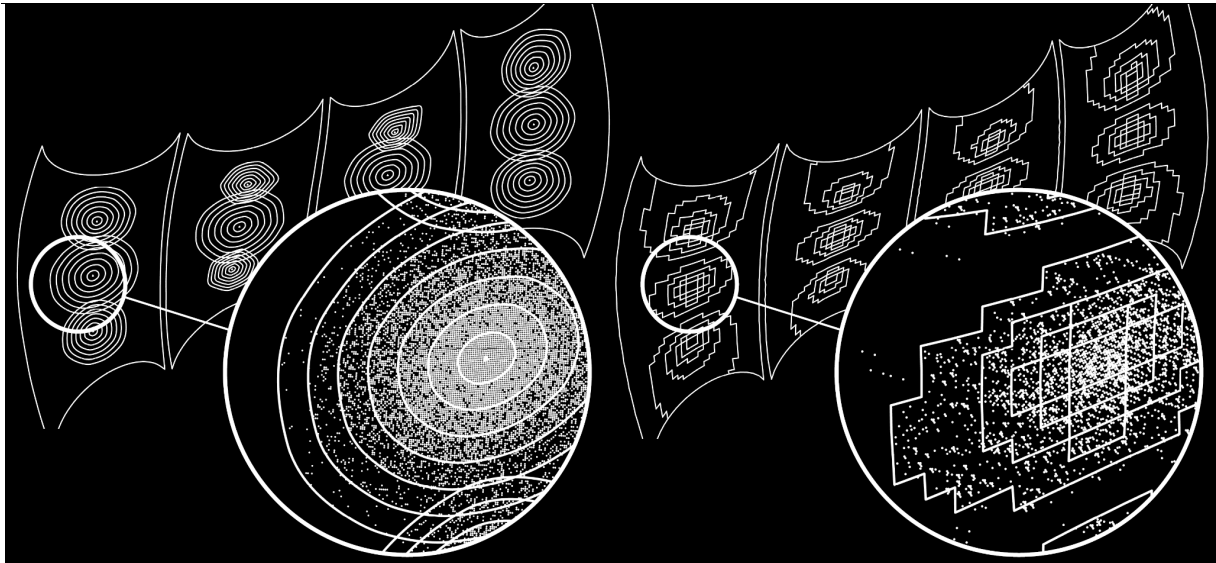


Figure 9. Material differentiation of knitting files of Zoirotia from 2021 (left) based on the planar offset vs. adjusted differentiation files from 2023 (right), based on the simulation-integrated mesh clustering, both using the geometrical analysis

4.2 Graded Knitted Ceiling Panels

The geometrical analysis is challenging to apply with the surfaces, that are not pulled perpendicular to its plane as it accounts for geometrical changes rather than the structural performance of the surface. Angled loading directions create a heterogeneous distribution of membrane surface tension, leaving some surface areas in compression, which results in textile wrinkling and underperformance (Figure 10). Insufficiently tensioned areas are preferred to be avoided within tensile membrane design as they reduce overall structural stability. For this reason and in order to maintain three-dimensional freedom of planarly produced CNC-knitted membranes, it is necessary to develop an alternative analysis approach that would lead to the generation of more suitable and well-performing knitting patterns, thereby preventing membranes from sagging when loaded in an angled direction.

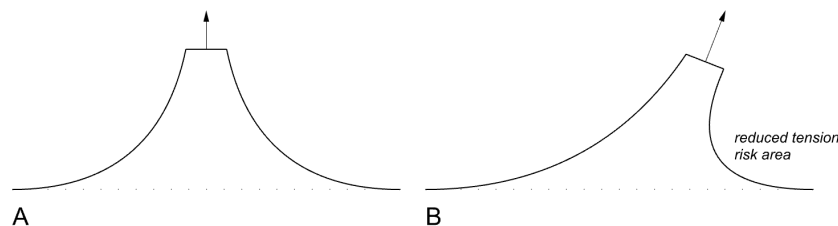


Figure 10: Perpendicular vs angled membrane loading

The second design case - Graded Knitted Ceiling Canopy, challenges and explores additional opportunities for CNC-knitted membranes material differentiation in order to permit loading direction freedom, while maintaining necessary surface tightness and expansion. This installation is a part of a workshop, held with CiA Computation in Architecture students, where the participants were testing developed by authors tools for exploring various membrane loading conditions under suspended and interconnected weights (Figure 11).

Membrane architecture: the seventh established building material. Designing reliable and sustainable structures for the urban environment.

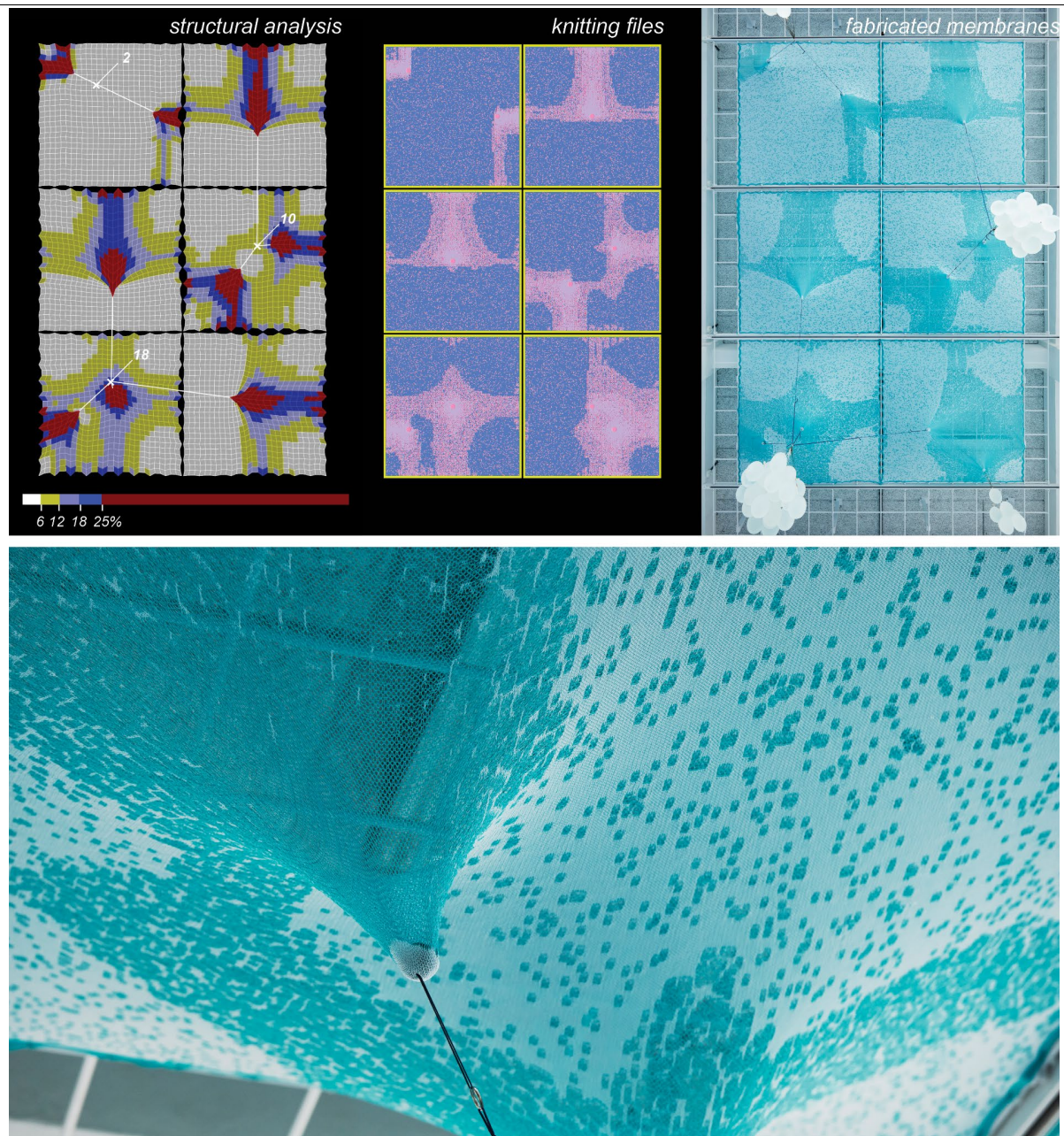


Figure 11: Structural analysis of graded panels, bitmap knitting files and the manufactured piece.

The chosen installation consists of six square textile panels made of digitally programmed CNC-knitted membranes, fixed to the ceiling. It achieves the three-dimensionality by textiles deformation under several interconnected suspended weights attached to the fabrics, thereby creating a situation where the membrane is loaded not perpendicularly, but in an angle. Consequently, this initiated the investigation into alternative patterning strategies, informed by the simulation and supported by structural analysis of surface tensile utilisation. Material programming allows the membrane expansion to be assigned only where it is needed, by concentrating larger stitches in areas of required greater stretch, while reducing stretchiness and

Membrane architecture: the seventh established building material. Designing reliable and sustainable structures for the urban environment.

therefore, the presence of large stitches in the areas of reduced tension, keeping the membrane tight.

For the reasons of method evaluation, for the same canopy design the geometric analysis based knitting pattern was prepared. In order to proof the statement that geometric analysis is not a suitable strategy for this loading case, the membrane displacement (in a shape of concentric circles around loading points) under the load is overlapped with the tension analysis, highlighted in red the areas of potential compression is provided below (Figure 12). The diagram allows us to conclude that geometric analysis would create material differentiations with larger surface area in the areas where the membrane is required to be tight and therefore structural evaluation-based analysis is necessary to be used here, to achieve a better membrane performance.

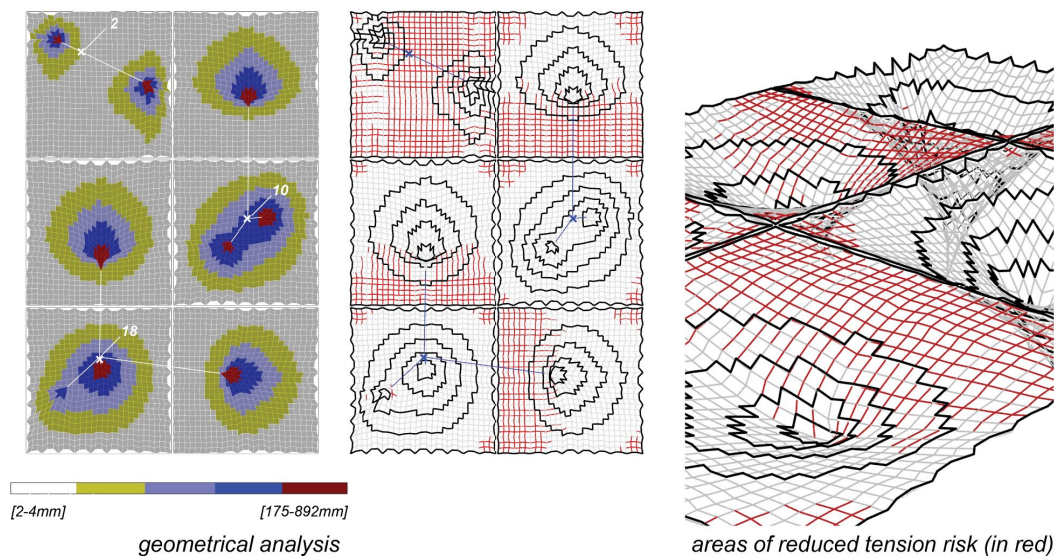


Figure 12: Diagram of material differentiation based on geometric analysis for evaluation purposes

4.3 Zoirotia 2.0 digital - 2023

The third case is a digital exploration of reapplying the method of structural analysis for material differentiation to the earlier mentioned design case of Zoirotia. This exploration allows for speculation on potential patterning outcomes of structural analysis application to a more complex design topology. The reapplication of the method results in a radically different patterning distribution in comparison to the geometrically driven approach in 4.1. In this pattern, a more sensitive approach to material differentiation is evident, as more areas of the membrane can be identified as requiring reduced or increased material density to achieve a geometrical membrane configuration as a result of stretching. A gradual change in differentiation can also be observed from the patterns once the membrane element is rotated in space or moved within the larger structure, which can be explained by the different gravity conditions applied to membranes as well as the interrelationships between membrane elements.

Membrane architecture: the seventh established building material. Designing reliable and sustainable structures for the urban environment.

In the diagrams below, we show potential patterning outcomes, applying a structural analysis for defining material differentiation models.

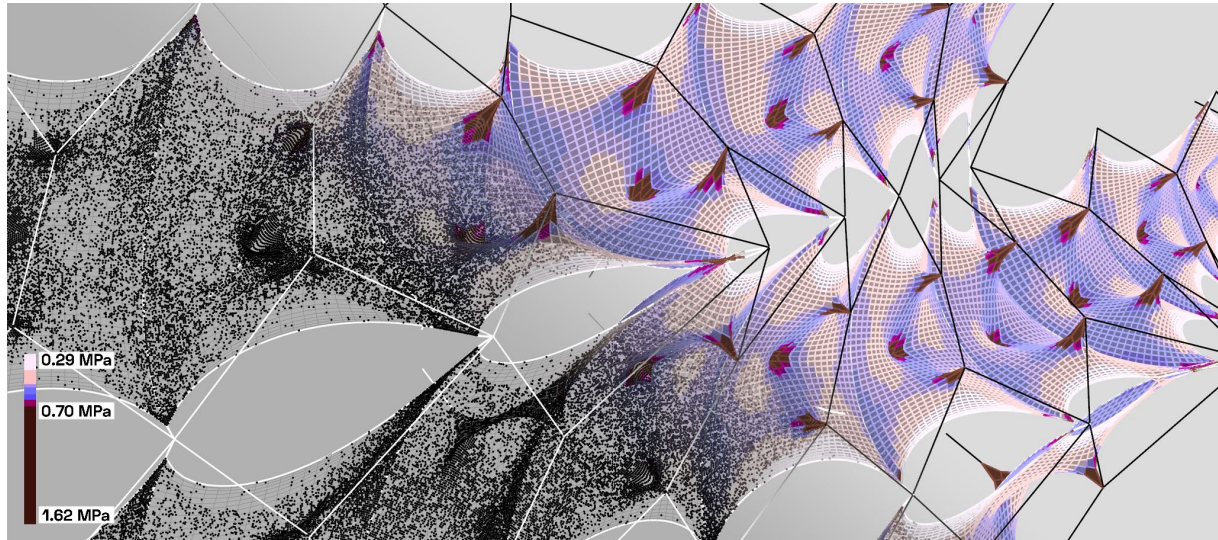


Figure 14: Zoirotia 2.0 digital exploration of structural analysis based material differentiation

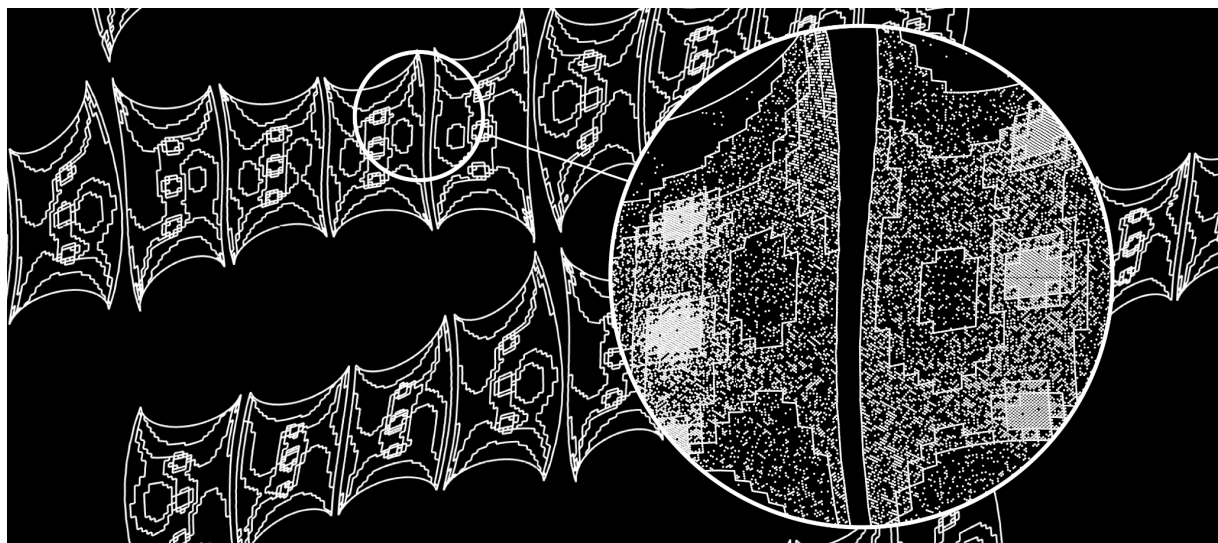


Figure 15: Diagram of material differentiation through the dithering of larger and smaller stitch types

5. Conclusion

Authors presented two methods that equally could be used for designing differentiation patterns for graded knitted membranes. The first, the *geometric* approach, operates within the membrane spatial displacement allowing the creation of clear and simple CNC-knitted patterns, concentrating the material property change mainly around the areas of applied loads. This method guarantees the efficient steer of the material property for expansion, if the load applied perpendicular to the plane of the membrane. The second method uses the *structural* analysis approach, which allows to take into consideration the structural performance of the surface. The resulting differentiation patterns suit better for the membrane loading conditions that are angled to the surface plane, which allows to expansion of the design space of CNC-knitted membrane structures.

Membrane architecture: the seventh established building material. Designing reliable and sustainable structures for the urban environment.

The presented methods contribute to the improvement of the robustness and the capacities of the workflow chain, used for the design, analysis and manufacturing of the CNC-knitted membranes. Thus, making it more convincing the use of CNC-knitted membranes in the field of membrane architecture, bringing them closer to become more and more used membrane material, that allows for a high degree of customisation and responds to demands, that sometimes cannot be answered by traditionally used woven-based materials.



Figure 16: Materially differentiated textile ceiling canopy

Acknowledgements

Zoirotia project involved multiple international institutions, to whom I address my gratitude. Special thanks to CITA, under the leadership of Mette Ramsgaard Thomsen and Martin Tamke, and the team, who pushed the boundaries of textile computational design: Y.Sinke, D. Albrechtsen, S.Hnídková, M. Seskas, N. Borpujari, V. Millentrup, M. Yan, J. Young, C. L. Xiuling, C. W.Chan, C. H. V. Carlström, C. Martinez Alarcon, and J. Aagaard Andersen. Additional thanks to structural engineers from Tragwerksentwurf of University of Kassel, Germany: J.Lienhard, D. Liu and manufacturing partners from Viola-Stils SIA, Kobleder GmbH, Karl Mayer Stoll Textilmaschinenfabrik GmbH and yarn sponsors from AMANN Group. I also would like to credit all the students, who took part in testing the digital tools and producing excellent and stimulating results during the workshop: A. Reigh Borbon, A. Krasheninnikova, A.Buckthal, A.Smith, C.Martinez, C.Ichniowski, D. Qiao, D.Bilesky, M. Kenzie Campbell, N. Elsgaard, S. Siefert, S. Henning, S. C. Liu, T. Wang, X. Luo, Y.-W. Yen.

References

- Adidas. (2017). *Knit for You*. <http://adidasknitforyou.com/>
<https://www.designboom.com/technology/adidas-knit-for-you-03-22-2017/>
- Brandt, C. (2016). *K2Engineering*.

Membrane architecture: the seventh established building material. Designing reliable and sustainable structures for the urban environment.

-
- David Rutten. (2007). *Grasshopper 3D*.
- Deleuran, A. H., Tinning Friis, I. K., Evers Leander, H., & Schmeck, M. (2015). Hybrid Tower, Designing Soft Structures. In M. Ramsgaard Thomsen, M. Tamke, & C. Gengnagel (Eds.), *Modelling Behaviour* (pp. 87–99). Springer Publishing.
- Liu, Y., Chai, H., & Yuan, P. F. (2020). Knitted composites tower. *RE: Anthropocene, Proceedings of the 25th International Conference of the Association for Computer-Aided Architectural Design Research in Asia, 1*, 55–64.
- Liu, Y., Hua, H., & Li, B. (2022). Exploration and design of knitted composites for architectural application: The MeiTing project. *Frontiers of Architectural Research*, S2095263522000061. <https://doi.org/10.1016/j.foar.2022.01.004>
- Mikucioniene, D., Halavska, L., Bobrova, S., Ielina, T., & Milasius, R. (2020). Ultra-Strong Knits for Personal Protective Equipment. *Applied Sciences*, 10(18). <https://doi.org/10.3390/app10186197>
- Piker, D. (2013). Kangaroo: Form finding with computational physics. *Architectural Design*, 83(2), 136–137. <https://doi.org/10.1002/ad.1569>
- Ramsgaard Thomsen, M., Nicholas, P., Tamke, M., Gatz, S., & Sinke, Y. (2019). Predicting and steering performance in architectural materials. *Architecture in the Age of the 4th Industrial Revolution - Proceedings of the 37th ECAADe and 23rd SIGraDi Conference - Volume 2, University of Porto, Porto, Portugal, 11-13 September 2019*.
- Ramsgaard Thomsen, M., Sinke Baranovskaya, Y., Monteiro, F., Lienhard, J., La Magna, R., & Tamke, M. (2019). Systems for transformative textile structures in CNC knitted fabrics – Isoropia. *Proceedings of the TensiNet Symposium 2019 Softening the Habitats*, 95–110.
- Ramsgaard Thomsen, M., Tamke, M., Karmon, A., Underwood, J., Gengnagel, C., Stranghöner, N., & Uhlemann, J. (2016). Knit as bespoke material practice for architecture: Acadia 2016. *Proceedings of the 36th Annual Conference of the Association for Computer Aided Design in Architecture (ACADIA)*, 280–289.
- Robert McNeel & Associates. (1980). *Rhinoceros 3D*.
- Sabin, J. (2013). My Thread Pavilion: Generative. *ACADIA Adaptive Architecture*.
- Sabin, J. (2021). *Data Knit* [Digitally Knit Textiles, Laser Cut Aluminum, Steel Frame, Custom Lighting System]. <https://www.jennysabin.com/dataknit>
- Sinke Baranovskaya, Y., Tamke, M., & Ramsgaard Thomsen, M. (2020). Simulation and Calibration of Graded Knitted Membranes. *ACADIA 2020: Proceedings of the 40th Annual Conference of the Association of Computer Aided Design in Architecture. 24-30 October 2020. Edited by B. Slocum, V. Ago, S. Doyle, A. Marcus, M. Yablonina, and M. Del Campo. 198-207*.
- Sinke, Y., Ramsgaard Thomsen, M., Albrechtsen, D. S. S., & Tamke, M. (2022). Design-to-production workflows for CNC-knitted membranes. *Hybrids & Haecceities*. ACADIA, Philadelphia, USA.
- Sinke, Y., Ramsgaard Thomsen, M., Tamke, M., & Seskas, M. (2022). Strategies for encoding multi-dimensional grading of architectural knitted membranes. *Towards Radical Regeneration*. DMS Design Modelling Symposium Berlin, Berlin, Germany.
- Šurc, D., Michel, D., Mirosnicenko, A., Artschwager, A., & Roeder, U. (2020). *Scan to Knit—From Body Scan Directly to the Knitting Machine*. <https://doi.org/10.15221/20.30>
- Tessmer, L., Goldstein, G., Herrera-Arcos, G., Korolovych, V., Bellisle, R., Paige, C., Shallal, C., Sahasrabudhe, A., Herr, H., & Anikeeva, P. (2022). 3D-Knit Spacesuit Sleeve with Multi-Functional Fibers and Tunable Compression. *Hybrids & Haecceities*. ACADIA 2022, Philadelphia, USA.



tensinantes2023 : TensiNet Symposium 2023 at Nantes Université

Membrane architecture: the seventh established building material. Designing reliable and sustainable structures for the urban environment.

Proceedings of the Tensinet Symposium 2023

TENSINANTES2023 | 7-9 June 2023, Nantes Université, Nantes, France

Jean-Christophe Thomas, Marijke Mollaert, Carol Monticelli, Bernd Stimpfle (Eds.)

Testing parameters for uniaxial short-term tensile tests of ETFE-foils and their connections

Dominik RUNGE*, Jörg UHLEMANN*, Natalie STRANGHÖNER*

*Institute for Metal and Lightweight Structures, University of Duisburg-Essen

Universitätsstraße 15, 45141 Essen, Germany

dominik.runge@uni-due.de

Abstract

The recently developed technical specification prCEN/TS 19102 acts as a precursor to a Eurocode for membrane structures and deals with textile fabrics as well as plastic foils in general and ETFE foils in particular. For the design of ETFE structures in the ultimate limit state (ULS), the corresponding design resistances of the base material as well as the area and edge weld seams are required. The design resistances are based on the short-term tensile strength of the foils or weld seams, resp., and the corresponding partial safety factor. The tensile strength at fracture of the ETFE base material and the welded connections can be assumed using conservative values or can be determined by experimental uniaxial short-term tensile tests. The tensile properties of the base material and the welded connections of ETFE foils are usually determined according to EN ISO 527-1 and -3 although for welded ETFE connections no specific test standard/guideline exist so far. This leads to the fact, that the testing parameters for determining the load bearing capacity of ETFE weld seams is not harmonized which might lead to deviating results.

From short-term tensile tests for ETFE base materials as well as for area and edge weld seams, it is well known that the load bearing capacities at fracture of the welded connections are mostly lower than the tensile strength of the corresponding base material. Beside this, the load bearing capacity at fracture of the welded connections can vary significantly within a test series and depend among others on the fabrication quality. Therefore, the load bearing capacity of welded ETFE foils is usually decisive in the ULS of the design concept of prCEN/TS 19102.

Within the framework of a German research project, the influence of different test parameters of uniaxial short-term tensile tests, e. g. test speed, test specimen geometry, on the stress-strain-behaviour of ETFE base material and especially on the load bearing capacity of ETFE area weld seams was investigated. The objective was to develop and define optimized and harmonized test parameters for the testing of ETFE area weld seams. The results of these research activities are presented in this paper.

Keywords: prCEN/TS 19102, ETFE, foils, weld seam, uniaxial testing, test parameters

1. Introduction

The thermoplastic fluoropolymer ethylene tetrafluoroethylene, short ETFE, has become increasingly popular as an extruded foil in architecture. However, there are still no standards

Membrane architecture: the seventh established building material. Designing reliable and sustainable structures for the urban environment.

neither guidelines available for the design of ETFE foil structures, the execution of the necessary weld seams as well as a harmonized product standard for ETFE foils.

Within the framework of the currently developed prCEN/TS 19102 as a precursor to a Eurocode for membrane structures, a concept for the design of ETFE structures has been developed. Within this concept, for the ultimate limit state design, the short-term tensile strength of the base material f_{t23} and the short-term tensile strength of area or edge weld seam f_{uw23} , which is in fact the load bearing capacity of weld seams, have to be determined. These values can be chosen as safe-sided values given in prCEN/TS 19102 or be derived as 5% fractile values of uniaxial short-term tensile tests. At least five specimens have to be tested at 23 °C.

The uniaxial short-term tensile tests are usually performed in accordance with EN ISO 527-1 and -3. These standards provide requirements and boundary conditions for the empirical determination of the material properties of plastics and plastic composites. ETFE area and edge weld seams are components. Herewith, they are not covered by these standards. This is a gap in standardisation. In the absence of a fitting standard or even guideline, the determination of the load bearing capacity of ETFE area weld seams is also performed in accordance with EN ISO 527-1 and -3. prCEN/TS 19102 provides additional rules to further harmonize foil testing and foil connection testing for architectural applications.

It is well established that the test results of plastics are highly dependent on the chosen test parameters, for example the test speed. This is especially the case for foils. EN ISO 527-1 and -3 do not provide specific values for the majority of test parameters but indicate acceptable ranges and allowed deviations the parameters should fall within. For the testing of ETFE foils, this results in a substantial number of varied test specifications, predefined by the individual test laboratory. However, the foundation of a test-based design is the reproducibility and comparability of the test results. The same is true for the empirical determination of the tensile properties within the context of the design approval and the manufacturer's quality control. Therefore, an optimised and standardised test method for determining uniaxial tensile properties of ETFE foils and their connections is crucial.

The German research project “Welded connections of ETFE foils in building construction: Standardisation of execution, testing and design” (WIPANO-ETFE for short), under the WIPANO initiative of the German Federal Ministry for Economic Affairs and Energy, has the primary objective of developing a standardised test method for a uniaxial short-term tensile test for ETFE area weld seams. In total, six project partners are involved in the project: University of Duisburg-Essen, Institute for Metal and Lightweight Structures, Essen Laboratory of Lightweight structures ELLF (UDE, project coordinator), Laboratory for Technical Textiles and Films of DEKRA SE (DEKRA), Vector Foiltec GmbH, Bremen (VF), se cover GmbH, Obing (SC), Taiyo Europe GmbH, Sauerlach (TE), formTL ingenieure für tragwerk und leichtbau GmbH (formTL), Radolfzell, all Germany. For the development of a harmonized test specification of ETFE area weld seams, the effect of various test parameters on the results of uniaxial short-term tensile tests of ETFE base material and area weld seams has been studied. On the basis of these tests, optimized test parameters, along with allowable tolerances, have been determined keeping in mind the practicability in daily practice. The investigated test parameters included the specimen geometry, the specimen preparation, the test speed as well as the type and cover of clamping. The sequence in which these test parameters have been optimised aligns with the order in which they are listed above. Herewith, firstly, the specimen geometry has been optimised, while keeping the remaining listed test parameters constant.

Membrane architecture: the seventh established building material. Designing reliable and sustainable structures for the urban environment.

An area weld seam consists of the base material, the weld itself, and the heat-affected zone on both sides of the weld. The load bearing behaviour of a weld seam is influenced by the base material, the geometry of the weld seam (width, thickness etc.), preparation of the weld seam, weld process, weld parameters, quality of the weld seam etc. One objective of the project is to define optimised test parameters for testing area weld seams in such a way that they comply with those testing parameters used for testing ETFE base material. Herewith, the daily testing practice shall be kept simple so that an ease of use can be guaranteed.

For this purpose, the project partners of WIPANO-ETFE have established a standardised test specification as a starting point, and subsequently varied individual test parameters. For example, a constant test speed of 100 mm/min and a line clamping of the specimen has been chosen as a starting point. This provides a consistent basis for systematically and controlled evaluation and optimisation of test parameters. In this research project, base material specimens and area weld seam specimens have been investigated in two different foil thicknesses, 100 μm and 250 μm . The base material and area weld seams of the same foil thickness come from the same production batch and foil product, ensuring comparability of the results. It is well known that ETFE foils have orthotropic material properties. For this reason, the uniaxial material properties have to be determined in both the extrusion direction (ED) and the transversal direction (TD). However, area weld seams are manufactured parallel to ED, so that only its load bearing capacity in TD is decisive for design. Hence, only the material properties of the base material and the area weld seams in TD were determined within the frame of the presented investigations.

2. Impact of the specimen geometry

2.1. General

For the examination of the impact of specimen geometry on the results of uniaxial tensile tests according to EN ISO 527-1 and -3 for the base material in TD and area weld seams, three different specimen types with different length-to-width ratios of the test area were investigated for two different foil thicknesses in the test laboratories of UDE (100 μm ETFE-foils) and DEKRA (250 μm ETFE-foils). To ensure the comparability of the test results from both test facilities, preliminary tests were carried out for this purpose. The different specimen types and foil thicknesses were tested at typical test temperatures of 23 °C and 50 °C.

2.2. Investigated specimen geometries

EN ISO 527-3 provides four different types of specimen geometries: a strip specimen (specimen type 2 (T2)) and three types of shoulder specimens. In the presented study, strip specimen T2, a modified version of it, see further explanations, and one shoulder specimen (specimen type 5 (T5)) have been investigated. Usually, in practice, strip specimens, not necessarily with the dimensions according to T2, but with individual dimensions, are used. Nevertheless, as some laboratories also use shoulder specimens, T5 has been chosen as well in this study.

EN ISO 527-3, 6.1.2 recommends using the strip specimen T2 for the determination of the tensile properties of foils and sheets, see Figure 1 (b). Two gauge marks are placed on this specimen type on defined positions for the measurement of the specimen elongation, which was carried out by extensometers (DEKRA) and optical displacement transducers (UDE). This way of detecting the deformation ensures that only uniaxial deformations within the area defined by the markers are detected. The recommended initial length between the clamps (L) is 100 mm \pm 5 mm. The marks should be placed at a distance (L_0) of 50 mm \pm 0.5 mm.

Membrane architecture: the seventh established building material. Designing reliable and sustainable structures for the urban environment.

According to EN ISO 527-3, 6.1.1, the specimen length L for plastics with high breaking strains can be reduced to 50 mm. At room temperature, a breaking strain of more than 400 % for ETFE base material is expectable, so that this modification according to EN ISO 527-3, 6.1.1 is usually applied for ETFE foils and is called modified specimen type 2 (MT2) by the authors, see Figure 1 (a). Due to the reduced specimen length, the marker for the measurement of the elongation cannot be placed on the test specimen anymore. Therefore, the elongation is only recorded by the crossbeam displacement of the testing machine. Herewith, the recorded elongation is influenced by the clamping region, i. e. by slip and multiaxial stress concentrations due to the disabled transversal contraction.

The shoulder specimen type 5 (T5) of EN ISO 527-3, 6.1.2 is given in Figure 1 (c). The strain of T5 was measured by an extensometer (DEKRA) or an optical displacement transducer (UDE). The investigated dimensions of the test area for the three different specimen types are presented in Table 1.

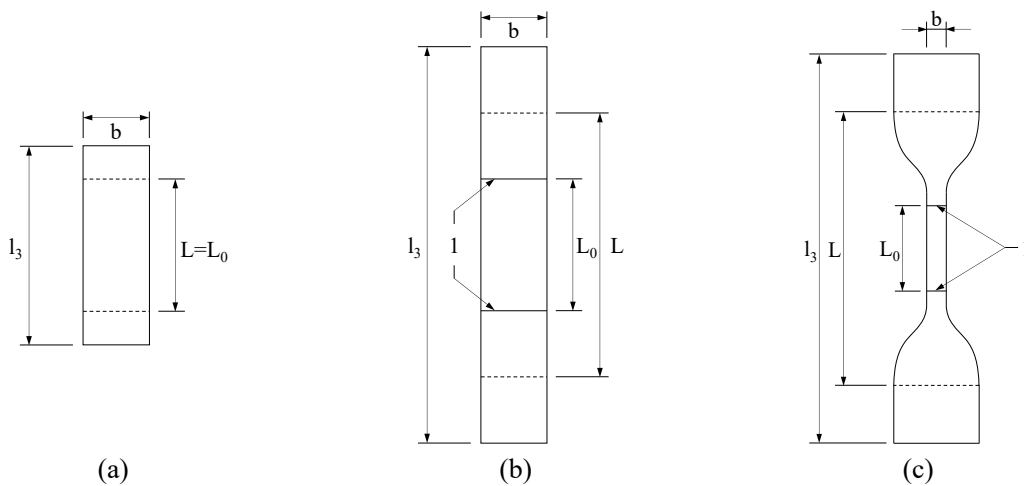


Figure 1: Investigated specimen types: (a) modified specimen type 2 (MT2) acc. to EN ISO 527-3, 6.1.1; (b) specimen type 2 (T2) acc. to EN ISO 527-3, 6.1.2; (c) specimen type 5 (T5) acc. to EN ISO 527-3, 6.1.2; b = width of the measuring field; l_3 = specimen length; L = gauge length; L_0 = length of the measuring field; 1 = gauge marks

Table 1: Measurements of the specimen geometry for different specimen types

Specimen type	L_0 [mm] x b [mm]	L [mm]	l_3 [mm]	$L_0:b$
MT2	50x10; 50x20*; 50x50; 80x10; 80x20; 80x50*	$L = L_0$	74 for $L_0 = 50$ mm; 104 for $L_0 = 80$ mm	5:1; 2,5:1; 1:1; 8:1; 4:1; 1,6:1
T2*	50x10; 50x20; 50x50; 80x10; 80x20; 80x50	100 for $L_0 = 50$ mm; 160 for $L_0 = 80$ mm	124 for $L_0 = 50$ mm; 184 for $L_0 = 80$ mm	5:1; 2,5:1; 1:1; 8:1; 4:1; 1,6:1
T5	50x10; 50x50	160	230	5:1; 1:1

*Only tested for 100 μ m base material and area weld seams

For the analysis of the test results, it has to be considered that the different clamp lengths of the different investigated specimen geometries combined with a constant test speed of 100 mm/min results in different strain rates $\dot{\epsilon}$. These different strain rates range from 200 %/min for the 50 mm short MT2 specimen to 62,5 %/min for the 80 mm long T2 specimen. The strain rate of the shoulder specimen is calculated to 150 %/min considering the parallel length between the

reinforced regions. The different strain rates influence the results of the tensile tests and are considered in the following analysis.

2.3. Impact of the specimen geometry on the tensile strength of ETFE base material

For the analysis of the impact of the specimen geometry on the tensile strength, the presented specimen geometries were investigated according to the standardised test specification mentioned before. Box plots were utilized as a graphical representation of the tensile strength. Additionally, statistical values like the average tensile strength $f_{u,mean}$, the 5% fractile value of the tensile strength $f_{u,5\%}$ and the correlating COV V acc. to EN 1990 are given. Figure 2 depicts the results of the MT2 specimens, 100 μ m foil, TD, room temperature 23 °C \pm 2 K with varying dimensions of the test area.

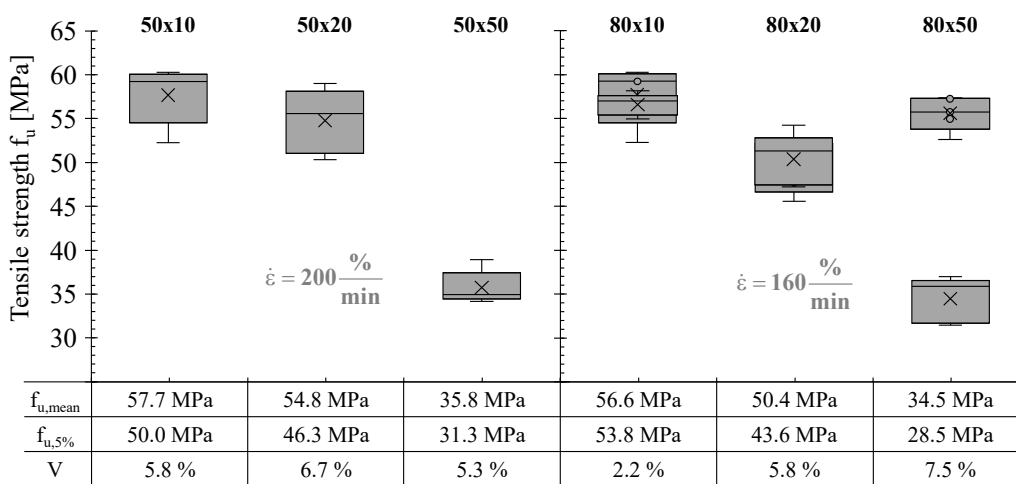


Figure 2: Box plots of the tensile strength and corresponding statistical values of 100 μ m base material for different geometries (L_0 [mm] x b [mm]), MT2, 23 °C, TD, $n = 5$

The results indicate a decrease of the tensile strength with increasing specimen width, especially when the tensile strength of the 50 mm wide specimens is compared to those achieved for the 10 mm and 20 mm wide test specimens. The slightly lower strength values for the specimen with $L = L_0 = 80$ mm, compared to the shorter specimens with $L = L_0 = 50$ mm can be attributed to the resulting lower strain rate. It is well known that a higher strain rate leads to higher strengths, e. g. Surholt et al. (2022). Furthermore, from the tests for the 100 μ m foils, it could be observed that the 50 mm wide samples regularly failed at the clamped edges whereas the 10 mm and 20 mm wide specimens usually failed in the test area.

Table 2 presents the average tensile strengths and corresponding statistical parameters for the 250 μ m foil which are in line with the results achieved for the 100 μ m ETFE foil, for the 10 mm and 20 mm wide test specimens. Contrary to the results for the 100 μ m foil, the 50 mm wide test specimen shows only a slightly smaller tensile strength as achieved for the 10 mm wide specimen.

The results of the investigations into various dimensions of the test area for specimen type T2 are illustrated in Figure 3. They are consistent with the observations achieved for the specimen type MT2, where a decrease of the tensile strength could be observed with increasing specimen

width. However, the achieved tensile strengths for specimen type T2 are significantly lower compared to those of the MT2 specimen (e.g. $\Delta_{50 \times 10} = 15,8 \%$). This is attributed to the significantly lower strain rate, as the T2 specimens have twice the length of the MT2 specimens.

Table 2: Uniaxial tension tests: MT2 base material, 250 μm , 23 $^{\circ}\text{C}$, TD

L_0 [mm] x b [mm] (5 test samples per test series)	50x10	50x50	80x10	80x20
$f_{u,\text{mean}}$ [MPa]	57.5	52.83	54.4	51.9
$f_{u,5\%}$ [MPa]	51.3	42.80	45.7	44.0
V [%]	4.7	8.2	6.9	6.5

For specimen types MT2 and T2, different strain rates result at the same test speed. This makes it difficult to compare the test results. For this reason, further tests were carried out for the T2 specimens, 100 μm thickness with a test speed that result in a strain rate of 200 %/min identical to the strain rate resulted for the already tested MT2 specimens. The average tensile strength of the new T2 tests was 56.4 MPa with a 5% fractile value of 47.2 MPa and a COV of 7.0%. These values are comparable to those achieved for the MT2 specimens with a thickness of 100 μm with the same test area dimensions, see Figure 2. This indicates that the specimen types MT2 and T2 provide similar tensile strengths for the 100 μm base material. The base material with a foil thickness of 250 μm was not tested with specimen type T2.

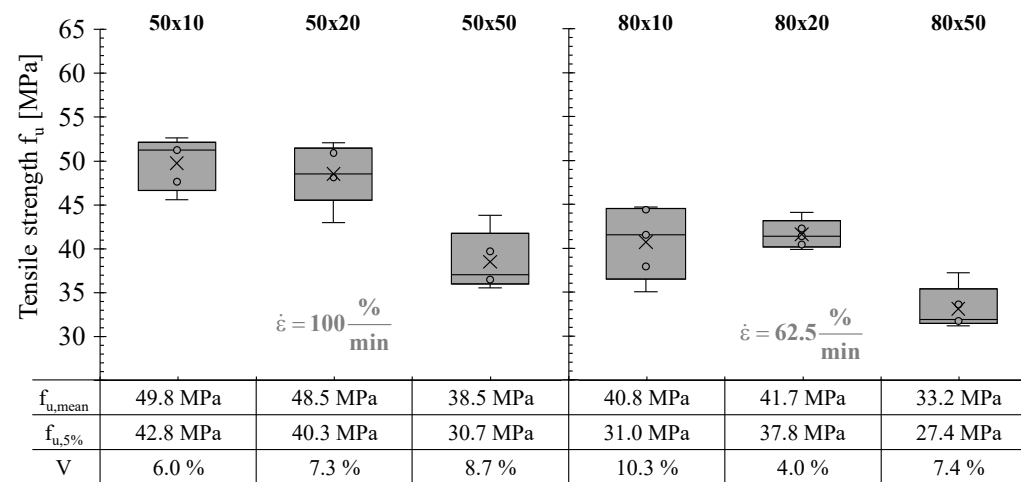


Figure 3: Box plots of the tensile strength and corresponding statistical values of 100 μm base material for different geometries (L_0 [mm] x b [mm]), T2, 23 $^{\circ}\text{C}$, TD, n = 5

By the test results for the shoulder specimen T5, it could be shown that the tensile strength decreases with increasing specimen width independent of the foil thickness. Considering the slightly lower strain rate due to the longer specimen length, the results of the specimens with the length-to-width ratio of 5:1 ($f_{u,\text{mean}} = 55.6 \text{ MPa}$, $V = 3.5 \%$) align with the outcomes of the strip specimens T2 and MT2. However, the tests with a specimen width of 50 mm show significantly higher tensile strengths ($f_{u,\text{mean}} = 41.8 \text{ MPa}$, $V = 6.2 \%$) compared to the results achieved for the strip specimens. This is likely due to the reinforcement (shoulder area) of the test specimens T5 in the clamping area. The T5 tests with the 250 μm foil show lower tensile

Membrane architecture: the seventh established building material. Designing reliable and sustainable structures for the urban environment.

strengths ($f_{u,mean} = 48.8$ MPa and $V = 9.2$ % (50x10), $f_{u,mean} = 38.2$ MPa and $V = 11.6$ % (50x50)) compared to those achieved in the MT2 and T2 tests independent of the foil thickness. One reason for this behaviour might be the specimen preparation. The specimens were prepared using a template and cutter knife. The curved shape of the shoulder specimens made the manufacturing process challenging. Defects in the curved areas cannot be completely ruled out, particularly for the thicker 250 μ m foil material. This effect is reflected by the comparably high COV of the thicker specimens.

For the investigations of the impact of the specimen geometry on the tensile strength of ETFE base material at elevated temperatures, the same test protocol used for the tests at 23 °C was also applied for the tests at 50 °C. Because of the limited height of the climate chamber and the even higher deformation of the material at elevated temperature, during testing the upper end of the test specimen is pulled out of the climate chamber, so that the part of the test specimen, which breaks, still lies in the climate chamber, but the pulled out upper part cools down during testing. This was the case for specimen types T2 and T5.

At elevated temperature, the 80 mm long T2 specimens did not break during testing due to the limitation of the crosshead travel, which was not sufficient to reach the breaking strain of this specimen type. The 50 mm long T2 specimens failed within the crosshead travel but showed an extraordinarily high COV with i. e. 18.8 % for the 10 mm wide specimens. This indicates a high influence of the different temperatures of the 50 mm long specimens in and out of the climate chamber. For this reason, the T2 specimens were not considered in the analysis. The T5 specimens were pulled out of the climate chamber during testing as well. However, the area that was pulled out included only the shoulder area of the samples. The temperature of the test area could be maintained at elevated test temperature. The T5 specimens broke within this unaffected area. Therefore, the results of the T5 specimens were evaluated. Nevertheless, it has to be kept in mind, that they might behave different. The results of the MT2 and T5 specimens are illustrated in Figure 4.

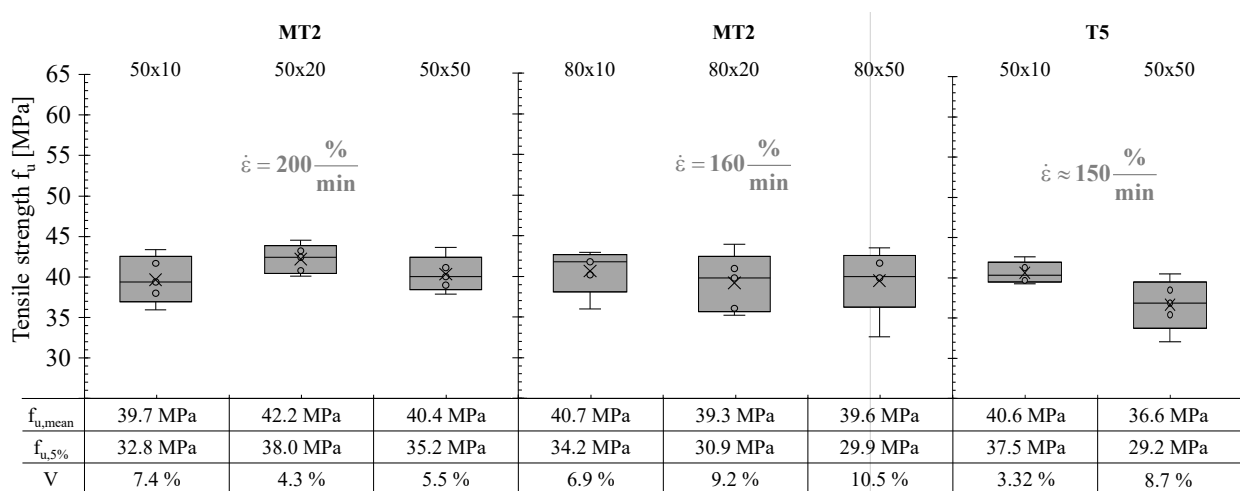


Figure 4: Box plots of the tensile strength and corresponding statistical values of 100 μ m base material for different geometries (L_0 [mm] x b [mm]), MT2 and T5, 50 °C, TD, $n = 5$

Membrane architecture: the seventh established building material. Designing reliable and sustainable structures for the urban environment.

The test results of the MT2 tests at elevated test temperatures indicate that the varying dimensions of the test area do not have a significant impact on the tensile strength. The average tensile strengths of the 100 μm foil for the various dimensions of the test area fall within a small range of 39.3 MPa to 42.2 MPa. The at 23 $^{\circ}\text{C}$ test temperature observed lower tensile strength for the 50 mm wide specimens cannot be confirmed for testing at 50 $^{\circ}\text{C}$. The results of the 250 μm foil support this observation. Typically for the testing of plastics at elevated temperatures, the level of the tensile strength is significantly lower compared to the tests conducted at room temperature.

2.4 Impact of the specimen geometry on the load bearing capacity of ETFE area weld seams

Table 3 presents the results of the investigation into the effect of the specimen geometry on the load bearing capacity of area weld seams for the MT2 and T2 specimen types. The average load bearing capacity of the same specimen type and foil thickness fall within the same range. No clear correlation between minor variations in the average load bearing capacity and the corresponding test area dimension can be observed. This indicates that the different investigated dimensions of the test area do not significantly impact the load bearing capacity of area weld seams for the specimen types MT2 and T2. The results of the 100 μm T5 specimen ($f_{u,\text{mean}} = 39,19 \text{ MPa}$ (50x10), $f_{u,\text{mean}} = 41,43 \text{ MPa}$ (50x50)) further extend this observation for the T5 specimen type.

Table 3: Uniaxial tension tests: MT2 and T2 area weld seam, 23 $^{\circ}\text{C}$, TD

L_0 [mm] x b [mm] (5 test samples per test series)			50x10	50x20	50x50	80x10	80x20	80x50
MT2	100 μm	$f_{u,\text{mean}}$ [MPa]	40.6	39.9	43.7	39.0	40.2	43.0
		$f_{u,5\%}$ [MPa]	34.9	32.4	38.4	36.3	36.8	38.4
		V [%]	6.0	8.1	5.2	3.0	3.6	4.5
	250 μm	$f_{u,\text{mean}}$ [MPa]	36.7	-	35.5	38.8	36.9	-
		$f_{u,5\%}$ [MPa]	33.3	-	23.1	36.8	33.4	-
		V [%]	3.9	-	14.9	2.2	4.1	-
T2	100 μm	$f_{u,\text{mean}}$ [MPa]	37.9	40.2	39.2	43.5	42.5	41.6
		$f_{u,5\%}$ [MPa]	35.4	32.6	31.7	38.9	38.6	34.4
		V [%]	2.8	8.0	8.2	4.5	3.9	7.5

As presented in Table 1, the 250 μm foils were only tested with the MT2 and T5 specimen types. For the 50 mm wide T5 specimens of the 250 μm foil an adapter has to be used for the clamping of the samples. In combination with the limited heights of the climate chamber, the 50 mm wide T5 specimens could not be tested until a fracture occurred. The 10 mm wide T5 specimens were tested without an adapter and failed within the climate chamber. Therefore, only the 10 mm wide T5 specimens could be considered in this analysis. Table 4 presents the results of the MT2 and T5 specimens. Similar to the conclusions of the tests of area weld seams at room temperature, the various investigated dimensions of the test area do not appear to have a significant impact on the load bearing capacity of the welded connection of the specimen type MT2. However, the tests for the 50 mm x 20 mm test area show a significantly reduced load

Membrane architecture: the seventh established building material. Designing reliable and sustainable structures for the urban environment.

bearing capacity compared to that achieved for specimens with a higher and lower specimen width and the same test area heights. One obvious explanation might be that other material-independent factors have influenced the load bearing capacity of this test series.

Table 4: Uniaxial tension tests: MT2 and T5 area weld seam, 50 °C, TD

L ₀ [mm] x b [mm] (5 test samples per test series)			50x10	50x20	50x50	80x10	80x20	80x50
MT2	100 μm	f _{uw,mean} [MPa]	39.3	32.8	37.7	36.3	35.9	35.7
		f _{uw,5%} [MPa]	34.5	28.5	35.5	32.9	34.2	34.1
		V [%]	5.2	5.6	2.5	4.0	2.1	1.9
	250 μm	f _{uw,mean} [MPa]	32.9	-	-	32.6	33.9	-
		f _{uw,5%} [MPa]	30.9	-	-	30.2	31.9	-
		V [%]	2.5	-	-	3.2	2.5	-
T5	100 μm	f _{uw,mean} [MPa]	40.6	-	36.6	-	-	-
		f _{uw,5%} [MPa]	37.5	-	29.2	-	-	-
		V [%]	3.3	-	8.7	-	-	-
	250 μm	f _{uw,mean} [MPa]	37.7	-	-	-	-	-
		f _{uw,5%} [MPa]	30.9	-	-	-	-	-
		V [%]	7.8	-	-	-	-	-

3. Impact of the specimen preparation

The uniaxial short-term tensile test is widely accepted as the method of choice for determining the uniaxial tensile strength of ETFE foils and the uniaxial load bearing capacity of their connections. The previous presented studies have shown that the ultimate tensile strength can differ significantly, potentially due to factors independent of the material. Hereby, the most important factor is the specimen preparation which involves mainly the cutting of the specimens to a predefined shape. Currently, a variety of cutting tools are used for the specimen preparation of ETFE base materials and area weld seams. For this reason, the impact of various cutting tools and methods on the results of uniaxial short-term tensile tests of ETFE base material and their connections was investigated, too. Multiple test series of uniaxial short-term tensile tests for ETFE base material and area weld seams were performed using two different preparation methods and one resp. five different cutting tools, see Figure 5.

The two preparation methods were a ruler or a template. Using the ruler, five different cutting tools were used: a rotary cutter, a scalpel with a new blade, a cutter knife with a new blade and a used blade and a lever cutter, see Figure 5. Using the template, only the cutter knife with a new blade was applied. The tests were conducted according to EN ISO 527-1 and -3 at room temperature and at a test speed of 100 mm/min using the MT2 specimen type with a test area of L = 50 mm by b = 10 mm. Two different foil thicknesses, 100 μm and 250 μm, were also considered. To obtain statistically significant results, 10 tests were performed per test series.

Membrane architecture: the seventh established building material. Designing reliable and sustainable structures for the urban environment.



Figure 5: Investigated cutting tools; (a) rotary cutter; (b) scalpel with a new blade; (c) cutter knife with a new blade (left) and a used blade (right); (d) lever cutter

Figure 6 illustrates the ultimate tensile strength of 100 μm ETFE base material prepared using the investigated cutting tools. The results indicate a significant impact of the cutting tool on both the tensile strength and its COV. Specimens prepared by cutter knife with a used blade exhibit a significantly lower average tensile strength and higher COV compared to those prepared with a new blade. The tests prepared by a cutter knife with a new blade provides the highest average tensile strength with 57.2 MPa (guided by ruler) and 56.3 MPa (cut with template), followed by the lever cutter and scalpel with both 54.2 MPa. The use of a template does not appear to have a significant effect on the tensile strength or the COV.

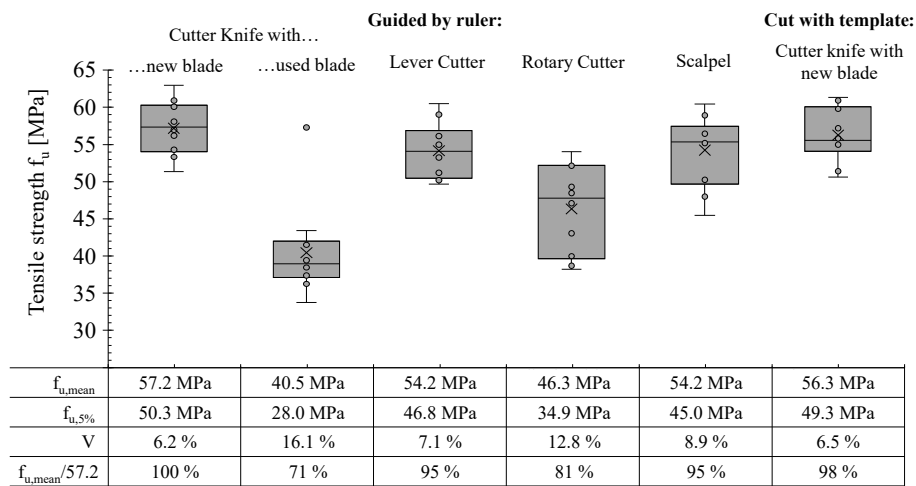


Figure 6: Box plots of the tensile strength and corresponding statistical values of 100 μm base material for different cutting tools and methods, 23 $^{\circ}\text{C}$, TD, n = 10

The results of the investigation into the effect of the preparation methods and cutting tools on the ultimate tensile strength for the 250 μm base material is presented in Table 5. The findings indicate that the 250 μm foil is less sensitive to the influence of the cutting tool and preparation method than the 100 μm foil. However, the results reflect the same effects of the different cutting tools and methods on the tensile strength that were observed for the 100 μm foils.

Membrane architecture: the seventh established building material. Designing reliable and sustainable structures for the urban environment.

Table 5: Uniaxial tension tests: different specimen preparation, base material, 23 °C, TD

10 test samples per test series	Guided by ruler				Scalpel	Template Cutter knife (New blade)
	Cutter knife with...		Lever	Rotary		
	New blade	Used blade	Cutter	Cutter		
$f_{u,mean}$ [MPa]	55.6	49.0	55.1	49.7	54.7	58.5
$f_{u,5\%}$ [MPa]	49.2	43.1	52.5	42.2	43.3	52.7
V [%]	6.0	6.3	2.4	7.9	10.9	5.1
$f_{u,mean}/55.6$	100 %	88 %	99 %	89 %	98 %	105 %

The results of the analysis of the impact of the investigated cutting tools and methods on the load bearing capacity of area weld seams of 100 µm foils are shown in Figure 7. The specimen preparation using a cutter knife with a new blade resulted in the highest load bearing capacity with 41.2 MPa (guided by ruler) and 42.9 MPa (cut with template). However, the variations in the load bearing capacity for the different cutting tools were minimal, indicating that the impact of the investigated cutting tools and methods on the load bearing capacity is negligible. The results of the 250 µm welded foils are consistent with the findings for the 100 µm welded foils, as shown in Table 6.

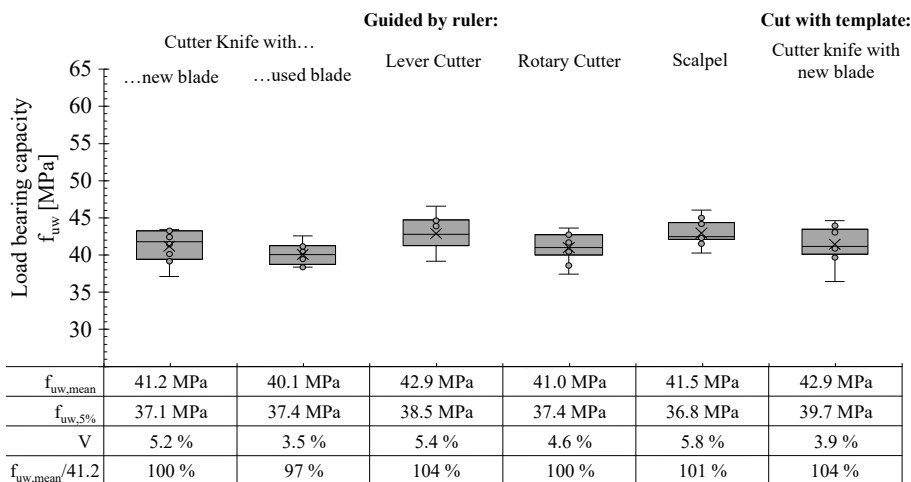


Figure 7: Box plots of the load bearing capacity and corresponding statistical values of 100 µm area weld seam for different cutting tools and methods, 23 °C, TD, n = 10

Table 6: Uniaxial tension tests: sample preparation, area weld seams, 250 µm, 23 °C, TD

10 test samples per test series	Guided by ruler				Scalpel	Template Cutter knife (New blade)
	Cutter knife with...		Lever	Rotary		
	New blade	Used blade	Cutter	Cutter		
$f_{uw,mean}$ [MPa]	39.0	38.8	39.0	38.4	39.2	40.7
$f_{uw,5\%}$ [MPa]	37.0	37.8	37.6	34.6	36.8	39.6
V [%]	1.5	1.4	1.9	5.1	3.3	1.4
$f_{uw,mean}/39.0$	100 %	99 %	100 %	98 %	101 %	104 %

Membrane architecture: the seventh established building material. Designing reliable and sustainable structures for the urban environment.

4. Conclusions

The objective of this study was to identify and optimize key factors that affect the accuracy and reliability of uniaxial short-term tensile test results for ETFE base material and area weld seams. Through extensive testing, it could be shown that the specimen type has only little influence on the ultimate tensile strength of the base material and the load bearing capacity of area weld seams. However, due to the increased effort and necessary equipment for testing specimen type T2 and T5, specimen type MT2 is recommended. Additionally, it could be observed that narrower specimens were more optimal for determining the ultimate tensile strength. Based on the parameters evaluated in the present investigation, a specimen length L_0 of 50 mm can be recommended. The investigation also revealed that the specimen preparation has a significant impact on the tensile strength of ETFE base material but not on the load bearing capacity of area weld seams. The recommended cutting tool and method is a cutter knife with a new blade. Overall, the use of a template provides slightly higher tensile strength.

In conclusion, it is important to note that the tensile strength derived from uniaxial short-term tensile tests is dependent on various factors beyond the materials properties. This means that the results of such tests should be considered in design as a material parameter with limitations. Additionally, the results of this study indicate that the load bearing capacity of area weld seams is less sensitive to these factors.

Acknowledgements

The authors would like to express their gratitude for the funding of this research by the German Federal Ministry for Economic Affairs and Energy within the framework of the research project “Welded connections of ETFE structures: Standardisation of execution, testing and design” (funding code: 03TN0011A). Additionally, the authors would like to extend their appreciation to the project partners for their valuable collaboration.

References

- prCEN/TS 19102:2022, Design of tensored membrane structures, final draft submitted to NEN (unpublished).
- EN ISO 527-1:2019, Plastics – Determination of tensile properties – Part 1: General principles (ISO 527-1:2019).
- EN ISO 527-3:2018, Plastics – Determination of tensile properties – Part 3: Test conditions for films and sheets (ISO 527-3:2018).
- EN ISO 1990:2021, Eurocode: Basis of structural design.
- Surholt F., Uhlemann J., Stranghöner N. (2022), Temperature and Strain Rate Effects on the Uniaxial Tensile Behaviour of ETFE Foils. In: *Polymers*, vol.14 (pp. 1 – 22).



tensinantes2023 : TensiNet Symposium 2023 at Nantes Université

Membrane architecture: the seventh established building material. Designing reliable and sustainable structures for the urban environment.

Proceedings of the Tensinet Symposium 2023

TENSINANTES2023 | 7-9 June 2023, Nantes Université, Nantes, France

Jean-Christophe Thomas, Marijke Mollaert, Carol Monticelli, Bernd Stimpfle (Eds.)

Living in the 7th element: Hans-Walter Müller's pneumatics

Katja Bernert*

*Dipl.-Ing. Architect, Mehler-Technologies, Rheinstr. 11, 41836 Hueckelhoven, Germany,
Katja.Bernert@freudenberg-pm.com

Abstract

Hans-Walter Müller designed and built pneumatics since the 1960s. His passion for textile architecture is not limited to designing and building temporary structures. Since 1971 he lives in an air supported fabric structure. The architect was born in Worms, Germany, in 1935. Müller studied in Darmstadt and Paris where he followed his interest in the performing arts. He did courses in Pantomime, acted as a magician in a cabaret and experimented with projections, putting static images into action. Parallel to joining an architect's office after his studies he further developed techniques and machines of his moving projections. He experimented with air-supported fabrics and foils as semi-translucent screen when putting the two-dimensional moving images into space. The fact that there was no additional supporting structure allowed him to work with an uninterrupted flow of surfaces. Hans-Walter Müller dedicated five decades of lifetime to the optimisation of his pneumatics – concentrating on one-layer structures. The presentation will explore how his work can serve as a trigger for using more fabrics in the built environment – not only for temporary dwellings but for the growing need of housing. Hans-Walter Müller certainly made-up for many restrictions when it comes to comfort – particularly at the beginning of his living in the 7th element. The presentation will show state of the art means and materials that facilitate using fabrics for housing.

Keywords: coated fabrics, pneumatic structures, fabrics for housing, experimenting with fabrics and foils, fabrics as a screen, insulated fabric structures, single layer, double layer

1. Introduction

Hans-Walter Müller's oeuvre links three topics that are most relevant in Tensile Architecture: light, lightness and movement. It is very interesting and a real pleasure to dive into the work of the French German architect and discover milestones leading him towards the liveable pneumatics that he calls "gonflables". Steps that – at that time – seemed quite far away from the architect's or urban planner's real occupation. From the retrospective point of view, pantomime and magic can be interpreted as inherent notions of pneumatics and Tensile Architecture in general.

Membrane architecture: the seventh established building material. Designing reliable and sustainable structures for the urban environment.

2. The beginnings in Paris

Regarding Hans-Walter Müller's experiences in Paris it is obvious that the city itself played an important role in his professional career which is essentially an artist's career. Worms, his home-town, and Darmstadt, the city where he studied, are just about 45 km apart. Except for the occasional visits to other university cities – mainly for gigs as a magician – it was the journey to the French capital that acted as turning point in Hans-Walter Müller's vita. Otherwise he would probably have continued his Darmstadt-way of working, with strong inputs of rationalists like Ernst Neufert for example.

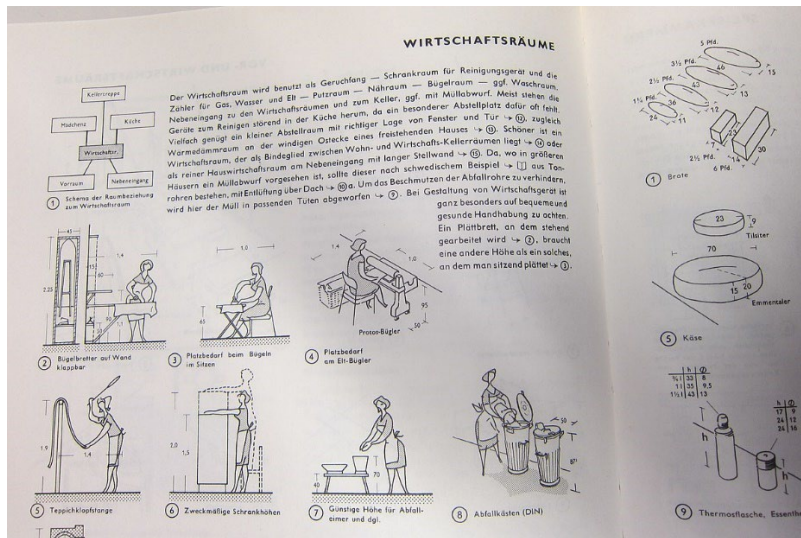


Figure 1: Ernst Neufert, Bauproduktionslehre, exemplary page on service facilities within a household, https://commons.wikimedia.org/wiki/File:Bladzijde_uit_Bauproduktionslehre.JPG



Figure 2: Ernst Neufert, Bauproduktionslehre, book title

When talking about his first experiences in Paris, Hans-Walter Müller highlights the role of the roaring sixties in the French capital, about the difficult living conditions and most of all about the interesting people he met like Hans Scharoun, the pioneer of organic architecture in Germany, or the German French artist Hans Hartung.

2.1. Pantomime

The concentration on the gist, on the most important message is what Hans-Walter Müller describes as the key learning when it comes to the merits of the time he spent pantomiming. Having experiences in drawing people's attention as a magician, it was his next step within the performing arts to dig deeper into pantomime. He did this in courses first and evolved his abilities quickly by choreographing his own programs. It was within the context of the Pantomime theatres that he came in touch with projections.

Membrane architecture: the seventh established building material. Designing reliable and sustainable structures for the urban environment.



Figure 3: Paris in the 1960s, Place du Trocadero, June 17, 1960 (Kodachrome by Ed Kanouse), Creative Commons licenced by Kent Kanouse, <https://www.flickr.com/photos/kkanouse/17163299225>

2.3. Projections

Hans-Walter Müller first experimented with the projection of images in his apartment. It was the power of coincidence that led him to experiments with sound and moving items within the setting of a strong light source. He describes the eureka effect of having some threads in front of the lens that fluttered in a seemingly random rhythm and – because projections always come in reverse – surrendering gravitation by standing and moving upright.

It is already at this early stage that we meet notions like light, rhythm or sound and the counterpart of gravity in Hans-Walter Müller's experiments.



Figure 4: Hans-Walter Müller in August 2019, under one of his „Klangstruktur mit Resonanzkugel“ (Structure sonore avec sphère de résonance). His inflatable house is in the background. https://commons.wikimedia.org/wiki/File:Hans-Walter_M%C3%BCller_Klangstruktur.jpg

2.4 Pneumatics

The first step into the world of pneumatics came with the need to have a three dimensional screen for projections in one of his performances. The choreography demanded for a curved surface that was not interrupted by any supporting means. A pneumatic structure was Hans-Walter Müller's obvious choice.

Membrane architecture: the seventh established building material. Designing reliable and sustainable structures for the urban environment.

Over the time he refined the technical equipment until the concept was ready to be taken from the stage, first into various exhibitions and then into the built environment. It is most obvious that particularly the step into the building scope needed space. In order to properly evolve his pneumatic experiments, Hans-Walter Müller moved away from down-town Paris, first to La Plaine Saint-Denis north of the peripheric and then to La Ferté-Alais south of Paris.

It is in La Ferté-Alais where he still lives among his various pneumatic and tensile structures. When he started the pneumatic itinerary in the 1960s, air supported fabric structures where not completely new. Nonetheless it was his innovative drive and in depth technological understanding combined with a fundamentally artistic approach that put pneumatics forward in terms of building technologies.

3. Living in the seventh element



Figure 5: living and working space of Hans-Walter Müller in La Ferté Alais

Hans-Walter Müller is probably the only pneumatics expert who knows these structures from decades of living and working within air-supported buildings. His grounds in La Ferté-Alais can be literally seen as the Mecca of Tensile Architecture. Like follies the different buildings and structures are hidden between the trees, foretelling of what Bernard Tschumi evolved a decade later in Parc de la Vilette – with boxes. Looking at the main time-scope of when Hans-Walter Müller’s structures came into being from the late 1960s till the end of the 70s there is another similar setting of innovative buildings sitting in a green environment. The international community in Auroville, Tamil Nadu, was mainly driven by French thinkers and architects. They developed a model town in the South Indian Jungle. Like Follies or Hans-Walter Müller’s pneumatic structures there are experimental but still liveable pieces of architecture set in the midst of a seemingly untouched green surrounding.

The interaction between nature and pneumatics plays an important role in Hans-Walter Müller’s oeuvre. Relating to a pneumatic structure he designed and built for a Tinguily exhibition he pointed out: “La nature et les volumes gonflables en harmonie, par ce qu’ils sont de la même famille constructive, la mécanique des fluids.”

Membrane architecture: the seventh established building material. Designing reliable and sustainable structures for the urban environment.



Figure 7: one of Hans-Walter Müller's gonflables set on his grounds in La Ferté Alais



Figure 8: one of the follies, Parc de la Vilette, concept Bernard Tschumi, 1983, <https://www.flickr.com/photos/victortsu/15950224982>



Figure 9: Auroville, exemplary house, credited by Sanyam Bahga - Own work, CC BY-SA 3.0, <https://commons.wikimedia.org/w/index.php?curid=17673986>



Figure 10: Milly-La-Forêt Accueil le Cyclope de J. Tinguely, photo and citation courtesy of Hans-Walter Müller

4. Conclusion

It is absolutely obvious that an ample oeuvre like that of Hans-Walter Müller can only be touched peripherally in a seven page paper. When looking at the German French architect's input on establishing fabrics and foils as the seventh building materials, his innovative impact cannot be overestimated. His proposals of decades of experimenting with pneumatics show that fabrics and foils are a grown-up building material. His extremely innovative handling of lightweight material in combination with his background as magician and pantomime experimenting with light and motion is a most prominent example for the seventh building materials' potential.

It is important to convey that these follies are not just pieces of art meant to address fellow architects or a similarly responsive audience. Hans-Walter Müller's oeuvre is an important showpiece of the fact that an ecological future in building technology is only possible with the contribution of lightweight materials like fabrics and foils.

Membrane architecture: the seventh established building material. Designing reliable and sustainable structures for the urban environment.

Knowing that citizens' engagement is most easily triggered by play it is obvious that Hans Walter Müller's playful approach additionally facilitates the promotion of fabric and foils as the seventh building material. His spheres of fabrics and foils are ideal promoters of lightweight architecture.



Figure 11: Hans-Walter Müller at work in La Ferté Alais

Acknowledgements

Hans-Walter Müller and my father were alumni at Darmstadt University, both studying architecture at the same time. I presume they did not know each other which is regrettable. Their professional career took completely different turns. Hans-Walter Müller caught up in bubbles, my father bound to boxes in the tradition of modernist architecture or more still American modernism around his favourite Frank Lloyd Wright. My own professional career path encloses both – first boxes and then bubbles. I am more than grateful for the influences which brought me there – the modernist boxes of my architects' family and the bubbles and saddle shapes from my itinerary within Textile Architecture.

References

Mehler Technologies GmbH, Textile Architecture team records, 1960s-ongoing

Meyer F., Baunetzwoche 596, BauNetz, Heinze GmbH, 2022

Stürzl R. (2022), Hans-Walter Müller und das lebendige Haus.



tensinantes2023 : TensiNet Symposium 2023 at
Nantes Université

Membrane architecture: the seventh established building material.
Designing reliable and sustainable structures for the urban
environment.

Proceedings of the Tensinet Symposium 2023

TENSINANTES2023 | 7-9 June 2023, Nantes Université, Nantes, France

Jean-Christophe Thomas, Marijke Mollaert, Carol Monticelli, Bernd Stimpfle (Eds.)

Finite element modelling of inflatable beams up to the ultimate stability phase

Laurent GORNET*, Jean-Christophe THOMAS

*GeM, Ecole Centrale Nantes/ Nantes University, France, Laurent.gornet@ec-nantes.fr,

*GeM, Nantes University, France, jean-christophe.thomas@univ-nantes.fr

Abstract

The aim of this paper is to examine three finite element models designed to simulate the behaviour of inflatable beam structures. These models are compared to each other on the example of an inflatable beam subjected to different boundary conditions. Experimentally measured vibration modes are used to show the relevance of the different models. The Timoshenko finite element beam model (T1) is based on a cubic interpolation for displacements and quadratic for rotations. The second model (T2) uses linear interpolation functions and sub-integration for rotations to avoid numerical locking phenomena. The last model (T3) is based on a quadratic interpolation of displacements and a reduced integration of rotations. The coupling between bending and torsion is taken into account. Finally, a mixed finite element approach combining pressurized beam elements with discretized cross-sections allows to take into account the nonlinear behaviour in the cross-section and drives the simulations to the loss of structural stiffness. The presented finite element models are implemented in a three-dimensional version in the finite element code Cast3M CEA.

Keywords: pneumatic structures, softening, structural membrane, sustainability

1. Introduction

In the literature there exist two classical beam models, the Euler-Bernoulli and the Timoshenko model. In the case of Timoshenko beams including shear effects, there are finite element approaches with linear, quadratic or cubic interpolation functions. These models are generally present in finite element software but not necessarily adapted to the treatment of swellable structures up to the ultimate stability phase. The choice of the interpolation functions allows to optimize the computation time or to obtain exact solutions for some loading cases [1-3]. In the case of inflatable beams, a Timoshenko finite element model with quadratic interpolation functions is presented in [2-3]. It corresponds to a finite element model with three nodes per element. The stiffness matrix is of dimension 9 by 9 in two-dimensional space. It should be noted that some components of the finite element model are under-integrated in order to avoid classical locking phenomena. In the case of an Euler-Bernoulli beam model, the choice of cubic interpolation functions allows to verify exactly the equilibrium equations. It therefore seems natural to use cubic functions to develop a

Timoshenko beam model (It3) [1]. This approach corresponds to a finite element model with two nodes per element. The stiffness matrix is of dimension 6 by 6 in a two dimensional space. The advantage of this model is that the equilibrium equations are verified and consequently there is no problem of incompatibility between the interpolation of rotations and displacements. Locking phenomena do not exist for cubic type interpolation functions. To conclude, a linear interpolation Timoshenko beam model (IT1) is proposed. The models (IT1 and IT3) can be used with meshed sections [5-6] incorporating nonlinear behaviour models to simulate the loss of stability of the inflated beam. These two finite element models have been implemented in Cast3M-CEA taking into account the center of torsion for complex cross sections. Static and vibratory responses of structures made of inflatable beams show the relevance of the proposed beam models.

2. Timoshenko beam models

This section recalls the kinematic assumptions of the derivation of a finite element model of beam with shear effects. The model will be subjected to small transformations following its pressurization. From a kinematic point of view, the so-called Timoshenko beam is made of a reference line and rigid cross sections. In the case of two symmetry axis for the cross section, the reference line passes through the centers of inertia of sections. We consider any section of the beam, M represents any point and G its center of gravity. The kinematic description of a rigid section is chosen in the following form:

$$\vec{U}(M) = \vec{U}(G) + \vec{\Omega} \wedge \vec{GM} \quad \text{avec} \quad \vec{\Omega} = \theta_y \vec{y} + \theta_x \vec{x} \quad \vec{GM} = y \vec{y} + z \vec{z}$$

In the case of a cantilever beam with a pressurized circular cross-section (p) subjected to a force F. we obtain the equilibrium equations and the boundary conditions on the generalized forces by using the principle of virtual works.

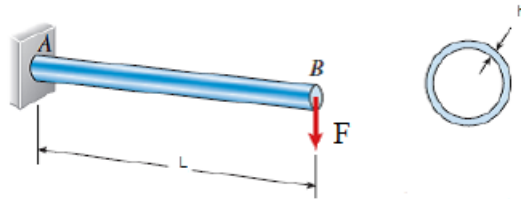


Figure 1: Pressurized beam (p) subjected to a bending force

The virtual work of internal forces $W_i^* = -\iiint_{\Omega} tr(\sigma \varepsilon(u^*)) d\Omega$ the both work of the boundary conditions and of the imposed load are written on the following form using the kinematics's Timoshenko of a rigid section: $\vec{U}^*(x, y) = v^*(x) \vec{y} - y \theta_z^*(x) \vec{x}$. The virtual work of the internal forces, work of the connections and work of the bending accelerations are:

$$W_i^* = -\int_0^l \left[M(x) \frac{d\theta_z^*}{dx} + T(x) \left(\frac{dv^*}{dx} - \theta_z^* \right) \right] dx$$

Membrane architecture: the seventh established building material. Designing reliable and sustainable structures for the urban environment.

$$W_e^* = Yv^*(0) + M \theta_z^*(0) - F v^*(l) \text{ et } W_{acc}^* = -\int_0^l \left[\rho S v^* \frac{d^2 v}{dt^2} \right] dx$$

From the generalized bending forces and the shear force appearing in the PTV $M(x) = \int_S -y \sigma_{xx} dS$ et $T(x) = \int_S \sigma_{xy} dS$ and elastic behavioral relations are

$$\sigma_{xx} = E \varepsilon_{xx} \quad \sigma_{xy} = 2G \varepsilon_{xy}$$

The generalized behavior laws are written in the following form taking into account the initial state of pressurization "p" of the beam and defining $P = p \pi R_0^2$:

$$M(x) = (E + P/S) I_z \frac{d\theta_z}{dx}, T(x) = k S \left(\frac{p}{k} + G \right) \left(\frac{dv}{dx} - \theta_z \right)$$

Equilibrium equations from the PTV:

$$\frac{dM(x)}{dx} + T(x) = 0 \quad \frac{dT(x)}{dx} = 0 \quad \forall x \in [0, l] \quad M(l) = 0 \quad T(l) = F$$

$$M(x) = F(x - l) \quad T(x) = -F$$

The analytical displacement solution resulting from the previous equations (Fig. 1) will be used as a reference to evaluate the performances of the various finite element models:

$$v(x) = -\frac{F}{\left(E + \frac{P}{S}\right) I} \left(l \frac{x^2}{2} - \frac{x^3}{6} \right) - \frac{F}{\left(\frac{p}{k} + G\right) k S} x$$

$$\theta(x) = \frac{F}{2 \left(E + \frac{P}{S}\right) I} (x^2 - 2 l x)$$

The analytical model takes into account the shear that corrects the Euler Bernoulli beam model. When the contribution of the shear effects is negligible, the Timoshenko's beam model should tend towards the Euler-Bernoulli model. Consequently, the first idea is to use a 3rd order polynomial to approximate the displacement of the Timoshenko model. Consequently, by using the definition of the shear deformation which is null in the Bernoulli model, we obtain:

Membrane architecture: the seventh established building material. Designing reliable and sustainable structures for the urban environment.

$$\frac{dM(x)}{dx} + T(x) = 0 \quad \frac{dT(x)}{dx} = 0$$

$$\text{where } M(x) = \left(E + \frac{P}{S}\right) I_z \frac{d\theta_z}{dx} \quad \text{and} \quad T(x) = k S \left(\frac{p}{k} + G\right) \left(\frac{dv}{dx} - \theta_z\right)$$

$$\left(E + \frac{P}{S}\right) I_z \frac{d^2\theta_z}{dx^2} + k S \left(\frac{p}{k} + G\right) \left(\frac{dv}{dx} - \theta_z\right) = 0$$

$$k S \left(\frac{p}{k} + G\right) \left(\frac{d^2v}{dx^2} - \frac{d\theta_z}{dx}\right) = 0$$

$$\text{Or } \frac{d^2M(x)}{dx^2} = 0 \quad \text{One gets } \frac{d^4v}{dx^4} = 0 \text{ in addition with } \varepsilon_{xy} = \frac{1}{2} \left(\frac{dv}{dx} - \theta_z\right) = 0 \Rightarrow \theta_z = \frac{dv}{dx} + c$$

$$\frac{d^2\theta_z}{dx^2} = \frac{12c}{\Phi_y G S k} \quad \text{with } \Phi_y = \frac{12 \left(E + \frac{P}{S}\right) I}{\left(\frac{p}{k} + G\right) k S}$$

2.1. Timoshenko's model IT3 order

The cubic polynomial solution represents an exact solution of the beam model $v(x) = a_0 + a_1 x + a_2 x^2 + a_3 x^3$. We determine the constants a_i as functions of the nodal unknowns of the finite element model. Using the conditions

$v(0) = v_1 \quad v(l) = v_2 \quad \theta(0) = \theta_1 \quad \theta(l) = \theta_2$. It should be noted that the interpolation functions $N_i(x)$ of the finite element model show the parameter Φ_y that is a function of the pressure. To construct the stiffness matrix, the finite element approximations are injected into the internal force work using the same interpolation functions for the virtual displacement fields as for the real fields. We obtain the finite element stiffness matrix K_{T3} .

$$v(x) = [N_1(x) \quad N_2(x)] \begin{Bmatrix} v_1 \\ v_2 \end{Bmatrix} \quad \theta(x) = [N_3(x) \quad N_4(x)] \begin{Bmatrix} \theta_1 \\ \theta_2 \end{Bmatrix}.$$

$$\int_0^l \left[\left(E + \frac{P}{S}\right) I_z \frac{d\theta_z}{dx} \frac{d\theta_z^*}{dx} + k S \left(\frac{p}{k} + G\right) \left(\frac{dv}{dx} - \theta_z\right) \left(\frac{dv^*}{dx} - \theta_z^*\right) \right] dx = \bar{U}^* K_{T3} \bar{U}$$

$$\bar{U}^T = [v_1 \quad \theta_1 \quad v_2 \quad \theta_2] \quad \text{with} \quad K_{T3} = \begin{bmatrix} 12 & 6l & -12 & 6l \\ & l^2(4 + \phi_y) & -6l & l^2(2 - \phi_y) \\ & & 12 & -6l \\ \text{Sym} & & & l^2(4 + \phi_y) \end{bmatrix}$$

The mass matrix of the IT3 model is presented only for bending. This matrix is determined from the work of the PTV acceleration quantities. The mass matrix of the IT3 model is

presented only for bending vibrations. This matrix is determined from the work of the PTV acceleration quantities. In this case the degrees of freedom $\vec{U}^T(t) = [v_1(t) \theta_1(t) v_2(t) \theta_2(t)]$ are a time function. The mass and stiffness matrices of the model are needed to determine the eigenvectors and eigenvalues of the inflatable structures. The responses of the structure to dynamic loading can be obtained using modal superposition or direct integration schemes. Three-dimensional eigenvectors of an arch are shown in Figures 5 and 6.

$$W_{acc}^* = -\int_0^l \left[\rho S v^* \frac{d^2 v}{dt^2} \right] dx = \vec{U}^{T*}(t) M_{T3} \vec{U}(t) \text{ the mass matrix:}$$

$$M_{T3} = \frac{\rho S l}{(1 + \phi_y)^2} \begin{bmatrix} 11/35 + m_{11} & 11/210 + m_{12} & 9/70 + m_{13} & -13/420 + m_{14} \\ & 1/105 + m_{22} & 13/420 + m_{23} & -1/140 + m_{24} \\ & & 13/35 + m_{33} & -11/210 + m_{34} \\ \text{Sym} & & & 1/105 + m_{44} \end{bmatrix}$$

$$m_{11} = 7/10 \phi_y + 1/3 \phi_y^2, m_{12} = (11/120 \phi_y + 1/24 \phi_y^2)l, m_{13} = 3/10 \phi_y + 1/6 \phi_y^2$$

$$m_{14} = -(3/40 \phi_y + 1/24 \phi_y^2)l$$

$$m_{22} = (1/60 \phi_y + 1/120 \phi_y^2)l^2,$$

$$m_{23} = (3/40 \phi_y + 1/24 \phi_y^2)l,$$

$$m_{24} = -(1/60 \phi_y + 1/120 \phi_y^2)l^2$$

$$m_{33} = 7/10 \phi_y + 1/3 \phi_y^2, m_{32} = (11/120 \phi_y + 1/24 \phi_y^2)l, m_{44} = (1/60 \phi_y + 1/120 \phi_y^2)l^2$$

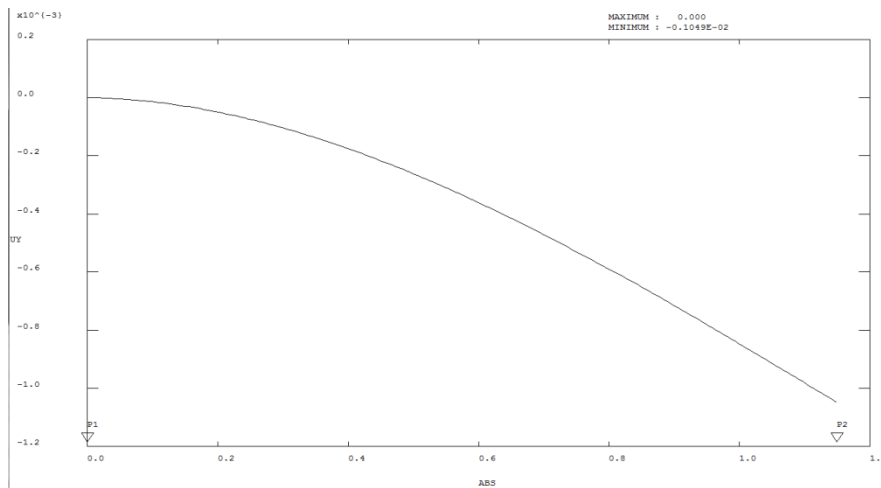


Figure 2: Timoshenko's inflatable beam. Displacement of the reference line for IT3 model. The finite element solution corresponds to the analytical one. Code Cast3M CEA

Table 1: Beam properties of the example Fig. 1.

Characteristics	value	Units
l	1.15	m
R	0.08	m
h	125 10 ⁻⁶	m
E	2500	MPa
G	940	MPa
k	0.5	

It should be noted that the IT3 model is equivalent to the analytical solution. This finite element formulation has been integrated into the Cast3M finite element code. The pressure-dependent mass matrix is used to determine the vibration eigenvectors and also to conduct simulations in the vibration domain. This IT3 model has a lower numerical cost than the three-node case which is quadratically interpolated (IT2 model [2]). In the following, a linear interpolation model is presented.

2.3. Timoshenko's model IT1 order

The Timoshenko finite element model with linear interpolation is presented. Two functions $N_i(x)$ are used to interpolate the displacement and rotation of the section. The use of identical interpolation for displacement and rotation leads to a locking phenomenon. One way to deal with this problem is to sub-integrate the strain energy due to shear into the work of the internal forces [7-8]. It should be noted that if the derivative of the displacement and rotation are interpolated with functions of the same order the locking phenomenon disappears with the reduced integration. This element is integrated in the Cast3M code and a simple modification of the elastic properties of the beam allows to treat examples of inflatable beams.

$$v(x) = [N_1(x) \quad N_2(x)] \begin{Bmatrix} v_1 \\ v_2 \end{Bmatrix} \quad \theta(x) = [N_1(x) \quad N_2(x)] \begin{Bmatrix} \theta_1 \\ \theta_2 \end{Bmatrix}$$

$$N_1(x) = 1 - \frac{x}{l} \quad N_2(x) = \frac{x}{l}$$

$$\int_0^l \left(E + \frac{P}{S} \right) I_z \frac{d\theta_z}{dx} \frac{d\theta_z^*}{dx} dx + \int_0^l k S \left(\frac{p}{k} + G \right) \left(\frac{dv}{dx} - \theta_z \right) \left(\frac{dv^*}{dx} - \theta_z^* \right) dx = \bar{U}^* K_{T1} \bar{U}$$

$$\bar{U}^T = [v_1 \quad \theta_1 \quad v_2 \quad \theta_2] \text{ with}$$

$$K_{T3} = \begin{bmatrix} \frac{S G_p}{l} & \frac{S G_p}{2} & -\frac{S G_p}{l} & \frac{S G_p}{2} \\ & \frac{E_p I_z}{l} + \frac{S l G_p}{4} & -\frac{S G_p}{2} & -\frac{E_p I_z}{l} + \frac{S l G_p}{4} \\ & & \frac{S G_p}{l} & -\frac{S G_p}{2} \\ \text{Sym} & & & \frac{E_p I_z}{l} + \frac{S l G_p}{4} \end{bmatrix}$$

$$\text{with } G_p = G + p / k \quad E_p = E + P / S$$

3. Finite beam elements with meshed sections

There are conventionally two methods to account for the nonlinear behaviour of a finite element beam model. The first method is to use nonlinear behaviour models between the generalized forces and the strains. This method is presented for elasto-plastic models in [9]. Coefficients are introduced in the behavioural model to take into account the shape of the cross-section. The second method consists in combining the ends of a Timoshenko beam finite element with a discretized section. This method allows the inclusion of a nonlinear model at each Gauss point of the sections [5-6]. The quasi-static response to a concentrated force of the T3 inflatable beam model as well as the frequencies and first eigenvectors calculated with the Cast3M code are presented in figure 1.

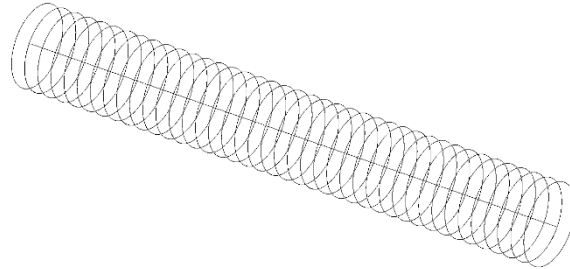


Figure 3: Model T3. Timoshenko Inflatable Beam elements combined with tube mesh sections.

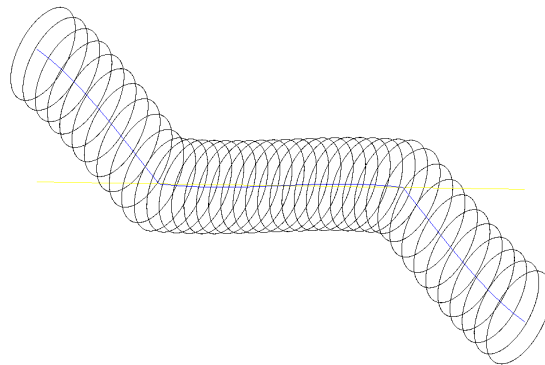


Figure 4: Model T1. Eigenvector at 1.3 Hz of an inflatable Timoshenko beam combined with meshed sections of tube. The beam is on two supports.

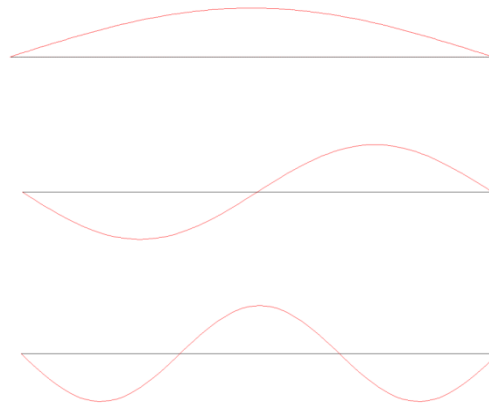


Figure 5: Model T3. The first three eigenvectors are associated with the eigen frequencies 4.91Hz; 13.059Hz, 21.148Hz of a Timoshenko T3 Inflatable Beam on two supports.

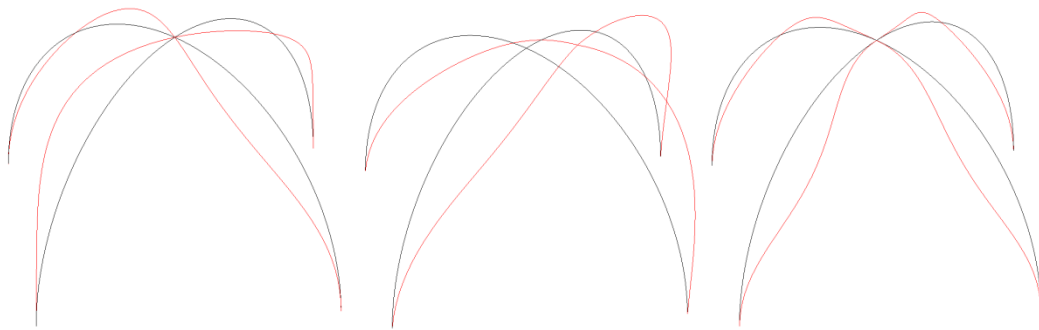


Figure 6: Three-dimensional embedded arch, model T3 (embedded boundary conditions). The first three eigenvectors are associated with the eigenfrequencies 6.011Hz; 6.782Hz, 10.87Hz of a structure consisting of inflatable beams.

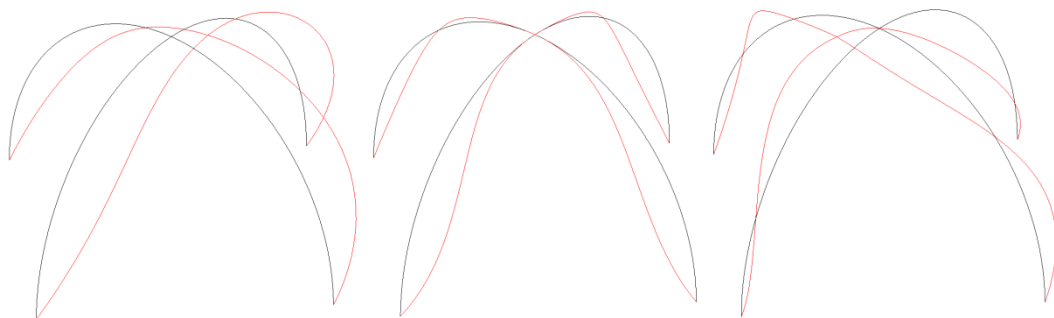


Figure 7: Three-dimensional arch, model T3 (boundary conditions supported). The first frequency is 1.205 Hz not shown. The three following eigenvectors are associated with the eigenfrequencies 3.388Hz (shape close to 1.205 Hz); 4.399Hz, 5.220Hz of a structure consisting of inflatable beams.

4. Conclusion

The work carried out at GeM has allowed the development of several finite element versions of the Timoshenko beam model dedicated to inflatable structures [1-4]. These Timoshenko models are cubic, quadratic or linear interpolation models. Only the cubic interpolation model is not subject to the locking phenomenon [1]. For the quadratic and linear interpolations, a selective integration called reduced integration of certain components allows to avoid the locking phenomena [7-8]. These models implemented in the Cast3M code can use all the functions of the finite element code. In particular, they can be associated with meshed sections in order to simulate beams up to the ultimate stability phase.

References

- [1] Jean-Christophe Thomas, Christian Wielgosz, *Deflections of highly inflated fabric tubes*, Thin-Walled Structures, Elsevier, 42 (7), pp.1049-1066, 2004.
- [2] Anh Le Van, Christian Wielgosz. *Finite element formulation for inflatable beams*. Thin-Walled Structures, Elsevier, 45 (2), pp.221-236. 2007.
- [3] A. Levan, C. Wielghosz, *Bending and buckling of inflatable beams: Some new theoretical results*. Mechanics and Engineering, 195, (52), 7264-7281, 2006.
- [4] Q.-T. Nguyen, J.-C. Thomas, and A. Le Van. *Inflation and bending of an orthotropic inflatable beam*. *Thin-Walled Structures*, 88 (0), 129 – 144 , 2015.
- [5] Spacone E, Filippou FC, Taucer FF. Fibre beam-column model for non-linear analysis of R/C frames: part I. formulation. *Earthquake Eng Struct Dynam*,25(7):711–26, 1996.
- [6] J. Mazars, P. Kotronis, F. Ragueneau, G. Casaux, *Using multifiber beams to account for shear and torsion*. Applications to concrete structural elements, Computer Methods in Applied
- [7] J.N. Ready, On locking-free shear deformable beam finite elements, *Computer Methods in Applied Engrg*. 149 -113-132, 1997.
- [8] J. Donea, L.G. Lamain, *A modified representation of transverse shear in C^0 quadrilateral plate elements*, Computer Methods in Applied Mechanics and Engineering, 63, 183-207, 1987.
- [9] DRJ Owen, E. Hinton, *Finite Elements in plasticity, theory and practice*, Pineridge Press, 1980.



tensinantes2023 : TensiNet Symposium 2023 at Nantes Université

Membrane architecture: the seventh established building material. Designing reliable and sustainable structures for the urban environment.

Proceedings of the Tensinet Symposium 2023

TENSINANTES2023 | 7-9 June 2023, Nantes Université, Nantes, France

Jean-Christophe Thomas, Marijke Mollaert, Carol Monticelli, Bernd Stimpfle (Eds.)

Analytical, numerical and experimental study of inflatable panels

Paul LACORRE, Anh LE VAN, Rabah BOUZIDI, Jean-Christophe THOMAS*

Institute of Research in Civil and Mechanical Engineering (GeM), CNRS UMR 6183

2 rue de la Houssinière, BP 92208, F-44000 Nantes, France

*Corresponding author: jean-christophe.thomas@univ-nantes.fr

Abstract

While most pressurized membrane structures have rounded shapes, an inflatable panel has two parallel flat sides: the inflated thickness of drop-stitch panels is set by the length of the high-strength threads that connect the upper and lower membranes, and the panel is finally sealed by lateral walls to make it airtight. Their light weight and small packed volume make them ideal for transportation and deployment, and they can be reused many times with different stiffness just by adjusting the inflation pressure. The literature dedicated to this specific component is scarce: pioneering works by NASA from the '60s proposed a plate-like model but more recent research efforts have been focused on inflatable beams or one-dimensional models of drop-stitch panels. This work investigates theoretical, computational and experimental aspects of pressurized plate-like structures. We propose a modern analytical theory based on the Mindlin-Reissner kinematics that accounts for shear and pressure-stiffening effects and compare analytical solutions with nonlinear finite element simulations as well as experimental data obtained from circular panels testing. The nonlinear equations of motion are derived from the principle of virtual power within the framework of finite deformations. Then, the equations are linearized around the inflated reference configuration and solved for a simply-supported circular panel subjected to a uniform load. The same problem is then treated using nonlinear 3D finite element analysis and investigated experimentally to assess the accuracy of the model. The results of this research can help guiding the design of inflatable panels and hopefully generalize the use of flat surfaces in load-bearing inflatable structures.

Keywords: inflatable panels, drop-stitch, pressurized membrane structure, large deformation, linearization, nonlinear finite element analysis, experiments, circular plate

1. Introduction

1.1. Inflatable panels

Pneumatic structures are structures that are stiffened by a pressure difference between the internal pressure and the ambient pressure, which can be caused by an overpressure or underpressure of the enclosed air volume; inducing a bi-axial pre-tension state in the fabric. This also generally means that the individual membrane systems, which enclose the air volume, are curved and wrinkle-free. Pneumatic structures are then able to transfer external loads by tensile forces into a substructure, into a primary structure or directly into the foundation. Many different curved shapes can be obtained with inflatables and the family of pneumatic structures can be divided into three subfamilies:

- air supported structures, which are often single membrane structures, such as air halls or inflatable roofs,
- air inflated structures, such as inflatable beams, columns, cushions, panels or mattresses,
- hybrid structures, which can be a combination of the above, or membrane reinforced.

Tensile fabric structures generally have opposing principal curvatures, and as such they belong to the anticlastic surfaces family (Figure 1). On the other hand, inflatable structures naturally have synclastic curvature (principal curvatures of the same sign), as can be seen with airbags; or single curvature (monoclastic), which is the case of inflatable tubes or cones. Some shapes (such as a torus) can even exhibit the three types of curvature.

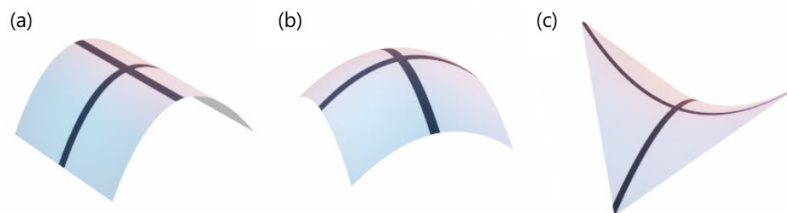


Figure 1: monoclastic (a), synclastic (b) and anticlastic (c) surfaces.

Numerous studies have been carried out over the last decades on simple elements such as inflatable tubes in order to provide design tools to study the behavior of inflatable tubes, cones and arches assemblies. The main challenge was to correctly quantify the influence of internal pressure on deformations and on the appearance of wrinkles or structural failure. Many of the team's works have highlighted the importance of the initial state of pressurization, and determined bending formulae by linearizing the mechanical equations obtained in total Lagrangian formulation (Nguyen 2015).

Once the behavior of one-dimensional structural elements such as beams and columns is mastered, it is logical to move on to plate elements which are two-dimensional elements. From the point of view of inflatable engineering, joining beams and panels can lead to lightweight constructions that are easy to implement by assembling the different elements.

Another kind of inflatable structures is the cushion wall, an airtight envelope where threads connect opposite walls, thus creating flatter shapes than the naturally curved shapes of the structures (see Figure 2). If the number of these threads is considerably increased, the so-called “drop-stitch” technology is obtained. The threads can be called “drop cords” or “drop yarns”. Figure 3 shows the interior of an inflatable panel, and in particular the large number of drop

Membrane architecture: the seventh established building material. Designing reliable and sustainable structures for the urban environment.

yarns that ensure the quasi-perfect flatness of the inflatable panel. In order to ensure the airtightness, the panel must be sealed with sidewalls, which can be seen in the right-hand view. The fabric is usually coated with PVC, made flame retardant and resistant to UV. The inflated thickness of drop-stitch panels is set by the length of the high-strength threads that connect the upper and lower membranes.

The production of inflatable panels is partly directed towards leisure, with sports equipment such as inflatable gymnastics mats, stand up paddles, floating platforms for boat maintenance and floating platforms to operate on water (Figure 4). Other applications involve inflatable movie screens or inflatable plane wings. There are also patents for inflatable wings, antennas, dams and rescue boards.



Figure 2: Inflatable structure with tubes, arches and cushion walls with inner threads. (© Vivien Laille, FlyPix.fr)

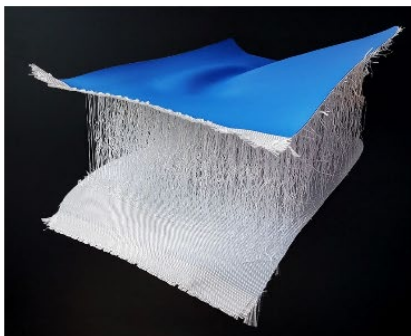


Figure 3: Cut-views of double-wall fabric with drop cords.



Figure 4: Floating decontamination platform. (© Écocréation)

Membrane architecture: the seventh established building material. Designing reliable and sustainable structures for the urban environment.

1.2. Previous works

The first mention of the “airmat” technology invented by the Goodyear Aircraft Company can be found in the research conducted at NASA by Leonard, McComb and Brooks (1960). They proposed a linear theory for inflatable panels using the principle of minimum total potential energy. They highlighted the similarities with the Mindlin–Reissner theory of thick plates.

Soon after, they analyzed the behavior of an inflatable cylindrical tube with two flat sides in an array of identical parallel tubes connected to each other (Kyser 1963). Such structures are lighter and easier to fold than drop-stitch structures with closely-spaced drop cords. It is interesting to note that this kind of tubular inflatable panel is currently a popular design choice for reentry vehicles in the space industry (Dillman 2013).

Dauids et al. (2021) carried out an experimental and computational study of the orthotropic behavior of the membranes in slender inflatable panels. The underlying equation are essentially one-dimensional, while managing to take into account the rounded edges that form when pressurized. They simulated the nonlinear (softening / stiffening) post-wrinkling response numerically by adapting a finite-element code they had previously worked on.

In this study which follows previous works on inflatable beams (Nguyen et al. 2015), analytical, numerical and experimental approaches are presented for inflatable panels. The 2D plate-like theory that was developed is based on the Mindlin–Reissner kinematics to allow shear deformation. To take the pressure into account, the formulation must be done in large deformations, large displacements and large rotations. The governing equations are obtained by using the principle of virtual power. Then the nonlinear equations are linearized around the inflated configuration with special emphasis on the importance of the terms relating to the inflating pressure. Then, the linear solution to the static bending problem of a simply-supported inflatable disk with uniform vertical load is given, and the analytical results are compared with numerical simulations obtained from a 3D-code dedicated to membrane structures, and with experiments on a 3-meter diameter inflatable panel.

2. Study of inflatable panels

2.1. Geometry of the panel

We consider structures where the mid-surface is a plane and all the quantities can be reduced to the plane, just like the study of beams was reduced to the study of quantities defined on the neutral fiber in the previous section.

First, we describe the reference configuration. The above and lower membranes are kept at a fixed distance H due to the presence of cords in drop-stitch panels (Figure 5). The thickness of the membranes is τ . The distance between the two membranes is $\tilde{H} = H - 2\tau$. Therefore, when integrating through the thickness, the considered interval is

$$T = \left[-\frac{H}{2}, -\frac{\tilde{H}}{2} \right] \cup \left[\frac{\tilde{H}}{2}, \frac{H}{2} \right]$$

Membrane architecture: the seventh established building material. Designing reliable and sustainable structures for the urban environment.

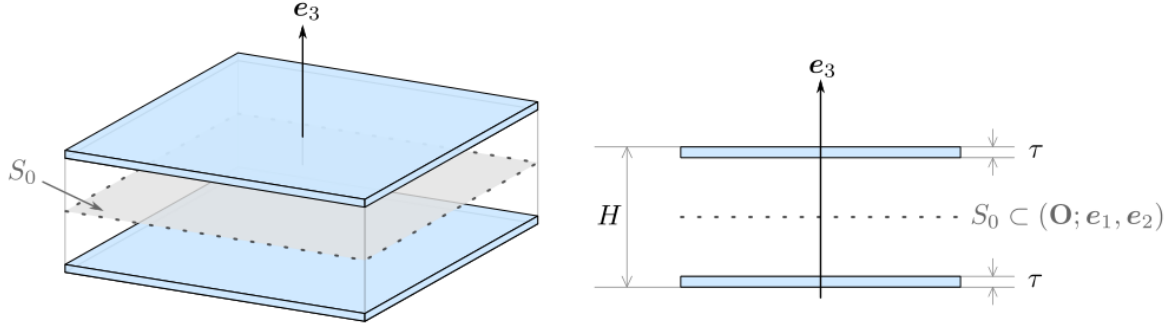


Figure 5: Reference configuration and cross-sectional view of the upper and lower membranes.

For a plate, the curvilinear basis at point \mathbf{Q}_0 is defined by

$$\forall i \in \{1,2,3\}, \quad \mathbf{G}_i = \mathbf{A}_i = \frac{\partial \mathbf{Q}_0}{\partial \xi^i}$$

And since the geometry is that of a plate, $\mathbf{A}_3 = \mathbf{G}_3 = \mathbf{e}_3$.

Second, we define the current configuration. For every point \mathbf{Q}_0 inside the membranes, there is a corresponding point \mathbf{P}_0 on the mid-surface S_0 . The displacement field is

$$\mathbf{U}(\mathbf{Q}_0, t) = \mathbf{U} + Z (\mathbf{a}_3 - \mathbf{e}_3)$$

where $\mathbf{U} \equiv \mathbf{U}(\mathbf{P}_0, t)$ is the displacement of the mid-surface, $\mathbf{a}_3 \equiv \mathbf{a}_3(\mathbf{P}_0, t)$ the fiber orientation field and $Z = \mathbf{P}_0 \mathbf{Q}_0$ the distance to the mid-surface.

In the current configuration, the local basis writes

$$\forall \alpha \in \{1,2\}, \quad \mathbf{g}_\alpha = \mathbf{a}_\alpha = \frac{\partial \mathbf{Q}}{\partial \xi^\alpha}$$

where \mathbf{Q} is the image of \mathbf{Q}_0 after deformation (the same goes for \mathbf{P}_0 and \mathbf{P}). Using these vectors, the Green strain tensor is defined as:

$$\mathbf{E} = E_{ij} \mathbf{A}^i \otimes \mathbf{A}^j = \frac{1}{2} (g_{ij} - G_{ij}) \mathbf{A}^i \otimes \mathbf{A}^j \quad (1)$$

where \mathbf{A}^i is the contravariant basis vector and $g_{ij} = \mathbf{g}_i \cdot \mathbf{g}_j = \mathbf{A}_i \otimes \mathbf{A}_j$ (with Einstein summation convention).

2.2. Derivation of the equations of motion

We propose a total Lagrangian formulation using the principle of virtual power:

$$\mathcal{P}_{int}^* + \mathcal{P}_p^* + \mathcal{P}_{ext \setminus p}^* = \mathcal{P}_{acc}$$

where the virtual power of internal forces is

$$\mathcal{P}_{int}^* = - \int_{\Omega_0} \boldsymbol{\Pi}^T : \mathbf{grad}_{\mathbf{Q}_0} U^*(\mathbf{Q}_0) \, d\Omega_0$$

Membrane architecture: the seventh established building material. Designing reliable and sustainable structures for the urban environment.

and \mathcal{P}_p^* is the virtual power of pressure forces, $\mathcal{P}_{ext\setminus p}^*$ the virtual power of external forces other than the pressure forces and \mathcal{P}_{acc} the virtual power of inertial forces (which vanishes in statics). The virtual velocity field is taken of the same form as the displacement field:

$$\mathbf{U}^*(\mathbf{Q}_0, t) = \mathbf{U}^* + Z \mathbf{a}_3^*$$

where \mathbf{U}^* is the virtual velocity of the mid-surface and \mathbf{a}_3^* is the virtual director vector $\mathbf{a}_3^* = \boldsymbol{\omega}^* \times \mathbf{a}_3$ ($\boldsymbol{\omega}^*$ is the virtual angular velocity vector).

Compared to a classical theory of plate, the main addition is the virtual power of pressure forces pushing the panel from the inside.

$$\mathcal{P}_p^* = \int_{\partial S} p \mathbf{n} \cdot \mathbf{u}^*(\mathbf{Q}) dS$$

which becomes, after all calculations are done: $\forall \mathbf{P}_0 \in S_0$,

$$\mathcal{P}_{p \rightarrow S_0}^* = \int_{S_0} \frac{p \tilde{H}}{\sqrt{A}} (\mathbf{a}_1 \times \mathbf{a}_{3,2} + \mathbf{a}_{3,1} \times \mathbf{a}_2) \cdot \mathbf{U}^* dS_0 + \int_{S_0} \frac{p \tilde{H}}{\sqrt{A}} (\mathbf{a}_3 \times (\mathbf{a}_1 \times \mathbf{a}_2)) \cdot \boldsymbol{\omega}^* dS_0$$

As for the edge: $\forall \mathbf{P}_0 \in \partial S_0$,

$$\mathcal{P}_{p \rightarrow \partial S_0}^* = \int_{S_0} p \tilde{H} \mathbf{U}^* \cdot (\mathbf{P}_{,\lambda} \times \mathbf{a}_3) d\lambda + \frac{p \tilde{H}^3}{12} \int_{\Lambda} \boldsymbol{\omega}^* \cdot \mathbf{a}_{3,\lambda} d\lambda$$

In the two equations above, the first integral gives rise to balancing pressure forces and the second integral to balancing moments. For more detailed comments and proofs of these results, we refer the reader to the corresponding paper (Lacorre 2022).

2.3. Inflated configuration

In practice, the dimensions of the structure are measured before inflation. However, our calculations take the inflated configuration as a reference. Therefore, one must be able to deduce the inflated lengths from deflated measurements. From infinitesimal strain theory calculations, the reference height is found proportional to the deflated height H_\emptyset :

$$H = H_\emptyset \left(1 + \frac{p}{d E_y A_y} \right)$$

where p is the inflation pressure, d the density of yarns (in number of yarns per square meter) and $E_y A_y$ the axial stiffness modulus of a single yarn (Young's modulus times section area). Now, assuming a rectangular panel the initial length L_\emptyset of one side:

$$L = L_\emptyset \left(1 + \frac{1 - \nu}{E} \frac{p(H_\emptyset - 2\tau)}{2\tau} \right)$$

Although the calculation is different, the same relationship applies to the radius of a circular panel. Some values are given for a circular panel in Table 1 for an axial stiffness of $E_y A_y = 100$ N and a density of threads $d = 30,000$ m⁻².

Membrane architecture: the seventh established building material. Designing reliable and sustainable structures for the urban environment.

Table 1: Radii and heights of the inflated panel before and after inflation ($E = 0.59$ GPa).

R_\emptyset (m)	H_\emptyset (cm)	p (kPa)	R (m)	H (cm)
1.5	10	30	1.504	10.10
		50	1.507	10.17
		70	1.510	10.23
		90	1.513	10.30
	20	30	1.509	20.20
		50	1.515	20.33
		70	1.521	20.47
		90	1.527	20.60

2.4. Linearized equations in statics

Hypotheses

In statics, every time-dependent term is cancelled. Furthermore, we assume small displacements and small rotations: the mid-surface displacement \mathbf{U} and the fiber rotation vector $\boldsymbol{\psi}$, as well as their derivatives, are assumed to be infinitesimal of the first order.

In what follows, the pressure-related terms are colored in blue.

Membrane problem

The linearized equations of motion are: $\forall t, \forall \mathbf{P}_0 \in S_0$,

$$\mathbf{N}_0: \mathbf{grad} \mathbf{grad} \mathbf{U}^P + \frac{E\tau}{1-\nu^2} [(1-\nu)\Delta \mathbf{U}^P + (1+\nu)\mathbf{grad} \operatorname{div} \mathbf{U}^P] + \mathbf{q} \cdot \mathbf{a}^\alpha = \mathbf{0}$$

where \mathbf{N}_0 are initial membrane forces due to inflation pressure and other pre-stresses. \cdot^P denotes the projection of a vector onto the plane $\mathbf{Oe}_1\mathbf{e}_2$.

The linearized boundary condition is: $\forall t, \forall \mathbf{P}_0 \in \partial S_0$,

$$\frac{2E\tau}{1-\nu^2} ((1-\nu) \mathbf{grad}_S \mathbf{U}^P + \nu(\operatorname{div} \mathbf{U}^P)\mathbf{I}) \cdot \mathbf{v}_0 + p\tilde{\mathbf{H}}[\mathbf{grad} \mathbf{U}^P \cdot \mathbf{v}_0 + \mathbf{U}_{,s_0}^P \times \mathbf{e}_3] = \mathbf{q}' \cdot \mathbf{a}^\alpha$$

where $\mathbf{grad}_S = \frac{1}{2}(\mathbf{grad}^T + \mathbf{grad})$.

Bending problem

The linearized equations of motion are: $\forall t, \forall \mathbf{P}_0 \in S_0$,

$$\mathbf{N}_0: \mathbf{grad} \mathbf{grad} W + p\tilde{\mathbf{H}}\operatorname{div} \boldsymbol{\psi} + \mathbf{q} \cdot \mathbf{a}^3 = \mathbf{0}$$

$$\frac{D^*}{2} [(1-\nu)\Delta \boldsymbol{\psi} + (1+\nu) \mathbf{grad} \operatorname{div} \boldsymbol{\psi}] + \operatorname{div}(\mathbf{grad} \boldsymbol{\psi} \cdot \mathbf{M}_0^{(2)}) - p\tilde{\mathbf{H}}(\boldsymbol{\psi} + \mathbf{grad} W) = \mathbf{0}$$

Membrane architecture: the seventh established building material. Designing reliable and sustainable structures for the urban environment.

where $D^* = \frac{E\tilde{\tau}H^2}{2(1-\nu^2)}$ the bending stiffness of the membranes.

The linearized boundary conditions are: $\forall t, \forall \mathbf{P}_0 \in \partial S_0$,

$$p\tilde{H}(\boldsymbol{\psi} + \mathbf{grad} W) \cdot \mathbf{v}_0 = \mathbf{q}' \cdot \mathbf{a}^3$$

$$\begin{aligned} D^*[(1-\nu)\mathbf{v}_0 \cdot \mathbf{grad}_s \boldsymbol{\psi} \cdot \mathbf{v}_0 + \nu \operatorname{div} \boldsymbol{\psi}] + \mathbf{v}_0 \cdot \mathbf{grad} \boldsymbol{\psi} \cdot \mathbf{M}_0^{(2)} \cdot \mathbf{v}_0 + \frac{p\tilde{H}^3}{12} \boldsymbol{\psi}_{,s_0} \cdot \mathbf{s}_0 \\ = (1 - \mathbf{v}_0 \cdot \mathbf{grad} \mathbf{U}^P \cdot \mathbf{v}_0) \Gamma^S \end{aligned}$$

and

$$\begin{aligned} D^*(1-\nu)\mathbf{s}_0 \cdot \mathbf{grad}_s \boldsymbol{\psi} \cdot \mathbf{v}_0 + \mathbf{s}_0 \cdot \mathbf{grad} \boldsymbol{\psi} \cdot \mathbf{M}_0^{(2)} \cdot \mathbf{v}_0 - \frac{p\tilde{H}^3}{12} \boldsymbol{\psi}_{,s_0} \cdot \mathbf{v}_0 \\ = -(2\mathbf{s}_0 \cdot \mathbf{grad}_s \mathbf{U}^P \cdot \mathbf{v}_0) \Gamma^S - (1 - \mathbf{s}_0 \cdot \mathbf{grad} \mathbf{U}^P \cdot \mathbf{s}_0) \Gamma^\nu \end{aligned}$$

3. Application example: simply-supported disk with uniform load

One of the simplest geometries for panels is a circular shape. The equations can be solved in the case of a uniform vertical load with the perimeter on simple support, making the problem axisymmetric. The two local equations are:

$$\frac{1}{r} \left(r(W_{,r} + \psi_r) \right)_{,r} = -\frac{q}{p\tilde{H}} \quad (2)$$

$$-K \left(\psi_{r,rr} + \frac{\psi_{r,r}}{r} - \frac{\psi_r}{r^2} \right) + p\tilde{H}(W_{,r} + \psi_r) = 0 \quad (3)$$

where $K = \frac{E\tilde{\tau}H^2}{2(1-\nu)^2} + \frac{pH^2\tilde{H}\tilde{\tau}}{4\tau}$ is the total bending stiffness. Taking into account the boundary conditions ($W(R) = 0$ and $\Gamma^\theta = 0$), the transverse deflection and fiber rotation fields are

$$\begin{cases} W(r) = q(R^2 - r^2) \left(\frac{1}{4p\tilde{H}} + \frac{1}{64K} \left(\frac{5K + K'}{K + K'} R^2 - r^2 \right) \right) \\ \psi_r(r) = \frac{q}{16K} r \left(\frac{3K + K'}{K + K'} R^2 - r^2 \right) \end{cases} \quad (4)$$

where pressure-dependent terms are highlighted in blue. Since the shear term $1/4p\tilde{H}$ is the main contribution to W , the solution is approximately quadratic. The fiber rotations ψ_r are very small (less than a degree).

Wrinkling load

Based on this linearized solution, one may compute the stresses and the load for which the stresses vanish (the wrinkling load). For very thin membranes ($\tau \ll H$) and reasonable pretension (average pressure and large panel height H), the limit load is

Membrane architecture: the seventh established building material. Designing reliable and sustainable structures for the urban environment.

$$q_w \approx \pm \frac{8p}{3 + \nu} \left(\frac{H}{R}\right)^2$$

Caution should be exerted when approximating wrinkling loads using linearized equations, as the onset of wrinkling happens in the nonlinear domain.

3.1. Numerical validation

The panel was modelled in an open source 3D finite element software (Evolver) using 12,288 triangular membrane elements as well as bar elements to connect the upper and lower faces. This 3D model of the structure accounts for all the material and geometric nonlinearities of the real system, such as the possibility for the fibers to become loose when the panel is crushed (which models the lack of compressive strength). The solution is found iteratively by updating the position of each of the 6,416 nodes using the conjugate gradient method to minimize the total potential energy. The results are presented in Table 2.

Table 2: Analytical and 3D finite element results for a simply supported circular inflatable panel ($q = 100$ Pa, $E = 2.5$ GPa).

p (kPa)	H_\emptyset (cm)	H (cm)	R_\emptyset (cm)	R (cm)	W_{FE} (mm)	$W_{analytic}$ (mm)	Relative Difference (%)	Wrinkling load q_w (Pa)	
30	10	10.10	1.0	1.000	9.17	9.11	0.7	734	
			1.5	1.501	22.10	22.59	-2.2	326	
			2.0	2.001	42.39	45.35	-6.5	183	
	20	20.20	1.0	0.999	4.49	4.33	3.7	2983	
			1.5	1.501	10.49	10.29	2.0	1323	
			2.0	2.002	19.86	19.59	1.4	743	
	50	10	10.17	1.0	1.001	5.79	5.72	1.2	1239
				1.5	1.502	14.98	14.94	0.3	551
				2.0	2.002	31.14	31.70	-1.8	310
20		20.33	1.0	1.000	2.72	2.66	2.3	5034	
			1.5	1.502	6.64	6.51	2.0	2232	
			2.0	2.004	13.13	12.86	2.1	1255	
70	10	10.23	1.0	1.001	4.32	4.27	1.2	1758	
			1.5	1.502	11.76	11.64	1.0	781	
			2.0	2.003	25.70	25.78	-0.3	439	
	20	20.47	1.0	1.001	1.98	1.94	2.0	7134	
			1.5	1.504	4.99	4.88	2.3	3164	
			2.0	2.006	10.20	9.95	2.5	1778	
90	10	10.30	1.0	1.002	3.50	3.46	1.4	2289	
			1.5	1.503	9.92	9.79	1.3	1017	
			2.0	2.004	22.51	22.43	0.4	572	
	20	20.60	1.0	1.003	1.57	1.54	2.0	9285	
			1.5	1.505	4.08	3.98	2.6	4119	
			2.0	2.008	8.56	8.33	2.8	2315	

Membrane architecture: the seventh established building material. Designing reliable and sustainable structures for the urban environment.

3.2. Experimental validation

Experiments were conducted at Nantes University on a large inflatable circular panel ($R_\phi = 3$ m, $H_\phi = 10$ cm) to validate the predictions of Equation (4). In order to do this, the deflection W was measured along a diameter of the panel before and after the load q_3 was applied.



Figure 6: Experimental setup to measure the deflection of circular inflatable panels at various inflation and load levels.

The measured deflection profiles $W(r)$ are presented and compared to analytical plots. The inflation pressure is specified on top of each figure, and the legend gives the surface load applied on the opposite side of the disk.

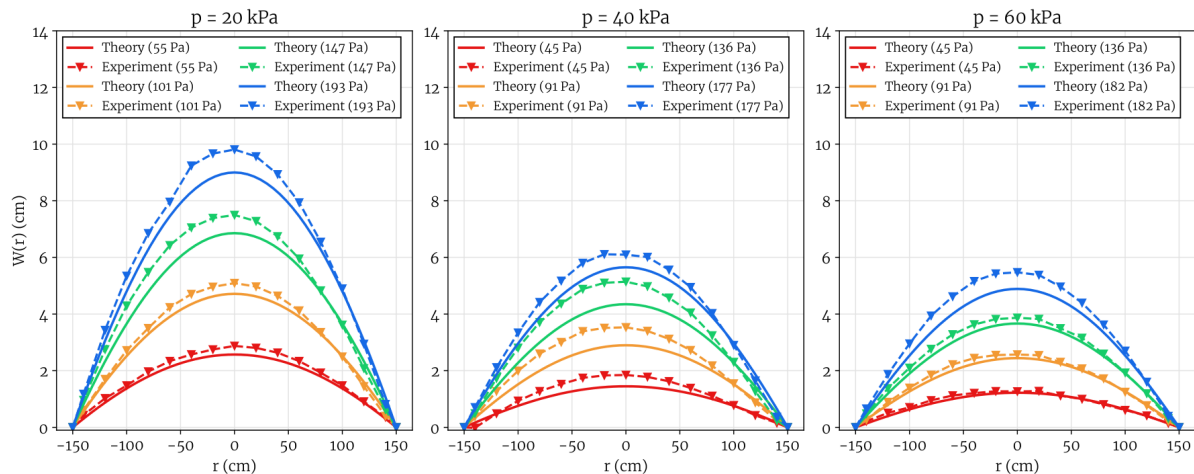


Figure 7: Experimental deflection profiles compared to the analytical solution (parameters: $R_\phi = 1.52$ m, $H_\phi = 10$ cm, $\nu = 0.25$, $E\tau = 390$ N/mm).

Membrane architecture: the seventh established building material. Designing reliable and sustainable structures for the urban environment.

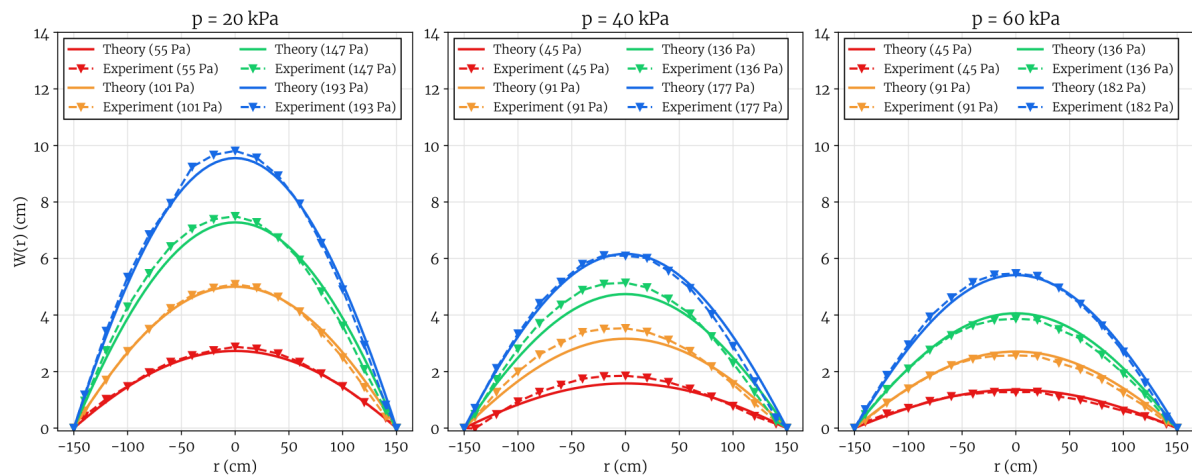


Figure 8: Experimental deflection profiles compared to the analytical solution with a smaller Poisson's ratio (parameters: $R_0 = 1.52$ m, $H_0 = 10$ cm, $\nu = 0.1$, $E\tau = 390$ N/mm)

Figure 7 shows the good agreement between experimental and theoretical deflections. However, the Poisson's ratio ν has not been measured: the value used in the analytical equations and the simulations was chosen arbitrarily ($\nu = 0.25$). By taking a smaller value such as $\nu = 0.1$, which is realistic and commonly found in the literature, the average relative error on the maximum deflection drops from 12% to 6% (Figure 8).

4. Conclusion

This research proposed an in-depth analysis of inflatable panels, taking into account their particular design. The large displacements are described by an appropriate kinematic field following the Mindlin-Reissner hypotheses. An analytical solution to the problem of static bending of uniformly loaded circular panel is proposed with its corresponding wrinkling load. It is found to be in good agreement with finite element solution and experimental results. Following these results, it will be easier to design membrane structures that incorporate inflatable panels as stiffening of load-bearing structural elements.

References

- Davids, W. G., Waugh, E., & Vel, S. (2021). Experimental and computational assessment of the bending behavior of inflatable drop-stitch fabric panels. In *Thin-Walled Structures*, 167, 108178.
- Dillman, R., DiNonno, J., Bodkin, R., Gsell, V., Miller, N., Olds, A., & Bruce, W. (2013, June). Flight performance of the inflatable reentry vehicle experiment 3. In *International Planetary Probe Workshop (IPPW-10)* (No. NF1676L-16379).
- Kyser, A. C. (1963). *A Contribution to the Theory of Pressure Stabilized Structures*. National Aeronautics and Space Administration.

Membrane architecture: the seventh established building material. Designing reliable and sustainable structures for the urban environment.

Lacorre, P., Le Van, A., Bouzidi, R., & Thomas, J. C. (2022). A plate theory for inflatable panels. In *International Journal of Solids and Structures*, 256, 111969.

Leonard, R. W., Brooks, G. W., & McComb, H. G. (1960). *Structural considerations of inflatable reentry vehicles* (Vol. 457). National Aeronautics and Space Administration.

McComb, H. G. (1961). *A linear theory for inflatable plates of arbitrary shape*. National Aeronautics and Space Administration.

Nguyen, Q.-T., Thomas, J.-C., and Le Van., A. (2015). Inflation and bending of an orthotropic inflatable beam. In *Thin-Walled Structures*, vol.88 (pp. 129 – 144).



tensinantes2023 : TensiNet Symposium 2023 at Nantes Université

Membrane architecture: the seventh established building material. Designing reliable and sustainable structures for the urban environment.

Proceedings of the Tensinet Symposium 2023

TENSINANTES2023 | 7-9 June 2023, Nantes Université, Nantes, France

Jean-Christophe Thomas, Marijke Mollaert, Carol Monticelli, Bernd Stimpfle (Eds.)

The calculation of large cable reinforced gas storage systems

Juergen Holl*, Peter Singer^a, Dieter Stroebel^b

*technet GmbH, Breitscheidstraße 4

Stuttgart 70174,

Germany, juergen.holl@technet-gmbh.com

Abstract

Today, computer models play an important role in the calculation of textile membrane and foil structures. In order to derive high-quality results from a model, the software used must enable a description of a structure that is as accurate and complete as possible. For pneumatically tensioned structures, the creation of the models and the static calculation is a challenge in many cases. A static calculation for membranes and foil structures is geometrically non-linear. The calculation requires the unstressed geometry and the material properties for all elements of the model. For the load case calculation, the external loads and, for pneumatic structures, also the internal pressures or volume data are required. Additional boundary conditions for pneumatic structures are that the loads are deformation-dependent and that the gas law must be considered in certain load cases. If the stresses in the membrane become so big that even the strongest membrane material can no longer bear the stresses, then the membrane must be reinforced with cable nets.

In this paper we show how in our software package the cable net reinforcements can be modelled together with the membrane in one system and then calculated. The cable net can slide on the membrane surface. In this way, it is possible to model the reality accurately.

Keywords: Pneumatic systems, gas storage, cable net, reinforcement.

1. Introduction

The calculation of pneumatic membrane structures includes form-finding, statics and cutting patterns. This paper deals with cable net reinforced pneumatic membranes, which are indispensable above a certain size in order to keep the membrane stresses within limits; sometimes, for example, also belts are used for gas holders (e.g. Forster B. and Mollaert).

Before we now present the individual steps in the generation of cable-mesh-reinforced pneumatic structures, we will discuss form-finding theory and the statics of pneumatic

Membrane architecture: the seventh established building material. Designing reliable and sustainable structures for the urban environment.

structures. Subsequently, we will show how arbitrary cable nets can be designed on the pneumatic surface and how the overall system, i.e. membrane and cable-net, is calculated.

2. Formfinding for Pneumatics

The theory of the form finding of mechanically and pneumatically membrane or foil structures has its basics in the well-known Force-Density Method (e.g. Stroebel and Holl). By specifying force densities (ratio between force S and stressed length l), the non-linear equilibrium equations become linear and can be solved without specifying initial values.

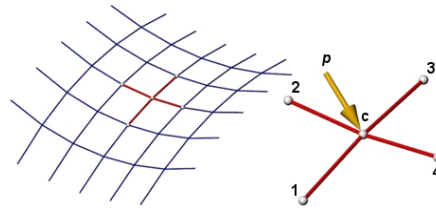


Figure 1: Four cables in point C

In the case of a point C connected by 4 cables to fixed points 1,2,3 and 4, the equilibrium conditions are as follows, where the external load vector can be expressed $\mathbf{p}^t = (p_x \ p_y \ p_z)$ (e.g. Ströbel, D. and Singer, P. et al).

$$\begin{aligned} (x_c - x_1) \frac{S_1}{l_1} + (x_c - x_2) \frac{S_2}{l_2} + (x_c - x_3) \frac{S_3}{l_3} + (x_c - x_4) \frac{S_4}{l_4} &= p_x \\ (y_c - y_1) \frac{S_1}{l_1} + (y_c - y_2) \frac{S_2}{l_2} + (y_c - y_3) \frac{S_3}{l_3} + (y_c - y_4) \frac{S_4}{l_4} &= p_y \\ (z_c - z_1) \frac{S_1}{l_1} + (z_c - z_2) \frac{S_2}{l_2} + (z_c - z_3) \frac{S_3}{l_3} + (z_c - z_4) \frac{S_4}{l_4} &= p_z \end{aligned} \quad (1)$$

If one specifies known force densities in (1), e.g. $q_1 = \frac{S_1}{l_1}$, and analogue for q_2, q_3 and q_4 , then the equations become linear and result in:

$$\begin{aligned} (x_c - x_1)q_1 + (x_c - x_2)q_2 + (x_c - x_3)q_3 + (x_c - x_4)q_4 &= p_x \\ (y_c - y_1)q_1 + (y_c - y_2)q_2 + (y_c - y_3)q_3 + (y_c - y_4)q_4 &= p_y \\ (z_c - z_1)q_1 + (z_c - z_2)q_2 + (z_c - z_3)q_3 + (z_c - z_4)q_4 &= p_z \end{aligned} \quad (2)$$

The coordinates of the point C (x_c, y_c, z_c) are the solution of these linear equations. In the following step we want to write the system above by considering m neighbours in the point C:

Membrane architecture: the seventh established building material. Designing reliable and sustainable structures for the urban environment.

$$\begin{aligned}
 \sum_{i=1}^m (x_i - x_c)q_i - p_x &= 0 \\
 \sum_{i=1}^m (y_i - y_c)q_i - p_y &= 0 \\
 \sum_{i=1}^m (z_i - z_c)q_i - p_z &= 0
 \end{aligned} \tag{3}$$

The energy which belongs to the system (1) can be written as:

$$\Pi = \frac{1}{2} \mathbf{v}^t \mathbf{R} \mathbf{v} - p_x(x - x_0) - p_y(y - y_0) - p_z(z - z_0) \Rightarrow stat. \tag{4}$$

The internal energy is the expression $\frac{1}{2} \mathbf{v}^t \mathbf{R} \mathbf{v}$. The vector $\mathbf{v}^t = (v_x \ v_y \ v_z)$ and the matrix $\mathbf{R} = \text{diag}(q_i \ q_i \ q_i)$ show this energy with respect to a single line element i . We can write the inner energy as $\frac{1}{2} q_i (v_x^2 + v_y^2 + v_z^2)$, precisely:

$$\begin{aligned}
 v_x &= x_i - x_c \\
 v_y &= y_i - y_c \\
 v_z &= z_i - z_c
 \end{aligned} \quad \mathbf{R} = \begin{bmatrix} q_i & 0 & 0 \\ & q_i & 0 \\ sym. & & q_i \end{bmatrix} \tag{5}$$

The chamber of a pneumatic structure has a volume V , which is made by an internal pressure p_i . The product from internal pressure and volume is a part of the total energy Π : a given volume V_0 leads directly to a specific internal pressure p_i : hence the total energy for the forming of a pneumatic chamber is

$$\Pi = \frac{1}{2} \mathbf{v}^t \mathbf{R} \mathbf{v} - p_x(x - x_0) - p_y(y - y_0) - p_z(z - z_0) - p_i(V - V_0) \Rightarrow stat. \tag{6}$$

The derivation of the total energy to the unknown coordinates and to the unknown internal pressure ends up with

Membrane architecture: the seventh established building material. Designing reliable and sustainable structures for the urban environment.

$$\begin{aligned}
 \frac{\partial \Pi}{\partial x} &= \sum_{i=1}^m (x_i - x_c) q_i - p_x - p_i \frac{\partial V}{\partial x} = 0 \\
 \frac{\partial \Pi}{\partial y} &= \sum_{i=1}^m (y_i - y_c) q_i - p_y - p_i \frac{\partial V}{\partial y} = 0 \\
 \frac{\partial \Pi}{\partial z} &= \sum_{i=1}^m (z_i - z_c) q_i - p_z - p_i \frac{\partial V}{\partial z} = 0 \\
 \frac{\partial \Pi}{\partial p_i} &= V - V_0 = 0
 \end{aligned} \tag{7}$$

In the system (6) the internal pressure p_i can be seen as a so-called Lagrange multiplier. The fourth row in (7) shows, that our boundary condition $V = V_0$ is obtained by the derivation of the energy to this Lagrange multiplier. The vector $(\frac{\partial V}{\partial x} \quad \frac{\partial V}{\partial y} \quad \frac{\partial V}{\partial z})$ describes the normal direction in the point (x, y, z) and the size is the according area. By a set of given force-densities for all elements and a given volume V_0 we end up with a pre-stressed and of course balanced pneumatic system with a volume V_0 and an internal pressure p_i .

3. Statics for Pneumatics

By introducing the constitutive equations for the membrane elements into the system (1), we extend the form-finding theory. Now the force-densities q from the form-finding are unknowns and they belong to the material equations.

$$\begin{bmatrix} \sigma_u \\ \sigma_v \\ \tau \end{bmatrix} = \begin{bmatrix} m_{11} & m_{12} & 0 \\ & m_{22} & 0 \\ sym. & & m_{33} \end{bmatrix} \begin{bmatrix} \varepsilon_u \\ \varepsilon_v \\ \Delta\gamma \end{bmatrix} \tag{8}$$

We must consider that the membrane axial-stress in u - or v - direction can be expressed as $\sigma_u = \frac{S_u}{b_u}$ and $\sigma_v = \frac{S_v}{b_v}$. b_u and b_v are the widths of the u - and v -lines. The force-densities q can be introduced now as: $S_u = q_u l_u$ and $S_v = q_v l_v$. The strains in u - and v -direction can be written as follows: $\varepsilon_u = \frac{l_u - l_{u0}}{l_{u0}}$ and $\varepsilon_v = \frac{l_v - l_{v0}}{l_{v0}}$. The angle difference $\Delta\gamma = \gamma - \gamma_0$ is needed for the shear-stress calculation. γ is the angle between u and v -direction; γ_0 refers to the ‘non-deformed start-situation’ without any shear-stress. The geometrical compatibility must be considered as follows: $l_i = \sqrt{(x_i - x_c)^2 + (y_i - y_c)^2 + (z_i - z_c)^2}$ and $\gamma = \arccos(\frac{l_u * l_v}{l_u l_v})$, in which $(l_u * l_v)$ means the inner (scalar-) product between u and v -direction. The shear-stress calculation is guaranteed also for a continuous membrane by the fact that the shear angle is between the non-deformed u - and v -direction of the material (e.g. Stroebel and Holl).

As already mentioned, additional boundary conditions must be fulfilled for pneumatic structures:

Membrane architecture: the seventh established building material. Designing reliable and sustainable structures for the urban environment.

1. The internal pressure loads are deformation dependent.
These loads are non-conservative. To get correct results software packages should consider these effects, especially also for wind loads.
2. Gas laws must be considered in certain load cases. For static calculations we recommend 4 calculation modes:
 - a) Given internal pressure p (snow)
 - b) Given volume V (water)
 - c) Given product $p \cdot V$ (Boyle-Mariotte, for example wind, p as absolute pressure)
 - d) Given product $\frac{p \cdot V}{T}$ (General gas equation, consideration of temperature, p as absolute pressure)

Mode c (consideration of gas-laws) enables the realistic behaviour of the internal pressure. This mode is important in case of e.g. fast wind gusts. Here the pump systems cannot update the inner pressure in the short time. We can see it as a closed system and by considering the temperature as constant we get the gas law of Boyle and Mariotte $p \cdot V = const$ in this case. Only if the gas law is fulfilled the membrane stresses get the correct size.

$$\begin{aligned}
 \frac{\partial \Pi}{\partial x} &= \frac{1}{2} \frac{\partial (v^t R v)}{\partial x} - p_x - \frac{\partial V}{\partial x} p_i = 0 \\
 \frac{\partial \Pi}{\partial y} &= \frac{1}{2} \frac{\partial (v^t R v)}{\partial y} - p_y - \frac{\partial V}{\partial y} p_i = 0 \\
 \frac{\partial \Pi}{\partial z} &= \frac{1}{2} \frac{\partial (v^t R v)}{\partial z} - p_z - \frac{\partial V}{\partial z} p_i = 0 \\
 \frac{\partial \Pi}{\partial p_i} &= V - V_0 = 0
 \end{aligned} \tag{9}$$

Equation (9) refers to mode c, here the constant value $(p_{abs} \cdot V)_0$ is the given product and row 4 of (9) must be fulfilled in iterations where the unknown internal pressure p_i is adapted.

4. Geodesic Lines and Slip Cables

Geodesic lines are solutions of a second order ordinary differential equation. In this paper, however, we will use some other definitions of the geodesic line, which show clearly that a geodesic line corresponds to a weightless prestressed cable stretched frictionlessly over a surface. A geodesic is a line whose geodesic curvature vector vanishes. This is only the case if the plane - created by the tangential and normal vector of the curve - is also the normal plane of the surface, i.e. the normal vectors of the curve and the surface normal vectors coincide at every point of the geodesic line. A prestressed cable on a surface can only be in equilibrium if it is normal, i.e. perpendicular, to the surface. Therefore, the equilibrium position of a prestressed (weightless) cable on a surface is a geodesic line and we define it as slip-cable.

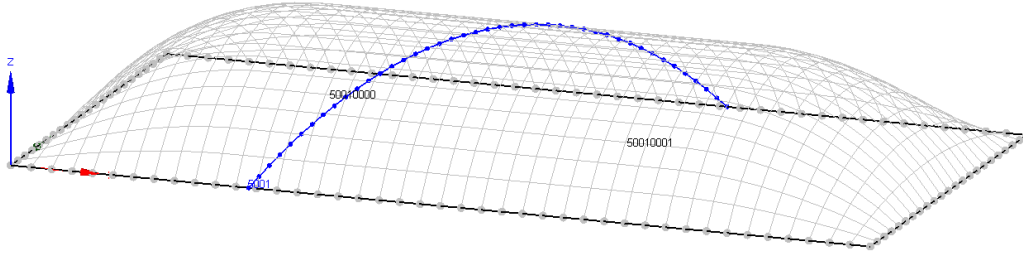


Figure 2: Geodesic/slip line over surface

We introduce now the slip-cables in the form-finding stage. Here we define a specific force F within the blue cable. Furthermore, we assume the number of the blue cable pieces from this single slip cable to be n , the stressed length in a cable to be l_i and the forcedensity to be q_i . So we have to add the following lines to equations (7).

$$q_i - \frac{F}{l_i} = 0, \quad i = 1, n \quad (10)$$

In case of static calculation, we assume to have the stiffness of the slip cable (EA) and the sum of all stressed lengths L and unstressed lengths L_0 .

$$L = \sum_{i=1}^n l_i \quad (11)$$

$$L_0 = \sum_{i=1}^n l_{0i}$$

Now the slip cable force densities q_i can be calculated as:

$$q_i = EA \frac{L - L_0}{L_0 \cdot l_i} \quad (12)$$

As $F = EA \frac{L - L_0}{L_0}$ we end up with the same force in all cable pieces.

The green cable (all points on it are fixed) in Figure 3 has the black vectors as reaction forces. The yellow lines show the normal vectors of the surface. The black vectors and the yellow lines are parallel. This means that the green cable is a geodesic line. You can also see in the top view the S-line, which is always obtained as a geodesic line in the case of a cylindrical surface.

Membrane architecture: the seventh established building material. Designing reliable and sustainable structures for the urban environment.

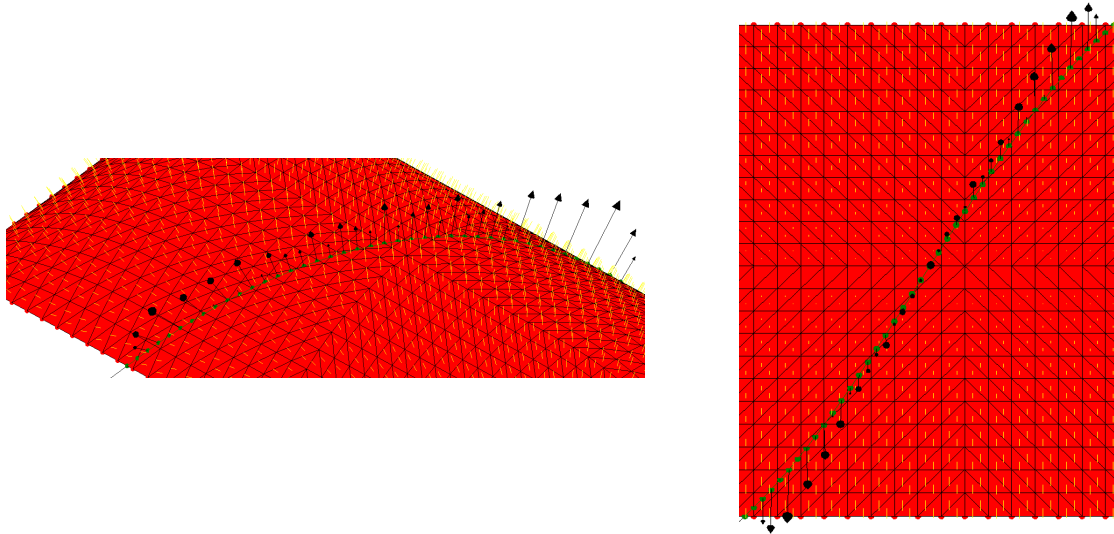
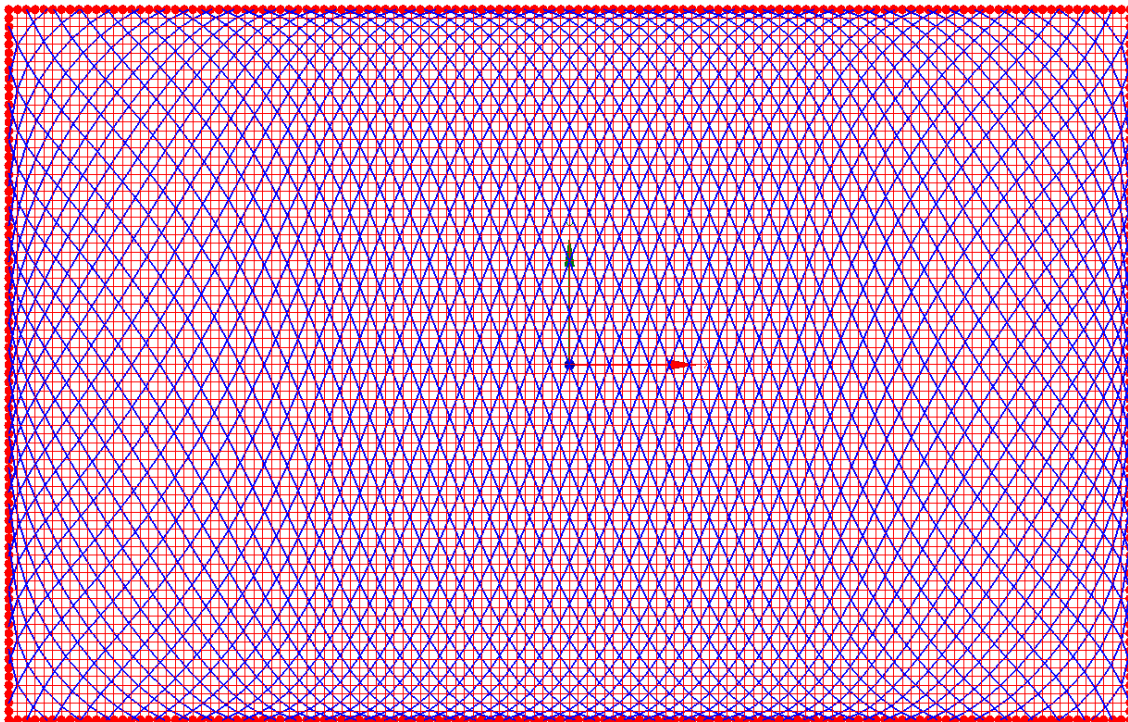


Figure 3: Slip line over cylindrical surface (side view left, plan view right)

This means for the calculation of pretensioned (weightless) cables on a pneumatic membrane that these cables are provided with a pretension and they slide friction-free on the surface until they reach an equilibrium position. The condition is therefore simply constant force and the surface forms the support.

5. Examples

Our software gives several possibilities to put cables or a cable onto a pneumatic surface. In the following example we generated an equidistant mesh on the surface.



Membrane architecture: the seventh established building material. Designing reliable and sustainable structures for the urban environment.

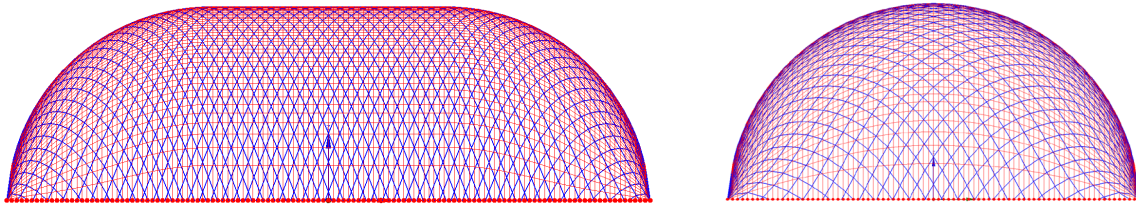


Figure 4: Big gas holder with equidistant cable mesh

The following picture shows that the cables constrict the membrane already in the load case of internal operating pressure.

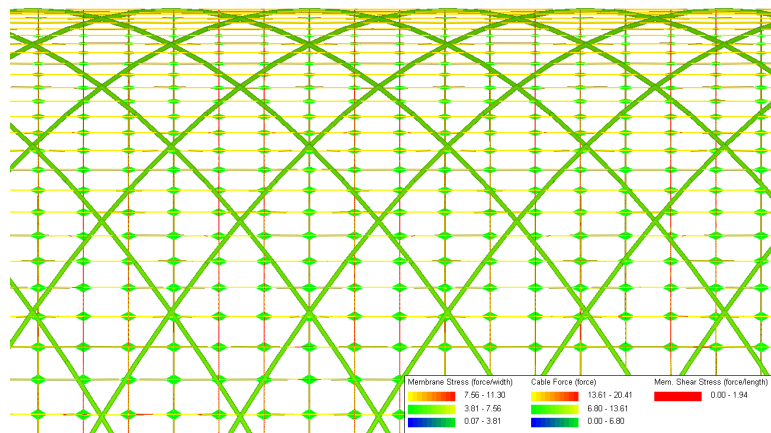


Figure 5: Constriction of the membrane by cables

When calculating pneumatic cable net reinforced membranes, the wind load cases are important and relevant for dimensioning.

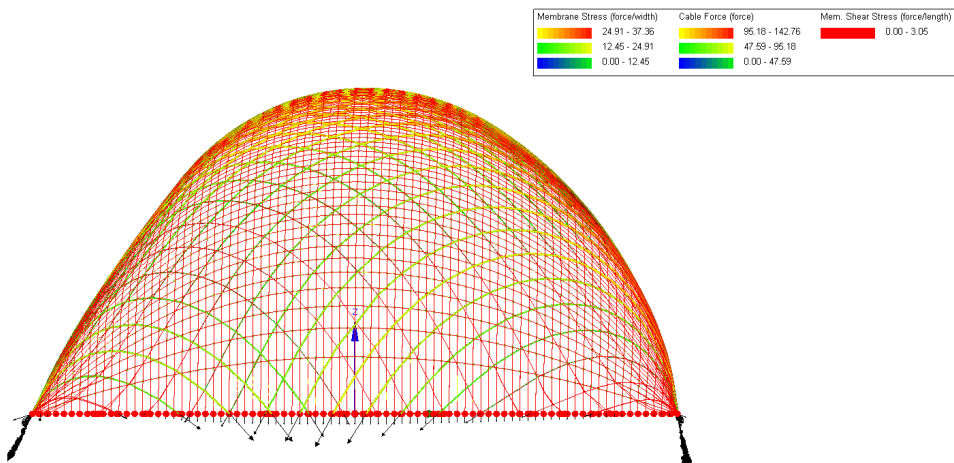


Figure 6: Deflected form under side wind

Snow loads should also be considered.

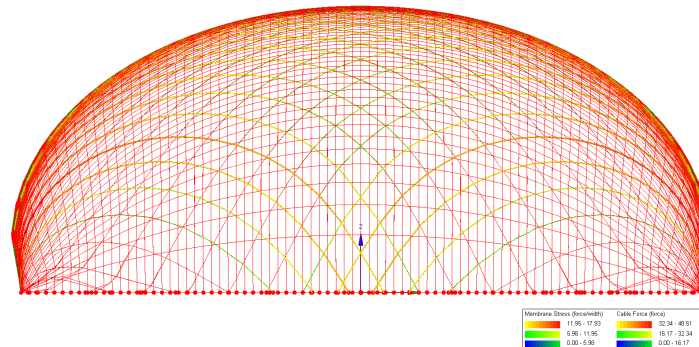


Figure 7: Deflected form under snow load

6. Conclusion

The calculation methods for form-finding and statics of pneumatic constructions are extended with the help of additional conditions for the combined calculation of cable or cable net reinforced pneumatic membrane constructions. These extended methods are built into the calculation programs. They lead to realistic results, as can be seen from many examples. Even the largest projects can be determined in acceptable calculation times.

References

Forster B., and Mollaert M. (eds.), European design guide for tensile surface structures: TensiNet, TensiNet, 2004.

Holl J., Stroebel D., “Fast model generation and static calculation of combined pneumatic and mechanically stressed structures”, X International Conference on Textile Composites and Inflatable Structures, Structural Membranes 2021, 13 – 14 September 2021.

Stroebel, D., Holl, J. “On the static calculation of biogas containers with radial and parallel cutting patterns”. IASS Annual Symposium 2019 – Structural Membranes 2019 Form and Force, 7 – 10 October 2019, Barcelona, Spain.

Ströbel, D., Singer, P., Holl, J. „Analytical Formfinding”, International Journal of Space Structures, Volume: 31 issue: 1, page(s): 52-61, March 1, 2016.

Ströbel, D. Singer, P, Holl, J: Holistic Calculation of (Multi)-Chambered ETFE-Cushions, Tensinet, TensiNet Istanbul, 2013.



tensinantes2023 : TensiNet Symposium 2023 at Nantes Université

Membrane architecture: the seventh established building material.
Designing reliable and sustainable structures for the urban environment.

Proceedings of the Tensinet Symposium 2023

TENSINANTES2023 | 7-9 June 2023, Nantes Université, Nantes, France

Jean-Christophe Thomas, Marijke Mollaert, Carol Monticelli, Bernd Stimpfle (Eds.)

Textile covers of biogas storage tanks - Interaction between Membrane behaviour and Operation of the Gas Membrane

Rosemarie Wagner*, Bernd Sum^a, Kai Heinlein^b

* KIT Karlsruhe Institute of Technology

Department of Building technology

Engelstrasse 7 D – 76131 Karlsruhe

Rosemarie.Wagner@kit.edu

^a KIT Karlsruhe Institute of Technology Hertzstrasse 16 76187 Karlsruhe

^b KIT Karlsruhe Institute of Technology Hertzstrasse 16 76187 Karlsruhe

Abstract

Two-layer, membrane covers over biogas storage tanks are economical, cost-effective and also efficient buffer storage to compensate for fluctuations in the power grid. The outer membrane, further referred to as the outer membrane, is an air-supported weather protection. The inner membrane, also called gas membrane, is used to store the gas produced from biodegradable materials, a mixture of methane, carbon dioxide, water and sulfur. Requirements for the gas membrane are considerably higher than for membranes used in textile architecture. Gas membranes must have high flexibility and be kink-resistant. When the gas storage tank is empty, the gas membrane lies folded on the support structure installed in the tank; when gas is produced, the gas membrane floats on the gas volume as a state of equilibrium between buoyancy due to the warmer and lighter methane as well as internal pressure in the gas space and the gas membrane's own weight with sulfur deposits and condensate as well as internal pressure in the support air space. Wind gusts are transmitted into the gas space by Boyle-Marriott's simplified law due to the required gas tightness. The gas diaphragms participate in load transfer at similar stiffnesses as the outer diaphragm and filled reservoir. The consequence of the large movements and folding is an occurring leakage of the gas membrane over the years, which has led to the recommendation in Germany to replace it with a new one after 6 years. Standards in which tests on the bending and buckling behaviour of coated fabrics are given and the evaluation is described only approximately represent the folding behaviour of the gas membrane. For this reason, a cover was reproduced on a scale of 1:10 and folding tests were carried out.

Keywords: biogas membrane, foldability, folding tests, permeability, flexibility

1. Introduction

The gas membranes in double-layer textile covers over digesters in biogas plants are subjected to requirements resulting from the gas production of organic matter. The gas production is dependent on the feeding times of the gas-producing bacteria and the demand for electricity, which is obtained from the biogas via engines. Consequently, there are three states for the gas membrane, which depend on the gas production. The gas chamber is empty, then the gas membrane lies folded on the supporting structure, which is installed in the tank. The supporting structures are either made of wood or a textile belt system with or without a polymer cable net made of plastic. The air pressure in the air volume acts on the folded gas membrane if the outer membrane is inflated. During gas production, the gas membrane floats on the internal pressure of the gas, which is higher than the internal pressure in the support air space. The internal pressure in the gas space increases until the gas membrane is tensioned. When the maximum internal pressure is reached, which is known as the limit value for the load-bearing capacity of the membrane, either gas must be burned or electricity must be generated, Fig. 1.

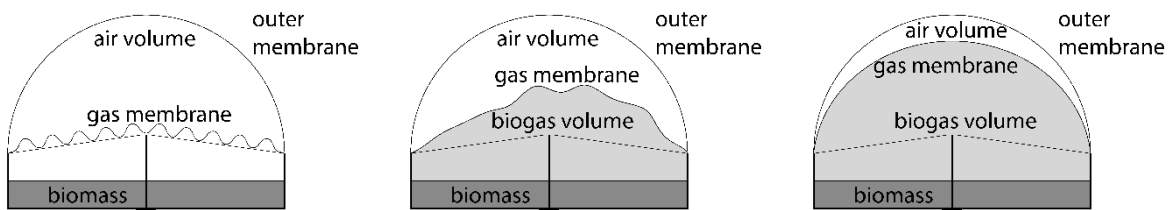


Figure 1: Shown are in principle the three different states of the gas membrane, no gas production (left), gas production (middle) and full gas space (right).

The gas is composed of methane, carbon dioxide and hydrogen sulfide. Continuous temperatures between 35°C and 40°C are necessary for gas production. Thermophilic bacteria still live at temperatures of 50°C. The humidity in the gas volume is continuously at 100% during operation. The accumulation of sulfur occurs from the hydrogen sulfide on the inside of the gas membrane, due condensation of moisture caused by the temperature difference between the inside of the gas membrane and the outside to the supporting air volume. If the gas membrane is made of coated fabric, the PVC coating is necessary as a permanently protecting of the polyester fabric. High gas humidity, folding and movement during gas production and the accumulation of sulfur require a flexible and durable coating. Damage to the coating due to rolling and buckling during folding leads to hydrolysis of the fabric under the above-mentioned conditions. The membrane becomes leaky and the fabric loses strength.

2. Folding Tests, State of the Art

Standardized tests on the kinking and folding resistance of PVC coated polyester fabric (PVC/PET), which are applicable, had been developed for tests in the elastomer and leather-textile industry. The characteristic of the tests is a folding of a sample in the middle of the sample, clamped in a test device and loaded with different load cycles. The test according to DIN ISO 132 - Elastomers - Determination of crack formation and crack growth is limited to homogeneous, flexible elastomers. The specimen is given a continuous cut in the center across its width. In the test, the lower specimen grip is moved up and down and the specimen is folded open and closed. The same procedure is used to examine the damage caused by needle punctures, Fig. 2.

Membrane architecture: the seventh established building material. Designing reliable and sustainable structures for the urban environment.

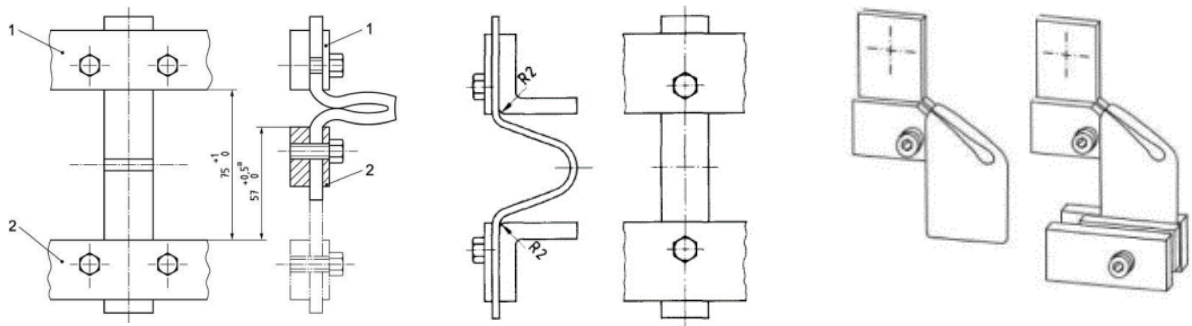


Figure 2: Shown are in principle the three different methods to test foldability of flexible materials, according to DIN ISO 132 (left), DIN 53340 (middle) and DIN EN ISO 32100 (right).

In the test DIN 53340 - Determination of the permanent folding behaviour of low-flexible leather, the test strips are clamped in a test device which has the same mode of operation as according to DIN ISO 132. The lower clamping is moved up and down. This test can also be used to examine undamaged and damaged specimens. The test setup and procedure according to DIN 53359 - Testing of artificial leather and similar fabrics - Permanent folding test are comparable to DIN ISO 132 and according to DIN 53340. Tests described in DIN EN ISO 32100 - Textiles coated with rubber or plastic - Flexometer method record the flexing process and the damage to the material. The specimen is folded lengthwise in the middle and then folded a second time at 90° to the fold. As the bottom clamp is moved up and down, the kink moves along the fold. Depending on the number of load cycles, the coating is damaged at the kink.

3. Folding and flexing processes of the gas membrane

The buckling resistance of gas membranes has hardly been methodically investigated so far. There is also a lack of information on kink and wrinkle resistance in the data sheets of membrane manufacturers. Due to safety regulations, the gas membrane in fermenters is hardly visible. Gas escaping is measured into the supporting air volume in case of leakage locally or at the exhaust air flap of the air volume. If the gas concentration increases, it can be assumed that the gas membrane is possibly leaking due to constant moving, buckling and folding. Questions that arise are what type of folds occur, does buckling occur, and does the folding pattern remain approximately the same with repeated filling and emptying. If the pattern changes, it is necessary to know the influencing variables that lead to different folding patterns. To investigate the behaviour of the gas membrane, observations were documented on an experimental storage tank. The special feature of this storage tank is the geometry of the textile cover. This is approximately a hemisphere. For a hemisphere, the shell area is two times larger than the base area. The gas volume of the experimental storage tank with a diameter of 15 m was accessible, filling and emptying was simulated with two radial fans.

A folding pattern, which was qualitatively repeated, became clear during emptying and inflating several times. If the internal pressure in the gas volume decreases during emptying and the pressure from above caused by an inflated air volume also has an effect. This pressure acts additional to the dead weight of the folded gas. The folded membrane is membrane is compressed onto the supporting structure. The weight at the pole is higher compared to the membrane itself due to the close seam spacing and a two-layer pole cap. The result is a faster lowering of the pole cap. The dead weight of the entire membrane counteracts the decreasing

Membrane architecture: the seventh established building material. Designing reliable and sustainable structures for the urban environment.

internal pressure with the air pressure above the membrane. The result is a settling of the gas membrane in radial folds starting from the container edge. The membrane form approximately the upper half of a torus, Fig. 3.



Figure 3: Placing the gas membrane on the belt system during emptying, Lowering the pole cap (right), radial folding form the tank edge (right).

Emptying the gas volume has another special feature for loading the gas membrane. If a lot of gas is removed in a short time, a negative pressure is also created in the gas volume. This additionally compresses the folded membrane more together with the dead weight and the internal pressure of the air volume. Furthermore, it was observed that the folding pattern can be repeated. This means that kinks at certain points increase with the number of times the gas is removed.

4. Set setup modelling the folding, unfolding and fulling process

Equations Several ways are possible to get an idea of how the type and frequency of wrinkling affects the coating and gas tightness. One method is to examine samples from gas membranes that have been removed due to age. For this purpose, the number of operations for emptying and filling should be known, in addition, unstressed original membrane should be available as a reference. The second possibility is to plan and build an experimental setup that reproduces the folding on a laboratory scale. Unfortunately, the availability of degraded gas membranes and the additional information is limited. Therefore, test rig was developed and material used as gas membranes in biogas storage systems were investigated. The size scale for the experiment is M 1:30 for a 15 m diameter biogas storage system and M 1:50 for a 25 m diameter storage system. The question of how to map the unfolding and folding from the circular base into a hemisphere without cutting is to be clarified. Membrane materials that actually require cutting are tested, in order to test the pure membrane in the experiment. The test setup is made of a steel cylinder with a diameter of 50 cm and a height of 70 cm. This is mounted airtight on a base plate. A fan for filling and emptying has been installed in this base plate. The membrane is clamped into the upper rim. This consists of two rings, which are cut out wave-shaped on one side. The membrane is clamped into this wave-shaped clamping rim. The membrane corresponds to a circular area with a diameter of 70 cm. This area is 1.96 times larger than the base area of the 50 cm diameter of the cylinder. During filling and emptying, kinks are created

Membrane architecture: the seventh established building material. Designing reliable and sustainable structures for the urban environment.

which also correspond to fulling. The load was applied via the fan over the base plate in the closed volume as overpressure and underpressure, Fig. 4.

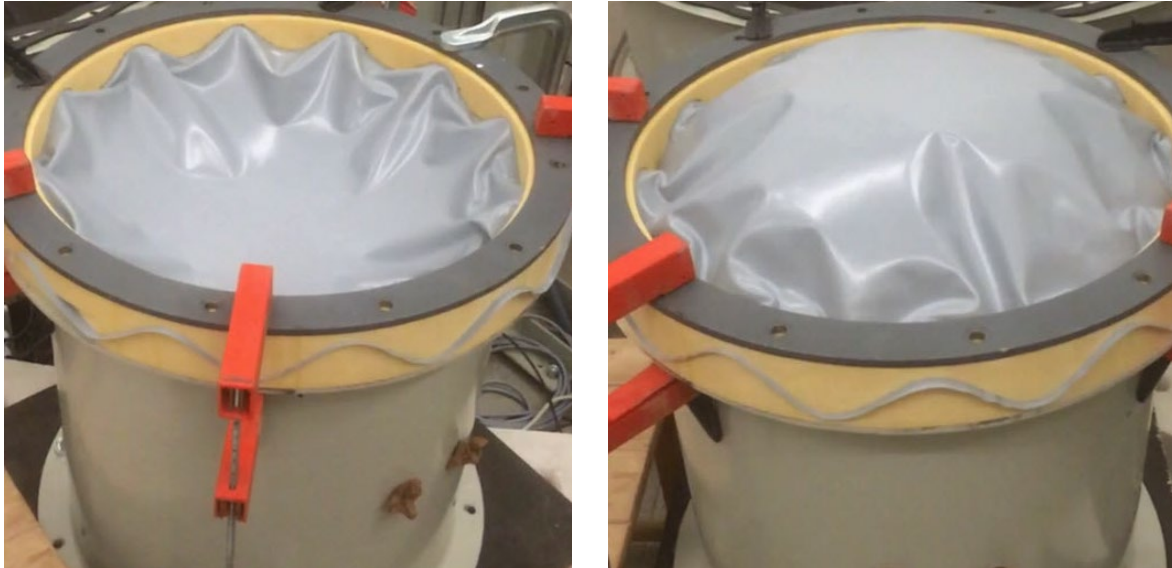


Figure 4: Membrane to be tested, after installation of the membrane (left); with internal pressure (right), (Photo Nicolas Hiltcher).

5. Test procedure

In order to investigate the behaviour of the polyester fabric coated on both sides with PVC and sealed with Top coat under buckling, folding and fulling processes, tests were carried out on several test pieces. Comparisons with wrinkle formations on the 15 m diameter test structure and the test structure in the laboratory provide a sufficiently accurate representation of the realistic material behaviour during a large number of cycles of filling and draining biogas. The omission of a cutting pattern for the membranes had an influence on the wrinkle formation, which are much closer together over the surface compared to the wrinkle patterns in reality.

Three types of membrane material were investigated from the same manufacturer, which are used as covers over biogas storage tanks. The membranes differ in weight with 800, 900 and 1050 g/m² and in tensile strengths warp/weft of 3400/3000, 4700/4500 and 6500/6700 N/5cm. The membranes are labelled as type 1, 2 and 3 for evaluation of the test results with increasing weight and tensile strength. The membranes had a top coat applied on one side. Therefore, different specimens were installed and tested with the top coat facing down and up in the test rig, Fig. 5.

Membrane architecture: the seventh established building material. Designing reliable and sustainable structures for the urban environment.

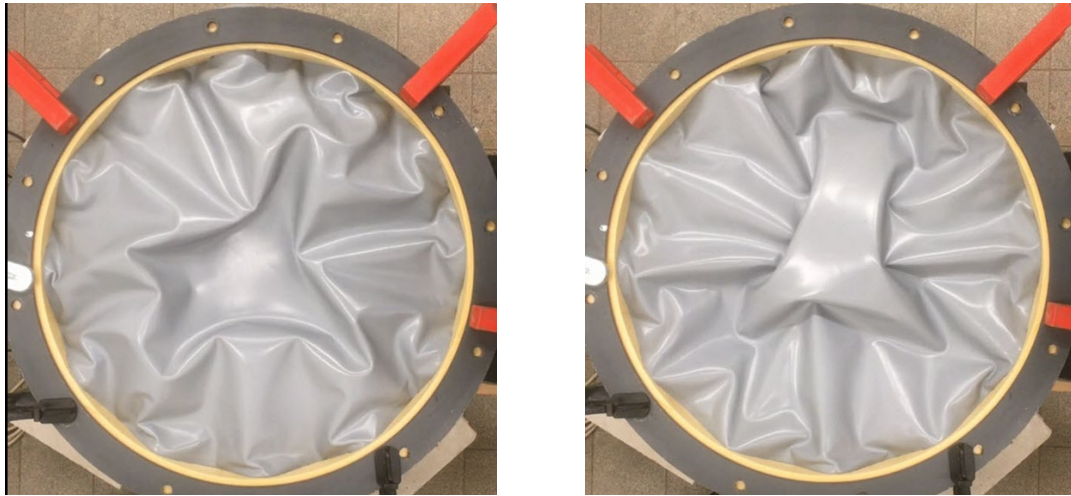


Figure 5: Folding, buckling and fulling of the membrane with maximum negative pressure (left) and positive pressure (right), (Photo Nicolas Hiltcher).

6. Evaluation of the tests

In order to detect damage in the membranes after a certain number of loading cycles, optical methods were used. Samples were taken from the tested membranes, with which uniaxial tensile tests were performed.

The optical methods are first a visual inspection by eye. Samples were examined by eye for damage. Clearly visible defects were marked for further examination in a subsequent step. This involved a classification into type and class of damage. This examination was performed with a microscope.

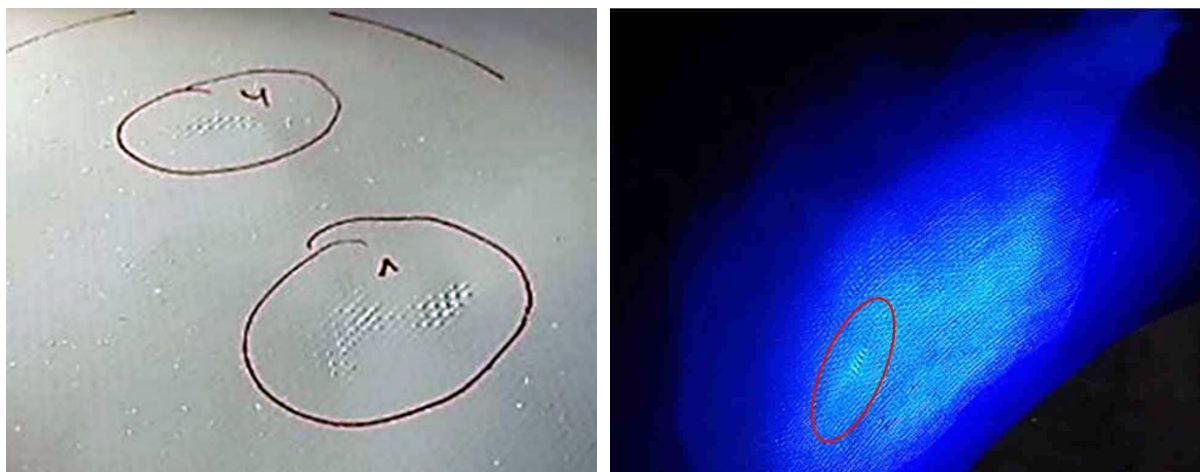


Figure 6: Visual inspection (left) and dye penetrant inspection (right), (Photo Nicolas Hiltcher).

To determine how far the damage has penetrated into the coating and the fabric, the dye penetrant test, as used for testing cast steel according to DIN ISO 4987. This method is normally used detecting failure in cast steel. The damaged sample was degreased on one side and coated

Membrane architecture: the seventh established building material. Designing reliable and sustainable structures for the urban environment.

with a fluorescent liquid. This liquid fills cracks and indentations in the membrane surface. In the case of deep cracks, the liquid even penetrates to the back of the membrane. The membrane is then cleaned with running water. With the aid of a UV lamp, cracks and defects can now be made visible. Classifications of the types of damage can also be made here, Fig. 6.

The classification was made in delamination of the coating by the fulling of buckles (Fig. 6 right) and linear defects, which were divided into short defects with a length less than 15 mm and long defects longer than 15 mm. The number of defects on the specimens was compared after a certain number of load cycles.

Counted Number of defects

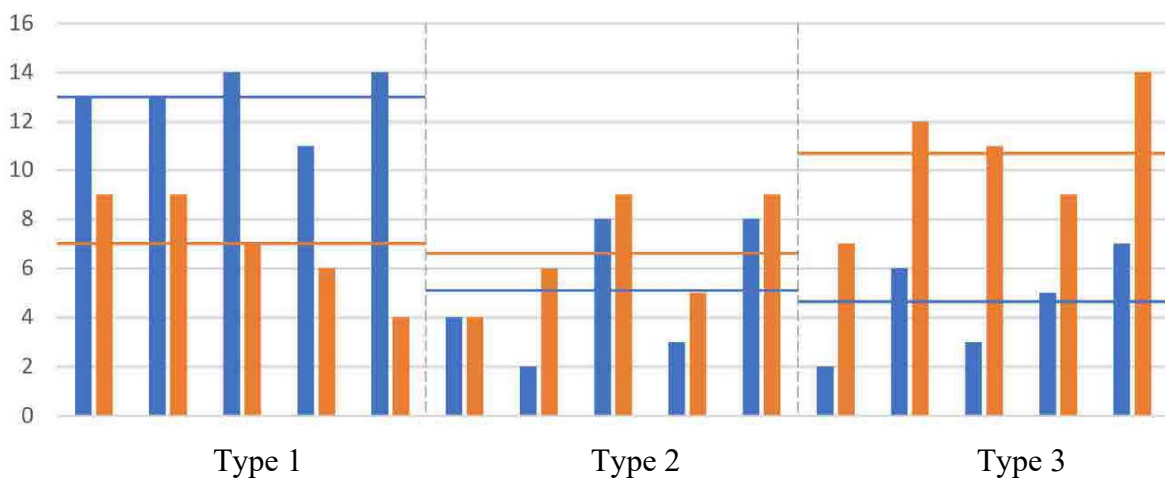


Figure 7: Number of failures after 200 load cycles for 5 specimens each, divided into short (blue) and long (orange) defects, (Ref. Nicolas Hiltcher).

It is noticeable from the mean values of the number (horizontal lines) that the medium-weight membrane has the lowest number of long defects compared to the other two and approximately the same number of short ones compared to the heavy material. In the lighter membrane material, significantly shorter cracks predominate. In the heavy material, the number of long cracks is high, Fig. 7. The reason may be the different structure of the fabrics, such as yarn count, weave type and thread twist, and a different thickness of the coating. Information on this was missing in the available data sheets.

Specimens 5 cm wide and 25 cm long were cut out of the pre-damaged membranes and uniaxially stretched to rupture. The warp threads in the samples are more or less, while care was taken into ensure this when cutting the samples. The folds are oriented parallel to the warp direction, see red lines on Figure 8. The maximum tensile strengths achieved show a variation higher than known from uniaxial tests. What is also striking in the tests is the fact that some values are below the values specified by the manufacturer, see table 1.

Membrane architecture: the seventh established building material. Designing reliable and sustainable structures for the urban environment.

Table 1: maximum tension strength after 1000 load cycles for 9 samples

Sample No.	maximum tension strength kN/5 cm], warp direction		
	Type 1	Type 2	Type 3
1	3,44	4,94	6,05 *
2	3,54	4,56 *	5,81 * *
3	3,51	5,16	6,85
4	3,75 *	4,71 *	6,72
5	3,58 *	5,00 *	6,55
6	3,01 * *	4,93 *	6,70 *
7	3,69 *	5,23 *	6,40 *
8	3,10 *	4,78	5,76 *
9	3,41 *	5,17 *	6,14 *
Data Sheet Producer	3,40	4,70	6,50
Weight [g/cm ²]	800	900	1050

* reached strength less than provided by the producer, * failure close to clamping, * failure with a crack

The result is that tensile strength and weight of the material influences the damage. Increasing both is related to higher density of the yarns and thickness of the coating. The stiffness of the yarns and interaction of warp and weft in the repeating folds reduces the strength of the yarns in warp direction. The nine samples are shown after failure, see. Fig. 8. Visible are the broken yarns and the fabric for the stiffer material. For flexible membranes the yarns have to be made of high strength filaments with lower density and more flexible coating.

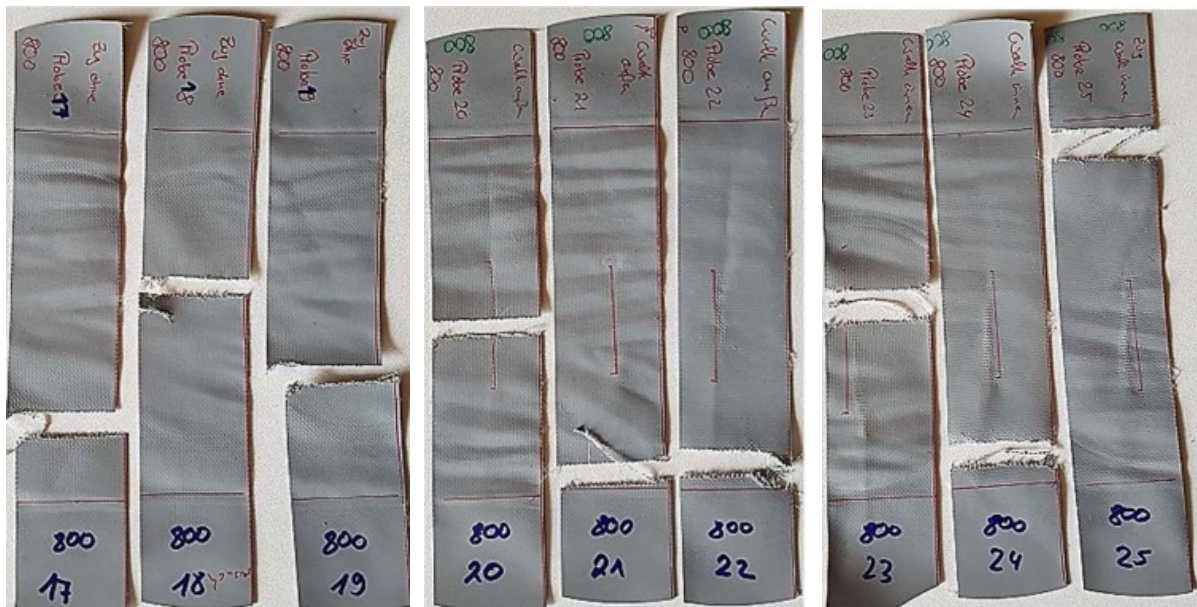


Figure 8: Tested Samples, Type 1 sample No. 1-3 (left), Type 2 sample No. 4-6 (middle) and Type 3 sample No. 7-9 (right), (Ref. Nicolas Hiltcher).

Membrane architecture: the seventh established building material. Designing reliable and sustainable structures for the urban environment.

7. Conclusion

In order to record the folding behaviour of a gas membrane in operation as realistically as possible, a test facility was built and used to investigate commercially available membranes that are used as gas membranes in biogas storage systems. It became clear from the investigations that the number of defects in the coating increases with the number of cycles. The weight and strength of the membranes has an influence on the type of defects. As a further step, it should be investigated whether the tensile strength and stress-strain behaviour of membranes pre-damaged in the folding test take on lower values after artificial aging. The conditions in the test chamber are to maintain the gas concentration of methane, carbon dioxide and hydrogen sulfide mixture as well as a temperature between 35°C - 50°C and 100% gas humidity. Testing of the gas tightness for the biogas is another clarification on the influence of the defects on the change of the properties by rolling and folding during in- and deflating of the gas membrane.

Acknowledgements

The work presented is based on investigations carried out as part of the research and development project "Research into new solutions for textile biogas storage systems; Subproject 1: Experimental determination of membrane properties" 2016 - 2019 carried out by the Department of building technology at the KIT. The project executing agency was the Agency for Renewable Resources FNR e.V. The funding agency was the German Federal Ministry of Food and Agriculture.

References

DIN ISO 132:2015-0: Elastomere oder thermoplastische Elastomere - Bestimmung der Rissbildung und Risswachstum (De Mattia).

DIN 53340:1979-07: Prüfung von Leder; Bestimmung des Dauer-Faltverhaltens wenig flexibler Leder.

DIN EN ISO 32100:2019-02: Mit Kautschuk oder Kunststoff beschichtete Textilien – Physikalische und mechanische Prüfungen - Bestimmung der Dauerbiegefestigkeit nach dem Flexometer-Verfahren.

DIN ISO 4987:2020-01: Stahlguß – Farbeindringprüfung.



tensinantes2023 : TensiNet Symposium 2023 at Nantes Université

Membrane architecture: the seventh established building material. Designing reliable and sustainable structures for the urban environment.

Proceedings of the Tensinet Symposium 2023

TENSINANTES2023 | 7-9 June 2023, Nantes Université, Nantes, France

Jean-Christophe Thomas, Marijke Mollaert, Carol Monticelli, Bernd Stimpfle (Eds.)

Design and execution of membrane structures according to CEN/TS 19102

Jörg Uhlemann*, Bernd Stimpfle^a, Natalie Stranghöner*

*Institute for Metal and Lightweight Structures, University of Duisburg-Essen, D-45117 Essen, Germany, joerg.uhlemann@uni-due.de

^a formTL ingenieure für tragwerk und leichtbau gmbh, D-78315 Radolfzell, Germany

Abstract

This paper reflects the progressive development of the first European design standard for membrane structures. It will be published in future as CEN/TS 19102 "Design of tensioned membrane structures". In addition to design rules, it will also contain provisional execution rules closely associated with the design concept. The current status of the planned regulations in these two fields design and execution is presented in this paper. It is an updated English version of [1].

Keywords: membranes, structures, design, execution, fabrics, foils.

1. State of development of prCEN/TS 19102

For some years now, the first European design standard for membrane structures has been developed by a large number of experts. The authors have reported on the development in several publications [2-4]. Since 2020, the draft standard has been listed under the number prCEN/TS 19102 "Design of tensioned membrane structures". The latest version submitted by the responsible project team is dated November 2021 [5]. It is currently being coordinated by CEN/TC 250 Working Group 5 "Membrane Structures" and the national mirror committees. The development is now approaching the final phase, in which the standard will be translated and then transmitted to the Formal Vote in the CEN member states. Afterwards it will be published in the CEN member states.

In addition to the core objective of the standard, which is to provide design and construction rules for membrane structures, execution rules and test procedures have been created that are coordinated with the design concept. These are presented in the form of informative or normative annexes of prCEN/TS 19102. Later – in the course of the hoped-for transfer of the CEN/TS into a Eurocode for membrane structures – these will then be standards in their own right, so that the design standard will be reduced to its core part.

This paper explains the current status of developments with regard to dimensioning and thus already provides an insight. The discussions in the committees, however, continue to be lively. This means that the state of affairs before the introduction may still change in parts. The authors

Membrane architecture: the seventh established building material. Designing reliable and sustainable structures for the urban environment.

expect, that this will affect not so much the design rules as the execution rules, which have recently been the subject of intense discussions.

2. Design of textile and foil structures

2.1. General

The main objective of prCEN/TS 19102 is to regulate the design of membrane structures made of both (coated) textiles and technical foils. The basis of all regulations is EN 1990 [6]. Within the scope of the present paper, supplementary explanations are given for [4] or regulations that have been changed in the meantime are presented.

For all membrane structures, a distinction is made between two partial safety factors on the resistance side: γ_{M0} for the verification of the base material and γ_{M1} for the verification of connections.

As a general rule, the required strengths derived from the verifications in the ultimate limit state and serviceability limit state are determined and communicated by the structural engineer on a project-specific basis. These strengths are to be supplied later by material producers and manufacturers and verified experimentally, see also the explanations on the design rules below.

In this paper, the many regulations of prCEN/TS 19102 are not presented in full for reasons of space and are reduced to the essential principles. prCEN/TS 19102 partly provides for further options to enable the verification to be more precise or individualized.

2.2. Design of textile structures

2.2.1. Verification in the ultimate limit state (ULS)

For the verification in the ultimate limit state (ULS) for woven structural elements, the design values of the membrane stresses in the yarn directions are compared with the design values of the strengths.

Strength losses of coated fabrics due to different physical influences, essentially high temperature, weathering, and long-term load exposure, are taken into account by modification factors. These must be determined experimentally for individual materials or connection types. In general, Eq. (1) must be observed.

$$f_{Ed} \leq f_{Rd} \quad (1)$$

f_{Ed} is the decisive design stress in the direction under consideration (checks in warp and fill direction are to be carried out separately from each other), f_{Rd} is the minimum strength of the material or connections measured in monoaxial short-term tensile tests at room temperature $T = 23^\circ\text{C}$ including the associated partial safety factors and the above-mentioned modification factors. In the case of PVC-coated polyester fabrics (PES-PVC) or PTFE-coated glass fibre fabrics (glass-PTFE), $\gamma_{M0} = 1.4$ is used for the material and $\gamma_{M1} = 1.5$ for connections.

The situation-dependent design strength f_{Rd} is calculated by dividing the characteristic short-term tensile strength at $T = 23^\circ\text{C}$ by the partial safety factor γ_M depending on the verification to be carried out and the strength modification factor associated with the corresponding design

Membrane architecture: the seventh established building material. Designing reliable and sustainable structures for the urban environment.

situation. Equation (2) represents this, whereby all modification factors are shown here for the introduction.

$$f_{Rd} = \frac{f_{Rd}}{\gamma_M \cdot k_{biax} \cdot k_{age} \cdot k_{dur,*} \cdot k_{temp,*} \cdot k_{size} \cdot k_x} \quad (2)$$

where

k_{biax} modification factor for biaxial effects,

k_{age} modification factor for environmental effects (ageing, deterioration),

$k_{dur,*}$ modification factor for various load durations (permanent, long-term, medium-term),

$k_{temp,*}$ modification factor for temperature effects (to be determined project-specifically, regularly on the safe side selected to 70°C),

k_{size} modification factor linked to the panel size, which takes into account the increasing risk of defects with a larger surface,

k_x is a variable for a modification factor for not yet specified effects.

Table 1 shows which of the presented modification factors are to be applied in which design situations. It also gives recommended value ranges for the most commonly used textile membranes, the PVC-coated polyester fabrics. The values k_{biax} and k_{age} are to be applied in all design situations, as biaxial stress conditions are always assumed and, to be on the safe side, the verification for aged material must always be carried out. The values given in Table 1 lie within certain bandwidths. The variations depend on the different materials and strength types (k_{age} , $k_{dur,*}$, $k_{temp,70}$), on the stress state (k_{biax}) or also on the location of an individual structure (k_{age}). If the specified maximum values are not used in the verification, the selected lower values must be experimentally verifiable or plausible. By "plausibility" above all the value k_{biax} is meant, which can be set to 1.0 in case of an (almost) monoaxial stress state, as is regularly the case in anticlastic membranes. For the determination of the k-factors, prCEN/TS 19102 will contain a normative annex, which proposes suitable test procedures for the determination of the k-factors.

2.2.2. Verification of the serviceability limit state (SLS)

Deformations of the membrane should be calculated. General deformation limits are not specified, they are to be determined individually between the contracting parties. However, the membranes must not hit other components, as this can lead to damage of the membrane, which can widen to cracks and eventually lead to failure.

The formation of snow and water ponds on the membrane surfaces should be avoided. If this cannot be ensured at all points, a detailed deformation calculation must be carried out with realistic values for snow, water or ice accumulation in the growing sag. For this deformation calculation, it is recommended to assume lower limits of the material stiffnesses and additionally also a reduced prestress condition.

Wrinkling in membranes is undesirable for both aesthetic and technical reasons. The appearance of a wrinkle signals locally insufficient prestress. This can lead to fluttering under wind loads and can damage the membrane in the long run. However, wrinkles cannot always be completely avoided. For example, wrinkles can inevitably occur in sharp angled corner areas. Therefore prCEN/TS 19102 does not require the complete avoidance of wrinkles, but

Membrane architecture: the seventh established building material. Designing reliable and sustainable structures for the urban environment.

rather the reduction as far as possible. The assessment should always be specific to the project. High differences in the principal stresses should be avoided both in the prestressed state and under extreme loads in order not to promote the formation of wrinkles.

Table 1: k-factors in design situations of the ULS of fabric structures, values or ranges of values for k-factors of PVC-coated polyester fabrics.

Design situation		$k_{biax} = 1,0-1,2$	$k_{age} = 1,1-1,4$	$k_{dur,P} = 1,4-1,8$	$k_{dur,L} = 1,3-1,7$	$k_{dur,M} = 1,1-1,2$	$k_{temp,70} = 1,5-2,0$	$k_{size}^* = 1,0$
1	Prestress	x	x	x			x	x
2	Prestress temporarily increased (pneumatic)	x	x		x		x	x
3	Snow > 1000 m altitude	x	x		x			x
4	Snow ≤ 1000 m altitude	x	x			x		x
5	Wind	x	x					x
6	Wind acting on fabric at elevated temperature	x	x				x	x

* If strength reduction due to the panel size is to be considered k_{size} may be calculated as

$$k_{size} = \left(\frac{50}{A}\right)^{\left(\frac{-1}{15}\right)} \text{ with } A \text{ is the panel surface in } m^2$$

The prestress (here the nominal value of prestress is meant, which is defined by the structural engineer) should be ensured over the entire service life of the membrane structure. Due to relaxation and irreversible strains after external load events, the prestress reduces over time. This can be compensated by a certain "overstressing" during installation or by a construction that can be re-stressed. For sufficient compensation, compensation values are determined by which the membrane panel - simplified - is shortened before installation to achieve a slightly higher initial prestress. To determine compensation values, prCEN/TS 19102 refers to the new European standard EN 17117-2 [7]. This standard provides a suitable framework for determining compensation values using biaxial tensile tests. This consists, among other things, of modules, from which a suitable load protocol for an individual project can be created, as well as a guideline for the evaluation of the tests. The standard deliberately leaves the users a great deal of freedom and does not make any restrictive or unavoidable provisions. Ultimately, the determination of compensation values for the different materials used in membrane structures remains very complex and highly dependent on the experience of the engineer carrying out the work. Gibson [7] gives an insight into the complexity.

The last serviceability provision of prCEN/TS 19102 concerns the control of tears. At regular maintenance, the structure should be checked for tears (meaning small initial cracks). Tears should be professionally repaired (as early as possible), e. g. by applying patches, or the membrane must be replaced.

Membrane architecture: the seventh established building material. Designing reliable and sustainable structures for the urban environment.

2.3. Design of foil structures

2.3.1. Verification in the ultimate limit state

In the ultimate limit state (ULS), the material or the weld seam is verified against fracture. According to equation (3), the following must apply:

$$f_{Ed} \leq f_{Rd,mod} \quad (3)$$

f_{Ed} is the decisive stress, f_{Rd} is the minimum of the material and weld seam strength measured in monoaxial short-time tensile tests at room temperature $T = 23^\circ\text{C}$, including the associated partial safety factors. In the case of ETFE foils, $\gamma_{M0} = 1.1$ for the material and $\gamma_{M1} = 1.15$ for the weld seam. For ETFE foils the following strengths may be assumed without further tests: for the material $f_{1Rd} = 40$ MPa, for the weld seam $f_{2Rd} = 30$ MPa. Thus, according to the current state of welding technology, the breaking strength at the weld seam is always decisive for ETFE foils.

The decisive strength value must still be modified to $f_{Rd,mod}$ depending on the design situation. This is also done here using various modification factors k , see Table 2. The modification considers, for example high temperatures of a design situation in summer or the strength-reducing effect of long-lasting loads from snow or water ponds (Eq. (4)):

$$f_{Rd} = \frac{f_{Rd}}{k_{biax} \cdot k_{age} \cdot k_{dur,*} \cdot k_{temp,*} \cdot k_{QL} \cdot k_x} \quad (4)$$

where

k_{biax} modification factor for biaxial effects,

k_{age} modification factor for environmental effects (ageing, deterioration),

$k_{dur,*}$ modification factor for various load durations (permanent, long-term, medium-term and short-term (Caution: short-term here means a "comparatively short-acting long-term load"; the resulting strength is not to be confused with the short-time tensile strength)),

$k_{temp,*}$ modification factor for temperature effects (0°C , 40°C or 50°C),

k_{QL} modification factor considering the manufacturers quality level,

k_x is a variable for a modification factor for not yet specified effects.

The modification factors are always to be used depending on the design situation. Table 2 clarifies which modification factors are to be applied in which design situations. The values k_{biax} and k_{age} are to be applied in all design situations, as biaxial stress conditions are always assumed and, to be on the safe side, the verification for aged material must always be carried out. For ETFE foils, however, both values can be assumed to be 1.0, since for these foils – in contrast to common woven fabrics – strength reductions have been proven neither from biaxial stress conditions nor from ageing. On the contrary, there is evidence of very good resistance to ageing, which is also due to the UV transparency. There are also contrary indications for the strength; at least for the first yield point, which can be observed well in biaxial tests, it is shown that it is higher under biaxial stress conditions than in monoaxial stress conditions [9].

Table 2 also gives an indication that prCEN/TS 19102 does not exclude the formation of water ponds. Ponding is considered acceptable when a limitation of the snow or water pond is proven

Membrane architecture: the seventh established building material. Designing reliable and sustainable structures for the urban environment.

or its expansion is limited by load-bearing elements, e. g. by additional cable support, which is activated in the event of ponding.

Table 2: k-factors in design situations of the ULS of foil structures, values or ranges of values for k-factors for ETFE foils.

Design situation	$k_{biax} = 1,0$	$k_{age} = 1,0$	$k_{dur,P} = 1,8$	$k_{dur,L} = 1,6$	$k_{dur,M} = 1,4$	$k_{dur,S} = 1,3$	$k_{temp,0} = 0,95 - 1,0$	$k_{temp,40} = 1,2$	$k_{temp,50} = 1,3 - 1,7$	k_{QL}^*
1 Prestress	x	x	x						x	x
2 Prestress increased pressure	x	x		x						x
3 Snow > 1000 m altitude	x	x		x			x			x
4 Snow ≤ 1000 m altitude	x	x			x		x			x
5 Wind	x	x								x
6 Wind acting on foil at elevated temperature 40°C	x	x						x		x
7 Wind acting on foil at elevated temperature 50°C	x	x							x	x
8 Water ponding	x	x				x				x

* Values for k_{QL} are:

- for connection verifications:
 - $k_{QL,1} = 1,3$ for QL 1 (low demands),
 - $k_{QL,2} = 1,15$ for QL 2 (medium demands),
 - $k_{QL,3} = 1,0$ for QL 3 (high demands),
- for the foil verification $k_{QL} = 1,0$.

In addition, for the verification of welds, a modification factor k_{QL} must also be applied. This takes into account the quality level of the manufacturer as verified by monitoring. Three quality levels are provided, which are directly linked to three different monitoring levels. The quality level QL1 is the basic level at which the manufacturing staff monitors itself. At QL2, production is monitored by a quality management system that is independent of the production and in the highest level QL3, the manufacturer is monitored by an independent external body. The values for k_{QL} foreseen in the current draft are also given in Table 2.

The usable strength resulting from this concept is so high that plastic strains may have to be expected. In many foil structures, plastic strains are not generally critical, e. g. in foil cushions. As long as they can be controlled by the structural engineer, they can be used deliberately to make the use of the foils more economical. For viscoelastic-plastic foils, such as ETFE foils, prCEN/TS 19102 therefore provides for a two-stage serviceability limit state (SLS) verification,

Membrane architecture: the seventh established building material. Designing reliable and sustainable structures for the urban environment.

in which either the limitation of the plastic strain is verified or simplified and on the safe side an elastic stress verification is carried out.

2.3.2. SLS: Limitation of plastic strain

In principle, the same general rules on deformations, water ponding formation, etc. apply to foil structures as to textile membrane structures (section 2.2.2). In addition, a stress verification is carried out for the foils which is explained in the following.

High utilization of the foils is achieved by allowing a limited amount of irreversible elongation. The limit can be defined for a specific project. If no project-specific plastic strain limit is defined, a maximum irreversible strain of 1% is suggested. In any case make sure that the foils used do not hit other components and thus are damaged.

The irreversible strains that occur are determined with the help of biaxial tensile tests that simulate long-lasting (snow) loads or cyclically acting wind gusts (Fig. 1). These tests are used to determine the maximum strains under load and, above all, permanent strains after loads. From the measured values irreversible strains can be assigned to stress levels, which are then used as limit stresses in the verification. In the cyclic tests, the stresses are increased step by step. Stiffening of the material is utilized in this way (Fig. 1b).

The normative Annex, which regulates these tests and their evaluation, stipulates that corresponding test results for three different temperatures 0°C, 23°C and 50°C are to be provided once for each foil product by the material producer. This ensures that they are available to all planners. Possible changes in the course of subsequent production are detected via regular monoaxial tensile tests. It should be noted that the results of the biaxial tensile tests vary significantly between different foil producers and foil products.

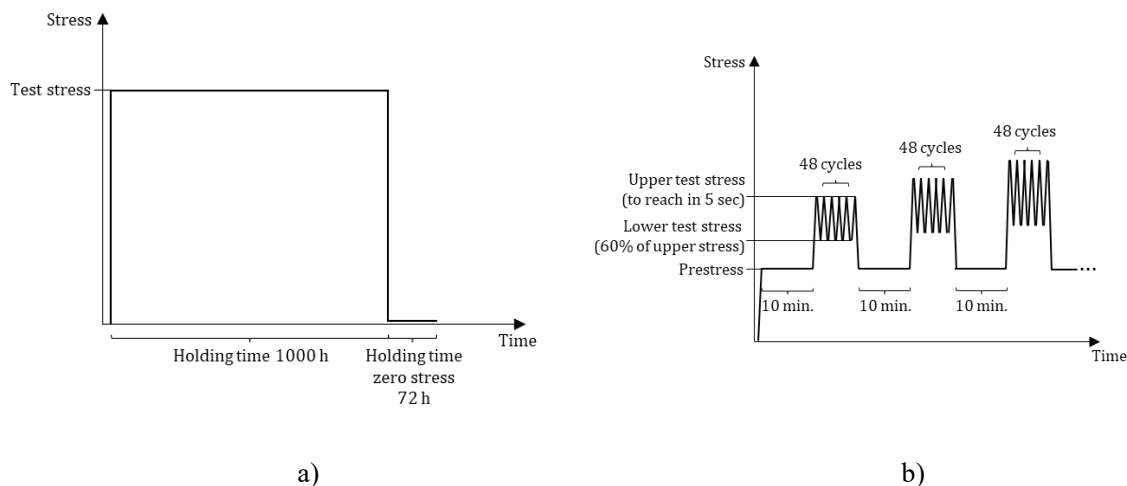


Figure 1: Load protocol for biaxial tension tests: creep tests (a) and biaxial hysteresis load tests (b), each simplified shown for only one material direction.

2.3.3. SLS: Elastic stress verification

Simplified, verification can be carried out in the elastic range. The elastic limit f_{el23} is used as the limit stress. This can be determined from biaxial or monoaxial tensile tests. In practice, monoaxial tensile tests are used, which are easy to perform. From test series with at least five specimens, the elastic limit is determined as the 5% fractile value. If no test results are available

Membrane architecture: the seventh established building material. Designing reliable and sustainable structures for the urban environment.

for the ETFE foil to be used, the approach $f_{e123} = 15$ MPa is recommended. It should be noted that also the elastic limit can vary significantly between different foil producers and foil products.

In the case of long-term loads such as snow or increased internal pressure in cushion structures over the winter months, it must be noted that creep strains can occur despite the "elastic" verification.

In the SLS too, physically induced modifications of the strength value (due to increased temperature, etc.) must be taken into account. While this is implicit in the biaxial test programs described above, it is covered in the elastic verification with modification factors. These are not necessarily identical with those in the ULS, both values as well as the fact that other factors are to be applied. For example, the value k_{QL} does not apply here, as the elasticity limit is a property of the base material and thus independent of the quality level of the manufacturer. On the other hand, for single-layer foil structures, however, an additional factor of $k_{single} = 1.1$ must be taken into account. The modification factor serves primarily to avoid significant plastic deformations and the associated loss of prestress in single-layer mechanically prestressed structures. This factor is to be applied to all design situations that could lead to significant irreversible strains, namely snow, wind and water ponding. It is not to be applied to prestress as high initial prestresses may be compensated by relaxation. Due to the relaxation processes that occur, a maximum prestress of 7.5 MPa is recommended. Table 3 summarizes the k-values for the SLS.

Table 3: k-factors in design situations of the SLS, values or ranges of values for k-factors for ETFE foils.

Design situation	$k_{biax} = 1,0$	$k_{age} = 1,0$	$k_{single} = 1,1$	$k_{dur,P} = 1,8$	$k_{dur,L} = 1,6$	$k_{dur,M} = 1,4$	$k_{dur,S} = 1,3$	$k_{temp,0} = 0,8$	$k_{temp,40} = 1,2$	$k_{temp,50} = 1,2 - 1,4$
1 Prestress	x	x		x						x
2 Prestress increased pressure	x	x			x					
3 Snow > 1000 m altitude	x	x	(x)		x			x		
4 Snow ≤ 1000 m altitude	x	x	(x)			x		x		
5 Wind	x	x	(x)							
6 Wind acting on foil at elevated temperature 40°C	x	x	(x)						x	
7 Wind acting on foil at elevated temperature 50°C	x	x	(x)							x
8 Water ponding	x	x	(x)				x			

() indicate that this value is only to be used for single-layer mechanically prestressed foil structures

Membrane architecture: the seventh established building material. Designing reliable and sustainable structures for the urban environment.

3. Execution of membrane structures

3.1. General

prCEN/TS 19102 is a design standard. Since many of the strength values required for the verifications in membrane structures have to be determined experimentally on a project-specific basis, it was obvious to develop execution rules at the same time. Following intensive and controversial discussions in the European and national committees a first draft for a minimum standard for the execution is now available. These rules are initially included in an informative annex to the design standard and serve as a basis for further refinement. The rules developed are closely related to the design concepts for textile and foil structures.

The aim is to separate the regulations for execution into an independent standard at the latest when CEN/TS 19102 is converted into a Eurocode.

This paper focuses on the particularly controversial issue of monitoring manufacturers and ignores for reasons of space the numerous other less controversial rules on the manufacture of membrane structures.

The basis for the monitoring rules is a division into three quality levels, which in turn are linked to three execution classes according to DIN EN 1990. Table 4 shows the different levels and interrelationships. The basic principle is that the higher the execution class and the associated consequences in the event of structural failure, the higher are the monitoring requirements for the manufacturers. This ensures in the case of complex and/or very large structures the necessary production quality and thus the reliability of the structure. On the other hand, this concept allows companies that specialize in smaller and/or less complex structures do not – justifiably – have to meet the same high requirements as those that also want to serve, for example, highly complex large structures. It also allows new firms to enter the market more easily.

Table 4: Relationship between execution classes and required quality levels of manufacturers.

Execution class	Required quality level	Examples of buildings and civil engineering works
EXC3	QL3	Grandstands, public buildings where consequences of failure are high (e. g. a concert hall).
EXC2	QL2	Residential and office buildings, public buildings where consequences of failure are medium.
EXC1	QL1	Agricultural buildings where people do not normally enter (e. g. storage buildings, greenhouses).

In principle, both the material producers (suppliers of textiles, coaters, foil producers) as well as the manufacturers must introduce and maintain a continuous factory production control. This includes written procedures, regular inspections, tests and evaluations and the use of the results

Membrane architecture: the seventh established building material. Designing reliable and sustainable structures for the urban environment.

to control the equipment, production processes and the membrane panels produced. Production control shall be based on:

- Incoming goods inspections,
- Control of processes,
- Calibration of testing equipment,
- Testing of manufactured products,
- Traceability.

In addition, the manufacturers must provide experimental proof of sufficient load-bearing capacities of the executed connections (surface seams, edge details) in laboratory tests before the start of production. This is explained in more detail in the following sections.

3.2. Continuous quality control of base materials production

For the material producers, there is no differentiation into different quality levels. At the time of material production, the producer often does not know what his material will be used for later. This means consequently that the quality must always meet the highest requirements.

3.3. Initial type testing of membrane panels

Initial type tests are to be carried out on surface seams and on edge details. They must be carried out once for a specific connection configuration. A connection configuration results from membrane material, seam width, edge profile geometry and material, keder diameter and material, etc.

The following applies to edge details in particular: they should be tested "as executed in the building", i. e. with the edge profile, keder rope etc. that are to be executed in the project. In this way, the decisive failure mode and load-bearing capacity can be determined. However, the edge profile may also be reinforced, so that only the membrane/foil and the keder are actually tested since the edge profile is verified separately anyway.

Partial safety factors should be applied in the verification according to the failure mode. This means that depending on whether metal components fail (e. g. bending up of the edge profile) or membrane or plastic components fail (e. g. crack at the seam edge, squeezing together and slipping out of the keder rope), partial safety factors are applied for metal components according to DIN EN 1993 [9] or DIN EN 1999 [10] or for structural membrane components according to prCEN/TS 19102 (plus modification factors if necessary). In case of failure in combination of metal and membrane components (e. g. slipping out of the keder rope due to squeezing together and bending up of the edge profile), the higher partial safety factor for membranes according to prCEN/TS 19102 should be applied.

According to prCEN/TS 19102, initial type tests should also be carried out at elevated temperatures "if required in the project". From the authors' point of view, the consideration of elevated temperatures is certainly necessary for most project regions in the world. As a standard, the temperature range for textile structures is $T = 70^{\circ}\text{C}$ for textile structures and $T = 50^{\circ}\text{C}$ for ETFE foil projects. Investigations in the past have shown that these temperatures reflect the highest values that can occur for the different materials in full sunlight. Depending on the project region and material colour, also lower temperatures can adequately cover summer conditions.

It is envisaged that initial type testing may be carried out by in-house or external testing laboratories. However, the testing laboratory should be accredited according to DIN EN

Membrane architecture: the seventh established building material. Designing reliable and sustainable structures for the urban environment.

ISO/IEC 17025 [12] and the test standard to be used (DIN EN ISO 1421 [13], DIN EN ISO 13934-1 [14] or DIN EN ISO 527-3 [15]) should be included in the list of accredited standards.

3.4. Continuous quality control of membrane panel production

The following applies to the manufacturers: Depending on the required quality level in a project, different strict measures for monitoring production are foreseen. In rudimentary QL1, production monitors itself. This can be done with the help of testing machines, but also by visual inspections and manual peel tests. The monitoring also includes inspections of the production site, machinery, storage facilities, test equipment, documentation, etc. In QL2 and QL3 the product inspections are carried out "directly" – meaning tests on a tensile testing machine – or "indirectly" – meaning tests of e. g. production parameters or peel tests. Someone independent of the production takes responsibility for these tests, e. g. a quality manager. The additional external monitoring in QL3 is to be carried out for each project, but however not more often than twice a year.

In contrast to initial type tests, tests in the frame of the continuous quality control only check the strength of the seam. This means that the test set-up for edge details can be simplified by, for example, using a project-independent, sufficiently rigid standard keder profile together with a steel keder which ensures breakage at the seam. The basic aim is to confirm the strengths from the initial type test.

Tests are only required at room temperature $T = 23^{\circ}\text{C}$, so they can be carried out by the manufacturers themselves – who usually do not operate temperature chambers on their testing machines. If the seam strengths at room temperature are sufficient, this also allows to confirm the strength at elevated temperatures. If no in-house testing machine is available, the tests can be handed over to external laboratories. Within the scope of continuous quality controls, no special competence requirements are placed on the internal or external laboratories; regular calibration of the testing machines is a prerequisite.

In quality levels 2 and 3, production controls must be documented and recorded and kept for at least ten years.

3. Conclusions and outlook

This paper presents the current state of development of the first European design standard for membrane structures, which is available as a draft standard in the form of prCEN/TS 19102 "Design of tensioned membrane structures". In addition to the core concern of the standard, the design, rules of execution were also developed which will be included in an informative annex to the design standard for the time being. In addition to the essential design rules, the paper presents excerpts of the controversially discussed execution rules for the supervision of the manufacturers.

The development of the standard has entered the final phase. The draft standard presented here will now be translated, submitted to the national mirror committees and published afterwards.

References

- [1] Uhlemann J., Stimpfle B. and Stranghöner N. (2022), Bemessung und Ausführung von Membrantragwerken nach prCEN/TS 19102, in: *Stahlbau*, vol. 91 (pp. 504-512).

Membrane architecture: the seventh established building material. Designing reliable and sustainable structures for the urban environment.

-
- [2] Stranghöner N., Uhlemann J., Mollaert M., Gosling P. (2014) The Development of a Eurocode “Tensile Membrane Structures”. Proceedings of the 37th IABSE International Symposium, Madrid, Spain, Sep. 3–5, 2014, pp. 1572–1578.
 - [3] Stranghöner N., Uhlemann J. (2016) Aktueller Stand der Normungsarbeit im Membranbau in: Stranghöner, N.; Saxe, K.; Uhlemann, J. [Eds.] 3. Essener Membranbau Symposium. Essen, 30. Sept. 2016. Aachen: Shaker Verlag.
 - [4] Stranghöner N., Uhlemann J., Maywald C., Stimpfle B. (2020) Materialprüfung und Bemessung im Zelt- und Membranbau in: Kuhlmann, U. [Ed.] Stahlbau-Kalender 2020. Berlin: Ernst & Sohn, pp. 455–509.
 - [5] prCEN/TS 19102:2021-11 (2021) Design of tensioned membrane structures. Final Draft submitted to NEN (unpublished).
 - [6] EN 1990:2010 Eurocode: Basis of Design.
 - [7] EN 17117-2:2021 Rubber or plastics-coated fabrics – Mechanical test methods under biaxial stress states – Part 2: Determination of the pattern compensation values.
 - [8] Gibson N. D. (2015) How to get a membrane structure off the drawing board. *Steel Construction*, vol. 8, No. 4 (pp. 244–250). <https://doi.org/10.1002/stco.201510034>
 - [9] Surholt F., Runge D., Uhlemann J., Stranghöner N. (2022) Mechanisch-technologisches Verhalten von ETFE-Folien und deren Schweißverbindungen. *Stahlbau*, vol. 91, No. 8 (pp. 513–523). <https://doi.org/10.1002/stab.202200039>
 - [10] EN 1993-1-1:2005 Eurocode 3: Design of steel structures – Part 1-1: General rules and rules for buildings.
 - [11] EN 1999-1-1:2007 Eurocode 9: Design of aluminium structures – Part 1-1: General structural rules.
 - [12] EN ISO/IEC 17025:2017 General requirements for the competence of testing and calibration laboratories.
 - [13] EN ISO 1421:2016 (2017) Rubber- or plastics-coated fabrics – Determination of tensile strength and elongation at break (ISO 1421:2016).
 - [14] EN ISO 13934-1:2013 Textiles – Tensile properties of fabrics – Part 1: Determination of maximum force and elongation at maximum force using the strip method (ISO 13934-1:2013).
 - [15] EN ISO 527-3:2018 Plastics – Determination of tensile properties – Part 3: Test conditions for films and sheets (ISO 527-3:2018).



tensinantes2023 : TensiNet Symposium 2023 at
Nantes Université

Membrane architecture: the seventh established building material.
Designing reliable and sustainable structures for the urban
environment.

Proceedings of the Tensinet Symposium 2023

TENSINANTES2023 | 7-9 June 2023, Nantes Université, Nantes, France

Jean-Christophe Thomas, Marijke Mollaert, Carol Monticelli, Bernd Stimpfle (Eds.)

Determination of ULS values of ETFE membrane structures according to Eurocode by using tensile strength measurements in quality control of production

Carl MAYWALD*, Torsten BALSTER^a, Delche LAZAREV^b

* Vector Foiltec GmbH

Steinacker 3, 28717 Bremen, Germany

Carl.Maywald@vector-foiltec.com

Abstract

The Euro Code 0 (EN 1990) is the harmonized basis of the European Union for structural design of buildings. It may unify European design rules, even though some EU countries are using the National Annex to consider local particularities.

However, the Euro Code itself is only a guideline to develop technical specifications for the structural design of ETFE membranes. Based on this concept the resistance design value R_d of the ETFE membrane and its joints is defined by measurements of the tensile strength.

The material properties of ETFE foils and their joints are characterized by a statistical distribution due to immanent production inaccuracies. Whereas the mechanical properties of the foil are defined by the extrusion and the properties of the polymer chain, the welding seams of the foil determine the value of the ultimate limit state ULS of the membrane. The statistical distribution of the tensile strength of the welds is defined by the variation of the welding process, i.e. the operation principle, the parameters of the different welding machines as well as by environmental conditions.

In this presentation the statistical parameters for the design value will be derived on the basis of the Eurocode. Accordingly, the maximum design values are calculated by using the statistical results of the quality control of the production. Vice versa, the threshold values for the production quality control were determined, i.e. the 5%-quantiles and mean values of tensile strength of the welding seams, which are certified by the external production audits twice a year.

Keywords: ETFE foil, structural membrane, performance, manufacturing, welding, quality control, ultimate limit states

1. Introduction

For the structural design of tensile membrane cladding systems in architecture, both the definition of serviceability limit state SLS as well as the definition of the ultimate limit state

Membrane architecture: the seventh established building material. Designing reliable and sustainable structures for the urban environment.

ULS are mandatory. Following the mandate of CEN/TC 250 “Structural Eurocodes” the workgroup 5 has prepared the Technical Specification for the design of membrane structures FprCEN/TS 19102:2022-05 (E) which strictly follows the regulations given in EN 1990:2021, Eurocode — Basis of structural and geotechnical design (EN 1990). For the application of ETFE foils as structural element two different systems are distinguished, single layer systems and cushion systems. For single layer systems, the viscoelastic-plastic deformation as a characteristic material performance of ETFE foils must be considered carefully by structural engineering, since plastic deformation is not allowed for single layer systems to keep the recommended prestress of approximately 6 MPa. For cushion systems elastic and plastic deformation is explicitly allowed since cushion systems automatically adapt to specific local wind loads. Thus, the limit state for serviceability of ETFE foil cushion systems is defined by 3 criteria only:

- Collision of the foil with parts of the supporting structure shall be avoided.
- The architectural aesthetic design should not be affected.
- Enhanced risk of water and snow ponding must be considered.

Anyhow, detailed information regarding mechanical performance of the ETFE foil material is required for both the mechanical prestressed and the pneumatically prestressed building cladding solutions. The test method for the analysis of the mechanical performance of ETFE foils can be found in Annex E “Test procedures to determine foil properties” of the Technical Specification for the design of membrane structures (TS 19102:2022-05 (E), p.73 ff). To achieve information regarding field loading response of ETFE foil under wind loads, biaxial hysteresis tests with discrete load levels simulating different wind gusts are recommended. The test speed is adjusted according to the duration and power of 2-5 seconds wind gusts. In Annex E4 “Biaxial hysteresis load tests for foils” it is recommended to perform 50 load cycles for each load level (15/7,5 MPa, 18/9 MPa, 20/10 MPa, 22/11 MPa, 24/12 MPa, 26/13 MPa), each one with loading and unloading time of 5 seconds (TS 19102, p.75 ff). Figure 1 shows one of the first tests that have been designed by Vector Foiltec in 2016. The load tests were performed at the Essener Labor für Leichte Flächentragwerke ELLF at the University of Duisburg-Essen.

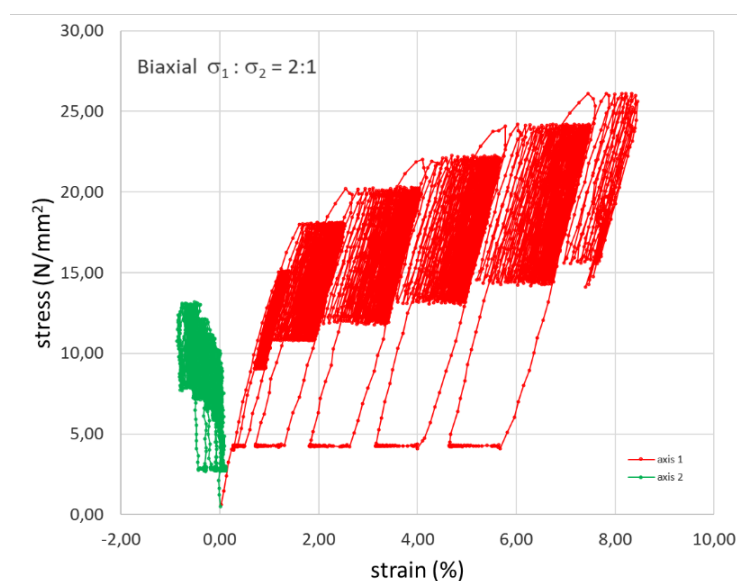
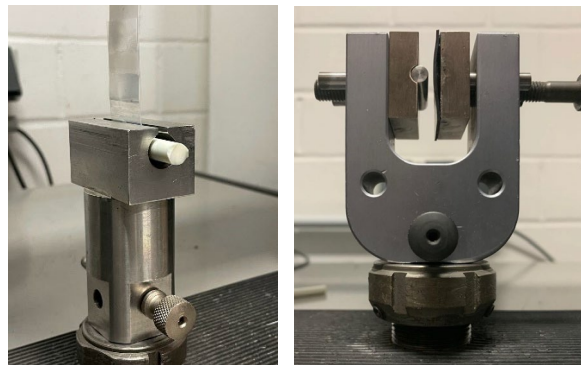


Figure 1: Stress-Strain diagram of biaxial tensile test. The load ratio is 2:1; basic load of 4 N/mm² according to 250Pa inner cushion pressure; 6 load levels: 15/7,5 MPa, 18/9 MPa, 20/10 MPa, 22/11 MPa, 24/12 MPa, 26/13 MPa; hysteresis frequency 50 x 5seconds

Membrane architecture: the seventh established building material. Designing reliable and sustainable structures for the urban environment.

The ultimate limit state ULS of an ETFE system is defined by the weakest point of the system which is the welded seam, either area welding or edge welding. For ETFE foil systems the welding strength is characterized by the load perpendicular to the weld. Thus, a monoaxial tensile test according to EN ISO 527-3 will provide information on the tensile strength of the ETFE weld. Detailed instructions regarding test conditions and procedures are given in the Annex I “Structural foils – Determination of tensile properties under uniaxial stress states” of prCEN/TS 19102 (TS 19102, p.97 ff).

For example, figure 2 shows standardized holders as uptake for Keder ropes for tests of edge welding (a) and as uptakes for foil, either single or multiple foils (edge welding):



a) Holder for Keder rope b) Linear pressing grips

Figure 2 a, b: Holder for monoaxial tensile tests for edge welding (a) and area welding (b). Copyright Vector Foiltec GmbH

2. Quality control and reliability management

Within the scope of EN 1990 the reliability required for structures shall be achieved by design in accordance with EN 1990 to EN 1999 and by appropriate execution and quality management measures. Different levels of reliability may be adopted inter alia for structural resistance and for serviceability. The choice of the levels of reliability for a particular structure should take into account relevant factors, including:

- The possible cause and /or mode of attaining a limit state.
- The possible consequences of failure in terms of risk to life, injury, potential economic losses.
- Public aversion to failure.
- The expense and procedures necessary to reduce the risk of failure.

The criteria for the design of different levels of reliability that apply to a particular structure as a whole and/or its components are defined in Annex B3.1 of the Eurocode EN 1990 as 3 Consequent Classes CC (EN 1990, p. 88) by considering the consequences of failure or malfunction of the structure (see table below):

Membrane architecture: the seventh established building material. Designing reliable and sustainable structures for the urban environment.

Table 1: Definition of consequences classes.

Consequences Class	Consequence for loss of human life, or economic, social or environmental consequences	Examples
CC3	High/severe consequences	Grandstands, public buildings where consequences of failure are high (e.g. a concert hall)
CC2	Medium/considerable consequences	Residential and office buildings, public buildings where consequences of failure are medium (e.g. an office building)
CC1	Low/negligible consequences	Agricultural buildings where people do not normally enter (e.g. storage buildings), greenhouses

Three examples for typical consequence class 3 CC3 buildings are shown in figure 3 a, b, c:

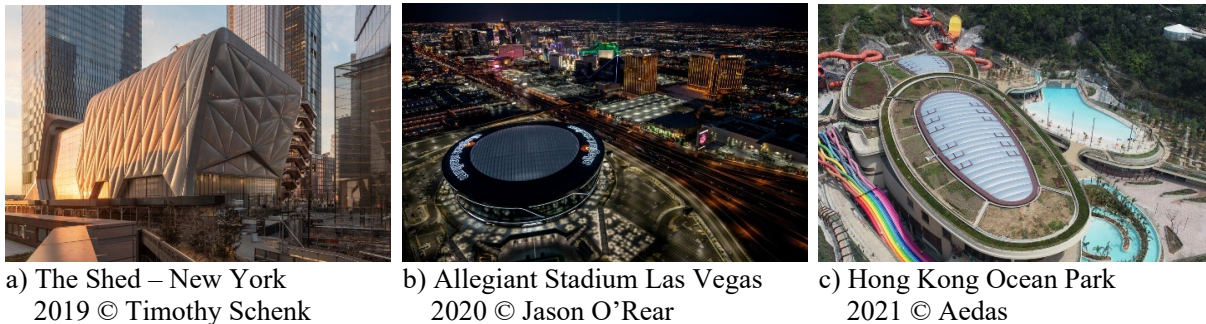


Figure 3 a,b,c: Three examples of ETFE cladding according to CC3

Figure 4 a and b shows two typical consequence class 2 CC2 buildings:



Figure 4 a and b: Three examples of ETFE cladding according to CC2

As mentioned before, consequence classes may be associated with reliability classes RC according to the Eurocode (EN 1990, p. 88). Within the context of the technical specification

Membrane architecture: the seventh established building material. Designing reliable and sustainable structures for the urban environment.

prCEN/TS 19102 (TS 19102, p.97 ff) reliability classes are named execution classes EXC. The execution classes (EXC) may be defined by the β reliability index concept.

Table 2: consequences classes associated with execution classes and the minimum 50 years reliability index β .

Consequences Class	Execution Class	Reliability index β (50 years)
CC3	EXC3	4.3
CC2	EXC2	3.8
CC1	EXC1	3.3

The execution classes may be associated with production inspection levels IL (see table 3):

Table 3: Execution classes associated with the quality level, i.e. verification of the data according to inspection

Execution Class	Quality Level	Minimum Requirements for Supervision
EXC3	QL3	As QL2 plus specific third-party inspection linked with the project.
EXC2	QL2	Inspection by the manufacturer's authorised representative, independent of the manufacturing personnel
EXC1	QL1	Self-inspection by the production

3. Calculation of the production specific design strength f_{Rd}

The following expression shall be satisfied at every location of the foil (TS 19102, p.36 f):

$$f_{Ed} \leq f_{Rd,mod}$$

where

f_{Ed} is the design principal foil stress in the considered direction; and

$f_{Rd,mod}$ is the design tensile strength of the foil or the connection related to the specific design situation.

The value for the partial factor for the resistance of ETFE foils and connections should be:

$$\gamma_{M0} = 1.1$$

$$\gamma_{M1} = 1.15$$

The partial safety factor for the resistance of connections γ_{M1} may be determined according to Formula (4.1). At least 30 series of minimum 5 tests per series from the last 6 month shall be available on connections of the base material under consideration. Welded seams and edge

Membrane architecture: the seventh established building material. Designing reliable and sustainable structures for the urban environment.

connections should be considered, as well as all welding machines and welders, for which this partial factor should be applied.

$$\gamma_{M1} = (1 - 1,64 * V_x)/(1 - 0,8 * \beta * V_x) \geq \gamma_{M0} \quad (4.1)$$

where

V_x is the mean value of the coefficient of variation of at least 30 series of minimum 5 tests per series from the production of the last 6 months [$V_x = (\text{standard deviation})/(\text{mean value})$]; V_x shall be validated by the tests carried out in the specific project on the specific detail. The coefficient of variation V_x shall not exceed 0,08 for the mean value and in the specific project.

β is the reliability index, $\beta = 3,8$; other values may be chosen depending on the reliability class of the project.

$$f_{Rd} = \min \begin{cases} f_{1Rd} = f_{u23}/\gamma_{M0} \\ f_{1Rd} = f_{uw23}/\gamma_{M1} \end{cases} \quad (4.2)$$

where

f_{u23} is the short-term tensile strength of the base material derived from uniaxial material tests at T=23 °C

f_{uw23} is the short-term tensile strength of a welded seam or edge connection derived from uniaxial tests at T=23 °C.

As threshold values for minimum required seam strength, $f_{uw23} = 30$ MPa as 5% fractile values for ETFE welding may be used. These values must be verified later by experiments.

4. The Vector Foiltec quality management system

Anyhow, equation 4.1 allows for a production-specific calculation of the partial factor γ_{M1} for area welding and edge welding by means of a continuous quality management system. Vector Foiltec has implemented a continuous tensile test system not only for the definition of production-specific partial factors but also for the definition of welding parameters for the different welding machines. The quality management system of the production is monitored twice per year for the time period between January and June and the time period between July and December by an external independent authorized surveyor. The quality management system does not distinguish between consequence classes. All classes are monitored according to EXC3. The threshold for fail is set to

$$\mu_R \geq 33 \text{ MPa and}$$

$$R_{5\%} \geq 30 \text{ MPa}$$

where

μ_R is the mean resistance value of 5 ETFE seam samples each and

$R_{5\%}$ is 5% fractile seam strength of ETFE seams for 5 samples each.

Since second half year of 2019, Vector Foiltec started to systematically analyze and document the data achieved from production quality control in order to provide a detailed quality assessment of the production.

Membrane architecture: the seventh established building material. Designing reliable and sustainable structures for the urban environment.

Figure 4 shows the trend curve of the average mean values of the tensile strength of all approved welding samples that have been produced by different welding machines within the production facility of Vector Foiltec in Bremen, Germany. The data comprise area welding and edge welding. Figure 5 shows the trend curve of the 5% fractile values of the tensile strength of all approved samples.

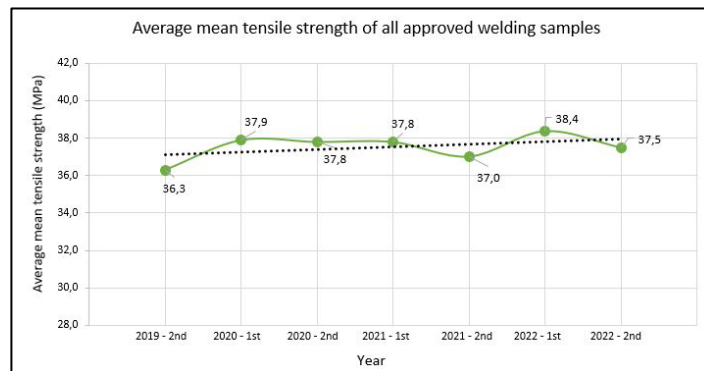


Figure 5: Average mean value of the tensile strength of all approved samples from 2nd half year 2019 until 2nd half year 2022 (7 inspection periods)



Figure 6: Average 5% fractile value of the tensile strength of all approved samples from 2nd half year 2019 until 2nd half year 2022 (7 inspection periods)

The trend curves shown in both figures make evident, that the quality management of the production contributes to constantly improved welding quality due to close cooperation between the test lab and the production. The variation is due to both, statistics and fluctuation of accuracy during production. The more detailed analysis of these data according to area welding, edge welding, printed foils, use of different welding machines, etc., will allow to identify and improve weak points in the production.

Accordingly, the partial factor γ_{M1} could be reduced significantly. Within the time period between 01.07.2022 and 31.12.2022 a total number of 2545 samples were approved, and 479 samples were not approved. The mean value R_m , the standard deviation σ_x , and the 5% fractile $R_{5\%}$ are shown in table 4:

Membrane architecture: the seventh established building material. Designing reliable and sustainable structures for the urban environment.

Table 4: tensile test of ETFE welding seams, 2nd half year 2022

	Number of samples	R_m MPa	σ_x	$R_{5\%}$ MPa
approved	2545	37.5	1.1	34.7
rejected	479	30.9	1.2	28.0

By means of these data, the design resistance can be calculated according to Equ. 4.2 as

$$f_{1Rd} = f_{uw23}/\gamma_{M1} \quad (5.1)$$

with

$$f_{uw23} = R_{5\%} = 34.7 \text{ MPa} \quad (5.2)$$

and according to Equ. 4.1

$$\gamma_{M1} = \frac{1-1.64*V_x}{1-0.8*\beta*V_x} = 1.061 \quad (5.3)$$

The result for the design strength, i.e. the design resistance, is

$$f_{1Rd} = \frac{34.7 \text{ MPa}}{1.061} = 32,71 \text{ MPa}. \quad (5.4)$$

Due to the more complicated setup of edge welding, we have extracted the welded seams done for the edges from the total number of welded seams. Results are shown in figure 5.

Table 5: tensile test of ETFE edge welding, 2nd half year 2022

	Number of samples	R_m MPa	σ_x	$R_{5\%}$ MPa
approved	748	36.2	1.2	33.1
rejected	301	30.5	1.3	27.1

By means of the data given in table 5, the design resistance can be calculated according to Equ. 4.2 as

$$f_{1Rd} = f_{uw23}/\gamma_{M1} \quad (5.5)$$

with

$$f_{uw23} = R_{5\%} = 33.1 \text{ MPa} \quad (5.6)$$

and according to Equ. 4.1

$$\gamma_{M1} = \frac{1-1.64*V_x}{1-0.8*\beta*V_x} = 1.071 \quad (5.7)$$

The result for the design strength, i.e. the design resistance, is

$$f_{1Rd} = \frac{33.1 \text{ MPa}}{1.071} = 30,92 \text{ MPa}. \quad (5.8)$$

Membrane architecture: the seventh established building material. Designing reliable and sustainable structures for the urban environment.

Following the postulate for the definition of ULS given in chapter 2 of this document, the weakest point of the system is identified as the edge welding. Thus, it is recommended to only use the data for the calculation of the design resistance for ULS of an ETFE system.

5. Conclusion

The prospective new industry standard prCEN/TS19102 Design of tensioned membrane structures will provide the choice of determination of the partial factor γ_{M1} and thus the determination of the design resistance R_d by two different methods:

- a) A simple method applying the Execution Class 2 and the corresponding reliability index β for all Consequent Classes. γ_{M1} will be 1.15.
- b) A more sophisticated method which not only allows for a production specific calculation of the partial factor γ_{M1} referring to the data from quality assessment and control but allows for improvement of the welding performance and γ_{M1} , respectively.

For the definition of the design resistance R_d , i.e. for calculation of ULS, it is strictly recommended to use the data of the weakest system point only. For ETFE cladding systems it is the edge welding.

6. References

- | | |
|--------------------|--|
| DIN EN 1990 | EN 1990 :2021-10 Eurocode: Basis of structural design, CEN/TC 250 Structural Eurocodes, Berlin, Germany, Beuth (2021). |
| TS 19102:2022-05 | FprCEN/TS 19102:2022-05 (E) Design of tensioned membrane structures, CEN/TC 250 (2022) |
| TS 19102, p.73ff | prCEN/TS 19102:2022-05 (E), Design of tensioned membrane structures Annex E (normative) Test procedures to determine foil properties, CEN/TC 250 (2022) |
| TS 19102, p.75 ff | prCEN/TS 19102:2022-05 (E), Design of tensioned membrane structures Annex E4 (normative) Biaxial Hysteresis Load Tests for foils, CEN/TC 250 (2022) |
| TS 19102, p. 97 ff | prCEN/TS 19102:2022-05 (E), Design of tensioned membrane structures Annex I (normative) Structural foils – Determination of tensile properties under uniaxial stress states, CEN/TC 250 (2022) |



tensinantes2023 : TensiNet Symposium 2023 at Nantes Université

Membrane architecture: the seventh established building material.
Designing reliable and sustainable structures for the urban environment.

Proceedings of the Tensinet Symposium 2023

TENSINANTES2023 | 7-9 June 2023, Nantes Université, Nantes, France

Jean-Christophe Thomas, Marijke Mollaert, Carol Monticelli, Bernd Stimpfle (Eds.)

On the design of membrane structures with the partial safety factor concept – a parameter study on the influence of structural and probabilistic properties

Martin FUBEDER^{*a}, Max TEICHGRÄBER^b, Daniel STRAUB^b and
Kai-Uwe BLETZINGER^a

^{*a} Chair of Structural Analysis, Technical University of Munich,
Arcisstraße 21, 80333 Munich, Germany,
martin.fusseder@tum.de

^b Engineering Risk Analysis Group, Technical University of Munich,
Arcisstraße 21, 80333 Munich, Germany

Abstract

The partial safety factor concept was developed for limit state functions that are linear or mildly non-linear. Structural membranes show a distinct non-linear behaviour and exhibit additional challenges due to their pre-stressing. Hence, the applicability of the partial safety factor concept to membrane structures needs to be studied. Previous investigations of the authors showed that the simplified design rules of EN 1990 (Eurocode 0) can lead to inconsistent reliability levels. Especially in case of membrane structures, the presence of pre-stress causes large deviations of the reliability compared to the linear target case. In this contribution, we conduct a parameter study to identify the influence of different parameters on the reliability of membrane structures. We study various pre-stress levels and different degrees of non-linearity in the relation between actions and their effects. Moreover, we investigate the effect of different probabilistic setups (distribution types and distribution parameters). We conclude with a discussion of the consequences of our investigations and an outlook to possible adaptation approaches of the partial safety factor concept with special focus on the particularities of membrane structures.

Keywords: structural membranes, partial safety factors, non-linear behaviour, semi-probabilistic safety concept, reliability analysis, Eurocode.

1. Introduction

Membrane structures appeal through their elegant double-curved shapes and lightness. These can be achieved by generating pre-stressed equilibrium surfaces through formfinding. Typically, membrane structures show a non-linear relation between external actions and their

Membrane architecture: the seventh established building material. Designing reliable and sustainable structures for the urban environment.

effects. Hence, the application of the semi-probabilistic safety factor concept for the structural design of membranes merits some deeper investigations. Recently, European efforts towards a harmonized standard in membrane design and verification have resulted in the Technical Specification (TS) on the “design of tensioned membrane structures” (Comité Européen de Normalisation (CEN), 2021) (TS), with the goal of developing a Eurocode on this basis. The TS provides a framework for the verification of the ultimate limit state (ULS) and serviceability limit state (SLS) based on EN 1990 (Comité Européen de Normalisation (CEN), 2002/2010). However, the EN 1990 provides only simplified rules for non-linear design problems. In addition to work on codification, research on reliability assessment of membrane structures has been conducted. For instance, there are studies of the general applicability of reliability analysis to membrane structures (Gosling, Bridgens, & Zhang, 2013) and reliability analyses of membrane structures that are modelled as cable-nets (Smedt, Mollaert, van Craenenbroeck, Caspeele, & Pyl, 2020b). Other research on membranes in the context of the safety concept concentrates on the determination of partial factors leading to a satisfying safety level. For example, there are investigations of the resistance uncertainty of membrane materials and recommendations of corresponding resistance partial factors (Zhang, Lu, Zhou, & Zhang, 2018) and attempts for the calibration of partial factors for pre-stress, wind and snow especially for membrane structures (Smedt, Mollaert, Caspeele, Botte, & Pyl, 2020a). The aforementioned works have in common that they use the partial safety factor concept, whose actual application for non-linear limit state equations is still an open research question. In this context, the authors (Fußeder, Teichgräber, Bletzinger, Straub, & Goldbach, 2021) investigated a basic case study of a membrane structure and showed that the simplified design rules of EN 1990 can lead to inconsistent reliability levels. Especially in case of membrane structures, the presence of pre-stress causes large deviations of the reliability compared to the linear target case. Previously conducted fundamental investigations (Teichgräber, Fußeder, Bletzinger, & Straub, 2023) contain a detailed parameter study to identify the influence of different parameters on the reliability achieved with the partial safety factor concept in the context of non-linear limit state functions. That parameter study shows that both the degree of non-linearity of the structural response and (semi-) probabilistic properties strongly affect the reliability.

The aim of this paper is to investigate the impact of the design rules in the partial safety factor concept on the structural reliability by a parameter study. In contrast to the above-mentioned fundamental parameter study, this contribution focusses on the particularities of membrane structures. In detail, we study an exemplary hyperbolic paraboloid with different pre-stress levels and different degrees of non-linearity in the relation between actions and their effects. Moreover, we apply different probabilistic setups (distribution types and distribution parameters) to investigate their interaction with the non-linear structural response. The paper is organized as follows: in Section 2 the partial safety factor concept is briefly introduced, Section 3 describes the fundamentals of the reliability assessment which is utilized in the parameter study in Section 4. Finally, Section 5 discusses the consequences of the parameter study and gives an outlook to possible adaptation approaches of the partial safety factor concept.

Membrane architecture: the seventh established building material. Designing reliable and sustainable structures for the urban environment.

2. The partial safety factor concept

The semi-probabilistic partial safety factor (PSF) concept is commonly implemented in design codes to verify structural designs. Within this paper we use the nomenclature of the PSF concept presented in EN 1990 (Comité Européen de Normalisation (CEN), 2002/2010). However, our investigations are general, and the conclusions extend to other design standards.

The EN 1990 (Eurocode 0) distinguishes between four PSFs: γ_f , γ_{sd} , γ_m and γ_{rd} . These cover the uncertainties related to the load model, the structural model, the material model and the resistance model, respectively. A PSF design needs to fulfil the inequality

$$\gamma_{sd} \cdot t_S(\gamma_f \cdot l_k) = e_d \leq r_d = \frac{1}{\gamma_{rd}} \cdot t_R\left(\frac{m_k}{\gamma_m}\right) \quad (1)$$

where l_k and m_k are the characteristic load and the characteristic material strength, e_d and r_d are the design load effect and the design resistance, t_S and t_R are functions provided by the structural model and the resistance model, which translate the load into the load effect and the material strength into the resistance.

However, the distinction of the four PSFs is only theoretical. In practice, EN 1990 applies only two factors γ_F and γ_M by combining the above PSFs as follows:

$$\gamma_F = \gamma_f \times \gamma_{sd} \quad (2)$$

$$\gamma_M = \gamma_m \times \gamma_{rd} \quad (3)$$

This leads to the question, if γ_F and γ_M should be applied prior (option a) or posterior (option b) to t_S and t_R :

$$(a) \quad e_d = t_S(\gamma_F \cdot l_k) \quad \text{or} \quad (b) \quad e_d = \gamma_F \cdot t_S(l_k) \quad (4)$$

$$(a) \quad r_d = t_R\left(\frac{m_k}{\gamma_M}\right) \quad \text{or} \quad (b) \quad r_d = \frac{1}{\gamma_M} \cdot t_R(m_k) \quad (5)$$

If t_S and t_R are linear functions, options (a) and (b) lead to the same design values. If non-linearities are present, this is not the case anymore. According to Paragraph 6.3.2(4) of the EN 1990, option (a) should be chosen if the load effects increase more than the loads and option (b) if they increase less. This simplified rule categorizes the non-linearity of structural systems into under- or over-linear behaviour and chooses the more conservative option.

3. Reliability assessment of structural designs

In this paper we focus on stress design in the ultimate limit state (ULS) of membrane structures. Hence, the structural model t_S equates the non-linear evolution of the maximal membrane stress in a certain direction during load application. We use a linear resistance model t_R . Therefore, we introduce a constant p , which can be interpreted as resistance design parameter. In case of an optimized material utilization, i.e., $e_d = r_d$, the PSF designs are given based on Equ. 4 and Equ. 5 as

$$(a) \quad t_S(\gamma_F \cdot l_k) = p \cdot \frac{m_k}{\gamma_M} \quad \text{or} \quad (b) \quad \gamma_F \cdot t_S(l_k) = p \cdot \frac{m_k}{\gamma_M} \quad (6)$$

Membrane architecture: the seventh established building material. Designing reliable and sustainable structures for the urban environment.

which leads to

$$(a) \quad p = \frac{\gamma_M \cdot t_S(\gamma_F \cdot l_k)}{m_k} \quad \text{or} \quad (b) \quad p = \frac{\gamma_M \cdot \gamma_F \cdot t_S(l_k)}{m_k} \quad (7)$$

as computation rule of the design factor p . Based on the PSF designs in Equ. 7 the limit state function g can be formulated as

$$g = p \cdot M - t_S(L) = \begin{cases} \frac{\gamma_M \cdot t_S(\gamma_F \cdot l_k)}{m_k} \cdot M - t_S(L) & \text{option (a)} \\ \frac{\gamma_M \cdot \gamma_F \cdot t_S(l_k)}{m_k} \cdot M - t_S(L) & \text{option (b)} \end{cases} \quad (8)$$

whereby M and L denote the random variables of the membrane material strength and the action. The probability of failure is defined as

$$\Pr(F) = \int_{\{g < 0\}} f_{LM}(m, l) dm dl \quad (9)$$

where f_{LM} is the joint probability density function of M and L . The reliability index β relates to the probability of failure through the standard normal cumulative probability distribution function:

$$\beta = -\Phi^{-1}(\Pr(F)) \quad (10)$$

In general, the integral in Equ. 9 cannot be solved analytically. Therefore, numerous techniques for approximate computation of the probability of failure were developed, e.g., First Order Reliability Method (Rackwitz & Fiessler, 1978) or subset simulation (Au & Beck, 2001). In case of only two basic random variables (M , L), standard numerical integration techniques also work well.

4. Parameter study

The aim of the parameter study is to investigate how the reliability index β varies for different membrane stress functions t_S and different probabilistic setups if the structure is designed with the PSF design rules presented in Section 2. Thereby we do not classify the stress functions into the categories over- and under-linear. Instead, we design all considered cases with options (a) and (b). To be able to compare the cases, we describe the stress functions t_S with the non-linearity measure introduced in (Teichgräber et al., 2023). The two components of the measure are defined as

$$\text{offset measure:} \quad y_0 = \frac{e_0}{e_k} \quad (11)$$

$$\text{curvature measure:} \quad \kappa = \frac{m_2}{m_1} \quad (12)$$

where $e_0 = t_S(0)$ is the pre-stress in case of membranes, $e_k = t_S(l_k)$ is the characteristic stress and $e_d = t_S(\gamma_F \cdot l_k)$ is the design value of the stress, $m_1 = \frac{e_k - e_0}{l_k}$ and $m_2 = \frac{e_d - e_k}{l_d - l_k}$.

Membrane architecture: the seventh established building material. Designing reliable and sustainable structures for the urban environment.

In all subsequent studies the partial safety factors γ_F and γ_M are chosen such the target reliability index of $\beta_{TRG} = 4.3$ is achieved for the linear case ($y_0 = 0$ and $\kappa = 1$). Thereby, we take $\gamma_F = 1.5$ as common value for variable actions in EN 1990 and calibrate γ_M such β_{TRG} is met in the linear case. The choice of β_{TRG} reflects the common range of nominal reliability indices in structural design (Köhler, Sørensen, & Baravalle, 2019). However, the results are not sensitive to minor changes of the target reliability index. If the reliability indices of the membrane designs are above/below β_{TRG} one can see them as conservative/non-conservative. Hence, the parameter study reveals under which conditions which PSF design option of EN 1990 lead to conservative or non-conservative designs of membrane structures.

4.1. Setup

The investigated structure is a hyperbolic paraboloid (hypar) which is shown in Figure 1. It is a slightly modified version of the hypar presented in Round Robin Exercise 4 (Smedt et al., 2017). The authors utilized the structure in their basic case study (Fußeder et al., 2021). The membrane has a Young's modulus of 600 kN/m, a shear modulus of 30 kN/m (both are pre-integrated over the thickness) and a Poisson's ratio of 0.4. The edge cables have a Young's modulus of 205 kN/mm² and a diameter of 12 mm. The structure has a fixed base area of 6×6 m and the height h is altered between 1 m, 2 m and 3 m (cf. coordinates of edge points in Figure 1). The membrane and its edge cables are fixed at its low and high points.

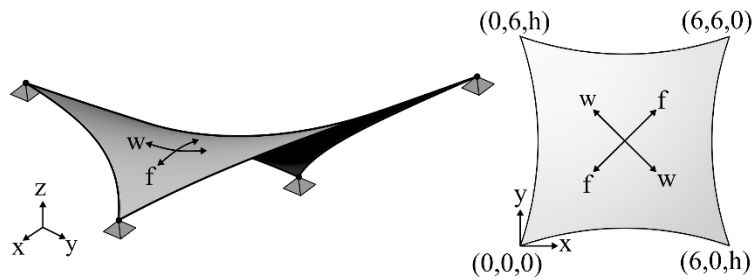


Figure 1: Investigated membrane structure with indication of warp (w) and fill (f) direction. The membrane is observed with three different heights h (1 m, 2 m and 3 m).

For structural design, an isotropic pre-stress of $p = 3.0$ kN/m and a cable force of $P = 30$ kN is utilized. Moreover, the membrane is subjected to a uniform snow load, which is acting in negative z -direction. Hence, the stress in warp direction (cf. Figure 1) is decisive for the design. Dead load is neglected in the study. For the load we assume a Gumbel distribution with mean $E[L] = 0.34$ kN/m² and a coefficient of variation $c.o.v.[L] = 0.3$ and for the tensile strength of the membrane we use a log-normal distribution with mean $E[M] = 1.0$ kN/m² and $c.o.v.[M] = 0.1$. The characteristic load is $l_k = 0.60$ kN/m² (98 % quantile of L) and characteristic tensile strength is $m_k = 0.84$ kN/m² (5 % quantile of M). The utilized distribution types are common choices for variable loads and resistances (Köhler et al., 2019) and the quantiles are based on EN 1990 (Comité Européen de Normalisation (CEN), 2002/2010).

The PSF design process and the reliability analysis of all observed cases are performed as described in Section 3. The procedure consists of three main steps:

- 1) Calibration of γ_M for the specific probabilistic setup (iterative PSF design with varying γ_M and proceeding reliability analysis based on linear static model until β_{TRG} is reached)
- 2) PSF design according to Equ. 7
- 3) Reliability analysis based on the limit state function defined by Equ. 8

4.2. Base case

The described structural and probabilistic properties in Section 4.1 define the base case of the parameter study. The non-linear evolution of the maximal membrane stress during load application is shown in Figure 2. The distributions of the decisive stress in warp direction due to $l_d = \gamma_F \cdot l_k$ and the position of the maximal stress can be seen in Figure 3. The non-linearity measures and the reliability indices of the three membranes of the base case are summarized in Table 1. All reliability indices are larger than β_{TRG} and thus all designs are conservative. The designs according to option (b) are even more over-designed. Furthermore, for option (b) we observe the trend that the reliability index strongly increases for higher values of γ_0 .

Table 1: Reliability indices β and non-linearity measures for the base case designed according to design options (a) and (b). Non-conservative/conservative designs are indicated by orange/green color.

height [m]	γ_M	reliability index β		non-linearity measure	
		option (a)	option (b)	κ	γ_0
1.0		4.58	5.17	1.07	0.42
2.0	1.23	4.46	5.03	1.23	0.53
3.0		4.60	5.40	1.10	0.61

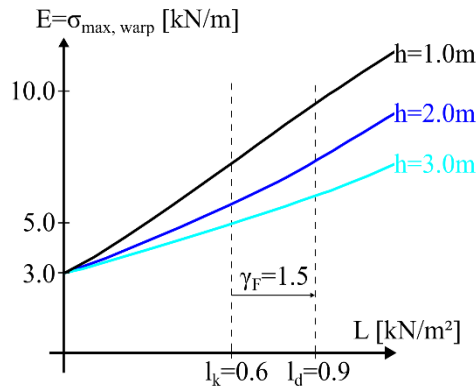


Figure 2: Action - effect of action diagram of stress in warp direction (w) under snow load for hypars with different height h .

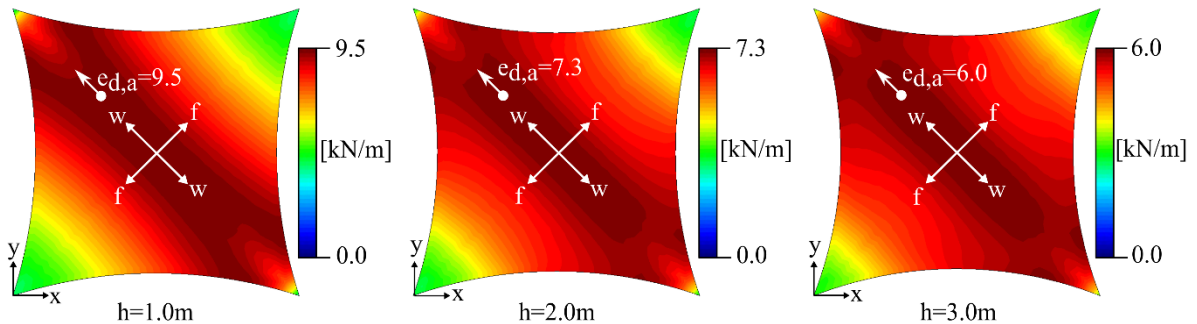


Figure 3: Distributions of stress in warp direction (w) due to load l_d for hypars with different height h . The white dot indicates the position of the maximal stress.

4.3. Effect of pre-stress

To investigate the effect of pre-stress, we vary the pre-stress of the membrane by $p \pm 1.0$ kN/m and the cable force accordingly by $P \pm 10.0$ kN. Since the probabilistic setup is unchanged, γ_M is the same as in the base case. The results are summarized in Table 2. We observe that all

Membrane architecture: the seventh established building material. Designing reliable and sustainable structures for the urban environment.

designs are conservative. The conservatism of the designs according to option (b) is particularly striking. For all three membranes with different heights, we observe that the reliability index is increasing with higher pre-stress. This trend can be found for both design options.

Table 2: Reliability indices β and non-linearity measures in case of varied pre-stress levels designed according to design options (a) and (b). The table contains additionally the results of the base case (bold). Non-conservative/conservative designs are indicated by orange/green color.

height [m]	setup p [kN/m] / P [kN]	γ_M	reliability index β		non-linearity measure	
			option (a)	option (b)	κ	y_0
1.0	2 / 20	1.23	4.55	5.01	0.97	0.28
	3 / 30		4.58	5.17	1.07	0.42
	4 / 40		4.64	5.44	1.09	0.52
2.0	2 / 20	1.23	4.42	4.63	1.38	0.39
	3 / 30		4.46	5.03	1.23	0.53
	4 / 40		4.67	5.56	1.10	0.61
3.0	2 / 20	1.23	4.38	4.72	1.43	0.49
	3 / 30		4.60	5.40	1.10	0.61
	4 / 40		4.83	6.02	1.06	0.68

4.4. Effect of the distribution types

Next, we alter the distribution types and use a normal distribution for both the load and the material strength. We perform this study for the base case membranes and additionally with varied pre-stress levels. As in the base case, we retain $E[M]$, $c.o.v.[M]$ and $c.o.v.[L]$ but choose $E[L]$ such that we receive the same characteristic load l_k as for the Gumbel distribution. Hence, the non-linearity measures are the same as in Section 4.3. Since the probabilistic setup is modified, γ_M is different compared to the base case. For the present setup, $\gamma_M = 0.95$ is sufficient to satisfy β_{TRG} in the linear case ($y_0 = 0$ and $\kappa = 1$). The results are summarized in Table 3 and show significant differences to the results with the initial distributions (cf. Table 2). In case of design option (a) all designs are non-conservative and we observe that the reliability index decreases when the pre-stress is increased. In contrast, all designs are conservative if option (b) is used. However, the reliability indices for option (b) are lower as for Gumbel/log-normal distributions and show less variation for the different membrane heights and pre-stress levels.

Table 3: Reliability indices β and non-linearity measures in case of normally distributed load and material strength designed according to design options (a) and (b). Non-conservative/conservative designs are indicated by orange/green color.

height [m]	setup p [kN/m] / P [kN]	γ_M	reliability index β		non-linearity measure	
			option (a)	option (b)	κ	y_0
1.0	2 / 20	0.95	3.95	4.50	0.97	0.28
	3 / 30		3.85	4.56	1.07	0.42
	4 / 40		3.65	4.60	1.09	0.52
2.0	2 / 20	0.95	4.15	4.43	1.38	0.39
	3 / 30		3.77	4.60	1.23	0.53
	4 / 40		3.38	4.60	1.10	0.61
3.0	2 / 20	0.95	4.07	4.57	1.43	0.49
	3 / 30		3.39	4.60	1.10	0.61
	4 / 40		3.08	4.57	1.06	0.68

Membrane architecture: the seventh established building material. Designing reliable and sustainable structures for the urban environment.

4.5. Effect of the uncertainty of material strength and load

To study the influence of the uncertainty of load and material, we alter the coefficient of variation of the material strength among 0.05, 0.1 and 0.15 and the coefficient of variation of the load among 0.1, 0.3 and 0.5. Please note that for each combination of the coefficients of variation an individual value of γ_M must be computed to satisfy β_{TRG} in the linear case ($y_0 = 0$ and $\kappa = 1$). Furthermore, the non-linearity measures differ for varying $c.o.v.[L]$. The results in Table 4 indicate that conservative designs are achieved in all cases except for those which are designed with option (a) and $c.o.v.[L] = 0.1$. For equal values of $c.o.v.[M]$ we observe in case of option (a) increasing reliability indices when $c.o.v.[L]$ is increased. For option (b), we can observe an opposite trend. In case of equal values of $c.o.v.[L]$ the reliability indices decrease if $c.o.v.[M]$ is increased. This observation applies to both design options.

Table 4: Reliability indices β and non-linearity measures in case of different coefficients of variations (c.o.v.) of load and material strength designed according to design options (a) and (b). The table contains results of the base case (bold). Non-conservative/conservative designs are indicated by orange/green color.

height [m]	setup			reliability index β		non-linearity measure	
	$c.o.v.[M]$	$c.o.v.[L]$	γ_M	option (a)	option (b)	κ	y_0
2.0	0.05	0.1	0.94	4.02	5.86	1.11	0.62
	0.05	0.3	1.26	4.51	5.13	1.23	0.53
	0.05	0.5	1.45	4.56	4.90	1.36	0.46
	0.1	0.1	0.93	3.53	5.26	1.11	0.62
	0.1	0.3	1.23	4.46	5.03	1.23	0.53
	0.1	0.5	1.39	4.50	4.82	1.36	0.46
	0.15	0.1	0.97	3.27	4.63	1.11	0.62
	0.15	0.3	1.22	4.39	4.91	1.23	0.53
	0.15	0.5	1.38	4.44	4.73	1.36	0.46

4.6. Summary and discussion of the parameter study

The parameter study shows that the reliability of membranes is strongly affected by both structural and probabilistic properties. Overall, we can see that all membrane designs with option (b) are conservative and in some cases strongly over-designed (e.g., the membranes with high pre-stress levels in Table 2). In case of option (a) in some cases non-conservative designs can be identified (e.g., cases on basis of normal distributions of load and material, see Table 3).

For design situations with Gumbel/log-normal distributions, we observe the trend that for increasing y_0 and decreasing κ , the reliability index for designs based on option (a) and (b) is increasing. In case of the hyper this behaviour of the non-linearity measure is achieved by either increasing the structural height or the pre-stress. However, the described trend is completely reversed if normal distributions are applied for load and material (cf. Table 3). Please note, the usage of Gumbel/log-normal distributions for load/material is more common and often more realistic in practical situations. The degree of uncertainty of load and material strongly also influences the reliability. For the combination of low coefficients of variation of load and material even non-conservative designs are achieved for option (a).

Some of the examined cases share the same side conditions (characteristic values, partial factors and probabilistic settings) as used in our general parameter study which is conducted with artificial bi-linear and quadratic t_S -functions (Teichgräber et al., 2023). For equal values of κ and y_0 , we observe good agreement between the findings and results of the survey at hand and those of the general parameter study. For instance, the observed relative difference of the

Membrane architecture: the seventh established building material. Designing reliable and sustainable structures for the urban environment.

reliability index based on the hypar and a quadratic ts -function with equal κ and y_0 is on average 1.6 % and maximal 7.9 %. This shows on the one hand the validity of the general parameter study for real-world structural models and on the other hand the suitability of the non-linearity measure for the hypar at hand.

5. Conclusion and outlook

The parameter study revealed the complexity of designing non-linear structures as membranes with the semi-probabilistic partial safety factor concept. A main reason for the complexity is that not only the degree of non-linearity of the structural response is crucial. In addition, the interaction with probabilistic properties (distribution types and parameters) also influences the reliability to a large extent. Hence, it is not possible to predict if conservative or non-conservative designs are achieved for a certain design option solely by characterizing with the non-linearity measures κ and y_0 or categories like over- and under-linear. However, the non-linearity measure could be used to define ranges of κ and y_0 in connection with pre-defined probabilistic settings which are common for membrane structures. Based on the ranges, recommendations could be made which design option is to be preferred for which measure of non-linearity. Thereby unnecessary over-design can be avoided in cases where both design options are conservative. A possibility to partly homogenize the reliability level could be to introduce an additional partial factor depending on the degree of non-linearity of the structural response. The results of the presented parameter study are based on a specific membrane structure (hypar). A target-oriented expansion is therefore the inclusion of other basic membrane shapes as those defined by (Knippers, Cremers, Gabler, & Lienhard, 2011). Other future research directions can be investigations in case of multiple load cases and uncertain pre-stress.

References

- Au, S.-K., & Beck, J. L. (2001). Estimation of small failure probabilities in high dimensions by subset simulation. *Probabilistic Engineering Mechanics*, 16(4), 263–277.
- Comité Européen de Normalisation (CEN) (2002/2010). *EN 1990: Eurocode: Basis of structural design (EN 1990:2002 + A1:2005 + A1:2005/AC:2010)*. Brussels.
- Comité Européen de Normalisation (CEN) (2021). *Design of tensioned membrane structures (prCEN/TS 19102:2021-04): (unpublished draft, publication expected 2022)*. Brussels.
- Fußeder, M., Teichgräber, M., Bletzinger, K., Straub, D., & Goldbach, A. (2021). Investigations on the design of membrane structures with the semi-probabilistic safety concept. In *10th edition of the conference on Textile Composites and Inflatable Structures*. CIMNE.
- Gosling, P. D., Bridgens, B. N., & Zhang, L. (2013). Adoption of a reliability approach for membrane structure analysis. *Structural Safety*, 40, 39–50.
- Knippers, J., Cremers, J., Gabler, M., & Lienhard, J. (2011). *Construction Manual for Polymers + Membranes: Materials / Semi-finished Products / Form Finding / Design*. München: Birkhäuser.
- Köhler, J., Sørensen, J. D., & Baravalle, M. (2019). Calibration of existing semi-probabilistic design codes. In *Proceedings of the 13th International Conference on Applications of Statistics and Probability in Civil Engineering, ICASP 2019*. Seoul National University.

Membrane architecture: the seventh established building material. Designing reliable and sustainable structures for the urban environment.

- Rackwitz, R., & Fiessler, B. (1978). Structural reliability under combined random load sequences. *Computers & Structures*, 9(5), 489–494, from <http://www.sciencedirect.com/science/article/pii/0045794978900469>.
- Smedt, E. de, Mollaert, M., Caspeelee, R., Botte, W., & Pyl, L. (2020a). Reliability-based calibration of partial factors for the design of membrane structures. *Engineering Structures*, 214, 110632.
- Smedt, E. de, Mollaert, M., Pyl, L., Gosling, P., Uhlemann, J., & Thomas, J.-C. (2017). *ROUND ROBIN Exercise 4: Reliability analysis of a simple membrane structure: a hyperbolic paraboloid*.
- Smedt, E. de, Mollaert, M., van Craenenbroeck, M., Caspeelee, R., & Pyl, L. (2020b). Reliability-based analysis of a cable-net structure and membrane structure designed using partial factors. *Architectural Engineering and Design Management*, 1–10.
- Teichgräber, M., Fußeder, M., Bletzinger, K.-U., & Straub, D. (2023). Non-linear structural models and the partial safety factor concept. *Structural Safety*, 103, 102341.
- Zhang, Y., Lu, Y., Zhou, Y., & Zhang, Q. (2018). Resistance uncertainty and structural reliability of hypar tensioned membrane structures with PVC coated polyesters. *Thin-Walled Structures*, 124, 392–401.



tensinantes2023 : TensiNet Symposium 2023 at Nantes Université

Membrane architecture: the seventh established building material. Designing reliable and sustainable structures for the urban environment.

Proceedings of the Tensinet Symposium 2023

TENSINANTES2023 | 7-9 June 2023, Nantes Université, Nantes, France

Jean-Christophe Thomas, Marijke Mollaert, Carol Monticelli, Bernd Stimpfle (Eds.)

Characterization of polyethylene structure membrane

Sherryl Anne PATTON

Intertape Polymer Group
50 Abbey Avenue, Truro, Nova Scotia, Canada
spatton@itape.com

Abstract

Polyethylene structure membrane has been used for more than 20 years to cover steel and aluminum framed buildings. These membranes can withstand high loads of wind, snow, and rain yet they are an unknown material in the world of tensile structures. To raise the awareness of polyethylene membranes they need to be characterized for their physical attributes, durability, recyclability, and other qualities. This characterization must be done according to some standards that only exist for PVC coated polyester fabrics. These standards have classes based on weight and strength. The results of the characterization and comparison to the PVC standards show polyethylene structure membranes that can meet or exceed the strength of material that is significantly heavier. The density of polyethylene is 35% less than PVC resulting in a lightweight material, but the manufacturing process used in the formation of the slit tapes for the scrim gives the material its high strength. From a physical strength perspective this study shows that polyethylene membranes can be a participant in the tensile structure arena. The classification system of structure membranes should not be limited to materials of specific weight but rather to strength and performance.

Keywords: polyethylene, structural membrane, performance, sustainability, alternative, lightweight, Cradle to Cradle.

1. Introduction

Polymers of many types are used extensively in our lives today. A few of the applications that come to mind range from carpets to blankets; from clothing to short-term lumber covers; from polymer lumber to permanent structure membranes. These applications can include a wide variety of polymers, but polyolefins are the group used in the manufacturing processes at Intertape Polymer Group (IPG) in Truro, Nova Scotia. Polyolefins include polypropylene and polyethylene; they are non-polar, non-porous, and inert in nature (Whittington, 1978). Polyolefins are used because they are low cost in processing but have an excellent performance record due to their high modulus, high tensile strength, and high chemical resistance (Miyagawa et al., 2007). Mendes et al. (2003) stated that polyolefins are both economically and commercially important. Of particular interest in this report is the group known as polyethylene having the chemical formula of $\text{CH}_3-(\text{CH}_2)_n-\text{CH}_3$ (Wypych, 2008). This group is divided into two main categories, low density polyethylene (LDPE) and high-density polyethylene (HDPE),

Membrane architecture: the seventh established building material. Designing reliable and sustainable structures for the urban environment.

by a benchmark density of 0.94 g/cm^3 (Wypych, 2008). Polyethylene has particularly good strength properties and is easily stabilized for outdoor exposure (Mendes et al., 2003). Stabilization of the polyethylene limits degradation which occurs during exposure to ultraviolet radiation and heat (Andrady et al., 1998).

The focus of this report is the polyethylene membrane manufactured by IPG that is used as a structure membrane. The structure membrane is used primarily in temporary or permanent steel framed structures. Permanent structures are intended to last more than 15 years to 25 years. This report will characterize polyethylene structure membrane as an alternative for use in tensile structures.

1.1. Introduction to manufacturing process

High density polyethylene (HDPE) resin pellets are used to produce the woven scrim substrate. The plastic pellets are melted in an extruder and extruded in a cast, or thin sheet then slit into narrow strips called slit tape. At this point, the molecules in the polymer are like a plate of spaghetti noodles. They are long but very randomly aligned. Because of this randomness the slit tapes are very stretchy and have low strength. The tapes are put through a process involving orientation and annealing which heats and stretches them in a very controlled manner. The molecules are aligned, and the tape becomes narrower and strong. The tapes are wound on spools for beaming and weaving. After weaving the substrate, also called scrim, is extrusion coated with molten polyethylene being applied to both sides. Figure 1. shows an example of the scrim and extrusion coatings.

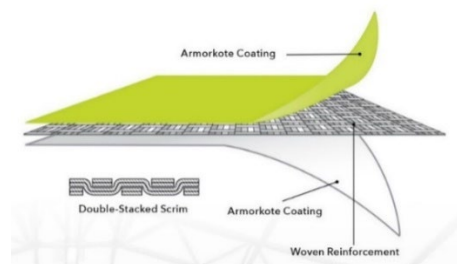


Figure 1: Diagrammatic representation of patented weave, courtesy of IPG.

The polyethylene structure membrane is a balanced weave. That is the warp and weft tapes have the same properties in denier and breaking strength; however, the resulting membrane is anisotropic because in the weaving process the warp tapes are in tension while the weft tape travels further to go over and under the warp tapes. Also, the warp direction is held in tension during the coating process while the weft direction is not. This results in a membrane that is usually stronger in the warp direction than it is in the weft direction.

1.2. Introduction to steel framed buildings

Briefly, the two main types of steel framed buildings are mono cover and Keder style. The one piece mono cover can be a smaller structure like the hoop frame shown on the left in Figure 2. This has the cover constructed as a single unit and pulled over the frame in the lengthwise direction of the building. This style of building is very inexpensive and of a more temporary nature. The Keder style of building, such as the one on the right in Figure 2. is constructed by pulling panels from one side of the building to the other through Keder extrusions then covering the Keder extrusion with a flap to make them completely waterproof. The Keder extrusion is

Membrane architecture: the seventh established building material. Designing reliable and sustainable structures for the urban environment.

on every truss. These buildings have a permanent foundation and are much larger with a clear span interior easily 100 metres wide.



Figure 2: On the left an example of a single cover steel framed building, photo courtesy of Les Industries Harnois. On the right an example of Keder style membrane buildings, photo courtesy of Norseman Group Ltd.

There are four basic designs of the steel framed membrane structure commonly in use today: Single Truss, Double Truss, I-Beam Sidewall, and Plate Girder. The Single truss building has trusses supporting the covering membrane that are only constructed of a single pipe following the curvature of the structure. See Figure 3. for an example of the single truss building style.



Figure 3: On the left an example of Single Truss building style, photo courtesy of Norseman Group Ltd. On the right an example of Double Truss building style, photo courtesy of GNB Global.

The double truss has two arches joined by steel webbing that follow the curvature of the membrane structure. The depth of the truss can change depending on the width and height of the structure. The trusses, whether they are single or double trusses are joined together with purlins. See Figure 3, on the right, for an example of the double truss style of structure.

The I-beam sidewall has a double truss roof structure, but I-beams are the supporting sidewalls, see Figure 4. The I-beams are so named because the beam is in the shape of an upper case I. This style gives a straight sidewall instead of a curvature that starts at the ground. It can still use membrane on the sidewall, rather than having wood or concrete sidewalls.



Figure 4: On the right is the I-beam Sidewall style, photo courtesy of Norseman Group Ltd. On the left is the Plate Girder style, photo courtesy of Accu-Steel.

Membrane architecture: the seventh established building material. Designing reliable and sustainable structures for the urban environment.

Like the I-beam sidewall is the Plate Girder style, see Figure 4. The plate girder is an I-beam with web plates, flanges, and stiffeners. According to www.structuralguide.com (2021) the plate girder can be used when high loads are anticipated, and they have a high degree of stability. The appearance of the plate girder is not the typical light membrane structure but more closely resembles a conventional metal building. The cover in Figure 4 is also a Keder cover with Keders on every plate girder steel member.

Polyethylene membranes have been used in the structures described above for over 20 years. The largest structures currently being constructed in these styles are 108 m wide and 220 m long. These are clear span structures.

2. Characterization of polyethylene membranes

2.1. Durability

The durability of structure membranes is important to understand. Permanent membrane structures are erected with the intention of more than ten years of service; however, during those years of service the polymer membrane is exposed to natural weathering such as heat and ultraviolet (UV) radiation. If polymer degradation can be understood, it may be possible to predict the lifetime of the building components made from polymeric resins and replacement protocol can be established (Khan and Hamid, 1995). The study of the “aging” process of polymers was important according to Tavares et al. (2003) because it can assist with the forecasting of the life span of the polymer.

The degradation noted by Andrady et al. (1998) ranges from surface discolouration, which affects the aesthetic appeal, to the loss of mechanical properties, which can seriously limit the performance. Mendes et al. (2003) concluded degradation can be on the molecular level affecting the crystallinity of the polymer chain leading to embrittlement and consequent loss of the property of elongation or ductility. Incorporating additives such as antioxidants and UV inhibitors during the manufacturing process can give heat and light stability to the polymers.

It has been suggested previously that understanding the degradation of polymers, and the rate of degradation, is beneficial to predict lifetimes and therefore replacement times of structure membranes. Intuitively the best way to study this would be in situ; however, this could mean waiting years to get results. To save time tests have been designed which accelerates the effects of weathering and most degradation studies are done in this manner.

A machine produced by Q-Panel Lab Products, known as a QUV machine, can be used for accelerated laboratory exposure. The QUV machine has two banks of fluorescent tubes that emit ultraviolet radiation at wavelength 340 nm and at a specified irradiance set point. The temperature and moisture levels are also controlled in this machine.

The machine operation and sample exposure are conducted following ASTM G154, “Standard practice for operating fluorescent light apparatus for UV exposure of nonmetallic materials”, and G151, “Standard practice for exposing nonmetallic materials in accelerated test devices that use laboratory light sources”. The exposure conditions are eight hours of UV at 60°C; four hours condensation at 50°C. The irradiance level of UV light setpoint is 1.35 W/m²/nm. The samples are rotated through the machine regularly during the exposure to ensure that each specimen receives an equal amount of radiation and that replicates are treated equally.

Membrane architecture: the seventh established building material. Designing reliable and sustainable structures for the urban environment.

Specimens are pulled from the QUV machine every 1000 hours. The exposed areas are examined for microscopic evidence of surface changes from degradation, crazing or cracking in the coating. The specimens are assessed for colour and gloss at the 1000 hour intervals as well. Finally, the specimens are assessed for physical strength by the strip tensile method ASTM D4851. According to the Canadian Building Code which adopted CAN/ULC S367 “Air-, Cable- and Frame-supported Membrane Structures” in 2009, this test is completed at 1000 hours and 4000 hours. Additionally, trapezoidal testing according to ASTM D4533 is conducted at the same exposure intervals. The exposed tests are compared to the strength of the retained samples to determine the percent retained strength.

Equation. 1. shows that retained strength can be expressed as:

$$\text{Retained Strength (\%)} = ((\text{Force}_o - \text{Force}_s) / \text{Force}_o) * 100 \quad (1)$$

Where Force_o is the strip tensile strength (or trapezoidal tear strength) of the base fabric
And Force_s is the strip tensile strength (or trapezoidal tear strength) of the exposed specimen.

2.2. Light transmission/translucency

Polyethylene structure membrane is a translucent material allowing a certain amount of light to pass through. Three interactions can take place; the light can be absorbed, transmitted, or reflected.

There are three main types of light in solar radiation: ultraviolet (UV) from 200 to 400 nm, Visible from 400 to 740 nm, and near infrared (NIR) from 740 nm and higher. Instrumentation can measure the spectral reflectance and transmission and the absorptance is calculated from Kirchhoff's Relationship shown in Equation. 2. where:

$$\rho + \alpha + \tau = 1 \quad (2)$$

The method used for this is ASTM E903 “Standard Test Method for Solar Absorptance, Reflectance, and Transmittance of Materials Using Integrating Spheres”. In this way we can determine the UV light, visible light, and NIR light that is either transmitted, reflected, or absorbed by the structure membrane. Because the polyethylene structure membrane is coated white on at least one side, if not both, no UV radiation passes through. It is blocked by the titanium dioxide (TiO_2) in the white coating.

The typical values of outdoor light levels in a moderate climate are given by Bögner-Balz (2019):

Illuminance -	Sunny summer day 100,000 Lux
	Cloudy summer day 20,000 Lux
	Cloudy winter day 3,000 – 5,000 Lux

These values are measured without any object or material between the sun and the measuring device. The values from ASTM E903 can be used to calculate the illuminance inside a single layer membrane building with the Equation. 3:

$$T_m = \frac{T_l}{1-r_l} \quad (3)$$

Membrane architecture: the seventh established building material. Designing reliable and sustainable structures for the urban environment.

Where T_m is the illuminance in the structure, T_1 is the transmittance of the membrane and r_1 is the reflectance of the membrane. The calculated T_m is the transmittance as it would be on a sunny day. In general, on a cloudy summer day the illuminance would be reduced by five times and a cloudy winter day it would be reduced by twenty times (Bögner-Balz, 2019). Table 1 lists the recommended light levels in various work areas according to Engineering Tool Box, 2004.

Table 1: Recommended light levels for various work areas (www.engineeringtoolbox.com, 2004).

ACTIVITY	ILLUMINANCE (Lux)
Warehouses, homes, theaters	150
Coffee break room, waiting rooms	200
Normal office work, auditoriums	500
Normal drawing work	1000
Detailed drawing work	1500-2000
Performance of very prolonged and exacting visual tasks	5000-20000

3. Welding

Polyethylene membranes can be heat welded using hot air or hot wedge welding equipment. Due to its inert nature, it cannot be welded using high frequency or RF welding. Most panel welding is done with hot air floor crawling machines. A panel weld is formed by overlapping two layers of membrane and inserting the nozzle, blowing hot air, between the layers. The typical weld width is 44 mm. The proper setpoint of temperature and speed is determined through experimenting with these variables and assessing the resulting welds for seam peel and seam shear. The setpoints on one machine can be a starting point; however, every machine is different depending on manufacturer and age. Other machine settings that can sometimes be adjusted are the nip pressure and/or the air velocity. The hot air floor crawlers are operated by nipping the membrane at the point the hot air is applied between a nip roller and the floor, so weights are applied to the top of the machine. Wedge welders are nipped at the point the hot wedge is applied between two nip rollers. The pressure can be adjusted between the two nip rollers on these types of welding machines.

In the process of finding ideal welding conditions, it is better to slow the machine down over increasing the temperature of the hot air. The dwell time is increased when the speed is reduced, and the coating of the membrane is given time to melt. When the temperature is simply increased the reinforcing base fabric is more likely to shrink or deform. If the reinforcing base fabric shrinks it can form puckers or distortion in the product. Distortions should be kept to a minimum. The more distorted the fabric becomes the less likely those distortions will be pulled out in the tensioning process during installation. Of greater concern is the reduction of strength of the base fabric if it is damaged by excessive heat during the welding process.

4. Weight – transportation and installation

The strength to weight ratio of polyethylene structure membrane is one of its most striking characteristics. The basis weight of the NovaShield™ FR Plus membranes is 407 gsm and yet the tensile strength of the membrane is approximately 45 kN/m. This weight has a huge consideration in the cost of transportation and the ease of installation. Large panels can be

Membrane architecture: the seventh established building material. Designing reliable and sustainable structures for the urban environment.

manipulated by labour in many cases. Not only is the weight to tensile strength ratio high the polyethylene membranes also have high tear strengths, exceeding 0.44 kN force much of the time.

5. Environmental considerations

The environment is such an important consideration. Sustainability is a huge focus of manufacturing companies in these recent years and in particular manufacturers of plastic which polyethylene structure membrane is. There have been many bans on plastics, especially single use plastics. Structure membranes are not single use plastics and indeed are stabilized to last 15 to 20 years, at least. But they are still plastic and as such under scrutiny in the manufacturing process, converting process, and end of life disposal. This type of examination is studying the circularity of a product, the entire life of a product from the birth to the grave. There are many study groups around the world and the one I will describe here is Cradle to Cradle Products Innovation Institute. This institute is a global entity with science based methods for evaluating products for their safety, circularity, and responsible manufacture with certification available.

5.1 Cradle to Cradle Certification

Cradle to Cradle certification, also called C2C certification, can be obtained after a product has been evaluated based on five categories. These five categories are: material health, material reuse, renewable energy and carbon management, water stewardship, and social fairness. Once assessed a product is assigned an achievement level for each of the categories. The lowest level achieved in any one of the categories is the level assigned to that product. The achievement levels are Basic, Bronze, Silver, Gold, and Platinum. A product requires certification renewal every two years showing continuous improvement. A description of the five categories (Cradle to Cradle Certified™ Products Program, 2021) follows:

The first of the five categories is Material Health. The chemicals used to manufacture a product are examined by a team of scientists to rate them on their safety for human and environmental contact. Assessment bodies accredited by the program will contact the suppliers as a confidential third party and evaluate all the raw materials that go into the constituent parts.

The second category is Material Reutilization. This is the rating on recyclability and is concerned with post-consumer recycled content (PCR) and post-industrial recycled content (PIR).

Thirdly the products are evaluated on Renewable Energy and Carbon Management. The assessment bodies look at the energy required to manufacture the product. The effort is to focus the manufacturer on using renewable energy rather than fossil fuels to reduce, or even eliminate, the production of greenhouse gases.

The fourth category is Water Stewardship. Water is a valuable resource and cannot be treated in a wasteful manner. Water is required in manufacturing processes but through upgraded equipment and state of the art chillers and reclaimers the amount needed can be significantly reduced.

Lastly, Social Fairness is considered. People are a part of manufacturing. A safe working environment is required, and a living wage is necessary.

Membrane architecture: the seventh established building material. Designing reliable and sustainable structures for the urban environment.

The NovaShield™ polyethylene structure membrane has a **Bronze** overall achievement level.

6. Membrane performance

The following tables contain the data for NovaShield™ FR Plus polyethylene structure membrane according to existing performance criteria.

Table 2: Elastic Moduli independent of stress ratio combination, courtesy of DEKRA, Stuttgart, DE

Elastic Moduli		Warp to weft stress ratio combination					
		1:1 2:1	1:1 1:2	1:1 1:0	1:1 0:1	2:1 1:0	1:2 0:1
Warp	kN/m	268	267	288	267	285	267
Fill	kN/m	282	315	273	312	262	313
Poisson Ratio warp and fill		0.15	0.10	0.12	0.10	0.08	0.11
Poisson Ratio fill and warp		0.15	0.09	0.12	0.09	0.09	0.10

Table 3: Characterization to DIN 18204-1 “Component for enclosures made of textile fabrics and plastic films – Part 1: Structures and tents. Requirements and performance classes and NovaShield™ FR Plus, courtesy of DEKRA, Stuttgart, DE:

Row	Parameter	Standard	Textile Fabrics			
			Class Z 1	Class Z 2	Class Z 3	NovaShield™ FR Plus
1	Carrier fabric	DIN EN ISO 2076	Polyester (PES)			HDPE
2	Coating	-	Soft polyvinyl chloride (soft PVC)			LDPE
3	Total area-related mass; g/m ²	DIN EN ISO 2286-2	≥ 450	≥ 580	≥ 650	407
4	Tensile strength; kN/5 cm; Warp/Weft	DIN EN ISO 1421, procedure 1	2.0 / 1.6	2.5 / 2.5	3.0 / 3.0	2.3/2.2
5a	Elongation at break,%		≥ 15 / ≥ 15			22/18
5b	maximum elongation at 10% of the tensile force according to line 4; %; Warp/Weft		≤ 2 / ≤ 6			1.5/1.2
6	Tear propagation resistance; kN; Warp/Weft	DIN EN 1875-3	0.1 / 0.1	0.13 / 0.13	0.2 / 0.2	0.5/0.4
7	Adhesive strength ^a N/5 cm	DIN EN 15619: 2014-07, Appendix B	100	100	100	80

Membrane architecture: the seventh established building material. Designing reliable and sustainable structures for the urban environment.

8a	Weld strength ^a ; b ^b 15 mm - <40 mm; kN/5 cm; Warp/Weft		DIN EN ISO 1421, procedure 1	at 23 ° C: min. 70% of the tensile strength according to line 4 at 70 ° C: min. 40% of the tensile strength according to line 4	23°C: 85% 70°C: 70%
8b	Weld strength ^a ; b ^b ≥ 40 mm; kN/5 cm; Warp/Weft			at 23 ° C: min. 80% of the tensile strength according to line 4 at 70 ° C: min. 60% of the tensile strength according to line 4	23°C: 85% 70°C: 70%
9a	Strength ^a f _{Ku} of the Keder connections; kN/5 cm	∅ 8 mm	DIN EN ISO 1421, procedure 1	at 23 ° C: 0.8 at 70 ° C: 0.30	TBD
9b		∅ 10 mm		at 23 ° C: 1.0 at 70 ° C: 0.60	TBD
9c		∅ 12 mm		at 23 ° C: 1.2 at 70 ° C: 0.80	TBD
a each individual value, at least					
b weld width					
The limit deviations of the test temperatures are ± 2 K.					

Table 4: Fire Classification DIN EN 13501

	NovaShield™ FR Plus
Fire Behaviour	B
Smoke Production	s1
Flaming Droplets	d0

Table 5: QUV testing for durability.

Specimen Code	FRU88X-6 4mil (Various Colour Combinations)			
	Warp		Weft	
	Average	Standard Deviation	Average	Standard Deviation
Retained Tensile Strength (%) 1000 hours	97	4.0	98	3.7
Retained Tensile Strength (%) 4000 hours	100	6.6	102	5.4
Retained Trapezoidal Tear (%) 1000 hours	104	9.3	104	11.4
Retained Trapezoidal Tear (%) 4000 hours	109	9.0	112	10.8

Table 6: Hemispherical Spectral Reflectance and Near Normal/Hemispherical Spectral Transmittance as evaluated by ASTM E903.

	% Reflectance			% Transmittance		
	UV	VIS	NIR	UV	VIS	NIR
White/white	12.2	90.7	80.2	0.0	6.4	11.5
Sandstone/white	10.6	64.8	75.3	0.0	2.7	9.3

·
Illuminance
Inside a single layer
of membrane NovaShield™ FR Plus

White/White 69,000 Lux
Sandstone/White 7,000 Lux

Membrane architecture: the seventh established building material. Designing reliable and sustainable structures for the urban environment.

7. Discussion

The purpose of this paper was to characterize the inherent nature and physical attributes of polyethylene membranes, show the history of their use in steel framed structures, and provide information for their use in tensile structures. This material has been used in covers for over 20 years, primarily in steel framed structures. The history is strong and world-wide having been used in Canada, United States, Mexico, Europe, China, Australia, and Israel, to name a few of the countries with polyethylene covered structures.

Structures covered with white coated polyethylene membranes are an extremely comfortable environment. The translucency of the material provides a well-lit interior. The membrane diffuses the light which means there are no shadows, nor are there bright and/or dim areas.

This polyethylene membrane has UV inhibitors added to the base fabric and coating to protect it from the degradative effects of the sun's radiation. Extensive testing has been performed on this membrane using accelerated weathering equipment. Real life data have been collected from structure covers that have been returned when new covers have been installed. Membranes that were exposed to weather and in use for 17 years maintained more than 90% tensile strength. Because of these data the life expectancy of the NovaShield™ non-FR and FR Plus is more than 15 years and the NovaShield™ FRU ELITE is more than 20 years.

Polyethylene is inert in nature and does not require the use of plasticizers for processing. Therefore, dirt and debris does not stick to membranes made of polyethylene and they are easily cleaned. Plasticizers can bloom to the surface and result in a surface that dirt will adhere to. Polyethylene does not provide a surface upon which micro-organisms will grow.

Polyethylene is combustible but can be fire retardant. The fire retardancy properties allow for the material to self-extinguish as it remains in contact with fire. This ability is to allow anyone in the building time to escape from the building. However, in real-life fire situations even the non-flame retardant covers have shown excellent performance by melting away from the heat of the fire.

Polyethylene is recyclable, and recycled polyethylene is used in many products. Polyethylene membranes are mixed with HDPE scrim covered with LDPE extrusion coating on both sides. This does limit the uses for the recycled material, but it is still in demand for many processes such as composite building materials and other industrial type products. IPG recycles the material by grinding the membrane material, re-processing it into pellet form and using it in the scrim or coating of material with less stringent property requirements, also plastic cores on which we wind finished and in-process material.

Certain polyethylene structure membranes are certified as being manufactured in a safe, circular, and responsible way, both considering the environment health and human health. This is a key factor to consider as people are becoming increasingly aware of the need for sustainable manufacturing processes. The material health category, as described in section 5.1, is separating materials into two groups; those that are safe for humans and the environment and those that are not safe for humans and the environment. The chemicals used in their manufacturing processes are evaluated and the rating is based on those chemicals. A list of banned chemicals has been established and is used in the evaluation of materials.

Membrane architecture: the seventh established building material. Designing reliable and sustainable structures for the urban environment.

Polyethylene membranes are half the weight of many structural membranes being approximately 400 gsm yet comparable in strength to membranes that weigh 700 to 900 gsm. This is a great benefit when thinking about the entire process of covering a structure. The membrane is lighter to handle in the converting process and bundling panels for transport. The transportation costs are lower than for heavier materials. Lifting the panels into place can use lighter equipment, this does depend on the size of the panel or cover, of course.

Polyethylene membrane is very easily welded using either hot air or hot wedge. This makes the welding process very speedy compared to high frequency welding or bar welding. In addition, there are no fumes or odours released during the welding, regardless of whether the material is flame retardant or non-flame retardant. Because of the high speed and the floor crawling welders that can be used the membrane is very well suited to long straight seams.

Polyethylene membranes have been used for more than 20 years withstanding storms of high winds, heavy rains, and snow loads. They are a lightweight, cost-effective alternative solution for membrane structures with their high tensile strength and excellent resistance to tearing. Table 4 shows one of several polyethylene membranes compared to classes of PVC coated polyester scrim. The tensile and tear strength meets or exceeds Class Z1 but the weight is less. A lighter weight is an advantage in handling, shipping, and installing, not a disadvantage. The density of polyethylene is approximately 35% lower than that of PVC coated polyester, with polyethylene density 0.94 g/cm³ and PVC density 1.4 g/cm³.

References

Andrady, A. L.; Hamid, S. H.; Hu, X.; Torikai, A. 1998. Effects of increased solar ultraviolet radiation on materials. *Journal of Photochemistry and Photobiology* 46: 96-103.

Bogner-Balz, H. 2019. *Lecture Notes: Materials – Mechanical and Physical Properties*. IMS Bauhaus.

Cradle to Cradle Certified™ Products Program, (2021) What Is Cradle to Cradle Certified™?. [online] Available at: <https://www.c2ccertified.org/get-certified/product-certification> [Accessed 30/01/2021].

Engineering ToolBox, (2004). Illuminance - Recommended Light Level. [online] Available at: https://www.engineeringtoolbox.com/light-level-rooms-d_708.html [Accessed 20/01/2021].

DEKRA Report on Biaxial Test and Young's Modulus determination of a PE coated HDPE fibre fabric, type FRU88X-6 400. 13/11/2020. DEKRA Automobil GmbH Laboratory for Technical Textiles and Films.

Khan, J. H.; Hamid, S. H. 1995. Durability of HALS stabilized polyethylene film in a greenhouse environment. *Journal of Polymer Degradation and Stability* 48: 137-142.

Mendes, L.C.; Rufino, E. S.; de Paula, F. O. C.; Torres Jr., A. C. 2003. Mechanical, thermal and microstructure evaluation of HDPE after weathering in Rio de Janeiro City. *Journal of Polymer Degradation and Stability* 79: 371-383.

Membrane architecture: the seventh established building material. Designing reliable and sustainable structures for the urban environment.

Miyagawa, E.; Tokumitsu, K.; Tanaka, A.; Nitta, K. 2007. Mechanical property and molecular weight distribution changes with photo- and chemical-degradation on LDPE films. *Journal of Polymer Degradation and Stability* 92: 1948-1956.

Structural Guide © 2021. Design: Plate Girder. [online] Available at: <https://www.structuralguide.com> [Accessed 29/01/2021].

Tavares, A. C.; Gulmine, J. V.; Lepienski, C. M.; Akcelrud, L. 2003. The effect of accelerated aging on the surface mechanical properties of polyethylene. *Journal of Polymer Degradation and Stability* 81: 367-373.

Tanaka, Yohei & Matsuo, Kiyoshi. (2011). Non-Thermal Effects of Near-Infrared Irradiation on Melanoma. 10.5772/38663.

Whittington, L. R. 1978. *Whittington's Dictionary of Plastics*. 2nd ed. Technomic Publishing Co, Lancaster, PA.

Wypych, G. 2008 *Handbook of Material Weathering*. 4th ed. ChemTec Publishing, Toronto, ON.



tensinantes2023 : TensiNet Symposium 2023 at Nantes Université

Membrane architecture: the seventh established building material. Designing reliable and sustainable structures for the urban environment.

Proceedings of the Tensinet Symposium 2023

TENSINANTES2023 | 7-9 June 2023, Nantes Université, Nantes, France

Jean-Christophe Thomas, Marijke Mollaert, Carol Monticelli, Bernd Stimpfle (Eds.)

Practical application of a stress-ratio dependent adaptive material model in the structural analysis of textile structures

Jörg Uhlemann*, Mehran Motevalli^a, Natalie Stranghöner*, Daniel Balzani^a

*Institute for Metal and Lightweight Structures, University of Duisburg-Essen, D-45117 Essen, Germany, joerg.uhlemann@uni-due.de

^a Chair of Continuum Mechanics, Ruhr-University Bochum, D-44801 Bochum, Germany

Abstract

Shortcomings of linear-elastic modelling for structural textile membranes are well known: their stress-strain behaviour under mono- or biaxial stress states is neither linear nor purely elastic. However, despite the fact that alternatives exist, the linear elastic approach is used in design practice. In this strongly simplified approach, one single set of “fictitious” elastic constants is determined based on several stress-ratio dependent stress-strain paths.

The procedure applied in this paper is based on a development of Motevalli et al. A bespoke set of elastic constants is used for each element, depending on the ratio of stresses in x and y direction of the element. The procedure is iterative. In each iteration step, stress ratios are checked in all elements and the material constants of each element are adjusted with regard to this ratio. In this way, numerous sets of elastic constants are applied. They are evaluated once prior to the structural analysis from a biaxial stiffness test.

This contribution presents how this adaptive procedure can be automated with commercial finite element software, using the example of the software package Sofistik controlled and evaluated by a higher-level Python script. It is shown that the iteration converges fast. Results are discussed compared to a usual linear-elastic approach using one single “best fit” set of fictitious elastic constants.

Keywords: structural analysis, textiles, membranes, linear-elastic, adaptive simulation

1. Introduction

Linear-elastic modelling for structural textile membranes is widely used in design practice, despite the fact that alternatives exist [8] that much better model the nonlinear stress-strain behaviour under mono- or biaxial stress states. In the strongly simplified linear-elastic

Membrane architecture: the seventh established building material. Designing reliable and sustainable structures for the urban environment.

approach, one single set of “fictitious” elastic constants is determined based on several stress-ratio dependent stress-strain paths. To evaluate the stiffness parameters from biaxial test results, usually a best fit approach is applied. The aim is to find the one set of elastic constants, that describes best all measured paths. But oftentimes, this is on cost of poor fits for single paths [1, 2].

Several proposals have been made to overcome the shortcomings of linear elastic modelling while holding the numbers of input parameters small. Minami et al. presented a multi-step approach based on the parameters of the linear elastic formulation with a stepwise use of the constitutive equations [3, 4]. Galliot & Luchsinger developed a nonlinear approach using normalized load ratios [5]. Only two new parameters were introduced to complement the plane stress orthotropic model. Another phenomenological approach is directly relating biaxial stresses to warp and fill strains, e. g. [6]. Although at least the method of Galliot & Luchsinger is implemented in the commercial software package Sofistik, however, up to now these methods are not widespread in practice. Particularly the evaluation of test results poses a challenge for the practice.

The material model [7] picked up here employs multiple sets of parameters of the simple linear-elastic formulation. For different stress ratios, different elastic constants are used. This allows a much better fit quality for each stress-strain path. At the same time the evaluation of recorded test data is simple and the simulation is robust and not computationally expensive. The parameters are elastic moduli and Poisson’s ratios which structural engineers are used to.

In the structural analysis, different materials are defined representing the different sets of elastic constants correlated to different stress ratios. During the analysis, the stress ratio is locally computed for every integration point within each finite element. Based thereon, the set of elastic constants is calculated as appropriate interpolation between those of the fitted stress ratios. Using these locally distributed parameter sets, the finite element analysis is performed. Afterwards, a new analysis is started, and the steps are repeated. This iterative approach is conducted until a predefined termination criterion is met. This procedure allows an easy-to-handle adaptive non-linear numerical simulation, optimizing the quality of the results of the structural analysis. It is referred to as the stress-ratio-dependent method (SRD method) in the following.

This contribution presents how this procedure can be automated with commercial finite element software, using the example of the software package Sofistik, controlled and evaluated by a higher-level Python script. It is shown that the iteration converges fast. Results are compared (i) to a usual linear-elastic approach using one single “best fit” set of fictitious elastic constants as well as (ii) to the nonlinear hyperelastic approach presented in [8]. It can be shown that the accuracy of the new adaptive analysis approach comes close to that of the nonlinear hyperelastic approach.

The SRD method, the practical application of which is demonstrated here, provides an alternative to the approach of Galliot & Luchsinger [5]. Unlike the method presented in [5], it copes with the orthotropic linear elastic material model present in every FE software product. Once sets of elastic constants are evaluated for a material product to be analysed and the programming of such higher-level routine is done for the used software environment, the additional efforts of the structural analysis are small while the accuracy is significantly increased.

Membrane architecture: the seventh established building material. Designing reliable and sustainable structures for the urban environment.

In this adaptive approach, the nonlinear stiffness behaviour of textile membranes can be covered quite well, even their oftentimes huge transverse contraction.

2. Implementation of the adaptive approach using commercial software

For the approach presented here, a higher-level program is required that generates input files, transfers them to the FE software, controls the FE software and reads out and analyses the results after a calculation. Furthermore, the applied FE software has to provide interfaces which enable to read out results from the data base by the higher-level program. Thus, the approach presented here needs advanced programming skills and good knowledge of the used FE software. Provided these skills are available, this method allows a more accurate and reliable analysis of structural textile membranes without huge efforts. Moreover, conventional stiffness parameters are used. That means, the engineer does not have to familiarise himself with new material laws and get used to new stiffness parameters. Well known and well understood elastic constants in the form of two tensile stiffness moduli and two Poisson's ratios are used.

The key difference to a traditional linear elastic analysis is the assignment of optimised stress-ratio dependent elastic constants to each finite element. The basis is therefore to know the resulting stress ratios in each element. This requires a preliminary calculation. It becomes clear that this leads to an iterative process. The iteration is carried out until one or more selected parameters converge, e. g., the deformation at a certain node.

Since the stress ratios are unknown before the initial calculation, it is sufficient to start with a single set of elastic constants that is applied to all elements. Up to this point, there is no difference to a conventional linear-elastic calculation. The initial set of elastic constants can be gained from a biaxial test and evaluation with standardized methods utilizing e. g. EN 17117-1 [1] or a similar procedure. In these methods, one single set of "fictitious" elastic constants is derived as a best fit for several, usually five stress ratios. The well-known disadvantage is that the best fit does not sufficiently fit all evaluated stress ratios.

For the following adaptive assignment of elastic constants during the iterations several sets of elastic constants are used. The recommendation is to determine one set of elastic constants for each tested stress ratio. In this contribution, this approach is further refined by interpolating stiffness moduli between these predefined stress ratios. Another option for refinement of course is to adapt the biaxial test by testing more than the usual five stress ratios. The author's experience is that either way, the refinement is worth it, the analysis results become noticeably better.

The higher-level programme picks up the input file for the finite element software and starts the analysis. Afterwards it reads out relevant results from the FE-model database, i.e. stresses in x and y directions at each integration point within each finite element. From these data the stress ratio σ_x/σ_y is calculated for each element. Based on the stress ratio of each element, a fitting set of elastic constants is evaluated. Subsequently, the input file for a new model is generated in which the set of elastic constants corresponding to the stress ratio is assigned to each element. The new input file is handed over to the finite element software and a new analysis is started.

Membrane architecture: the seventh established building material. Designing reliable and sustainable structures for the urban environment.

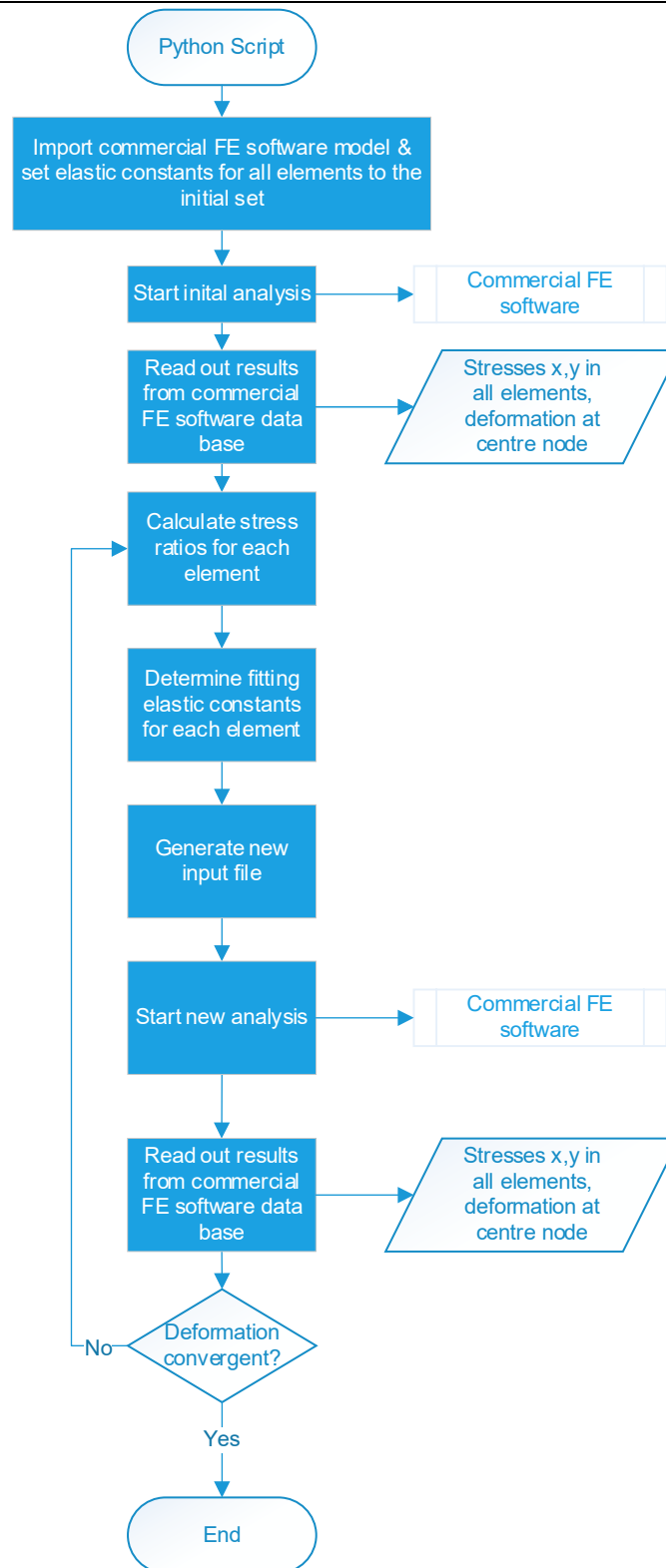


Figure 1: Flow chart for the adaptive structural analysis using a higher-level Python script and a commercial FE software

Membrane architecture: the seventh established building material. Designing reliable and sustainable structures for the urban environment.

For this paper, Python 3.10 [9] is used to set up the higher-level script. Sofistik 2023 [10] is used as commercial finite element software. As more or less every finite element software, Sofistik provides interfaces to read results via multiple programming languages from the database. These are implemented in the Python code [11]. Figure 1 depicts a flow chart for the adaptive structural analysis using a higher-level Python script and Sofistik as FE software.

3. Example analysis and validation

In the example presented here, a simple textile membrane structure is analysed, see Figure 2. The structure is a plane square of 1400 mm x 1400 mm. For reasons of comparison to the analysis in [7], the prestress is set to zero. The external load acting on the structure is a surface load orthogonal to the membrane surface of $p = 7 \text{ kN/m}^2$.

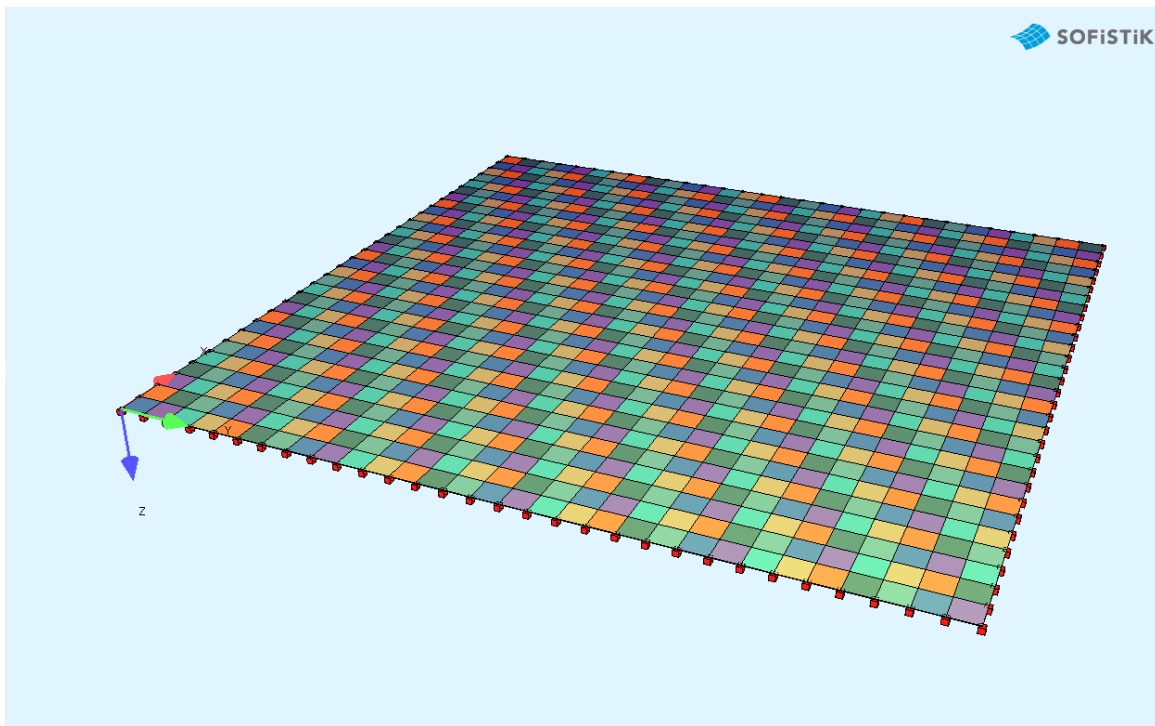


Figure 2: Plane textile membrane structure as example

It is assumed that the membrane material is a PTFE-coated glass fibre fabric with the following “fictitious” elastic constants achieved from a biaxial test according to [12]: $E_x = 1842 \text{ kN/m}$, $E_y = 174 \text{ kN/m}$, $\nu_{xy} = 0,146$ [7]. Using the reciprocal relationship [1], the second Poisson’s ratio can be calculated as $\nu_{yx} = E_x \cdot \nu_{xy} / E_y = 1842 \cdot 0,146 / 174 \cong 1,55$. These values are taken as the initial set of elastic constants assigned to each element. The discussion of the shear modulus is excluded in this contribution. It is assumed to be $G = 60 \text{ kN/m}$ in the example.

The stress and deformation results of the initial analysis using these stiffness values are given in Figures 3 and 4.

Membrane architecture: the seventh established building material. Designing reliable and sustainable structures for the urban environment.

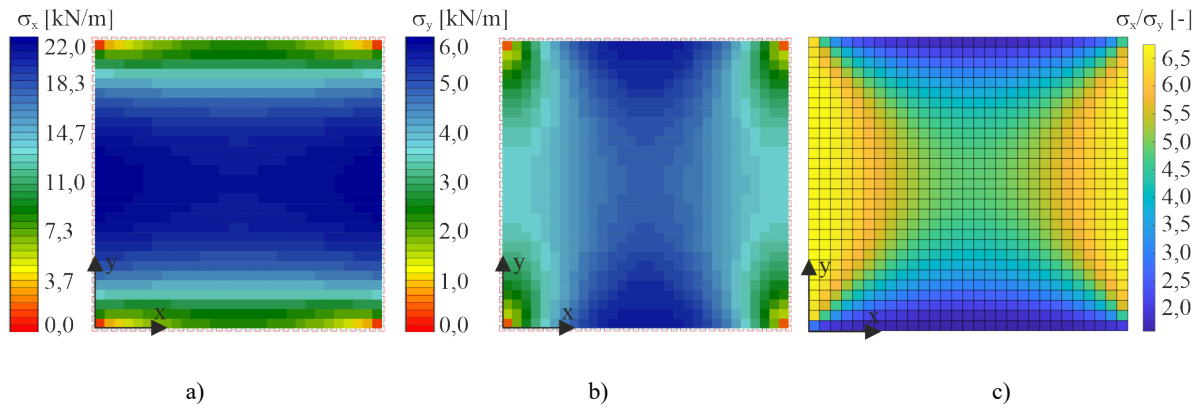


Figure 3: Stress results of the initial analysis: a) stresses in x-direction, b) stresses in y-direction, c) stress ratios x/y

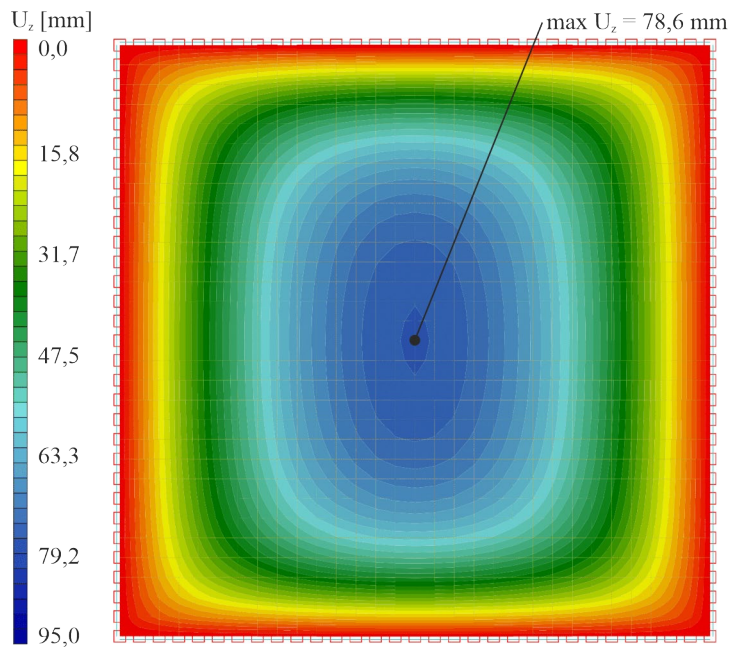


Figure 4: Deformation results in z direction, initial analysis

For the adaptive approach starting with the first iteration, in analogy to [7], nine sets of adaptive elastic constants are used for nine experimental stress ratios. The stress ratios that were tested in separate biaxial tests were: 1:0,125 | 1:0,25 | 1:0,5 | 1:0,75 | 1:1 | 0,75:1 | 0,5:1 | 0,25:1 and 0,125:1. The stiffness values fitted to the measured stress-strain paths of these stress ratios are given in Table 1. Here, Poisson's ratio ν_{yx} is considered a fixed quantity. The value is adopted from the initial sets of constants. Consequently, ν_{xy} is then a dependent quantity to be calculated via the reciprocal relationship. The number for each set of constants is given in Table 1.

In addition, between the nine stress ratios, stiffness moduli E_x and E_y are linear interpolated. During this, the dependent quantity ν_{xy} is adjusted every time. This is handled automatically in the FE software.

Membrane architecture: the seventh established building material. Designing reliable and sustainable structures for the urban environment.

Table 1: Adaptive stiffness values assigned to nine tested stress ratios warp/fill.

Stress ratio Parameter	1:0,125	1:0,25	1:0,5	1:0,75	1:1	0,75:1	0,5:1	0,25:1	0,125:1
E_x	1100	1152	1253	1354	1173	895	757	526	421
E_y	86	124	148	177	190	175	165	154	159
ν_{xy}	0,12	0,17	0,18	0,20	0,25	0,30	0,34	0,45	0,59
ν_{yx}	1,55								

Performing the iterative analysis, convergence of the deformation U_z of the central node is observed. The termination criterion is set here to $\Delta U_z \leq 0,1$ mm. For the performed analysis it turns out that this property converges very fast after only one iteration step, see Figure 5. Figure 5 also shows that the deformation difference at the central node between the initial analysis (iteration step 0) and the converged adaptive analysis (iteration step 1) is considerable with a quantity of ca. 18%. This indicates the importance of an advanced structural analysis of textile structures.



Figure 5: Deformation results in z direction of the central node vs. iteration steps

The stress and deformation results of the last iteration step performed, step 8, are given in Figures 6 and 7.

Membrane architecture: the seventh established building material. Designing reliable and sustainable structures for the urban environment.

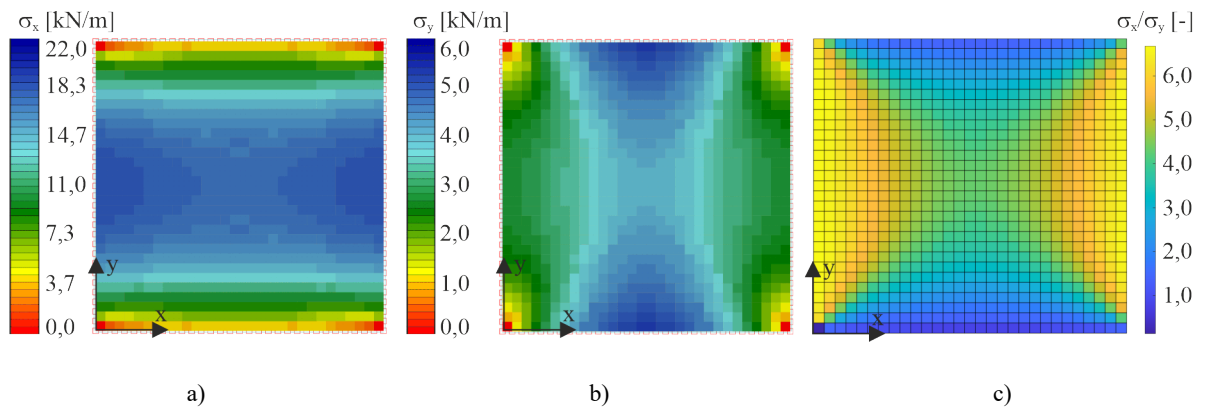


Figure 6: Stress results of the last iteration step: a) stresses in x-direction, b) stresses in y-direction, c) stress ratios x/y

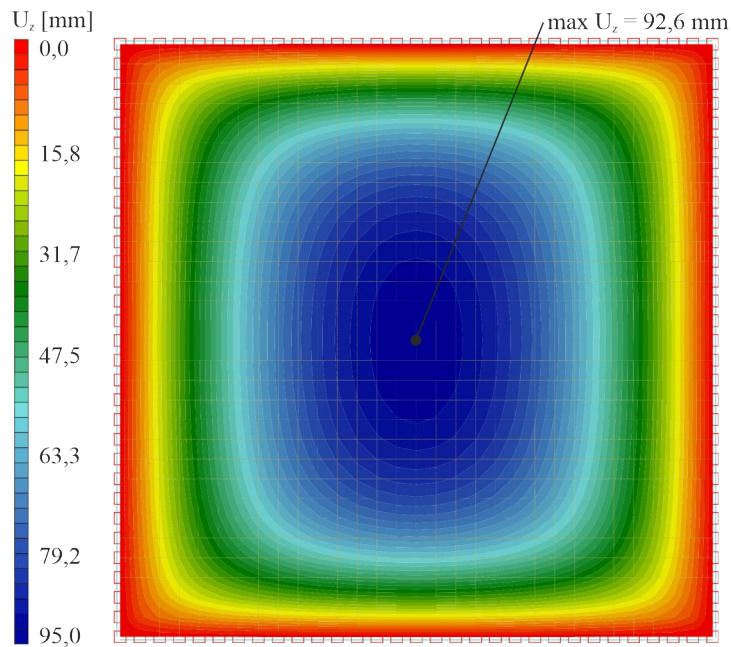


Figure 7: Deformation results in z direction, last iteration step

Design-relevant maximum stress and deformation values observed from the initial analysis and the adaptive approach are listed and compared in Table 2. It can be seen that regarding stresses the values reduce with the sophisticated adaptive analysis. This fits to the higher calculated deformation.

Membrane architecture: the seventh established building material. Designing reliable and sustainable structures for the urban environment.

Table 2: Comparison of results from the initial analysis and the last iteration step of the adaptive analysis.

Result Parameter	Initial analysis	Adaptive analysis	Difference [%]
Max σ_x [kN/m]	21,8	18,7	17
Max σ_y [kN/m]	5,4	5,3	2
Max U_z [mm]	78,6	92,6	18

Compared to the results using the nonlinear hyperelastic approach taken from [7] it is observed that the results of the adaptive linear-elastic approach fit very well. This indicates the validity of the results.

4. Conclusions

The practical implementation of a recently proposed advanced numerical simulation method for textile fabrics based on stress-ratio dependent material parameters within the linear elastic plane stress constitutive model is presented. This method reacts on varying stress ratios in finite elements during an iterative analysis. It requires a higher-level routine which controls and handles a commercial finite element software.

Actually, it is an effort to programme the higher-level script that handles the commercial finite element software. This script must be fitted to the software environment used. But when this is done once, an easy-to-use tool for enhanced numerical simulation of textile structures is available. It allows to achieve enhanced structural simulations of the non-linear anisotropic stress-strain behaviour of textiles while using easy to handle and intuitively understandable linear-elastic stress-strain-modelling.

Stress ratio dependent sets of elastic constants are required as input stiffness parameters. They have to be determined once for the material to be analysed. As stress-strain paths do not deviate significantly in repeated biaxial tests, databases can be set up for common textile membrane products. In the meantime, as well as for unknown materials, adequate biaxial tests have to be performed and evaluated.

The results of an example calculation indicate that these efforts are worth it. Stress and deformation results show to be much more accurate when compared to a hyperelastic nonlinear material model as a reference.

Acknowledgements

The authors wish to express thanks for the funding of this research by the Deutsche Forschungsgemeinschaft (DFG – German Science Foundation) in the framework of the research project „Characterization and modelling of the nonlinear material behaviour of coated fabrics for textile architecture“ (projects STR 482/5-2, BA 2823/10-2). Moreover, the programming work by Basel Daoud Rajha B.Sc. for the Python script is gratefully acknowledged.

References

- [1] EN 17117-1:2018, Rubber or plastics-coated fabrics – Mechanical test methods under biaxial stress states – Part 1: Tensile stiffness properties
- [2] Schröder, J., Balzani, D., Stranghöner, N., Uhlemann, J., Gruttmann, F., Saxe, K. (2011), Membranstrukturen mit nicht-linearem anisotropem Materialverhalten - Aspekte der Materialprüfung und der numerischen Simulation. In: *Bauingenieur*, vol.86, No. 9 (pp. 381-389).
- [3] Minami, H., Yamamoto, C., Segawa, S., Konoy, Y. (1997), A method for membrane material nonlinear stress analysis using a multi-step linear approximation, In: IASS International Symposium on Shell and Spatial Structures, Singapore.
- [4] Minami, H. (2006), A multi-step linear approximation method for nonlinear analysis of stress and deformation of coated plain-weave fabric. In: *Journal of Textile Engineering*, vol.52, No. 5 (pp. 189-195).
- [5] Galliot, C., Luchsinger, R.H. (2009), A simple model describing the non-linear biaxial tensile behaviour of PVC-coated polyester fabrics for use in finite element analysis. In: *Composite Structures*, vol.90, (pp. 438-447).
- [6] Bridgens, B.N., Gosling, P.D. (2004), Direct stress-strain representation for coated woven fabrics. In: *Computers and Structures*, vol. 82 (pp. 1913-1927).
- [7] Motevalli, M., Balzani, D. (2022), Enhancement in the Numerical Simulation of Textile Fabrics by Local Calculation of Stress-Ratio-Dependent Material Parameters. In: *Proceedings in Applied Mathematics and Mechanics*, 22/9/2022.
- [8] Motevalli, M., Uhlemann, J., Stranghöner, N., Balzani, D. (2019), Geometrically nonlinear simulation of textile membrane structures based on orthotropic hyperelastic energy functions. In: *Composite Structures*, vol. 223. Doi: 10.1016/j.compstruct.2019.110908.
- [9] Python.org, 2022, Python 3.10.9 documentation, accessed 24/1/2023, <https://docs.python.org/3.10/>
- [10] Sofistik 2023, Manual.
- [11] SOFiSTiK AG, 2022, CDB-Interfaces-Python, accessed 17/1/2023, https://www.sofistik.de/documentation/2022/en/cdb_interfaces/python/_python.html
- [12] MSAJ/M-02-1995, Testing Method for elastic constants of membrane materials.

TOPIC 3
Structural membrane:
an answer to issues of the 21st century





tensinantes2023 : TensiNet Symposium 2023 at Nantes Université

Membrane architecture: the seventh established building material. Designing reliable and sustainable structures for the urban environment.

Proceedings of the Tensinet Symposium 2023

TENSINANTES2023 | 7-9 June 2023, Nantes Université, Nantes, France

Jean-Christophe Thomas, Marijke Mollaert, Carol Monticelli, Bernd Stimpfle (Eds.)

Textile Architecture with or versus today Challenges in built Environment

Rosemarie Wagner*

*KIT Karlsruhe Institute of Technology

Engelstrasse 7 D – 76131 Karlsruhe

Rosemarie.Wagner@kit.edu

^a KIT Karlsruhe Institute of Technology Engelstrasse 7 76131 Karlsruhe, Germany

Abstract

Textile architecture as we know it today was developed in the 1950s last century. It is founded the early works of Frei Otto (1925-2015). After nearly 70 years, the question arises to what extent this building technique has established itself as the seventh building material. The applications are very broad, ranging from sun sails to façades, roofing of conditioned rooms and large stadium roofs. It can therefore be assumed that membrane structures are state of the art. If the use of resources, recyclability, avoidance of CO₂ emissions and economical consumption of available energy during production and use are set as requirements for membrane buildings, the effects of today's planning and building become visible. Building material properties are reduced to a few parameters, design tools allow structures that exclusively express design intentions, and numerical structural analysis makes it possible to prove the load carrying behaviour and build them. Membrane materials still lack the homogeneity in properties that is given in building materials such as steel, concrete or masonry. Despite automation, tolerances in production are considerably greater and lead to deviations in the design. A few aspects are shown that should be known in order to plan and build safe, durable, responsive membrane structures. This also includes paying attention to energy use and the environment.

Keywords: textile architecture, membrane structures, design, material, function

1. Introduction

Tents made of cotton, flax, hemp and animal hair can be found as mobile dwellings on all continents and in any early cultures. They are known as military tents in the Roman Empire, in the Middle Ages until the 19th century and are remaining so to this day. The vela over Roman amphitheaters (Graefe, 1979), the circus and fairground tents in the earlier centuries, textile shades for events of high-ranking personalities of the nobility, trade and the church are all well-known, Fig. 1a. All these structures had in common a sensitivity to high winds due to the lack of stabilization against flapping. Vela were retracted and circus tents had so-called storm poles to prevent the textile fabrics from flapping too much.

Membrane architecture: the seventh established building material. Designing reliable and sustainable structures for the urban environment.

Using natural yarns from plants safety and durability required the replacement of membranes or of the total structures after a few years. Permanent membrane structures are hardly to found in literature of the history in architecture. The only textile like structures which last more than hundred years was a tin canopy at the castle guard in Detmold, Germany, based on a design of Karl Friedrich Schinkel (1781 – 1841), Fig. 1b and is copying textile roof.



Figure 1a: Detail from Munich Oktoberfest Heinrich Adam, Oktoberfest, 1823; Schloss Nymphenburg, Marstallmuseum, Germany



Figure 1b: Tin canopy, Detmold castle guard, 1836, Detmold city archives

The publication of the dissertation by Frei Otto in 1954 and the early tent structures together with the company L. Strohmeier Konstanz Germany initiated the development of double-curved, prestressed membranes as light roofs (Otto, 1976). In the following 15 years this cooperation resulted in a large number of membrane buildings for temporary and permanent use. Of these, the membrane roofs at the Federal Garden Show in Cologne in 1957 and the Swiss National Exhibition in Lausanne in 1964 are probably the best known. What is obvious about this period between 1954 and around 1980 in Germany is that very few of the buildings still exist today. Most of them were either dismantled after defects due to ageing or damage and replaced by other buildings, in very rare cases again as membrane buildings. Of the few membrane buildings still in use, the membranes have now been replaced in almost all of them. There was a lack of experience and knowledge about the material properties of the coated fabrics, such as biaxial tensile strength, weather resistance and ageing behaviour. The variety of possible shapes was limited to those whose geometry and load-bearing behaviour could be described by analytical methods. The establishment of the Institute for Lightweight Structures in 1964 onwards at the Technical University of Stuttgart, Germany, and the research program SFB 64 Tensile Structures (1970-1985) were therefore characterized by the development of the fundamentals for the design and construction of flexible, prestressed and permanent textile structures. This included modelling and experiments to describe the material behaviour. The emergence of computer technology at this time led to the development of the finite element method for the structural analysis of doubly curved structures (Argyris, Angelopoulos, Knudson, & Schneider, 1979). The so-called force density method was developed to determine the geometry of prestressed membranes or membranes supported by internal pressure (Schek, 1976). There were the first approaches to create sections numerically. The knowledge gained during this time was incorporated into standards and is now state of the art.

Membrane architecture: the seventh established building material. Designing reliable and sustainable structures for the urban environment.

The question is whether the technical developments and scientific knowledge gained in the last 50 years is sufficient enough to use textile architecture for future buildings with the current challenges. Are we today in a position to design and build membrane structures that guarantee a service life of 50 years according to DIN EN 1990-1-1 Table 2.1 for buildings and other ordinary load-bearing structures?

Some Manufacturers of coated fabrics are talking today of a service life of 30 years. Although mechanical and environmental impacts and maintenance certainly have a strong influence on durability. Despite computer aided design, numerical simulation methods for wind analysis, structural analysis and heat transfer, numerical cutting pattern and digital plotting, defects and damage still occur today. Textile architecture has become established in the last 70 years, its contribution to teaching and research is small compared to conventional construction methods made of reinforced concrete, steel, wood, glass or masonry. Consequently, the number of buildings with membranes also has a small contribution to the numbers of new buildings to be constructed.

If ecological criteria such as recyclability, emissions and pollution are considered, textile buildings are no exception in the building industry. The *Silent Spring* by Rachel Carson, 1962 (Carson, 1962) and *"The Limits to Growth. A Report for the Club of Rome's Project on the Predicament of Mankind"*, 1972 (Maedows, Maedows, Renders, & Behrens, 1972) were published in the early days of tensile structures in Germany. In the last 50 years, building has been designed and build in a certain belief. Saving resources and protecting the environment can be achieved only with technical solutions such as thermal insulation, regenerative energies, computer-controlled interior conditioning and adaptable building materials, components and buildings.

What does the future of membrane structures look like. Will the number of textile buildings increase compared to conventional construction methods, can building materials be developed that require less resources, are more environmentally friendly and more recyclable than those available on the market today? Will digital planning methods, including Building Integrated Modelling (BIM) and automated production, make it possible to guarantee acceptance and service life over more than 50 years? Or are membrane buildings a possible answer to the fast living world of today with constantly changing demands on the use of buildings?

Offering solutions for this comprehensive task is impossible for a person with a modest field of expertise. Science in engineering means observing, perceiving, recognizing relations and deriving operationalizable functions. With this in mind, a few aspects will be mentioned for the building materials, the numerical design tools and some notes to architectural aspects.

2. Membrane Materials

Architects are interested in the surface texture, colour and light transmission among others. Depending on the use, the fire behaviour is also in demand. For membranes, a textile surface is preferred, but like light transmission, this is lost through a coating. Strengths, stress-strain behavior, tear propagation and reduction factors for designing are relevant for structural engineers. Heat flux, the heat transfer coefficient and radiation properties are required by building physics and companies for confection need values for seam behaviour, adhesion between coating and fabric as well as foldability. These characteristic values are carried out in short-term tests according to corresponding standards and are available in data sheets from the manufacturers. Some of these standards come from the polymer technology, artificial leather and leather industry. Till today, only some of the requirements are adapted to prestressed membrane constructions, e.g. tear propagation and foldability. Short-term ageing tests to investigate durability over time are also rather rare. The values provide an indication of ageing under assumptions of the environmental conditions.

Membrane architecture: the seventh established building material. Designing reliable and sustainable structures for the urban environment.

These may change or there are other influencing factors on the site. Resource use and environmentally relevant factors tend to be disregarded. Whereas for the few building materials of historical buildings there was sufficient experience for the preservation of weathered surfaces, today there is a lack of awareness of the visual ageing of surfaces exposed to the environment. It is assumed without questioning that the surfaces are not subject to any ageing processes and remain clean. Depending on the surface condition and the design of seams, cable or clamp boundaries, a scheduled or an unscheduled run-off of rainwater, soiling on the membranes up to the formation of bacteria, fungus, moss and algae occurs; even with higher quality membranes. Optical ageing has a direct correlation to an early failure only under certain circumstances. Discoloration due to environmental influences reduces the value of the building and its acceptance by users. The loss of intangible values of buildings quickly leads to demounting and is favoured by technical defects.



Figure 2a: PTFE/Glass fabric after 11 years



Figure 2b: PVC/PET fabric after 5 years

Cleaning is time-consuming, requires knowledge of cleaning agents and methods, and safety measures for walking on the roof surfaces. A rain-cleanable surface is possible with an additional dirt- and water-repellent layer or a specially structured surface. The additional layer is made of other polymers. Questions of compatibility and disposal have to be solved. The structuring of the surface requires an additional operation in the production of the membranes. Welding of two strips along a seam needs to remove the structured top on one strip. The most practicable approach today, but one that is rather rare, is to include the aspect of optical ageing already in the planning stage. However, this requires knowledge of rainwater run-off, concepts for details, connections and joints, as well as an idea of how membrane surfaces may age without losing their appearance.

While there was still a lot of experimentation with membrane materials till the last forty years, two composite materials are used for textile architecture today, with a few exceptions. These are, in different versions, PVC-coated polyester fabrics and PTFE-coated glass fabrics. The current state of the art in terms of durability, use of resources and environmental impact is described below for the two composite materials.

Today, polyvinyl chloride is the third most produced plastic after polyethylene PE and polypropylene PP. It is obtained from 43 % crude oil and 57 % rock salt. Rock salt is split into chlorine gas and caustic soda by means of electrolysis (Elsner, Eyerer, & Hierth, 2012). Chlorine gas is combined with ethylene obtained from crude oil to get vinyl chloride, which is then used to produce long-chain polymers. In research, there are currently approaches from China to obtain ethylene from waste and residual materials (Chen, et al., 2019).

Membrane architecture: the seventh established building material. Designing reliable and sustainable structures for the urban environment.

Pure PE, PP and PVC have no long-term resistance. Short-wave UV radiation and higher temperatures lead to discoloration, embrittlement and reduction of mechanical strength when oxygen in the air gets into reaction with the surface. Active carbon black with 2-2.5% by volume (Elsner, Eyerer, & Hierth, 2012) reduces this chemical ageing. The processing of pure PVC powder into coatings on woven or knitted fabrics with a higher resistance requires the addition of plasticizers up to 50% of PVC (Baur, Drummer, Osswald, & Rudolph, 2022) antistatic agents, stabilizers, flame retardants, dyes, fillers, lubricants and processing aids. Plasticizers migrate and PVC coatings are sealed with a lacquer coating, e.g. acrylic. Very few of these additives are biodegradable, making composting almost impossible. The recycling of soft PVC into the technical material cycle is made more difficult by the high plasticizer content. Thermal recycling is costly due to the high chlorine content. PVC is partly replaced by thermoplastic elastomers to avoid the use of chlorine. These coatings are mixtures of soft EPDM with hard polypropylene (TPO) or of soft polyester and hard polyurethane (TPU). Both mixtures have a low ageing resistance without additives. These make biodegradation more difficult, but it is possible to return them to the material cycle. Isocyanate is used to reactivate polyurethane (Niesner, 2022).

Polyester (PET) ranks fifth in Europe in terms of plastic demand and processing. Polyester is decomposed by hydrolysis when exposed to moisture and higher temperatures. Samples stored in 40° C warm water for 7 days, which are additionally pre-stressed, show a decrease of the uniaxial tensile strength depending on the amount of pre-stressing (Müller-Rochholz & Bronstein, 1994). When planning membrane structures, areas that heat up due to solar radiation and moisture are to be avoided. Examples are clamping near the ground floor or low points where moisture remains. UV radiation, together with the effect of atmospheric oxygen and temperature over a longer period of time, leads to the decomposition of pure polyester. The consequences are a reduction in tensile strength and elongation at break. Usually, the coating with the appropriate finish protects against this. Polyester occurs in nature, e.g. in cork, is biodegradable without additives and can be obtained from renewable raw materials (Behr & Seidensticker, 2018).

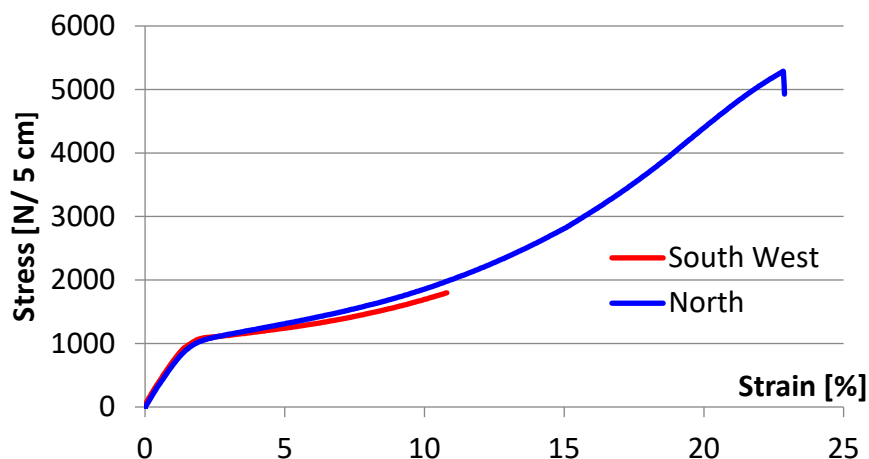


Figure 3: Stress-strain diagram of a PVC/PET fabric with moisture and solar radiation (south West) and without solar radiation (north)

Polymers with fluorine such as PTFE, PVF, PVDF, FEP and ETFE have a high weather resistance even without additives. However, this excludes composting. Thermal recycling is costly due to the fluorine that is released. Today, PTFE is broken down into monomers using ultrasound, thermal, photochemical or mechanical energy, which in turn are used to produce polymers (Niesner, 2022).

Membrane architecture: the seventh established building material. Designing reliable and sustainable structures for the urban environment.

Glass fibre fabric is generally presented as very durable. Frei Otto already had a different experience for the membrane of the entrance arch to the Federal Garden Show in Cologne 1957 (Otto, 1976). The structure was dismantled and was to be rebuilt a year later. However, the membrane was brittle and had only little strength left. It is known from heritage conservation that glass corrodes when exposed to moisture, high temperatures, alkaline and acidic media. For glass fiber, the corroding of the surface means the loss of compressive prestress and thus of tensile strength. The described influences are covered by reduction factors of the uniaxial tensile strength. However, these do not consider the environmental conditions, e.g. on a busy road or on the edge of a city in the countryside, nor the annual rainfall and places where moisture may penetrate the fabric.

The conclusion from the above is for textile architecture either to achieve technically and creatively high-quality buildings with a long service life. This requires careful planning, checking the durability of the coating and careful handling during installation in order to avoid defects and damage to the coatings. These lead to earlier failure of the load carrying fabric, regardless of the material used. The alternative is to replace the membranes at regular intervals. This should already be considered during the planning stage. The membranes should either be compostable or recyclable into the technical material cycle with little effort.

3. Numerical Design Methods

The effort to plan double-curved and pre-stressed membrane structures was possible mainly with sophisticated modelling and measuring technology at the beginning of these building technique. Soap skin models were used for the first designs. These were photographed, often with a grid in the background, to obtain information about the geometry. The transfer to a model with the properties of the membranes was done with fabrics, thin cables or chains.

Small measuring devices were attached to the boundaries and stay cables to analyse the load-bearing behaviour. For the fabrication, a negative mould was made of plaster from the fabric models, which were used to determine the cutting pattern. For the seams, curvilinear rulers were used to map the course of geodesic lines on the three-dimensional surfaces of the plaster models. The physical and geometric laws behind the individual steps made it possible to map this process to numerical simulation and software tools had been developed. Today, there is a multitude of programs that can be used for designing membrane structures in the steps of form finding, structural analysis and cutting pattern based on discrete, numerical models.

The so-called form finding is derived from the soap skin models, namely to create a spatially curved surface. The geometry is derived for a given boundary from the surface tension of the soap film. The relationship between geometry and tensions is implemented in software in different approaches. The difference lies in the modelling of the discrete surfaces and the formulation of the equilibrium conditions. The surfaces are modelled with single mass points connected by springs. The equilibrium of the spatial geometry is determined by oscillating the masses and damping them via the springs until they are at rest. The geometry is determined by the mesh geometry, the chosen masses and the damping property of the springs. This is a very powerful method, because only the vectors of acceleration and velocity in points have to be determined in each calculation step. All animations of moving fabrics are digitally generated in this way (Bender, 2014). It corresponds to shape finding in Rhino/Grasshopper, for example. Moving mass points creates shapes, but it has to be proved whether these shapes can also be represented with the material properties of the membranes.

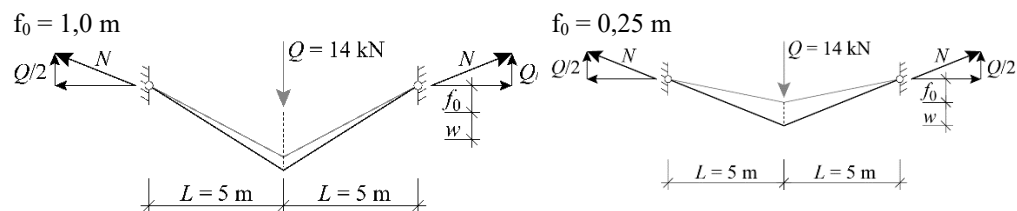
Membrane architecture: the seventh established building material. Designing reliable and sustainable structures for the urban environment.

However, a development can be seen in the use of knitted fabrics instead of woven fabrics for the membrane surfaces. The great flexibility of the knitted fabric due to the warping of the loops does not require any cutting and approximately reproduces the geometry calculated with spring-mass models. In membrane structures, this way of defining equilibrium shapes has been known for a long time under the term "dynamic relaxation".

A set of points and link created in the plane with different meshes can be brought into equilibrium by linearizing the equilibrium of forces at each node. The ratio of force/edge length, called force density, remains constant when the two nodes are moved on a plane. The fixed points where the mesh is calculated into equilibrium have to be at different heights in the z-direction. The geometry depends on the assumed forces in each link in the plane initial state and is independent of the mesh geometry. This method is known as the "force density method". It is also powerful, because no material law is necessary to determine the equilibrium in one calculation step.

Linearization of nodal equilibrium is impossible for finite elements such as triangles or quadrilaterals because the force densities change with the change in geometry of the triangles or quadrilaterals during iteration to equilibrium. Determining the equilibrium geometry using the finite element method is based on geometrically non-linear calculations with the Green-Lagrange displacement-distortion relationship. However, this only applies to small angular distortions. If these become too large in one iteration step, no equilibrium is possible or very many small iteration steps become necessary. Compared to the exact kinematic condition, other geometries result. The error due to the simplification in the Green-Lagrange condition adds up with each iteration step.

Table 1: Deformation and forces according to the different approaches of the deflection-strain relation



	Deformation w [m]	Cable force N [kN]	Deformation w [m]	Cable force N [kN]
Theory I	0,125	17,846	1,899	70,087
Theory II	0,113	16,032	0,5796	21,125
GL-Strain	0,107	16,115	0,4028	26,842
Geom. nonlinear	0,108	16,106	0.4049	26,754

For the behaviour under external influences, a material law of the coated membranes is necessary. In the meantime, there are national, European and international standardised procedures for determining the parameters of the simplified orthotropic material law. However, the stresses and deformations depend not only on the characteristic values but also on the curvature in which the warp and weft run. At any point on a doubly curved surface, an orthogonal tripod can be placed in the tangential plane to the surface. If a warp thread passes through this point, the surface and line normal only coincide if the warp thread has the course of a geodesic line. Unfortunately, this is very rarely the case, warp and weft consequently run at an oblique angle to each other.

The warp and weft course are determined by the direction of the cutting paths. The more the thread orientation deviates from the main curvature direction of the surface, the greater the rotation angle between them. According to Frei Otto, a slight deviation of the thread orientation from the main direction of curvature facilitates assembly. There is compliance due to the adjustment and twisting. Tolerances are easier to compensate because the change in geometry leads to less stress in the membranes.

Membrane architecture: the seventh established building material. Designing reliable and sustainable structures for the urban environment.

The methods for determining the cutting pattern today convey a precision which, however, can hardly be maintained in production despite cutting plotters. The welding of curved seams is done manually. The setting of welding marks makes it easier to produce the seams, because it enables tacking before welding together. Inaccuracies add up unfavourably. With an elongation stiffness of 600 kN/m and a length error of 0.1%, this results in a tension of 0.6 kN/m. With a pretension of 3 kN/m, this corresponds to 20% too little or too much after assembly.

The conclusions are that the numerical design methods represent a virtual world. This contains models which, however, have comparatively little in common with reality, depending on the calculation method, the material properties, the orientation of warp and weft according to the main curvature of the double curved surface, the tolerances during manufacturing and mounting. Together with the environmental conditions, these certainly have an influence on the durability of the textile covers.

4. Architectural Aspects

After almost 70 years of textile architecture, as imitated by Frei Otto with his dissertation, the status of this building method is still very diffuse compared to conventional building methods. Membrane buildings came into fashion in Germany in the 1960s and 1970s, fitted the times and were planned and built by other architects. As a result of the lack of experience and knowledge in dealing with these buildings, the majority of membrane buildings were dismantled after a short time. There are only a few that have survived the test of time. The reasons for this are a high level of identity of the owners and users of the buildings, planning and construction that allows for use and ageing without the building losing its value, and maintenance that is appropriate to the effort involved.



Figure 4a: Textile canopy entrance building spa garden Bad Wildbad, Germany 1964, Archive Bauamt Pforzheim



Figure 4b: situation today, removed structure

Textile architecture has an incredible breadth of applications compared to other construction methods, from small structures as shading to large stadium roofs as weather protection. However, this is limited. Membrane structures are singularities by their design and are getting their appearance, if no conventional buildings are too close to them. In this context, it is permissible to ask how many membrane buildings a city can tolerate, and in what proximity to each other and to neighbouring buildings. It also depends on the social environment in which the membrane buildings are erected. In an environment with a higher potential for conflict, vandalism is possible, especially if the membranes are at heights that can be reached and damaged by people.

Membrane architecture: the seventh established building material. Designing reliable and sustainable structures for the urban environment.



Figure 5a: Textile Cover PH Ludwigsburg, Germany 1980, replacement 2010, (Ref. Institut für Massivbau, University Stuttgart)



Figure 5b: Situation today with vandalism in 2016 on the left side

Using membranes for roofing conditioned interior spaces is rather the exception. This may be due to the multi-layered structure of the envelopes, which require additional design, construction and building costs compared to conventional roof structures. In addition, there are the large volumes under the membranes that need to be heated and cooled. For some, this could be considered as a waste of energy in these days. Uses such as sports halls, shopping centres, community halls, corridor roofing in office buildings causes flatter textile roofing, often with little curvature. This approach deprives the membrane of their lightness and their appearance due to the necessary and sometimes heavy-looking substructures made of steel or wood. The consequence of this is to critically question membrane structures for certain uses or to give the membrane roofs the space they need for these uses in order to work in a balanced relationship to the installations. This raises the question of how architects who have mainly dealt with conventional buildings are prepared for this. In addition, there is the very rudimentary knowledge of building materials, designing methodology and, derived from this, the idea that numerical designs can be translated into reality as if modelled. This leads to decisions that contradict the nature of prestressed membranes. The responsibility is handed over to executing companies that are supposed to implement the almost impossible. The durability and long life are depending of the fabric is mostly depending on the acceptance of the user during the life span. This is closely related to the appearance and the identification of the owner.



Figure 6: Tanzbrunnen Köln, 3 times replacement of the fabric, one-time replacement of the cables, build 1957, picture 2016

Membrane architecture: the seventh established building material. Designing reliable and sustainable structures for the urban environment.

5. Conclusion

The future and lifespan of membrane structures will be determined much more by the understanding of the building materials, the interplay of form and force, and the ideas about the three-dimensional spaces than is necessary for conventional buildings made of reinforced concrete, steel and wood. It is possible to build membrane structures because the numerical design tools, some of the material properties and the automatic cutting pattern are available and can be used by anybody with in a short time of training. The acceptance, the life time and the durability require a more holistic knowledge and experience which can only be reached if one engages physical and sensitive with these structures.

References

- Argyris, J., Angelopoulos, T., Knudson, W., & Schneider, S. (1979). *WIDESPAN Benutzerhandbuch – ein Programmsystem zur statischen und dynamischen Berechnung von weitgespannten Flächentragwerken. Mitteilung 50/1978 SFB 64 Weitgespannte Flächentragwerke*. Stuttgart: Inst. f. Statik u. Dynamik d. Luft- u. Raumfahrtkonstruktionen.
- Baur, E., Drummer, D., Osswald, T. A., & Rudolph, N. (2022). *Saehteling Kunststoff Handbuch*. München: Hanser Verlag.
- Behr, A., & Seidensticker, T. (2018). *Einführung in die Chemie nachwachsender Rohstoffe*. Berlin: Springer.
- Bender, J. (2014). *Dynamiksimulation in der Computergraphik*. Karlsruhe: KIT Scientific Publishing.
- Carson, R. (1962). *The Silent Spring*. Greenwich, Conn. USA: Fawcett Publications, Inc.
- Chen, R., Su, H.-J., Liu, D., Huang, R., Meng, X., Cui, X., . . . Deng, D. (07. November 2019). Highly Selective Production of Ethylene by the Electroreduction of Carbon Monoxide. *Angewandte Chemie Volume 59 Issue 1*.
- Elsner, P., Eyerer, P., & Hierth, H. (2012). *Kunststoffe Eigenschaften und Anwendungen*. Heidelberg: Springer Verlag.
- Graefe, R. (1979). *VELA ERUNT, Die Zeldächer der römischen Theater und ähnlicher Anlagen*. Mainz am Rhein, Germany: Philipp Zabern.
- Maedows, D., Maedows, D., Renders, J., & Behrens, W. (1972). *The Limits to Growth*. New York, USA: Univers Books.
- Müller-Rochholz, J., & Bronstein, Z. (1994). *Einfluß der Zugbeanspruchungen auf das Hydrolyseverhalten von Polyester - PET*. Stuttgart: Fraunhofer IRB Verlag.
- Niesner, R. (2022). *Recycling of Plastics*. München: Carl Hanser.
- Otto, F. (1976). *Mit Peter Stromeyer durch die Jahre 1953 - 1976. IL 16 Zelte Tents, Burkhardt, B.; Otto, F.; Schmall, I. (Hrsg.), Mitteilungen des Instituts für Leichte Flächentragwerke, Universität Stuttgart*. Stuttgart: Karl Krämer.
- Schek, H. (1976). *Über Ansätze und numerische Methoden zur Berechnung großer netzartiger Strukturen. Habilitation*. Stuttgart: Institut für Anwendungen der Geodäsie im Bauwesen.

The Pathways to Zero Carbon for Tensioned Membrane Architecture: ongoing actions and next steps

Bruce Danziger, SE*, Carol Monticelli, *architect PhD.*^a

* Danziger Engineering Collaborative, Inc., 7402 McConnell Ave, Los Angeles, CA 90045, USA,
bruce.danziger@danzigerec.com

^a Professore Associato in Tecnologia dell'Architettura, Politecnico di Milano, Dip. di Architettura, Ingegneria delle Costruzioni e Ambiente Costruito, Textiles Hub - Interdept. Lab., Via G. Ponzio 31, Milano, 20133, Italy

Abstract

The authors want to share insights on the process for assessing the environmental impacts of tensioned membrane structures. They will discuss how to learn and share effective methods to quantify and reduce the embodied carbon of lightweight structures and to describe the advancements of research on this topic with the adoption of carbon accounting methods for current design practice.

Various professional organizations have founded efforts to reduce embodied carbon in the built environment. Typically, these organizations are based upon geographic regions and specific disciplines with separate, yet similar, declarations and commitments for architects, structural engineers, MEP engineers and Contractors. The authors will present a global vertically integrated carbon reduction strategy for the tensioned membrane industry seeking to capture the collective efforts across design, manufacture, supply, install, maintain and ownership.

The AEC industry is currently focused on the global warming potential (GWP) of the built environment. The embodied and operational carbon of building construction are a major contributor to greenhouse gasses. The first steps towards embodied carbon reduction strategies include a declaration of commitment, education, collecting data, establishing benchmarks and setting reduction targets. The presentation will share draft declarations and plans carbon reduction for tensioned membrane structures with many of aspects of collaboration and input identified for the rest of the industry including

architects & designers, manufacturers, suppliers, builders and clients, owners, and stakeholders).

The authors will present the draft declarations and plans to solicit dialogue. The intent is to facilitate wide industry adoption of similar declarations and plans for embodied carbon reduction that includes:

1. Education - sharing resources, methods and carbon accounting tools
2. Reporting – carbon accounting and sharing project data
3. Reduction Strategies – making plans, collecting data, establishing benchmarks, setting carbon reduction targets
4. Advocacy – promoting carbon reduction on projects, getting more EPD data from suppliers and manufacturers, promoting the industry's contributions to carbon reduction
5. Implementation - transfer collected knowledge to design practice

Keywords: sustainability, carbon dioxide equivalent (CO₂eq), global warming potential (GWP), environmental product declaration (EPD), embodied carbon action plan (ECAP), lightweight structures, structural membrane)

References

- [1] C. Monticelli and A. Zanelli, "Life Cycle Design and efficiency principles for membrane architecture: towards a new set of eco-design strategies", *International Symposium on "Novel structural skins – Improving sustainability and efficiency through new structural textile materials and designs*, (2016).
- [2] T. Finlay, "The Carbon Footprint of Long Span Structures: Review of the Millennium Dome and Subsequent Tensile Systems", *Proceedings of the IASS Annual Symposium 2020/21 and the 7th International Conference on Spatial Structures*, (2021).



**tensinantes2023 : TensiNet Symposium 2023 at
Nantes Université**

Membrane architecture: the seventh established building material.
Designing reliable and sustainable structures for the urban
environment.

Proceedings of the Tensinet Symposium 2023

TENSINANTES2023 | 7-9 June 2023, Nantes Université, Nantes, France

Jean-Christophe Thomas, Marijke Mollaert, Carol Monticelli, Bernd Stimpfle (Eds.)

Integrating sustainability aspects in the teaching of lightweight structures and their comparison with common structures

Heidrun BÖGNER-BALZ*, Sarah VON DER WETH^a, Karsten MORITZ^a

*HFT – Hochschule für Technik Stuttgart

Schellingstr. 24, 70174 Stuttgart

heidrun.boegner-balz@hft-stuttgart.de

^a IMS BAUHAUS® Archineer® Institutes e.V., Dessau, Germany

Abstract

The positive development of the construction industry with regard to CO₂ emissions in recent years seemed to initiate the turnaround in the sector. Now the trend is going backwards. Despite increased investments in energy efficiency and lower energy intensity, the construction sector's energy consumption and CO₂ emissions have risen again to an all-time high since the COVID 19 pandemic, according to a new report. “Years of warnings about the impacts of climate change have become a reality,” said Inger Andersen, Executive Director of the United Nations Environment Programme (UNEP). “If we do not rapidly cut emissions in line with the Paris Agreement, we will be in deeper trouble.” [6]

Construction has evolved over millennia, whereby a large proportion of buildings and civil engineering structures have been designed with an emphasis on not using too much material. But in view of the threat of global warming, mass extinction of species, energy crisis, finite fossil resources and the not inconsiderable contribution of construction, it is essential to include aspects of sustainability in every building. The awareness that we need to counteract global warming and think and plan sustainably has grown considerably over the last decades. We do have the knowledge of how the building industry can reduce environmentally harmful actions in theory, but a fast implementation seems at the moment to be the biggest problem. This challenge raises the question of which possibilities we have in structural design and especially in the design of lightweight structures to promote a rapid and continuous conversion towards sustainable and environmentally friendly design into everyday building design and practice. One key point besides awareness of the situation is to create a basis of understanding and tools for those who are involved in the building industry in order to make the right decisions towards more sustainable solutions in project planning and execution but also for being able to explain and provide well-founded calculations. Thus, teaching and research may contribute to a more rapid change in rethinking sustainable construction.

Membrane architecture: the seventh established building material. Designing reliable and sustainable structures for the urban environment.

This paper explains a teaching concept for this purpose, which is intended to promote the understanding and learning of sustainability aspects for reducing environmental impacts in construction. The teaching concept is intended to create an understanding of the considered selection of materials, comparison of materialized building components through to the sustainability concept of entire buildings and lightweight construction in three simple stages. In addition, students should explicitly understand how the approaches they learn can be applied in practice.

Keywords: teaching sustainability, sustainability concepts, lightweight structures, environmental impact, global warming potential lightweight structures, comparison of environmental impacts of lightweight and common structures

1. Current status and postulated goals

According to a study by the UN Environment Program, in 2021 the construction and building sector was responsible for 37 percent of global energy-related CO₂ emissions, which corresponds to about 10 gigatons of CO₂ per year (figure 1), surpassing even the previous maximum from the year of 2019 [2].

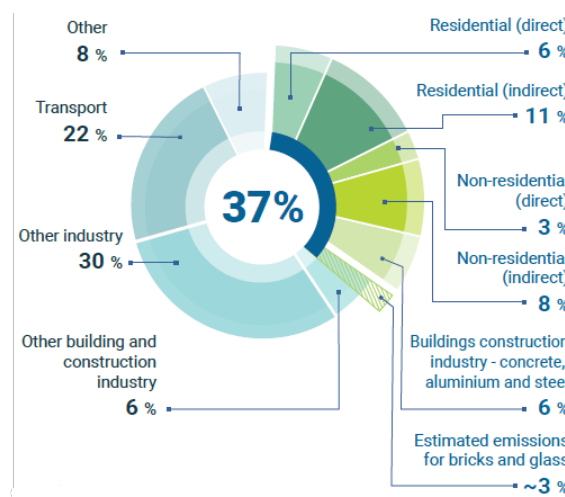


Figure 1: Share of buildings in global energy and process emissions in 2021 [5]

So how do we get back to reducing environmental impacts starting with embodied emissions from the construction of new buildings, the use of buildings and the refurbishment of existing buildings to the necessary levels to meet global environmental goals and stop and reverse the renewed upward trend in CO₂ emissions?

In addition, we have to consider that not only the emissions of harmful greenhouse gases have to be drastically reduced, resources conserved, energy saved and the amount of waste reduced - and all this with a continuously increasing population and increasing demands of people for comfort and standard of living.

With this goal in mind, it is the task of teachers and researchers in engineering and architecture to achieve a high level of quality, that means the harmony of form, function, construction, economy and ecology of buildings under the premise of sustainability [2], [3]. Here, the technical possibilities available to us or in prospect and the knowledge of socio-ecological

Membrane architecture: the seventh established building material. Designing reliable and sustainable structures for the urban environment.

relationships and long-term consequences must be taken into account. Today's design and construction has been enriched by the criterion of sustainability and has therefore also become significantly more complex [4].

2. Implementing sustainability in teaching of lightweight structures

In [1] the authors of the paper have already stated that the strategy to develop a detailed and comprehensive understanding of sustainable construction methods should start in smaller units and steps from the bottom up (figure 2).

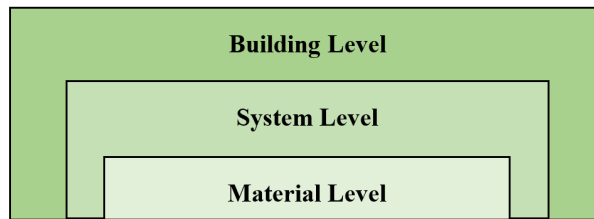


Figure 2: Building Levels of consideration [1]

The material level starts with deepened knowledge of structural materials including raw materials and their origin and availability, production processes, energy consumption, environmental impact and durability. Students will get to know and how to handle Environmental Product Declarations (EPDs) as neutral and objective considered documents including all environmentally relevant properties of the specific building materials. The content data usually covers as far as possible all effects a material has on its environment. Ideally, the entire life cycle of the material is taken into account. In this level also future perspectives may be shown. Which efforts are currently being undertaken by the building industry to improve environmental aspects of individual materials? How are these developments influencing future assessments, recyclability and lifetime of materials? Are there new materials with less environmental impacts available besides the commonly used ones [1]?

At the system level, different structures or assemblies, made of different materials or using different construction methods are investigated. This next step level will be based on the knowledge of the materials and their environmental impact previously taught. Advanced students calculate and evaluate life cycle assessments (LCA) based on the structural calculations of different structural systems. Different material designs for building components such as walls, ceilings, roofs, etc. are calculated and compared with each other. Building physics aspects, for example energy transfer and sound transmission through building components, are included in here [1].

Finally, life cycle assessments (LCA) of total structures and buildings will be carried out at the building level. Different solutions and their effects on the LCA are compared and evaluated. Here, also the interactions with the environment are intended to be taken into account.

The aim is that the students are trained to develop an understanding of the environmental impact of building materials (level 1), building systems and components (level 2) and complete building structures (level 3). Finally, the students should be able to make decisions about suitable combinations of structures and materials with regard to the life cycle assessment of a building. They will know at which points they will have to change something in order to significantly improve the LCA or a desired certification for the respective building (e.g. DGNB, BREEAM, LEED) [1].

Membrane architecture: the seventh established building material. Designing reliable and sustainable structures for the urban environment.

3. Teaching levels of sustainability from bottom to top on the example of the P&S Building for the African Union

3.1 Initial situation and comparison of common and lightweight solutions

The approx. 430.0 m² oval-shaped roof has dimensions of approx. 25.30 m x 20.00 m and is being built as a covering over the atrium of the newly built Peace and Security Building of the African Union in Addis Ababa, Ethiopia. The roof is planned as a building closure and is supported on the reinforced concrete attics. The original design envisaged a steel and glass roof variant - option 01 (figure 3).

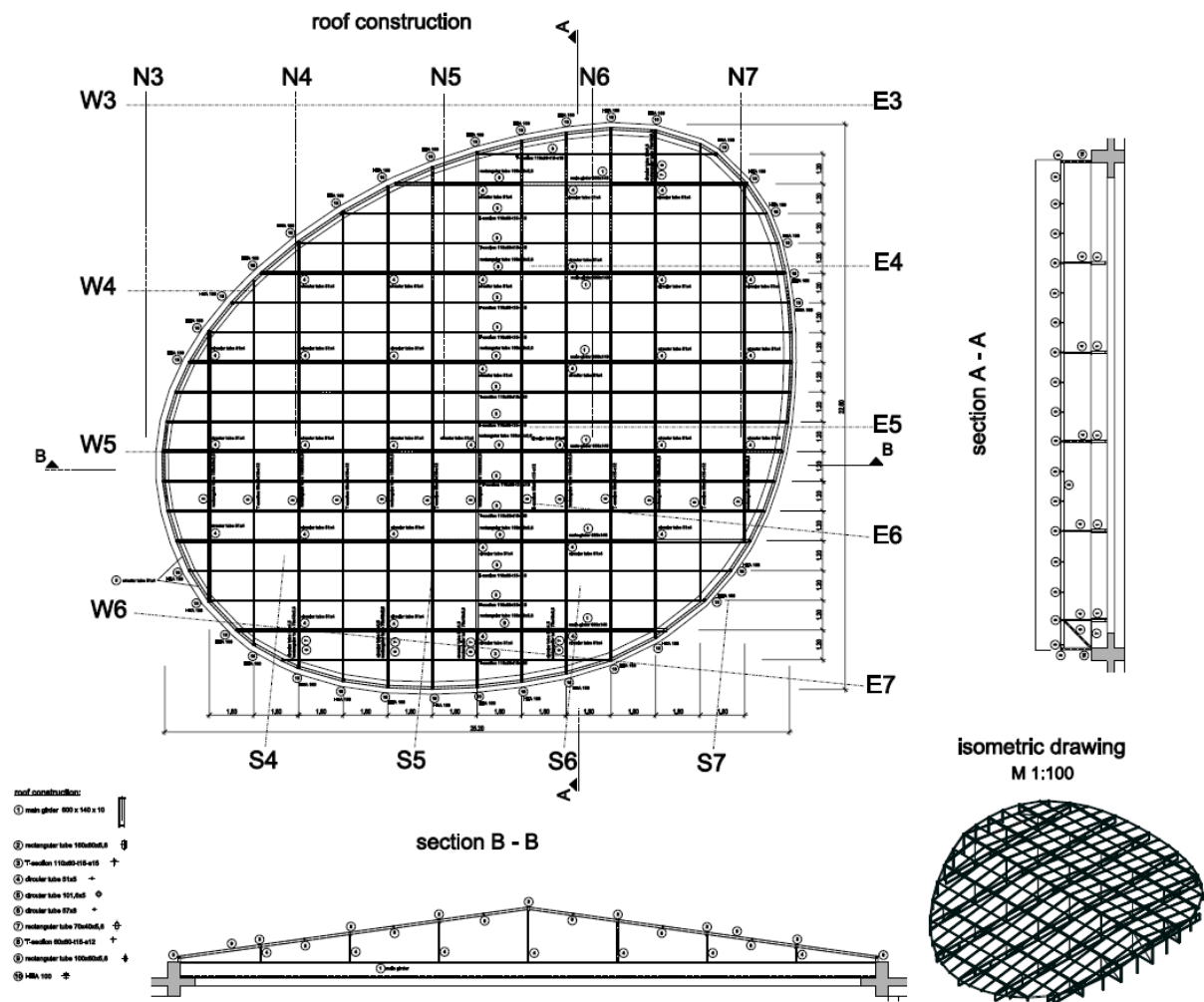


Figure 3: Option 01 – Steel-glass-roof - Position plan

The steel-glass roof is supported by 6 main girders, which carry the rest of the steel framework including the glass panes and transfer the loads to the edge attic construction. The glass elements are arranged at a gradient of 8° and consist of a laminated insulated safety glass inside and a toughened safety glass outside. Due to high earthquake load zone (level IV) the steel-glass roof solution has been reconsidered.

In order to save material and achieve the same effect of a light-flooded atrium area, an alternative proposal was to use an ETFE cushion construction - option 02 (Figure 4 and 5).

Membrane architecture: the seventh established building material. Designing reliable and sustainable structures for the urban environment.

Positionsplan

Grundriss Dach

Windlast Sag: $w_{s,k} = -0.59 \text{ KN/m}^2$
 Windlast Druck: $w_{d,k} = +0.24 \text{ KN/m}^2$
 Regenlast Druck: $r_{s,k} = +0.20 \text{ KN/m}^2$
 pneumatischer Druck Kissen: 300 Pa

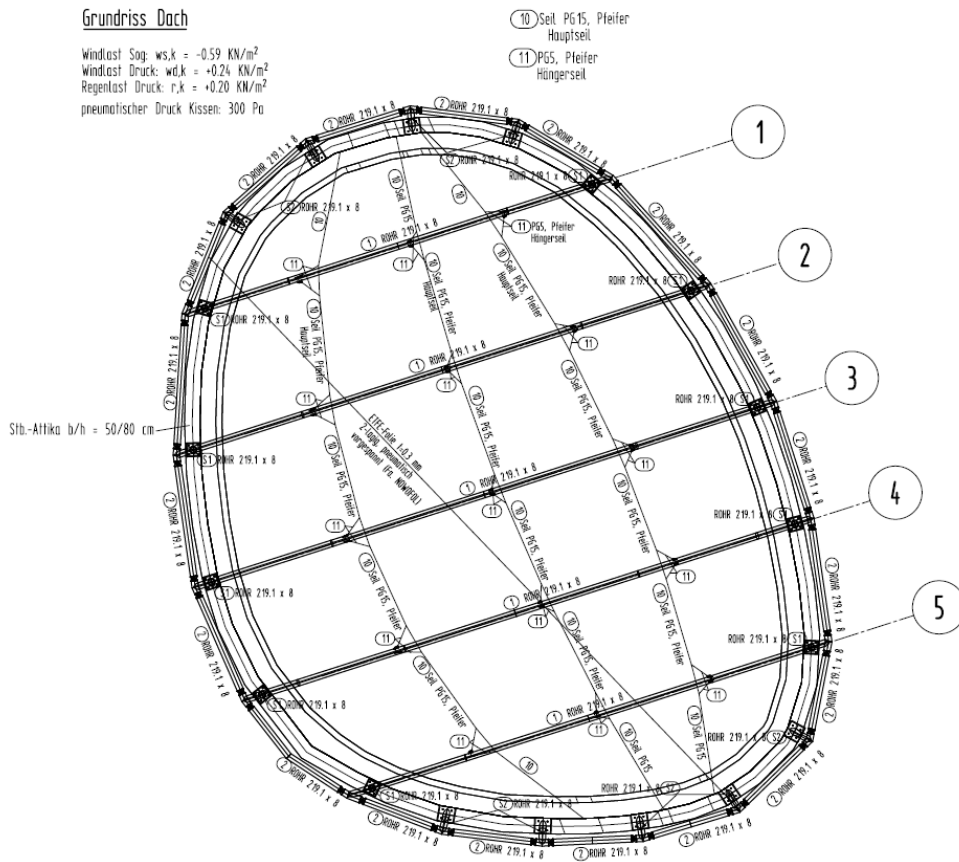


Figure 4: Option 02 - ETFE-cushion-roof - Position plan

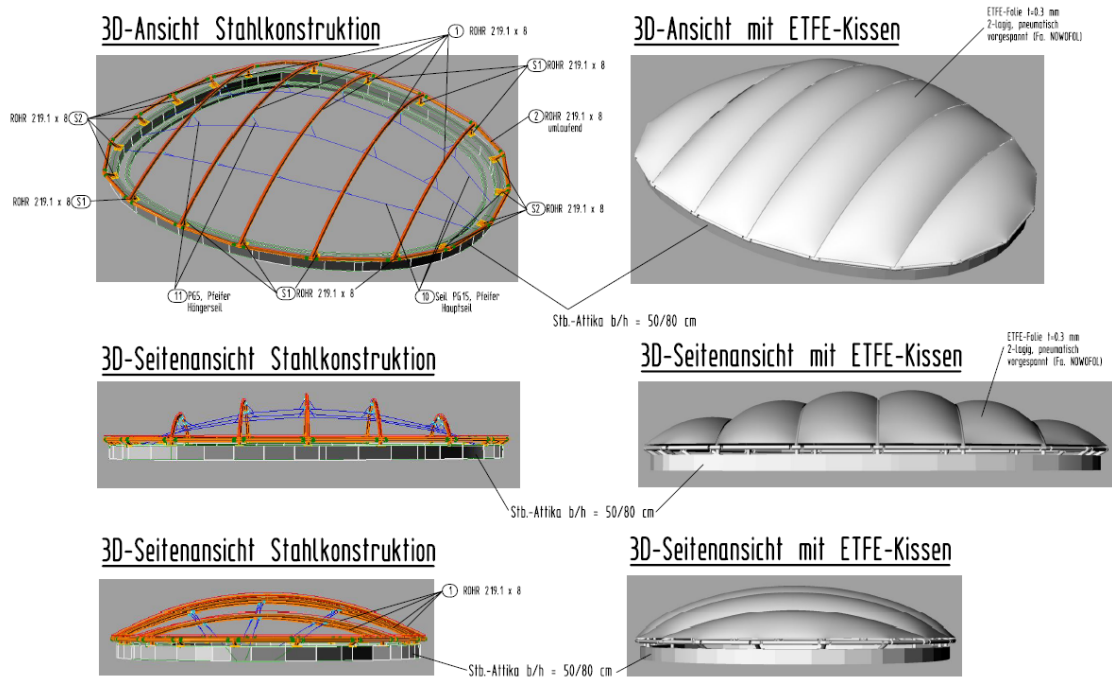


Figure 5: Option 02 - ETFE-cushion-roof - Visualization of Cushion Structure

Membrane architecture: the seventh established building material. Designing reliable and sustainable structures for the urban environment.

The roof envelope consists of a 2-layer pneumatically prestressed ETFE cushion. The primary structure is again a steel structure. The steel structure consists of 5 arched beams supported by columns on the attic. The roof is intended to have a slight cantilever over the reinforced concrete attic, i.e. the roof area is slightly larger than the opening in the ceiling. The radii of the arches are different. For transverse stiffening, the arches are each braced with 3 inclined cables. In the remaining outer edge area, the cushions are braced via a jointed ring beam.

The two variants are compared and evaluated below in the sustainability categories of material, system and overall structure.

3.2 Comparison of a lightweight and a common structure on Material Level

The first level is the material level. The focus of this example is on the handling of environmental product declarations, which enable a comparison between both envelopes, in this paper with regard to the global warming potential.

Lightweight construction requires materials that have high strength at the lowest possible weight. The design weight of a light surface structure, such as a membrane structure, can be significantly less than 1/50 to 1/100 of the weight of a solid structure, such as concrete or glass [2], [3]. Air-supported foil cushions form an extremely light-weight construction, because they consist of a volume of air that is enclosed airtight by at least two layers of thin ETFE-foils. The foils in this example are each 0.3 mm thick, so that the entire cushion weighs only about 0,7 kg/m² (without the frame). The glass option weighs about 50 times more than this.

But weight is not the only important factor at the material level. The environmental impact of the material itself is a criterion worth considering. In order to have enough quantified environmental information about the life cycle of a product to make comparisons between products with the same functions, environmental product declarations (EPD) are used for benchmarking. An EPD is a document in which the environmentally relevant properties of a specific product are presented in the form of neutral and objective data. This data covers, as far as possible, all the effects that the product can have on its environment. Ideally, the entire life cycle of the product is taken into account. An environmental assessment of the roofing materials (without the steel structure) based on the respective declarations [7],[8],[9] shows that the same area can be covered with an ETFE cushion construction with approx. 60% less CO₂ emission than with glass.

Table 1: LCA Analysis of the two different covering materials

Glass-Cover				Global warming potential														Total				
Option	Declaration Code	Product definition	Dimension	Product stage			Use Stage							End-of-life stage					Benefits after D			
				A1	A2	A3	A4	A5	B1	B2	B3	B4	B5	B6	B7	C1	C2			C3	C4	
Toughened safety glass (exterior)	M-EPD-FEV-GB-002000	1 m ² area and 1 mm glass thickness	8 mm 460,00 m ²	12.732,80	0,00	0,00	0,00	0,00	0,00	0,00	0,00	0,00	0,00	0,00	0,00	0,00	105,98	34,78	158,98	102,67	-1.435,20	
Laminated insulated safety glass (inside) 4-16-4	M-EPD-MIG-GB-002000	1 m ² area insulating glass units - double glass configuration	460,00 m ²	14.549,80	0,00	0,00	0,00	0,00	0,00	0,00	0,00	0,00	0,00	0,00	0,00	0,00	12.282,00	110,40	36,80	156,40	105,80	
Sum [to CO2 equiv.]:				27,28	0,00	0,00	0,00	0,00	0,00	0,00	0,00	0,00	0,00	0,00	0,00	0,00	12,39	0,15	0,20	0,26	-1,33	38,94
ETFE-Cover				Global warming potential														Total				
Option	Declaration Code	Product definition	Dimension	Product stage			Use Stage							End-of-life stage					Benefits after D			
				A1	A2	A3	A4	A5	B1	B2	B3	B4	B5	B6	B7	C1	C2			C3	C4	
ETFE Foil t = 0.3 mm double layer; pneumatically pre-stressed, p = 300 Pa	EPD-TAL-20190092-ICB1-EN	Material Example! 1 m ² of Taiyo Europe's TensoSky®-System (double layer)	460 m ²	17.130,40	0,00	294,95	0,00	0,00	0,00	0,00	0,00	0,00	0,00	34,78	0,00	0,00	0,00	17,10	724,50	0,00	-3.017,14	
Sum [to CO2 equiv.]:				17,13	0,00	0,29	0,00	0,00	0,00	0,00	0,00	0,00	0,03	0,00	0,00	0,02	0,72	0,00			-3,02	15,18

Membrane architecture: the seventh established building material. Designing reliable and sustainable structures for the urban environment.

3.3 System Level

The glass option weighs around 15 times more than a comparable ETFE cushion system incl. aluminium frames, gutter, keder etc. [9] which effects the primary structure enormously. The primary supporting structure of ETFE foil cushions has therefore to transmit less load to the foundations and can be made more filigree using less weight. In addition, the span that can be achieved with such cushions is relatively large, in this case 4,00 m, which also saves weight. The steel glass roof, on the other hand, requires a support grid with a dimension of 1.80 x 1.20 m. This results in a significantly higher quantity of steel. The weight advantage is included at various points in the ecological balance (Life Cycle Assessment or LCA) of components and buildings, for example during manufacture, transport, assembly and disassembly, as well as during the preparation for reuse of the components.

Before the evaluation can take place on the basis of the material, a structural analysis must be carried out that defines the required cross-sections. Based on this, a quantity calculation of option 01 and option 02 have been carried out.

At the second level, the system level, also an intelligent selection of the structural system for each structural component of the building needs to be carried out. This means for example filigree component cross-sections that are adapted to the material, the construction and the stress. They are achieved, for example, by avoiding bending stress, by preferring tensile to compressive stress, or by short-circuiting forces (example: tension and compression ring of a spoked wheel). Supporting elements that are based on the force path of the shape-determining load case or adaptive systems reacting on the load distribution, or structures that have a density distribution corresponding to the stress profile also meet the criterion of structural lightweight construction [2], [3]. If we add to the above compared roofing material the rest of the structure, i.e. all steel and concrete components, the difference of 60% less CO₂ emission will remain. The reason for this is that with a sophisticated static system and the difference in weight of the covering material, the steel [10] and concrete [11] also increases or decreases proportionally.

Table 2: LCA Analysis of the glass and ETFE cover system variants including primary structures

Glass-Cover				Global warming potential																	Total	
Option	Declaration Code	Product definition	Dimension	Product stage			Use Stage							End-of-life stage				Benefits after D				
				A1	A2	A3	A4	A5	B1	B2	B3	B4	B5	B6	B7	C1	C2		C3	C4		
Toughened safety glass (exterior)	M-EPD-FEV-GB-002000	1 m ² area and 1 mm glass thickness	8 mm 460,00 m ²	12.732,80	0,00	0,00	0,00	0,00	0,00	0,00	0,00	0,00	0,00	0,00	0,00	0,00	105,98	34,78	158,98	102,67	-1.435,20	
Laminated insulated safety glass (inside) 4-16-4	M-EPD-MIG-GB-002000	1 m ² area insulating glass units - double glass config.	460,00 m ²	14.549,80	0,00	0,00	0,00	0,00	0,00	0,00	0,00	0,00	0,00	0,00	0,00	12.282,00	110,40	36,80	156,40	105,80		
Steel Structure + 10%	EPD-BFS-20180116-IBG2-DE	pro Tonne Baustahl	33,98 to	38.400,51	0,00	0,00	0,00	0,00	0,00	0,00	0,00	0,00	0,00	0,00	0,00	0,00	0,00	62,53	0,00	-14.034,88		
Attica 500 x 650 mm	EPD-IZB-20180101-IBG1-DE	1 m ³ Beton	24,85 m ³	4.894,71	96,90	26,83	-248,46	0,00	0,00	0,00	0,00	0,00	0,00	0,00	77,02	298,16	149,33	0,00	0,00	-531,71		
Sum [to CO2 equiv.]:				70,58	0,10	0,03	-0,25	0,00	0,00	0,00	0,00	0,00	0,00	0,00	12,47	0,44	0,41	0,26	0,00	-15,90	68,13	
ETFE-Cover				Global warming potential																	Total	
Option	Declaration Code	Product definition	Dimension	Product stage			Use Stage							End-of-life stage				Benefits after D				
				A1	A2	A3	A4	A5	B1	B2	B3	B4	B5	B6	B7	C1	C2		C3	C4		
ETFE Foil t = 0.3 mm double layer; pneumatically pre-stressed, p = 300	EPD-TAL-20190092-ICB1-EN	Material Example! 1 m ² of Taiyo Europe's TensoSky®-System (double layer)	460,00 m ²	17.130,40	0,00	294,95	0,00	0,00	0,00	0,00	0,00	0,00	34,78	0,00	0,00	17,10	724,50	0,00	0,00	-3.017,14		
Steel Structure	EPD-BFS-20180116-IBG2-DE	pro Tonne Baustahl	10,12 to	11.437,56	0,00	0,00	0,00	0,00	0,00	0,00	0,00	0,00	0,00	0,00	0,00	0,00	18,62	0,00	0,00	-4.180,28		
Cable + 10%	EPD-BFS-20180116-IBG2-DE	pro Tonne Baustahl	0,07 to	73,56	0,00	0,00	0,00	0,00	0,00	0,00	0,00	0,00	0,00	0,00	0,00	0,00	0,12	0,00	0,00	-26,89		
Attica 200 x 300 mm	EPD-IZB-20180101-IBG1-DE	1 m ³ Beton	3,78 m ³	744,66	14,74	4,08	-37,80	0,00	0,00	0,00	0,00	0,00	0,00	0,00	11,72	45,36	22,72	0,00	0,00	-80,89		
Attica 500 x 800 mm	EPD-IZB-20180101-IBG1-DE	1 m ³ Beton	27,20 m ³	5.358,40	106,08	29,38	-272,00	0,00	0,00	0,00	0,00	0,00	0,00	0,00	84,32	326,40	163,47	0,00	0,00	-582,08		
Sum [to CO2 equiv.]:				34,74	0,12	0,33	-0,31	0,00	0,00	0,00	0,00	0,03	0,00	0,10	0,39	0,93	0,00	0,00	0,00	0,00	-7,89	28,45

Membrane architecture: the seventh established building material. Designing reliable and sustainable structures for the urban environment.

The comparison of the global warming potential of the two solutions shall be shown below (Figure 6 and 7).

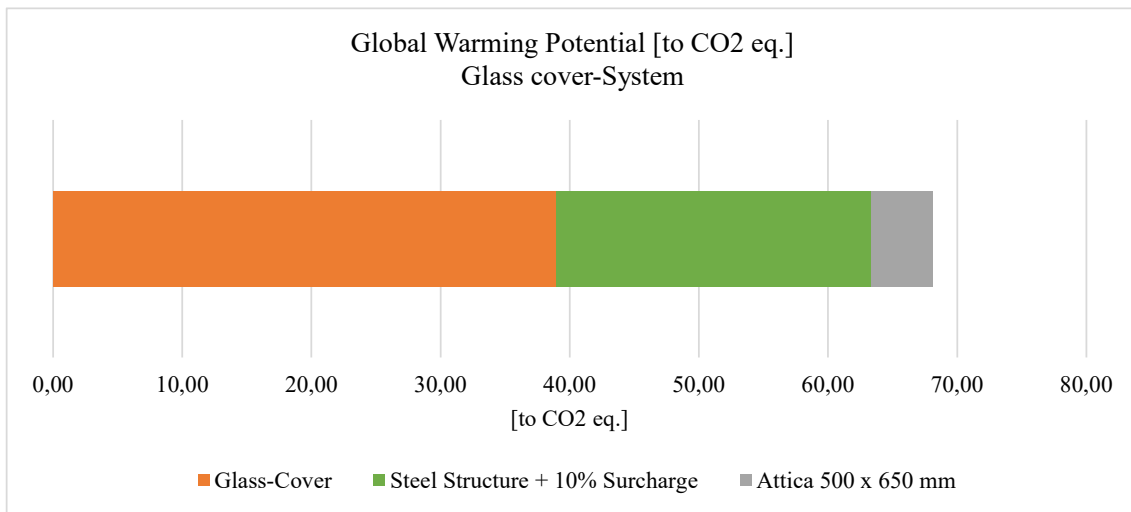


Figure 6: Visualization of LCA Analysis of the glass cover

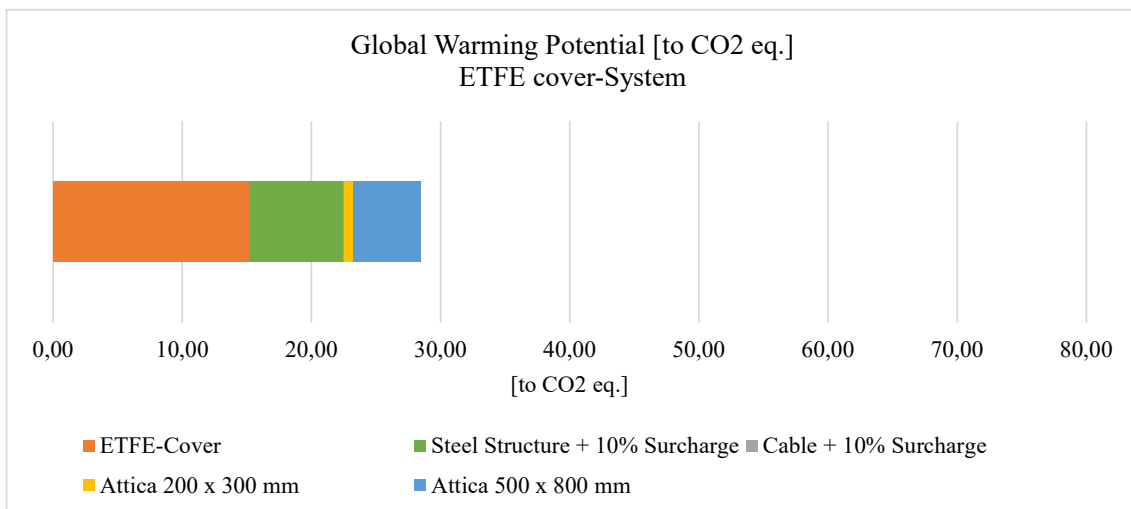


Figure 7: Visualization of LCA Analysis of the ETFE cover

This simple comparison, based on the material level, shows that a material analysis via the EPDs is already worthwhile in terms of a sustainable construction. The reduction of weight through light long-span structures has a significant influence on the primary structure and the entire building, whereby the use of resources and embodied emissions can be saved.

For this reason, the ETFE cushion will be examined in more detail as the preferred variant in the following.

The foil cushion (option 02) meets the criterion of structural lightweight construction perfectly, since they consist exclusively of tension elements and one pressure element: air. The thin foils transmit the tensile forces, the air cushion enclosed between them transfers the load via pressure into the respective load-dissipating foil (figure 8). The upper foil supports wind suction and the lower foil supports wind pressure. Bending and thus stability problems do not exist with foil cushions. The cushions are a closed system which, as long as the tensile loads at both ends of the single cushion are equal, stabilizes the steel arches. At the end cushion there is no

Membrane architecture: the seventh established building material. Designing reliable and sustainable structures for the urban environment.

counterpart which is why the edge beam experiences a bending stress due to the hinged support. With regard to the overall static system, this is not optimal. A continuous compression ring would be better suited as a stand-alone system to transport only compressive stresses and not bending moments. For transport and assembly, however, the division of the outer ring into individual links is helpful.

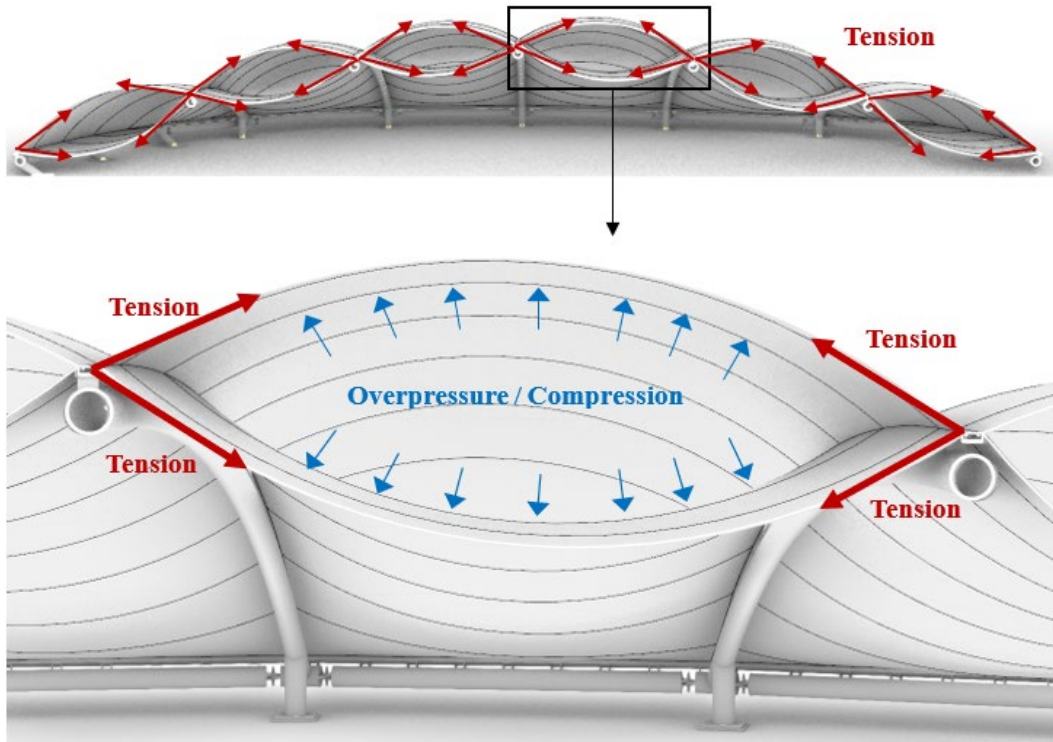


Figure 8: Structural System of a Foil Cushion

At the edge, the planner chose a rigid edge beam, which transfers the lateral tensile load of the cushions via bending moments. This is not optimal from the point of view of structural lightweight design and might in other solutions be replaced by a ring or cables.

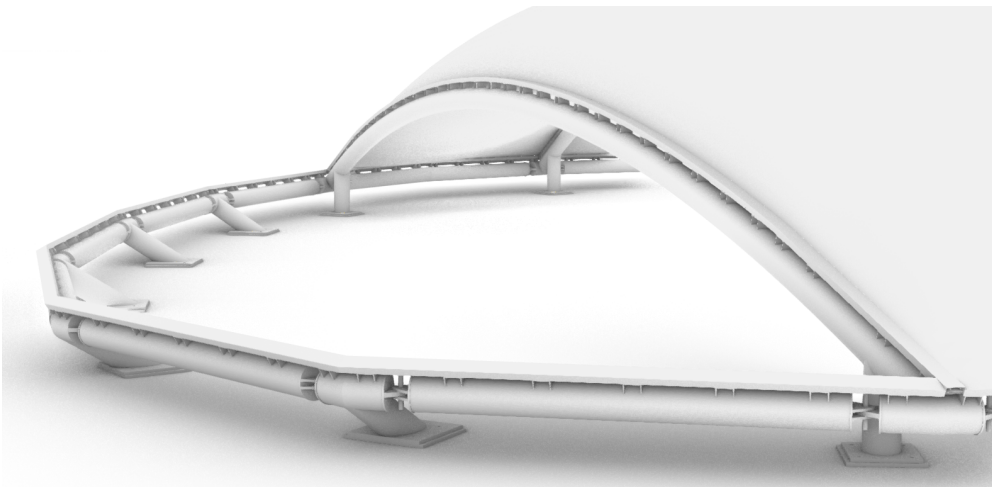


Figure 9: Edge of the EFE-Cushion structure

Membrane architecture: the seventh established building material. Designing reliable and sustainable structures for the urban environment.

3.4 Building Level

ETFE foil cushions can not only be used as a building enclosure with a load-bearing function, but also offer other possibilities in addition to light penetration. In this case, photovoltaic modules are attached to the cushion to generate solar energy for the pumps that regulate the internal pressure of the cushion. If the top layer is, for example, printed, pigmented or provided with a radiation-influencing coating, the solar transmission and energy transfer into the building may also be controlled. The amount of radiation that is transmitted through the cushion into the interior can be adjusted to reduce mechanical air conditioning but still allows enough light to pass through and thus saving energy.



Figure 10: ETFE cushion atrium roof including photovoltaic modules

The ETFE foil cushion thus fulfils the desire for a transparent supporting structure that can even control the incidence of light and shading, as well as energy generation with the use of photovoltaic modules, here by providing additionally a symbolic design option.

4. Conclusion and Outlook

The applicability of the bottom-up educational concept for the sustainability aspects of structures has been demonstrated using the example of the P&S building for the African Union in Addis Ababa, Ethiopia. And furthermore a comparative study for the global warming potential of a lightweight structure made of ETFE cushion has been confronted with the one of a common glass-steel option. From the material level comparing the weight of the envelope

Membrane architecture: the seventh established building material. Designing reliable and sustainable structures for the urban environment.

materials of both solutions, to the system level taking into account the weight of the primary structure of the two transparent atrium roof solutions and an LCA for the GWP including considerations of further optimization possibilities the educational levels have been described up to the building level. In further studies more environmental aspects will need to be included into the LCA on the system level to the detailed investigation and calculation of certification systems on the building level. In this first study already the advantages of a lightweight structure compared to a common solution could be shown.

References

- [1] Bögner-Balz, H., Moritz, K. and Von der Weth, S. (2022) Sustainability Aspects in lightweight construction: How can education improve the state of the art of sustainable construction?, *Advanced Building Skins, Proceedings* S. 112 ff, Bern 2022
- [2] Moritz, K. (2009) *Entwurfsaspekte von ETFE-Folienpneus / Design Aspects of ETFE-Foil Cushions, Innovativ Konstruieren / Innovative design, Special Issue, Detail Business Information GmbH, München*
- [3] Moritz, K. (2011) *Funktionaler Leichtbau – Möglichkeiten mit ETFE-Folien-Fassaden / Functional Lightweight Construction - Possibilities with ETFE-Foil-Facades, Looking into the Future, 3rd VDI Conference, Düsseldorf*
- [4] Moritz, K. (2020) *Form follows Sustainability, Essay, Architectural Membrane Association (AMA), www.amaforum.com, Dessau*
- [5] *United Nations Environment Programme (2022) Global Status Report for Buildings and Construction: Towards a Zero-emission, Efficient and Resilient Buildings and Construction Sector. Nairobi, download 12.02.2023*
- [6] *CO₂ emissions from buildings and construction hit new high, leaving sector off track to decarbonize by 2050 (2023) UN, download 08.02.2023*
- [7] M-EPD-FEV-GB-002000 – flat glass, toughened safety glass and laminated safety glass
- [8] M-EPD-MIG-GB-002000 – Insulating glass units double and triple glass configurations
- [9] EPD-TAI-20190092-ICB1-EN – TensoSky®-System with Fluon® ETFE-film
- [10] EPD-BFS-20180116-IBG2-DE – Baustähle: Offene Walzprofile und Grobböeche
- [11] EPD-IZB-20180101-IBG1-DE – Beton der Druckfestigkeitsklasse C25/30



tensinantes2023 : TensiNet Symposium 2023 at Nantes Université

Membrane architecture: the seventh established building material. Designing reliable and sustainable structures for the urban environment.

Proceedings of the Tensinet Symposium 2023

TENSINANTES2023 | 7-9 June 2023, Nantes Université, Nantes, France

Jean-Christophe Thomas, Marijke Mollaert, Carol Monticelli, Bernd Stimpfle (Eds.)

The environmental performance of membrane structure: OCMW Zoutleeuw case study.

Zehra Eryuruk ^{a,*}, Marijke Mollaert ^b, Danny Van Hemelrijck ^a, Lars De Laet ^b

^{*}Vrije Universiteit Brussel (VUB) Dept. Mechanics of Materials and Constructions,

Pleinlaan 2, 1050 Brussels

Zehra.eryuruk@vub.be

^a Vrije Universiteit Brussel (VUB) Dept. Mechanics of Materials and Constructions, Pleinlaan 2, 1050 Brussel, Belgium

^b Vrije Universiteit Brussel (VUB) Dept. Architectural Engineering, Pleinlaan 2, 1050 Brussel, Belgium

Abstract

Membrane structures are lightweight spatial structures made of tensioned membranes. They are mostly structurally optimized and highly efficient, prefabricated and designed for a varying lifetime. Like with conventional construction systems, it is important to understand and assess the ecological impact of these lightweight constructions.

This research studies the environmental performance of membrane structures by analysing a case study, the ‘OCMW Zoutleeuw’ canopy. In addition, the LCA of the membrane case study is compared with the LCA of a canopy made from steel with a similar size and function. Although the design is different, it allows to see some intrinsic qualities for both.

The literature review shows that few LCA studies on membrane structures have been performed and that LCA data for these structures are still very limited or even not available (such as data for structural steel cables, ETFE-foils, or PTFE-fabric). The existing data in Environmental Product Declarations need to be verified to interpret the results. Generally, the research shows that the impact of the product stage (A1-A3) on the environmental indicators is high, while the ‘end-of-life’ stage (C1-C4) and the ‘benefits and loads beyond the system boundaries’ stage (D) can also have a non-neglectable impact, certainly for temporary structures.

The LCA of the considered membrane structure and of the steel canopy shows that the Global Warming Potential (GWP) for the membrane structure is lower, even if the membrane is replaced during the service life of the canopy, while the available end-of-life processes of the steel/aluminium canopy are beneficial.

Keywords: lightweight structures, structural membrane, sustainability, environmental impacts, life cycle assessments (LCA)

Membrane architecture: the seventh established building material. Designing reliable and sustainable structures for the urban environment.

1. Introduction

Membrane structures are structures made of tensioned fabrics or foils and supported by a primary structure. These structures are lightweight structures, which is one of the biggest advantages of these constructions. It is possible to create large spans with a low amount of material.

While other building technologies engage in ‘ecological’ aims, only little research has been done on how to integrate the Life Cycle Assessment (LCA) into the design and analysis of tensile surface structures [1].

The aim of this paper is to investigate the environmental performance of a membrane case study by means of evaluating the Global Warming Potential (GWP) indicator. Then, the values of the membrane case study will be compared with those of a steel canopy.

The LCA of the two projects is done with the tool OneClickLCA. The tool supports the methodology of the Centre for Environmental Studies (CML) of the University of Leiden as well as the tool for the Reduction and Assessment of Chemical and other Environmental Impacts (TRACI) of the United States Environmental Protection Agency [2]. All the datasets in the tool comply with ISO 14040/14044 [3][4] and most parts also with the EN 15804 standard [5]. The LCA analysis is done following the CML methodology.

To understand the environmental performances of a product, a material, or a construction, a deep analysis of the life cycle is needed. The LCA process starts from raw material extraction going through production, transport, consumer use, and finally disposal and recycling. Figure 1 gives an overview of the different stages considered in the LCA.

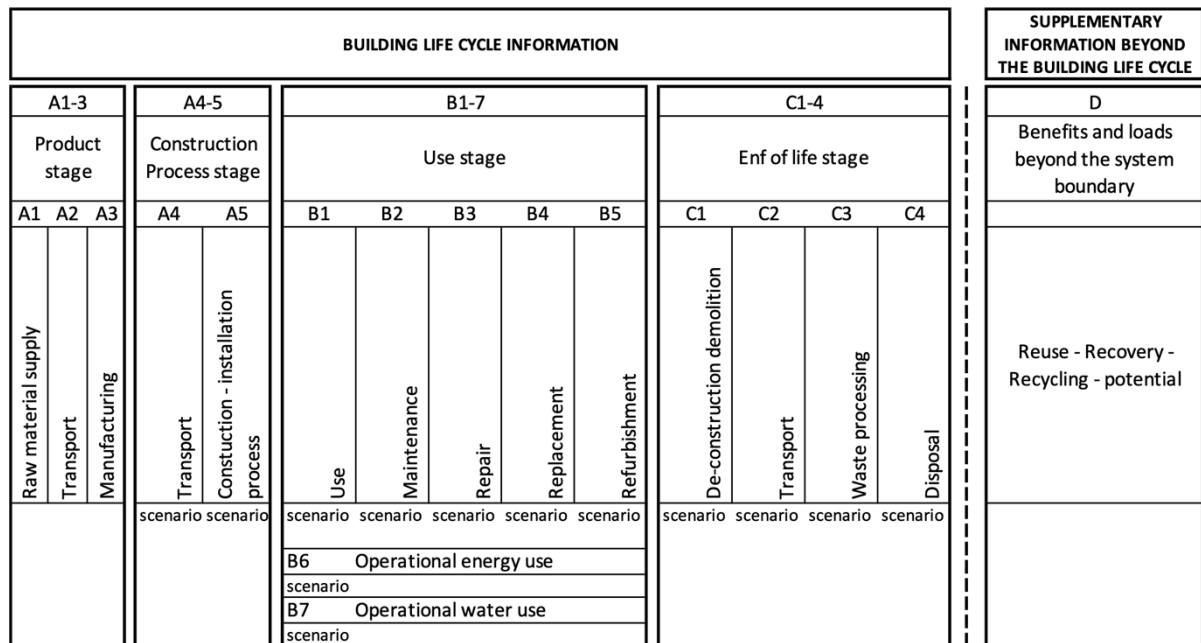


Figure 1: LCA process according to EN 15804+A1:2013 [5]

The LCA assessment tool OneClickLCA gives an overview of the environmental impact per module of the LCA and per building parts classification. It is possible to extract the

Membrane architecture: the seventh established building material. Designing reliable and sustainable structures for the urban environment.

environmental impact per building part e.g., foundation, roof, load bearing elements, etc. The building parts classification is applicable for general constructions, but it should be slightly different for membrane structures. For this reason, we added a new classification for membrane structures in the LCA tool, containing the following parts: (1) foundation, (2) primary structure, (3) membrane/foil, (4) edge cables, (5) system cables, (6) corner plates and accessories.

2. Case study 1: OCMW Zoutleeuw

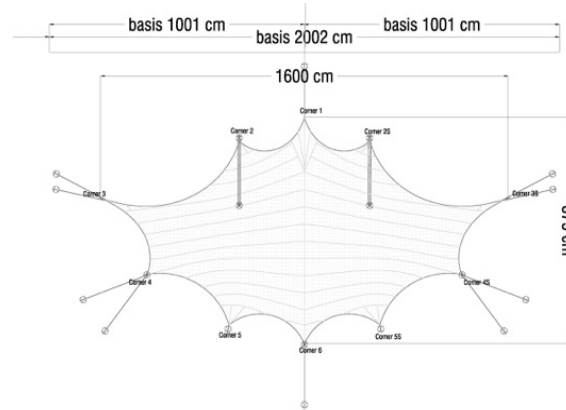


Figure 2: OCMW, Zoutleeuw, ©The Nomad Concept

The membrane structure is designed and executed by The Nomad Concept in 2012 for the OCMW organisation located in Zoutleeuw, in Belgium [6]. The structure has a length of 16 m and a width of 9 m. The total covered area is approximately 64 m².

2.1. Input Data for LCA

The skin of the structure is executed in PTFE-glass fabric from the supplier Verseidag. The fabric type is Duraskin® B 18039 GF type II with a weight of 800 gr/m². Since the environmental performance of the PTFE-glass fabric is not known, the LCA of this project is conducted with a PVC-polyester fabric (VALMEX FR900 Mehler Technologies [7]). 135 m² of fabric was ordered for this project, with a wastage of 25%.

Input data for the LCA assessment is listed in Table 1, specifying the quantity for each building element and the data used (generic data of OneClickLCA or a specific EPD).

Table 1: CS1, input data

Material	Quantity	EPD or Generic Data (GD)
Foundation	30 m ³	GD: Ready-mix concrete, C25/30 CEM I
Steel reinforcement	488 kg	GD: Reinforcement steel, 80% recycled content
Fabric	135 m ²	EPD: VALMEX FR900 Mehler Technologies [7]
Stainless-steel columns	237 kg	GD: Hot rolled stainless steel
Edge cables (incl. thread terminals)	19,52 kg	EPD: Prestressed steel [8]
System cables (incl. fork terminals)	31,69 kg	EPD: Prestressed steel [8]
Stainless-steel corner plates	191,2 kg	GD: Hot rolled stainless steel

Membrane architecture: the seventh established building material. Designing reliable and sustainable structures for the urban environment.

For the transport phases of the LCA different trajectories are applicable depending on the material. Table 2 shows the distances between two facilities and the mode of transport.

Table 2: CS1, transport distances (km)

Transport	Distance	Type of transport
Fabric		
Fabric supplier (DE) → Manufacturing company (PL)	1.046	Group transport, trailer combination
Tailoring company (PL) → The Nomad Concept (BE)	1.223	Group transport, trailer combination
Stainless-steel columns and plates	370	Group transport, trailer combination
Concrete foundation	60	Concrete mixer truck
Stainless-steel cables and accessories		
Supplier → Assembling facility (NL)	681	Group transport, trailer combination
Assembling facility (NL) → The Nomad Concept (BE)	194	Delivery van
All material delivery to site	80	Group transport, trailer combination

At the end of life, the concrete of the foundation will be crushed to aggregates, the metal construction elements will be recycled, and the fabric will be incinerated. Energy recovery from the incineration is considered as a benefit in the module D of the LCA.

For this LCA analysis the construction site operation (B1), repair (B3), annual energy consumption (B6) and the water use (B7) are omitted. The service life of the project is 50 years, hence the fabric needs to be replaced after 25 years (typically for PVC-polyester fabric) or after 30 years (for PTFE-glass fabric).

2.2. Results of LCA

Table 3 and Figure 3 represent the results for the Global Warming Potential (GWP) per module of the LCA. The GWP is 12.542 kgCO₂eq for the whole LCA process. The most impactful are the modules A1 to A3 with a value of 9.790 kgCO₂eq. The second most impactful are the modules B4 and B5, concerning the replacement of the material after 25 years with a value 948 kgCO₂eq. Module A4 represents the transportation to the site and has a GWP of 593 kgCO₂eq. The construction and installation process are represented in module A5 and have a GWP of 630 kgCO₂eq. The A5 module contains mostly a by default given percentage of material wastage on site. Modules C1 to C4 represent the end-of-life situation and have a GWP of 581 kgCO₂eq.

Module D quantifies the net environmental benefits or loads, resulting from reuse, recycling and energy recovery, from the net flows of materials and exported energy exiting the system boundary. The GWP for module D is 2.280 kgCO₂eq, this value is not counted in the total GWP value.

Table 3: CS1, Results GWP – Life-cycles stages

Result category	Global warming (kg CO ₂ eq)	%
A1-A3 Construction Materials	9.790	78,06%

Membrane architecture: the seventh established building material. Designing reliable and sustainable structures for the urban environment.

A4	Transportation to site	593	4,73%
A5	Construction/installation process	630	5,02%
B4-B5	Material replacement and refurbishment	948	7,56%
C1-C4	End of life	581	4,63%
D	External impacts (not included in Total)	-2.280	
	Total	12.542	100%

Beside considering the LCA modules it is possible to analyse the results for the building parts (Figure 4 and further Table 9). From the total GWP results for the building parts it can be derived that the concrete foundation is the most impactful material. The concrete foundation represents 74,88% (9.400 kgCO₂eq) of the total GWP. The second impactful material is the membrane with 17,05% (2.100 kgCO₂eq). All the steel, including primary structure, cables, corner plates and accessories, is 8,07% (1.020 kgCO₂eq) of the total GWP.

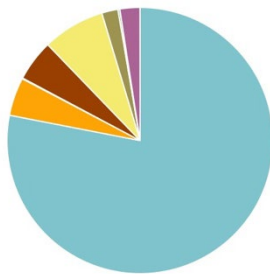
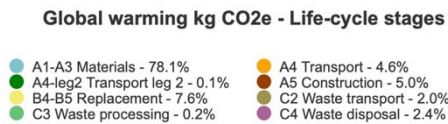


Figure 3: CS1, GWP - LCA stages

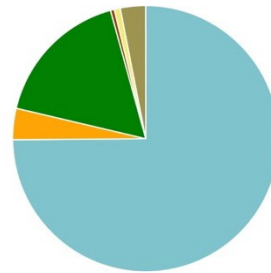


Figure 4: CS1, GWP – Classifications

3. Case study 2: Pavillon Place de Gaulle

The pavilion at the square Place Charles de Gaulle in Eure, France is designed by Lafayette architecture office and engineered by Bollinger + Grohmann engineering office [9][10]. The structure has been designed in 2022 and is currently under construction.

This structure, although different, but similar in size and function, was chosen as a second case study to be able to evaluate the LCA results of the membrane canopy. The circular structure has an outer diameter of 12m and an opening with a 4,8m diameter. The total covered surface is 95m². The height of the structure is approximately 4m.

Membrane architecture: the seventh established building material. Designing reliable and sustainable structures for the urban environment.

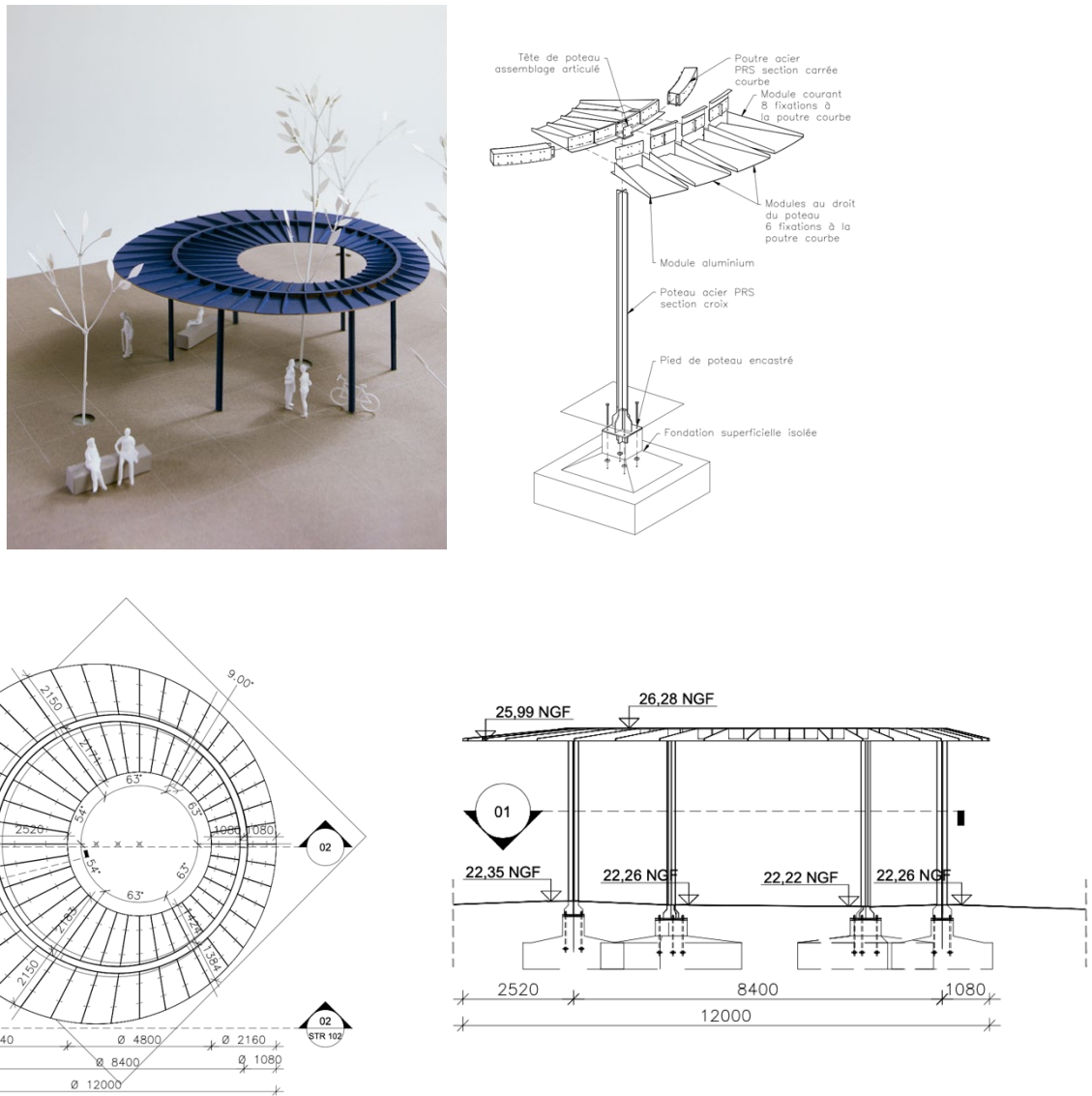


Figure 5: Pavillon Place de Gaulle, © Lafayette Archi, Bollinger and Grohmann

3.1. Input Data for LCA

Based on the bill of materials of this project, Table 4 gives an overview of the materials used for this LCA assessment.

Table 4: CS2, input data

Material	Quantity	EPD or Generic Data (GD)
Foundation		
Blinding concrete	12,7 m ³	GD: Ready-mix concrete, C12/15 CEM I
Concrete	19,94 m ³	GD: Ready-mix concrete, C35/45 CEM I
Steel reinforcement	3589,92 kg	GD: Reinforcement steel, 80% recycled content

Membrane architecture: the seventh established building material. Designing reliable and sustainable structures for the urban environment.

Reconstituted welded steel column	2254 kg	EPD: Reconstituted welded steel used as structural element [11]
Reconstituted welded steel column top and bottom	338 kg	EPD: Reconstituted welded steel used as structural element [11]
Paint coating	25 m ²	EPD: Anti-corrosive paints [12]
Cover plates	0,54 m ²	GD: Hot-dip galvanized steel sheets
Reconstituted welded steel beams	2166 kg	EPD: Reconstituted welded steel used as structural element [11]
Reconstituted welded steel beam connection elements	324,90 kg	EPD: Reconstituted welded steel used as structural element [11]
Paint coating	30 m ²	EPD: Anti-corrosive paints [12]
Stainless-steel screws	50kg	GD: Stainless steel screws
Aluminium sheets	114 m ²	GD: Aluminium sheet
Cover plates	0,54 m ²	GD: Hot-dip galvanized steel sheets

The reinforcement steel is assumed to have 80% recycled content. The wooden formwork is not taken into consideration. The 6 columns are welded steel columns. The columns are hot galvanized and have paint coatings. The column tops are covered with a sheet, assumed to be hot-dip galvanized. The 6 beams forming the circle are curved 230mm square section beams with a thickness of 12mm. The beams are hot galvanized and have paint coatings. The covering material of the canopy is made from folded aluminium sheets of 6mm thick. Due to the missing information the wooden formwork, anodization and galvanisation processes described in the bill of materials are not taken into consideration for this assessment.

For the transport phases of the LCA default values of OneClickLCA are taken into consideration. Table 5 gives the default values used for the transport.

Table 5: CS2, transport distances (km)

Transport	Distance	Type of transport
Foundation		
Blinding concrete	60	Concrete mixer truck
Concrete	60	Concrete mixer truck
Reinforcement steel	370	Group transport, trailer combination
Reconstituted welded steel columns and beams	370	Group transport, trailer combination
Aluminium sheets	470	Group transport, trailer combination
Hot-dip galvanized steel sheets	370	Group transport, trailer combination

At the end of life, the concrete will be crushed to aggregates and all the metal components (steel and aluminium) used for the structure will be recycled.

Membrane architecture: the seventh established building material. Designing reliable and sustainable structures for the urban environment.

For this LCA analysis the construction site operation (B1), repair (B3), annual energy consumption (B6) and the water use (B7) are omitted. The service life of the project is 50 years. Paint coatings need to be refreshed every 10 years [12].

3.2. Results of LCA

Table 6 and Figure 6 represent the results for the GWP per module of the LCA. The GWP is 31.594 kgCO₂eq for the whole LCA process. The most impactful are the modules A1 to A3 with a value of 28.700 kgCO₂eq. The second most impactful is the module A5, construction and installation process, which has a GWP of 1.270 kgCO₂eq. The A5 module contains mostly a by default given percentage of material wastage on site. Module A4 represents the transportation to the site and has a GWP of 751 kgCO₂eq. The material replacement and refurbishment, modules B4-B5, in this case the refreshment of the painting, has a GWP of 153 kgCO₂eq.

The GWP for module D is 24.300 kgCO₂eq, this value is not counted in the total GWP value.

Table 6: CS2, Results GWP – Life-cycles stages

Result category		Global warming (kg CO ₂ eq)	%
A1-A3	Construction Materials	28.700	90,83%
A4	Transportation to site	751	2,38%
A5	Construction/installation process	1.270	4,02%
B4-B5	Material replacement and refurbishment	153	0,49%
C1-C4	End of life	720	2,28%
D	External impacts (not included in Total)	-24.300	
Total		31.594	100%

The total GWP results for the building parts of this case study (Figure 7 and further Table 9) show that the three materials, concrete, steel and aluminium have almost the same impact. The concrete foundation represents 39,15% (12.300 kgCO₂eq) of the total GWP. The roof, which represents the aluminium sheet covering, is 25,18% (7.940 kgCO₂eq) of the total GWP. All the steel, including columns, beams, connection plates and screws is 35,67% (11.300 kgCO₂eq) of the total GWP.

Membrane architecture: the seventh established building material. Designing reliable and sustainable structures for the urban environment.

Global warming kg CO₂e - Life-cycle stages

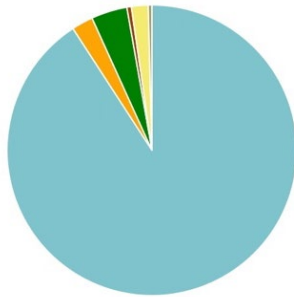


Figure 6: CS2, GWP - LCA stages

Global warming kg CO₂e - Classifications

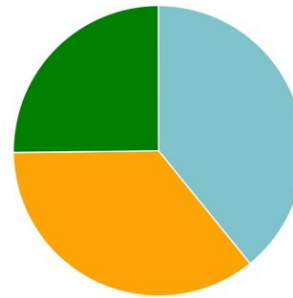
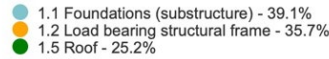


Figure 7: CS2, GWP - Classifications

4. Comparing the case studies.

General data for the two case studies is listed in Table 7. The service life of the two case studies is 50 years. For CS1 a replacement of the fabric is considered after 25 years and for CS2 the painting needs to be replaced every 10 years. The weight of the concrete foundation for both cases is quite similar. For that reason, only the weight of the steel structure and the skin are considered. The self-weight/m² covered area of CS1 is 7,77 times lower than for CS2. The skin represents 20% of the total self-weight (excluding foundations) for CS1 and 26% for CS2.

Table 7: Evaluation CS1 & CS2

	CS1	CS2
Service life	50 years	50 years
Service life skin/coating	25 years	10 years
Size	16mx9m	Dia 12m
Covered area	64m ²	95m ²
Structure (steel)	479,41kg	5133kg
Skin (membrane/aluminium)	135m ²	114 m ²
	122kg	1800kg
Self-weight/ m ²	9,4kg/ m ²	73kg/ m ²
%Skin (self-weight)	20%	26%

It is not correct of course to compare in absolute values two different constructions with different sizes. However, by comparing the values per square meter and looking at ‘order of magnitudes’, we hope to gain some ‘qualitative’ insights in the LCA of a membrane structure and a steel/aluminium canopy. To evaluate the two case studies, the GWP is calculated per

Membrane architecture: the seventh established building material. Designing reliable and sustainable structures for the urban environment.

square meter of covered area. The membrane structure (CS1) has a covered area of 64m² and the steel canopy structure (CS2) has a covered area of 95m².

Table 8 gives for the two case studies the GWP per covered area for all modules of the LCA. Case study 2 has a larger GWP per m² compared to case study 1 with a factor of 1,7. This difference is mainly due to the modules A1 to A3, which represent the construction materials. The GWP per m² for the modules A1 to A3 for CS2 is 2 time higher than for CS1. The modules A4, A5 and C1 to C4 for the two case studies have similar values. The replacement of the fabric for CS1 and the replacement of the painting for CS2 are represented in module B4-B5. The GWP per m² for the module B4-B5 of CS1 is 7,5 times higher compared to CS2 and this is due to the higher environmental impact of the PVC coated polyester fabric compared to paint.

The GWP per m² for module D for CS2 is almost 7 times higher than for CS1. This shows that the recycling process has a greater benefit. The GWP of module D is not included in the total GWP of the case studies, but if benefits beyond the system boundary are to be included, the total GWP/m² for CS1 is 160 kgCO₂eq/m² (196-36 kgCO₂eq/m²) and for CS2 is 77 kgCO₂eq/m² (333-256 kgCO₂eq/m²).

Table 8: Results GWP per m² covered area – Life-cycles stages for CS1 & CS2

Result category		CS1: GWP (kg CO ₂ eq)	CS1: GWP/m ² (kg CO ₂ eq/m ²)	CS2: GWP (kg CO ₂ eq)	CS2: GWP/m ² (kg CO ₂ eq/m ²)
A1-A3	Construction Materials	9.790	153	28.700	302
A4	Transportation to site	593	9	751	8
A5	Construction/installation process	630	10	1.270	13
B4-B5	Material replacement and refurbishment	948	15	153	2
C1-C4	End of life	581	9	720	8
D	External impacts (not included in totals)	-2.280	-36	-24.300	-256
Total		12.542	196	31.594	333

The GWP per m² covered area can also be specified per building part.

The two case studies are shown in Table 9. The membrane structure (CS1) has a concrete foundation, steel elements include the columns, system cables, edge cables, fixing accessories for cables and corner plates, and a PVC coated polyester membrane roof covering. The steel structure with aluminium roof covering (CS2) has a concrete foundation, the steel elements include the columns, the beams and assembling pieces, and an aluminium sheet roof covering.

The GWP per m² covered area for the concrete foundation is comparable for the two case studies. For the steel elements the GWP per m² is 7,5 times higher for CS2 than for CS1. For the roof, which is a membrane material for CS1 and aluminium sheets for CS2, the GWP per covered area for CS2 is 2,5 times higher than CS1.

Membrane architecture: the seventh established building material. Designing reliable and sustainable structures for the urban environment.

Table 9: Results GWP per m² covered area – Building parts for CS1 & CS2

Building Parts	CS1: GWP (kg CO ₂ eq)	CS1: GWP/m ² (kg CO ₂ eq/m ²)	CS2: GWP (kg CO ₂ eq)	CS2: GWP/m ² (kg CO ₂ eq/m ²)
Foundation	9.400	147	12.300	130
Steel elements	1.020	16	11.300	119
Roof covering (Membrane or aluminium)	2.100	33	7.940	84

5. Conclusion

This research investigated the environmental performance of a membrane case study by means of evaluating the Global Warming Potential (GWP) indicator. The values of the membrane case study were compared with a steel canopy. Two completely different projects are compared, meaning the conclusions should be seen in this perspective.

Regarding the comparison between CS1 and CS2, where the covering material is a membrane material for CS1 and aluminium sheets for CS2, it is shown that the total GWP per m² covered area for the membrane is for these case studies 1,7 times lower compared to the aluminium covering material.

The tensioned fabric works as a structural element in tension and all connections are pinned. By designing lightweight, it is possible to create more with less. Using a minimum amount of material gives an advantage on the environmental impact of the primary structure. For this reason, the impact of steel for the membrane structure is lower compared to the stiff frame structure.

Figure 8 gives an overview of GWP/m² covered area for CS1 and CS2. The membrane structure is known for being lightweight and it is shown in this study that the self-weight/ m² covered area for a membrane structure (not considering foundations) is much lower compared to a more traditional canopy. This gives an advantage with a lower GWP/m² covered area. The biggest advantage of CS2 is on the end-of-life scenario, all material is recyclable and the environmental benefits resulting from the recycling potential is higher than for the membrane structure.

Membrane architecture: the seventh established building material. Designing reliable and sustainable structures for the urban environment.

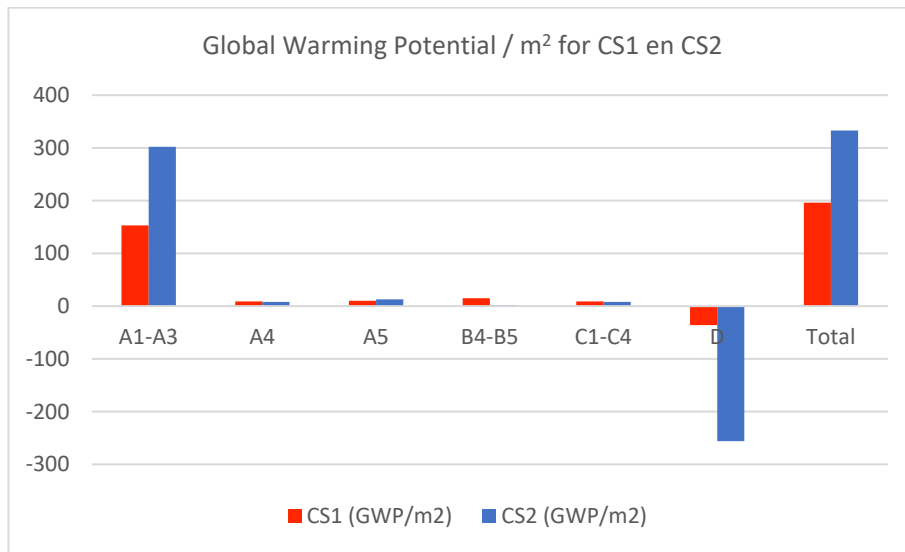


Figure 8: Comparison CS1 & CS2, LCA modules

The membrane as material is a composite material and the end-of-life treatment for now is incineration or landfill. Further research is needed to improve the end-of-life scenarios.

Following this study, the membrane structure is well positioned in terms of environmental performance compared to a canopy made of aluminium and steel.

It is in this research not the intention to weigh up the architectural qualities of both projects against each other. The intention is, however, to indicate that the choice of shape and material must be made consciously, including the criteria of environmental performance.

Acknowledgements

The authors would like to thank the companies “The Nomad Concept” and “Bollinger and Grohmann” for providing the data of their projects.

References

- [1] Monticelli C., Zanelli A. (2016), Life Cycle Design and Efficiency Principles for Membrane Architecture: Towards a New Set of Eco-design Strategies. In: *Procedia Engineering*, vol. 155 (pp. 416-425).
- [2] <https://www.epa.gov/chemical-research/tool-reduction-and-assessment-chemicals-and-other-environmental-impacts-traci>
- [3] ISO 14040:2006. “*Environmental management - Life cycle assessment - Principles and framework*”. International Standardization Organization, Geneva, Swiss, 2006.
- [4] ISO 14044:2006. “*Environmental management - Life cycle assessment - Requirements and Guidelines*”. International Standardization Organization, Geneva, Swiss, 2006.

Membrane architecture: the seventh established building material. Designing reliable and sustainable structures for the urban environment.

[5] EN15804:2012 +A1. “*Sustainability of construction works - Environmental product declarations - Core rules for the product category of construction products*”. European Committee for Standardization (CEN), 2013.

[6] <https://nomadconcept.eu/portfolio/ocmw-zoutleeuw/>

[7] 2012, VALMEX ®FR900 Mehler Technologies GmbH, Environmental Product Declaration IBU, Germany

[8] 2020, Siderurgica Latina Martin S.p.A., Environmental Product Declaration Kiwa BCS Öko-Garantie GmbH - Ecobility Experts, Germany

[9] <http://www.lafayette.archi/fr/projets/pavillon-vernon>

[10] <https://www.bollinger-grohmann.com/en.projects.pavillon-place-charles-de-gaulle.html?f=current>

[11] 2022, Centre Technique Industriel de la Construction Métallique (CTICM, producteur de la FDES), Environmental Product Declaration INIES, France.

[12] 2019, International AkzoNovel, Environmental Product Declaration Stickting MRPI®, Netherland.

[13] EN 15978:2011. “*Sustainability of construction works - Assessment of environmental performance of buildings - Calculation method*”. European Committee for Standardization (CEN), 2011.

[14] Forster B., and Mollaert M. (eds.) (2004), European design guide for tensile surface structures: TensiNet, TensiNet.

[15] <https://www.oneclicklca.com>



tensinantes2023 : TensiNet Symposium 2023 at Nantes Université

Membrane architecture: the seventh established building material. Designing reliable and sustainable structures for the urban environment.

Proceedings of the Tensinet Symposium 2023

TENSINANTES2023 | 7-9 June 2023, Nantes Université, Nantes, France

Jean-Christophe Thomas, Marijke Mollaert, Carol Monticelli, Bernd Stimpfle (Eds.)

A comparative LCA between a Textile Façade Retrofit and conventional solutions

Giulia Procaccini*, Carol Monticelli ^a

*Ph.D Candidate, ABC Department, Politecnico di Milano, Via Ponzio 31, 20133 Milan (Italy), email: giulia.procaccini@polimi.it

^aAssociate Professor, ABC Department, Politecnico di Milano, Via Ponzio 31, 20133 Milan (Italy)

Abstract

Building skins play a crucial role in achieving the goal of the carbon neutrality of the building stock within 2050, as they account for 20-30% of the overall global energy consumptions. Therefore, it drives an assessment of the potential impact of widespread façade retrofit as a means to improve building sector energy performances and to reduce energy consumptions and related carbon emissions.

Architectural textiles present high advantages and potentials in façades applications thanks to their intrinsic properties, unveiling great potentialities in retrofit solutions.

This paper assesses both the impact and the advantages of the employment of textiles materials in retrofit applications in terms of Life Cycle Assessment (LCA) and Life Cycle Costing (LCC) in comparison with conventional methods. The analysis aims to validate the existing results about the potentialities of these materials in case of first life proving their efficiency also in retrofit practices.

The research is conducted through a comparative LCA and LCC audit for evaluating the potentialities of innovative Textile Façade Retrofit Strategies (TFRS). The research aims at evaluating the environmental potentialities of TFRS through the integration within the design phase of the environmental dimension of the material, the optimization of the construction phase and an appropriate design. The outcome of the analysis showcases which parameters make TFRS competitive in the field, revealing further considerations for the optimization of the material and its application.

Keywords: Textile Façades, Envelope Retrofit, Resilient Constructions, Sustainability, LCA, Environmental impact, Lightweight Structures

1. Introduction

The raised awareness about the environmental vulnerability, with the general need and research for sustainable solutions and resilient approaches is affecting even the construction sector, which represents one of the larger energy consumers worldwide. Despite the advanced age of

Membrane architecture: the seventh established building material. Designing reliable and sustainable structures for the urban environment.

the European building stock, the expectation towards their service life is still long. The consequent need for the renovation of the asset, through fast, low-cost and environmental-friendly solutions, opens up the research to potential applications of membranes over existing façades.

Indeed, if the use of membranes in vertical walling systems started in the advertising industry [Monticelli et al. 2013], nowadays, thanks to their intrinsic and valuable properties such as lightness, thinness and flexibility, they are being used more and more in the building field with different applications [Chilton J., 2010; Pohl and Pohl, 2010]. It follows that the retrofit of buildings to improve their environmental performances represents an expanding field for fabrics and foils.

The analysis of the environmental impact of a TFR solution allows designers in developing retrofit proposals based on overall environmental performances of lightweight façades. A comparative analysis between a textile retrofit solution and conventional ones helps in determining which are the parameters that make one solution more sustainable than the others.

This investigation, based on a Case-Study, intend to compare three different façade retrofit designs which, based on similar approaches but achieved with different materials, highlight the differences in terms of both environmental and economic impacts, proving how the design choices affect the outcome [Monticelli et al.2017]. The analysis focuses merely on the outer layer of the façade, considering the energetic performances of the existing building as “constant” throughout the three options. The aim of the analysis is to detect which are the parameters that majorly affect the results, therefore making textiles competitive as materials for the façade retrofit. The achieved data will be helpful for further research steps both at the production level and at the application level: they will influence manufacturers in the optimization of the product as well as designers supporting their decision into to the design phase.

2. Methodology

The methodology applied for the analysis consists of a LCA and a cost comparative analysis between the identified Case-Study and two hypothetical alternative solutions. In accordance with ISO 14040 and ISO 14044 [ISO 14040, 2021; ISO 14044, 2021], the LCA framework was selected for this analysis and structured in five sections: (i) goal and scope definition; (ii) system boundaries and functional unit; (iii) life cycle inventory analysis; (iv) life cycle impact assessment; (v) result interpretation and comparison with previous analyses.

The software One Click LCA was used for running the analysis. Its internal database integrates data from nearly all of the available EPD platforms around the globe, complying with EN15804 and/or ISO 14025 standards. The EPD included in the analysis have been taken from the global databases ecoinvent and GaBi. The databases served as the primary source for obtaining the life cycle inventory data of all manufacturing process voices related to the building materials involved in the comparisons. The sustainability metrics in the paper consists in the investigation of the building carbon footprint in accordance with the LCA methodology.

2.1. Goal and scope definition

The main goal of the LCA and LCC analysis is to investigate and to compare the environmental impact of three different façade retrofit solutions applied as the finishing layer within a façade restyling intervention on two existing façades of a tertiary building. Considering that the

Membrane architecture: the seventh established building material. Designing reliable and sustainable structures for the urban environment.

application of membranes over existing façades represents the current practice in the use of textiles in cases of façade retrofitting for tertiary architecture, it serves as a typological case-study for façade retrofit interventions achieved with membranes.

Located in Darfo Boario Terme (BS), Italy, the “Iperal Shopping Mall -Adamello” underwent restoration in 2015: its two main existing façades were partially substituted with a textile one. The current analysis aims at comparing the Case-Study with two hypothetical façade retrofit alternatives achieved respectively with a system made of (a) polycarbonate panels and a second one made of (b) perforated aluminium panels. The two alternatives have been designed according to their characteristics that allow for a result of a translucent effect. The material choice was additionally affected by the technological system, which, in all the three cases, requires a similar substructure for the fixing of the elements. Polycarbonate panels have considered in order to compare same end-of-life treatments in relation to various amounts of materials, too.

This LCA assesses the carbon footprint of three distinct façade solutions, with the goal of understanding both the relationship between the environmental impacts of each system's fixing tools and cladding layers, and the effects of partial element replacements during the building façade's life cycle, including the demolition phase and end-of-life waste treatment. The study focuses on identifying the environmental impacts of the materials over their pre-use phases until the transports to the building site and, successively, over their substitution and demolition phases, determining which aspect of each technology has to be improved in order to reduce the overall environmental impact caused by façade systems.

The results of the analysis are expected to assist both manufacturers in the optimization of the waste treatment phase and designers with a better understanding of building material selection and system improvement from the life cycle perspective. Considering that open mesh fabrics (PES/PVC), Polycarbonate panels and Aluminium perforated panels have important differences in their material composition and system size, these were considered in order to design the modularity of the façade, to dimension the fixing systems and consequently to compute the material flow chart, with relation to the functional unit.

2.2. System boundaries and functional unit

The processes examined within this LCA deals with the Product Stage A1-A3 phase, the A4-A5 Construction phases (transportation to the building site and installation process), the B4-B5 Replacement and Refurbishment stages and C1-C4 end-of-life phase. The operational phase, excluding the Replacement and Refurbishment stages, is omitted as it is considered "constant." This is because the analysed façade restyling focuses solely on its outer layer, without interfering with the existing structure or external partitioning wall system. However, the B6 phase (operational energy use) is an exception, as it is influenced by the design and characteristics of the finishing layer. Thus, this study analyses the environmental impact only of the pre-use phase, leaving for a further analysis the study of the effect of the finishing system on the operational energy use.

The functional unit for the LCA consisted in the two main façades of the commercial building with a height of 11,10 m and a length of 163,25 and 167,80 m, respectively. Within the comparison of the three alternatives, two coatings have been considered as a constant: the wall paint, which accounted for 1011 sqm of the total of the two façades, and the expanded galvanized steel sheet which had been used for marking the entrances to the building, for a total of 582 sqm. The technical textile cladding, for a total of 2390 sqm, and its substructure (with

Membrane architecture: the seventh established building material. Designing reliable and sustainable structures for the urban environment.

variable kg) represent the core materials whose application has been compared to the one of (a) polycarbonate panels and (b) perforated aluminium panels.

2.3. Life cycle inventory analysis

The specification and quantities about the case-study itself (in terms of extension of the project, existing structure etc.) and those ones related to the textile façade retrofit intervention (with regard to the quantities of the material used, the cost and time of the project) have been provided by the structural designer and manufacturer of the system. Consequently, the two hypotheses in polycarbonate panels and perforated aluminium panels have been developed respectively: the above-mentioned data have been adapted to the hypothesized solutions based on the data acquired through the Literature Review.

2.3.1 Case – Study

For the membrane cladding, two different types of membranes have been used: technical textiles in PES/PVC open mesh, one preventing the 97% of heat gains when it is installed as outer layer, and the second one which presents a high resistance to UV rays, rain and wind combined to a high breathability for humidity regulation and thermal insulation. The juxtaposition of these two allowed the creation of a uniform and continuous façade surface, with the first membrane applied over the opaque façade and the second over the windows areas. The technology adopts a system based on aluminium profiles and steel fixing elements for the substructure, on top of which the pre-tensioned membrane is assembled. The design of the facade has been achieved with a PES/PVC open mesh with a weight of 0,42kg/sqm and a thickness of 0,45mm, which has been pre-tensioned into rectangular aluminium frames for a total of 1752 lm. The steel fixing elements contribute for a total weight of 1250 kg (0,033 kg/unit). The service life of the material has been considered in 15 years, as indicated in its EPD and its end-of-life treatment consists in the plastic-based material incineration, according to the current state of the art for the material.

Table 1: Case-Study – Textile cladding

	MATERIAL	QUANTITY	UNIT WEIGHT	KG TOT	SERVICE LIFE	END OF LIFE
Sub-structure	EPS extruded aluminum profiles frame	1752 lm	1,58 kg/lm	2768,16 kg	As building	Aluminum recycling
	Clips	37886 units	0,033 kg/unit	1250,24 kg	25 years	Steel recycling
Cladding	Pre-tensioned membrane Soltis 92 sandblasted beige colour	1210 sqm	0,42 kg/sqm	1003,8 kg	15 years	Plastic-based material incineration
	Pre-tensioned membrane Soltis 92 biting colour	1180 sqm				
	Expanded metal panels in pre-painted galvanized steel type fils model esperia RAL 7046, 1019, 8012	582 sqm	7850 kg/mc	18000 kg	As building	Steel recycling
	Existing masonry painting	1011 sqm	0,69 kg/sqm	697,6 kg	10 years	Landfilling

2.3.2 Option 1 – Polycarbonate panels:

In the case of polycarbonate panels as outer layer, a translucent multi-wall cellular polycarbonate cladding has been considered. It presents very strong resistance to the degrading effects of solar radiation and has excellent thermal properties that allow for immediate energy savings. The panels considered have a dimension of 700x2000 mm, a thickness of 60 mm and a weight of 72 kg/sqm.

Membrane architecture: the seventh established building material. Designing reliable and sustainable structures for the urban environment.

The panels are supported by vertical and horizontal aluminium profiles for a total of 1576 lm placed along the façade without the extra support of any clip as the system foresees a male-female joint between the panels.

The service life of the material has been considered in 25 years and its end-of-life treatment consists in the plastic-based material incineration, as indicated in its EPD.

Table 2: Opt. 1 – Polycarbonate panels cladding

	MATERIAL	QUANTITY	UNIT WEIGHT	KG TOT	SERVICE LIFE	END OF LIFE
Sub-structure	Uprights in extruded aluminum profiles	360 lm	1,58 kg/lm	2490,08 kg	As building	Aluminum recycling
	Crossbars in extruded aluminum profiles	1216 lm				
Cladding	Polycarbonate panels	2390 sqm	72 kg/sqm	172080 kg	30 years	Plastic-based material incineration
	Expanded metal panels in pre-painted galvanized steel type fils model esperia RAL 7046, 1019, 8012	582 sqm	7850 kg/mc	18000 kg	As building	Steel recycling
	Existing masonry painting	1011 sqm	0,69 kg/sqm	697,6 kg	10 years	Landfilling

2.3.3 Option 2 – Aluminium perforated panels:

The option of aluminium perforated panels as cladding system foresees the use of perforated metal sheets with two different percentage of perforation and different patterns, in order to resemble even more the choices adopted in the case-study. Aluminium perforated metal sheet, in addition to their aesthetical pleasantness and their ease of formation and fabrication, are very light, therefore representing a favourable material for cladding applications, particularly when weight is an important parameter.

The sheet considered have a dimension of 1000x2000 mm, a thickness of only 2 mm and a weight of 8.5 kg/sqm.

The panels are supported by a frame of vertical and horizontal aluminium profiles for a total of 4856 lm placed along the entire façade.

The service life of the material has been considered in 20 years with an end-of-life treatment of aluminium recycling.

Table 3: Opt. 2 – Aluminium perforated panels cladding

	MATERIAL	QUANTITY	UNIT WEIGHT	KG TOT	SERVICE LIFE	END OF LIFE
Sub-structure	Uprights in extruded aluminum profiles	2424 lm	1,58 kg/lm	7672,48 kg	As building	Aluminum recycling
	Crossbars in extruded aluminum profiles	2432 lm	1,58/lm			
Cladding	Perforated aluminum panels pattern 1	1210 sqm	8,5kg/sqm	20315 kg	20 years	Aluminum recycling
	Perforated aluminum panels pattern 2	1180 sqm				
	Expanded metal panels in pre-painted galvanized steel type fils model esperia RAL 7046, 1019, 8012	582 sqm	7850 kg/mc	18000 kg	As building	Steel recycling
	Existing masonry painting	1011 sqm	0,69 kg/sqm	697,6 kg	10 years	Landfilling

2.3.4 Constant data:

Membrane architecture: the seventh established building material. Designing reliable and sustainable structures for the urban environment.

All the three options include some materials which represent a constant throughout the analysis. These materials are:

- Wall paint for exterior use, which has a thickness of 0.44 mm and a weight of 0.678 kg/sqm. Its service life is reported in 10 years with a waste treatment of landfilling;
- Expanded galvanized steel sheets, used for marking the entrance. These sheets have dimensions of 1000x2000 mm with a thickness of 4 mm and a weight of 7850 kg/m³. Their substructure has not been considered since it represents a constant too. The waste treatment for this material consists of steel recycling;
- For the aluminum profiles the same material has been adopted in the three different options, differentiating it only in terms of linear meters. Its weight is of 1.58 kg/m and its waste treatment consist of aluminum recycling. Additionally, it must be clarified that the material applied is realized with the 85% of recycled aluminum.

Lastly, for what concerns the A4 phase of the transport, the default data given by each EPD have been adopted. However, as it will be clarified better in the analysis of the result section, the transportation phase affects only slightly the final impact.

3. Analysis of the Results

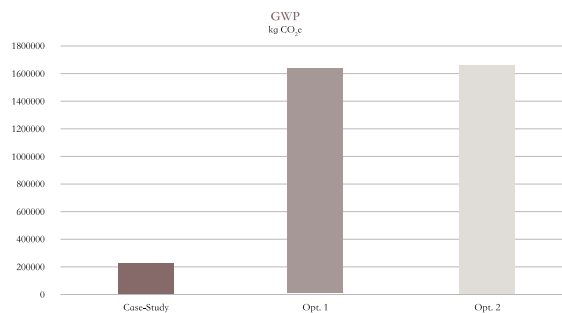


Figure 1: Overall GWP comparison among the three options (unit kg/CO₂e)

Overall, the comparison of the three options exhibits a visible difference between the Global Warming Potential (GWP) of the Case-Study in comparison with the Opt.1 – Polycarbonate Panels and Opt.2 – Perforated Aluminium Panels [Figure 1]. Indeed, if the Case-Study deploys its GWP at 216952.8 kg/CO₂e, Opt. 2 and Opt. 3 differs of only 0.5% reaching 1652425,09 kg/CO₂e and 1660713,48 kg/CO₂e respectively. While the construction phase of the three options accounts for similar kg/CO₂e, what highly contribute to the total difference are the production of the materials (A1-A3 phase), the waste processing (C3 phase) and the substitution of the components (B4-B5) for what concerns the Opt.1 and the Opt.2 [Figure 2] respectively.

A closer look within the environmental impact of each solution helps in the evaluation of the higher impactful parameters and their consequent optimization.

Membrane architecture: the seventh established building material. Designing reliable and sustainable structures for the urban environment.

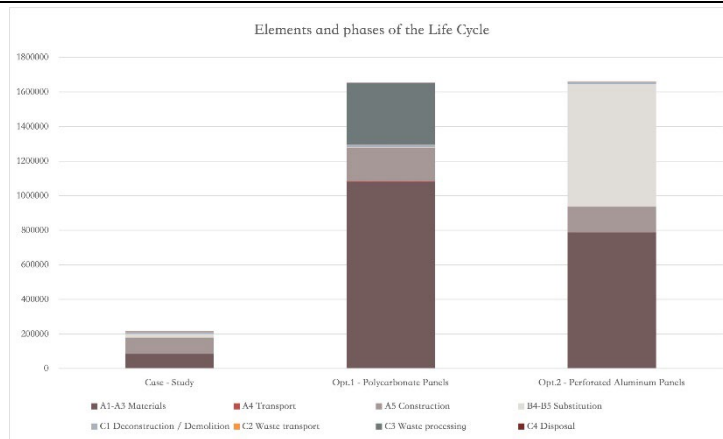


Figure 2: Comparison analysis of the GWP of the three options: elements and phases of the Life Cycle

3.1 Case – Study:

The Case-Study represents the least environmental impacting strategy, with a difference of around 1,5 million of kg/CO₂e in comparison with the two alternatives, despite the almost similar values for what concern the A5 phase.

As represented in Figure 3, the phases that contribute the most to the total environmental impact are the A1-A3 and the A5 (with a ratio of almost 1/1), followed by B4-B5 and C1.

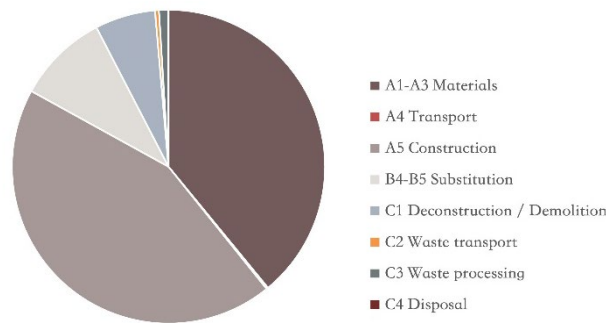


Figure 3: Case-Study: Global Warming kg/CO₂e per Phases of Life Cycle

Fig. 4 combines Fig. 3 with the analysis of the impacts of each material per phase: if galvanized steel accounts for the highest impact in the production of the materials (A1-A3), the technical textile represents the most impacting one for what concern the substitution phase (B4-B5), despite its replacement occurs only once after 15 years along the entire life cycle of 30 years. Fastening system, which will be replaced after 25 years, and wall paints, whose replacement occurs every 10 years, also share an impact in the substitution phase, on the contrary of galvanized steel. However, the above-mentioned materials account for the least in the production phase (A1-A3), therefore just slightly affecting the overall impact.

Membrane architecture: the seventh established building material. Designing reliable and sustainable structures for the urban environment.

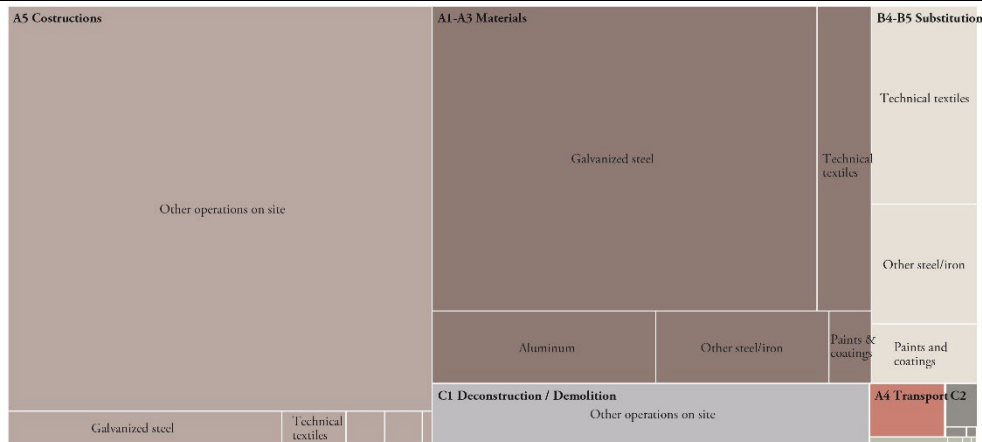


Figure 4: Case-Study: Resource treemap by Phases of Life Cycle - subtype

3.2 Option 1 – Polycarbonate panels:

Similarly to the Case-Study, the Opt.1 – Polycarbonate panels involve the application of plastic based materials. The main difference between the two is that technical textiles weight for 0,42 kg/sqm while polycarbonate panels have a weight of 72 kg/sqm. Consequently, their impact is completely different. Indeed, in the Opt.1, A1-A3 phases account for the higher share of the impact and, within it, the plastic products share the majority [Fig. 5-6], with a ratio of 5,5/1 between A1-A3 and A5 phases. It follows that their contribution is the higher also in the A4 and C3 phases. Considering that the service life of the material corresponds to the building service life (30 years), B4-B5 share an almost insignificant value in this option because the main material is never replaced. On the contrary, its end-of-life process corresponds to the plastic-based material incineration, with its related high impact.

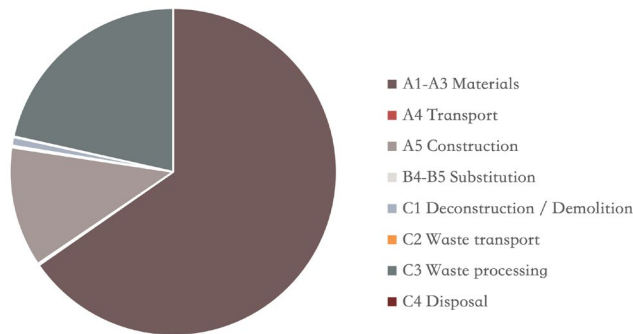


Figure 5: Opt. 1: Global Warming kg/CO₂e per Phases of Life Cycle

Membrane architecture: the seventh established building material. Designing reliable and sustainable structures for the urban environment.



Figure 6: Opt. 1: Resource treemap by Phases of Life Cycle - subtype

3.3 Option 2 – Perforated aluminium panels:

The Opt.2 – Perforated aluminium panels is characterized by an extensive use of aluminium, being applied as coating of the entire façade. It follows that it contributes for the most both in the material production (A1-A3), as well as in the substitution phase (B4-B5) which occurs after 20 years of service life [Fig. 7-8]. If the ratio between A1-A3 and A5 accounts for around 5,3/1, what must be highlighted is the ratio between A1-A3 and B4-B5 which, in this case, lines up at around 1/1 (compared to the one of the case-study which is 4/1 and for the one of the opt.1 which is non-equivalent).

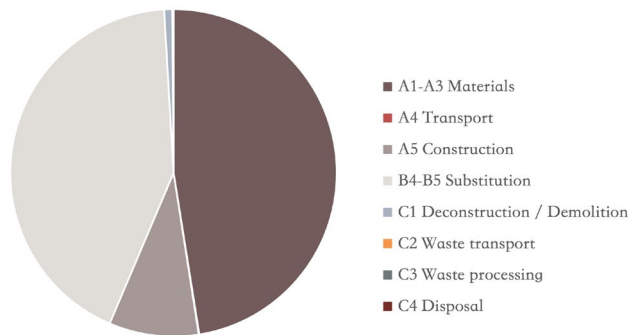


Figure 7: Opt. 2: Global Warming kg/CO₂e per Phases of Life Cycle

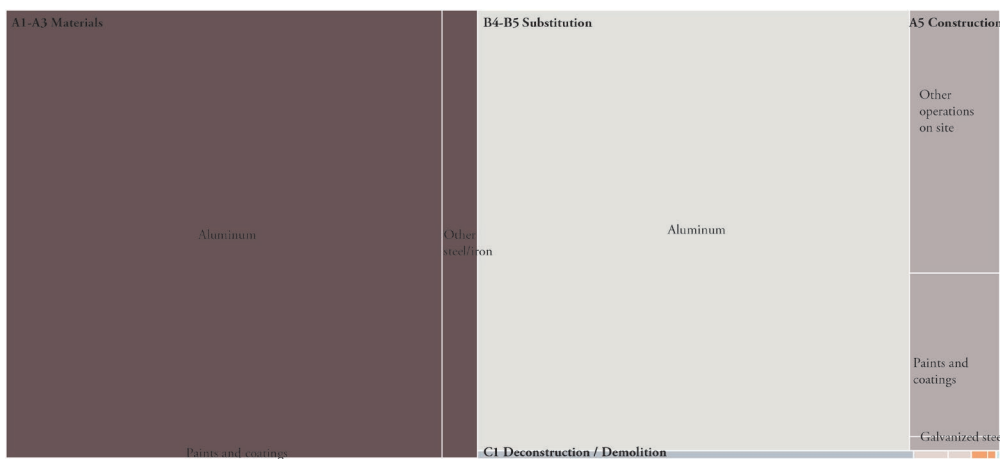


Figure 8: Opt. 2: Resource treemap by Phases of Life Cycle - subtype

4. Discussion

The three analysed design options accounts for almost similar impacts with relation to the construction phase. Nevertheless, while A5 contributes the most to the total life cycle of the case-study, it represents only the third impacting phase both in opt.1 and opt.2, highlighting how the materials applied in the two alternatives have higher impacts in terms of materials production (A1-A5), substitution (B4-B5) and waste processing (C3). With respect to the three alternatives, what can be pointed out is:

- Following the construction phase (A5), which accounts for the most, the total impact of the case-study is affected by A1-A3 and B4-B5 phases. Similar values for A1-A3 are showcased by most of the materials used, except for the galvanized steel. Considering that this material is present in the same quantities throughout the three options and it is almost irrelevant in the other solutions, it testifies how little is the impact of the other materials applied in this strategy. Additionally, the substitution (B4-B5) represents the third impacting phase due to the replacement of the technical textiles and the fastening system. Consequently, further analysis should focus on the extension of the service life of the membranes. The correct optimization of the fastening system allows for the minimization of the construction phase, which is highly affected by it.
- On the contrary, B4-B5 does not impact at all the Opt. 1 since the plastic products applied have a service life of 30 years. In parallel, the construction phase (A5) represents only the third impacting phase because what account most are A1-A3 and the C3 phases due to the production and incineration of high quantities of plastic products. However, it must be pointed out that the multi-wall polycarbonate presents excellent thermal properties which could potentially have quite different effects on the operational energy use, thus influence the final choice of over-cladding system.
- Lastly, in the Opt. 2, similar values between A1-A and B4-B5 are displayed. All of this is affected by the aluminum which is the most used material in the strategy. Indeed, despite that the aluminum is applied for the substructure in all the three strategies, it is extensively applied in this option, with a substructure that accounts for almost three times higher than in the other two strategies. Considering that its service life is as long as the one of the building, it contributes to A5 phase but not to B4-B5 phases which are affected after 20 years only by the replacement of the perforated aluminum panels.

With regard to the economic impact, only the material purchases have been considered, evaluating their costs in relation to the number of replacements that occur due to the service life of each material. Further analysis will focus on a complete LCC estimation, evaluating also the transportation phase and the construction one.

The comparison among the three alternatives presents the case-study as the cheaper, thanks to the textiles which account for the minimum expense in comparison with the other materials. The consequent total expense deploys at 247,39 €/sqm, despite the required replacement of the textiles and its fastening system [Table 4].

Membrane architecture: the seventh established building material. Designing reliable and sustainable structures for the urban environment.

Table 4: Case-Study – Cost per sqm

	MATERIAL	QUANTITY	€/SQM	SERVICE LIFE	REPLACEMENT	FINAL COST
Sub-structure	EPS extruded aluminum profiles frame	1752 ml	36,13	As building	/	100000,00
	Clips	37886 units	0,53	25 years	1	40000,00
Cladding	Pre-tensioned membrane Soltis 92	2390 sqm	25,10	15 years	1	120000,00
	Expanded metal panels in pre-painted galvanized steel type fils model esperia RAL 7046, 1019, 8012	582 sqm	160,00	As building	/	93120,00
						353120,00
TOTAL €/SQM						247,39 €

The Opt. 1 is similarly impacting from an economic perspective: indeed, it takes advantage of the lack of replacement for its cladding system, therefore limiting its values at 287,08 €/sqm [Table 5]. Lastly, Opt. 2 is the one with higher economic impact: the cladding in perforated aluminium panels has a high expensive value and it is even replaced once along the life cycle. Consequently, the total strategy has a cost of 567,08 €/sqm [Table 6].

Table 5: Opt. 1 – Cost per sqm

	MATERIAL	QUANTITY	€/SQM	SERVICE LIFE	REPLACEMENT	FINAL COST
Sub-structure	Extruded aluminum profiles (uprights&crossbars)	1576	57,08	As building	/	89958,08
Cladding	Polycarbonate panels	2390	70,00	30 years	30 years	167300,00
	Expanded metal panels in pre-painted galvanized steel type fils model esperia RAL 7046, 1019, 8012	582 sqm	160,00	As building	/	93120,00
						350378,08
TOTAL €/SQM						287,08 €

Table 6: Opt. 2 – Cost per sqm

	MATERIAL	QUANTITY	€/SQM	SERVICE LIFE	REPLACEMENT	FINAL COST
Sub-structure	Extruded aluminum profiles (uprights&crossbars)	4856 ml	57,08	As building	/	277180,48
Cladding	Perforated aluminum panels pattern 1	1210 sqm	100,00	20 years	1	242000,00
	Perforated aluminum panels pattern 2	1180 sqm	75,00	20 years	1	177000,00
	Expanded metal panels in pre-painted galvanized steel type fils model esperia RAL 7046, 1019, 8012	582 sqm	160,00	As building	/	93120,00
						789300,48
TOTAL €/SQM						567,08 €

5. Conclusion

The study aimed to determine which parameters have the greatest effect on the environmental impact of a façade retrofit solution. It compared three different alternatives achieved respectively with a textile cladding, polycarbonate panels and perforated aluminium panels in order to highlight which phase of the life-cycle is by most affected by the application of one material or the other.

Membrane architecture: the seventh established building material. Designing reliable and sustainable structures for the urban environment.

The results pointed out that the material production (A1-A3) is generally the most impacting phase, together with the construction (A5) and/or substitution (B4-B5) phases. The deconstruction/demolition phase (C1) and the waste processing (C3) variably affect the overall environmental impact depending on the source of the material applied and its final treatment. In line with previous analysis [Monticelli et al. 2013], the study highlighted that, despite the same quantities of sqm used for technical textiles, plastic products and perforated aluminium panels, the thickness of the material highly affects the total weight affecting the amount of substructure and, consequently, the overall environmental impact. In addition to it, to consider to recycle the material at the end of its life instead of incinerating it highly affect the outcome, as it is showcased by the comparison of perforated aluminium panels with plastic products. This opens up further considerations about the end-of-life of textile products, considering to optimize even more their environmental impact through the improvement of their end-of-life treatment.

References

- Chilton, J. (2010), Tensile structures - textiles for architecture and design. In Pohl G. (Edited by), *Textiles, polymers and composites for buildings*. Cambridge: Elsevier Ltd., 229-257.
- Cremers J. (2014), Environmental impact of membrane and foil materials and structures – status quo and future outlook. In *Technical Transactions Architecture*, 7-a, Poland.
- ISO 14040 (2021), Environmental management — Life cycle assessment — Principles and framework, Geneva, International Organization for Standardization (ISO).
- ISO 14044 (2021), Environmental management — Life cycle assessment — Requirements and guidelines, Geneva, International Organization for Standardization (ISO).
- Monticelli, C.; Zanelli, A.; Centrulli, M. (2017), Application and validation of eco-efficiency principles to assess the design of lightweight structures: case studies of ETFE building skins. In *Proceedings of the IASS Annual Symposium 2017 “Interfaces: architecture. engineering. science”* September 25 - 28th, 2017, Hamburg, Germany, Annette Bögle, Manfred Grohmann (eds.).
- Monticelli C. and Zanelli A. (2016), Life Cycle Design and efficiency principles for membrane architecture: towards a new set of eco-design strategies. In *Procedia Engineering*, Science Direct Elsevier, n. 155, pp. 416 – 425.
- Monticelli, C.; Zanelli, A.; Campioli, A. (2013), Life cycle assessment of textile façades, beyond the current cladding system, TensiNet Symposium, Istanbul, (pp. 467-476).
- Pohl, J.; Pohl, G. (2010), The role, properties and applications of textile materials in sustainable buildings. In Pohl G. (Edited by), *Textiles, polymers and composites for building*, Cambridge: Elsevier Ltd, 258-289.
- Thinkstep AG. (2021). LBP-GaBi, University of Stuttgart: GaBi Software System, Leinfelden-Echterdingen / Germany, 2011
- Wernet, G., Bauer, C., Steubing, B., Reinhard, J., Moreno-Ruiz, E., & Weidema, B. (2016). The ecoinvent database version 3 (part I): Overview and methodology. *International Journal of Life Cycle Assessment*, 21(9), 1218-1230. doi:10.1007/s11367-016-1087-8



tensinantes2023 : TensiNet Symposium 2023 at Nantes Université

Membrane architecture: the seventh established building material. Designing reliable and sustainable structures for the urban environment.

Proceedings of the Tensinet Symposium 2023

TENSINANTES2023 | 7-9 June 2023, Nantes Université, Nantes, France

Jean-Christophe Thomas, Marijke Mollaert, Carol Monticelli, Bernd Stimpfle (Eds.)

ATLAS architectural membrane as a core element for larger and energy efficient air domes

Alexandra SONNENBERG*, Dusan OLAJ^a

* Sattler PRO-TEX GmbH

Sattlerstraße 45, 8077 Gössendorf, Austria

Alexandra.Sonnenberg@sattler.com

^aDUOL doo, Kapalniska pot 2, 1351 Brezovica, Slovenia

Abstract

The properties of membranes allow nearly unlimited possibilities for the realization of building projects.

A membrane (=skin) has the great potential to take on countless material-specific requirements and functions: covering, protecting, separating, self-cleaning, fire-resistant, fire-retardant, opaque, green, eco-friendly, inexpensive, tear-resistant, durable and aesthetical.

No other architecture creates maximum spans with minimal use of material and energy. Fabrics are characterized by flexibility in combination with a low weight per unit area. Thanks to its range of special characteristics such as tensile strength, elastic performances, translucency and higher yarn density, large areas can be covered and thus extraordinary structures can be built.

For the success of a project, the right choice of material is crucial. Including the membrane supplier at an early stage of the project ensures that all advantages of a membrane regarding costs, longevity and maintenance intensity can be used to its fullest extent.

Keywords: aesthetics, strength, air domes, lightweight system, membrane system, sustainability, performance, Stability of values, manufacturing, durability

1. Introduction

Membrane construction combines architecture with modern design and function. Because of its modern and futuristic form, we often find membrane buildings in exposed locations.

Architectural membranes are not just a decoration or a design element. They are given an extraordinary role. Through the applied pre-stressing, architectural membranes become the static part of the structure; they take on a dual function.

Membrane architecture: the seventh established building material. Designing reliable and sustainable structures for the urban environment.



Figure 1: Tashkent Stadium, SATTLER GROUP

The design of a membrane structure is complex because the shape is the result of a form-finding process due to the bending flexibility of the material. After determining the shape and the external loads, the membrane material is calculated. At this point, the selection of the right membrane material is important. Aspects such as strength, manufacturing, membrane system and performance play a significant role. The process is influenced by design/aesthetic and technical parameters.

2. Weaving as the main aspect of PES/PVC coated fabrics

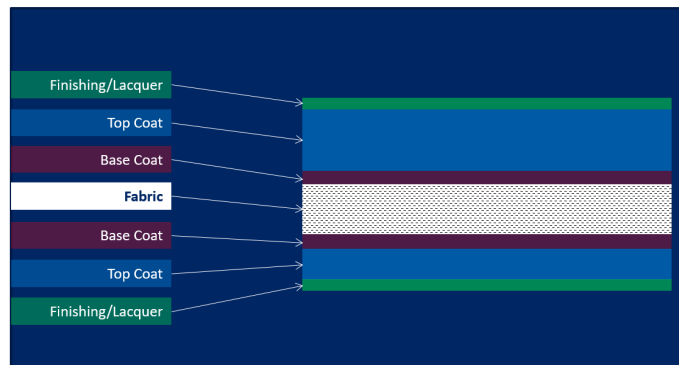


Figure 2: structure of a PES/ PVC membrane

2.1. Structure of a membrane

PES/PVC is a multi-component, coated architectural fabric. The processing of the polyester yarns on the loom takes place at the beginning of the production process. The PVC coating is then applied to the raw fabric as a highly viscous coating compound in a multi-layer process dependent on the manufacturer (plastisol or calander method). Finally, the surface is refined by a finish coating, which defines the handling, soil repellency, performance and durability of the membrane.

Table 1: PES/PVC coated fabrics layer structure

Fabric:	* thermoplastic and partially crystalline polymer
---------	---

Membrane architecture: the seventh established building material. Designing reliable and sustainable structures for the urban environment.

	<ul style="list-style-type: none"> * backing fabric made of synthetic polymers (polyethylene terephthalate = PET) * fineness of the fibre is measured in detx² * PET fibre is dimensionally stable * fibre has a decisive influence on the material behaviour of the fabric * takes over the function of the load-bearing element * it is responsible for the mechanical parameters such as maximum tensile forces and tear resistance
Coating:	<ul style="list-style-type: none"> * protective function for the yarn from damage * stabilises the yarn * enables weldability of the membrane * enables processing * together with the finishing, it ensures impermeability to moisture and air
Finishing:	<ul style="list-style-type: none"> * provides the aesthetics * prevents the plasticisers from leaking and thus brittleness * protection against the effects of moisture * protection against plasticiser migration * ensures dirt repellency and longer warranty * responsible for durability of the membrane

2.2 Weave

Woven fabrics are created by crossing warp and weft threads. They are characterized by the various orthogonal crossings of two thread systems.

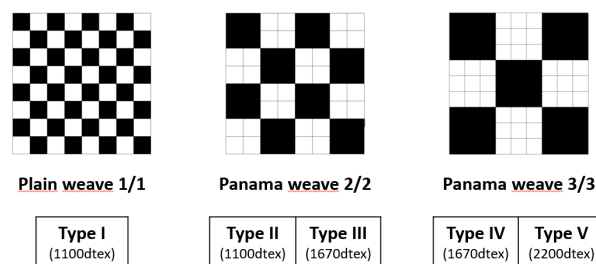


Figure 3: plain and panama weave structures

2.2.1. plain-weave: One warp thread (yarn thickness 1100 dtex) is crossing a weft thread in one point (1/1) This chessboard-like connection creates two identical fabric sides.

2.2.2 panama-weave: Panama-weave is a further development of the plain weave. If two/three warp threads (yarn thickness 1100 - 2200 dtex) are crossing two/three weft threads in one loop point, we call it panama – weave (2/2 and 3/3) (Fig. 3). The advantage of panama weave is that the more threads and the stronger the yarn, the stronger the fabric. However, it has the

Membrane architecture: the seventh established building material. Designing reliable and sustainable structures for the urban environment.

disadvantage that with more threads crossed together, there are more loop points, which make the fabric very rough and sensitive to dirt.

2.2.3 ATLAS weave: A weaving technique known from the clothing industry is used as an innovative and new weaving product line for architectural membranes. If we change the weave structure, as in the ATLAS weave, these wrap points can be reduced (atlas= smooth). The weft thread runs completely straight over 4/or more warp threads and it has only one loop point and with the next weft thread it is offset by another 4/or more warp threads. The ATLAS weave is easily recognized by two-sidedness of the fabric. While the weft threads dominate on the upper side of the fabric, the warp threads predominate on the reverse side. This has the advantage of a much flatter fabric on the one hand, fewer loop points and a higher yarn density. More threads in the fabric mean more strength.



Figure 4: characteristics of ATLAS weave

To optimize the weave structure more weft threads on the upper side of the membrane were used and the result is a much flatter fabric on the one hand, fewer loop points and a higher yarn density (Fig. 4).

3. Which properties of a membrane are decisive for a project?

The choice of the right membrane material depends on various factors. The following aspects are decisive:

1. Durability and stability of values
2. Mechanical performance

The resistance of a coated fabric to load-dependent and load-independent effects are achieved by various work steps in the fabric production process. The basic parameters of a membrane are often fixed, but individual project-specific requirements can always be included. Architectural membranes are often fabricated to specific customer needs. Yarn thicknesses, weaves, base fabric, coating and lacquering can be used to react to different effects and influences.

3.1 Durability

3.1.1 Coating

As already explained, the basis of a fabric and also the function of the load-bearing element comes from the weave.

Membrane architecture: the seventh established building material. Designing reliable and sustainable structures for the urban environment.

This report uses different projects to show which additional project-specific features and material properties play a decisive role in the production process with regard to coating, finishing and composition.

In 2021, we were engaged by the company DUOL to develop a PES/PVC membrane for the largest air dome in the Middle East, called Al Maryah, which was to be built with an area of 8.750 sqm.



Figure 5: External view of Sports dome Al Maryah

The core elements of this project were the construction of one of the largest air domes in one of the most climatically difficult regions. A lightweight material with high tensile forces was needed. A durable material that could withstand the extreme weather conditions in the Middle Eastern desert. Greater protection was needed, including better UV protection. A group of weaving engineers focuses on the technological advancement of high quality and functional coated membranes. Two main activities form the core of the research. The first is about a smooth surface to prevent pollution, especially with regard to desert sand. The second is of a more practical nature. If some dirt does stick, the surface of the membrane should be easy to clean.

Protection of the fabric is generally achieved by applying a coating in paste form. Coatings have specific formulations which increase the levels of performance such as fire retardance, fungal resistance or colour pigmentation. A coating is characterised by its weight in g/m^2 and in thickness measured as the distance between the top of the fabric's yarn and the outer surface of the coating. There is a proportional dependence of the fabric protection on the coating thickness. The weaving process and the coating process cause differences in the waviness of the warp and weft yarns. While the warp thread is kept under tension during the under tension during the manufacturing process and thus has a more stretched thread the weft thread shows a higher waviness. This increased waviness of the weft thread leads to a softer weft thread. The multiple thread guidance in the Atlas weave leads to lower thread waviness in warp and weft direction compared to Panama weave (Fig. 6).

Membrane architecture: the seventh established building material. Designing reliable and sustainable structures for the urban environment.

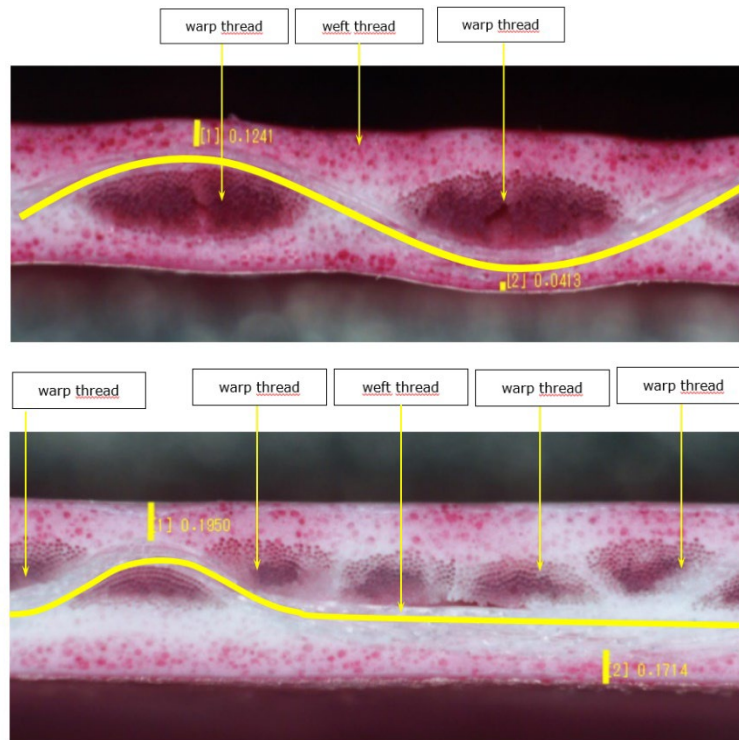


Figure 6: Cross-section Panama and ATLAS weave

The coated fabric produced in this way now exhibits identical, significantly reduced waviness in both yarn directions. The deflection of the warp and weft threads is minimized and the fabric is almost flat. This brings the benefits of equal coating thickness over the back of the thread. The PET yarns are covered with a thicker PVC-coating which increases the protective function of the fabric (Fig. 7).

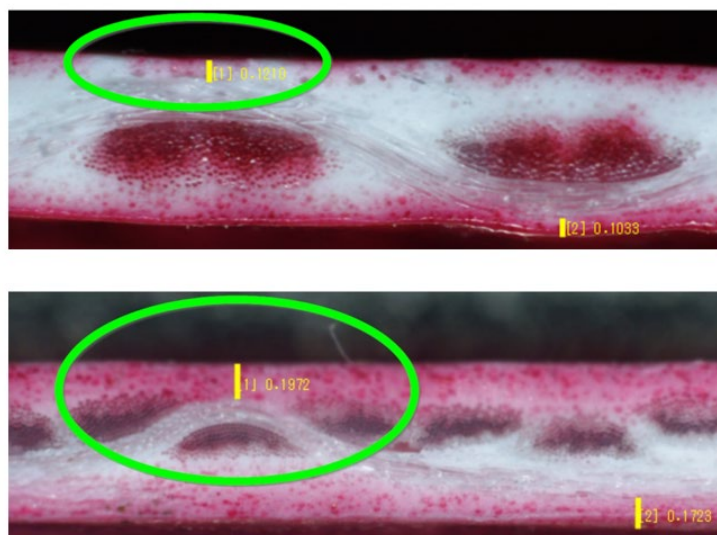


Figure 7: coating thickness over the back of the thread- Panama and ATLAS weave

Membrane architecture: the seventh established building material. Designing reliable and sustainable structures for the urban environment.

3.1.2 Finishing

The resistance of the membrane is influenced by the coating component PVC (polyvinyl chloride) with plasticizer content. In order to prevent the plasticizers from escaping and thus the fabric coating from becoming brittle, especially at high outside temperatures, PES/PVC fabrics are provided with a lacquer. By applying a PVDF (fluoroplastic) based lacquer in the coating process, the resistance of the weather side of the outer membrane can be increased. Here, a difference is made between non-weldable lacquers, which have to be polished off in the finishing process, and weldable finishes.

To achieve better protection against UV rays, the membrane is additionally equipped with a multi-layer structure with UV protection. UV light damages the membrane as the sunlight penetrates the lacquer.

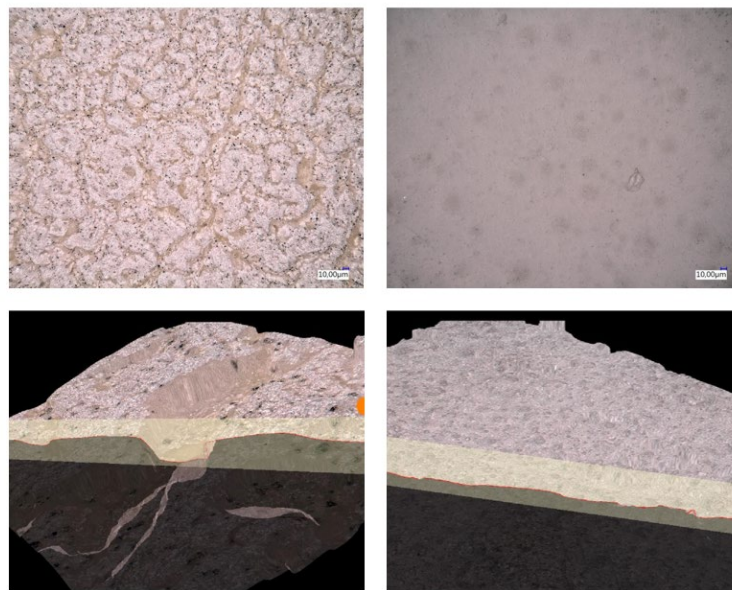


Figure 8: Microscope image of the membrane surface Panama and ATLAS weave

The protective function of the finishing is reduced and the PVC coating is exposed to direct sunlight. The result is extreme damage to the polyester base fabric and loss of strength.

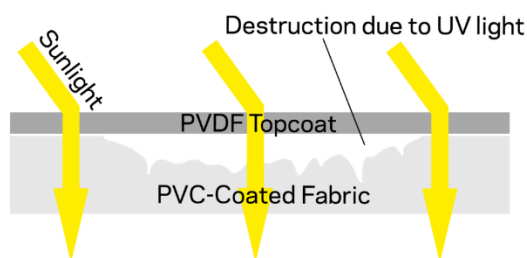


Figure 9: UV-light damages the membrane

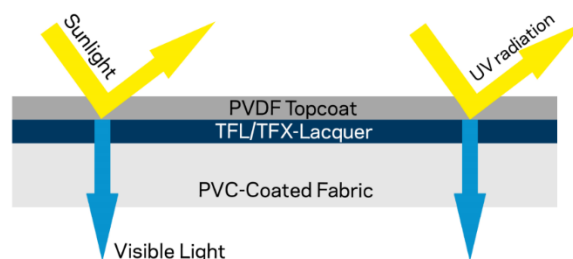


Figure 10: UV-protection by ATLAS

The addition of a multi-layer surface treatment significantly increases the UV protection. The application of an additional UV-Primer blocks the penetration of the damaging UV-radiation, similar to a suntan lotion.

Membrane architecture: the seventh established building material. Designing reliable and sustainable structures for the urban environment.

The application of a TiO₂ UV primer works on a physical principle and does not decompose like a chemical UV blocker; therefore, it offers long-term protection.

As the PVC coating is not damaged by UV-radiation and delamination of the lacquer is prevented, the polyester fibres remain protected.

The protective function of the coating is maintained and the transmission of visible light is not affected by the UV blocker.

3.1.3 lightweight system

Another project specific requirement was the local site conditions in the Middle East. Necessary was a type of membrane that is primarily intended for extremely hot regions where solar shading is essential. In most of the European regions, a high level of light transmission is usually required to bring natural light into the interior of a building. Coated fabrics are very light, so one advantage is very high light transmission, which allows adequate daylighting. In this Al Maryah project, however, the exact opposite was needed. Sunlight had to be kept away from the sports dome. The requirement was to develop an opaque membrane that could withstand heat of up to 70 degrees Celsius. The task was to develop a blackout version without increasing the weight of the material, as the static and technical project requirements did not allow any additional loads.

In terms of production technology, the blackout function involves the application of an additive dark blocking layer to protect against light transmission.

With a conventional weave such as Panama weave 3x3, a thicker blocking layer is necessary due to the rougher surface. This leads to a higher material weight. With the smooth ATLAS weave, the blackout line can be applied significantly thinner, so that the additional feature does not increase the weight of the fabric.

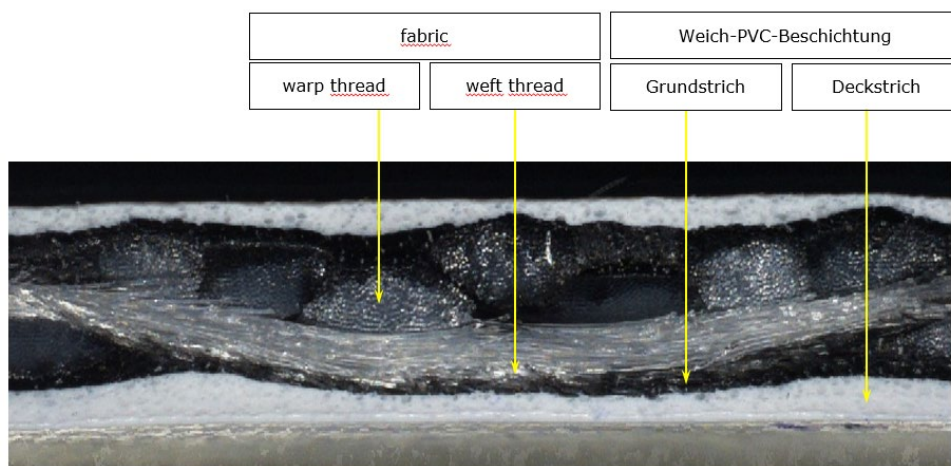


Figure 11: Cross-section Blockout

3.1.4 membrane system

With regard to the thermal environment, an intelligent, flexible building was required. In conventional buildings, the thermal capacity of roof reduces the effects of rapid changes in outside temperature. In contrast, a membrane is extremely thin. The surface temperature of the

Membrane architecture: the seventh established building material. Designing reliable and sustainable structures for the urban environment.

membrane can fluctuate rapidly over the course of a day. It is obvious that materials with a thickness of one millimetre do not have good insulating properties. To improve the climatic behaviour inside the air dome a multi-layer construction with an insulated membrane system was developed.

The outer second skin functions as a "climate cover". In principle, the outer membrane of the Al Maryah air dome takes over the function of the main load-bearing membrane and is determined on the basis of the external wind load pressure and the internal pressure. It also represents the first and most important "protective shield" from external climatic conditions. In the UEA region, the considered wind speed is 165 km/h. Together with the high temperatures (+54C) and the desert sand in the air, the membrane has to withstand high thermal and mechanical loads.

In addition to the climate cover, an intermediate temperature zone is created as a buffer zone, which reduce heat transfer through the building skin. A high insulating material is fixed on the inner membrane. The insulation in the air dome is a completely independent layer. It is attached to the inner air envelope in such a way that it can be quickly disassembled, reinstalled or easily retrofitted. Special pattern drawings are made for the insulation, based on the pattern of the inner air dome. Multiple insulation panels are joined together to create a large, continuous insulation layer over the inner dome membrane. It is important that it be continuous to avoid thermal bridging. The attachment to the inner membrane needs to be rigid and flexible at the similar time. Furthermore, a fixed connection point between the insulation and the inner membrane is required, which nevertheless provides enough flexibility to allow the entire insulation with its additional weight to move on the inner membrane. The most important point in the construction of an air dome is to tension and connect all the insulation to the floor and then lift the insulation together with the inner dome fabric. The membrane itself must have sufficient tensile and tear strength to support the weight of the insulation during operation and installation. The membrane must also be flexible as we allow small movements to avoid tearing the insulation.

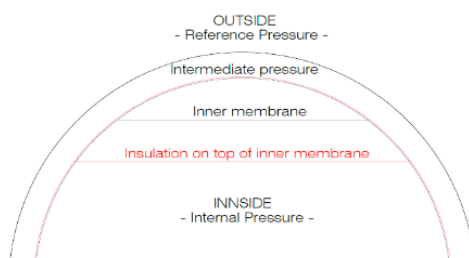


Figure 12: Pressure explanation

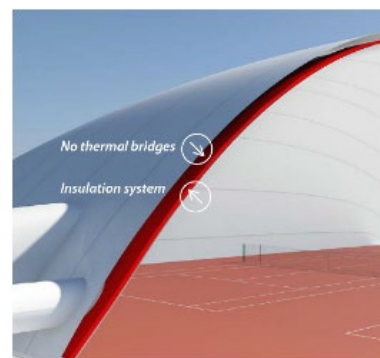


Figure 13: Membrane system

3.1.5 performance

Applying insulation to the inner dome membrane also increases the sound insulation value of the air dome.

Considering only the double diaphragm systems with empty cavity, it can be seen from figure 14, that the spacing of the diaphragms only has an influence in the low frequency range up to 1000 Hz and has no influence at higher frequencies. A doubling of the diaphragm spacing brings on average 3 dB to the single-number value R_w .

Membrane architecture: the seventh established building material. Designing reliable and sustainable structures for the urban environment.

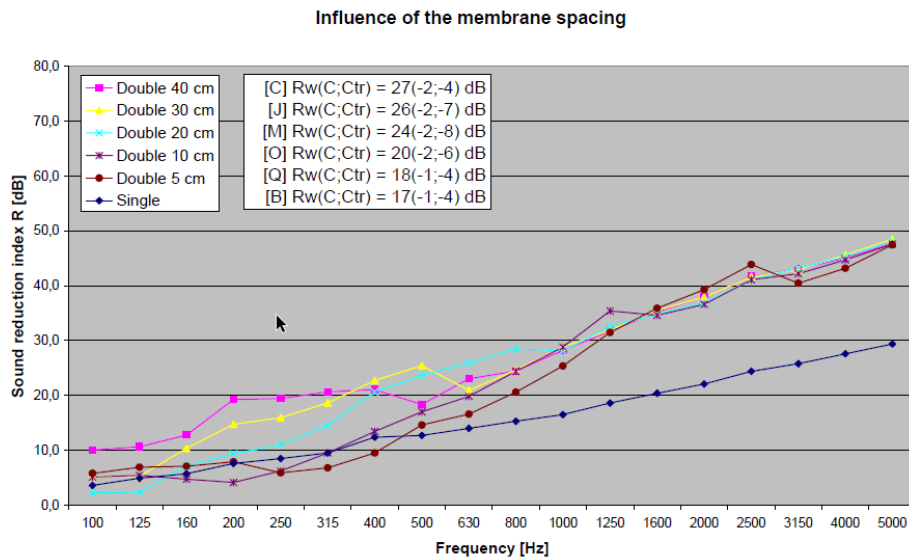


Figure 14: Empty cavity measurements – influence of membrane spacing, Contex-T (2008), Test report, Sound reduction index of double membranes

Filling the cavity with an absorbent has a further influence on the spectrum of the sound reduction index. Due to the additional mass and the additional viscous losses in the cavity, the sound reduction index increases further. The first centimetres of the absorbent have the greatest effect. The first thickness resonance is completely attenuated by any absorbent. Here 40 cm of the absorber has a surface mass of 14 kg/m² compared to a 2-layer Type IV membrane of about 2.8 kg.

A further increase in the density of the filling leads to further increases in sound attenuation, especially at high frequencies, as the flow resistance increases.

Studies have shown that the position of the absorber plays only a minor role.

3.2 Mechanical performance

3.2.1 Elastic behaviour

In no other building sector is the interaction between production quality on the one hand and project requirements on the other as pronounced as in membrane architecture. The next project should show these relations.

This is a reconstruction of a membrane covering. In order to protect the historically parabolic reflector antenna in Raisting (erected in 1964) from external influences of weather, it was encased in a pneumatically prestressed membrane, 49 m in diameter and 34 m high, constructed as a spherical section. The 5200-square-meter cover, which was only 1.0 millimetres thick and weighed 10.5 to was manufactured in one piece. Waste, membrane joints and seams had to be carefully calculated, as these details have an essential effect on the material consumption. Careful consideration has to be given to the overall economics of the project and proper material management.

Membrane architecture: the seventh established building material. Designing reliable and sustainable structures for the urban environment.



Figure 15: Radome Raisting

The membrane behaviour has an influence here. The material behaviour cannot be compared with that of conventional, rigid materials. While a linear elastic and isotropic stress-strain relationship is assumed for conventional components, this assumption cannot be made for fabrics due to their complex behaviour. Fabrics, as used in membrane constructions, are nonlinear, anisotropic and non-elastic.

As already described in chapter 2.2, the manufacturing and coating process of textile membranes causes the characteristic waviness of the fabric threads. The curvature of the threads depends on the weave, the weaving and coating process. In the untensioned state the warp thread is less curved than the weft thread, since the weft thread is kept under tension during the manufacturing process. One consequence of the different geometry is the much lower stiffness of the fabric in the weft direction. While the less curved warp yarns quickly reach their final stiffness the weft yarns must first achieve their stronger curvature first by stretching. Only after reaching a more stretched geometry, the weft yarns also have their final stiffness.

The crossing of the warp and weft threads leads to interactions at the crossing points. This interaction of the fabric threads makes a significant contribution to the pronounced non-linear force-elongation behaviour of fabrics.

The following biaxial tests were done according to DIN EN 17117. This test was implemented in order to define the modulus of elasticity. Modulus of elasticity under tensile stress describes the relationship between stress and relevant elongation of the material when it is deformed due to the impact of a tensile force.

A biaxial, thread-parallel tensile test is performed on a standardised cross-shaped test sample. First, a biaxial preload is applied to the cross sample.

The following load cycles 3x 1:1, 3x 2:1, 3x 1:1, 3x 1:2, 3x 1:1, 3x 1:0, 3x 1:1 and 3x 0:1 are applied successively (Fig. 16). These force combinations are kept constant during the application of the load. The maximum test force was set at 20% of the respective breaking strength in warp and weft. A tension of 1.2 kN/m was set as the minimum pretension.

Membrane architecture: the seventh established building material. Designing reliable and sustainable structures for the urban environment.

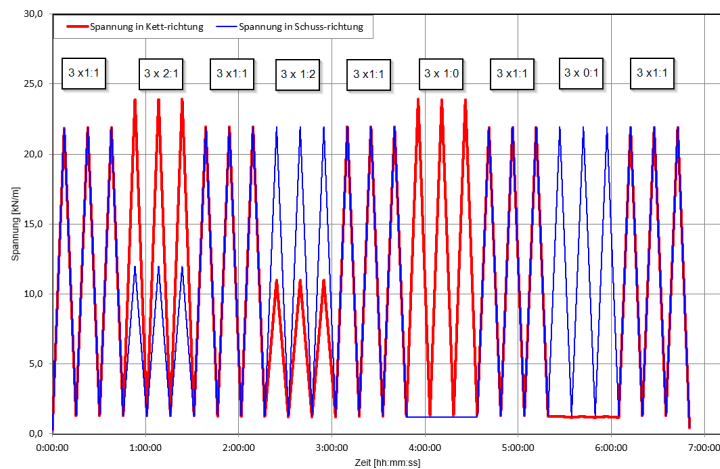


Figure 16: Lastgeschichte im Biax-Versuch

1:1: First, the force in warp and weft direction is increased in parallel up to 22kN/m test force.
 2:1: Next, the force in the warp direction is increased up to a maximum test force of 24kN/m. Similarly, a test force of 11kN/m is applied in the weft direction.

The following 1:1 load is then followed by the cycle 1:2 with a switched application of the forces (warp direction 11kN/m and weft 24 kN/m).

After another 1:1 loading, the loading cycle 1:0 follows. While the force in the weft direction remains constant at the pre-tensioning level, the force in the warp direction is constantly increased up to the maximum test force.

After a final 1:1 loading cycle, the test configuration is once again 0:1 relation and the force in the weft direction is increased three times up to the maximum test force.

This study is intended to investigate the biaxial behaviour under idealised load conditions. In real structures, different loads and load conditions will occur depending on the geometry and load.

Figure 17/17a+18/18a show a comparison of the biaxial time-elongation diagrams for ATLAS and Panama. It can be seen that over the complete test period and after overcoming the initial elongation, the more homogeneous weave is reflected in a lower impact of the fabric directions on each other. The structure of the material also reduces the difference in elongation between warp and weft.

The result of this comparison is that, compared to an ordinary weave structure, the smaller difference in elongation between warp and weft direction can be read in the balance of the curves. The tension differences are smaller. The material behaves less anisotropically. For our radome project, we were able to take advantage of this property. There is the same tension in all directions in the radome. That means we measure the same inner pressure at every point of this pneumatic form. Another great task in the radome project were the surface seams. The new covering consists of diagonally running panels, which should reduce their deformation from wind loads. The up to 42m long seams follow great circles and also run diagonally. The required load transmission from 5-6 overlapping layers with seam strength of 70% at a temperature of 70 °C could be implemented. The condition of the seam depends on the one hand, on the production parameters such as the duration of heat and pressure applications and, on the other hand, on the properties of the membrane.

Membrane architecture: the seventh established building material. Designing reliable and sustainable structures for the urban environment.

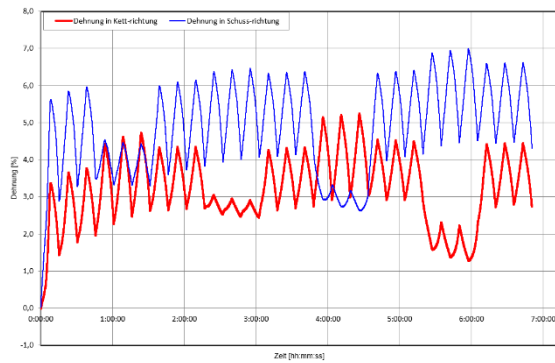


Figure 17

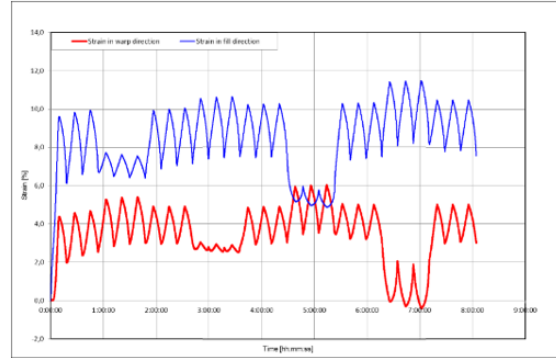


Figure 18

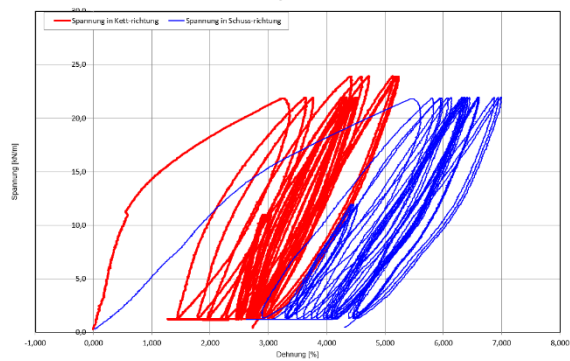


Figure 17a: E-modulus diagram, ATLAS

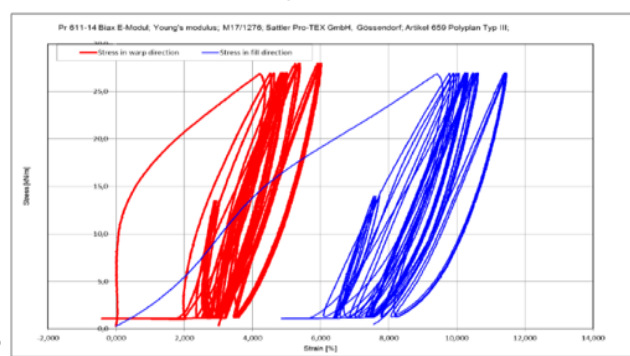


Figure 18a: E-modulus diagram, Panama

4. Conclusion: submission of contributions

This article is intended to illustrate that every task in textile architecture is an interplay of many project participants - an interdisciplinary team that is confronted with the diverse challenges of the building.

In regards to performance, building use, cost optimisation, longevity, installation and reduction of maintenance intensity, the early involvement of all project participants is target-oriented and efficient. It is important to define the specific project requirements. The performance of the membrane could be defined via the parameters yarn thickness, weave, coating and lacquer.

Adaptive elements such as the constructive multi-layer design of the membrane structure make another major contribution to this. To improve the performance of the membrane skin, additional adaptive elements such as the number of layers that make up the building cover could be increased. We have shown that the use of a multi-layer construction could reduce heat transfer through the building cover and improve the acoustic properties of the enclosed space. Of course, a multi-layered construction can do even more. Controlling daylight, reducing the risk of condensation between layers, or avoiding the drum effects of rain and hail.

But this article attempts to give an overview of the material aspects of PES/PVC coated fabrics. Individual aspects have been singled out and explained. It is only a small but exemplary selection from the repertoire of material possibilities

Membrane architecture: the seventh established building material. Designing reliable and sustainable structures for the urban environment.

References

Fröb U. (1979), Membrankonstruktionen, Leichtbaukonstruktionen Teil 1, Neuartige Membranstoffe

Mollaert M. (2000), The Design of membrane and lightweight structures (pp. 89 – 94)

Brian Forster, Mollaert M., European design guide for tensile Surface Structures

Saxe K., Stranghöner N., Uhlemann J., Membranbau Symposium 2014, Membranwerkstoffe: Zusammenhang zwischen Bauaufgabe und Materialauswahl

Seidel M., Bauen mit biegeweichen Tragelementen, Materialien biegeweicher Tragelemente, Ernst & Sohn 2008

Weller F., Membranbau Symposium 2016, Die häufigsten Probleme bei der Umsetzung der Planung in die Ausführung von Membranbauwerken

Contex-T (2008), Test report, Sound reduction index of double membranes



tensinantes2023 : TensiNet Symposium 2023 at Nantes Université

Membrane architecture: the seventh established building material. Designing reliable and sustainable structures for the urban environment.

Proceedings of the Tensinet Symposium 2023

TENSINANTES2023 | 7-9 June 2023, Nantes Université, Nantes, France

Jean-Christophe Thomas, Marijke Mollaert, Carol Monticelli, Bernd Stimpfle (Eds.)

T-shade: experimental case study conducted to reuse t-shirts as a tensile-shading system

Amirhossein AHMADNIA*, Gergely Mátyás JELINEK^a, Aina RADOVAN^a, Giacomo ONTANO^a, Mana Hosseinpour ROUDSARI^a, Salvatore VISCUSO^b, Alessandra ZANELLI^c

*Textile Architecture Network, Dip. of Architecture, Built-environment and Construction Engineering,
Politecnico di Milano, Italy
Amirhossein.ahmadnia@polimi.it

^a Student of Design of Ultra-Lightweight Building System, School of Architecture, Politecnico di Milano, Italy

^b Textile Architecture Network, Dip. of Architecture, Built-environment and Construction Engineering,
Politecnico di Milano, Italy

^c TextilesHUB - the Interdepartmental Research Laboratory on Textiles and Polymers, Politecnico di
Milan, Italy

Abstract

The T-Shade system is a sustainable and cost-effective solution for urban shading constructed from fashion waste that reduces the adverse effects of solar radiation and brings comfort to urban environments. This paper presents the development, evaluation, and potential of the T-Shade system, which is designed and structurally analysed using computational algorithms and form-finding methods. Experimental studies have shown that T-Shade can effectively reduce the amount of solar radiation entering the building while preserving daylighting conditions, and its modularity enables it to be easily installed and adapted to various urban contexts and dimensions. The system was constructed in 2021 at the campus of Politecnico di Milano, demonstrating its real-world application. T-Shade aims to address the increasing demand for sustainable shading systems by promoting comfort and sustainability in urban areas by combining functionality, sustainability, and affordability. The proposed solution is an example of how upcycling practices can lead to innovative and sustainable solutions for urban challenges. The paper concludes by highlighting the importance of sustainable shading systems and the role of upcycling practices in promoting sustainable practices in urban areas.

Keywords: Reuse, Urban shading, sustainability, upcycling, T-Shade, cost-effective, Ultra-lightweight, computational form-finding.

Membrane architecture: the seventh established building material. Designing reliable and sustainable structures for the urban environment.

1. Introduction

Clothing is responsible for 2-10% of environmental impact across various sectors, making it a significant contributor. Clothing consumption is projected to increase by 63% by 2030, from 62 million tons in 2015 to 102 million tons (Global Fashion Agenda & The Boston Consulting Group, 2017). The textiles industry, deeply ingrained in society and culture, is among the most polluting industries globally. Moreover, the production of raw materials for the textile and clothing industries has the biggest total environmental impact (Da Silva et al., 2021). Majority of the raw materials used originate from either agriculture or petro-chemical industry of which both are responsible of vast amounts of emissions. The textiles industry faces considerable pressure to meet increasing demand due to a growing population, increasing wealth, and consumerism in emerging markets, and the rise of fast fashion in developed countries. Claudio (2007) defines fast fashion as "a possibility to produce clothing at increasingly lower prices, making consumers consider clothing as disposable." The fast-fashion business model is based on copying styles from high-end fashion and delivering them in a short time, at low prices, and typically with low-quality materials in large volumes and due this to be thrown away after wearing them maximum seven-eight times (European Parliament, 2019). As a result, there is a significant strain on natural resources, which has caused severe environmental impacts and social problems. Furthermore, the overproduction of textiles and changes in consumer patterns have resulted in vast quantities of used and unsold textiles ending up in developing countries, while most post-consumer waste is disposed of as waste. (Wang, 2006; Beton et al., 2006; Zamani et al., 2014).

One of the major issues is the enormous amount of waste generated, with 92 million tonnes of garments ending up in landfills each year, which is equivalent to a rubbish truck full of clothes every second. This trend is expected to continue, with fast fashion waste predicted to increase to 134 million tonnes per year by the end of the decade. Dyeing and finishing, along with yarn preparation and fibre production, are some of the most resource-intensive processes in the industry, contributing to 3% of global CO₂ emissions and over 20% of global water pollution. These processes rely heavily on energy-intensive methods using fossil fuels (source:Earth.Org).



Figure 1: The wasted clothes were collected by the HUMANA company

The table below shows the data on global fiber production in 2021 (source: textileexchange.org). In the face of a total production of 111 million tons, it emerges that the two dominant classes are Polyester and Cotton.

Membrane architecture: the seventh established building material. Designing reliable and sustainable structures for the urban environment.

Table 1: Global fiber production in 2021 based on: textileexchange.org

Type of fiber	Polyester	Other Syntactic fiber	Cotton	Other Vegetable fiber	Animal Fibers	Artificial (cellulosic matrix)
Percentages	54	10	22	5.9	1.6	6.4

This paper proposes the learning-by-doing development of an ultra-lightweight shading system constructed of wasted t-shirts as a way to utilize discarded t-shirts in the construction industry. Its goal is to raise awareness about the significant amount of textile clothing that is thrown away every year, which has a substantial environmental impact due to the water, energy, and chemicals consumed in its production and service life (EURATEX, 2019).

2. Problem statements

2.1. The application context: the urban shading-system

Cities are rapidly growing, resulting in increased urbanization and its associated challenges. Urban shading systems, including natural and artificial means of providing shade, are essential for creating comfortable and sustainable urban environments (Jiang et al., 2017) due to the need to create comfortable public spaces for gathering people as well as to improve human well-being for urban inhabitants (Source: www.yale-nus.edu). Existing gaps in urban shading systems require further investigation and attention. These gaps include the need for comprehensive design and integration guidelines considering local climate, building orientation, and urban morphology (Jiang et al., 2017). Further research is necessary to evaluate the performance of different shading techniques in various urban contexts, considering their impact on microclimatic conditions, energy consumption, and human comfort (Jiang et al., 2017). Equity and accessibility should be addressed to ensure fair access to shaded spaces, address social justice concerns, and avoid disparities (Webb et al., 2020). Increasing public awareness and fostering community engagement through education and outreach initiatives are essential for successful implementation (Webb et al., 2020). Collaboration among stakeholders, including policymakers, urban planners, architects, and researchers, is crucial to developing comprehensive guidelines, conducting evaluations, promoting equity, and raising awareness for the sustainable and inclusive integration of urban shading systems.

2.2. The material: wasted clothes

Currently, individuals purchase an average of 13 kg of new clothing per year, of which less than 1% is recycled for new clothing, while 13% is reused in other industries such as insulation and mattress fillings (Zanelli et al., 2020). Recycling and reusing of wasted clothes have become an increasingly important topic in recent years due to the negative impact of textile waste on the environment. According to Beton et al. (2006), the overproduction and shifting consumer patterns in the fashion industry have led to significant amounts of used and unsold textiles ending up in developing countries, while most post-consumer waste ends up in landfills. To address this issue, various recycling and reuse strategies have been developed. For instance, mechanical recycling involves shredding and spinning old textiles into new yarns, while chemical recycling breaks down the fibers into their basic components to produce new materials (Hu et al., 2021). Reuse strategies include donation to charities, resale markets, and upcycling,

Membrane architecture: the seventh established building material. Designing reliable and sustainable structures for the urban environment.

which involves transforming old clothes into new products with higher value (Zamani et al., 2014).

Despite the potential benefits of recycling and reuse, there are also challenges associated with these strategies, such as the cost and complexity of the recycling process and the lack of demand for recycled materials (Hu et al., 2021). Additionally, there is a need for more education and awareness among consumers to encourage a shift towards more sustainable consumption patterns (Goworek et al., 2019). Nonetheless, recycling and reusing of wasted clothes have the potential to reduce the environmental impact of the fashion industry and create a more circular economy.

The raw materials used in the products are not only valuable but also have potential to be utilized for construction industry, as they are or by shredding into their raw materials. Emerging technologies on sorting discarded textiles exist; simultaneously, utilization in construction sector may prove lower processing requirement and faster applicability in comparison to recycling textiles waste back into consumer garments.

2.3. Form-finding and Computational design process

Despite the advancements in computational design and form-finding methods, there are still gaps in the field when it comes to utilizing wasted materials as structural elements. While techniques like mesh relaxation can create optimized shapes for tensioned structures, there is a lack of strategies for incorporating discarded materials into the design process. This gap presents an opportunity to explore how wasted clothes, for example, can be integrated into the form-finding process to create sustainable and cost-effective designs. By addressing this gap, we can move towards a more circular economy where discarded materials are repurposed and reused in innovative ways.

3. Research questions and objectives: Can wasted T-shirts be used as a membrane for urban shading systems?

The research question of whether wasted t-shirts with acrylic sources can be used as a membrane for urban shading systems is an interesting and relevant topic for sustainable design. With the growing concern about the environmental impact of textile waste and the need for sustainable urban solutions, repurposing discarded t-shirts as shading membranes could be an innovative and eco-friendly approach. However, this research question presents several challenges that need to be addressed, such as the durability and strength of the material, the production process, and the feasibility of using this material for large-scale urban shading systems. Investigating these challenges could provide valuable insights into the potential use of textile waste in sustainable urban design. This paper presents a learning-by-doing project that mostly involved the form-finding and fabrication of a temporary waste-based shading system.

4. The project approach and methodology

The project approach involves collecting discarded t-shirts from HUMANA, a multinational social enterprise, and processing them in the TextilesHUB laboratory to create a repurposed fabric. The digital form-finding technique will be employed using Kangaroo, a grasshopper plugin, to optimize the shape of the shading membrane based on the physical properties of the repurposed fabric while Finite Element Analysis (FEA) with Karamba evaluates its structural performance. The selected t-shirts will be interconnected to create a cohesive membrane and

Membrane architecture: the seventh established building material. Designing reliable and sustainable structures for the urban environment.

installed on-site as an urban shading system. The methodology will include a series of physical testing and evaluation to assess the durability and strength of the material and the feasibility of using it for large-scale urban shading systems. This research aims to contribute to the development of sustainable design solutions and demonstrate the potential for transforming waste into valuable resources.

The T-Shade, a temporary shading system, was installed on the Politecnico di Milano campus during the summer 2021, taking advantage of low wind loads on non-windy days. As the project is still under development, the structure is not yet a permanent solution. Further enhancements are being explored to ensure its strength and stability under varying wind conditions. The temporary installation serves as a prototype to gather valuable insights and feedback, informing the ongoing development of the T-Shade as a robust and reliable urban shading system.

4.1. Collecting the wasted T-shirts

In order to explore the potential of using wasted t-shirts as a material for urban shading systems, a source of such t-shirts was identified in HUMANA, a multinational social enterprise operating in 45 countries. HUMANA collects discarded clothing via 5,000 bins located across 1,200 municipalities in Italy, with an annual intake of approximately 20,000 tons of clothing (4,000 tons sorted) (Source: Interview with Karin Bolin in mid-2022 published on Youtube by progettolabelab). Around 150 wasted t-shirts were brought from HUMANA (The clothes selection center of Pregnana Milanese) to the TextilesHUB laboratory and those that were not significantly damaged were selected to be used as a membrane in the next step. However, there exists a non-textile fraction of discarded clothing that is contaminated with non-recyclable materials such as metals or plastics. The challenge of recycling t-shirts lies in the diversity of their composition, the presence of potential chemical contaminants, and the difficulty in separating out non-recyclable materials. To address these challenges, a clustering approach was employed to group t-shirts with similar characteristics and enable efficient processing for reuse or recycling. Acrylic is a synthetic polymer that is commonly used in textile production. The wasted t-shirts used in the t-shade project are made of acrylic fiber. According to the Textile Exchange's Preferred Fiber and Materials Market Report (2021), an estimated 1.7 million tonnes of acrylic fibers were produced in 2020, giving acrylics a 1.57 percent share of the world's fiber market.

4.2. Mesh Relaxation Form-finding and FEA

Kangaroo, a plugin for Grasshopper, offers a form-finding method called mesh relaxation, which utilizes a balance between forces and geometry to create optimized shapes for tensioned structures such as textile membranes. These structures require complex form-finding methods due to their non-linear behaviour under load. The mesh relaxation method can simulate the forces acting on the structure and create an efficient shape that minimizes material usage and maximizes structural performance. Understanding a structure's behaviour under load is crucial in designing lightweight, tensile structures, and the mesh relaxation method aids in creating efficient and cost-effective designs. The mesh relaxation method shares similarities with other structural form-finding techniques for fabric-formed concrete structures design, such as dynamic relaxation. Mesh relaxation and its application in Kangaroo are detailed by Piker (2013).

To simulate the behaviour of t-shirts as shading devices in urban areas using Kangaroo, information on the elastic modulus and yield strength of t-shirts is required. Therefore, based

Membrane architecture: the seventh established building material. Designing reliable and sustainable structures for the urban environment.

on (source: matweb.com), the elastic modulus of t-shirts made of acrylic would fall within the range of 2.76 to 3.3 GPa, and the Ultimate Tensile Strength would fall within the range of 44.9 - 86.0 MPa and elongation at break is from 33 to 64% (Grishanov, 2011).

The form-finding process of T-Shade using Kangaroo was performed to create a temporary shading solution in the summer of 2021. In this process, the T-Shade was designed to be suspended from three anchor points that were located on the facades of existing buildings, and a cable was used to hang the membrane. To preserve the environment, a hole with a radius of 50 cm was included in the design to accommodate a tree.

The form-finding process using Kangaroo to simulate the behaviour of the T-Shade resulted in the identification of the maximum deformation points in the membrane structure. The analysis indicated that the corners of the T-Shade experienced the highest degree of deformation, as evidenced by the red color coding in the corresponding figure (figure 2.2). This finding is consistent with the behaviour of membrane structures under load, where corners and edges are known to experience more significant stresses and deformations due to the concentration of forces in these areas. The identification of these areas of high deformation will be useful in determining the areas of the structure that may require additional reinforcement to maintain stability and longevity over time.

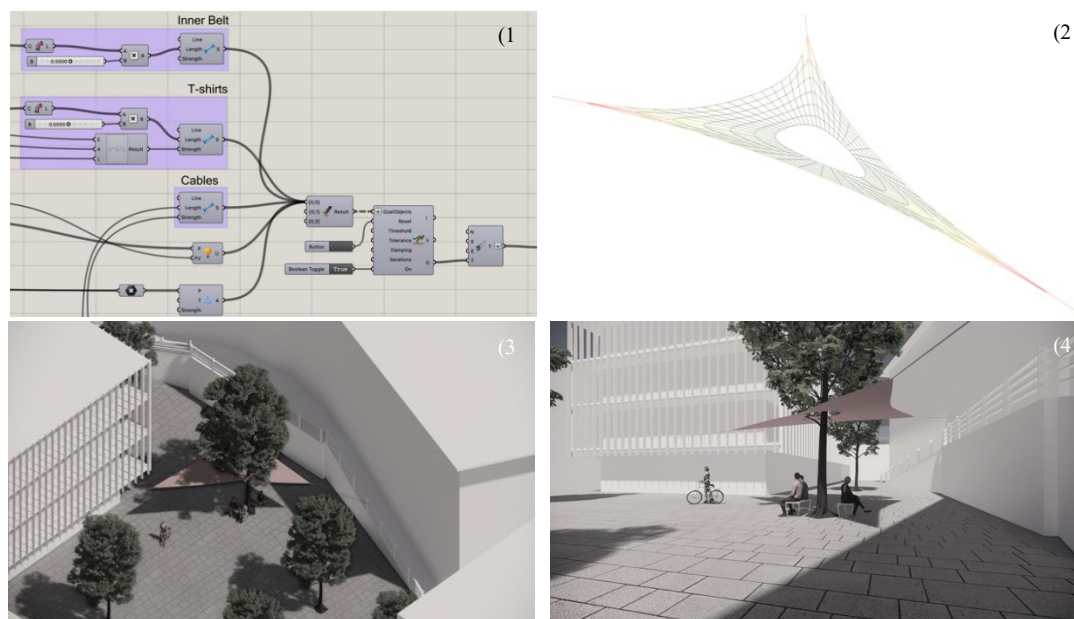


Figure 2: Form-finding process through Kangaroo plugin

To evaluate the structural behaviour of the t-shirt membrane, the form-finding results obtained from Kangaroo were imported into Karamba 3D as a mesh. The analysis in Karamba was performed on the membrane as a shell element, considering a zero bending stiffness to account for its inherent flexibility. Moreover, the membrane was subjected to pre-tensioning to capture its actual behaviour under different loading conditions. The loads considered in the analysis included wind loads and the self-weight of the membrane. However, it should be noted that the installation of the T-Shade took place during the summer and was temporary, and as such, the wind loads were not explicitly considered in the calculation. The FEA results indicated a high utilization percentage, primarily influenced by the effect of wind load. These findings highlight the importance of considering wind loads and ensuring structural stability for the long-term

Membrane architecture: the seventh established building material. Designing reliable and sustainable structures for the urban environment.

performance of the membrane, especially for permanent installations. Figure 3-1 showcases the percentage utilization of the membrane under wind load, while Figure 3-2 presents the corresponding structural model view, with weak points that are normally located beside the anchor points and the reaction forces of supports.

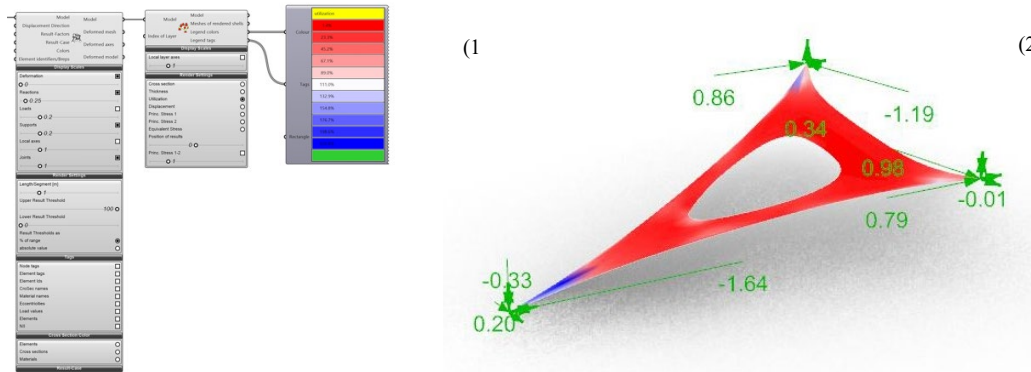


Figure 3: FEA analysis of T-Shade

4.3. Prefabrication procedures

After collecting the wasted t-shirts from HUMANA and completing the digital form-finding process, which allowed us to determine the cutting pattern of the membrane and the number of t-shirts required to cover the target area, the next step was to create a large membrane by connecting the t-shirts together. Each t-shirt provided four connection points, with one located on each short sleeve and two near the corners of the bottom part. The aim was to create a continuous and uniform surface to serve as an urban shading system. In order to connect the t-shirts together, grommets were used at each connection point. Grommets are commonly used in fabric structures for their ease of installation and durability, and were suitable for connecting the t-shirts due to their light weight and flexibility. The use of grommets also allowed for quick and easy assembly of the membrane on site, as well as easy disassembly for storage and reuse in future installations. This connection process was carried out for a total of 54 t-shirts by four non-professional students in the TextilesHUB laboratory, and it was completed within two days. The resulting membrane was a unique and sustainable material that was ready for installation as an urban shading system.



Figure 4: Connection of wasted t-shirts using grommets to create a large membrane for urban shading system.

Membrane architecture: the seventh established building material. Designing reliable and sustainable structures for the urban environment.

4.4. On-site Installation

During the final stage of the T-Shade project, the on-site installation of the membrane was carried out on the Leonardo campus of Politecnico di Milano. The installation process involved hanging the T-Shade membrane from three anchor points to create an effective urban shading system. The membrane was carefully positioned and adjusted to ensure proper coverage and maximum shading efficiency. This process was challenging due to the size of the membrane and the need to position it accurately in order to maximize its performance. The installation was carried out with the help of the project team, which included a group of 5 architectural students in 6 hours. Overall, the on-site fabrication and installation of the T-Shade project was a success, and the final product provided a functional and aesthetically pleasing urban shading system for the campus.



Figure 5: T-Shade after installation

Based on the provided information, the T-Shade made from wasted t-shirts had a total weight of 12 kg and could cover an area of 29 square meters. This makes the T-Shade an effective and lightweight solution for urban shading. The use of wasted t-shirts as a material not only provides a sustainable alternative to traditional shading systems but also allows for the reuse of discarded clothing. Overall, the T-Shade project showcases the potential of using innovative materials and design strategies for sustainable and eco-friendly solutions in the built environment.

5. Conclusion

In conclusion, this project demonstrates the potential for the innovative reuse of waste materials in architectural design. By repurposing wasted acrylic t-shirts as a membrane material for an urban shading system, this project challenges the conventional approach of using these materials solely as fillers. The use of digital tools such as Kangaroo, Grasshopper, and Mesh Relaxation enabled the creation of a precise and optimized membrane design. The resulting T-Shade structure not only provides effective shading for gathering spaces but also creates a unique aesthetic and spatial quality. Moreover, the fast and easy fabrication process, carried out by a group of non-professional students, highlights the potential for low-cost and accessible fabrication techniques. Overall, the T-Shade project represents a promising example of

Membrane architecture: the seventh established building material. Designing reliable and sustainable structures for the urban environment.

sustainable and innovative architectural design, showcasing the possibilities of repurposing waste materials to create functional and aesthetically pleasing structures. As such, it represents a valuable contribution to ongoing efforts towards a more sustainable built environment. The project aims to raise awareness in the scientific community about the vast amounts of wasted t-shirts and the need to implement circular practices for their reuse instead of resorting to landfilling or incineration.

Acknowledgements

We would like to express our gratitude to the students of the Design Ultra-Lightweight Building System (DULBS) course at Politecnico di Milano during the academic year of 2020-21 for their tireless efforts in designing and fabricating this project. Their dedication and hard work were crucial to the success of this research endeavour. Additionally, we would like to thank HUMANA Company (the Clothes Selection Center of Pregnanza Milanese) for providing the wasted t-shirts. Their support and contribution were invaluable in making this project possible. We also extend our appreciation to the TextilesHUB Laboratory at Politecnico di Milano for providing the facilities and resources for conducting the experiments. Without the support of these organizations and individuals, this project would not have been possible.

References

- Beton, L., Hogg, C., & Wang, X. (2006). Garment collecting: practices and challenges. *Journal of Fashion Marketing and Management*, 10(3), 259-270. <https://doi.org/10.1108/13612020610669792>
- Claudio, L. (2007). Waste couture: Environmental impact of the clothing industry. *Environmental Health Perspectives*, 115(9), A449-A454. <https://doi.org/10.1289/ehp.115-a449>
- Da Silva, C. J. G., Fernandes, S. C. M., Barud, H. S., & Ribeiro, S. J. L. (2021). Bacterial cellulose biotextiles for the future of sustainable fashion: a review. *Environmental Chemistry Letters*, 19, 2967-2980. <https://doi.org/10.1007/s10311-021-01214-x>
- Dezeen. (2019). Harry Nuriev fills transparent sofa with worn Balenciaga clothing. <https://www.dezeen.com/2019/12/03/harry-nuriev-balenciaga-clothing-sofa/>
- Designboom. (2013). Clothes covered building for Marks & Spencer shwopping campaign. <https://www.designboom.com/art/clothes-covered-building-marks-spencer-shwopping-campaign/>
- Designboom. (n.d.). Atelier Belge's plof bench made from shredded textile leftovers. <https://www.designboom.com/design/atelier-belge-plof/>
- Dexigner. (2016). Scottish designers turn unwanted clothing into fashion collections. <https://www.dexigner.com/news/28674>
- Earth.Org. (2021). Fast fashion waste statistics. Earth.Org. <https://earth.org/statistics-about-fast-fashion-waste/#:~:text=1.,on%20landfill%20sites%20every%20second.>
- EURATEX, The European Apparel and Textile Confederation. (2019). Prospering in the circular economy.

Membrane architecture: the seventh established building material. Designing reliable and sustainable structures for the urban environment.

-
- European Parliament. (2019). Environmental impact of the textile and clothing industry. Retrieved from [https://www.europarl.europa.eu/RegData/etudes/BRIE/2019/633143/EPRS_BRI\(2019\)633143_EN.pdf](https://www.europarl.europa.eu/RegData/etudes/BRIE/2019/633143/EPRS_BRI(2019)633143_EN.pdf)
- Gessato. (2018). Demode: Recycled clothing tiles by Bernardita Marambio. <https://www.gessato.com/demode-recycled-clothing-tiles-by-bernardita-marambio/>
- Global Fashion Agenda & The Boston Consulting Group. (2017). Pulse of the Fashion Industry.
- Goworek, H., Fisher, T., Cooper, T., & Woodward, S. (2019). The sustainable clothing market: An evaluation of potential strategies for UK retailers. *International Journal of Retail & Distribution Management*, 47(2), 170-186. <https://doi.org/10.1108/IJRDM-05-2018-0117>
- Grishanov, S. (2011). Structure and properties of textile materials. In M. Clark (Ed.), *Handbook of Textile and Industrial Dyeing* (Vol. 1, pp. 28-63). Woodhead Publishing. <https://doi.org/10.1533/9780857093974.1.28>
- Hu, G., Zhang, J., Feng, Y., Li, B., & Li, G. (2021). Textile waste recycling: A review. *Journal of Cleaner Production*, 295, 126295. <https://doi.org/10.1016/j.jclepro.2021.126295>
- Jiang, Y., Hou, L., Shi, T., & Gui, Q. (2017). A Review of Urban Planning Research for Climate Change. *Sustainability*, 9(12), 2224. <https://doi.org/10.3390/su9122224>
- MatWeb. (n.d.). Acrylic (PMMA) Resin, Pellets. Retrieved February 10, 2023, from <https://www.matweb.com/search/datasheet.aspx?bassnum=O1303&ckck=1>
- MVRDV. (n.d.). House of clothing. <https://www.mvrdv.nl/projects/182/house-of-clothing>
- Piker, D. (2013). Kangaroo: Form Finding with Computational Physics. *Architectural Design*, 83, 136-137. <https://doi.org/10.1002/ad.1569>
- Textile Exchange. (2021). Preferred Fiber and Materials Market Report. Retrieved from https://textileexchange.org/app/uploads/2021/08/Textile-Exchange_PREFERRED-Fiber-and-Materials-Market-Report_2021.pdf
- Wang, Zhongyin. (2016). Sustainable Fashion Supply Chain: Lessons from H&M. *Sustainability*, 8(12), 1266.
- We Heart. (2013). Bernardita Marambio: The Reliving Room. <https://www.we-heart.com/2013/09/30/bernardita-marambio-the-reliving-room/>
- Webb, S., Holford, J., Hodge, S., Milana, M., & Waller, R. (2020). Learning cities and implications for adult education research. *International Journal of Lifelong Education*, 39(5-6), 423-427. DOI: 10.1080/02601370.2020.1853937.
- Yale-NUS College. (n.d.). Urban Studies Programme - Why Urban Studies. Retrieved from <https://www.yale-nus.edu.sg/urban-studies/overview/programme/why-urban-studies/>
- Zamani, B., Strøm-Andersen, J., & Kopnina, H. (2014). Reuse and recycling of clothing and textiles—a network approach in the UK. *Journal of Cleaner Production*, 83, 155-162. <https://doi.org/10.1016/j.jclepro.2014.06.019>

Membrane architecture: the seventh established building material. Designing reliable and sustainable structures for the urban environment.

Zanelli, A., Monticelli, C., & Viscuso, S. (2020). Closing the Loops in Textile Architecture: Innovative Strategies and Limits of Introducing Biopolymers in Membrane Structures. In S. Della Torre, S. Cattaneo, C. Lenzi, & A. Zanelli (Eds.), *Regeneration of the Built Environment from a Circular Economy Perspective* (pp. 287-298). Springer. https://doi.org/10.1007/978-3-030-33256-3_25

Proceedings of the Tensinet Symposium 2023

TENSINANTES2023 | 7-9 June 2023, Nantes Université, Nantes, France

Jean-Christophe Thomas, Marijke Mollaert, Carol Monticelli, Bernd Stimpfle (Eds.)

Comparison of PE coated PE weave to PVC coated PES weave

ir Rogier Houtman*, ir. Laura Dings*

*Tentech BV, Rotsoord 9A, NL3523CL Utrecht, Nehterlands, Ahmed@tentech.nl, Rogier@tentech.nl

Abstract

This paper handles about the comparison of a weave made out of Polyethylene and coated with Polyethylene material to the more traditional PVC coated Polyester weaves. A comparison will be made on aging, weld capacity, creep and temperature influence. It will be investigated whether it is possible to determine the material reduction parameters described in the prTS19102.

Benefits and drawbacks of both materials will be compared as well as the production and installation procedures.

The PE/PE material is widely used in US and Canada and known for its low environmental impact. It might be an alternative for PVC coated Polyester weave.

Keywords: material research, environmental impact, creep, temperature effects, stiffness, installation, confection.



Figure 1: External view of a PE / PE membrane for an indoor tennis court

Membrane architecture: the seventh established building material. Designing reliable and sustainable structures for the urban environment.

1. Introduction & objectives

The company IPG Intertape Group produces PE coated PE weave, called Novashield Elite for architectural applications. IPG commissioned Tentech to investigate the possible differences between, amongst others, Novashield Elite and PVC-PES.

1.1. Introduction

In both Europe and North America, there is a long tradition of using lightweight materials for covering temporary and semi-permanent structures. This began in North America with, among others, the Ringling Bros. and Barnum & Bailey Circus, which travelled around in giant cotton tents as early as 1871. In Europe there was a similar development. From a certain point in time on, this started to deviate. In North America the material Polyethylene becomes more and more popular made as the so called tape weave and also coated with Polyethylene. The company IPG created high strength tapes enabling strong weaves. In Europe the Polyester weave became more popular having a PVC coating.



Figure 2: advertisement of the Barnum&Bailey Circus 1899 (Wikipedia)

Strange enough, both materials developed their own market in both continents, leaving aside what the development has been in other continents, which have not been considered. One could say that certain building types have emerged that lend themselves ideally to one material or another. The interesting thing about this is that it is not immediately clear why these differences arose and whether the materials could be exchanged without question.

Membrane architecture: the seventh established building material. Designing reliable and sustainable structures for the urban environment.

It is a fact that both materials require a similar, yet specific way of processing, which means that one fabric cannot simply be swapped with another, even though there are no immediate construction-technical obstacles to this. It therefore has more to do with how fabricators set up their production and what machinery they have at their disposal. These are parameters that are less controllable because they often involve larger investments.

However, given the fact that a PVC-coated Polyester fabric is a composite material that can be recycled, but not in an easy way, and in these days there is an increasing need to use materials that can be recycled properly, the question becomes interesting whether PE-coated PE fabric can be an alternative to PVC-coated Polyester.

To get acquainted with the material, the authors visited a building in the Netherlands equipped with a PE coated PE fabric. At the time of visits, the building has been standing for about 10 years. The building is shown in Figure 1.

At first sight, it is not visible that the fabric is not a PVC coated Polyester. As a matter of fact, when the building had just been erected, the author had already gone to see it, not realizing that it was a PE coated PE fabric. Also still after 10 years the building envelope looks like a normal tensioned membrane roof out of PVC coated Polyester. Of course, one is going to see differences if one knows what to look for.

Typical for the building style of PE-coated PE fabrics, is the use of linear support at fixed distances, a bay distance of approx. 5m. The fabrics are produced in panels of 5m, but tightened in such a way as to create a double curvature in the membrane.



Figure 3: inside picture of the tennis court (the orange gravel dust everywhere discloses it is a tennis court)

Membrane architecture: the seventh established building material. Designing reliable and sustainable structures for the urban environment.

2. Quantitative comparison

If fabric is going to be used as a structural material, one of the first questions is what is the strength of the material and what is the stiffness of the material. For comparison, 2 fabrics are compared here, an IPG NOVASHIELD PE/PE fabric and a Type I PVC/POLYESTER fabric.

Table 1. An example selection of yarns to suit the set criteria, and their mechanical properties.

Fabric type	Tensile strength	Width	Stiffness (direct)
	N/5cm (Warp / Weft)	Mm	kN/m (Warp/ Weft)
IPG Novashield Elite	2309 / 2131	3657	+/- 300 / 300
PVC-PES Type 1	3000 / 3000	3000	+/- 800 / 700

At first glance, the Novashield Elite material is a 'tight' Type 1, at least belongs to the lighter materials. A mainstream fabric strength has been taken for the PVC-PES fabric.

The stiffness of the Novashield fabric is also lower than the PVC-PES fabric. This is obvious due to the weaker fabric, but can also be an advantage under external loads.

To do a test on this, 2 fabric panels are modelled in the FEM software EASY FSC from Technet GmbH.

Fabric panel of 5x20m, with pretension of 1 kN/m' both in warp and weft (see Figure 4).

The left panel is with IPG Novashield, the right panel is with a Type II fabric.

If we apply the stiffnesses according to the table and we load the panels with wind in the same way, we get an indication of the differences in stress (see Figure 5).

Membrane architecture: the seventh established building material. Designing reliable and sustainable structures for the urban environment.

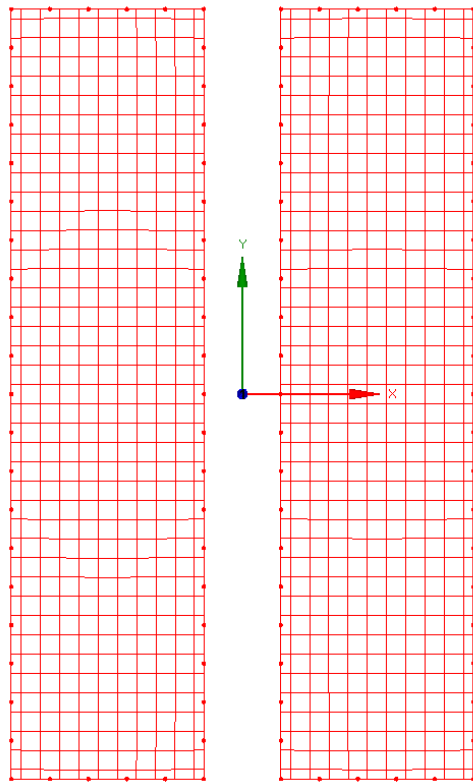


Figure 4: left panel Novashield Elite fabric, right panel PVC-PES fabric

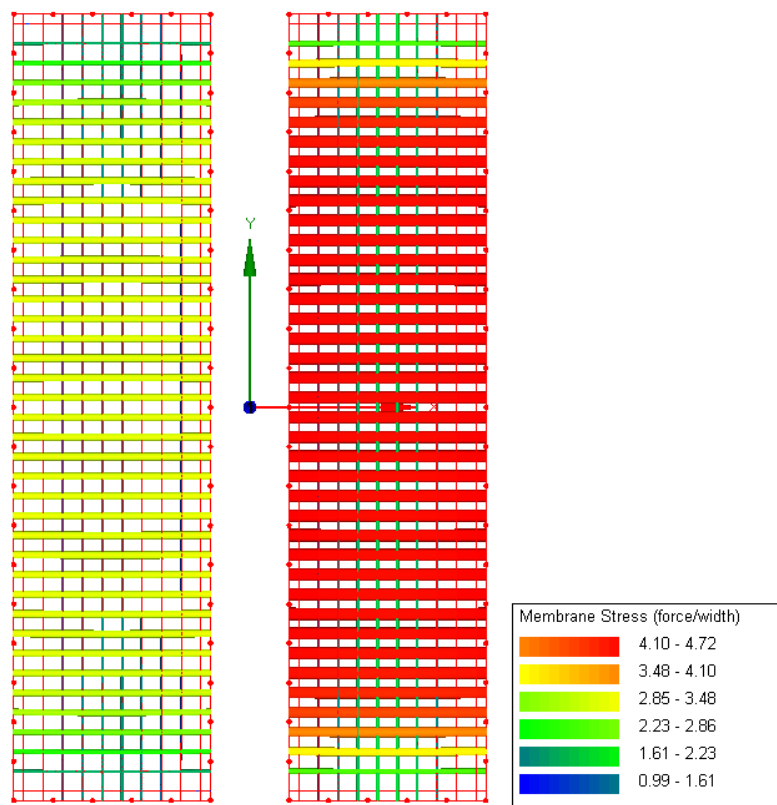


Figure 5: stresses in left panel Novashield Elite fabric, right panel PVC-PES fabric, kN/m'

Membrane architecture: the seventh established building material. Designing reliable and sustainable structures for the urban environment.

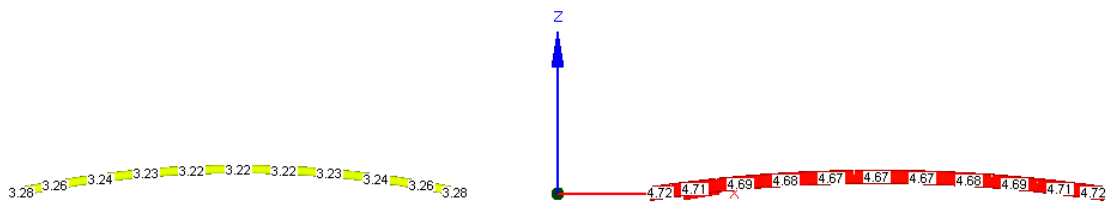


Figure 6: stresses in left panel Novashield Elite fabric, right panel PVC-PES fabric, kN/m' in cross section

So, in the Novashield there is 3.22 kN/m, in the PVC-PES fabric there is 4.67 kN/m

- ➔ $4.67 / 3.22 = 1.44$ times lower.
- ➔ This will be one of the benefits
- ➔ This will also be a drawback for more flat roofs, as they will have sooner snow accumulation.

This might explain why a lot of applications with Novashield material have a steep roof inclination as this facilitates snow shedding.



Figure 7: Typical applications of Novashield Elite material (Itape 2023)

References

Houtman, R. (2021) 21.04.3568_ME01_Test Protocol," internal report Tentech 2021.

Patton, S. (2021) Characterization of Polyethylene Structure Membrane: Anhalt University of Applied Science, 2021

Intertape (2023) IPG INTERTAPE NOVASHIELD <https://www.itape.com/wp-content/uploads/2022/12/FIRST-SUSTAINABLE-STRUCTURE-FABRIC.pdf>

Wikipedia

https://en.wikipedia.org/wiki/Ringling_Bros._and_Barnum_%26_Bailey_Circus#/media/File:Barnum_&_Bailey_greatest_show_on_Earth_poster.jpg



tensinantes2023 : TensiNet Symposium 2023 at Nantes Université

Membrane architecture: the seventh established building material. Designing reliable and sustainable structures for the urban environment.

Proceedings of the Tensinet Symposium 2023

TENSINANTES2023 | 7-9 June 2023, Nantes Université, Nantes, France

Jean-Christophe Thomas, Marijke Mollaert, Carol Monticelli, Bernd Stimpfle (Eds.)

Advancing the Design of Sustainable ETFE Membrane Structures: Insights from the Lighten Consortium Project

Mohammad Hosein Nejabatmeimandi^{*,c}, Alessandro Comitti^{a,b}, Luis Seixas^{a,b}, Adrian Cabello^c, Adam C. Bown^c

^{*}Department of Civil, Environmental and Mechanical Engineering, University of Trento, Trento, IT,

mh.nejabatmeimandi@unitn.it

^a Department of Mechanical Engineering, University College London, London, UK.

^b CAEMate s.r.l., Bolzano, Italy, IT.

^c Tensys Ltd, 122 Wells Road, Bath, UK

Abstract

The construction industry is a significant contributor to CO₂ emissions and energy consumption due to its high material use. ETFE membrane structures offer a potential route to reduce some of these impacts, by being lightweight and fully recyclable, thus reducing material consumption. It is popular among designers due to its desirable properties such as high stiffness and durability, but a lack of understanding of how time and temperature affect its mechanical properties has limited its use in sustainable buildings. The Lighten Consortium is working to improve the design of sustainable membrane structures using ETFE through material characterization and the development of a constitutive model. Additionally, the research group is investigating instability mechanisms in lightweight tension structures caused by environmental loads. This paper presents the progress of the Lighten Consortium project and explains an analysis method that couples CFD and FE techniques to predict and ultimately prevent instabilities.

Keywords: Lightweight structures, Structural membrane, Sustainability, ETFE models, Flutter

1. Introduction

1.1. Tensile Structures: A Sustainable Solution for the Built Environment

Construction is a major contributor to global energy consumption and carbon dioxide emissions, accounting for 36% and 39% respectively, which is more than transportation, at 33%, and industrial activities at 29% (IEA, & UNEP. 2018). As population and floor area continue to increase, so will the demand for energy in building construction, especially in urban areas in Asia and Africa (United Nations. 2021). To address this issue, it is important to implement low-carbon building technologies to reduce CO₂ emissions, design resource-efficient buildings, and reduce transportation needs. Finding and implementing appropriate new technologies is a major challenge in the building industry.

Membrane architecture: the seventh established building material. Designing reliable and sustainable structures for the urban environment.

Tensile or membrane-based structures can be a sustainable solution for the built environment. While traditional structural materials use compressive, bending, or compressive/tensile mechanisms to bear external loads, tensile structures rely solely on tension actions to do so. Therefore the use of lightweight textile membranes in place of heavy materials like steel, timber, and concrete in many applications, may result in more efficient load-bearing and reduced energy consumption and emissions from transportation and construction. (Seidel, 2009, Koch, 2004).

Lightweight membranes also have the benefit of durability and long lifespan. In the past, these types of structures were only used for temporary installations due to limitations in the materials available. However, with advances in coatings, or with the use of foils, the average lifespan of membrane structures can be up to 30 years or more. This increased durability has encouraged the use of membrane structures in a wide range of building applications, including cladding, roofing, and facades, in exhibitions, and stadiums, providing attractive envelopes while minimizing resource use (De Focatiis and Gubler, 2013).

1.2. ETFE Models for Building Design and Analysis

Ethylene Tetrafluoroethylene (ETFE) is a fluorine-based plastic that has gained popularity in the construction industry for its unique properties and potential for sustainability and offers many benefits such as energy efficiency, durability, and cost-effectiveness (Huang et al., 2014). It is also highly resistant to UV radiation and has a self-cleaning ability, making it easy to maintain (Mahdavi et al., 2016). ETFE has been used in a variety of building projects around the world, including the Beijing National Aquatics Center (also known as the "Water Cube") and the Allianz Arena in Munich. One of the major advantages of ETFE is its transparency and ability to transmit natural light, making it an ideal material for use in structures such as atria and skylights. However, there is a lack of understanding of the constitutive behaviour of this material, particularly in relation to creep. Creep is the time-dependent deformation of a material under a constant load and is a result of the movement and relaxation of the material's molecular chains (Wu et al., 2019). Creep behaviour, particularly at high temperatures, can lead to permanent deformations and changes in the material's properties (Meng et al., 2018) and more importantly from a structural perspective, result in changes in the prestress in the material.

Accurately modelling the creep behaviour of ETFE is important for designing and analysing structures using this material. However, the creep behaviour of ETFE is complex and depends on temperature and the type of loading (Meng et al., 2018). In addition, ETFE has nonlinear and anisotropic properties making it difficult to develop a precise constitutive model that can accurately predict the behaviour of the material under different loading conditions (Wu et al., 2019). As a result, there is a need for more research on the constitutive behaviour and creep behaviour of ETFE in order to improve the accuracy of models for this material and optimize its use in building envelopes.

It is important to have a comprehensive understanding of ETFE's behaviour under different loads in order to design and ensure the safety of structures made from it. Neglecting to fully comprehend ETFE's response and alterations in pre-stress caused by relaxation or creep can result in structural failures or deformations that threaten the functionality of a building. Therefore, it is essential to enhance our knowledge of ETFE.

1.3. Lighten project

The Lighten project is a research program funded by the European Union that aims to develop innovative and sustainable building technologies using lightweight materials. The project aims

Membrane architecture: the seventh established building material. Designing reliable and sustainable structures for the urban environment.

to reduce the environmental impact of the building sector through the development of technologies that permit the reduction in the use of traditional materials such as steel and concrete and by promoting the use of recyclable building components. The ultimate objectives of the Lighten program are four-fold:

- I) Determine a linear and non-linear constitutive model to characterise the viscoelastic behaviour of ETFE.
- II) Determine temperature and strain rate-dependent yield criteria.
- III) Use hybrid machine learning techniques to characterise the plastic behaviour of ETFE.
- IV) Investigate potential dynamic instabilities in tensioned ETFE skins.

It is item 4 above, which is the particular subject of this paper. A simplified version of the constitutive model has been explained and the nonlinear dynamic behaviour of wind-induced vibration of prestressed tension structures has been investigated numerically.

2. Material modelling

2.1. Viscoelastic modelling - initial results

The accurate modelling of material behaviour is essential for the safe and efficient use of membrane materials in tensile structures. Single foil membranes in boundary-tensioned structures are particularly sensitive to changes in external conditions such as temperature and loads, which can severely affect structural performance. Loss of pre-stress due to these factors can lead to loss of functionality. These structures are also prone to aeroelastic instabilities. To optimize and control the design of a tensile structure, it is necessary to take into account time and temperature dependence in the constitutive model.

ETFE has been shown to be greatly affected by time and temperature effects, showing creep (Li, Y., & Wu, M., 2015), softening with higher temperatures (Moritz, K., 2007) and stiffening with higher strain rates (Galliot, C., & Luchsinger, R. H., 2011). Nevertheless, no comprehensive material model to enable a conscious structural design exists to date. Moreover, no official regulations yet exist to guide the design process and verification.

The most valuable document to guide the design of ETFE structures is provided by Tensinet Guidelines (Houtman, 2013), which suggests the use of a linear elastic material model, with the stiffness values changing according to the load case. In particular, different elastic moduli for short and long term loads are provided. It has already been shown by Cabello and Bown (Cabello, A., & Bown, A. C., 2019) that the construction of a reliable model is needed to achieve a confident design of ETFE structures. In fact, in this paper, the author re-factored the nonlinear thermoviscoelastic model created by Bosi and Pellegrino (Bosi, F., & Pellegrino, S., 2018) to match some experimental data of ETFE and applied it to common load cases for ETFE structures. Comparing those results with what is suggested by the current guidelines (Houtman, 2013), it is shown how the design of ETFE is currently unsafe in certain conditions.

In the Lighten project (LIGHTEN MSCA project, 2021), a constitutive model is in development, following a phenomenological approach. An extensive experimental campaign has been executed in order to achieve a deep understanding of the material behaviour, investigating uniaxial and biaxial properties through constant strain rate tests, blister tests of different shapes, oscillatory tests, and creep and relaxation conditions. Through the procedure, the strain rates, the frequencies, and the temperatures have been varied in order to comprehensively capture the material response in an adequate range for the application in

Membrane architecture: the seventh established building material. Designing reliable and sustainable structures for the urban environment.

buildings. This campaign led to a preliminary constitutive model built in the linear viscoelastic region of the material. This model was shaped using the mechanical analogy rheological modelling, employing a Generalized Kelvin-Voigt element to describe the multiaxial stress-strain response. The linear viscoelastic model can include temperature dependence in its response through applying the Time-Temperature Superposition Principle (Brinson, H. F., & Brinson, L. C., 2008). The strain response $\varepsilon(t)$ consequent to a variable stress history $\sigma(t)$ can be expressed by applying the Boltzmann superposition principle as

$$\varepsilon(t') = \int_0^{t'} D_0 + \sum_{i=1}^N D_i \left(1 - e^{-\frac{t'-s}{\tau_i}}\right) \frac{d\sigma(t')}{ds} ds, \quad (1)$$

where D_0 and D_i represent the instantaneous and the transient stiffnesses of the material, while τ_i indicates the relaxation times of the Prony series. The preliminary constitutive relation is working satisfactorily to predict an extended set of independently acquired experimental data. The nonlinearity of ETFE will need to be captured in future extensions of the model, currently in development as a modification of the linear viscoelastic material law.

2.2. Yield criterion – initial results

When membrane materials are implemented in engineering applications, one of the most important aspects is the definition of their design limits. Ignoring these limits can lead to failure, or over-designed structures, the latter significantly increasing material usage. One of the limits that structural engineers must consider in the case of ETFE, especially in structures undergoing cyclic loading, is the onset of plasticity, because irreversible and sometimes unpredictable deformations are created from that point onward. This mechanical limit can be defined for ductile materials through yield criteria, used to evaluate if a multiaxially stressed structure is at risk of entering plasticity.

Several past studies (Galliot, C., & Luchsinger, R. H., 2011) have shown that ETFE onset of plasticity is highly dependent on time and temperature. Characterizing these dependencies correctly is essential to build a time temperature-dependent yield criterion that can predict the ETFE onset of plasticity in multiple conditions. The temperature can affect dramatically the material's yield strength since there is a reduction in higher temperatures, which can lead to unsafe design if not accounted for. Concerning the time effect, currently, it is mostly neglected or oversimplified in design practices and recommendations (Houtman, 2013), however, the viscous behaviour of ETFE can cause the material entering plasticity at lower stress levels when a long-term load is present.

Different authors, such as (Zhao, B., & Chen, W., 2021) and (Sun, G. et al. 2022), tried to model the ETFE yield strength time and temperature dependencies through a yield law. However, these expressions lacked further implementation. During the Lighten material modelling campaign, a mathematical expression that can predict the yield stress with temperature and strain rate as independent variables was also developed based on the uniaxial experimental results. This first approach, completely phenomenological, has shown to be able to predict the onset of plasticity with significant accuracy. The mathematical expression was then further implemented into a known criterion, as Von Mises, which allowed to change of the yield loci accordingly. As it is possible to observe in Figure 1, the von Mises yield criterion expands/contracts with the time and temperature effects resulting in different plasticity onsets.

In the future, other yield models that can represent the time and temperature effects of ETFE will be considered and implemented into the von Mises yield function. These models will be

Membrane architecture: the seventh established building material. Designing reliable and sustainable structures for the urban environment.

less phenomenological than the proposed mathematical expression, which will help explain the plasticity behaviour in structural membranes, such as ETFE.

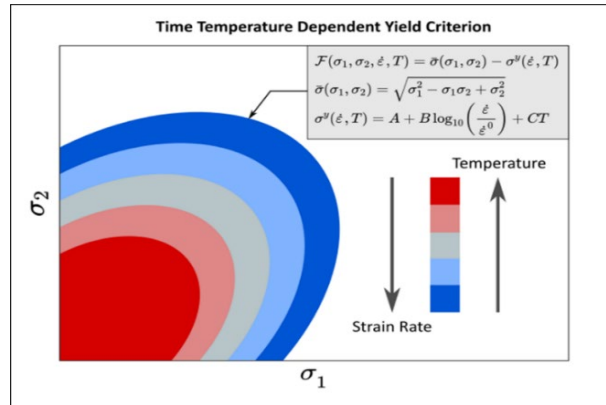


Figure 1: Time temperature-dependent yield criterion representation.

2.3. Application of the preliminary models

As mentioned, preliminary tools have been developed and are currently under validation and extension to a more accurate formulation. In the following, the application of the linear viscoelastic model to replicate independently acquired test data is shown, together with the yield criterion application. In particular, the stress and time values of an experimental data set have been fed into the model, which was able to return a corresponding strain, plotted in Figure 1a, where the test temperature was 40 °C. Moreover, Figure 1b shows creep tests with ‘instantaneous’ loading, at a temperature of 0 °C. For both load cases, the creep stress was 3 MPa. Each sample is composed of a set of 3 specimens tested, in the ETFE machine direction (along the extruded roll). The viscoelastic model can predict the material behaviour by knowing the temperature and either the strain or the stress time-history. In these examples, the stress history was an input to the model, that could provide a simulated strain. The evaluation of the simulated strain rate allowed the computation of the yield point evolution in time.

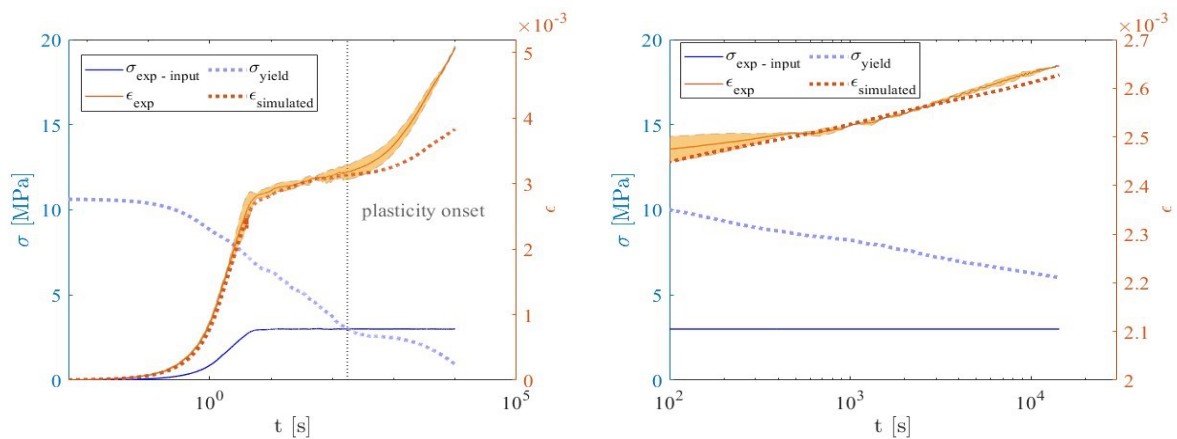


Figure 2: Comparison of the viscoelastic model and yield criterion with 4h creep tests data at 40 (a) and 0 (b) °C. The corresponding strain and yield point can be accurately predicted until the plasticity onset by inputting the recorded stress at the given time.

Figure 2a. shows an accurate prediction of the strains in a constant strain rate and subsequent creep phase. However, the two measures of strain develop a clear discrepancy after an initial

Membrane architecture: the seventh established building material. Designing reliable and sustainable structures for the urban environment.

agreement. The unloading of this sample for a sufficient time span showed a permanent strain, which can explain the disagreement between the model and the data with the onset of plasticity. Additional confirmation of this hypothesis is obtained through the application of the yield law, which shows that the yielding happened in a similar time frame. Figure 1b shows instead an instantaneous creep test at 3 MPa and 0 °C, which did not enter plasticity according to the recovery phase the specimen underwent, analogously to what was described above. The yield criteria and the linear viscoelastic model have excellent agreement with the data in this case.

These application examples show the potential of the combined use of a time and temperature-dependent constitutive model and yield criterion, that can be applied to cushions and single foil applications in order to predict the creep strains, the stress relaxation and the plasticity onset. Future works will extensively validate this approach on independently acquired data. Such powerful tools will need, in future applications, a correct guideline on the design load cases, that should be defined with time-history profiles to allow for a correct evaluation of the material state.

3. Instabilities in tension structures

3.1 Introduction

ETFE structures are susceptible to instabilities such as wrinkling and flutter under certain loading conditions. The onset of these instabilities may also be influenced by the nonlinear and anisotropic properties of ETFE, which in turn are affected by factors such as temperature. (Meng et al., 2018). Instabilities have to be avoided as they can pose a hazard due to dynamic amplification of stresses, fatigue of materials, excessive rotations at the connections, which combined, may eventually lead to structural failure. Pre-stress is the initial stress applied to a structure and improves its stability and capacity to resist external loads (Li et al., 2018). Losses of pre-stress can lead to deformations and instabilities in the structure (Meng et al., 2018). Therefore, it is important to ensure that the pre-stress levels are properly designed, considered and maintained.

3.2 Flutter and VIV instabilities

Flutter instability is a type of aerodynamic instability that can occur in tensioned single-skin structures. It happens when the surface starts to uncontrollably vibrate or oscillate in response to wind forces and can lead to structural damage or failure. Several factors can affect the potential of flutter instability such as area, weight and pre-stress. When the wind blows over the roof, it can generate fluctuating surface pressure that can cause the roof to vibrate. If the natural frequency of the roof's vibration matches the frequency of the wind, the vibration can become self-sustaining, leading to flutter. This can be dangerous as it can cause large amplitude movement and even lead to structural failure (Muc et al., 2019).

Vortex-induced vibration (VIV) is a phenomenon that can occur when a fluid, such as wind or water, flows past a solid object. As the fluid flows past the object, it can shed vortices from the upstream and downstream sides of the object which can cause an oscillating force on the object. This can lead to low amplitude and high-frequency vibrations, which can cause fatigue in the structure over time (Dowell. 1984).

It is well established in the engineering and scientific literature that instability issues related to wind can lead to significant failures in the building industry. One notable example of this is the destruction of the Georgia Dome during the 1995 Atlanta Olympics, which failed despite the structure undergoing thorough wind-resistant designs. According to a study by Dowell, the

Membrane architecture: the seventh established building material. Designing reliable and sustainable structures for the urban environment.

collapse of the Georgia Dome's cable-supported Teflon roof was caused by a combination of factors, including a design flaw in the cable support system, and wind speeds that exceeded the design wind speeds used in the original calculations. (Dowell et al., 1996).

To elaborate more on these instabilities, a detailed examination of FSI simulation modelling and governing equations is presented, the approach to model flutter is validated, and its application to ETFE is demonstrated.

3.3 Governing equations

To determine the forces acting on the structure, the fluid-flow equations in both dynamic and elastic coupling need to be solved. In dynamic coupling, the structure responds to force by solving the rigid body dynamics equations. In elastic coupling, we need to solve the stress equilibrium equations using strain-displacement relations and material constitutive laws. To calculate the shear and pressure forces acting on the structure, we solve the Navier-Stokes equation and continuity equation for an incompressible flow, as described in Equ. 2.

$$\begin{aligned} \nabla \cdot u &= 0 \\ \frac{\partial u}{\partial t} + (u \cdot \nabla)u &= -\frac{1}{\rho} \nabla P + \mu \nabla^2 u \end{aligned} \quad (2)$$

Where u is the velocity, t is time, ρ is the fluid density, P is pressure, and μ is the kinematic viscosity.

The governing equations of the solid are defined with the equilibrium stresses and the strain-displacement relations which relate the internal deformation of the body with its displacement field. Equ. 3. defines the governing equations of the solid.

$$\begin{aligned} \nabla \cdot \sigma + f &= \rho a \\ \epsilon_{ij} &= \frac{1}{2} \left(\frac{\partial u_i}{\partial x_j} + \frac{\partial u_j}{\partial x_i} + \frac{\partial u_k}{\partial x_i} \frac{\partial u_k}{\partial x_j} \right) \end{aligned} \quad (3)$$

Where σ is the Cauchy stress tensor, f is the volume forces, a , ϵ , and u are respectively the acceleration, strain, and displacement at a particular node of the object.

When wind blows over a structure that is under tension, it causes turbulence and friction, leading to initial movements. These movements then affect the airflow and cause changes in surface pressure, as described by Bernoulli's equation. According to Bernoulli's equation, as speed of airflow over the peaks of the disturbance becomes higher and over the troughs becomes lower, this causes a decrease in pressure over the peaks and an increase over the troughs (Equ.2), which amplifies the disturbance. Since these pressure changes are proportional to the disturbance amplitude, they have the same effect as a negative stiffness. When the negative stiffness exceeds the tension of the fabric, large displacement can occur without any resistance. (Williams. 1990).

Membrane architecture: the seventh established building material. Designing reliable and sustainable structures for the urban environment.

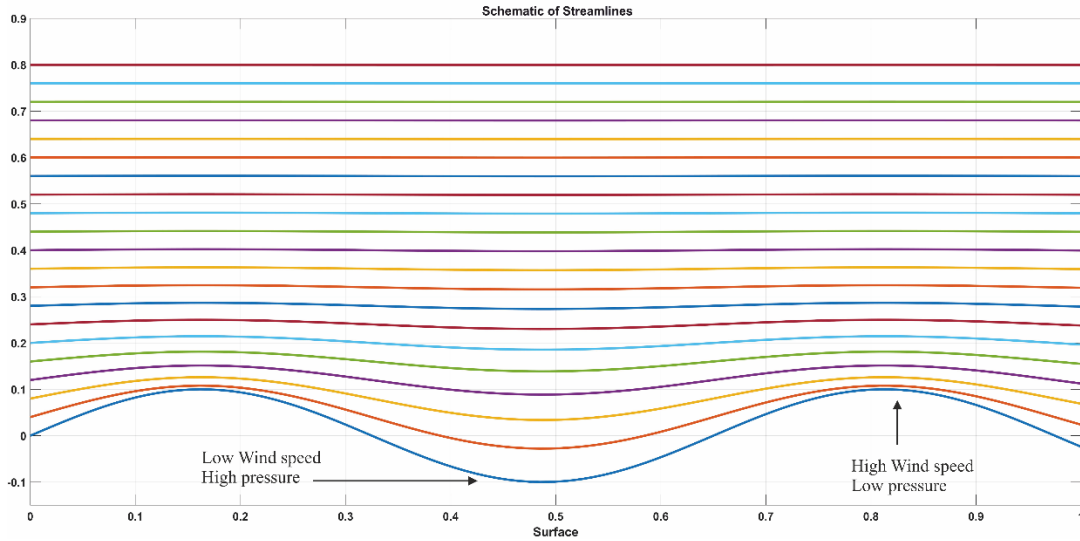


Figure 3: Streamlines over a tensioned structure with out-of-plane disturbances.

Figure 3. shows the streamlines and displacements on a surface. These displacements could be avoided by an adequate amount of prestress. The relation between the critical prestress and wind velocity is defined in Equ. 4. As the wind velocity approaches the critical value, a dynamic amplification of the out-of-plane movements is expected.

$$\frac{1}{2} \rho V_{crit}^2 = \frac{\pi T}{2\lambda} \quad (4)$$

Where ρ is the fluid density, T is the pretension force in the wind direction, and λ is the wavelength (Williams. 1990).

3.4 Modelling approach and Validation

To apply the coupled system of equations outlined previously, we need to employ a FSI approach. Fluid-solid interaction (FSI) involves the interaction between fluid dynamics and structural mechanics. In this type of application, a fluid exerts forces on a solid structure, causing it to deform. The deformation of the structure also affects the movement of the fluid, changing the flow field. To model and solve for both the fluid and solid domains, two different tools and methods are used. The fluid domain is solved using the finite volume method, which involves dividing the domain into small control volumes (cells) and converting partial differential equations into algebraic equations. The solid domain is solved using the finite element method, which involves dividing the domain into smaller elements. Data is frequently exchanged at intervals called coupling steps, which allows for the full solution of the fluid-solid interaction to be obtained. In mechanical coupling, the CFD model passes loads to the stress model, which includes both pressure and wall shear stress. The stress model then passes resultant displacements to the CFD model. The displacements are used as an input for the mesh morpher in the fluid domain. In the CFD model, an incompressible flow and K-Omega turbulence model is used. The inlet boundary is Velocity Inlet with constant value, and the outlet boundary is modelled as a Pressure Outlet, the bottom is no-slip wall, and the top and sides of the domain are specified as Symmetry boundaries. The dynamic implicit method is used for the stress model.

Membrane architecture: the seventh established building material. Designing reliable and sustainable structures for the urban environment.

In order to validate the coupling a solid square plate, moment connected to the base is then subjected to a 10 m/s mean wind velocity. The weight and stiffness of the plate are selected such that the first eigenmode has a frequency of around 4 Hz and the first twisting mode has a frequency of around 20 Hz. The dimensions and material properties are shown in Figure 4. and table 1.

Table 1: Details of the simulation

Material properties	Young's modulus	38.4 MPa
	Poisson's ratio	0.3
	Density	4096 kg/m ³
Mesh definition	Mesh	C3D8R elements
	FE elements number	1600
Assumption	Model	Linear elastic material
	Loading	Dynamic step

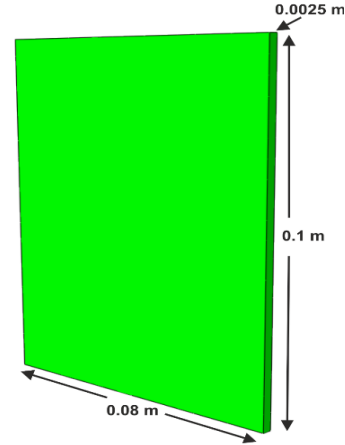


Figure 4: Dimensions of the plate.

The natural frequencies of the plate are calculated and the first three eigenmodes for bending and twisting are shown in Figure 5.

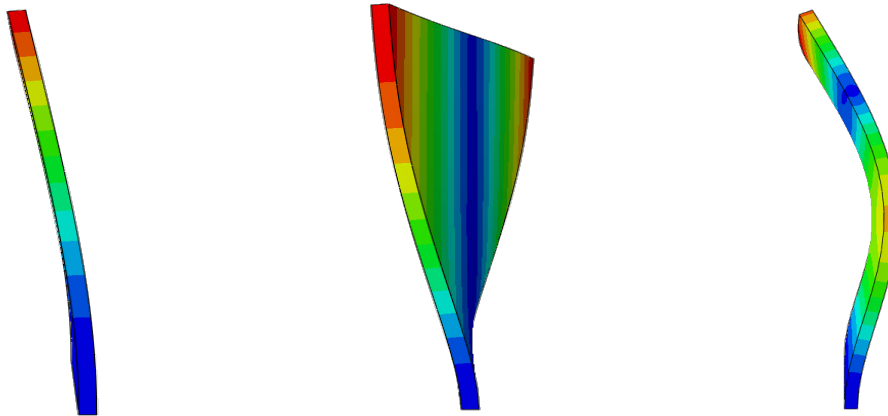


Figure 5: The first three eigenmodes at 3.97, 19.9, and 24.6 Hz respectively

Since the flow is passing over the plate, vortices form at the back of the body and detach periodically from either side, forming the Kármán vortex street (Williamson & Govardhan, 2004). When the vortex shedding frequency matches the resonance frequency of the bluff structure, VIV happens, and the structure vibrates with harmonic oscillations generated by its energy. The frequency of vortex shedding is given by the Strouhal number (non-dimensional),

$$\frac{f L}{U_0} = St (Re) \quad (5)$$

where f is the Strouhal or vortex shedding frequency, L is the body length and St is the Strouhal number. For a plate in the laminar flow $St \sim 0.2$ (Matty, R. R. 1979). Considering that for the

Membrane architecture: the seventh established building material. Designing reliable and sustainable structures for the urban environment.

mean velocity of 10 m/s, the shedding frequency is close to 20 Hz. Therefore, a deflection with respect to the second eigenmode is expected. Figure 6. shows the displacement of two nodes on the top corners of the plate for different frequencies. In second mode, the corners of the plate are out of phase with each other and twisting mode is observed.

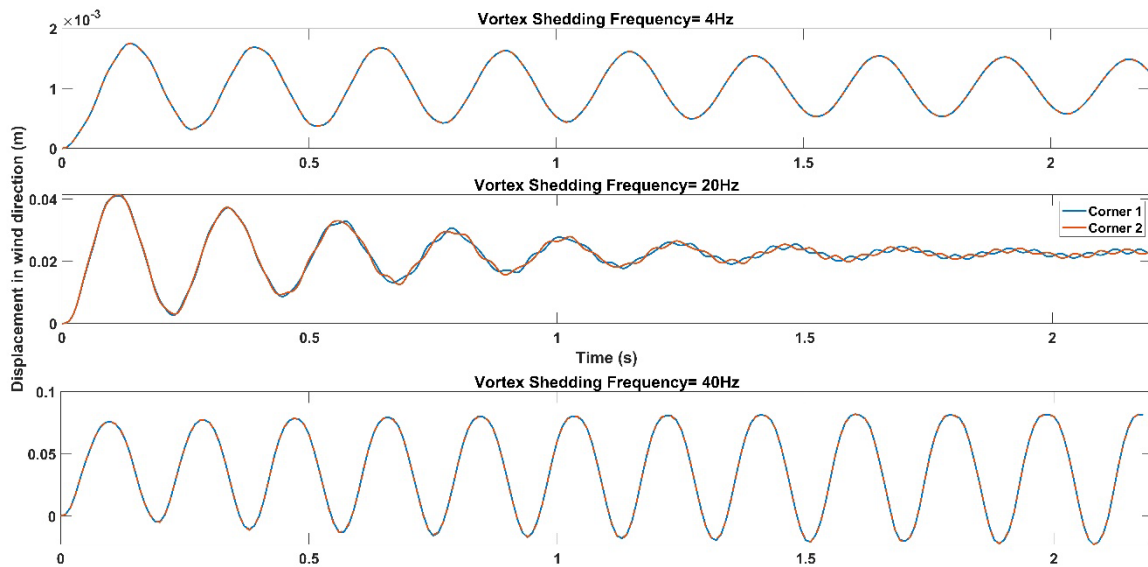


Figure 6: Effect of vortex shedding frequency of the plate motion.

3.5 Application to a single skin, flat tensioned ETFE structure

Flat tensioned structures may be prone to aeroelastic instabilities as the pre-stress is lost via creep. As an illustration, a representative flat panel of ETFE, with dimensions of 10 meters in length and 4 meters in width, is subjected to a mean wind speed of 25 m/s and air density of 1.18 Kg/m³. The panel is simply supported on all four edges. The wind exerts surface forces on the panel, which can cause vibration and deformation. These movements can lead to the oscillation of the panel. The simulated panel was modelled using 16,000 solid C3D8R elements with Young's modulus of 816 MPa, a Poisson ratio of 0.42, and a density of 1740 kg/m³ under different uniaxial stress in wind direction as explained in figure.8. It is shown that any alteration in pre-stress can lead to potentially large vibrations.

The structural element is expected to develop moving or standing waves when there is not enough prestress in the model. In Figure 7. the movements are illustrated.

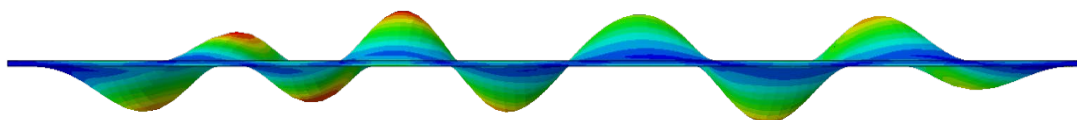


Figure 7: Magnified movement (10 times) in an unstable panel with no prestress.

As explained before, by using Equ.4. the critical velocity at which the wind is able to generate enough out-of-plane force to start movements in the panel is calculated. According to Equ.4, by staying above the critical prestress (700 KPa for the assumed panel) out-of-plane displacements are negligible. Therefore, when the prestress is lower than this value, the large

Membrane architecture: the seventh established building material. Designing reliable and sustainable structures for the urban environment.

movements appear. The new constitutive model and FSI tool to simulate aeroelastic instabilities have shown to be useful, and it is expected to continue to be a valuable tool for engineers.

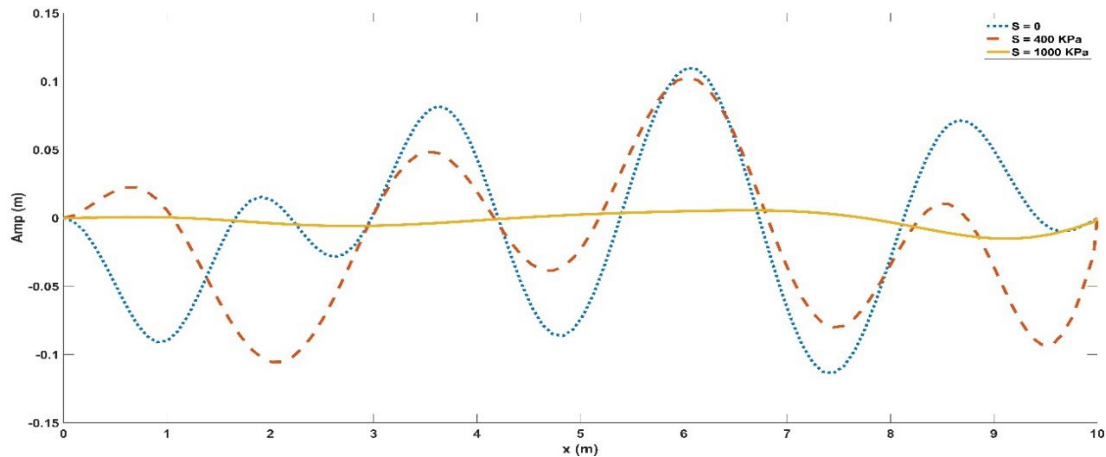


Figure 8: Comparison between the displacement with different prestress at the same time step

The next step is to integrate the ETFE model under development by the LIGHTEN research group into the structural solver of the FSI simulations in order to replicate creep and simulate a structure that starts off stressed and stable, but becomes unstable as pre-stress is lost due to creep.

4. Conclusion

An understanding of ETFE is essential to effectively design and analyse structures made from it. The goal of the Lighten project is to gain a deep understanding of ETFE behaviour and develop a predictive model for use in various conditions. One important aspect of ETFE structures to consider is the instabilities that can occur in structures under natural external loads like wind. Not addressing these instabilities can lead to structural failure. This paper presents a simple governing model, examines the importance of aerodynamic instabilities in tensile structures using FSI simulations. The results demonstrate the impact that prestress can have on the stability of a structure and the potential for large deformation.

Acknowledgements

The authors gratefully acknowledge the support from the EU and the H2020- MSCA-ITN-2020-LIGHTEN-956547 grant.

References

- Bosi, F., & Pellegrino, S. (2018). Nonlinear thermomechanical response and constitutive modelling of viscoelastic polyethylene membranes. *Mechanics of Materials*, 117, 9-21.
- Federico Bosi. LIGHTEN project. 2021. url: <https://lighten-itn.eu/>.
- Brinson, H. F., & Brinson, L. C. (2008). *Polymer engineering science and viscoelasticity. An introduction*, 99-157.
- Cabello, A., & Bown, A. C. (2019, October). Using a nonlinear thermo-viscoelastic constitutive model for the design and analysis of ETFE structures. In *Proceedings of IASS Annual Symposia (Vol. 2019, No. 23, pp. 1-18)*.

Membrane architecture: the seventh established building material. Designing reliable and sustainable structures for the urban environment.

De Focatiis, D. S., & Gubler, L. (2013). Uniaxial deformation and orientation of ethylene–tetrafluoroethylene films. *Polymer Testing*, 32(8), 1423-1435.

Dowell, E.H. (1984). Vortex-induced vibrations. *Annual Review of Fluid Mechanics*, 16(1), 423–455. <https://doi.org/10.1146/annurev.fl.16.010184.002235>.

Dowell, J.H., Ricles, J.M., & Caughey, T.K. (1996). "Investigation of the Collapse of the Georgia Dome Cable-Supported Roof" *Journal of Wind Engineering and Industrial Aerodynamics*, 63(1), 17-36.

Galliot, C., & Luchsinger, R. H. (2011). Uniaxial and biaxial mechanical properties of ETFE foils. *Polymer testing*, 30(4), 356-365.

Houtman R. (2013), *TensiNet European Design Guide for Tensile Structures*. Appendix 5: Design recommendations for ETFE foil structures.

Huang, Y., Li, S., Li, Y., & Li, H. (2014). ETFE as a new option for sustainable building envelopes: A review. *Renewable and Sustainable Energy Reviews*, 37, 657-665.

IEA, & UNEP. (2018). International Energy Agency and the United Nations Environment Programme—Global Status Report 2018: Towards a Zero-Emission, Efficient and Resilient Buildings and Construction Sector. *Glob. Status Rep.*, 73.

Koch K.-M. (2004), *Membrane structures: innovative building with film and fabric*, Prestel Publications.

Li, Y., Li, S., Li, H., & Huang, Y. (2018). Buckling and post-buckling Behaviour of ETFE membranes: A review.

Mahdavi, A., Roudsari, M. S., & Aliabadi, M. (2016). ETFE: A sustainable material for building envelopes. *Energy and Buildings*, 112, 280-290.

Matty, R. R. (1979). *Vortex shedding from square plates near a ground plane: an experimental study* (Doctoral dissertation, Texas Tech University).

Meng, X., Li, S., Li, H., & Li, Y. (2018). A review of constitutive models for ethylene tetrafluoroethylene. *Materials*, 11(9), 1471.

Moritz, K. (2007). *ETFE-folie als tragelement* (Doctoral dissertation, Technische Universität München).

Muc, A., Flis, J., & Augustyn, M. (2019). Optimal design of plated/shell structures under flutter constraints—A literature review. *Materials*, 12(24), 4215.

Seidel M. (2009), *Tensile surface structures: a practical guide to cable and membrane construction*, John Wiley & Sohn.

United Nations. (2021) *Global Status Report for Buildings and Construction: Towards a Zero-emission, Efficient and Resilient Buildings and Construction Sector*. Tech. rep. Nairobi: United Nations Environment Programme, 2021.

Williams, C. J. K. (1990). Travelling waves and standing waves on fabric structures. *Structural Engineer*, 68(21/6).

Williamson, C. H., & Govardhan, R. (2004). Vortex-induced vibrations. *Annual review of fluid mechanics*, 36(1), 413-455.

Wu, J., Li, S., & Li, H. (2019). Review of constitutive models for ETFE membrane structures. *Frontiers of Structural and Civil Engineering*, 13(4), 558-571.



tensinantes2023 : TensiNet Symposium 2023 at Nantes Université

Membrane architecture: the seventh established building material. Designing reliable and sustainable structures for the urban environment.

Proceedings of the Tensinet Symposium 2023

TENSINANTES2023 | 7-9 June 2023, Nantes Université, Nantes, France

Jean-Christophe Thomas, Marijke Mollaert, Carol Monticelli, Bernd Stimpfle (Eds.)

Lightweight ideas for a built environment beyond concrete

Katja Bernert*

*Dipl.-Ing. Architect, Mehler-Technologies, Rheinstr. 11, 41836 Hueckelhoven, Germany,
Katja.Bernert@freudenberg-pm.com

Abstract

A space suit is a home – as is the liveable textile bubble. Following this path the article will literally dwell in options for using textiles in between the dimensions of a shirt and a pneumatic house – exploring the options of energy savings when limiting our heated comfort zone to a minimum. The 1960s are a valuable starting point for this evaluation. The escapist notion of what Haus Rucker Co did when covering a whole villa with a huge pneumatic structure is an example for textile options if all other means stopping the climatic collapse fail. Taking the same artists' proposal for the documenta art exhibition in Kassel serves as a more optimistic example of what a tensioned structure can do for limiting energy consumption to the direct personal realm. Peter Cook and Archigram set examples when proposing the inhabited capsules as house models for the future – their future which is our present. The presentation will explore if these 60 year old ideas are ready to be transformed into a possible answer to nowadays energy saving needs. It delivers the proof that within the last 60 years innovative lightweight structures transformed fabrics and foils into a grown-up seventh building material.

Keywords: lightweight, sustainability, pneumatics, bubbles, spheres, recycling, upcycling, fabrics, foils, comfort zone, seventh building material

1. Introduction

“Architects need to stop thinking exclusively in buildings” said designer Hans Hollein in his article “Everything is architecture!” (Hollein H. 1968, in: *Schrift für Architektur und Städtebau*). If a space suit can be a home according to this scheme, is the same true for our second or third skin? Is there a means of transporting the thermal blanket principle to a broader scale by using fabrics and foils as building materials? The basis for this investigation is a positive answer to this question: Yes, there is an unexploited option for using fabrics and foils to make our built environment more sustainable. There are lightweight ideas with building materials beyond concrete. Fabrics and foils are ready to be established as the seventh building material.

Membrane architecture: the seventh established building material. Designing reliable and sustainable structures for the urban environment.

The starting point for this study is a look into the past. Around 60 years ago, there were suggestions – more pieces of art than architecture – that tackled the society’s response to changing environmental conditions. That was about half a century before talking about imminent climate change was omnipresent in the daily discourse.

The awareness for a more sustainable built environment has changed dramatically within the last 60 years – so has the perception on plastics as main source for fabrics and foils. Whereas the graduate in the so called film was still told that there is a great future in plastics, polymers or PVC in general is now more a no-go material for architects. Along its generally unpleasant connotation, the polymer-industry is now facing additional sourcing challenges as a raw-oil based material.

Taking this as a background it must be assessed if it is now the right point in time to put the visionary approaches of the past on the next, more user-friendly level.

2. Textiles in units between house and blouse

Our first association with fabrics relates to our second skin. The material for our clothes are textiles - mostly woven, sometimes knit or felted, only rarely extruded. They prevent us from nakedness and keep us well-tempered. Today’s highly functionalized fabrics keep the cold out, allow water to transpire. Sometimes they are even smart when illuminating in the dark or highlighting body parts of patients in hospital that are threatened by too much pressure.

Apart from needing textiles in our direct intimate realm we use fabrics and foils for structures like tents or canopies. Here again they are means of protection, helping us to withstand environmental input like rain or UV radiation.



Figure 1: space suit, creative commons licensed



Figure 2: James Vaughan, fashion model in a bubble, photographer Melvin Sokolsky, creative commons licensed

<https://www.flickr.com/photos/40143737@N02/6346077837/>

Membrane architecture: the seventh established building material. Designing reliable and sustainable structures for the urban environment.

There is yet another scope in which fabrics play a role as our second or rather third skin: a space suit for example houses the astronaut when exposed to outer space. The pop-up festival tent gives privacy in an environment that is focused on proximity and togetherness. Both are means to further limit our exposure to the environment – beyond the mere physical or visual protection.

These are examples of textile and tensile units in between the size of a blouse and a house. It is this scope which needs further investigation – be it when looking at fabric and foils as the seventh building material or when exploring sustainable options of lightweight tensile structures.

2.1. Haus Rucker Co

The Viennese group of artists and architects Haus Rucker Co. was founded in the late 1960s. In many of their works they tackle the interrelation of human beings with their environment. Within their assessment the environment is often a harassing factor.

2.1.1. Exhibiting in Krefeld against environmental odds

A climax of these thoughts is their proposal for an exhibition in Krefeld. The villas of the Verseidag founders Lange and Esters were only recently converted into exhibition spaces when the Haus Rucker Co exhibition took place in 1971. The title “Cover. Survival in a Polluted Environment” illustrates the artists’ dystopic view on the matter. The response to this life-threatening scenario is all the more utopian: a temporary pneumatic structure covering an entire villa. The translucent polyvinyl coated polyester fabric contrasting Mies van der Rohe’s Modernist architecture is a highlight of early fabric architecture.



Figure 3: Haus Rucker Co, 1971, COVER installation project, Haus Lange, Krefeld, © Kunstmuseen Krefeld, Manfred Vollmer, Artothek

2.1.2. Exhibiting in Kassel at documenta 5 and in Hamburg

Only one year later, Haus Rucker Co had the opportunity to further develop their pneumatic objects on a far bigger scale – not in terms of the structure’s scale but in terms of publicity.

Membrane architecture: the seventh established building material. Designing reliable and sustainable structures for the urban environment.

They installed a bubble on the front side of documenta's main building Fridericianum. The unit was equipped with two artificial palm trees and a seating accommodation.

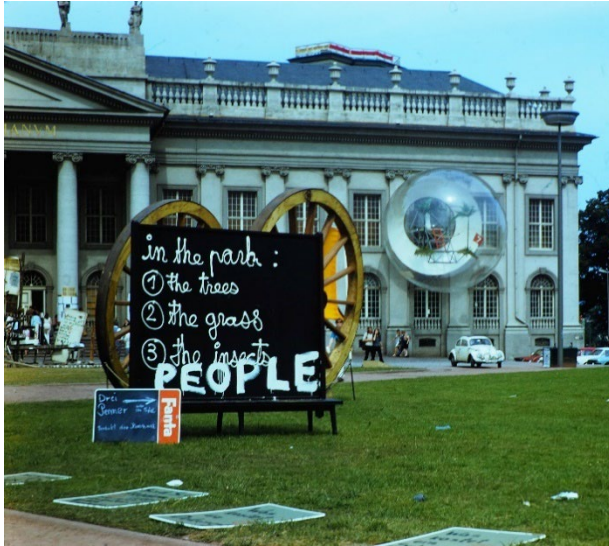


Figure 4: Haus Rucker Co at the documenta 5 art exhibition in Kassel, 1972, bubble on the outside of the Fridericianum building, Creative Commons Licence



Figure 5: Haus Rucker Co, "Oase Nr. 7", Museum für Kunst und Gewerbe, Hamburg, Creative Commons Licence

Again, in 2010, they were able to repeat this scheme in Hamburg, at the Museum für Kunst und Gewerbe. Both structures are hinting at the same idea: because the environment is more and more harassing, mankind in this case in the single unit of one person, needs to withdraw into protected spaces. The bubble unit becomes the direct personal realm. The airlock is not only a pneumatic device but mainly a gate meant to keep the dangerous environment outside so that the individual is protected against all odds in the secluded inside.

2.2. Archigram

The work of Architect Peter Cook within the Archigram group is mainly characterized by ideas about modular living. Archigram imagined future forms of living as an addition of capsules housing the citizens or serving as cultural hubs with equipment for the city's social functions. Pneumatic spheres of fabrics and foils are one option for the single units, rectangular shapes – similar to state of the art schemes with container units as building parts of a stadium for example – are another option for structural units.

Membrane architecture: the seventh established building material. Designing reliable and sustainable structures for the urban environment.

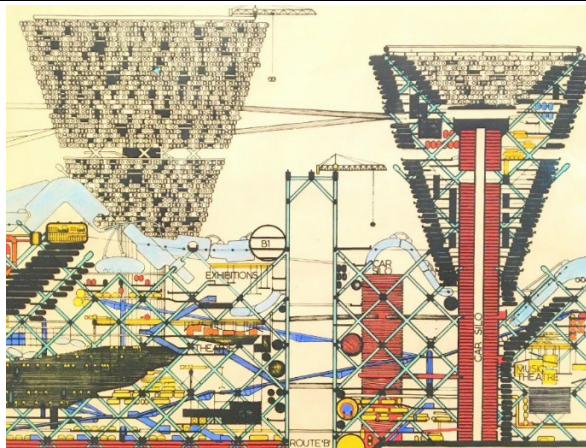


Figure 6: Peter Cook's "Plug-In City", Creative Commons licenced on:
<https://www.flickr.com/photos/wyliepoon/49224543288/in/photostream/>

Thinking in modules was the key to making these schemes very flexible and hence sustainable. The adaptive building skins that we are talking of today are a direct link to what Archigram invented about 60 years ago.

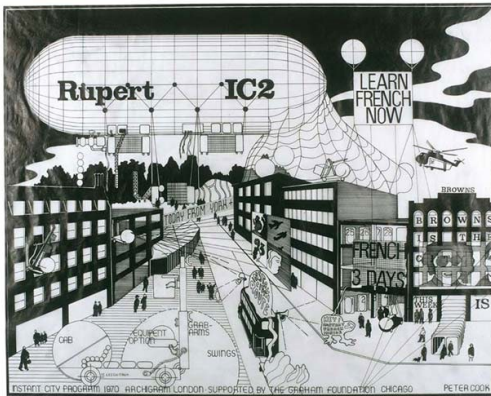


Figure 7: Peter Cook (Archigram), Instant City (Rupert IC 2), 1969, drawing, © Philippe Magnon

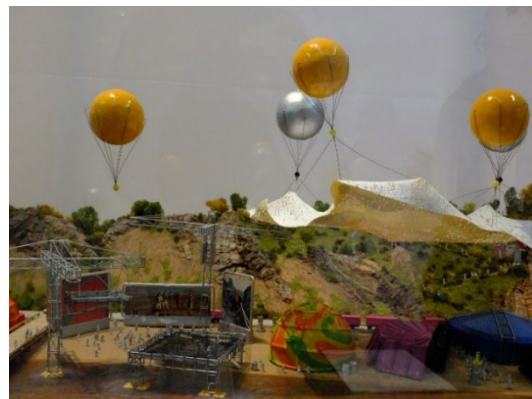


Figure 8: Peter Cook (Archigram), Instant City, photo of mock-up, Creative Commons licenced on:
<https://www.flickr.com/photos/11561957@N06/46875988314>

Instant City, an Archigram project of the late 60s, suggests an airship containing all the cultural resources of a metropolis. Moving from site to site, not restricted by a building, it redefined the city as a temporary event, much like a festival, rather than a location fixed in space. This is yet another sustainable notion which comes with the flexibility of such a modular scheme. It is obvious that this idea can only work when using fabric and foils as lightweight materials for these playful schemes.

Membrane architecture: the seventh established building material. Designing reliable and sustainable structures for the urban environment.

2.3. Hans-Walter Müller

Hans-Walter Müller designs and builds pneumatics since the 1960s. His passion for textile architecture is not limited to temporary structures. Since 1971 he lives in an air supported fabric structure.

Already very early he experimented with air-supported fabrics and foils as dwellings. In contrast to what Archigram suggested, his proposals were very realistic, he actually lived and worked in one of his pneumatic structures and does so still.

Looking at Hans-Walter Müller's work and his enthusiasm for fabric and foils can certainly trigger more use of these materials in the built environment – for example for the growing need of housing.



Figure 9: Hans-Walter Müller in August 2019, under one of his „Klangstruktur mit Resonanzkugel“ (Structure sonore avec sphère de résonance). His inflatable house is in the background. https://commons.wikimedia.org/wiki/File:Hans-Walter_M%C3%BCller_Klangstruktur.jpg

2.4. José Miguel de Prada Poole

In a TensiNews article that was published shortly after de Prada Poole's death in 2021 it was pointed out that the Spanish architect and pioneer of pneumatic structures was in tune with Buckminster Fuller or Frei Otto when it comes to options for building with less material. Their resource-sensitive way of structural and architectural design is still state of the art and definitely pathbreaking when looking at today's challenges.

De Prada Poole was particularly passionate about using air as the most available and hence most sustainable supporting material, respectively structural element.

Membrane architecture: the seventh established building material. Designing reliable and sustainable structures for the urban environment.



Figure 10: Instant City by José Miguel de Prada Poole, photo credit courtesy of Josep Llorens

2.5. Frei Otto

Of course Frei Otto's work serves for relating fabrics to tangible ideas for the build environment – we can certainly find notions of sustainability in his work. One of the most important merits of his work is introducing lightweight materials as a playful way of architecture as in the Olympic Stadium in Munich.

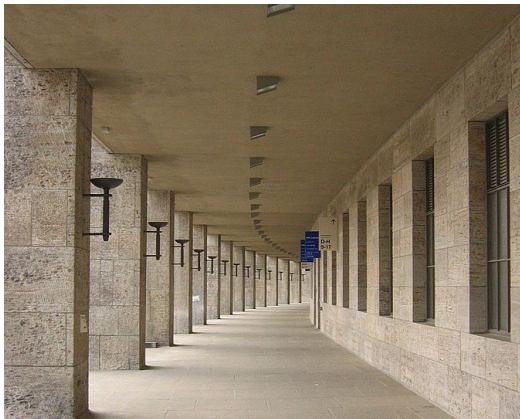


Figure 11: Werner March's Olympic Stadium Berlin for the Games 1936, here the status of the early 21st century, renovation by gmp architects, https://de.wikipedia.org/wiki/Datei:IMG_Olympiastadion_Gang.JPG



Figure 12: Olympic Stadium in München, structural design Frei Otto, Wikimedia-licenced © Jorge Royan

When looking at Frei Otto's sketch books we find more in depth assessment of the interrelation of human beings with their (built) environment – all hinting at the fact that there must be a sustainable, lightweight way of minimizing people's input. Essentially these notes are early evaluations of the citizen's environmental footprint.

Membrane architecture: the seventh established building material. Designing reliable and sustainable structures for the urban environment.



Figure 13: Circular cut of a Frei Otto sketchbook page

There are surprisingly few up to date answers for a more sustainable use of fabrics and foils as building materials. The proposals from the fabric industry for example extend to declaring PVC/Polyester Materials as recyclable – failing to put this option into reality most of the times and having failed in making this option true or at least feasible for Glass/PTFE fabrics altogether. Hinting at the options for recycling (which is essentially a downcycling) is definitely not enough to get away from raw oil based material consumption. The concept of being lightweight in the first place and saving raw material by using recycled (upcycled!) PET bottles for the fabric are certainly important steps towards a more sustainable fabrics industry.

Beyond these examples that are limited to the doing of the material producers we need to explore options and necessary steps to establish fabrics and foils as the seventh building material with a truly sustainable notion.

3. Learnings for today

From the Tensile Architecture point of view it is absolutely clear that surrendering the right angle helps to solve today's environmental challenges: if lightweight structures with curved shapes replace what we still take for granted as our built environment – boxes in the dimension of houses – we respond to today's needs for downsizing. We make dock-in stations inhabitable, that is to say that we redefine the personal realm in a manageable, movable size

In essence we surrender the “my Home is my castle” habitus. At this very moment this scheme seems frightening - be it by harassing our traditional concept of living or be it by introducing new materials to shape our personal realm and essentially reshape our urban environments.

If we take serious what Hollein said in 1967 “Everything is architecture!” we must be frank enough to dwell in innovative tensile units between the dimensions of a blouse and a pneumatic house. That does not necessarily lead us into a bubble the size of what Haus Rucker Co suggested for documenta 5, imagining all of us in a matrix-like structure with the balloons that house us. It can be as simple as the single person using a thermal hoody when living in a 200 sqm villa instead of keeping the whole place in 21° condition.

This is far from the escapist notion of what Haus Rucker Co suggested when covering the Lange villa with a pneumatic structure in order to withstand climate change. Rather transferring it into the hygge, that is to say cosy corner and hence giving the scheme of smaller units per person a

Membrane architecture: the seventh established building material. Designing reliable and sustainable structures for the urban environment.

more positive notion. That works in cold temperatures as well as in hot climates. Whereas hygge is more associated to Scandinavian cosiness it is the well-tempered fresh unit on the Arabian peninsula for example.



Figure 14: original Fiat 500.
<https://pxhere.com/en/photo/657070>



Figure 25: SUV car
<https://pxhere.com/de/photo/934553>



Figure 36: SUM, Sustainable Urban Mobility.
<https://www.opel.de/fahrzeuge/rocks-e/uebersicht.html>

A comparative look at individual mobility is an eye opener: here we are obviously one step ahead. The transformation from taking cars with the notion “the bigger the better” to accepting micro-cars for the new SUM, Sustainable Urban Mobility, is in full swing. Starting point here again was a very similar sized car from the late 1950s, as for example the original Fiat 500.

3.1. Energy savings as focal point

The mobility example shows that downsizing is a key to making transport more sustainable. The savings on energy can easily be detected during production – using lightweight material is an important milestone in mobility.

This learning from mobility can easily be transformed into the built environment. It is more than obvious that tensile architecture holds the key to many of these transformation processes. The material is lightweight, modules are replicable and can be added within a matrix that holds the structure’s service functions. The flexibility of these structures is a key to a quick response to changing demands. Whereas the design life can hence be prolonged to a far extend there still is an end of life scenario – either by recycling the components that can easily be separated or by using the parts yet again in another structure.

Being lightweight is the integral advantage of fabric and foils as building materials. The drawback of having raw oil based products as the base material can literally be diffused by using for example upcycled PET bottles as the raw material for the fabric.

Textiles are one of the eldest materials to serve as a second skin for human beings. While we accept a thermal blanket or even a foil as a cover to re-energize respectively keep energy close to our bodies, we would not necessarily accept a foil in a wider sense, giving us a bigger realm for deployment. There is great potential in exploring this realm in between house and blouse – particularly when looking at the units we need to heat respectively cool. It is the responsibility of people involved in tensile architecture to explore this space in between the second skin and the building skin. Establishing fabric and foils along the traditional building materials is one step, looking at the dimensions of the envelopes we build is yet another.

Membrane architecture: the seventh established building material. Designing reliable and sustainable structures for the urban environment.



Figure 17: Hoody for individual thermal comfort



Figure 18: Runner keeping warm under a thermal blanket, photo by Marco Verch, creative commons licensed

<https://www.flickr.com/photos/149561324@N03/36880396074>

4. Conclusion

The motto that architects need to stop thinking exclusively in buildings must be complemented by the notion not only to think in bricks and concrete when it comes to materials. It must be supplemented by the idea that houses in their traditional shape are not the only spaces apt to house a human being. Space is a luxury with eight billion people on earth, well-tempered space the more.

Fabrics and foils are a means to downsize our personal realm to reasonable units. 60 year old proposals show that this is not necessarily a limitation. Innovative ideas with lightweight material as Hans-Walter Müller has been producing over the last decades are prominent examples for fabrics and foils as a grown-up seventh building material.

It is important to communicate that these bubble ideas are no spleen of some hippy architects. They are part of the sustainable concepts that our built environment is so urgently asking for. An ecological future in building technology is only possible with the contribution of lightweight materials like fabrics and foils, plus a reassessment or rather revalidation of our need for space. Hans-Walter Müller and José Miguel de Prada Poole have proofed the feasibility of living in a bubble.

Membrane architecture: the seventh established building material. Designing reliable and sustainable structures for the urban environment.



Figure 19: José Miguel de Prada Poole, Smart Structure, 1968,

<https://www.tumblr.com/pradapoole/3091222826/smart-structure-1968-autor-jose-miguel-de-prada>



Figure 20: Hans-Walter Müller's workshop

At this point in time it is most important to transform these 60 year old concepts into livable spaces. Today's material technology allows the actualization of these visions of the past and take the step to realizations on a bigger scale. The steadily growing number of lightweight foil structures as replacement for glass roofs is a prominent example for this transformation in our built environment. While these structures become more common in our urban environments it is clear that we are certainly not meant to be living in bubbles lined up in prefab grids.

A transformation of the visionary thoughts of the 1960s comes true by giving lightweight materials a chance to compete with bricks and concrete. This can be actively done by facilitating the use of fabrics and foils through a fixed set of rules and norms – as does the Technical Specification for example. The lack of regulations has been one of the biggest bottlenecks for tensile structures in the past, along the fact that at universities fabrics and foils still play a minor role at the side of the classics like glass and bricks for example. Sustainability needs and a fresh look on lightweight structures in the architects' and engineers' education is about to put fabrics and foils on the next level. There are great future possibilities deriving from university projects like the adaptable building skins at the university in Aachen, the fabrics lab at Polimi in Milan or the adaptive test tower at the ILEK in Stuttgart – to name just a few.

In a passive way lightweight materials are better off just by looking on the Carbon Footprint of concrete for example. From the material's perspective there must be a closer look on alternatives to raw-oil based material and to circularity that sources materials within the tensile architecture realm and brings them back into the same when closing the loop in an end of life scenario.

From a design perspective fabrics and foils are apt to transform our sense of space from the living-in-a-box principle to units that are far more flexible than rooms that are enclosed by brick walls. A fabric wall, as for example a curtain wall, is an ephemeral means to transform spaces into adjustable units. Recent research into the building-physics of tensile structures allow an optimistic outlook on making these flexible walls into first skins that insulate the spaces they surround.

The playful bubble approach facilitates the promotion of fabric and foils as the seventh building material. As the idea of a tiny car like the Rocks-e model in the above example appeals to the

Membrane architecture: the seventh established building material. Designing reliable and sustainable structures for the urban environment.

modern urban citizen, tensile structures have a great potential to attract attention and to be valued as an added value while being a limitation at the same time.

Citizens' engagement is most easily triggered by play. Like Haus Rucker Co engaged visitors of documenta 5 in Kassel 50 years ago, tensile architecture can now re-engage sustainably sensitive people with spheres of fabrics and foils. The appeal of a pneumatic structure can significantly help to relate sustainability by using lightweight materials on the one hand and a reasonable unit-size for an ecological use of resources on the other.

Acknowledgements

When preparing this article I led a workshop at the Arts School in Bremen, HfK. Within the workshop the students of various design units explored soap film models. It was their first venture into the world of tensile structures. For me it was a most valuable eye opener. Dwelling in the world of Textile Architecture limits our thinking to well established forms and hence tends to make us blind for new input. I am very grateful for the innovative interchange – be it in Bremen or coming from 60 year old ideas of architects and artists.

References

- Beccarelli P., Corne E. et al. (eds.), TensiNews, Newsletter No. 42 (2022), José Miguel de Prada Poole, article by Josep Llorens (pg. 6-9)
- Beccarelli P., Corne E. et al. (eds.), TensiNews, Newsletter No. 39 (2020), Bubbles to live and work in, article by Evi Corne (pg. 15)
- Cook P., Archigram (1973) by Praeger Publishers
- Documenta retrospective, available online, accessed on January 18th 2023, https://www.documenta.de/de/retrospective/documenta_5#
- Forster B., and Mollaert M. (eds.) (2004), European design guide for tensile surface structures: TensiNet, TensiNet.
- Haus-Rucker-Co, Oase Nr. 7, Documenta 5, 1972, accessed on January 18th 2023, <https://elephant.art/iotd/haus-rucker-co-oase-nr-7-documenta-5-1972/>
- Hollein H. (1968), „Everything is architecture“, originally published in Bau: Schrift für Architektur und Städtebau 1/2 | 1968
- Mehler Technologies GmbH, Textile Architecture team records, 1960s-ongoing
- Meyer F., Baunetzwoche 596, BauNetz, Heinze GmbH, 2022
- Prieto González N. 2013, La arquitectura de José Miguel de Prada Poole : teoría y obra, available on <https://ruc.udc.es/dspace/handle/2183/11917>, accessed on January 18th 2023
- Stürzl R. (2022), Hans-Walter Müller und das lebendige Haus.
- Sustainable Urban Mobility, accessed on January 18th 2023, https://ec.europa.eu/commission/presscorner/detail/en/qanda_21_6729 and <https://www.eltis.org/it/mobility-plans/11-what-sustainable-urban-mobility-plan>



**tensinantes2023 : TensiNet Symposium 2023 at
Nantes Université**

Membrane architecture: the seventh established building material.
Designing reliable and sustainable structures for the urban
environment.

Proceedings of the Tensinet Symposium 2023

TENSINANTES2023 | 7-9 June 2023, Nantes Université, Nantes, France

Jean-Christophe Thomas, Marijke Mollaert, Carol Monticelli, Bernd Stimpfle (Eds.)

HOW LIGHTWEIGHT ARCHITECTURE CONTRIBUTE to SUSTAINABILITY & DECARBONIZATION STRATEGY?

Thomas BONNEVILLE*

***SERGE FERRARI Group**

ZI – BP54 – 38110 LA TOUR DU PIN CEDEX – France

thomas.bonneville@sergeferrari.com

Abstract

Facing the reality of climate change, the building industry needs to reduce its impacts, especially one of them: carbon footprint. With their inherent material efficiencies, lightweight tensile structures can seriously challenge this goal and become a significant part of building materials.

Through study cases, and with the support of Structure Engineers [1] and Specialized Environmental Consulting Engineering [2] this paper highlights:

- the real lightness of tensile solution,
- and the sustainable benefits of tensile envelope, compared against non-tensile equivalent functionalities (metal and other material).

The structure under investigation is a micro climatic roof in Chrifia golf club house (Morocco, 2015). This application has been designed with an absolute minimum of material $\sim 4,5\text{kg/sqm}$, including membrane, masts and cables.

Moreover, without re-inventing concepts that are already available, this paper gives the benefits of a tensile envelope in terms of:

- Thermal comfort,
- Optical comfort,
- Acoustic comfort,
- Hygrometry comfort.

Membrane architecture: the seventh established building material. Designing reliable and sustainable structures for the urban environment.



Figure 1: External view of the micro climatic roof: Chrifia golf club house – Morocco
Architect: Youssef Melehi, Rabat – Morocco / Engineering: Prat SA – France /
Membrane fabrication & installation: Ametema – Morocco / Membrane: Serge ferrari Flexlight
1202 S2 – 1500 sqm

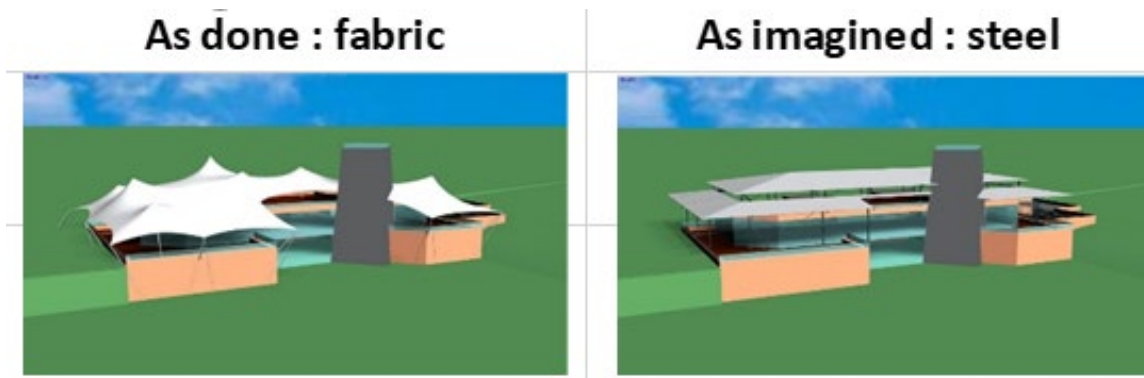


Figure 2: comparative carbon footprint for a fabric and a steel roof

Keywords: structural membrane, sustainability, lightness, lightweight building material, carbon footprint, embodied carbon, CO₂, tensile shading, tensile building envelope, EPD, thermal comfort, optical comfort, glare control, acoustic comfort, hygrometry comfort.

1. Introduction

The building and construction sector is a key sector for sustainable development. The construction, use and demolition of buildings, generate substantial social and economic benefits to society, but may also have serious negative impacts on the environment.

The building and construction sector accounts for the largest share in the use of natural resources, by land use and by materials extraction. Energy use, liquid and solid waste generation, transport of construction materials and consumption of hazardous materials are examples of

Membrane architecture: the seventh established building material. Designing reliable and sustainable structures for the urban environment.

negative environmental impacts from this sector. In Europe, buildings are responsible for 40-45% of total energy use, contributing to significant amounts of carbon dioxide CO₂ emissions.

A number of national and international initiatives and efforts have been developed by the building and construction sector itself to promote more sustainable buildings. Nevertheless, beyond conventional materials, the building industry would benefit from taking an interest in structural membranes to achieve the objectives of the Kyoto Protocol and the United Nations Framework Convention on Climate Change.

CO₂ emissions are currently greatest in industrialized countries, although estimates suggest that developing countries will increasingly contribute to global warming in the coming decades. In the United States of America, CO₂ emissions per capita equal 20,1 tons, almost twice those of countries such as China and Brazil, 16 times higher than India and 50 times higher than Nigeria and Sudan. If high populated developing countries follow the same unsustainable production and consumption path as developed countries, the consequences will be significant. The challenge is to determine how industrialized countries can manage their environmental impacts, while developing countries can achieve economic growth in a sustainable way.

The presentation consists of 3 parts.

Part 1 is the basis of what we can achieve today with the current product portfolio available on the market (plain fabrics, mesh fabrics, acoustic inner layer...).

Part 2, “from Mass to Membrane” illustrates that we can do more with less material (Less raw material and less overall product).

Part 3 opens the subject of integrating recycled content into the fabric.

2. Part 1 : TENSILE ENVELOPE : PRESENT & FUTURE

During decades, a tensile roof was dedicated to shading structure only. Indeed, it was installed as a single layer to ensure a protection against sun, rain, snow and sand, according to the territory and climate requirements. Nowadays, we can build a complete membrane envelope to ensure the comfort of a 21st century building. The combination of multilayers: Serge Ferrari Opaque, Translucent or Transparent fabrics & conventional materials, achieve comfort goals.

Membrane architecture: the seventh established building material. Designing reliable and sustainable structures for the urban environment.



Figure 3: Hygrometry & Thermal comfort in a cold country for a carpentry workshop

SALVOS halls (Finland): 126 m x 33 m x 5,9 m high, free span / Double layer Insulated wall 200mm >> $U=0,18 \text{ W/sqm/K}^\circ$ / Double layer Insulated roof 400mm >> $U=0,12 \text{ W/sqm / K}^\circ$

3. Part 2: LESS IS MORE

The Chrifia Golf club in Morocco has been selected for assessment as an example of tensile structure. The building was designed in a light way with structural efficiency as a key driver and as a result an absolute minimum of material has been achieved with the primary and secondary structure (masts, cables, fittings and membrane) obviously combining a small weight of 4,5 kg/m².

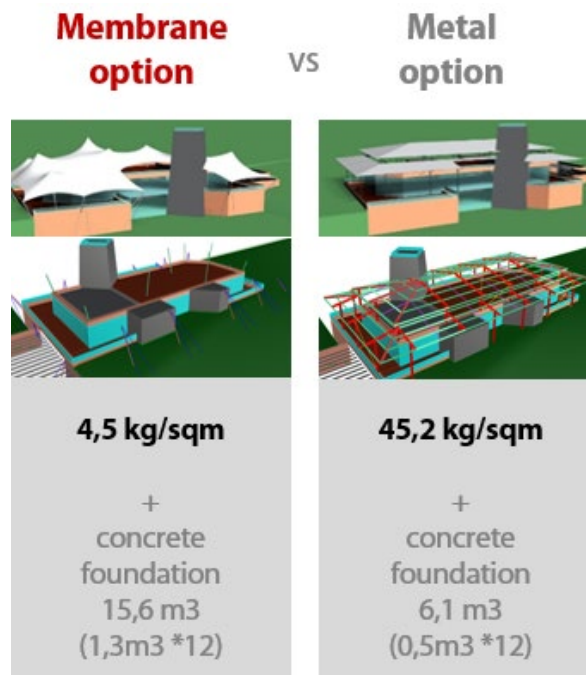


Figure 4: Comparative weight of solution Preconstraint 1202 from Serge Ferrari Group vs Metal option

Membrane architecture: the seventh established building material. Designing reliable and sustainable structures for the urban environment.

3.1 Embodied carbon for an overall life cycle of 50 years

Results for the embodied carbon assessment are shown below. Even in a protective scenario with a refit after 25 years of the fabric solution, it is immediately obvious that Preconstraint Tensile roof has an embodied carbon value significantly below the solution made with conventional material, that is to say entirely in steel.

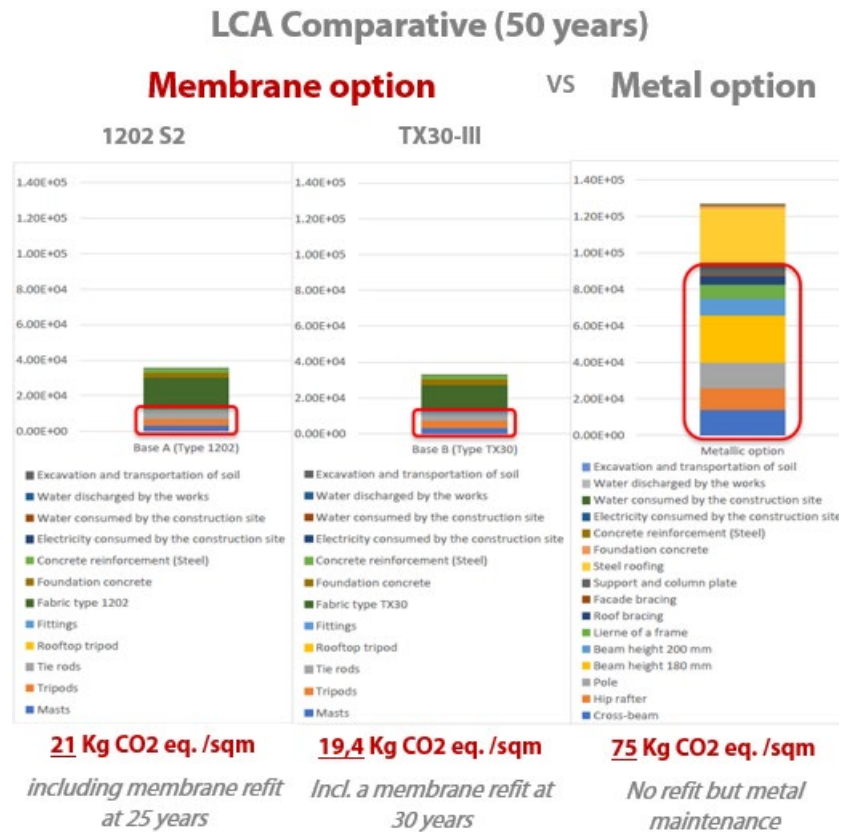
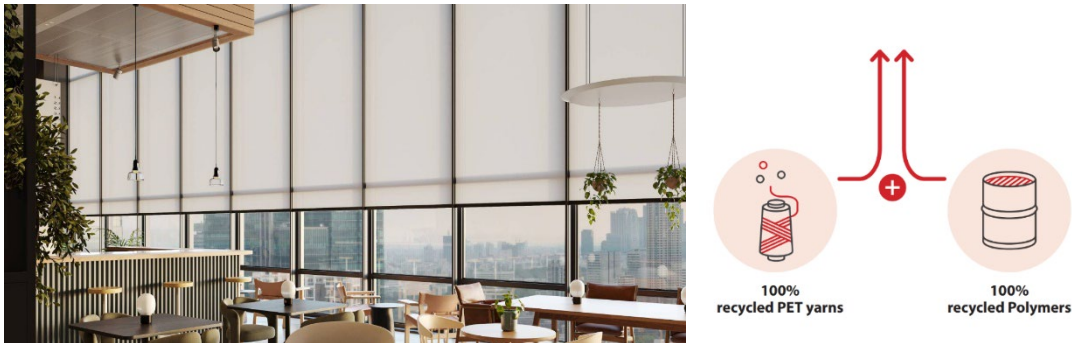


Figure 5: Comparative carbon footprint of solution Preconstraint 1202 and TX30.3 from Serge Ferrari Group vs Metal option; Including Primary & secondary structure + roof material + foundations

Membrane architecture: the seventh established building material. Designing reliable and sustainable structures for the urban environment.

4. Part 3: RECYCLED CONTENT INSIDE

We open a new chapter of the structural membrane by using recycled content into the fabric. Our first Structural Mesh with 100% recycled Polyester is an example of this new generation of material. Mainly used for outer skin of a building envelope, this mesh combines thermal comfort, glare control and less environmental impacts. In parallel, we developed architectural fabrics with 100% recycled Polyester yarns + 100% recycled polymers from post consumer's waste.



Figures 6 & 7: office building (Tur) with Soltis Loop Sunmate made with 100% r-pet & 100% r-polymers

Loop is a new generation of innovative products, made of 100% recycled materials, which embodies our sustainable approach: "+ = 0". This formula reflects our will for lighter, more durable and high-performance membranes, without any additional environmental impact. Aiming at saving natural resources, the Loop range is a forerunner of tomorrow, when we will be able to do even more with less. Loop - the first range of composite membranes on the market made of 100% recycled polyester yarns and polymers.

5. Conclusion: How Tensile fabrics can contribute to the Sustainability and Decarbonization strategy of the Building Industry?

During the TENSINANTES2023 symposium, the presentation will highlight through examples and case studies, how Tensile fabrics can contribute to the Sustainability and Decarbonization strategy of the Building Industry. The brief presentation led to the following conclusions:

- Solutions already available in the range of Serge Ferrari group can achieve a good level of performance in terms of Thermal, Optical, & Acoustic comfort, while being reliable and safe.
- The equivalent embodied CO2 for tensile structure can be successfully assessed and compared against other similar structures.

Membrane architecture: the seventh established building material. Designing reliable and sustainable structures for the urban environment.

- The Chrifia Golf Club in Morocco, the International Grand Airport in Turkey, the Leviathan Sculpture in France, combined with Translucent and Transparent fabrics commonly shows that lightness value can be achieved through an ultra-efficient structural design.
- Efficient structural geometry is key to driving embodied carbon down to the lowest realistically achievable levels.
- The choice of the structural membrane compared to other conventional solutions has a very significant impact on the embodied carbon of the entire building construction.

Acknowledgements

All partners represented into the presentation through case studies and applications: Building owners, Architects, consultants, membranes specialist and installers, photographers.

References

- [1] J.PRAT, *Comparative study, tensile structure vs metal roof – PRAT SA 2021*
- [2] J.LACOMBE and S.BARRET, *Comparative study, tensile structure vs metal roof – Tribu.E 2022*
- [3] PALOS VERDES, *Heat & Visual comfort with energy efficiency – Silver Spur Sotheby's reality offices California USA – 2015*
- [4] CALVO VAN TRAN and GREEN AFFAIR (Bream), *Wings campus – Head office of Airbus Group (F) – 2016*
- [5] ZUH visuals- 2022 & 2023



tensinantes2023 : TensiNet Symposium 2023 at
Nantes Université

Membrane architecture: the seventh established building material.
Designing reliable and sustainable structures for the urban
environment.

Proceedings of the Tensinet Symposium 2023

TENSINANTES2023 | 7-9 June 2023, Nantes Université, Nantes, France

Jean-Christophe Thomas, Marijke Mollaert, Carol Monticelli, Bernd Stimpfle (Eds.)

6dTEX – Sustainable Composite Structures from 3D Print on 3D Textile

Claudia Lüling*, Sascha Biehl, Roxana Tennert, Marina Chernychova^a Gözdem Dittel^a,
Thomas Gries^a

* Frankfurt University of Applied Sciences, Nibelungenplatz 1, 60318 Frankfurt, Germany, clue@fb1.fra-uas.de

^a ITA, Institut für Textiltechnik of RWTH Aachen University, Aachen, Germany

Abstract

Lightweight building in architecture originates from tent structures and nomadism – as opposed to massive structures built from stone, for example. The combination of a loadbearing structure (supports and beams) and a skin (fabric, felt, membranes) reduces weight and material with simultaneously high functionality. A perfect solution from the past with potential for a future, where less material consumption is a crucial necessity. In contrast to traditional manufactured, cost- and failure-intensive structures, the combination of 3D printing technologies with 3D textiles (6dTEX) is intended to create integratively manufactured skeleton structures that are equally load-bearing with minimal material consumption. The fabric serves as a skin and absorbs tension forces, with the thickness of the 3D textile geometry providing more space for additional functions like insulation and light modulating options, etc. The 3D print pattern on the textile on the other hand provides the necessary loadbearing support for absorbing compression forces – replacing traditional supports and beams with a pattern that can follow the flow of forces. Ultimately, the 3D printed, skeleton structure of a high-density material together with the porous 3D fibre structure of the textile becomes an individually prefabricated, lightweight and gradable system, ready to use on site for applications in architecture. The findings so far show promising results for applications in the wall and ceiling area and in two different materials groups: 3D printing with concrete on 3D AR glass fabrics and 3D printing with rPETG from recycling sources on recyclable PES fabrics. The findings also show the technical challenges and possibilities of 3D printing on multilayer textiles in contrast to printing on 2D textiles.

Keywords: spacer fabrics, monomaterials, additive manufacturing, form finding, 3D manufacturing processes

1. Introduction

Lightweight construction is a driver for resource and energy efficiency, including in the construction industry. The aim is to develop recyclable, highly functional and material-reduced components. Disruptive approaches, incorporating classic lightweight construction methods (tent and skeleton structures) and solid construction methods (clay, brick and concrete), are opening up new possibilities. The combination of archaic textile processes such as braiding,

Membrane architecture – the seventh established building material. Designing reliable and sustainable structures for the urban environment.

weaving, knitting or warp-knitting using anisotropic materials, together with essentially isotropic solid construction materials such as concrete, opens up new sustainable, constructive as well as aesthetic possibilities. This is done especially in the context of cutting-edge, additive 3D manufacturing techniques. In solid construction, these are 3D printers that are now being used to create 3D-printed houses from concrete but also from clay or sand. The state of the art is essentially LDM processes for concrete printing (3DCP), with alternative research being conducted on "shotcrete printing" (Kloft, H. et al., 2019) and generally with mineral materials also on binder jetting techniques for sand printing or on glass printing from recycle (Ramsgaard et al., 2020), as well as in other material groups on metal printing and printing with biomaterials (Goidea et.al, 2020, FraunhoferUMSICHT, 2022).

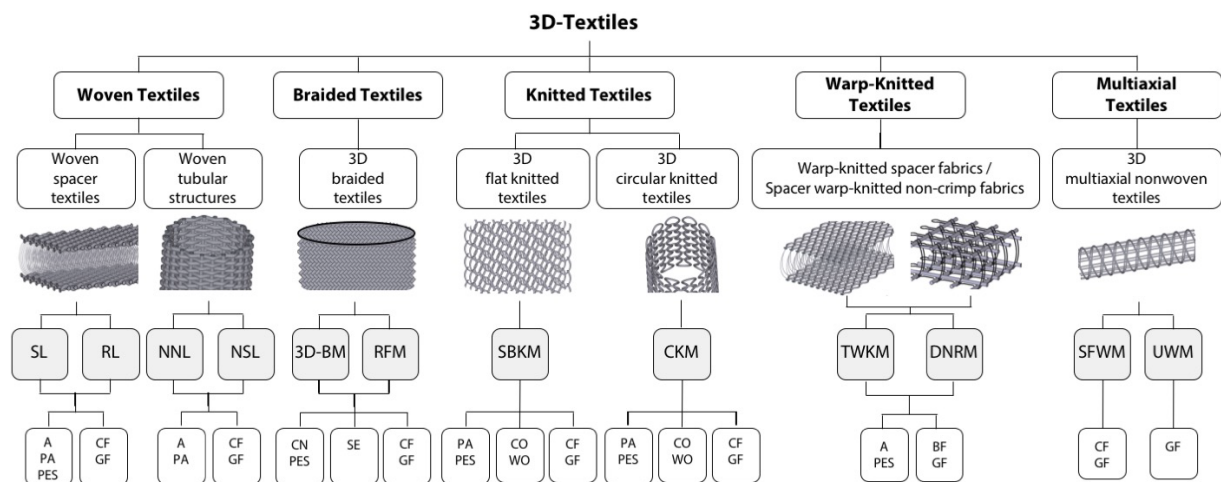


Figure 1: 3D Textile Techniques (©ITA): Lines 1 and 2 Textile typologies; Line 3 Textile machinery: SL, Standard loom; RL, Ravier loom; NNL, Narrow needle loom; NSL, Narrow shuttle loom; 3D-BM, 3D-Braiding machine; RFM, Radial braiding machine; SBKM, Straight bar knitting machine; CKM, Circular knitting machine; DNRM, Double needle bar raschel machine; TWKM, Tricot warp-knitting machine; SFWM, Single filament winding machine; UWM, Ultrasonic welding machine; Line 4 Material groups: S, synthetic; B, biological; M, mineral; Line 5 Materials: A, aramid; BF, basalt fibres; CF, carbon fibres; CN, surgical sewing thread; CO, cotton; GF, glass fibres; PA, polyamide; PES, polyester; PP, polypropylene; K, ceramic; SE, silk; WO, wool, ©ITA

However, additive 3D technologies also include processes for the production of technical 3D textiles, so-called spacer textiles (Fig. 1). Their applications in the building industry have so far been limited to use as a filter medium; now and then they become visible as fog traps or are used in interior finishing as mattress pads or upholstery. In research, studies on the topic of ge3TEX (“Woven, Knitted, Foamed: 3D Textiles for the Building Envelope”) have showed further potential (Lüling at al., 2021). The results were recognized in the DGNB Sustainability Challenge in the "Research" category. 6dTEX is investigating the extent to which, in addition to foaming as in ge3TEX, the combination of additive 3D printing and 3D textile manufacturing processes can be used to develop sustainable, prefabricated building envelope components that combine the advantages of skeletal and solid construction. Research is being conducted on textile-reinforced 3D-printed composite components from the same material group in a mineral-based and polymer-based variant. The project identifies similar material groups for 3D printing as for 3D textiles with the aim of developing lightweight, material-saving and recyclable mono-

Membrane architecture – the seventh established building material. Designing reliable and sustainable structures for the urban environment.

material composites. The respective textile and print manufacturing processes are installed with a view to adhesion and composite effect, and components for the building sector are developed from the new composite material at scale from the meso to the macro level.

2. Methodology

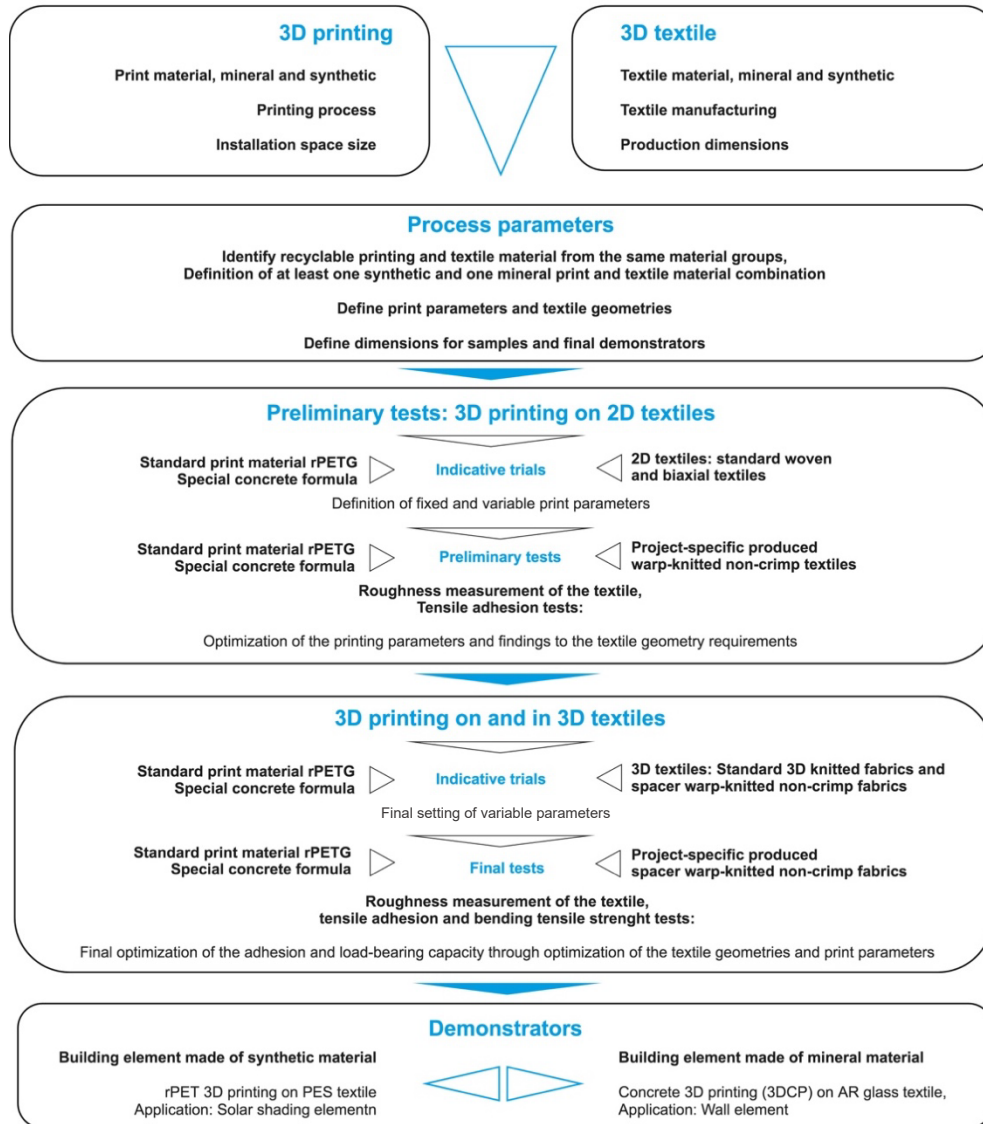


Figure 2: 6dTEX research design, ©FRAUS

The research design is based on an iterative experimental series. Figure 2 shows the general approach, starting from the synchronization of the composite materials, i.e. the identification of a synthetic and a mineral composite variant, the optimization of the process parameters for adhesion improvement via printing tests first on surfaces of 2D textiles and then on 3D textiles, and finally printing tests on and into the textiles for different demonstrators.

3. Results

3.1. Process parameters

Due to a lack of references on 3D printing on 3D textiles, research on 3D printing on non-elastic 2D textiles was evaluated (Narula et al., 2018; Pei et al., 2015; Gorlachova et al., 2021; Grothe et al., 2020; Čuk et al., 2020; Malengier et al., 2018; Cuevas et al., 2020).

For adhesion, an important 3D printing parameter is the Z-Offset, and for 2D textiles the porosity of the textile structure, as also shown in the latest research (Popescu et al., 2022). With regard to materiality in these studies printing materials and textile materials come from different material groups, which makes recycling difficult. Unlike 6dTEX, none of the previous studies aim to produce a mono-material from 3D printing and textile materials. Also unlike 6dTEX, none of the studies pursues the goal of depositing the printing material specifically into the textile structure, which is only possible through the multilayer textile structure of the 3D textile. In this context and for 6dTEX in particular the characteristic parameters of the 3D textile and the chosen 3D printers need to be considered.

6dTEX uses spacer warp-knitted non-crimp fabrics, which were developed especially for the reinforcement of concrete (el Kadi et al., 2019). Figure 3 shows the complex machine technology. Similar to a woven fabric, the geometry of the two cover surfaces is defined by the warp and weft threads, which, however, are not woven together but warp-knitted. For optimal absorption of tensile loads, they thus lie straight and without undulation in the space. The warp-knitted threads hold them mechanically in position. The interaction of the warp and weft threads decisively determines the geometry and the porosity in particular of the cover areas to be printed. It is decisive for the mechanical adhesion between print and textile material. In the case of the warp threads it is defined by the needle occupancy of the leads, and in the case of the weft by the minimum and maximum distances of the weft feeders. The spacing pile threads, in turn, define the height and resilience of the 3D textile.

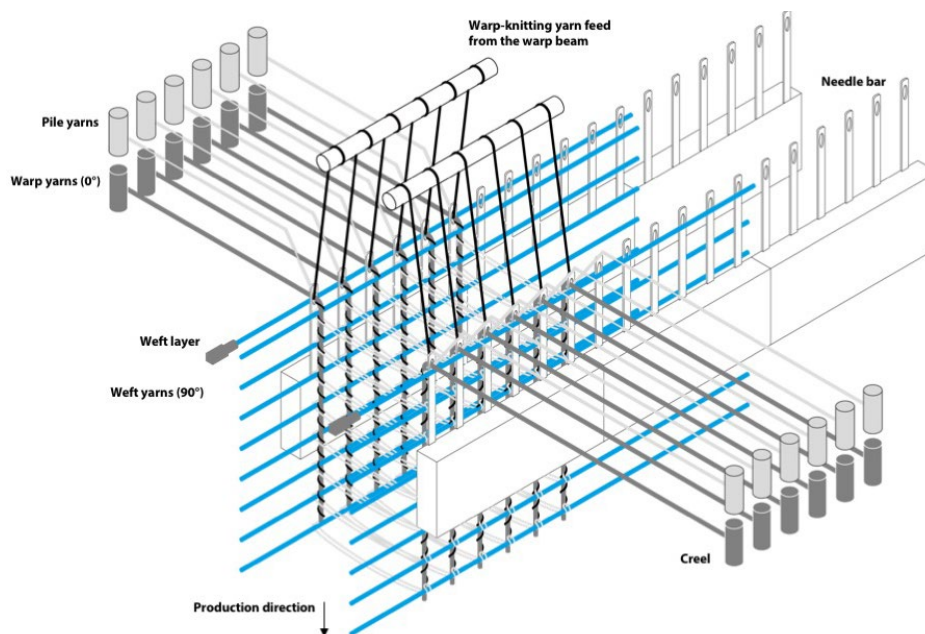


Figure 3: Principle of the production of spacer warp-knitted non-crimp fabric (blue weft yarns, grey warp yarns, black war-knitting yarn, light grey pile yarns) ©FRAUAS

Membrane architecture – the seventh established building material. Designing reliable and sustainable structures for the urban environment.

The 3D print parameters for 6dTEX are determined by the project-specific chosen print materials: 3D FDM print with polymer-based materials like PET and 3D LDM print for 3D print with mineral-based materials like concrete. For both material groups and depending on the printer technology the Z-offset and G-code need to be altered, as shown in Figure 4.

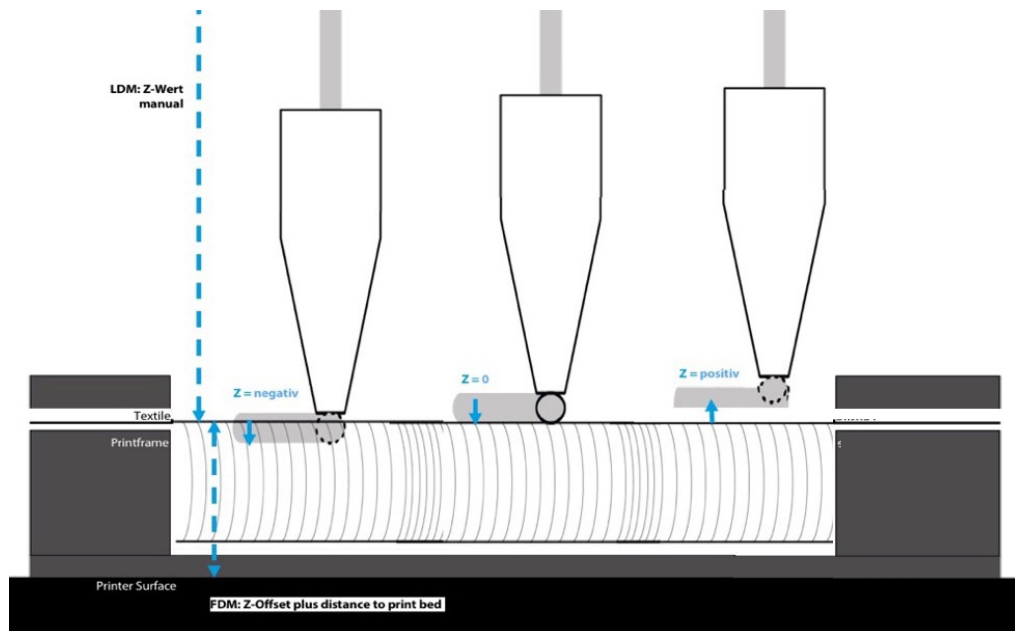


Figure 4: FDM/ LDM 3D print Z-offset adjustment; ©FRAUAS

For the final 3D printing on 2D as well as 3D textiles, a frame is developed that can be attached to the build platform of both the FDM and LDM printers (Fig. 5). The frame is used to clamp the 2D textile or the top cover layer of the 3D textile between two battens so that the textile can then be stretched without wrinkles and evenly in all directions. The tension provides a surface that withstands the pressure of the extruder and allows the printing filament to penetrate deeper into the textile.

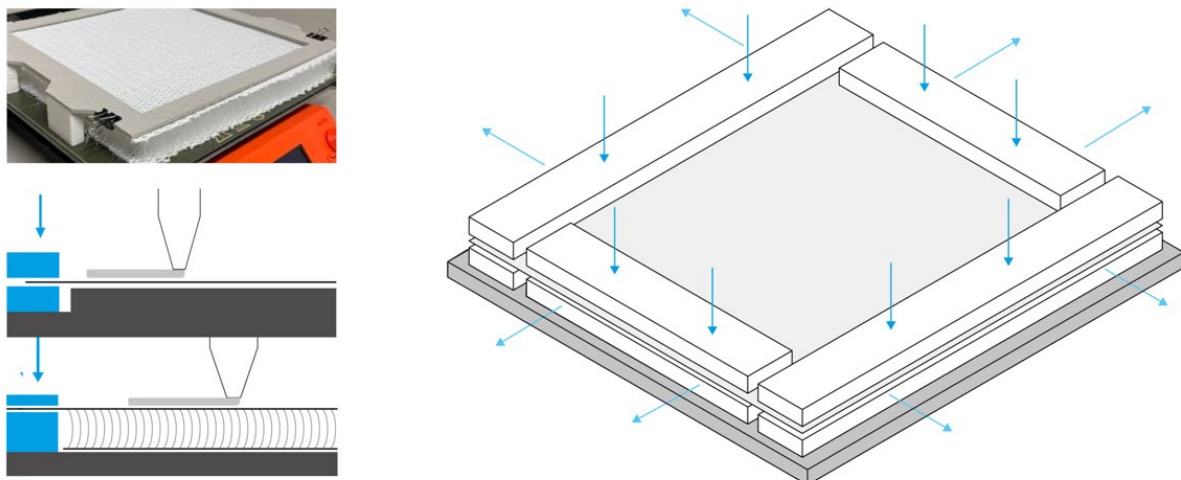


Figure 5: Attachment of 2D and 3D textiles for the build platform of the FD and /LDM 3D printer;
Top left: Preliminary tests with clamps, ©FRAUAS

Membrane architecture – the seventh established building material. Designing reliable and sustainable structures for the urban environment.

3.2. Preliminary Tests: 3D Print on 2D Textile

3.2.1 Composite from polymer-based materials

In the preliminary tests on 2D textiles, investigations were initially carried out with printed and textile materials from the following four material groups: PA, PETG flame-retardant, rPETG and PP. For recycling reasons, the goal is to combine 3D printing and textile materials from identical or at least similar material groups. The respective print material was initially printed as squares on marketable 2D fabrics of the same materiality.

The summary of the preliminary tests shows the qualifying tensile results of the tests in terms of peel and tensile adhesion in relation to the misprint rate or reproducibility, the material cost per kg, the level of printing requirements in terms of process steps, and the recyclability of the filaments. The high misprint rate and difficult handling in the printing process combined with the poor peel and tensile adhesion test results of PA led to its exclusion from further tests. The material combinations of PETG flame retardant, rPETG and PP were then investigated further. The adhesion between 3D printing and the 2D fabrics was also determined via quantifying tests. Various compression die geometries were investigated and tested in the preliminary trials. As a result of the print form, a tensile adhesion stamp with a cylindrical base with a 50 mm diameter and a clamping surface for the testing machine was printed on the textile. After evaluating the test results, it was decided to use a combination of rPETG as the printing material and PES textile. Finally, project-specific textiles were designed with two different porosities and adhesion test and flexural bending were conducted. Figures 6 and 7 show the results.

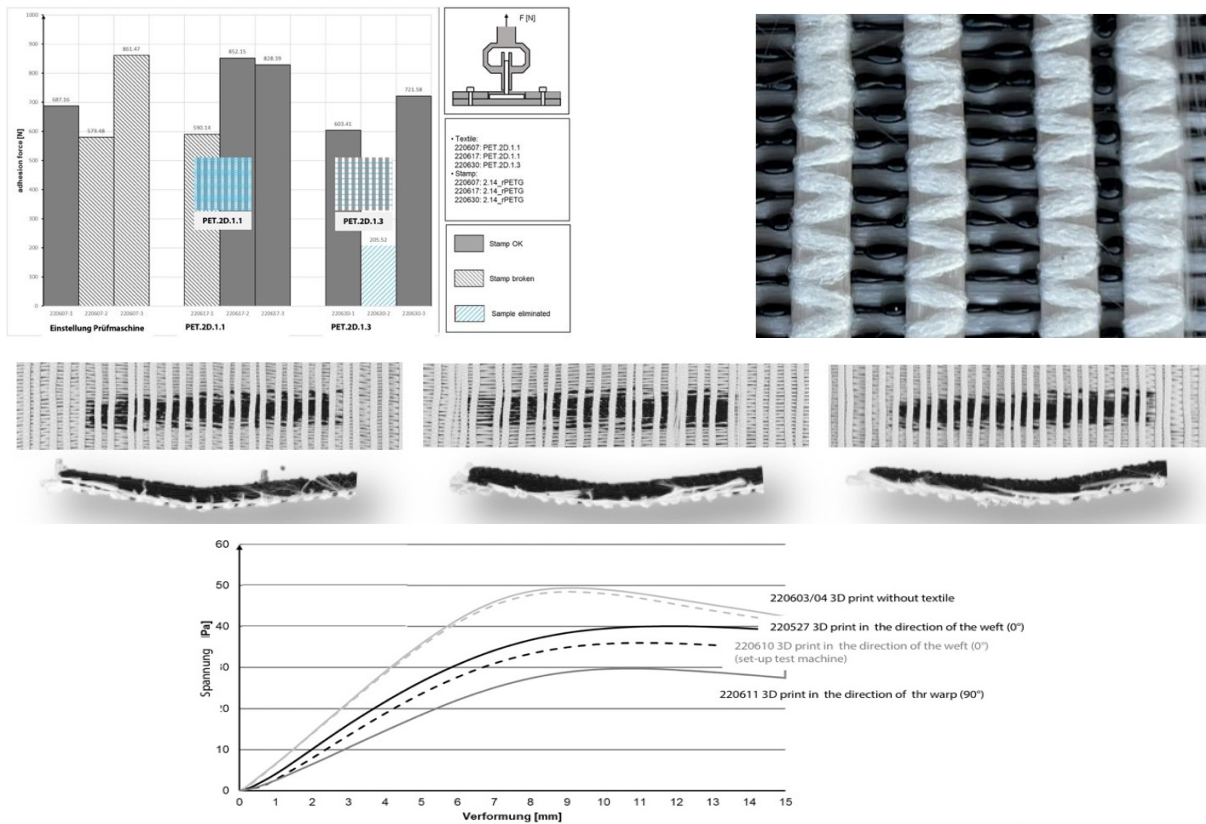


Figure 6: 3D FDM rPETG printing on 2D PES textiles; Top: Adhesion tests and view of the reverse side of the PES textile; Bottom: Bending tensile strength tests with pictures of three specimens printed in the direction of the weft ©ITA and FRAUAS

Membrane architecture – the seventh established building material. Designing reliable and sustainable structures for the urban environment.

The results show better adhesion on the denser surface with a regular and similar pattern of fibres and holes and a rather thick weft roving. In terms of bending, the results show better results if the print is made in direction of the weft yarns. They also show that the material properties (bending tensile strength) of the sole rPETG material is better without the textile. This is probably related to the notches that appear at the interface of the print and textile material on the lower surface of the 3D printed specimens

3.2.1 Composite from mineral-based materials

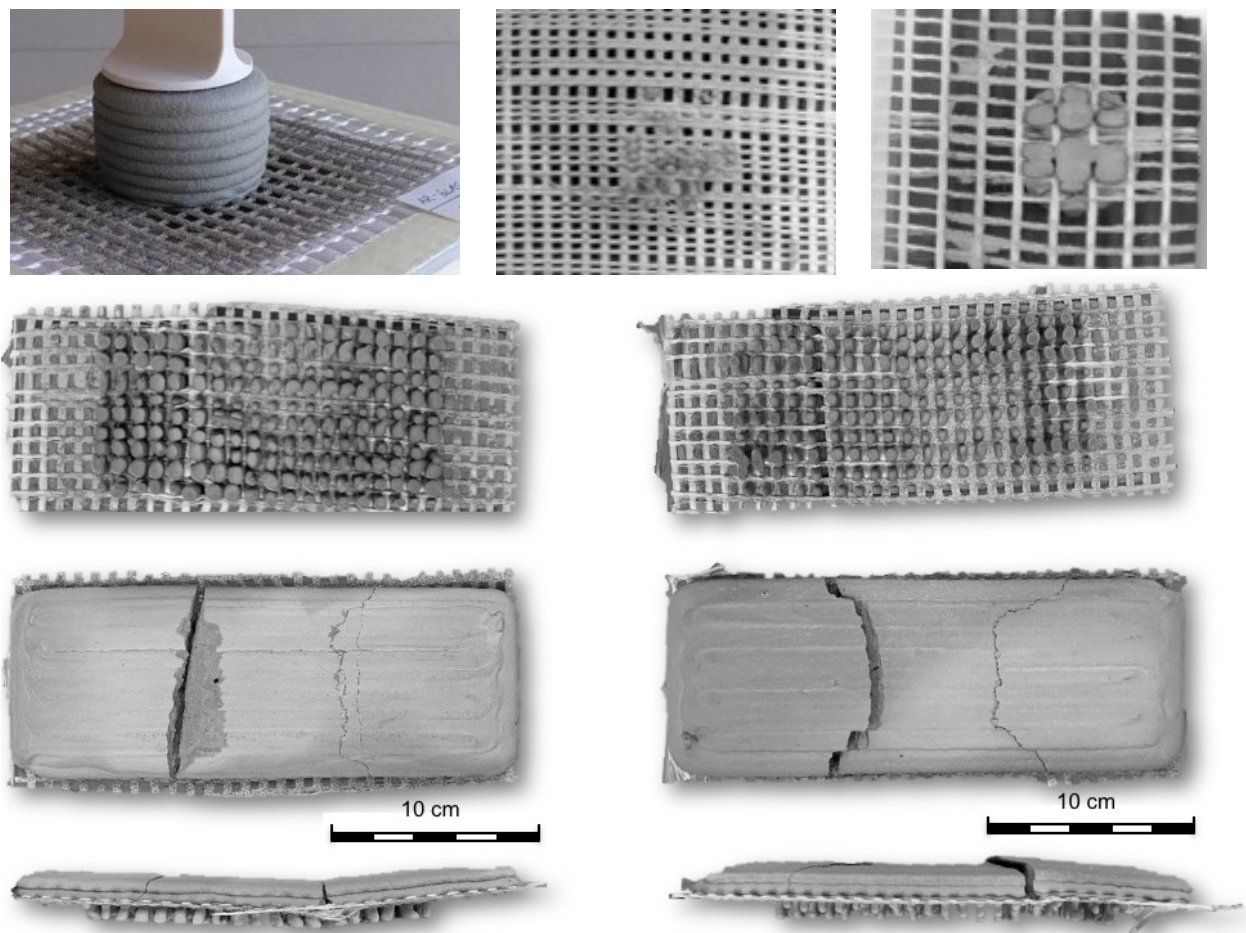


Figure 7: 3D LDM concrete printing on 2D glass textiles; Top left: Specimen adhesion tests; Top right: Adhesion tests seen from below; Bottom: Bending tensile strength tests ©ITA and FRAUAS

Nine different 2D glass textiles were designed and produced on a 2D machine for warp-knitted scrims – comparable to the former production of 2D PES textile. The geometry of the 2D surface is similar to the latter 3D textile. After evaluating the adhesion of nine simple concrete pre-casts on the 2D textiles, five of them were selected for the preliminary 3D concrete printing. Figure 7 shows the specimens for the adhesion and bending tests. Contrary to the rPETG/PES tests, the 3D concrete printing has a much better adhesion once the weft yarns are thin and the concrete is able to enclose the individual rovings. These anticipated benefits will later also be demonstrated with 3D textiles. The first bending tests also show differing results to the rPETG/PES tests. The bending tensile force increases compared to the specimen made of pure concrete. The coating of the textile (not crucial for adhesion) might become relevant for bending

Membrane architecture – the seventh established building material. Designing reliable and sustainable structures for the urban environment.

tests, as the findings for textile reinforced concrete show. The final tests will be executed in 2023.

3.3. Tests: 3D Print on 3D Textile

3.3.1 6dTEX composite from polymer-based materials

Based on the behaviour of the PES rovings in the 2D textile fabrication process (e.g. deformation of the warp and weft rovings), four spacer warp-knitted non-crimp fabrics were designed and produced from PES rovings. They differ in terms of the porosity of the surface layers as well as the design of the pile threads that keep the surfaces apart. All four were used for 3D rPETG printing. The results with regards to adhesion and bending tensile strength tests are shown in Figure 8. Like the 2D textile results, the results with 3D textiles show that adhesion increases with weft roving thickness and uniform surface distribution of larger closed and smaller open areas. Overall, the adhesion on the 3D textile is more than twice as high than on the 2D textile. One reason for this might be the warp-knitting fibres, which increase the roughness of the textile. Additional microscopic studies are currently under way to prove this assumption.

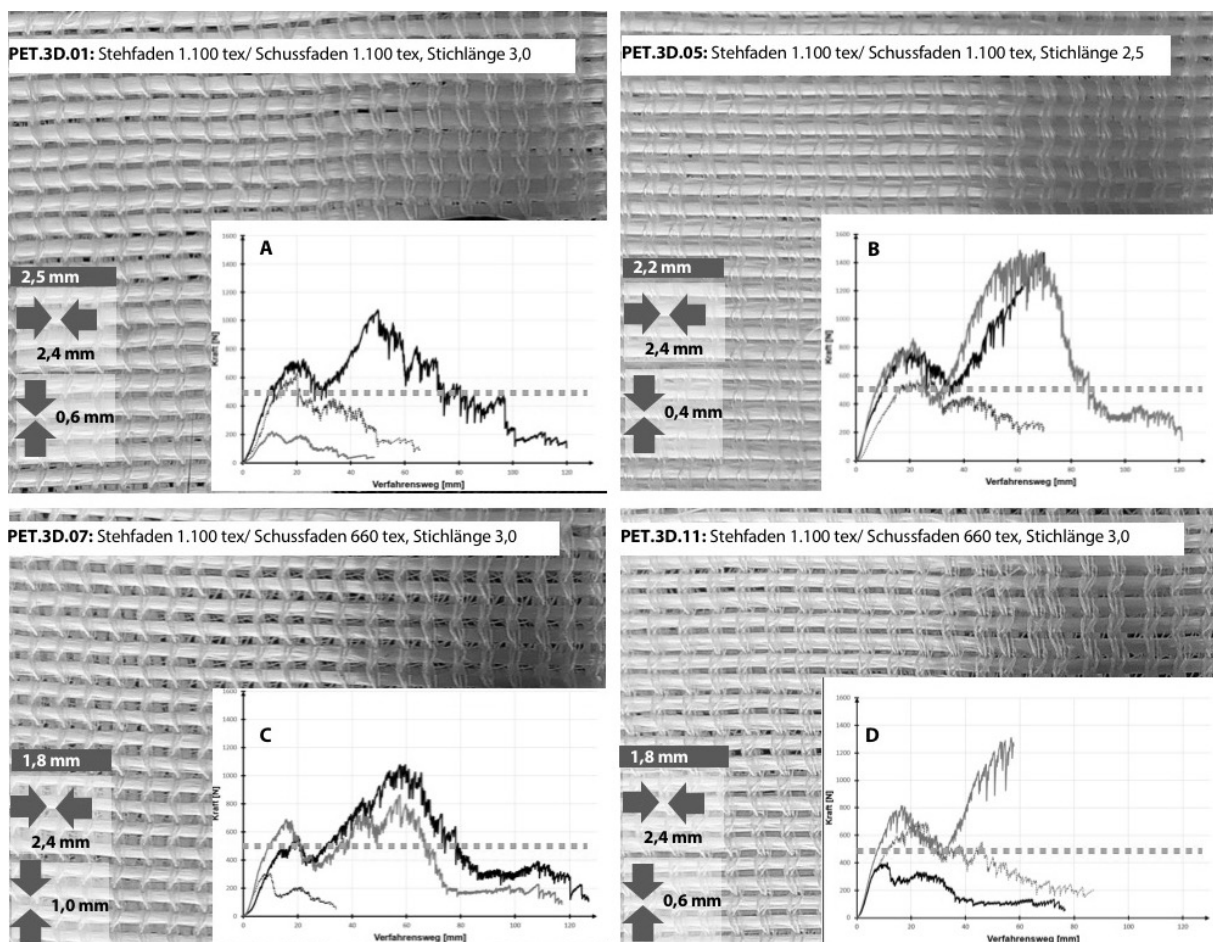


Figure 8: 3D FDM rPETG printing on 3D PES textiles, adhesion tests, ©ITA and FRAUAS

Bending tensile strength tests were also executed on the four 3D textiles. The results do not differ much from the tests with 2D PES textiles. Like with the adhesion tests, the most positive results were once again achieved with textile no. PET.3D.05 with thick weft rovings and smaller openings in the surface than with the other surfaces.

Membrane architecture – the seventh established building material. Designing reliable and sustainable structures for the urban environment.

3.3.2 6dTEX composite from mineral-based materials

Based on the behaviour of the glass rovings in the 2D textile fabrication process (e.g. deformation of the warp and weft rovings), once again four spacer warp-knitted non-crimp fabrics were designed and produced. Figure 9 shows the surface design of the four 3D textiles and the making of 3DCP specimens for adhesion tests. The specimens are currently under production, and the tests will be carried out at the beginning of 2023.

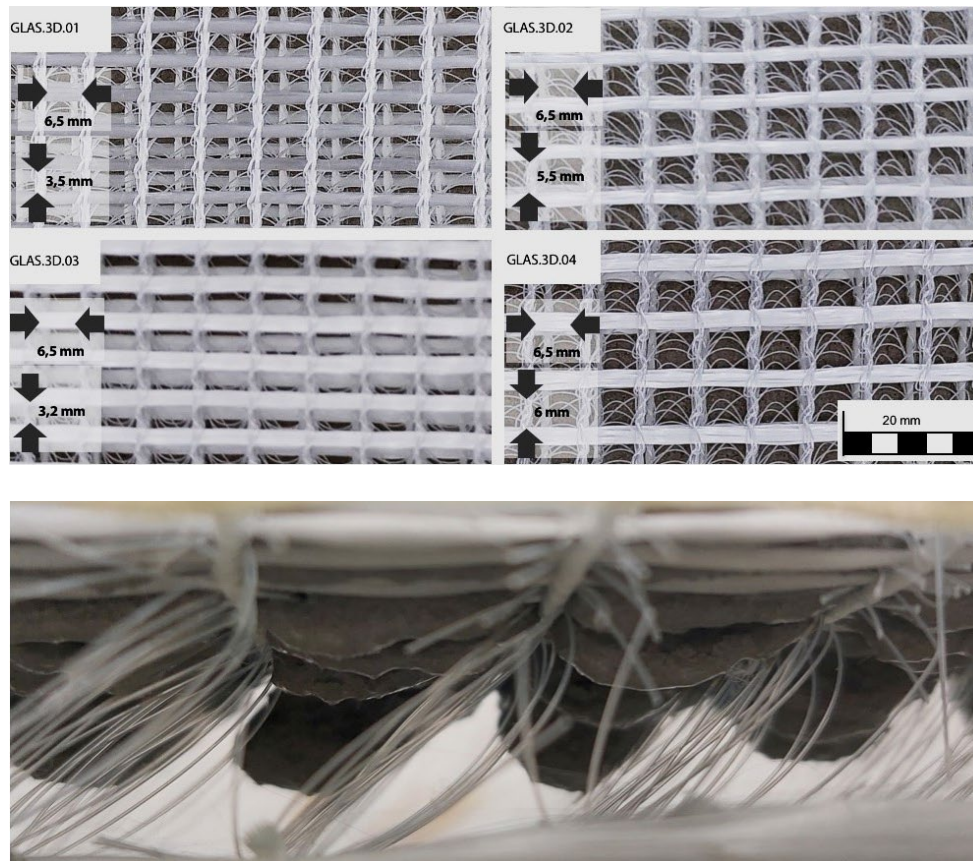


Figure 9: 3D LDM concrete printing on 2D glass textiles; Top – Design of project-specific textile geometry; Bottom – 3D concrete print on 3D textile, section through the 3D textile; targeted penetration of different amounts of concrete allows the production of structures of different densities © FRAUAS

3.3. Demonstrators

The potential fire classifications of the new 6dTEX composites are a determining factor for possible building applications. It is expected that the polymer-based version (rPETG/PES) could be classified in the flame retardant (B1) range, while the mineral-based version (concrete/glass) will achieve a maximum classification in the region of A2, also due to the fact that the pile threads are from PES. The polyester composite of PES textile and rPATg from recycle is fully recyclable. The recyclability of the composite of glass fibers and concrete is equivalent to that of textile concrete. The recyclability of the composite of glass fibers and concrete is equivalent to that of textile concrete. Compared to conventional, solid textile concrete structures or concrete canvas, the filigree, skeleton-like 3D printed concrete structure requires less material and thus less CO₂-intensive cement. The two-layer 3D textile, in turn, offers various possibilities for closing the actual wall surface, such as filling with mineral or bio-based lightweight materials for construction applications.

Membrane architecture – the seventh established building material. Designing reliable and sustainable structures for the urban environment.

The initial findings so far show possibilities: one for secondary building components with less stringent requirements such as solar shading devices from a polymer-based 6dTEX; and the other for primary building components with higher requirements such as ceiling or wall elements from a mineral-based 6dTEX. One of the envisioned elements for solar shading can change its own translucency, which can be preset to different densities via the textile structure. Figure 10 shows an initial textile design with the two described stages of open and closed solar protection. The mechanism works without the use of hinges or joints, and can be moved through the specific 3D printed elements that will be added on the opaque zones. The envisioned elements in terms of ceiling or wall elements have skeleton structures with beams and columns, 3D printed on a lost formwork with additional functions such as tension load-bearing capacities or thermal or sound insulating options (Fig. 10).

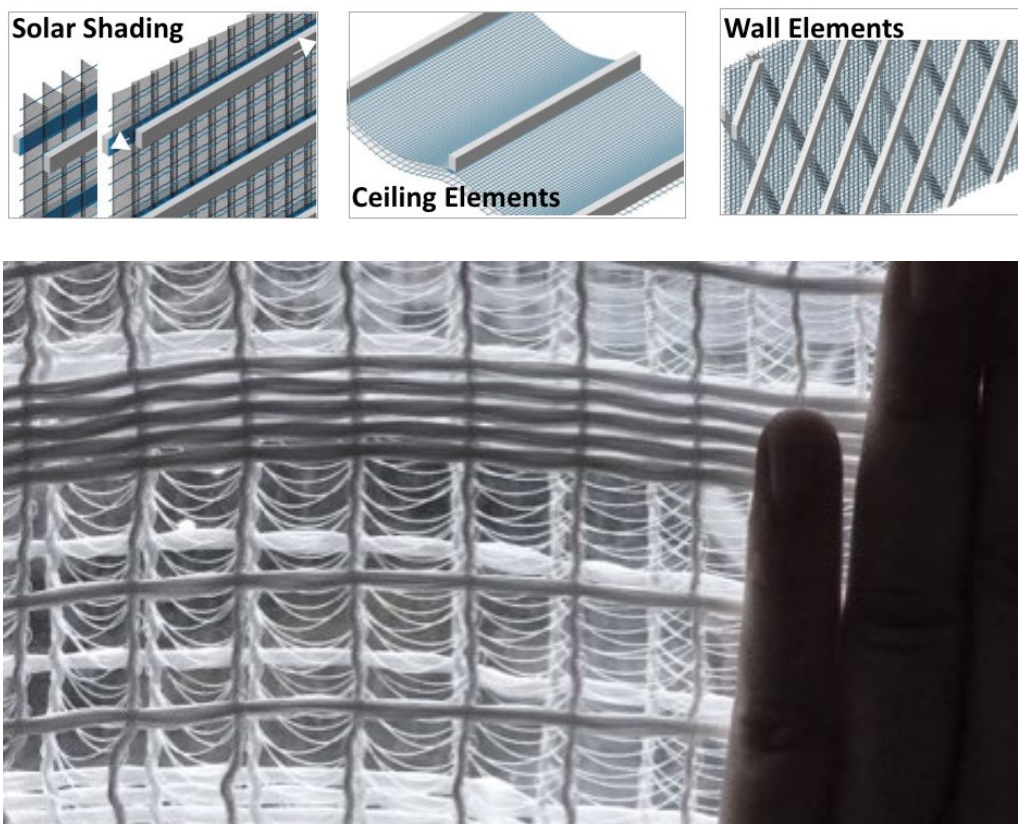


Figure 10: Top – Design options for applications from 6dTEX; Bottom – Solar shading device with preset translucency for different densities via the textile structure © FRAUAS

4. Conclusion / Outlook

The findings so far show the added value of combining manufacturing processes that were previously considered separately. The printed 3D structures are effective for stabilization, while the 3D textiles contribute equally to reinforcement, as lost formwork or as light filter. Prefabricated semi-finished, self-supporting building elements could be produced.

It is demonstrated for both material groups how the mechanical adhesion can be increased by an appropriate Z-Offset in interaction with specially designed textile surfaces. The design of the textile surface in relation to porosity, roughness, undulation is decisive here. Data is currently being collected via laser scanning with the aim of being able to clearly define and

Membrane architecture – the seventh established building material. Designing reliable and sustainable structures for the urban environment.

replicate the textile geometry. With regard to the increase in mechanical strength through textile reinforcement of the printed material concrete in combination with 3D glass fibre textile is particularly successful. Ongoing tests show an increase in the bending flexural strength absorption of the mineral-based 6dTEX version. A big difference between the two material versions of 6dTEX is the fact that the print materials from synthetic sources are available in a great variety and the processing is relatively easy. By contrast the formulas for printable concrete are still under development and they are very sensitive in processing. This makes reproducible printing results on the textile still challenging.



Figure 11: Upscaling, ceiling and wall elements from 3D textiles combined with 3D concrete printing
© FRAUAS

Figure 11 shows initial attempts to upscale the process using commercially available, patented concrete formulations and a large 3D printer. A ceiling and a wall element were produced according to the drawings in Fig. 10. The process was very successful, the adhesion between the concrete and the textile surface developed for it is very good, as is the precision of the concrete geometry. The next step is to test the mechanical strength of the overall composite and the stability of the textile to further evaluate the practical suitability of the elements as lightweight components. Fig. 12 shows initial application options for polyester components. Here, 3D printing serves as a connection and at the same time as a supporting beam structure for the production of spatial textile lightweight structures with lower fire protection requirements. In this case, the function of the 3D textile is in the area of shading or passive cooling in combination with humidification.

Membrane architecture – the seventh established building material. Designing reliable and sustainable structures for the urban environment.

By combining additive 3D processes, recyclable lightweight components with graded material densities can be designed for reliable and sustainable structures for the urban environment. They can be individually manufactured, depending on the requirements profile.

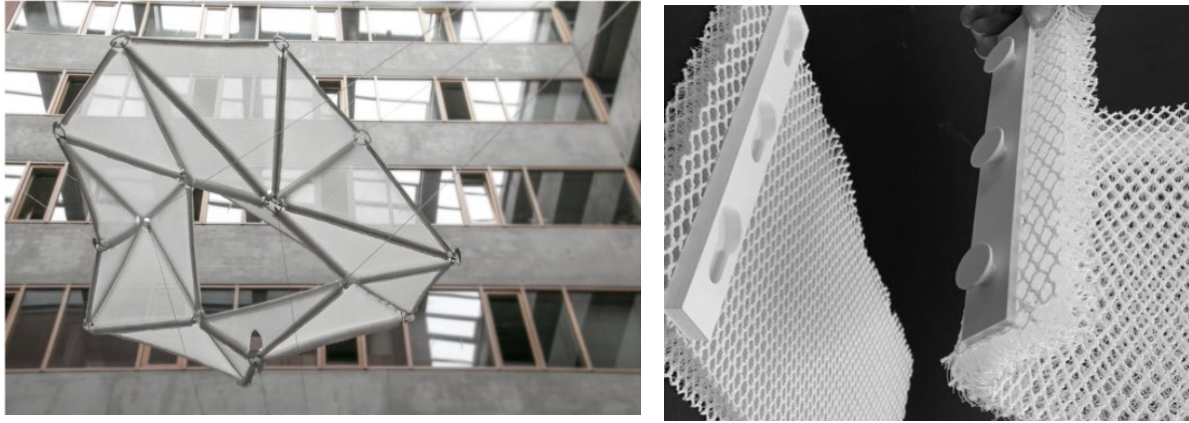


Figure 11: Installation using 6dTEX as a means to join and stabilize a spatial textile lightweight structures via 3D printed two-part beams, © FRAUAS

Acknowledgements

This paper and the research behind it would not have been possible without the exceptional support of the “Zukunft Bau Forschungsförderung” of the Federal Ministry for Housing, Urban Development and Building, the collaboration between FRAUAS and ITA Aachen and all the research assistants and students who helped.

References

- Čuk, Marjeta; Bizjak, Matejka; Muck, Deja; Kočevlar, Tanja Nuša (2020), 3D PRINTING AND FUNCTIONALIZATION OF TEXTILES. University of Novi Sad, Faculty of Technical Sciences, Department of Graphic Engineering and Design. Access: doi: 10.24867/GRID-2020-p56
- El Kadi, M.; Tysmans, M., Verbruggen, S., Vervloet, J., De Munck, M., Wastiels, J., Van Hemelrijck, D. (2019), Experimental study and benchmarking of 3D textile reinforced cement composites. Access from > journals.elsevier.com/cement-and-concrete-composites
- FraunhoferUMSICHT, (2022), FungiFactoring. Access: <https://fungifactoring.de/fungi-factoring/projekt-steckbrief/> [retrieved on 13.04.2022].
- Goidea, Ana; Andreen, David; Floudas, Dimitrio (2020), Pulp Faction: 3D printed material assemblies through microbial biotransformation. In Fabricate.London
- Gorlachova, Maryna; Mahltig, Boris (2021), 3D-printing on textiles – an investigation on adhesion properties of the produced composite materials. Journal of Polymer Research, 2021, 28:207. Access: doi: 10.1007/s10965-021-02567-1

Membrane architecture – the seventh established building material. Designing reliable and sustainable structures for the urban environment.

- Grothe, Timo; Brockhagen, Bennet; Storck, Jan Lukas (2020), Three-dimensional printing resin on different textile substrates using stereolithography: A proof of concept. *Journal of Engineered Fibers and Fabrics*, 15, p. 1-7. Access: doi: 10.1177/1558925020933440
- Kloft, H., Hack, N.; Mainka, J., Brohmann, L., Herrmann, E., Ledderose, L., Lowke, D. (2019), Additive Fertigung im Bauwesen: Erste 3-D-gedruckte und bewehrte Betonbauteile im Shotcrete-3-D- Printing-Verfahren; *Bautechnik*. 96(12), p. 929-938
- Lüling, C., Rucker-Gramm, P., Weilandt, A. et al.: Advanced 3D Textile Applications for the Building Envelope, in: *Applied Composites Materials* 29, 343–356 (2022). <https://doi.org/10.1007/s10443-021-09941-8>
- Lüling, C.; Rucker-Gramm, P.; Weilandt, A.; Schneider, J.; Bauder, H-J.: G3TEX – Multifunctional monomaterials made from foamed glas-, basalt- or PET- based 3D textiles, 04/21 *Proceedings Powerskin*, S.37 - S.50 (2021)
- Lüling C., Beuscher, J.: 4dTEX – Exploration of Movement Mechanisms for 3D Textiles Used as Solar Shading Devices. *Powerskin Conference Proceedings* p. 159–172 (2019)
- Malengier, Benny; Hertleer, Carla; Cardon, Ludwig; Van Langenhove, Lieva (2018), 3D Printing on Textiles: Testing of Adhesion. *J Fashion Technol Textile*, 2018, p. 4. Access: doi:10.4172/2329-9568.S4-013
- Narula, A.; Pastore, C. M.; Schmelzeisen, D.; El Basri, S.; Schenk, J.; Shajoo, S. (2018), Effect of knit and print parameters on peel strength of hybrid 3-D printed textiles. *Journal of Textiles and Fibrous Materials*, 1:1-10. Access: doi:10.1177/2515221117749251
- Pei, Eujin; Shen, Jinsong; Watling, Jennifer (2015), Direct 3D printing of polymers onto textiles: Experimental studies and applications. *Rapid Prototyping Journal*, 2015, 21/5, p. 556–571. Access: doi: 10.1108/RPJ-09-2014-0126
- Diana Popescu and Cătălin Gheorghe Amza (2022) 3D Printing onto Textiles: A Systematic Analysis of the Adhesion Studies; DOI 10.1089/3dp.2022.0100
- Ramsgaard Thomsen, Mette; Tamke, Martin; Sparre-Petersen, Maria; Buchwald, Emil Fabritius; Hnídková, Simona (2020), Silica - A circular material paradigm by 3D printing recycled glass. *Proceedings of the 38th eCAADe Conference*. vol. 2, 128, Berlin, pp. 613-622



tensinantes2023 : TensiNet Symposium 2023 at Nantes Université

Membrane architecture: the seventh established building material.
Designing reliable and sustainable structures for the urban environment.

Proceedings of the Tensinet Symposium 2023

TENSINANTES2023 | 7-9 June 2023, Nantes Université, Nantes, France

Jean-Christophe Thomas, Marijke Mollaert, Carol Monticelli, Bernd Stimpfle (Eds.)

Architecture for Pigs

Maxime Durka*

*Sioen Coating, Fabriekstraat 23, B-8850 Ardoorie.

Maxime.durka@sioen.com, Tel: +32.51.74.16.06

Abstract

Biogas production has the potential to provide three benefits for green energy, waste management, and bio-fertilizers. The process involves converting organic waste materials, such as agricultural waste and food scraps, into methane-rich biogas through anaerobic digestion. This biogas can then be used to generate electricity and heat, reducing the reliance on fossil fuels. Additionally, the waste materials are broken down, reducing the amount of waste in landfills, and the process produces nutrient-rich fertilizer for crops. In summary, biogas production can play a significant role in creating a sustainable future. In recent decades, membrane materials have been used and improved to become a proven solution for covering the roof of anaerobic digesters. Coated textiles, with advanced technical properties such as good gas barrier properties, flexibility, and durability, are ideal for this application. The aim of this paper is to provide the reader with a clear understanding of biogas production and the focus on the impact of some plasticizers which can be used for the development of a gas membrane in anaerobic digesters.

Keywords: biogas; biomethane, green energy production, gas permeation, flexible roof.

1. Biogas, the power from the dung

Biogas is a type of renewable energy that is formed from biogenic matter in the absence of oxygen, consisting primarily of methane, carbon dioxide, and water vapor. It is produced from various sources, including agricultural and food waste, industrial waste, and wastewater. While the biogas industry has faced obstacles to widespread adoption due to technical, economic, and environmental challenges, it has still experienced rapid growth in recent years. In Europe, the biogas sector currently produces over 19 billion standard cubic meters of biogas, with projections indicating growth to 35 billion standard cubic meters by 2030.[1]

National and international entities have conducted feedstock analyses to evaluate the viability of biogas production. Recent reports have also emphasized the profitability of side products

Membrane architecture: the seventh established building material. Designing reliable and sustainable structures for the urban environment.

National and international entities have conducted feedstock analyses to evaluate the viability of biogas production. Recent reports have also emphasized the profitability of side products generated by biogas plants, such as CO₂ and digestates, which reduce reliance on fluctuating gas prices.[2]

The EU commission has established a program to support the growth of the biogas industry within the frame of EU energy security and to support the goals of the EU green deal.

2. From organic wastes to biogas

A biogas plant operates on a principle similar to that of a cow's stomach. Microorganisms found in cow dung break down organic waste to produce methane through a series of biological processes. To be suitable for this process, a substrate must have a high level of biodegradable organic matter and should not contain any digestion-disturbing elements.

Animal waste is the primary source of biodegradable material for farm projects, but its methanogenic potential is low compared to other biomass sources. Agricultural plant materials, such as silage, straw, and crop residues, have high carbon content and good degradability, making them ideal for co-use in biogas production.

Anaerobic digestion, a process in which microorganisms called methanogens break down organic matter in the absence of oxygen, is used to produce biogas. This process occurs in a closed system called an anaerobic digester or bioreactor, and it involves four stages: hydrolysis, acidogenesis, acetogenesis, and methanogenesis (Figure 1).

During hydrolysis, complex biopolymers are broken down into simpler molecules, and acidogenic bacteria produce volatile fatty acids and alcohols during acidogenesis. Methanogens then use these acids to produce methane during methanogenesis. Balancing the nutritional needs and environmental conditions of acid-forming and methane-forming microorganisms is essential to prevent instability in the reactor. Inhibitory substances can also affect the process, leading to a reduction in production or total failure of the process.

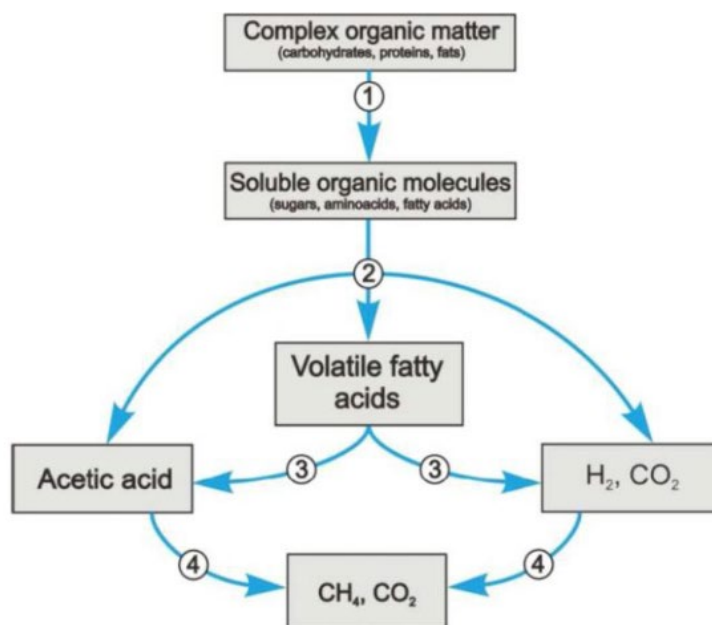


Figure 1: Anaerobic pathway of digestion of organic material

Membrane architecture: the seventh established building material. Designing reliable and sustainable structures for the urban environment.

Approximately 50% of the biogas produced is biomethane (Table 2), biogas has a calorific value of around 6-20 MJ/m³ whereas biomethane's calorific value is 35-40 MJ/m³.

Biogas can be used in cogeneration units to generate energy and heat, but the yield of electricity is moderate. Biogas can be purified and the biomethane (CH₄) separated from other gases to be injected directly into the natural gas grid.

The purification path represents today the biggest part of the new anaerobic digester projects, but also the usual upgrade realized on existing biogas installations. Other by-products, such as CO₂ and digestate, are being investigated and promoted for their potential to make the biogas industry more circular.

Table 2: Biogas composition

Component of generated biogas	Content (%)
Methane (CH ₄)	50-75
Carbon dioxide (CO ₂)	25-50
Nitrogen (N ₂)	0-10
Hydrogen (H ₂)	0-1
Hydrogen sulphide (H ₂ S)	0-3
Oxygen (O ₂)	0-2

3. The architecture of a biogas installation

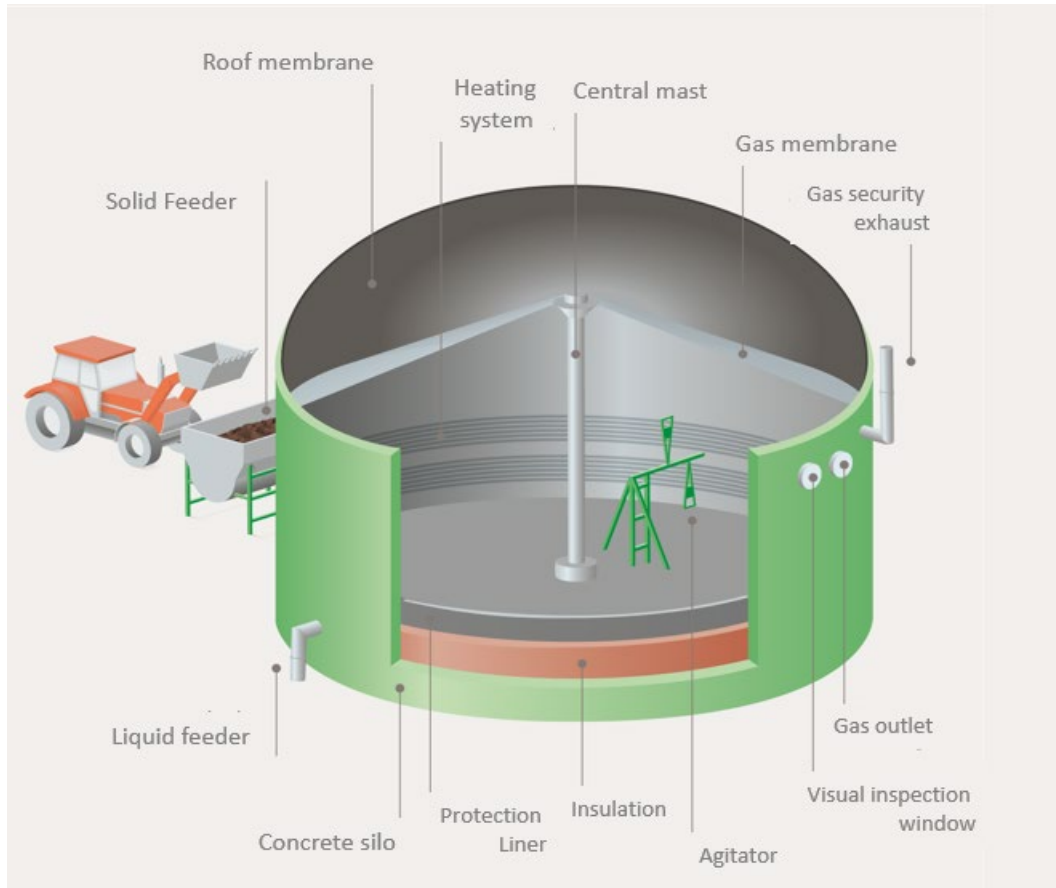
The choice of process for digestion depends on factors such as the type of feedstock, the ratio, and the incorporation method. Liquid phase is the most commonly used method, and it works well for mixtures with less than 18-20% dry matter. To ensure proper mixing, digestate recirculation may be used. For projects involving only solid manure, the solid route may be more appropriate.

During incorporation, it is important to carefully consider the type of material being used. Liquid materials are typically stored in tanks and pumped into the digester several times per day using eccentric screw pumps, chopper pumps, or lobe pumps for thicker substances. Solid materials are loaded into a hopper connected to the digester by an endless screw or a piston. This is also the stage where any undesirables such as pebbles, strings, or metals must be removed. It may be necessary to include a crusher and a stone trap depending on the type of manure being used.

The digester itself may be constructed of concrete or stainless steel and may be semi-buried. To ensure the optimal conditions for digestion, the parts of the digester in contact with the gas are protected against corrosion. The size of the digester must be calculated carefully to ensure sufficient residence time for the bacteria to express the methanogenic potential while maintaining a sufficient organic load. To maintain optimal conditions, the digester must be sealed, and temperature and pH levels must be maintained while ensuring there is no oxygen present.

Membrane architecture: the seventh established building material. Designing reliable and sustainable structures for the urban environment.

Material flows are quasi-continuous, with one cubic meter of digested material being evacuated for every cubic meter of feedstock incorporated. The digester's roof consists of a double membrane, with the outer membrane providing structural support and protection from weathering elements, and the inner membrane acting like a lung, inflating or deflating during gas generation and extraction (Scheme 1). The double membrane roof is being over pressured from 5-25 mbar. In Europe, the process is typically run at a constant temperature between 35 and 42°C using the mesophilic temperature regime.



Scheme 1: Overview of anaerobic digestion reactor (adapted from ADEME brochure)

Before the gas membrane has reached its maximum capacity, the biogas is being stored in a gas holder system, or being used to generate heat and electricity in a side CPH unit, or the gas is being purified thanks to a complex gas scrubbing system before being normalized (pressure, odour,...), verified (purity) and injected in the natural gas grid.

The solid and liquid content has generally a residence time in the digester is around 40 days. For 1 m³ of feedstock entering, 1m³ of digestate is being evacuated. The digestate is being filtered to separate the liquid and the solid parts. Both of them are used to fertilize the fields depending on the soil and crops need.

Recent studies have highlighted the need to regulate carefully the incoming and outgoing fluxes of matters, pressure and temperature in order to maintain a robust and performing process.[3] Due to the complex pathways of anaerobic digestion together with the side products generated, both biological selections together with numerous additives have been developed to buffer and increase the CH₄ yields.

Membrane architecture: the seventh established building material. Designing reliable and sustainable structures for the urban environment.

4. Technical textiles at the service of Biogas plants

There are numerous technical textiles located near the biogas plant, and their main purpose is to create reliable and durable barriers against the dispersion of odors and matter in the environment. This allows for efficient storage and delayed processing. The focus of this discussion, however, is on the peculiarities of gas membranes and outer membranes used in anaerobic digester units, and not on these other applications.

Roof membranes, also known as outer membranes, need to be resistant to weathering conditions while maintaining their structural shape against various factors such as wind, snow, gas production, and degassing. To achieve this, a positive pressure system (including compressors and gas sensors) is used to adjust the overall pressure of the structure to the calibrated values. These overpressures can range from 5 to 50 mbar.

Therefore, the detailing of the membrane and the overall project must be executed meticulously to ensure the smooth operation for a minimum of 10 years. Overall, the structural approach of the roof membrane is not significantly different from the air positive structures commonly encountered in tensile architecture business. Currently, the most commonly used materials for roof membranes include PVC-coated polyester fabrics, EPDM membranes, and PE foils.

Gas membranes, on the other hand, face different challenges. They are not directly exposed to environmental conditions but are instead subjected to a hot, humid, and chemically rich environment due to the anaerobic digestion process. In these harsh conditions, gas membranes need to maintain their gas holding capacity and flexibility. Therefore, several measures are implemented in anaerobic digesters to ensure a minimum lifespan of 5 years for the gas membranes. For instance, the use of a center mast and connected belts prevents physical contact between the gas membrane and slurry, which could otherwise cause degradation and loss of function.

Additionally, the production of side products such as ammonia, hydrogen sulfide, volatile organic acids, and terpenes during anaerobic digestion can rapidly degrade the gas membrane if proper chemistry is not implemented. In most cases, this degradation leads to a loss of flexibility and gas barrier performance, ultimately resulting in the cessation of biogas production and costly operations to clean and repair the structure before resuming routine operations. The presence and composition of these side products are frequently monitored and depend on the biological processes and feedstock composition.

As a company with over 20 years of experience in biogas applications, we have installed our membrane products in more than 80 countries, encountering various conditions and uses. This extensive expertise has led to the development of three ranges of gas membrane products. In the next part of this discussion, we will focus on PVC coated polyester fabrics as gas membranes.

5. Gas membranes, performance requirements and evaluations

To assess the performance and suitability of biogas membranes, we conducted a series of tests that consider the application conditions mentioned above. Firstly, we performed characterizations of the mechanical and physical properties of the membranes, such as tensile strength and adhesion, following our standard internal quality control procedures. These procedures are based on the guidelines outlined in the "Prospect for European Guidance for the Structural Design of Tensile Membrane Structures" [4].

Membrane architecture: the seventh established building material. Designing reliable and sustainable structures for the urban environment.

Secondly, certain regions, like Germany, have published advanced guidelines for biogas plant safety. For example, the TRAS120 specifies rules for membranes, including requirements such as flame retardancy for the roof, surface resistance within a specific range to ensure conductivity and prevent electrostatic charge, outer membrane tensile strength and tear strength thresholds, reflection of thermal radiation to counteract heating from the sun and unnecessary overpressure in the storage tank, and inner membrane methane permeability limits at a specific pressure difference [5]. When necessary, our biogas membrane products for anaerobic digester roofs are developed and tested in accordance with these guidelines.

Thirdly, due to the variety of feedstocks and side products generated during the biological reactions, we have developed advanced specialty products to enhance the durability of the flexible roof. Although these tests are not officially covered by any guidelines, they are crucial for creating a reliable installation. In addition to locally monitored projects, we have developed two sets of tests to provide innovative and purpose-fit roof membrane products to the market.

The first type of test is typically conducted at specific biogas production sites, and it provides valuable information about the membrane's general behavior and performance degradation (Figure 2).

The second type of test is performed in laboratory conditions to further investigate and characterize the causes of performance loss observed in the field. The materials exposed during these tests undergo advanced surface and atomic analyses conducted internally and with the assistance of competent laboratories.

We have observed rapid performance loss, including degradation and loss of flexibility, in certain applications involving feedstocks derived from specific branches of the food industry and waste processing of fats and flavour derivatives.



Figure 2: Field test exposing the gas membrane to raw biogases before conducting material analyses.

One critical degradation mechanism of the gas membrane is the "loss of plasticizers," which refers to the membrane material becoming more rigid over time, resulting in the loss of gas barrier properties.

This de-plasticization is, to our knowledge, caused by two main factors: 1) hydrolysis of ester plasticizers in the presence of water, alcohols, and temperature, catalysed by acidic or basic conditions, and 2) displacement of plasticizers through concentration exchange in the presence of organic aliphatic derivatives, catalysed by heat.

Membrane architecture: the seventh established building material. Designing reliable and sustainable structures for the urban environment.

To test and prevent such degradation, we developed various membrane specimens and subjected them to representative and simplified biogas atmospheres. We evaluated the degradation and oxidation of PVC plasticized coatings using FT-IR and SEM EDX analyses, and the comparative results are summarized in Table 2.

Table 2: Comparative resistance against different chemicals released during anaerobic digestion

Specimen		1	2	3	4
Formulated with		Phtalate derivatives	Sulfonated phenyl esters	Adipic esters	Rubber derivatives
Compatibility					
Gas	Water			+++	
	Methane			+++	
	Ethane			+++	
	Propane			+++	
	Butane			+++	
	Pentane & higher hydrocarbons			-	
	Carbon dioxide			+++	
	Nitrogen			+++	
	Hydrogen			+++	
	Hydrogen sulfide	+	++	+	+++
Acids	Sulfuric acid <10% sol.	++	+++	++	+++
	Acetic acid <10% sol.		++		+++
	Phosphoric acid <10% sol.		++		+++
Bases	Soda <10% sol.			+++	
	Ammonia <30% sol.			+++	

Membrane architecture: the seventh established building material. Designing reliable and sustainable structures for the urban environment.

Alcohols	Methanol			–		
	Ethanol <30% sol.	+	+		++	+++
	Propanol <30% sol.	+	+		++	+++
	Isobutanol <1% sol.	+	+		++	+++
	Glycol				+++	
	Glycerin				+++	
Oil	Citrus	–	–		–	++
	Organic oils (soja, olives...)	–	–		+++	++
	Orange				–	
Hydrocarbons	Gasoline / Kerozene	–	–		+	++
Solvents	Acetone				–	
	Benzene				–	
	Terpene, limonene <5% sol.	–	–		–	++
	Toluene				–	
UV		++	++	++		–

Based on the results obtained, we have reasonable confidence in the following conclusions:

1. Phthalates or sulfonated phenyl esters (specimens 1 & 2) demonstrate stability against hydrolysis conditions. Therefore, it is reasonable to use gas membranes formulated with these substances for crop wastes and manure feedstocks. Moreover, these formulations exhibit good UV resistance, making them suitable for agricultural biogas membranes.

2. The adipic ester formulation shows similar resistance against hydrolysis conditions, albeit with slightly higher hydrolysis rates compared to the previous formulations. Additionally, we observed better performance in terms of resisting plasticizer exchanges when hydrocarbons and oils are present as slurry components in the anaerobic digester.

3. Among the tested specimens, specimen 4 exhibited superior performance, acting as a superhero against the investigated de-plasticization mechanisms. However, it has one clear drawback: poor resistance against UV exposure. As a result, it can only be used as a gas

Membrane architecture: the seventh established building material. Designing reliable and sustainable structures for the urban environment.

membrane for double-layer anaerobic digesters and is not suitable for low-tech, single-layer digesters. This formulation seems to be the solution for challenging and aggressive feedstocks (such as food, oil, agricultural, and industrial waste) that trigger both de-plasticization mechanisms, scope of this investigation.

6. Conclusions and perspectives

Biogas production plays a crucial role in fostering a sustainable future. Over the past few decades, membrane materials have emerged as a proven solution for covering the roofs of anaerobic digesters, and continuous advancements have been made to enhance their performance. Coated textiles, possessing advanced technical properties such as excellent gas barrier capabilities, flexibility, and durability, are particularly well-suited for this application.

In this study, we conducted an analysis of various plasticizers in relation to the derivatives produced and present in anaerobic digesters. Through our investigation, we were able to identify several key and complementary benefits associated with different formulations. Furthermore, ongoing research is focusing on surface treatments aimed at improving gas barrier properties and resistance. Additionally, significant efforts are being dedicated to developing suitable insulation membranes, aiming to achieve high-performance and reliable technologies for anaerobic digestion processes.

References

[1] https://www.europeanbiogas.eu/_trashed-3/ accessed the 07.03.2023

[2] <https://www.europeanbiogas.eu/beyond-energy-monetising-biomethanes-whole-system-benefits/> accessed the 02.05.2023

[3] S. Sarker et al., A Review of the Role of Critical Parameters in the Design and Operation of Biogas Production Plants, *Appl. Sci.* 2019, 9, 1915

[4] <https://publications.jrc.ec.europa.eu/repository/handle/JRC132615>, accessed online the 02.05.2023

[5] <https://www.kas-bmu.de/tras-endgueltige-version.html>, accessed online the 02.05.2023



tensinantes2023 : TensiNet Symposium 2023 at Nantes Université

Membrane architecture: the seventh established building material.
Designing reliable and sustainable structures for the urban environment.

Proceedings of the Tensinet Symposium 2023

TENSINANTES2023 | 7-9 June 2023, Nantes Université, Nantes, France

Jean-Christophe Thomas, Marijke Mollaert, Carol Monticelli, Bernd Stimpfle (Eds.)

An innovative solar shading device for outdoor thermal comfort

Adriana ANGELOTTI^{*,b}, Alara KUTLU^{a,b}, Salvatore VISCUSO^{a,b}, Andrea ALONGI^{*,b},
Alessandra ZANELLI^{a,b}

^{*}Politecnico di Milano, Energy Department

v. Lambruschini 4A, 20156 Milano, Italy

adriana.angelotti@polimi.it

^a Politecnico di Milano, Department of Architecture, Built environment and Construction engineering, v. Ponzio 31, 20133 Milano, Italy

^b Politecnico di Milano, Interdepartmental Laboratory for Textiles and Polymers (TetxilesHub), v. Ponzio 31, 20133 Milano, Italy

Abstract

This study illustrates the design, the development and the testing of an innovative solar shading device to be installed in outdoor urban spaces, with the aim to provide better thermal comfort during summer. The device consists in either a single or a double membrane tensioned through a flying mast and hung to existing poles and trees. Adjustable corner joints facilitate the installation and dismantling by the users and guarantee adaptation to most urban spaces. The double membrane configuration is proposed in order to reach a very low solar transmissivity, while an adequate air gap between the two layers allows cooling by ventilation. Two 25 m² prototypes were created and installed side by side in an outdoor space in the Politecnico campus in Milan, Italy: a single layer device (based on a standard white membrane) and a double layer one (adopting a standard white membrane on the top and a low emissivity membrane on the bottom). The experimental campaign showed that the latter can provide better thermal comfort, since the mean radiant temperature under the double layer device was found to be lower (about 3°C on average and about 5°C at maximum) than under the single membrane.

Keywords: lightweight structures, membrane, thermal emissivity, solar reflectivity, solar shading, thermal comfort, mean radiant temperature, urban space.

1. Introduction

Outdoor thermal comfort is a relatively new and emerging field of research and design (Johansson et al. 2014). Providing urban spaces with adequate thermal comfort conditions, especially during summer, enhances the use of the public space by the citizens, promoting urban sociability. At the same time, the more the citizens spend their free time outdoor, the less energy is potentially consumed to provide mechanical air conditioning indoor.

Membrane architecture: the seventh established building material. Designing reliable and sustainable structures for the urban environment.

However, achieving adequate comfort conditions outdoor during summer is becoming more and more challenging due to the climate change. Heat waves phenomena are becoming more frequent and intense. Thus, there is an increasing demand for strategies and solutions impacting on the urban microclimate in different phases, ranging from the early design of the public space to its renovation and adaptation.

Sun shading is key to mitigate heat stress during summer, as it helps to maintain a low Mean Radiant Temperature. The latter is defined as the “uniform temperature of an imaginary enclosure made of black surfaces in which the radiant heat transfer from the human body equals the radiant heat transfer in the actual non-uniform enclosure” (ASHRAE 2001). Therefore, it summarizes into a single index the effect of the many radiative heat transfers between a body and its surrounding environment. While indoor the Mean Radiant Temperature is mainly related to infrared radiation from the building surfaces, in outdoor environments it is largely influenced by solar radiation.

Solar control in outdoor environments can be achieved through either trees or artificial devices made up of textiles or membranes. When comparing thermal comfort conditions for pedestrians under trees and under sun sails shading an entire urban canyon, Kantor (Kantor et al. 2018) found that the first were more effective, either because the tree canopies have a lower solar transmissivity than fabric sails or because the evapotranspiration provides an additional cooling effect. However, the greening strategy is more easily adopted in the design phase of a new urban area, while using textiles or membranes to shade sunny open areas is a simple, reversible and flexible intervention that can renovate an existing urban space, turning it into a comfortable niche. Artificial shading devices are often canopies installed in urban canyons at the rooftop level (Paolini et al. 2014), as in traditional urban design in Mediterranean countries, or lightweight structures at the ground level, such as the Palenque pavilion developed for the Expo international exhibition held in Sevilla, Spain, in 1992.

This study focuses on the design, the development and the testing of an innovative solar shading device based on membranes, to be installed in outdoor streets and squares to improve thermal comfort during summer. The research has manifold objectives: on the one side to widen the possibilities of application of sun shading to different urban spaces by developing adaptable devices, on the other side to improve the microclimatic mitigation performance of artificial shading devices. To the latter purpose, non-conventional membrane materials, featuring a low thermal emissivity, and double layers configuration are investigated.

After describing the concept of the shading device, the development of two prototypes is reported. Finally, the results of an experimental campaign comparing their performance are illustrated and discussed.

2. The urban solar shading device concept

The basis for the urban solar shading device is the membrane kit. Each membrane kit consists of a membrane layer, a supporting element or flying mast and two belts forming a cross. By using only one membrane kit, a single layer shading device is obtained: the flying mast is connected in a reversible way on one side to the membrane and on the other side to the belts, so that a pre-tensioned lightweight structure is created (Figure 1, top). The structure can then be hung to four existing poles or trees by means of additional cables, suitably tensioned. The design challenge is the development of adjustable corners joints, able to facilitate the installation and dismantling by the users and guaranteeing adaptability to most urban spaces. If

Membrane architecture: the seventh established building material. Designing reliable and sustainable structures for the urban environment.

properly tensioned, the shape of the device allows to prevent the rain accumulation on the membrane.

A good solution to improve the performance of extremely thin and flexible membrane materials - which in many cases cannot themselves offer adequate thermal performances - is to use a multi-layer design approach (Knippers et al., 2011). Multi-layer systems combine a variable number of layers made of materials with specific functions (e.g., permeability to water, light and noise, thermal insulation, radiation reflection and fire resistance) to provide better thermal and optical performance such as reduced U-values compared to a single material (Göppert & Paech, 2015).

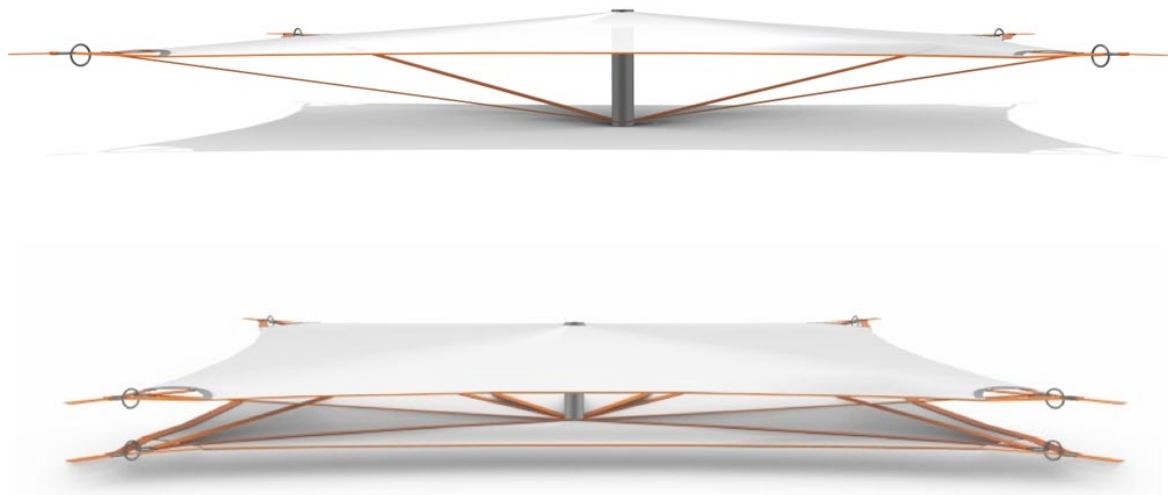


Figure 1: Single layer (top) and double layer (bottom) shading devices

Based on these premises, the concept focused on a modular approach for the ongoing developing shading system: in fact, two membrane kits can be used to create a double layer shading device, which appears as a modular implementation of the single membrane device achieved by adding a bottom membrane (Figure 1, bottom). To use lightweight flexible materials correctly, it is first necessary to accurately determine the physical properties of the individual materials in order to evaluate the contribution of each layer that composes the multi-layer envelope system. Nevertheless, even if the contributions of individual components are known, also the order and assembly method in which the layers are placed affects the overall performance of the system. Since the double layer device is symmetrical, it is possible to switch the top and bottom membranes, investigating the impact of materials with different solar and thermal properties and the influence of their position.

The double membrane configuration is characterized by a lower solar transmissivity with respect to the single layer one; at the same time, an adequate air gap between the two layers helps to keep cool the bottom membrane, which is the one exchanging heat with the persons below. The height of the flying mast determines the maximum width of the air gap (Figure 1, bottom).

Membrane architecture: the seventh established building material. Designing reliable and sustainable structures for the urban environment.

3. Development of the prototypes

Two prototypes with membrane area of about 25 m² were designed by the research group and realized by Canobbio Textiles Engineering srl (Figure 2): a single layer and a double layer one, based on membrane materials produced by Ferrari Textiles. The fabric form of both layers is computer generated using specific software for the industry. This 'form' is then converted into flat panel which can then be cut out to create paper patterns, or the information can be used by a plotter/cutter.



Figure 2: The manufacturing of the prototypes at the Canobbio Textile Engineering factory

The single layer device is based on a standard white membrane. The double layer one adopts the same standard white membrane for the top layer and a low emissivity membrane for the bottom one, with the low emissivity side facing the ground. The solar and thermal properties of the membrane materials derived from the technical data sheet are reported in Table 1, where it has to be mentioned that the two sides of the standard white membrane are the same, while the low emissivity membrane features a special aluminium coating on one side, leading to different thermal emissivities on the two sides. The low emissivity membrane material is usually adopted for solar control inside buildings, so that the use proposed in this work can be considered non-conventional.

Because of the nature of the technical fabrics used, the presence of the double curve and the process of manufacturing, tension is always required in order to induce the correct shape and take out any minor creases in the fabric. This tensioning can take many forms: from simply hand pulling a canopy into place and Velcro fixing, to tensioning a corner of a canopy with a rigging screw or turn buckle, depending on the size of the structure and the use. In this case, two plastic hollow pipes 80 cm long with a diameter of 10 cm serve as flying masts; tubes are then fastened to the corners of the canopies by means of adjustable belts and Velcro fixings. Although the flat fabric is not specifically stretchy, it will stretch a very small amount

Membrane architecture: the seventh established building material. Designing reliable and sustainable structures for the urban environment.

particularly across the bias of the fabric (Knippers et al., 2011). For that reason, the stretch amount must be compensated and thus the additional length has to be deducted from the panel size. In the tested prototypes, the manufacturer adopted a compensation of 1%.

Membrane	τ_{sol}	ρ_{sol}	ϵ
Standard white (Preconstraint 502-8102 white)	10%	76%	0.9
Low emissivity (Soltis low-e 99-2061E)	6%	68%	0.9 (A side) /0.35 (B side)

Table 1: Solar transmissivity, solar reflectivity and thermal emissivity of the membrane materials adopted in the prototypes

4. Experimental campaign

4.1 Experimental methods

The two prototypes were installed side by side in an outdoor space in the Politecnico campus in Milan, Italy (Figure 3). The campaign lasted for two weeks in September 2021. The experimental site is a green area with an almost regular array of trees, so that the shading devices were hung to 6 trees overall. During the day, the trees could partially shade the devices, yet the orientation of the trees and of the devices was such that shading by the trees happened almost in the same way contemporarily on the two devices.

It was not possible to install the two devices on the same ground surface, so that one was placed over grass and the other over a cement pavement covered with clear gravel. In order to avoid any influence of the different ground cover on the comparison, in the first part of the campaign the single membrane device was placed over grass, while in the second part it was placed over the cement pavement. The opposite happened to the double membrane device.

The measurement set up consisted of a mobile data acquisition system and two small dataloggers, equipped with several sensors. Below each prototype a standard black globe thermometer was installed at the conventional height of the center of a standing person, namely 1.1 m from the ground. A third globe thermometer was placed in the sun close to the prototypes. On the bottom side of the single layer device and on the bottom side of the lower membrane of the double layer device a thermocouple was placed, in order to measure the surface temperature of the membrane directly radiating towards the ground and towards any person below the devices. The temperature of the ground surface shaded by each prototype was measured by means of two thermocouples. Further, the main microclimatic parameters were measured, namely air temperature and humidity by means of a thermo-hygrometer, wind velocity at 1.1 m height through an ultrasonic anemometer and global solar irradiance on the horizontal in open field by means of a solar radiometer. Data were acquired every 30 s in the central hours of the day.

The Mean Radiant Temperature (MRT) below each shading device and in open field was then calculated from the globes temperature, the air temperature and the wind speed data, averaged every 5 minutes. Air temperature and humidity as well as wind speed can reasonably considered equal below the two sun shading devices, while the Mean Radiant Temperature was expected to be different for two reasons: the solar radiation transmitted is different and the thermal radiation emitted towards an underlying person by the bottom surfaces is different. Therefore, the measurements were aimed at verifying the existence of a difference in the MRT produced

Membrane architecture: the seventh established building material. Designing reliable and sustainable structures for the urban environment.

by the two prototypes, resulting in a different thermal comfort perceived by a person standing alternatively under them.



Figure 3: The two prototypes installed side-by-side in the Politecnico campus

4.2 Experimental results

4.2.1 Installation test

Installing the prototypes allowed to identify some key aspects able to ease and speed up the installation and dismantling phases. First of all, it might occur that existing supports (poles, trees) for hanging the shading devices are not arranged symmetrically with respect to the membrane geometry. Therefore, the membrane corners should be equipped with multiple or redundant connections that can be steered at least in two directions per side, allowing to properly tension the kit in any condition.

Furthermore, Velcro was chosen as the most important element for regulating the length of the crossed tapes stabilizing the kit. Even if this device made the prototyping easier to be managed, it proved to be very uncomfortable during the installation stage, as it requires the operator is able to maintain the tension through the force exerted by his/her own arms, thus losing a clear reference of the length reached by the entire system of tension. This problem can be easily remedied with the integration of turnbuckles at the end of the crossed belts, close to the corresponding flying mast.

The requirement of interchangeability for both membrane layers – the above and the below ones – is guaranteed only if the kits are completely independent from each other, i.e., each membrane is stabilized by its flying mast and by its system of crossed ribbons. To speed up the prototyping and installation stages, this was only partially done during the experimentation in the campus site, in which the surrounding trees only permit to set up an irregular hanging system for the membrane kits. The single-layer and double-layer shading devices - installed side by side (Figure 3) - do not appear perfectly tensioned as the lower membrane was not installed independently, but simply hung from the upper one. If this has not invalidated the thermal comfort test, it is certainly to be considered an ineffective fallback, but potentially dangerous for the stability of the entire structure over time. In fact, the lower membrane hanging from the

Membrane architecture: the seventh established building material. Designing reliable and sustainable structures for the urban environment.

upper one does not work properly as it is not able to resist the wind load and can potentially accumulate rainwater until it collapses. Therefore, to install the double layer device using an irregular hanging points layout, the two membrane kits must be firstly pre-coupled and tensioned in mid-air and then raised to the desired distance (based on the optimal air gap for ventilation) using the turnbuckles, missing in the current version of the prototype.

During the experimental campaign the two shading devices proved to be able to resist to the modest urban wind in Milano. Further efforts could be devoted to identify the wind load resistance of the structure.

4.2.2 Thermal comfort test

The MRT trend in open field and under the two prototypes is shown in Figure 4 and Figure 5 for a representative day of the first and second part of the monitoring campaign respectively, named day 1 and day 2. As already explained, during the first part of the campaign, and thus on day 1, the single membrane device is over grass and the double membrane device is over the cement pavement, while they are exchanged during the second part of the campaign, and thus on day 2. In both cases the advantage of sun shading is evident, as both shading devices largely decrease the MRT with respect to the open field unshaded situation. It can be noticed from Figure 4 and Figure 5 that the grass surface remains always cooler than the cement surface, up to about 5°C more, probably because evapotranspiration occurs more effectively. As expected then, the ground surface conditions are not fair under the two prototypes. However, it is found that MRT below the double membrane device is always lower than under the single membrane, both when the latter is over the cooler ground surface (day 1, Figure 4) and when it over the warmer ground surface (day 2, Figure 5). In other words, the double membrane device performs better whatever the kind of ground cover, as it is more clearly shown in Figure 6, where the MRT data of the single membrane device plotted against the MRT data of the double membrane device remain generally above the bisector of the chart, with comparable trends in both days. The MRT difference is equal on average to 3.1°C with a maximum of 4.6°C during day 1, while it is on average 2.5°C with a maximum of 5.4°C during day 2.

By analyzing the temperature of the membrane surface facing downwards in each prototype, it was found that they do not differ significantly and systematically, namely sometimes the single membrane surface is the coolest but often the situation is reversed (Figure 7). Indeed, thermal energy radiated by the membrane surface towards the ground and the person depends on the membrane temperature but also on thermal emissivity, so that the temperature alone does not define the radiative heat transfer between the membrane and the underlying person.

Membrane architecture: the seventh established building material. Designing reliable and sustainable structures for the urban environment.



Figure 4: Monitoring data in a representative day of the first part of the campaign (“day 1”)

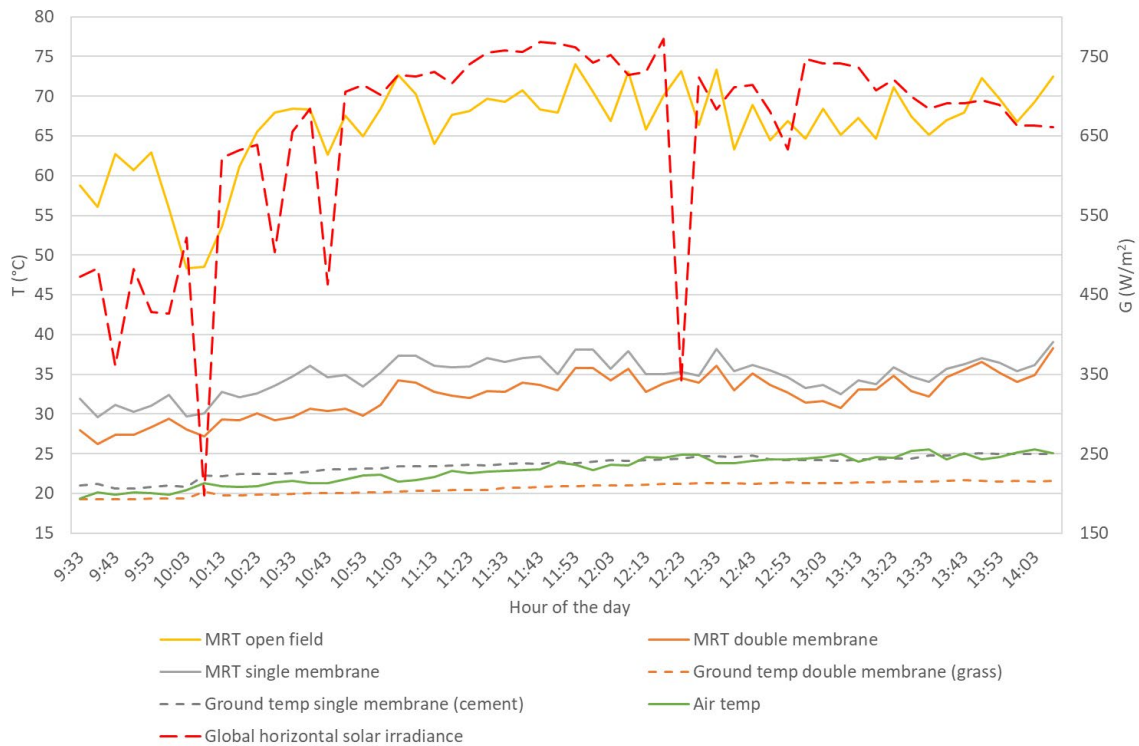


Figure 5: Monitoring data in a representative day of the second part of the campaign (“day 2”)

Membrane architecture: the seventh established building material. Designing reliable and sustainable structures for the urban environment.

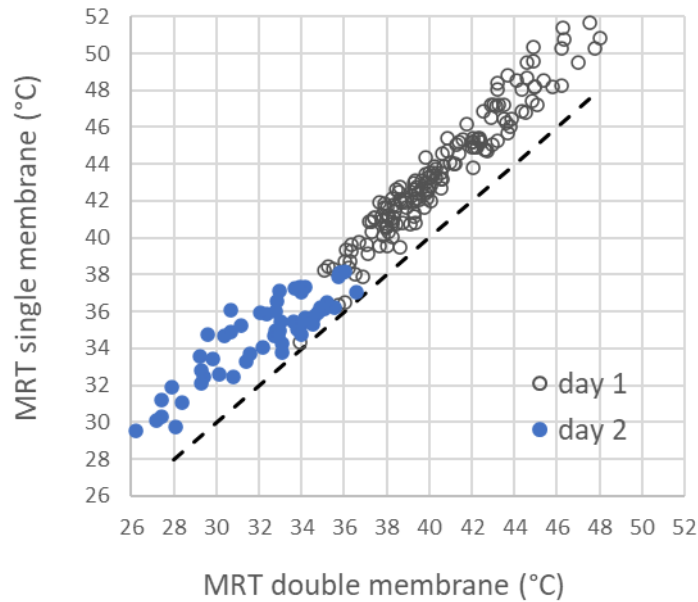


Figure 6: Mean radiant temperature below the single membrane device versus the same under the double membrane device (days 1 and 2)

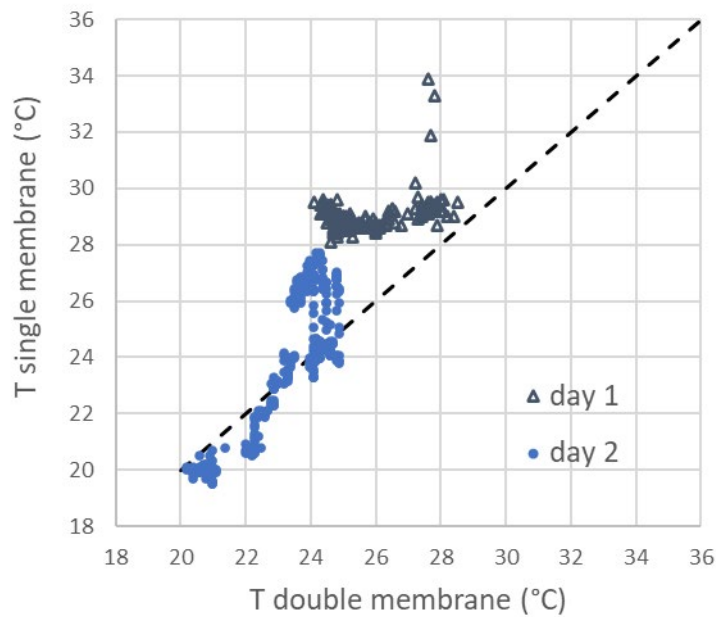


Figure 7: Surface temperature of the membrane of the single layer device versus surface temperature of the bottom membrane of the double layer device (days 1 and 2)

Membrane architecture: the seventh established building material. Designing reliable and sustainable structures for the urban environment.

Conclusions

The research designed and developed a flexible solar shading device for mitigating heat stress during summer in open urban spaces. Testing the prototypes allowed to identify some key aspects able to ease the installation and dismantling phases, such as the opportunity to equip the membrane corners with redundant connections, and the necessity to pre-couple and tension the two membrane kits before raising at the design height. Moreover, the experimental campaign allowed to verify that a double membrane configuration featuring a low emissivity surface towards the ground is able to reduce significantly the Mean Radiant Temperature with respect to a single layer configuration based on a standard white membrane. Further developments of this study will investigate to which extent the better performance of the double membrane device is due to the adoption of two layers or to the use of a low emissivity membrane. To this purpose, field tests will be performed on different shading devices configurations and membrane materials, thanks to the modularity of the designed devices. Moreover, a simulation model is being developed, allowing to analyse the energy balance of the shading devices and to generalise the experimental results.

Acknowledgements

The research was carried out in the framework of the Polisocial Award Grant 2017: “West Road Project, a device for activating networks and public spaces through the diffused neglected areas”. The Authors warmly thank Ferrari Textiles for providing the membrane materials and Canobbio Engineering Textiles srl for manufacturing the prototypes.

References

- R. and A.C.E. American Society of Heating (2001), ASHRAE Handbook Fundamentals, SI Edition.
- Göppert, K., Paech, C. (2015), High-performance materials in façade design: Structural membranes used in the building envelope. *Steel Construction*, 8(4), 237-243.
- Johansson E., Thorsson S., Emmanuel R., Krüger E. (2014), Instruments and methods in outdoor thermal comfort studies – The need for standardization. In: *Urban Climate*, vol. 10 (pp. 346–366).
- Kántor N., Chen L., Gál C. V. (2018), Human-biometeorological significance of shading in urban public spaces—Summertime measurements in Pécs, Hungary. In: *Landscape and Urban Planning*, vol. 170 (pp. 241–255).
- Knippers, J., Cremers, J., Lienhard, J., & Gabler, M. (2011), Construction manual for polymers + membranes: materials, semi-finished products, form-finding, design. Basel: Birkhäuser Verlag.
- Paolini R., Mainini A., Poli T., Vercesi P. (2014), Assessment of thermal stress in a street canyon in pedestrian area with or without canopy shading. In: *Energy Procedia*, vol. 48 (pp. 1570 – 1575).



tensinantes2023 : TensiNet Symposium 2023 at Nantes Université

Membrane architecture: the seventh established building material.
Designing reliable and sustainable structures for the urban environment.

Proceedings of the Tensinet Symposium 2023

TENSINANTES2023 | 7-9 June 2023, Nantes Université, Nantes, France

Jean-Christophe Thomas, Marijke Mollaert, Carol Monticelli, Bernd Stimpfle (Eds.)

Suntex: weaving solar energy into building skin

Dr. Pauline van Dongen^a, Ellen Britton Bsc^a, Ing. Anna Wetzel^a, , ir. Ahmed Mohamed Ahmed*, ir. Stefanie Ramos*, Dr. Mariana Popescu^b, ir. Rogier Houtman *

^a Studio Pauline van Dongen, Westervooredijk 73HE, 6827 AV Arnhem, Netherlands,
pauline@paulinevandongen.nl

^b TU Delft - Civil Engineering & Geosciences Department 3MD, Room 6.52, Stevinweg 1 - 2628 CN Delft,
Netherlands, M.A.Popescu@tudelft.nl

*Tentech BV, Rotsoord 9A,NL3523CL Utrecht, Netherlands, Rogier@tentech.nl

Abstract

The key objective of this research project is to “create a new architectural textile, Suntex, by interweaving thin film solar cells and electrically conductive yarn into a structural technical textile, so it can generate energy while it is providing shade, structure or an aesthetic update to a building.”

Textile is an inherently sustainable building material because it is lightweight. Moreover, its flexibility provides great design freedom and its transparency makes it very suitable for façade cladding, maintaining views to the outside while providing solar shading. Suntex is a solar textile, currently in development, meant for textile architecture applications like textile façades. By combining three qualities, namely providing the building with energy generation, solar shading and a unique aesthetic appearance, which also promotes the acceptance of solar technology, it offers a positive climate impact.

Suntex can be considered as a new type of membrane material for Building Integrated Photovoltaics (BIPV). With this innovative, constructive fabric, enormous surfaces that are still unused can be outfitted

Solar energy, currently the cheapest source of energy, holds great opportunities for a sustainable future (Scheer, 2005). One of the characteristics of solar systems is that they are decentralised and energy production facilities are located closer to where energy is consumed, a factor that is particularly attractive given the uncertainty of the global energy market in 2022. However, solar panels on the roofs of homes and offices, especially in high-rise buildings, are not sufficient to meet energy demand (TNO, n.d; Middelhaue, 2021).

Façades have great potential, especially in low-latitude urban areas where the low sun generates greater solar potential on the vertical surface than on rooftops in the winter months (Horn et al. 2018).

The combination of thin-film solar technology with textiles is not new (Smelik et al., 2016; Kuhlmann et al., 2018; Nathanson 2021), and solutions range from highly experimental

Membrane architecture: the seventh established building material. Designing reliable and sustainable structures for the urban environment.

research in the laboratory stage to more applied approaches that are already commercially available (Satharasinghe et al., 2020). The simplest and most common approach is to attach the flexible solar panel to the surface of the textile, for example by gluing, sewing or laminating. However, these mounting methods are difficult to implement industrially and are limited for architectural applications in terms of mechanical properties, modularity and design potential. So far, this method has been used commercially in architecture by the US company Pvilion.

Suntex, an architectural textile currently under development and initiated by Studio Pauline van Dongen, takes a different approach. Thin-film solar panels and electrical circuits (composed of conductive yarn) are integral to the construction of the textile by being directly combined in the weaving process. With the aim of being both a standardised and easily customizable with energy-generating potential.

This paper presents the first results of testing and development process of this weave. Based on insights into the development process and experiment results so far, it evaluates the feasibility from a technical and design perspective.

Keywords: Textile architecture, solar textile, energy innovation, lightweight structures, BIPV

1. Research & Innovation objectives

The key objective of this research project is to “create a new architectural textile, SUNTEX, by interweaving thin film solar panels and electrically conductive yarn into a structural technical textile, so it can generate energy while it is providing shade, structure or an aesthetic update to a building.” The textile should be suitable for retrofitting onto existing buildings (for example, as a façade second skin), to increase the sustainability credentials of building stock, in addition to applications such as temporary tensile structures like tents, marquees and awnings. The textile should help progress awareness and subsequently also acceptance of renewable energy generation in our immediate living or working environment.

From a structural standpoint, textiles are required to meet strength and stiffness criteria as well as water, UV-light, and fire resistance for durable load bearing applications. Typical architecture textiles are coated fabrics such as polyvinyl chloride (PVC) coated polyester (PES) fabrics and polytetrafluoroethylene (PTFE) coated glass fabrics, where the coating provides protection against weathering agents, and the fabric weave within the coating is the load-carrying element. Uncoated fabrics are similarly used in an architectural context but to a limited extent since without a coating, achieving comparable durability becomes challenging. In terms of strength, architecture fabrics are classified into categories from type I to type V, corresponding to tensile strengths of about 3000 N/5cm to 10,000 N/5cm, respectively. The strength should be verified in both weave directions and in areas of seams using relevant standardised tensile strength tests. Type I fabric, thus, offers the minimum required tensile strength for a viable fabric. It is also necessary that the fabric does not show too much remaining strain under loading so as not to lose functionality prior to failure. In addition, architecture fabrics are required to provide a sufficient level of fire retardancy which is demonstrated by the fabric's ability to undergo combustion, the extent of smoke production, and the production of molten droplets, as indicated by the Euroclasses for fire reaction classification. A polymeric coating is considered sufficient for water and UV-light resistance; however, for uncoated fabrics, these properties should be verified.

Membrane architecture: the seventh established building material. Designing reliable and sustainable structures for the urban environment.

In light of the aforementioned criteria, the SUNTEX fabric is designed to attain a type I fabric with a strength of approximately 3000 N/5cm in both warp and weft directions. The fire behaviour objective is set to meet at least EN 13501 class B-S2, D0.

To guarantee a functional solar fabric, not only is the structural behaviour important, but also the practicality and environmental impact are crucial. These aspects were translated into the following preset objectives:

1. A lightweight material of up to 1200 g/m² with a solar panel active area to textile surface ratio of approx. 50/50;
2. A material that can be rolled up;
3. A modular system that can be put together in (differently shaped) strips into 3D curved fabrics, whereby the various electrical circuits are connected by means of interconnects;
4. An energy yield of approximately 20 Wp/m² (Peak watt at STC) of composite solar textile (given this is only 50% coverage of active OPV area); which may seem relatively little compared to traditional silicon solar panels, but the characteristics of OPV mean it can be used in this context in a way traditional silicon solar panels could not;
5. A sunlight transmission factor of 20 to 30%;
6. A fully recyclable material, whereby the solar cell structures can be separated from the textile, with a lifespan of 10 - 15 years.

2. Design Process

The design process of the textile itself is informed by the requirements outlined in Section 1, and broadly follows these steps repeatedly (forming an iterative loop):

1. Material selection (as detailed in Section 2.1).
2. Textile development Process (see Section 2.2).
 - a. Structure/Weave design (including solar panel integration method).
 - b. Sample creation.
3. Sample evaluation (Testing, as detailed in Section 2.1).
4. Analysis and review of the materials and weave design, then return to the material selection stage (not described in this paper).

2.1 Material selection

2.1.1 Photovoltaic material selection

The type of photovoltaic technology to be integrated had to be selected primarily. Organic photovoltaic film (OPV) was chosen for a number of reasons; It is a flexible, thin-film material (as can be seen in Fig. 1) produced in a low-carbon roll-to-roll manufacturing process. It is composed of organic, non-toxic materials which are abundant and can be recovered at end-of-life. Due to this composition, it is semi-transparent and can be created in different colours (see Fig. 2). Additionally, the materials and production process mean that this technology has the theoretical potential to provide electricity at a lower cost than first- and second-generation solar technologies (USA Department of Energy, 2022), and it can have an energy payback time (the time required by an application to generate as much energy as is consumed during its

Membrane architecture: the seventh established building material. Designing reliable and sustainable structures for the urban environment.

production) around 10 times shorter than that of other solar technologies (ASCA®, EPBT 2021).

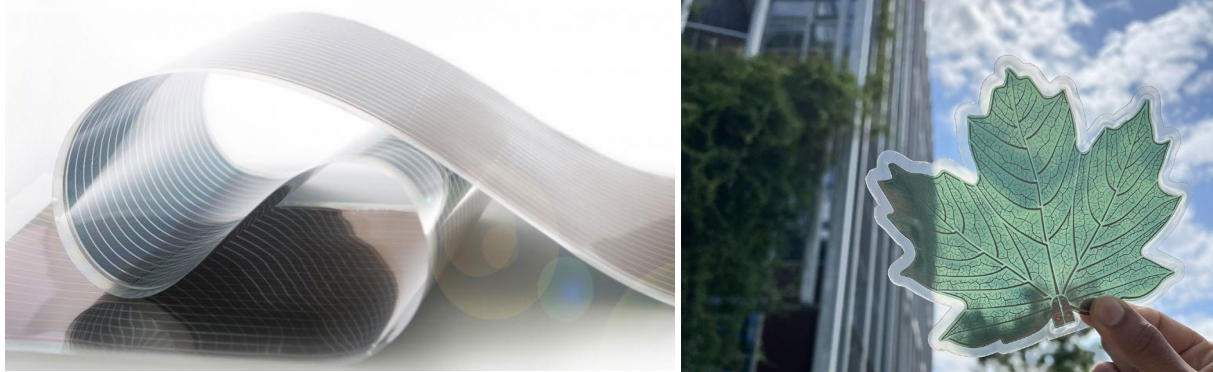


Figure 1. ASCA Organic Photovoltaic Film, flexibility apparent. (Image courtesy of ASCA®)

Figure 2. ASCA Organic Photovoltaic Film; transparency, colour and freeform possibilities apparent. (Image courtesy of ASCA®)

2.1.2 Yarn Selection

The continuous challenge with Suntext is the requirement to combine several “unusual” materials in one weaving process to make up the functional module. Alongside the OPV films (which mechanically, act like PET film), materials like a conductive track (that connects the solar panels), transparent monofilament (to secure the solar film) and high-tenacity yarns (that give the required tensile strength) are inevitable to use when making Suntext. All of the materials have rather different properties in terms of flexibility, elasticity or breaking-load which all need to be considered before, during and after the textile has been woven. During the hands-on research materials were assessed on how well they harmonise and complement each other so that their combined properties add up in the weave to make Suntext an energy-harvesting architecture type 1 fabric.

The important factors for the selection of materials and structure of the fabric include:

- A high-tenacity main yarn, used in warp and weft, that is readily available and has a textile look and touch
- A high-tenacity main yarn, used in warp and weft, that when woven has a tensile strength of 3000N/5cm (criteria type 1 architectural fabric)
- A transparent warp yarn (“float yarn”) in combination with a specific weave pattern to hold the OPV films in place without putting strain or load on them or covering them entirely
- A conductive yarn, used in warp and weft, that enables a functioning circuit which connects the OPV films with each other and enables a connection to transfer the energy to an outlet
- All materials complying with fire-retardancy, durability and weather resistance standards for textile architecture

Based on these factors, examples of chosen textiles and their mechanical properties can be seen in Table 1.

Membrane architecture: the seventh established building material. Designing reliable and sustainable structures for the urban environment.

Table 1. An example selection of yarns to suit the set criteria, and their mechanical properties.

Component type & function	Example	Diameter [mm]	Linear Density [dTex]	Breaking Force [N]	Breaking Tenacity [cN/dTex]
MAIN YARN	MSP rPET	n/a (flat yarn)	1100	84.3	7.54
FLOAT YARN	Filva Monofilament	0.40	1600	27.45	1.72
CONDUCTIVE YARN	Karl Grimm High Flex 3981	0.42	2325	27.468	1.181

2.2 Textile development process

The main focus of the textile development is the weave structure strategically designed around the integration of OPV films. This makes it similar to Saxion University's Texenergie/Texenergy research project (Hurenkamp, 2020), where OPV films were woven into a textile to make indoor window blinds (among other things). Because these use cases are very different, the material choices for Suntext and the weave structure are also different.

The main goal for Suntext is that the high-strength yarns described in section 2.1.2 take on most of the tensile load, and that the "floating" structures around and on top of the OPV hold the film strips in place without overloading or shading these strips. The purpose of this is to avoid electrical efficiency losses of the OPV. Therefore, an iterative process began, in which different material combinations, patterns and weave patterns were tested and evaluated with respect to Suntext's processability and functionality, first on a hand loom and later on an industrial sample loom. The woven demonstration models and samples were extensively tested to investigate their structural and tensile behaviour to verify or refute material choices, weaving patterns and set-ups.

Besides the choice of material, the loom also plays an important role. Industrial looms are usually single-purpose and cannot be adapted to switch from one material to another, especially in terms of preparing the warp beams and general set-up, which can take months. To enable a more flexible development process, most Suntext samples were initially tested on a hand loom (Louët Erica) and later replicated on an industrial sample loom (CCI Evergreen).

Membrane architecture: the seventh established building material. Designing reliable and sustainable structures for the urban environment.

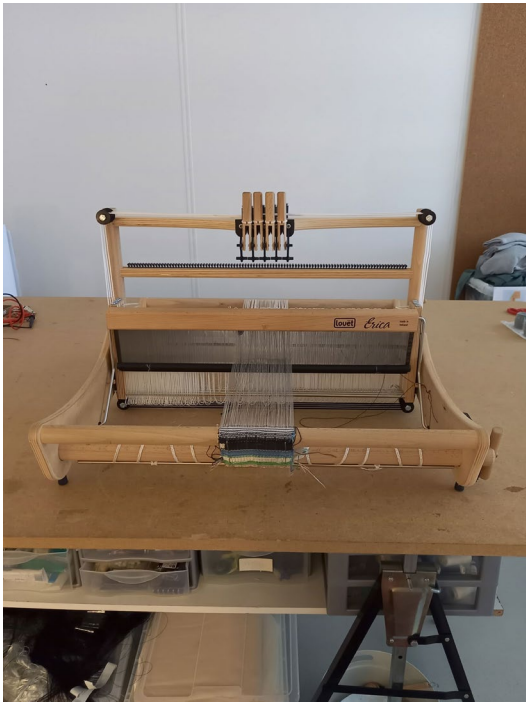


Figure 3. Louët Erica Handweaving Loom

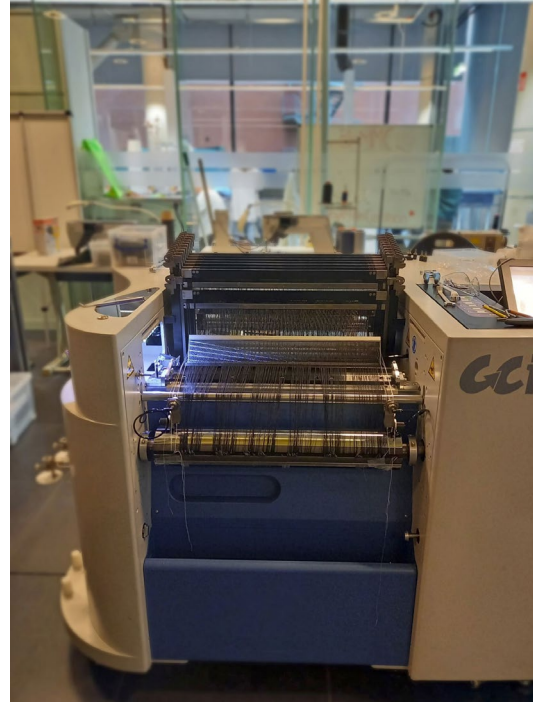


Figure 4. CCI Evergreen Sampling Loom

3. Experimental Testing & Review

3.1 Textile Evaluation Tensile Strength

The results are summarised in Table 2 and can be seen graphed in Figure 8. The data showed substantial failure loads, averaging 2781.4N for the regular specimens and 2545.2N for the specimens with ‘solar film’ (SF) integrated in ‘float’ structures (Figure5). This strength reduction of only 8.49% in the more irregular ‘solar film’ (SF) specimens, verifies the weaving strategy of implementing single-sided floats (with plain/twill backing) to integrate the solar films.



Figure 5. Sutex V2 Specimens after testing to failure. Regular specimens labelled “Twisted rPET W1-3” are referred to as “Sutex V2 W1-3” in this paper, and Solar Film specimens labelled “Twisted rPET SC W1-3” are referred to as “Sutex V2 SF W1-3” in this paper.

Membrane architecture: the seventh established building material. Designing reliable and sustainable structures for the urban environment.

Table 2. Suntex V2 specimen information and tensile test results (as logged by Instron 1122 tensile testing machine used)

General Information		Weave specifications			Test results	
Category	Specimen name	Pattern	Warp density (yarns/cm)	Weft density (yarns/cm)	Elongation (%)	Failure load (N/5cm)
Regular Specimens	Suntex W1	V2 Plain weave	10	11	13.3	2646.23
	Suntex W2		10	11	15.0	2959.46
	Suntex W3		10	11	12.7	2738.56
Solar Film (SF) specimens	Suntex SF W1	V2 Plain/Twill backing layer at SF 'floats'	10	16.6	9.7	263.44
	Suntex SF W3		10	16.6	10.6	2547.77
	Suntex SF W3		10	16.6	10.21	2542.64

The digital image correlation (DIC) analysis (Figures 7 and 8) data correlates with the data logged by the Instron 1122 tensile testing machine used (summarised in Table 2). The DIC analysis of the solar film specimens is particularly interesting (Figure 8); lower strain can be observed at the solar film sections compared to the adjacent woven sections, which implies that the solar cells are not under any stresses that could cause a loss of function before fabric failure. This indicates that the weave design strategy to integrate the solar film in a way that it would not be subject to large tensile loads is successful, and supports the viability of this approach and the textile itself.

The results are, however, limited to the warp direction only, and to verify the fabric strength, the weft direction should also be tested. Furthermore, due to the samples being handwoven, non-uniform stressing of the specimens is most likely to happen which might cause failure at a lesser load than potentially possible; therefore, upcoming tests should be performed on fabrics woven on a power loom. Nonetheless, these results show the rPET Suntex V2 is a promising configuration to achieve the desired strength, and inform the next iteration, Suntex V3.

Membrane architecture: the seventh established building material. Designing reliable and sustainable structures for the urban environment.

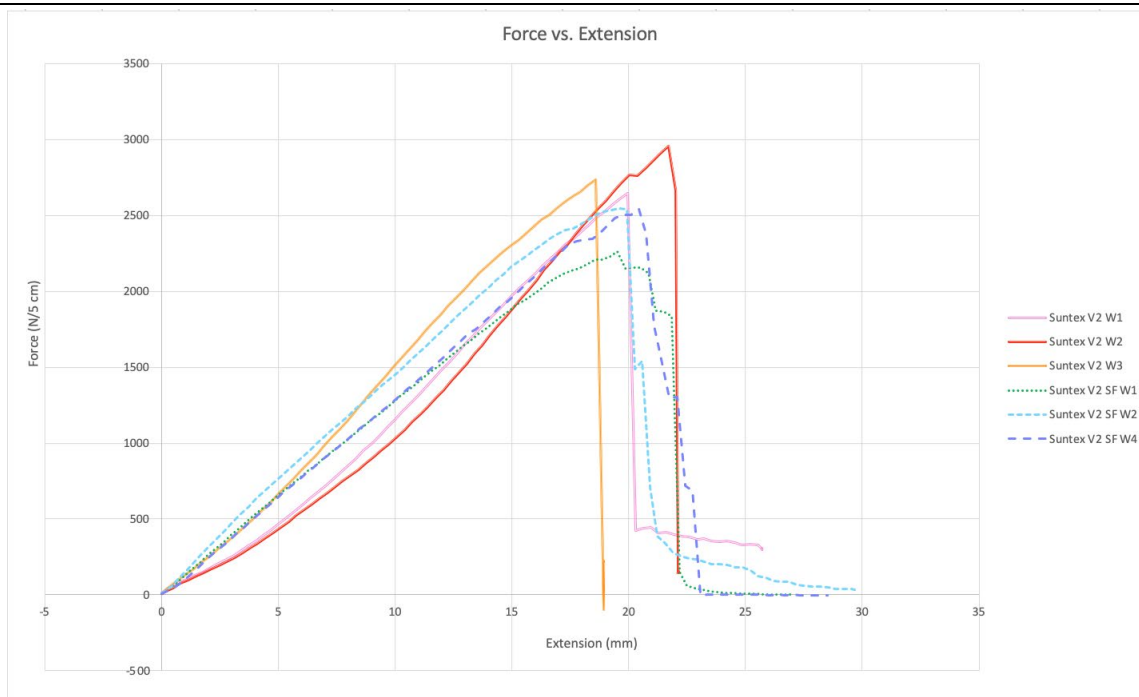


Figure 6. Suntext V2 specimens' force-extension behaviour.

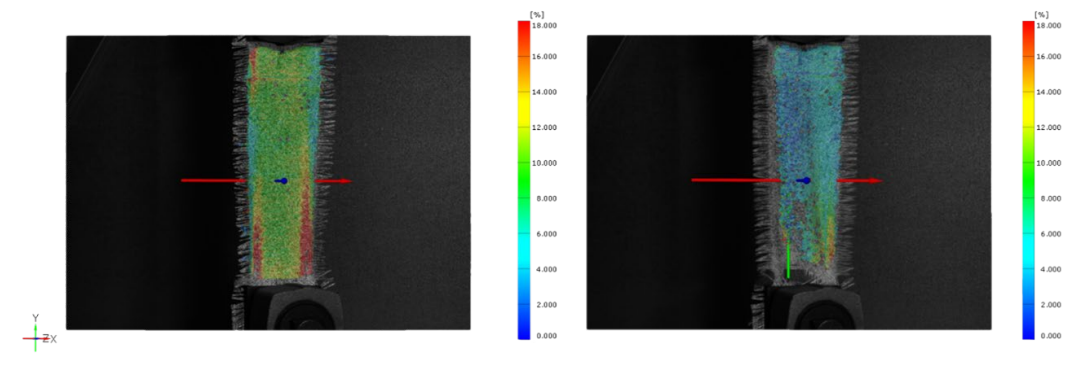


Figure 7. Specimen 'Suntext W3' strain field along the longitudinal direction at failure (left) & directly after failure (right).

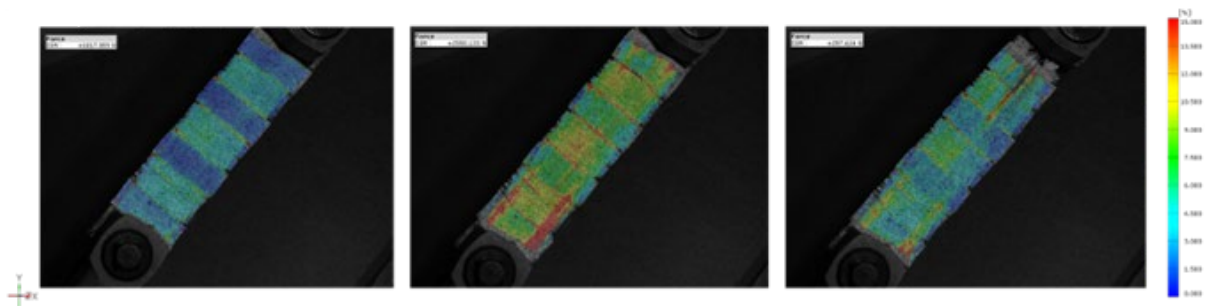


Figure 8. Specimen 'Suntext V2 SF W2' strain field at approximately 1 kN load (left), at maximum load (middle), and after failure (right).

Suntext V3 samples have been woven on a power loom (CCI Evergreen), using the same rPET yarn as Suntext V2 for the 'main yarn' but with some of these warp yarns replaced with monofilament (which is used as the float yarn to hold the solar film in place). Weaving it on

Membrane architecture: the seventh established building material. Designing reliable and sustainable structures for the urban environment.

the power loom facilitated a denser weave, which should result in a stronger overall textile. However, the weaker monofilament replacing some of the rPET warp yarns may counteract this effect. Conclusive mechanical testing has not yet been performed, to investigate these theories and the mechanical strength of this latest iteration.

3.2 Textile Evaluation Shear Behaviour

It is well known that the determination of shear characteristics of advanced composites is one of the most difficult types of mechanical static tests. One of the principal difficulties of the development of a shear test method for these materials is to induce a stress state of pure shear in a gauge section of the specimen which has to be only subjected to a shear stress of a constant magnitude (Ramos, S., 2023). Out of all available tests illustrated in section 3.1, in order to evaluate shear stresses and angles, three picture frame tests were executed. The choice of the number of tested specimens is limited due to the sample availability.

Usually, on a picture frame test, all the corners of each frame are pinned. When the fabric is loaded into the frame, it is clamped on all edges to prevent slippage. The corners of a sample are cut out to allow the tows to rotate without wrinkling the fabric. Thus, it appears that each sample has four flanges. With the fabric properly aligned and tightly clamped in the frame, the distance between two opposing corners is increased with the aid of the tensile testing machine, and therefore the tows begin to reorient themselves as they shear.

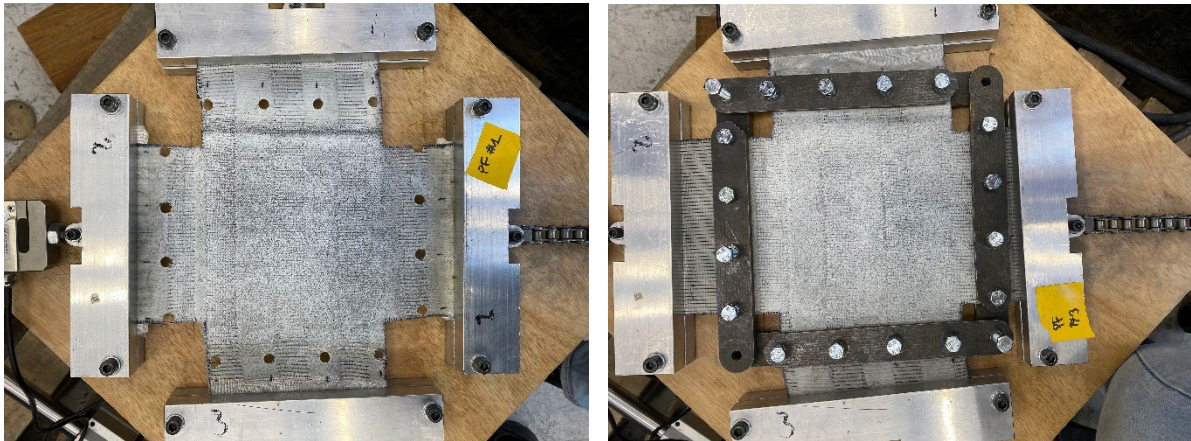


Figure 9: PF set up. Trial specimen in pretension position in biax

Figure 10: PF set up. Trial specimen with picture frame installed

As seen in the literature review the angle can be calculated from a picture frame test based on the measured tensile machine displacement. It is often assumed that the shear strains are uniform in the gauge area such that a global shear force and shear strain can be obtained from kinematic and static analysis of the frame. It is, however, common practice to use either Digital Image Correlation (DIC) measurements or to manually check the fibre angles from pictures of the test as a validation (Ramos, S., 2023). In this case, a 3D DIC was used, therefore the strain field was measured by two cameras positioned under different angles with respect to the measured object.

As mentioned, the testing procedure has been done following EN- 17117, which is the standard for coated fabrics as shear standards for uncoated fabrics do not exist yet.

Membrane architecture: the seventh established building material. Designing reliable and sustainable structures for the urban environment.

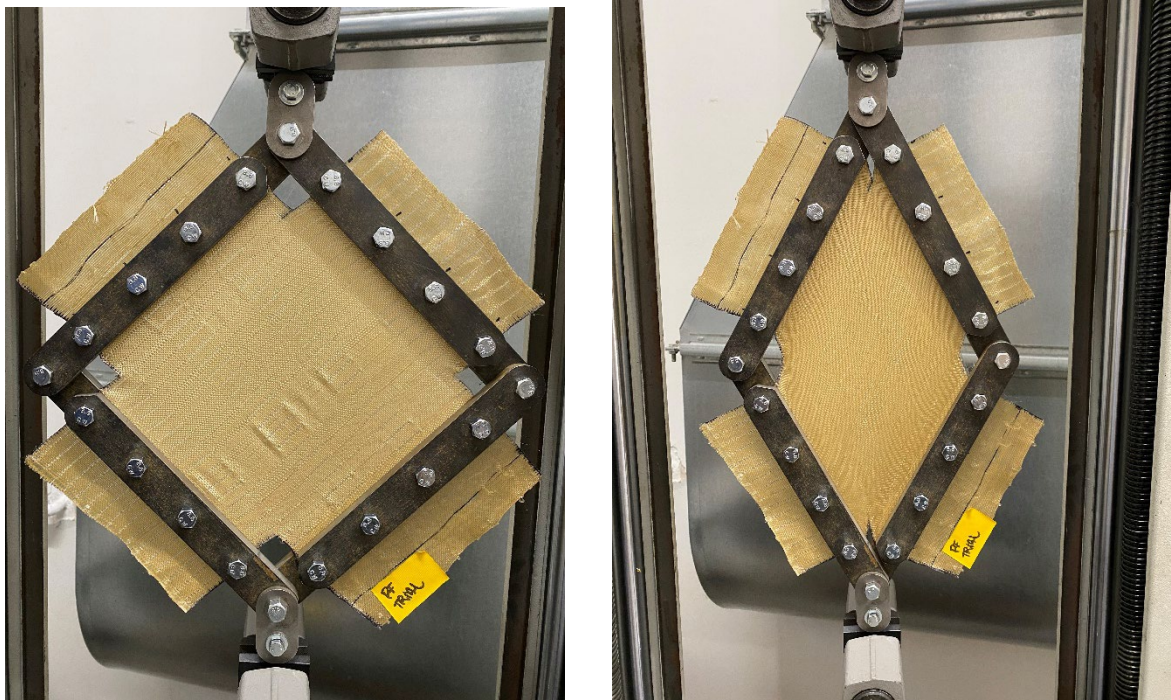


Figure 11: PF set up. Trial specimen initial position in mono-ax
Figure 12: PF set up. Trial specimen after deformation



Generated with GOM Software 2022

PF01 final stage

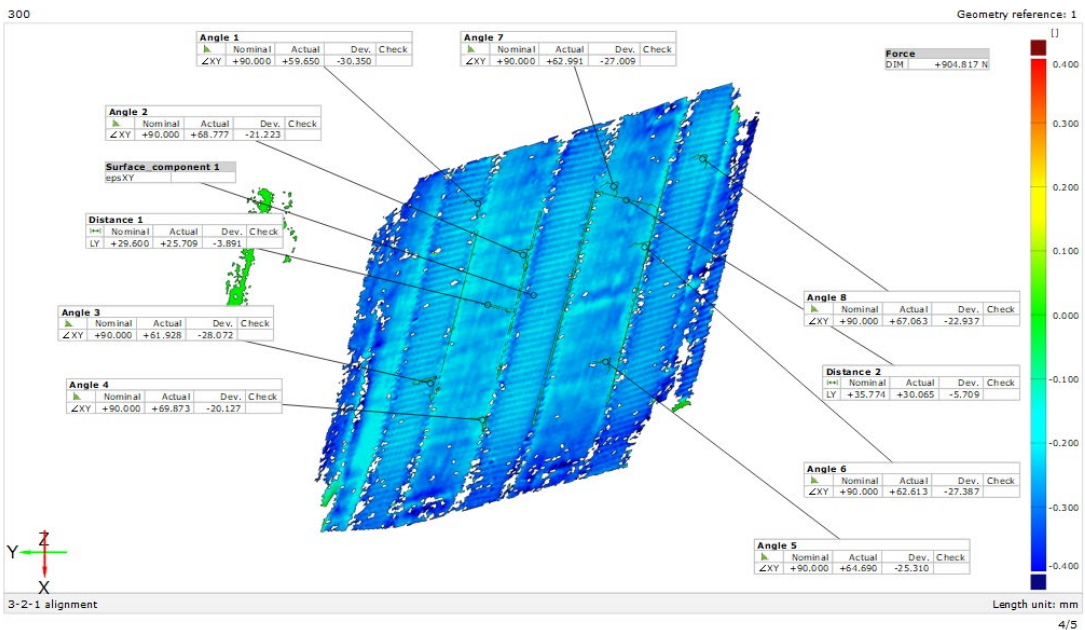


Figure 13: PF set up. DIC correlation of Trial specimen after deformation

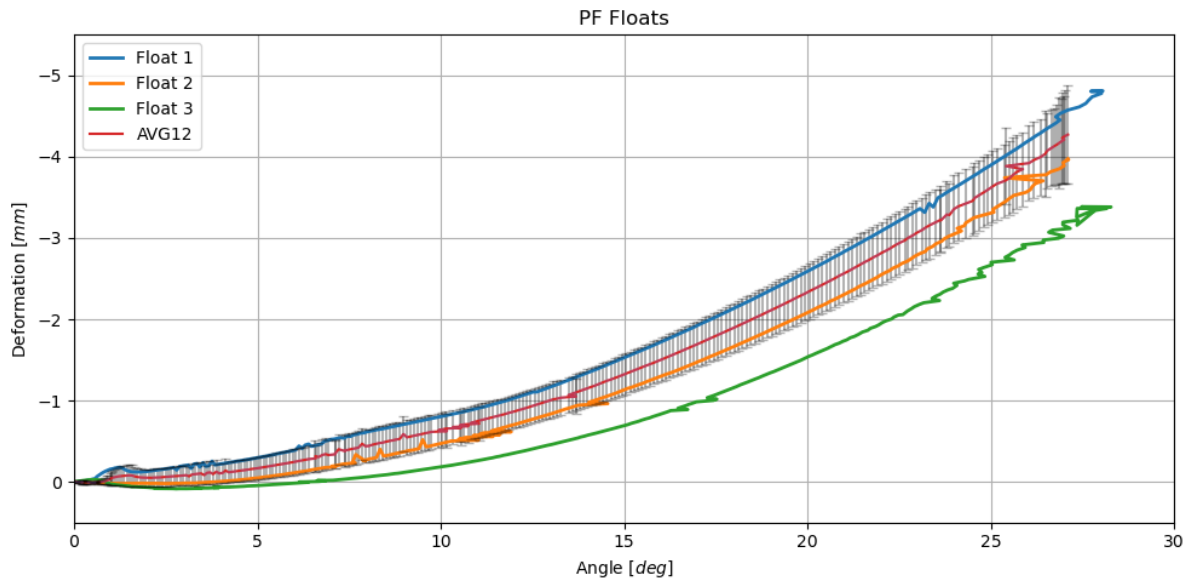


Figure 14: Deformation-angle graph

The picture frame was mounted in the monoaxial tensile machine Instron 1122 and DIC (Digital Image Correlation) system was used to measure the elongation and strain field along the specimens. The chosen testing rate was 0.5 mm/s (displacement-controlled test). Tests were performed on 11/08/2022 at TU Delft Stevin Lab II.

The deformation-angle graph in Figure 14 represents the shortening of the weave floats. The initial average width of all floats is 30 mm, as the width of OPV strips is 25mm the maximum feasible shortening width is 5mm. The average float deformation of specimens PF01 and PF02 (AVG12) is considered representative of all specimens. The limit of 5mm has not been reached during testing, meaning up to 27 degrees of shearing angle the OPV strips will not undergo any compressive stress

4. Conclusion

This paper outlined the textile design and development process for Suntex, followed by the preliminary results obtained through experimental testing of samples. These test results validated the feasibility of the textile.

If Suntex can be developed into an industrial off-the shelf and customizable architectural textile, it can support large-scale use. However, for this to happen more research is needed to solve the challenges described. Therefore the iterative loops of the development process outlined in this paper will be continued until May 2023. To evaluate an industrial production of Suntex further, a dialogue with industry partners will be started with the clear aim to evolve Suntex into a industrially manufacturable type I architectural textile.

Acknowledgements

With thanks to; a MIT R&D subsidy provided by the Dutch Ministry of Economic Affairs and Climate, which funds this two-year project; Saxion University of Applied Sciences, Holst Centre, Solliance and CT-Stevin II Lab TU Delft for collaboration.

Membrane architecture: the seventh established building material. Designing reliable and sustainable structures for the urban environment.

References

- Smelik et al (2016) *International Journal of Fashion Studies*, Volume 3, Issue 2, Oct 2016, p. 287 – 303
- ASCA® (2021). Material Datasheet. Retrieved from https://www.asca.com/wp-content/uploads/2021/07/Generic_data_sheet_EN.pdf
- ASCA®, Efficiency Increase (2021). Asca increases performance of Organic Solar cells by integrating new semiconductors Retrieved from <https://en.asca.com/latest-news/asca-increases-performance-of-organic-solar-cells-by-integrating-new-semiconductors>
- ASCA®, EPBT (2021). Focus on the Energy Payback Time of the Asca Film. Retrieved from <https://en.asca.com/latest-news/focus-on/focus-of-the-energy-payback-time-of-the-asca-film>
- Dongen, P. (2019). *A Designer's Material-Aesthetics Reflections on Fashion and Technology*. Doctoral Thesis Eindhoven University of Technology. ArtEZ Press
- Dongen, P., Britton, E., Wetzell, A., Houtman, R., Ahmed, A., Ramos, S. (2023). *Suntex: Weaving Solar Energy Into Building Skin*, Powerskin volume 10, number 2, *Journal of facade design & engineering* 2022, TU Delft, Delft
- Fan, Z., De Bastiani, M., Garbugli, M., Monticelli, C., Zanelli, A., & Caironi, M. (2013). Experimental investigation of the mechanical robustness of a commercial module and membrane-printed functional layers for flexible organic solar cells. Retrieved from <https://www.sciencedirect.com/science/article/abs/pii/S1359836816308216>
- Horn, S., Bagda, E., Brandau, K., & Weller, B. (2018). Einfluss der Bauwerkintegrierten Photovoltaik in Fassaden bei der energetischen Bilanzierung von Gebäuden (Teil 1). *Bauphysik*. [Influence of building-integrated photovoltaics in facades on the energy balance of buildings (Part 1). *building physics*] 40, 68–73. doi:10.1002/bapi.201810007. Retrieved from <https://onlinelibrary.wiley.com/doi/abs/10.1002/bapi.201810007>
- Hurenkamp, A. (2020). *TexEnergie: solar cells and textiles as a match made in heaven*. Retrieved from: <https://www.saxion.nl/>
- Kuhlmann, J.C., de Moor, H.H.C., Driesser, M.H.B., Bottenberg, E, Spee, C.I.M.A. & Brinks, G.J. (2018). Development of a Universal Solar Energy Harvesting System Suited for Textile Integration Including Flexible Energy Storage. *Journal of Fashion Technology & Textile Engineering* S4:012. doi: 10.4172/2329-9568.S4-012

Membrane architecture: the seventh established building material. Designing reliable and sustainable structures for the urban environment.

Middelhauve, L., Girardin, L., Baldi, F. & Maréchal, F. (2021). Potential of Photovoltaic Panels on Building Envelopes for Decentralized District Energy Systems. *Frontiers in Energy Research*, 15 October 2021. <https://doi.org/10.3389/fenrg.2021.689781>

Mohamed Ahmed, A. (2022). *Structural Solar Textile*, TU DELFT

Nathanson, A. (2021). *A History of Solar Power Art and Design. Part III 5. Textiles and Wearables*. Routledge

Ramos, S. (2023). *Shear Characterisation of a novel woven solar cell integrated textile for tensile structures application*, TU DELFT

Satharasinghe, A.S., Hughes-Riley, T., & Dias, T. (2020) A Review of Solar Energy Harvesting Electronic Textiles. *Sensors* 20(20):5938 DOI:10.3390/s20205938 Retrieved from https://www.researchgate.net/publication/328043412_Aesthetic_impact_of_solar_energy_systems

Scheer, H. (2005). *A Solar Manifesto*. Routledge.

Smelik, A., Toussaint, L., & Van Dongen, P. (2016). Solar fashion: An embodied approach to wearable technology. *International Journal of Fashion Studies*, Vol 3, Nr 2, 1 October 2016

USA Department of Energy (2022). *Organic Photovoltaics Research*. Retrieved from: <https://www.energy.gov/eere/solar/>



tensinantes2023 : TensiNet Symposium 2023 at Nantes Université

Membrane architecture: the seventh established building material.
Designing reliable and sustainable structures for the urban environment.

Proceedings of the Tensinet Symposium 2023

TENSINANTES2023 | 7-9 June 2023, Nantes Université, Nantes, France

Jean-Christophe Thomas, Marijke Mollaert, Carol Monticelli, Bernd Stimpfle (Eds.)

Integration of the fog water harvesting system in lightweight structure design for emergency camps

Maria Giovanna DI BITONTO*, Nathaly Michelle RODRIGUEZ TORRES*, Nicolò Elio GIORGETTI*, Alara KUTLU*, Alessandra ZANELLI*

*ABC Department, Textile Architecture Network

Politecnico di Milano

mariagiovanna.dibitonto@polimi.it

Abstract

Growing concerns over water scarcity worldwide have led to research about technologies that have the potential to obtain water from non-traditional sources, implementing water collectors as alternative infrastructure to supply water in territories where the fog phenomenon is recurring (Schemenauer and Cereceda, 1994). The Large Fog Collector, a device commonly used for fog harvesting, is a textile-tensile structure composed of a mesh, two poles, and cables. The paper aims to integrate this technology in the lightweight structure design, for its application in emergency camps. Taking advantage of the vertical development of the device, this tensile structure shall be integrated into shelter envelopes, in order to promote resilient installations and make the structured water self-sufficient. The paper explores the design criteria for the development of a novel concept of a Smart Water Collecting Envelope (SWCE) integrated into an emergency shelter. Firstly, the SWCE is thought of as a possible add-on of two emergency shelters: (a) the “Multipurpose Shelter” (MP), designed by PoliMi with the collaboration of IFRC and produced by Ferrino; and (b) the “Cocoon Textile Unit”, designed by PoliMi with the collaboration of Sioen. Both shelters are the results of the European project S(p)eedkits (Zanelli 2016, Viscuso et al 2019, Ferrino 2023). The new concept of SWCE can promote air and water purification, as well as a shading effect; reducing the use of cooling systems, energy demand, and the ecological footprint. Depending on the Fog Liquid Water Content (Klemm et al., 2012), the water can be used for basic human needs or in an optimal scenario also for domestic uses. Starting from the SWCE concept, the authors evaluate the opportunities and the limits of integrating similar devices to other family tents available on the market and study the applicability of the SWCE concept to a wider scale of the emergency camp.

Keywords: Fog water harvesting, water self-sufficiency, smart façade, textile architecture, resilient construction

1. Introduction

Water is essential to life and health. In emergencies it is often not available in adequate quantity or quality, thus creating a major health hazard.

To meet the need for shelter for catastrophic event refugees, emergency camps are planned. Tents are lightweight structures, composed of textiles and a supporting structure, able to be rapidly assembled and disassembled to the need. One of the main issues in planning an emergency camp is hygiene matter. In fact, camps are usually located in areas that are not prepared with an adequate water supply and sanitation systems. Water is usually obtained by the nearest water resource, which can be surface water or underground basin, extracted thanks to small wells. Often these resources are contaminated and far from the camp settlement, therefore water should be transported by truck and stored in water towers.

However, many emergency events worldwide are located in areas affected by fog. Since ancient times fog has been documented to be an efficient source of water for communities who lived in arid areas (Fessehaye et al. 2017). The device able to extract water from air is the Fog Collector, a lightweight textile-based structure.

By meeting the needs of the people hosted in the shelters and taking advantage of the technical composition of the tents, the camps can be provided with an alternative source of water which is fog. Achieving in this way one of the objectives of The Water, Sanitation, and Hygiene (WASH), by guaranteeing that people have access to safe and sufficient water.

2. Ongoing research on how to exploit water through textiles

Like plants, fog collectors are designed so that when the cloud mass passes through them, these drops are trapped in the mesh they have (Cereceda, 2000). They have evolved significantly in terms of construction, design, and material.

The collection of fog water dates back several centuries, such as in the Canary Islands (Spain), where the collection has been carried out for approximately 2,000 years. In its beginnings, trees such as the olive tree were used as fog catchers; perhaps, they were the first source of water collection (Román, 1999). However, fog harvesting is mostly documented since the 16th century, when it was applied in the Basin of Mexico and the Atacama Desert. Chile has been considered the pioneer country in this technology, where the first research and models of mist collectors were born. This technique is beginning to grow in developing countries. Currently, they are used in different Latin American countries (Chile, Mexico, Peru, Ecuador, Colombia, Guatemala, Jamaica, and the Dominican Republic), Spain, South Africa, Namibia, Oman, Croatia, Yemen, and the Cape Verde Islands in Africa.

2.1. Fog phenomenon

Fog is a meteorological phenomenon, that consists of water droplets suspended in the air. From a physical point of view, when a saturated mass of air, reaches its dew point, fog is generated. There are, however, different mechanisms and conditions for achieving this state, for which it is necessary to distinguish fog depending on the formation of its process: radiation fog, formed by radiative heat loss; advection fog, the result of the mixing of two parcels of saturated air initially at two different temperatures; orographic fog, formed for the ascending movement and resultant cooling of an air parcel (Roach, 1994).

Fog is characterized by three parameters: the size distribution of droplets, their concentration, and their content in condensed water. These parameters depend, mainly, on the formation

Membrane architecture: the seventh established building material. Designing reliable and sustainable structures for the urban environment.

process, the meteorological and geographical conditions, and the duration of the phenomenon (Schemenauer and Cereceda, 1994).

Many territories worldwide are affected by the fog phenomenon, some of them are located in arid areas, while others are in territories that will face a hydric crisis in the upcoming years. Since ancient times, in arid fog oases, the populations adapted to those extreme conditions; here some sort of fog collector has been developed (Klemm et al., 2012). Some fog harvesting projects have been mapped, in Figure 1.

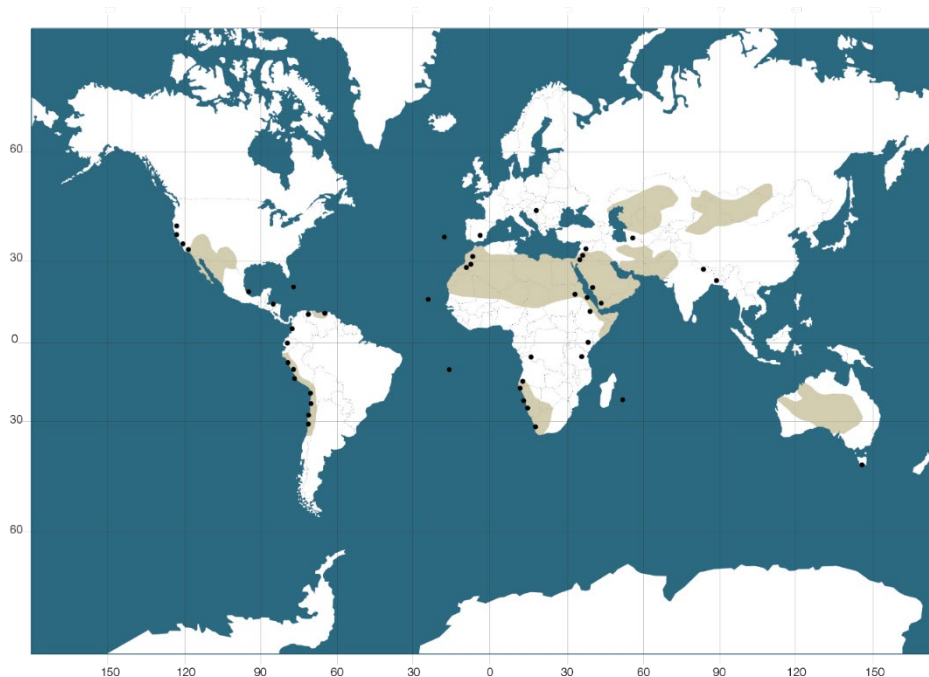


Figure 1: Map of fog harvesting projects. Elaborated by the author M.G. Di Bitonto, based on several authors

2.2. Fog collectors

Fog collectors are structures composed of two poles, a mesh that is made in different sizes and placed perpendicular to the wind direction, a gutter that receives the collected water, and a whole system of supports. The structure design is very simple and the materials implied are very humble, such as wooden poles, ropes, and Raschel mesh, which is the common mesh used in agriculture. It is a system environmentally friendly due to the amount of water that is extracted from a cloudy mass is minimal, it does not even intercept 1% of the total water that is displaced by the wind, therefore the structure could hardly alter the ecosystems (Cereceda, 2000). Moreover, it is considered “new water”, meaning that the water that is extracted from the fog does not come from another hydrological system (river, aquifer, etc.) and if it is not used, it will evaporate when the atmospheric conditions change.

2.2.1. Two-dimensional fog collectors

- Standard fog collector (SFC): Described in a 1994 paper by Schemenauer and Cereceda. It is a piece of research instrumentation made to certain standards to provide a consistent measurement of the fog water collected anywhere fog exists. It is composed of a rigid frame for a fog-collecting mesh of 1 m² and is set up such that its base is 2m above the ground and its top is 3m above the ground. It is designed for research purposes, for example, to determine the

Membrane architecture: the seventh established building material. Designing reliable and sustainable structures for the urban environment.

water collection potentiality of a location and the performance of a certain mesh. One standard fog collector of 1 m² of mesh, typically collects an average of 5 L per day throughout the year. On some days no water is produced. On other days as much as 30 L can be generated.

- Large fog collector (LFC): Has a fog-collecting area of 48 square meters. It is composed of two poles, Raschel mesh, and tension cables. The collecting panel is not included in a rigid frame, it allows the sail effect (Figure 2).
- Vertical fog collector (VFC): Designed by Aqualonis, is a two-dimensional collector with rigid frames. Its improvement concerning the LFC consists of a more rigid and stable structure, in which the collecting panels are no longer horizontal but vertical. Moreover, it also applies an innovative mesh, the 3DEA, a 3D mesh that seems to be more efficient than the common Raschel mesh.

2.2.1. Three-dimensional fog collectors

- Micro-diamond: Ideal for capturing fog carried by multidirectional winds. An example of this fog collector is the one designed in Antofagasta in 1956. The problem related to this structure is that not all the panels are perpendicular to the ground, therefore the drainage of water and its collection is not very efficient (Román, 1999).
- Cylindrical fog collectors: Ideal for capturing environmental fog without a main wind direction, as is the case with the structures built by Warka Water in Ethiopia.
- Box fog collectors, like the Nieblagua collectors, are paraparallelepiped structures, where the main face is oriented through the most common wind direction. It is composed of several mesh layers placed inside. The mesh used is the Mosquitera net. This structure can collect also the fog droplets that pass through the first mesh layer, resulting in a higher collection (Figure 3).



Figure 2: Large Fog Collector by Fog Quest



Figure 3: Nieblagua structure, Canary Islands

2.2.2. Geographical conditions

Fog harvesting is most effective at wind speeds of 4 to 10 m/s, therefore windward places should be prioritized, maintaining a particular distance from sources of humidity, like oceans, lakes, rivers, and seas. Winds that flow consistently in one direction, such as trade winds, and are also able to transport clouds are optimal for fog collection. No wind barriers must exist within a few kilometers of the site. In this way, the standard fog collector can be placed in an exposed area such that the mesh surface faces the prevailing winds that would be expected during most fog events.

Membrane architecture: the seventh established building material. Designing reliable and sustainable structures for the urban environment.

3. Emergency Events

Every year occur 400 hazardous events in the world, caused by human behavior or by natural effects. These events cause the loss of human lives and the demolition of villages and houses. Two fundamental aspects of the design in an emergency are the impossibility to forecast the disaster and the need for quick response. CRED (Centre for Research on the Epidemiology and Disaster) defines a disaster as “a situation which overwhelms local capacity, necessitating a request to national or international assistance”. Disasters occur when vulnerabilities and hazards sum up.

Natural disasters are natural phenomena caused by rapid or slow onset of events. They are not directly caused by human beings, but they are geological transformations or climatic changes, which however are very often influenced by human behavior.

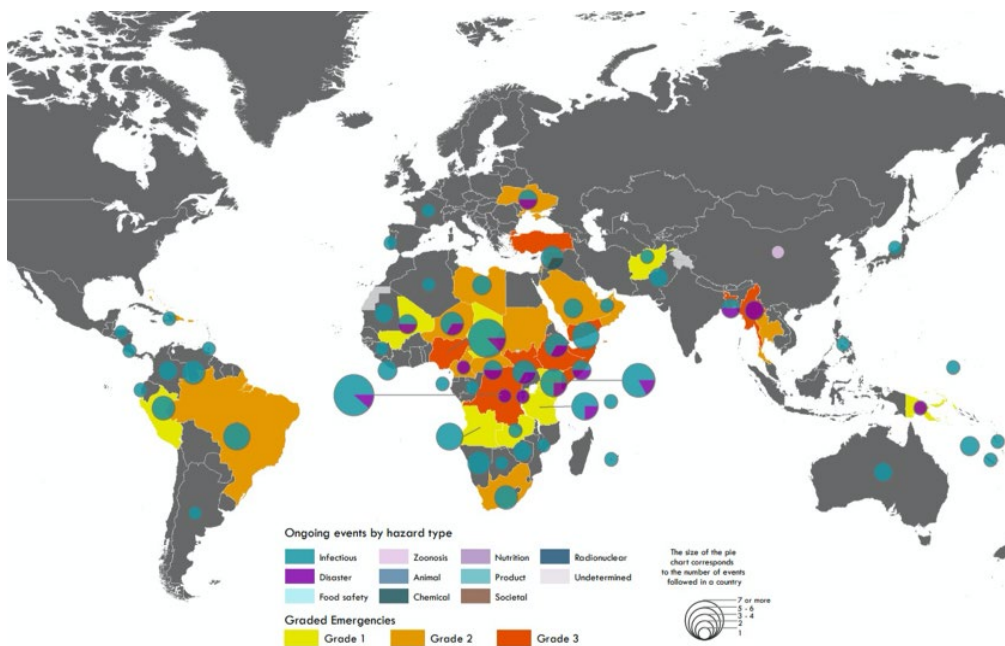


Figure 4: Map of global ongoing health emergencies. Elaborated by the author N.E. Giorgetti, based on the source: WHO (World Health Organization) database

Generally, environmental impacts, most often caused by human action, facilitate the occurrence of a natural disaster. Natural disasters can be divided into three specific groups:

1. Hydro-meteorological: floods, storms, droughts, extreme temperatures, landslides, and avalanches.
2. Geophysics: earthquakes, tsunamis, volcanic eruptions.
3. Biological: epidemics, insect infestations.

To meet the need for rapid and effective assistance to natural and non-natural disasters, humanitarian associations such as UNHCR (United Nations High Commissioner for Refugees) and ICRC (International Committee of the Red Cross) have implemented a global safeguard plan. In addition to the humanitarian associations, the WHO (World Health Organization) also

Membrane architecture: the seventh established building material. Designing reliable and sustainable structures for the urban environment.

acts in the field of emergencies by cataloging and classifying countries according to their health situations and the causes of the emergencies in progress.

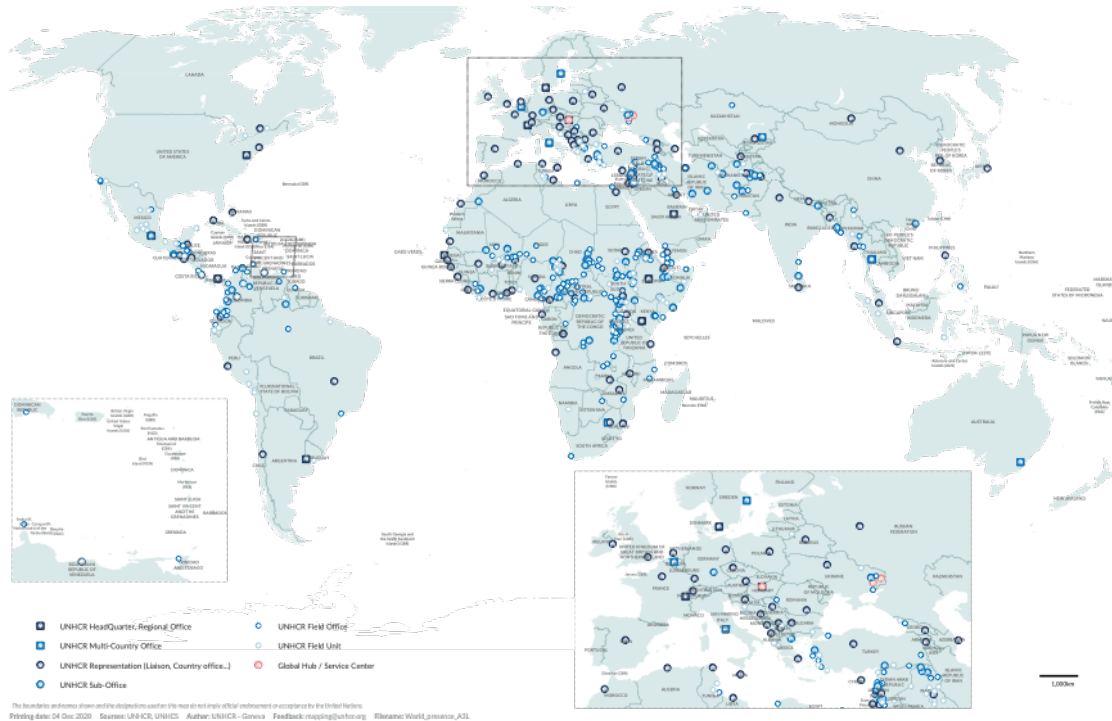


Figure 5: Map of global presence of UNHCR. Elaborated by the author N.E. Giorgetti, based on the source UNHCR (United Nations High Commissioner for Refugees) database

3.1. Emergency shelters

For responding to an emergency event, emergency camps are often required. People left without a refuge, are in need of shelter, and for this reason, emergency camps are developed. For being considered a shelter, a covered space should be safe and should protect people from outside attacks. It implies the protection from climate and external conditions, but also the privacy of people hosted. Providing shelters doesn't mean only the supply of family units, but also the access to all those facilities necessary in order to rebuild community life. Unfortunately, emergency situations are not easily predictable and happen suddenly. Furthermore, stays in emergency camps are eventually long-lasting. For these reasons, the emergency shelter should be adaptable to different crises, locations, and inhabitants. The portability of the building artifact allows the possibility to move them to different places. For being portable the architecture needs to be characterized by structural lightness. This entails system reversibility, allowing the assembling and disassembling of the solution several times. The lightness of emergency products considers also the problem of transportation in impracticable areas, influencing the final weight, dimensions, and materials choice. Logistics is an important aspect of emergency planning, in all the sectors involved.

Emergency shelters must comply with three standards:

1. Logistics: weight less than 40-60 kg, small packaging volume;
2. Physical: the tent must provide at least 3.5-4.5 m² per person, adequate height, ventilation, fire safety, protection from insects and dangerous animals, heat-cold protection;
3. Social: ease of assembly, modular assembly, privacy.

Membrane architecture: the seventh established building material. Designing reliable and sustainable structures for the urban environment.

In emergency camps, water and sanitation are critical constituents for survival immediately after and during the initial stages of a disaster (GWC, 2009). Therefore, the availability of sufficient water of the highest achievable standard in the immediate aftermath of a disaster is a crucial factor to take care of the sick, providing for human consumption, safeguarding basic hygiene, supporting search & rescue efforts, and ensuring that both the productive and commercial activities get back to normal as fast as possible.

Therefore the camps require small-scale centralized water treatment and supply systems to provide appropriate quantities of drinking water.

3.1.1. Multipurpose Tent

Textile Architecture Network (TAN) of Politecnico di Milano together with Ferrino SpA, which is the commercial partner that was responsible for the manufacturing of the T2 - Multipurpose Tent, carried out a partnership both for the design optimization of the tent and its production (Viscuso et al., 2019). The final product Multipurpose tent can be used for many different functions and purposes such as storage, hospital, dispensary, school, and office.



Figure 6: Mounted multipurpose tent



Figure 7: Possible shelter connection and different inner layouts

The complete design procedure of the shelter was carried out following various requirements such as MSF, IRC, and IFRC Standards which are largely applied in the emergency field; but primarily with paying close attention to requirements given as Target Product Profiles (TPPs) for the shelters and others NFIs (Non-food items) by UNICEF. The ground area of the tent is made of polyester-coated PVC fabric and covers a total of 48m². Instead, for the rest of the tent fabric poly-cotton was used. The structural frame is composed of aluminium poles with a diameter of 35 mm and a thickness of 3mm joined together with steel cross pieces (Viscuso et al., 2019). The stability of the system is assured by the tensioning ropes located on the edges and the anchoring system which fixes the tent firmly to the ground. To be adaptable to different climate zones in case of need, an additional shading layer made by a polyester net and other inside partitions are separately available in the tent kit. The Multipurpose shelter allows the possibility to be repeated as many times as needed for the sake of flexibility and different uses since they can be connected to each other length- and width-wise. Multipurpose tent is available in two sizes of 48 m² and 75 m² (Ferrino, 2023).

3.1.2. Cocoon Tent

The concept consisted in a complete living accommodation fixed onto whatever structural element by means of polyester belts. It allows creating a confined, winterized space to assure intimacy and protection. The amount of material needed oriented towards more lightweight insulating materials instead to foam boards, such as a non-woven polyester fabric with thickness

Membrane architecture: the seventh established building material. Designing reliable and sustainable structures for the urban environment.

of 20 mm. Sheltering literature demonstrates that structural components (timber, steel profiles modules, bamboo etc.) and plastic tarpaulins are largely recoverable in local markets and their use is directly linked to traditional construction practices. All the obtained concepts presented a high connectivity score with both structures provided into other shelter-kits due to rings that permit pretension textiles. They were also connectable to the ‘Clever Roof’ kit, which works as shade net in hot climates. The aptitude of the shelter to adapt itself to local buildings or wherever existing structural elements permit to hang the panelling by means of few accessories (e.g. ropes and small anchors) provided within the relative kits (Viscuso and Zanelli, 2016).

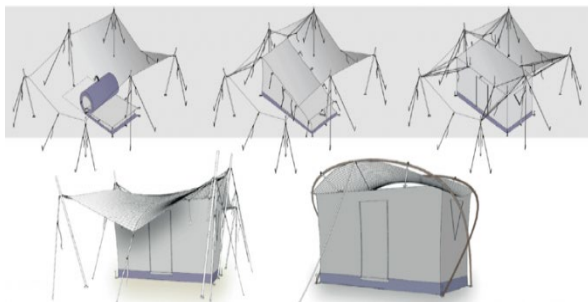


Figure 8: Mounting scheme shows the Cocoon's versatile connectivity to various structures

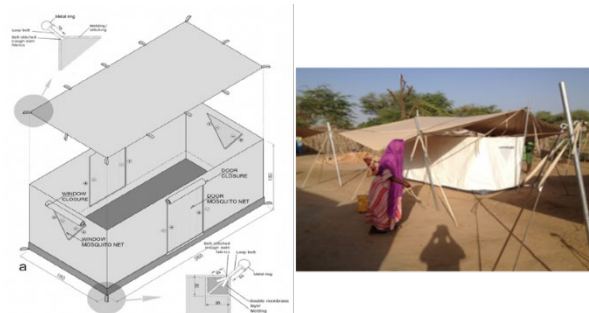


Figure 9: Cocoon tent design scheme and a mounted tent in Senegal, 2016

3.1.3. UNHCR - Lightweight Emergency Tent

This type of tent provided by UNHCR is a double fabric canvas structure that can accommodate 4 to 5 people (the standard that requires at least 3.5mq per person is not met, reaching a value of 3.3mq per person at maximum capacity). Air circulates through vents and screened windows to prevent the intrusion of insects and disease-carrying animals. The entrance is through two opposing doors on the short sides which allow an easy escape route in case of fire. To guarantee privacy, the designers have equipped each curtain with a fabric capable of dividing the internal space in order to allow women to change and/or parents to sleep separately from their children. The partition can also be used to create a semi-public space. The tent can be set up quickly and easily by two people as the structure is made up of simple arches with traditional poles. Multiple tents can be joined together by communicating with doors to create a longer tunnel.



Figure 10: Mounted lightweight emergency tent



Figure 11: Emergency camp with lightweight emergency tent

3.1.4. Rofi Rapid 608 Inflatable Tent

Unlike the previous tents, the construction system is completely different: the structure is not metallic and heavy, but light and pneumatic. The extremely rapid assembly (from 5 to 30 minutes) of the ROFI RAPID 608 tent does not require the presence of specialized and qualified

Membrane architecture: the seventh established building material. Designing reliable and sustainable structures for the urban environment.

operators as it is simply necessary to have a compressor to inflate the pneumatic arches. The company produces this type of shelter in three different lengths: 6, 8 and 10 metres; all with a width of 6 meters as standard to make connections possible (transversal or in continuity) between several units, or with different elements such as special vehicles. Internal ventilation and air exchange are allowed by the presence of windows with three protective layers (transparent layer, mosquito net and shading layer). The tent is also supplied with a kit to improve privacy: the internal spaces can be divided thanks to the application of special curtains; this improves the versatility of the tent which without structural or morphological modifications is able to be used for different functions: as a field hospital, as offices, as a single or multi-family home, etc.



Figure 12: Mounted Rofi Rapid Tent



Figure 13: Cross-wise connection of Rofi Inflatable Tents

3.1.5. Summary Comparison Table

The following Table 1 shows the comparison summary of the aforementioned tents:

Table 1: Tents comparison table

Name	Manufacturer	Dimension	Surface	Height	Weight	Structure	Structure Material	Cover Material
MULTIPORPOSE	Ferrino	6x8 or 6x12 m	48 or 72 mq	3 m	342 or 511 Kg	External framework	Aluminium	Polyester with polyurethane coating
UNHCR - LIGHTWEIGHT EMERGENCY TENT	Ferrino	5.50x3.10 m	17 mq	2.10 m	40 Kg ca.	Internal semicircular framework	Fiber glass	Outer shell: Polyester Inner tent: Cotton-Polyester fabric
COCOON	-	3.60x1.80 m	6.50 mq	1.80 m	-	External poles structure	Aluminium	Non woven polyester fabric
RAPID 608 INFLATABLE TENT	Rofi	6x6 or 8x6 or 10x6 m	36 or 48 or 60 mq	3 m	336 Kg	Pneumatic framework	Air	PVC coated fabric

4. Proposal of smart water collecting envelope for emergency response

Two proposals for adaptation to existing tents on the market were studied, based on their connecting elements and mounting systems. Figures 1, 4, and 5 can help us understand in which areas, the following proposals can be installed, by the overlapping of these maps. In this sense, the areas where there is a correlation between the frequent phenomenon of fog and the frequency of hazards and then the presence of emergency camps. It is the case in some parts of North and Southwest of Africa, Central West of South America, and the Mediterranean area. The proposals suggest the integration of the fog harvesting device on existing tents, analysed in the previous part, by adjusting its components. It is important to underline that at the moment the tents investigated rely on external hydric supplies for water use, while the proposals are meant to make them nearly water self-sufficient by integrating fog water collecting mesh in the structure.

Membrane architecture: the seventh established building material. Designing reliable and sustainable structures for the urban environment.

4.1. SWCE integrated into the collective shelter T2 Multipurpose tent

For the first type of tent described, the SWCE is developed as an extension of the outer layer of the tent; the water collecting flagship modules are fixed on top of the roof. When several multipurpose tents are clustered into field hospital, then additional inclined SWCE modules may be used during the day to shade intermediate tunnels between the tents, and at night they may collect dew or fog water. The joints for the structural frame of the Multipurpose Tent are made up of three different kinds including; 5-way, 3-way ground, and T-ground connectors. 5-way connectors are used to join the tent's aluminium poles to each other. The connection capability of these joints allows for rotation and configuration with other supplementary pieces. With this reasoning, the connectors on the sides when turned about 245 degrees, allow the opportunity to locate the poles orthogonally for the frame of a fog collector. Instead, the joint at the center top in its original position already enables for the integration of additional poles on its upper section. In case of need, the rotation of side joints can also give the possibility to directly connect two or more tents to each other from the diagonal structural poles.

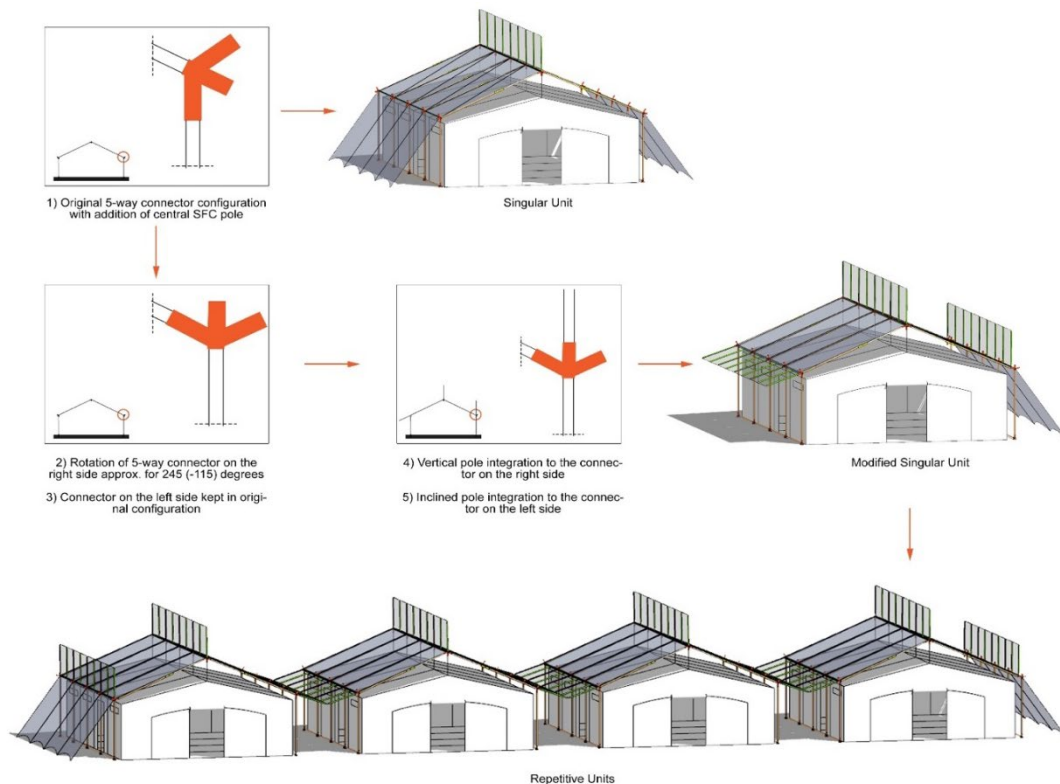


Figure 14: Process proposal scheme for the integration of fog collectors to Multipurpose Tent

4.2. SWCE integrated into the “cocoon family kit” in a wider emergency camp

For the second type of tent described, an emergency camp settlement system based on hexagonal private spaces was designed. The Cocoon tent has been made self-supporting and can be arranged as desired within the private area. The enclosure, made up of six meshes of about 9 square meters, has a dual function: during the day the six surfaces remain lowered to provide privacy for families; during the night, on the other hand, one or more meshes can be raised using a system of pulleys and can perform the function of fog collector. Each fog collector is equipped with an independent water drainage system connected to a small tank. By estimating an average of about 5 l/m²/day, and assuming the use of one mesh at a time for a

Membrane architecture: the seventh established building material. Designing reliable and sustainable structures for the urban environment.

single hexagon, each housing unit could have around 45 liters of drinking water available per day, which in emergency conditions could be sufficient for a small family unit. The settlement is designed to have the fog collector system in staggered positions to prevent the wind from undergoing large variations in terms of speed and direction. The hexagonal shape of the fence allows to maximize the collection of water as the most perpendicular surface to the wind direction can be chosen. This feature allows emergency organizations to be able to use this solution even in areas where there are no winds from constant directions over time. Furthermore, the shading system is designed with a fabric that is ideal for collecting rainwater and morning dew. In this way it is possible to increase the production of drinking water.

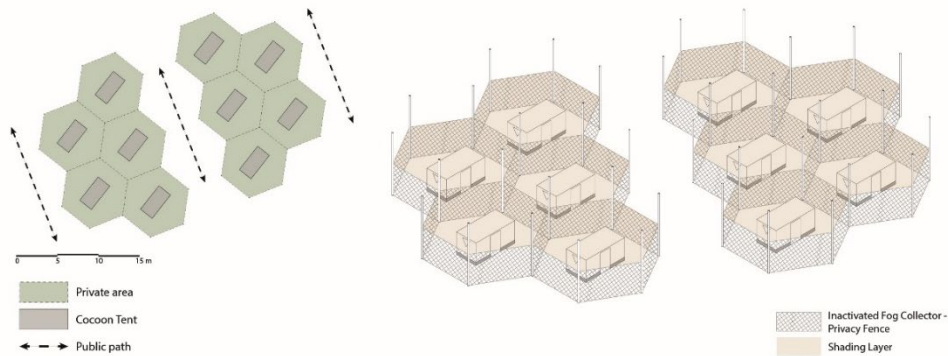


Figure 15: Emergency camp settlement and Daytime operation of the mesh system

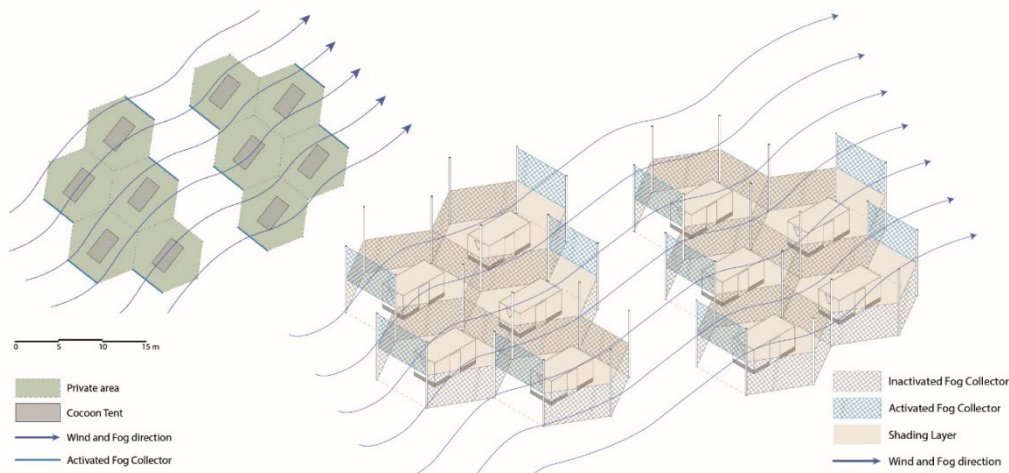


Figure 16: Night-time fog harvesting situation with only one mesh per hexagon

Membrane architecture: the seventh established building material. Designing reliable and sustainable structures for the urban environment.

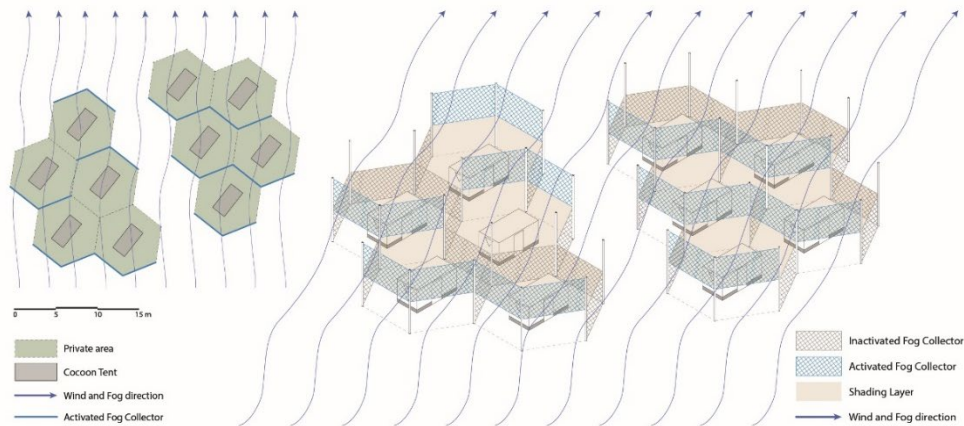


Figure 17: Night-time fog harvesting situation with two meshes per hexagon

Conclusion

The research proposes an alternative water supply system for the humanitarian sector, taking advantage of the weather conditions of the location. From the analysis of the fog harvesting system and the exploration of different shelter compositions, it emerged that the water collection system can be integrated with the design of emergency camps. Two solutions have been explored, the first one is based on the different use of the elements that form a shelter, the Multipurpose tent; while the other, is a shading system that can be integrated into a different kind of tent design, which create an enclosed semi-private place for familiar scale tent. In both cases, it is estimated a collection of about 40liter per day, which is a good result considering that the minimum required per person in emergency situations is 10-20 liters (De Buck et al., 2015). However, since the weather conditions are unpredictable, fog water probably won't fulfill the whole hydric demand of a camp, but it can be a great support system in those locations where another freshwater resource is not available. Besides, the proposed devices are very simple and easily installable, moreover, they have multiple functions, creating private gardens, providing shading, and also water.

References

- Azad, M., Ellerbrok, D., Barthlott, W., & Koch, K. (2015). Fog collecting biomimetic surfaces: Influence of microstructure and wettability. *Bioinspiration & Biomimetics*, 10, 016004. doi:10.1088/1748-3190/10/1/016004
- Cereceda, P. (2000). Los atrapanieblas, tecnología alternativa para el desarrollo rural. *Revista Medio Ambiente y Desarrollo*, 51-56. European Environment Agency. (10 de 12 de 2019).
- De Buck, E., Borra, V., De Weerd, E., Vande Veegaete, A., & Vandekerckhove, P. (2015). A systematic review of the amount of water per person per day needed to prevent morbidity and mortality in (post-) disaster settings. *PLoS One*, 10(5), e0126395.
- Ferrino Spa, Multipurpose Collective Shelter. Available at: <https://www.ferrino.it/en/shop-en/equipment/first-aid-line/tents/98080mww-high-performance-tent-48mq.html> (last access: January 2023)

Membrane architecture: the seventh established building material. Designing reliable and sustainable structures for the urban environment.

-
- Ferrino Spa, UNHCR Lightweight emergency tent. Available at: <https://www.ferrino.it/en/shop-en/equipment/first-aid-line/tents/97058wfp-light-weight-emergency-tent.html> (last access: January 2023)
- Fessehaye, M., Abdul-Wahab, S. A., Savage, M. J., Kohler, T., Gherezghiher, T., & Hurni, H. (2017). Assessment of fog-water collection on the eastern escarpment of Eritrea. *Water international*, 42(8), 1022-1036.
- GWC (2009). WASH Cluster Coordination Handbook. GWC.
- Klemm, O., Schemenauer, R. S., Lummerich, A., Cereceda, P., Marzol, V., Corell, D., ... & Fessehaye, G. M. (2012). Fog as a fresh-water resource: overview and perspectives. *Ambio*, 41(3), 221-234.
- Roach, W. T. (1994). Back to basics: Fog: Part 1-Definitions and basic physics. *WEATHER-LONDON-*, 49, 411-411.
- Rofi Protecting People, Rofi Rapid Inflatable Tent. Available at: <https://www.rofi.com/rapid-608> (last access: January 2023).
- Román, R. (1999). Obtención de agua potable por métodos no tradicionales. *Ciencia al día Internacional*, 2(2).
- Schemenauer, R. S., & Cereceda, P. (1994). A proposed standard fog collector for use in high-elevation regions. *Journal of Applied Meteorology and Climatology*, 33(11), 1313-1322.
- Schemenauer, R. S., & Joe, P. I. (1989). The collection efficiency of a massive fog collector. *Atmospheric Research*, 24(1-4), 53-69.
- Viscuso, S., Dragoljevic, M., Monticelli, C., & Zanelli, A. (2019). Finite-element analysis and design optioneering of an emergency tent structure. In *TENSINET SYMPOSIUM 2019*, 208-219.
- Viscuso, S., & Zanelli, A. (2016). Insulated membrane kit for emergency shelters: product development and evaluation of three different concepts. *Procedia Engineering*, 155, 342-351.
- Zanelli et al. (2016) Report on S(p)eedkits project. in “Politecnico di Milano: Stories of Cooperation at PoliMi (2011-2016)”, available at: chrome-extension://efaidnbmnnnibpcajpegclefindmkaj/http://www.polisocial.polimi.it/wp-content/uploads/2016/12/libro_bianco.pdf (last access: January 2023)



tensinantes2023 : TensiNet Symposium 2023 at Nantes Université

Membrane architecture: the seventh established building material.
Designing reliable and sustainable structures for the urban environment.

Proceedings of the Tensinet Symposium 2023

TENSINANTES2023 | 7-9 June 2023, Nantes Université, Nantes, France

Jean-Christophe Thomas, Marijke Mollaert, Carol Monticelli, Bernd Stimpfle (Eds.)

Challenges of measuring sound absorption of ETFE membranes in a laboratory

Yannick SLUYTS*, Monika RYCHTARIKOVA^a, Christ GLORIEUX^b

* KU Leuven, Faculty of Architecture Campus Brussels and Ghent

^aKU Leuven, Faculty of Architecture Campus Brussels and Ghent

^bKU Leuven, Department of Physics and Biophysics

yannick.sluyts@kuleuven.be

Abstract

At present, the acoustic comfort in spaces covered with ETFE membranes (and membrane structures in general) has not been extensively discussed in literature. To assess the acoustic comfort in any room, it is of primary importance to determine how much sound is absorbed by room boundaries (walls, windows, roof, floor). From this, basic room acoustic parameters such as the reverberation time, the sound pressure level distribution in the given room, and the speech intelligibility can be extracted. If conventional building materials are absorbing sound, then this is typically because they are porous or based on cavity resonance. The non-reflected sound energy is dissipated into heat. If an ETFE roof or wall membrane or cushion does not reflect sound, then this is because incoming sound is transmitted to the outdoor environment. This high sound transparency, which occurs at low frequencies, makes it challenging to determine the acoustic absorption coefficient in a classical reverberant chamber setting as described by ISO354, due to the transmitted sound being back reflected in the room by the floor under or the wall behind the membrane. Here we report on two alternative scenarios/measurement setups. First, an experiment in which an ETFE sample membrane was placed in a reverberant room, using a box that was filled with absorbing material., and second, making use of transmission chambers in which sample is placed in the opening between the two rooms. The results were found to be in line with expectations, indicating transparency and thus high effective absorption at low frequencies and high reflectivity towards high frequencies.

Keywords: ETFE, acoustics, sound absorption, ISO354, ISO10140-2, acoustic transparency

1. Introduction

ETFE membranes have a few mechanical characteristics that are relevant for the acoustic characterization. The membranes have a high flow resistance (to air), this allows them to be used for the application of inflated cushions. The membranes have low surface mass and a young's modulus of around 1GPa. The critical frequency of ETFE membranes of typical thickness of a few hundred micrometers is typically much higher than the highest audible frequency (see Equ. 1).

$$f_c = \frac{c^2}{\pi h} \sqrt{\frac{3\rho(1-\nu^2)}{E}} = 306,5 \text{ kHz} \quad (1)$$

Where: density $\rho = 1750 \text{ kg/m}^3$, young modulus $E = 1 \text{ e9 Pa}$, $\nu = 0,45$, speed of sound $c = 343 \text{ m/s}$, and thickness $h = 2,5 \text{ e-4 m}$

This implies that, for a single membrane, across the entire audible frequency range, the acoustic behaviour of a membrane is governed by the mass law (Rindel, 2017).

The acoustic characterization of thin membranes has been described in literature by different authors. Sakagami et al. (Sakagami, 1994), (Sakagami et al., 1998) proved that thin membranes with a high flow resistivity do not absorb any sound energy internally and that virtually all the transmitted sound energy is equal to the absorbed energy. For a thin and light membrane that results in a high transmission (=effective absorption) at low frequencies (near 100%) and a low sound transmission (= effective absorption) at high frequencies. Furthermore, the tension of the membrane has no impact on the sound transmission and absorption of the system. These findings have been explored and confirmed in the following references: (Hashimoto et al., 1991), (Guigou-Carter et al., 2008) and (De Geetere, 2011).

In practice, we often find that membranes are implemented in cushions. The effect of this configuration on the sound absorption coefficient has not been modelled extensively in literature. De Geetere (De Geetere, 2011) modelled and measured the sound transmission of multiple layered membrane systems. The membrane layers were parallel to each other in his experiments. Cushions consist of membranes that are clamped together at the edges, changing the boundary conditions.

Traditionally, the measurement of absorption and transmission of building materials can be performed by relying on rather low transparency. Since thin membranes are quite transparent, in traditional settings, the sound that is trespassing them remains present in the measurement room, affecting the total sound field. Traditional methods thus need adaptation to take this into account. In the next section two adapted methods are described.

2. Methods

Two common ISO procedures in building acoustics, ISO354 and ISO10140 were chosen to be adapted to obtain α_{eff} , R and IL . These are respectively the effective sound absorption coefficient, the sound reduction index R , and the insertion loss IL . The absorption coefficient is expressed in %; a higher percentage indicates a higher degree of absorption. In the case of ETFE it

Membrane architecture: the seventh established building material. Designing reliable and sustainable structures for the urban environment.

indicates a higher degree of transparency. The sound reduction index R is a measure for sound energy that is reduced while going through the sample, expressed in dB. A higher number indicates a better sound insulation. The absorption coefficient in this context is different than for conventional absorbing materials. While in conventional materials the absorption happens at the boundary or in the material, with thin membranes the absorption is provided on the condition that nothing is behind the membrane to reflect the energy back through the membrane. This is why the acoustic measurement of a transparent sample in a laboratory environment is challenging, more details are included in the following chapters. To distinguish the “absorption” of membranes we use the terminology “effective absorption”, α_{eff} .

2.1. ISO 354

The ISO354 method for measuring the absorption coefficient requires the use of a reverberation chamber with a sufficiently long reverberation time and a high diffusivity. A reverberation chamber (Figure 1) has smooth walls with a high surface mass and stiffness (painted armed concrete). The background noise in this room is reduced to sound levels < 0 dB thanks to high sound insulation of boundaries and box-in-box construction placed on springs in the case of the Laboratory of Acoustics of the Department of Physics and Astronomy of KU Leuven.



Figure 1. Picture of the reverberant room during a demonstration

The calculation of the absorption coefficient is possible by comparing the sound field with the sample present and without it. If the sample has absorbed any sound, the sound field is altered, and the reverberation time is shorter. Sound energy is physically converted into heat, usually by air friction. In the case of porous materials, the most common type of absorbers used in architecture today, the porosity and density of the fibrous materials dictate how much sound is absorbed by friction internally. Using Equ. 2, as described in ISO354, allows for the extraction of the sound absorption area of the test sample.

$$A_T = A_2 - A_1 = 55.3V \left(\frac{1}{c_2 T_2} - \frac{1}{c_1 T_1} \right) - 4V(m_2 - m_1) \quad (2)$$

where:

Membrane architecture: the seventh established building material. Designing reliable and sustainable structures for the urban environment.

V is the volume, in cubic meters, of the empty reverberation room
 c_1 is the propagation speed of sound in air at the temperature during measurement 1
 c_2 is the propagation speed of sound in air at the temperature during measurement 2
 T_1 is the reverberation time, in seconds of the empty reverberation room
 T_2 is the reverberation time, in seconds of the reverberation room with the sample present
 m_1 is the power attenuation coefficient, in reciprocal metres, calculated according to ISO9613-3 using the climatic conditions that have been present in the empty reverberation room measurement. The value of m can be calculated from the attenuation coefficient α , which is used in the ISO 9613-1.

The absorption coefficient α_s can be calculated using the following formula:

$$\alpha_{eff} = \frac{A_T}{S} \quad (3)$$

where:

A_T is the equivalent sound absorption area of the test sample

S is the surface area of the test sample in square meters

While placing some porous material on the floor in the reverberation chamber does represent the practical application quite well, placing a flat membrane on the floor in the reverberation chamber does not. Sound waves, especially at low to mid frequencies easily pass through a thin membrane and reflect off the floor. Next, pass through the membrane once again. Effectively, the floor of the reverberant chamber (the “solid backing”) and any resonances in the cavity between the membrane and the floor determine the absorption coefficient. To represent a membrane that is hung on the interface between inside and outside as in ETFE enclosed building constructions, a different approach is needed. To mimic open air behind a membrane (like in practice) a thick layer of glass wool (61 cm) was placed inside a wooden box (see Figure 3.). This box was then covered with the ETFE membrane. In this manner, sound passing through the membrane was absorbed inside the glass wool, just as it was not reflected by any object in practical applications (see Figure 2).

Membrane architecture: the seventh established building material. Designing reliable and sustainable structures for the urban environment.



Figure 2. Picture of the Mediacité shopping center roof canopy consisting of ETFE cushions. This structure has been designed by Ron Arad Architects in cooperation with Vector Foiltec GmbH. From the perspective of the room enclosed by the cushions, there is only open air behind the cushions. All the sound energy that passes through the membranes will not be reflected back inside.

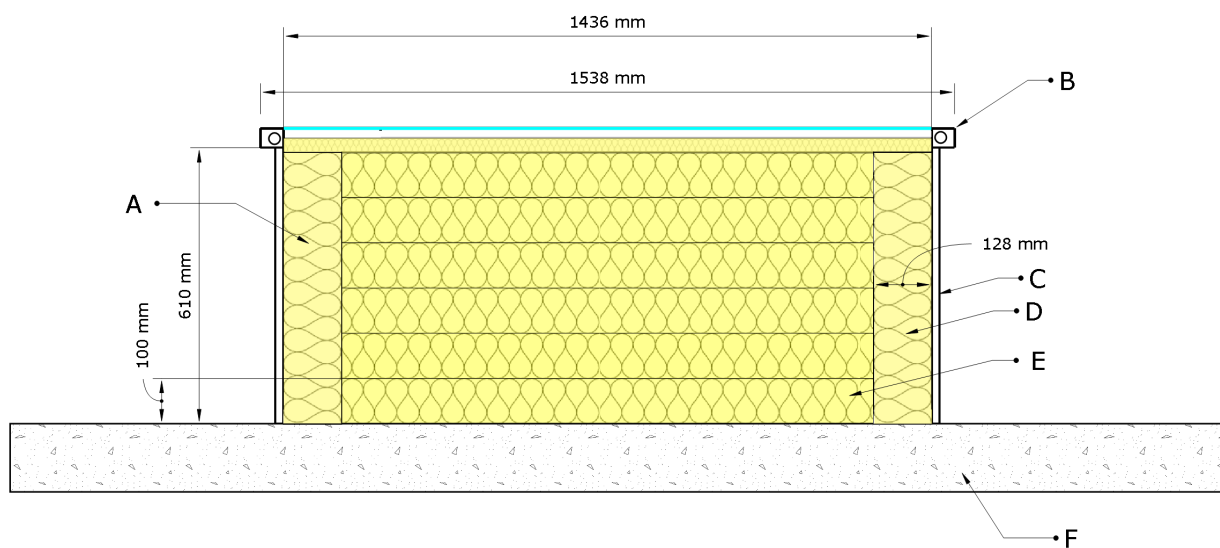


Figure 3. Section of the box used for this experiment and the sample (ETFE membrane of thickness 250 μm).

To remove the absorption added due to the wooden box, the empty box was also measured separately in the reverberation chamber. The resulting absorption value was then subtracted from the absorption coefficient values with sample. The measurement was repeated with a second identical box adjacent to the first one, resulting in a surface area of the ETFE of 4.16m². While the minimum surface area is 10m² for this ISO method, we compared results from a measurement with one (A) and two (B) boxes to check for consistency. (Sluyts et al., 2022)

Membrane architecture: the seventh established building material. Designing reliable and sustainable structures for the urban environment.

2.2. ISO 10140

The ISO10140 method for measuring the sound transmission loss of a building element requires the use of transmission rooms. These are two adjacent rooms that feature an opening between them. The opening allows for a test element to be inserted. The construction of the rooms is such that it allows for the extraction of the transmission spectrum of only the test element in frequencies 50 or 100 Hz and above. The measurement requires a high surface mass of the boundaries of the room and some decoupling of both rooms. In the Laboratory of Acoustics of KU Leuven, the rooms consist of thick (40 cm) walls with a cavity in between them filled with mineral wool. Furthermore, the rooms are resting on springs, so that even low frequencies cannot be transmitted via their foundations. This results in a very high airborne sound transmission loss. The ISO 10140 method calculation is rather simple, it requires subtracting the energy average in the source room from the receiving room and adjusting for the absorption area in the receiving room.

$$R = L_1 - L_2 + 10 \lg \left(\frac{S}{A} \right) \quad (4)$$

Where: L_1 (dB) is the energy average sound pressure level in the source room, L_2 (dB) is the energy average sound pressure level in the receiving room, S (m^2) is the surface area of the test specimen, A (m^2) is the equivalent sound absorption area in the receiving room.

The high sound transparency of ETFE membranes in the low frequencies poses a problem. At the moment of the measurement, the sound energy passes through the membrane(s), reflects on the boundaries of the receiving room and reflects back towards the sample where it is transmitted again. With most traditional building elements such as windows, doors, walls with a minimum surface mass of about 20 kg/m^2 , most of the energy is transferred only in one direction, from the source room (L_1) to the receiving room (L_2).

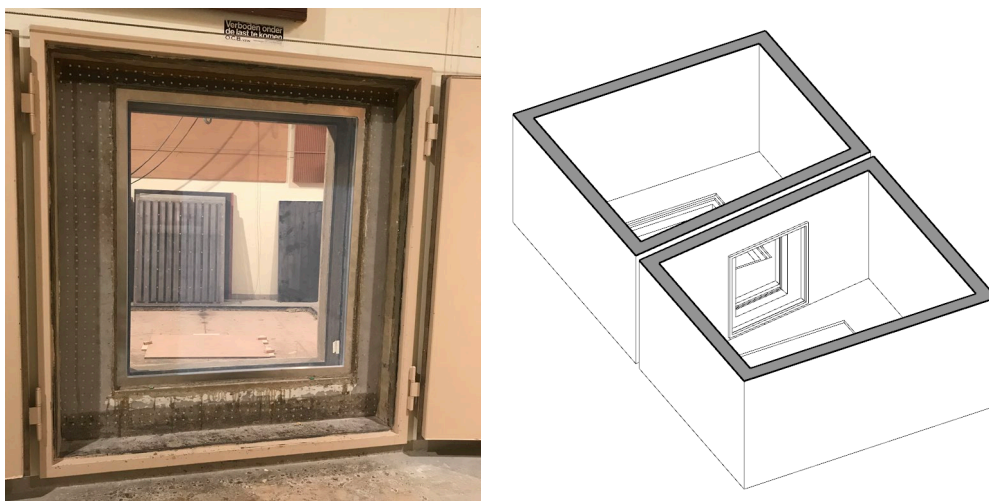


Figure 4. Picture of the test setup in the transmission rooms (view from the source room) (left) and 3d section cut of the transmission rooms with the opening visible (right), the same membrane used in the reverberant room is place in between two rooms here.

Membrane architecture: the seventh established building material. Designing reliable and sustainable structures for the urban environment.

The surface mass of ETFE membranes that are typically used in architecture is less than 0,5 kg/m² (more if multiple layer systems are used). At low frequencies the transmission loss TL is expected to be around 1dB. This reduction is almost negligible. This means that some sound energy will find its way back to the source room, the energy average in the receiving room is therefore underestimated with the conventional ISO140 calculation method. The energy average in the source room is overestimated, resulting in a smaller delta between the two rooms (especially in the low frequencies). The transmission loss through the sample is then virtually higher this way.

As an example: if some other building element has an R value of 10dB, the total sound reduction for the sound coming back to the source room is a little less than 20 dB (the room boundaries of the receiving room do absorb a bit of sound energy, but very little in the low frequencies in practice, some sound energy is also converted into heat due to diffraction around the edge of the opening). A 20 dB difference means that the returning sound energy (that went through the sample twice) only represents 1% of the total energy in the source room (Eq. 6). L_1 (the energy average in the source room) is only very strictly affected. In the case of the ETFE membrane used in this experiment, the sound returning to the source room will only be reduced by about 2dB at low frequencies. This means that the returning sound energy represents still 63% of the total energy (Eq. 7).

$$p_0 = 2 * 10^{-5} Pa \quad (5)$$

$$\frac{p_0 * 10^{60/10}}{p_0 * 10^{80/10}} = 0,01 \quad (6)$$

$$\frac{p_0 * 10^{78/10}}{p_0 * 10^{80/10}} = 0,63 \quad (7)$$

In view of the above, to reveal the “true” transmission loss of this highly transparent material, we have slightly altered the calculation method to reveal the “true” transmission loss of this highly transparent material. We have used two methods; both involve repeating the measurement without any sample in the opening.

By calculating the R value according to ISO10140 (Eq. 4) for the empty opening we obtain the transmission loss of the opening, which is not 0 dB as is often assumed (Martin, 2008). For a relatively small opening (1,53x1,35m in this case), there are some effects at play that prevent all the energy in source room from reaching the receiving room besides the absorption of the boundaries. Among them is the diffraction around the edge of the opening. The R values per third octave band for the small opening the Laboratory of Acoustics at KU Leuven is displayed in the Figure 5.

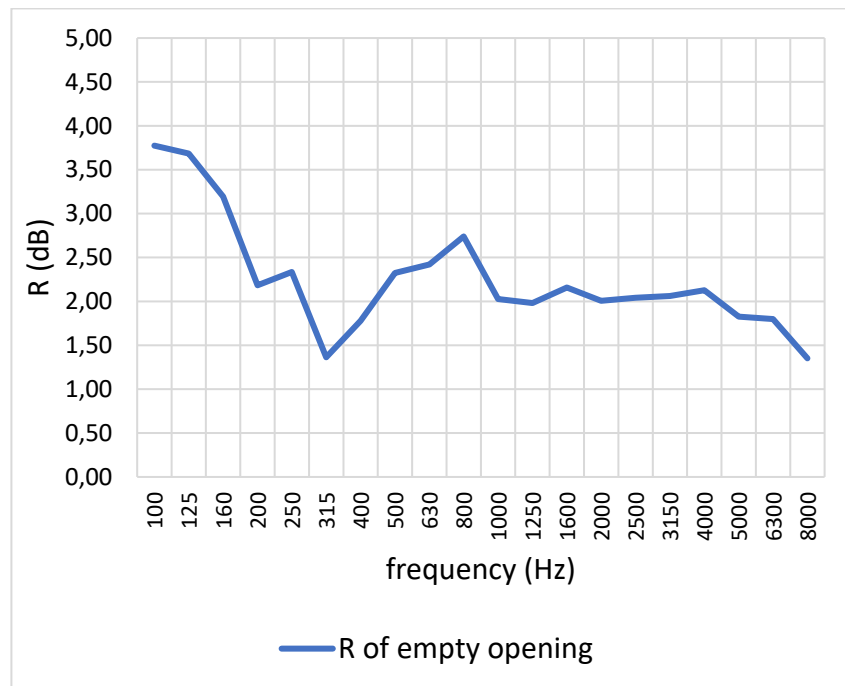


Figure 5 R value of the empty opening in the Laboratory of Acoustics of KU Leuven calculated according to ISO10140

The following step is to subtract the R value with sample (the ETFE membrane) from the R value without a sample.

$$R_{\text{ref empty}} = R_{\text{opening}} - R_{\text{ETFE}} \quad (8)$$

The second approach involves the calculation of the insertion loss (IL). The energy averaged L_p in the receiving room **without** sample should be subtracted from the energy averaged L_p in the receiving room **with** sample.

$$IL = L2_{\text{empty}} - L2_{\text{ETFE}} \quad (9)$$

3. Results & discussion

For both types of measurements, the minimum number of measurement combinations according to the ISO standard has been respected. In both measurements the atmospheric conditions were met and logged carefully to take the effect of air absorption in the rooms into account.

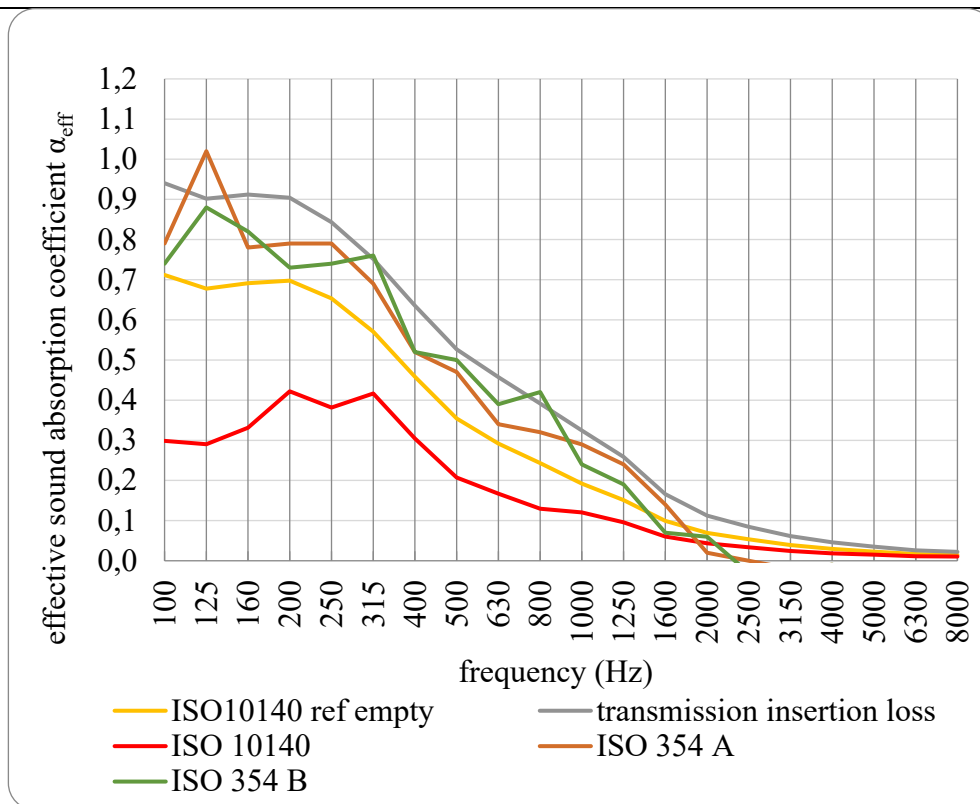


Figure 6 comparison of α_{eff} values from the transmission room measurements and reverberant room measurements.

The α_{eff} spectrum obtained through the adapted ISO354 approach with a box in the reverberant room is relatively high at the low frequencies but goes to below 0 from 2500 Hz onwards, this is an unphysical result. It is not clear what caused this, the effect of the humidity in the room has been accounted for (as per ISO354 requirements), it might be that the sample is too small as the ISO standard suggests (4.16m² instead of a minimum of 10m²), even though both sizes of samples give similar results.

The conventional ISO10140 method yields an absorption coefficient that is relatively low compared to expectations. As mentioned earlier this is due to the energy returning to source room and making the transmission loss virtually higher (and the effective absorption lower).

When using the adapted ISO10140 method (with empty opening as reference) as in (Eq. 4), the calculated transmission loss becomes lower, and the effective absorption becomes higher.

The insertion loss method yields a higher α_{eff} than the two other methods in the transmission room. The transmission loss is the lowest for this method.

The α_{eff} spectrum obtained with the insertion loss method is comparable (slightly higher) to the α_{eff} spectrum obtained in the reverberant room with the ISO 354 box method, except at high frequencies (where the box method yields unphysical results).

3. Conclusion

The effective absorption of a thin ETFE membrane has been determined using two measurement methods, one in the reverberant room and second in transmission rooms. The high transparency of the membrane in the low frequencies required the adaptation of conventional methods (according to ISO354 and ISO10140) to avoid measuring sound energy that passes through the membrane twice or more.

The insertion loss in the transmission rooms and the absorption-based method involving a box in the reverberant room result in a similar α_{eff} between 100 Hz and 2500 Hz. As is described by the theory in the literature, these thin membranes are transparent at low frequencies and more reflective at high frequencies.

References

- De Geetere, L. (2011). *Bouwakoestische prestaties van meerlaagse membraansystemen*.
- Guigou-Carter, C., Sallee, H., & Normand, X. (2008). Acoustic performance of membrane based multilayered systems with improved thermal inertia characteristics. *J. Acoust. Soc. Am.*, 123(5), 3815–3815.
- Hashimoto, N., Katsura, M., Yasuoka, M., & Fujii, H. (1991). Sound insulation of a rectangular thin membrane with additional weights. *Applied Acoustics*, 33(1), 21–43. [https://doi.org/10.1016/0003-682X\(91\)90063-K](https://doi.org/10.1016/0003-682X(91)90063-K)
- Martin, B. (2008, November). What is the Sound Transmission Loss of an Open Window? *Acoustics and Sustainability*. Acoustics 2008, Victoria, Australia.
- Rindel, J. H. (2017). *Sound insulation in buildings*. CRC Press.
- Sakagami, K. (1994). A note on the acoustic reflection of an infinite membrane. *Acustica*, 80, 569–572.
- Sakagami, K., Kiyama, M., Morimoto, M., & Takahashi, D. (1998). Detailed analysis of the acoustic properties of a permeable membrane. *Applied Acoustics*, 54(2), 93–111. [https://doi.org/10.1016/S0003-682X\(97\)00085-6](https://doi.org/10.1016/S0003-682X(97)00085-6)
- Sluyts, Y., Glorieux, C., & Rychtarikova, M. (2022). *Effective absorption of architectural ETFE membranes in the lab*. Nordic Acoustic Association.



tensinantes2023 : TensiNet Symposium 2023 at
Nantes Université

Membrane architecture: the seventh established building material.
Designing reliable and sustainable structures for the urban
environment.

Proceedings of the Tensinet Symposium 2023

TENSINANTES2023 | 7-9 June 2023, Nantes Université, Nantes, France

Jean-Christophe Thomas, Marijke Mollaert, Carol Monticelli, Bernd Stimpfle (Eds.)

Greentexx: Advanced tensile architectural membranes for active and passive cooling of the outdoor & indoor environments via vertical gardens

Benny F.G. PYCKE*, Maxime DURKA^a, Joost WILLE^a

^{*}, ^a Sioen Industries NV

Fabriekstraat 23, 8850 Ardoorie, Belgium

benny.pycke@sioen.com

Abstract

European cities are increasingly suffering from the effects of climate change, and more specifically urban heat stress, as a result of combined heat and drought spells. Greentexx® is an innovative multilayer textile composite to leverage the ample vertical space in cities by mounting cooling vertical gardens. The Greentexx® composite was engineered building on SIOEN's tensile architecture, confectioning, and construction experience. During the Interreg 2-Sea COOL TOWNS project, numerous Greentexx® demonstrators were installed in the public space in municipalities across Belgium and the Netherlands. In parallel, SIOEN conducted experiments to determine the cooling potential of the vertical gardens. Up to 5°C of cooling was observed at 50 cm of the vertical garden compared to a conventional (reference) concrete wall using an array of weather stations. Greentexx® vertical gardens were also observed to be substantially cooler (35 - 39 °C) compared to the naked concrete wall (52 - 57°C) during the day. Because Greentexx® vertical gardens do not heat up as much as regular walls, it is believed that urban heat stress can contribute to mitigating the urban heat island effect when installed in larger numbers across the city.

Keywords: lightweight structures, sustainability, performance, vertical gardens, green wall, urban heat stress

1. Introduction

Cities and its inhabitants are increasingly experiencing the impacts of climate change, and more particularly the associated heat waves, drought spells, and (flash) floods. The health impacts of urban heat- and drought-related phenomena are grouped under the umbrella term, urban heat stress.

Indeed, during heat waves sensitive subpopulations (such as the elderly, children, and infants) are particularly susceptible to the combined effect of excessive heat and dehydration. In several countries peaks in mortality rates are clearly identifiable during periods of heat waves, resulting in excess mortality. Deaths that may not have occurred if the issue had been described better and if adequate measures had been taken to mitigate/counteract the effects of climate change

Membrane architecture: the seventh established building material. Designing reliable and sustainable structures for the urban environment.

and the resulting urban heat stress. During the COOL TOWNS project, the concept of ‘flip-flop distance’ has been proposed by the researchers, a model wherein cooling features (e.g. a park, trees, shade sail, water feature, vertical garden, or their combination) are available within a specific radius, i.e. an easily walkable distance from every spot in the city.

Seemingly in contrast with drought and heat waves, annual storm incidence and severity has increased also as a result of climate change, requiring both centralized and decentralized solutions to slow the flow of stormwater to the sewers, canals, and rivers. Across the European continent numerous instances are reported every year of excessive storms resulting in floods and property damages.

‘Blue-green intervention’ is an umbrella term for all (infrastructural) measures to counteract both urban heat stress and storm-associated floods. Yet, there remains a dearth of information on the individual quantitative contributions these blue-green interventions have to mitigate urban heat stress and stormwater-associated floodings. Such information could be valuable also maximize their impact also, by tweaking intervention-specific parameters. Blue-green interventions may cover horizontal spaces: incl. permeable pavement, green roofs, or water features, but they may also cover vertical spaces: incl. soil-bound climbing plants, and/or vertical gardens/green walls. Vertical gardens are the latest addition to the list of blue-green interventions. They are comprised of: a mounting structure, a substrate material (e.g. Greentexx® by SIOEN), an automated fertigation unit most often with dripper hoses, and perennial plants.

2. The product: properties and installation

Greentexx® (www.greentexx.com) is an evolution of SIOEN’s advanced tensile architecture tarpaulins. Five additional layers of SIOEN textiles have been added to our TA tarpaulins to give it the ability to support plant growth on the long term. As a result, the Greentexx® composite material consists of a PVC-coated tarpaulin, three layers of technical felt, and two layers of PVC-coated mesh fabric. Each individual layer was researched and developed specifically with the application of vertical gardens in mind in terms of strength, water management, rooting efficiency, breathability, and flame retardancy. The composite as a whole is certified B-s2-d0 with a PVC-coated glassfiber fabric and C-s2-d0 with a PVC-coated polyester fabric.

The composite weighs approximately 3.5 kg/m² dw and can hold tenfold its weight in water when it is applied horizontally. It is produced in rolls of 25 lm and a width of 185 cm, of which 165 cm is foreseen with a fixed planting pocket pattern. There are two fixed planting pocket patterns available, namely for 30 plants/m² (15cm x 23cm pockets) or 45 plants/m² (15 cm x 15 cm pockets). Along both edges of the composite (10 cm strips on each end) hook-and-loop fastening tapes are added with the option of adding keders for rapid installation of the composite. As a result, up to 100 m²/day has been reached with two installers on aerial work platforms. The edges to which the hook-and-loop fastening tapes are added are foreseen to house 1-2 dripper lines every 165 cm. In term so each pocket of 15 cm of 23 cm is fed with at least two drippers each.

Greentexx® can be shipped with or without waterproof tarpaulin. With tarpaulin, the product is confectioned with keders to mount the product in dedicated profiles, whereas when shipped without tarpaulins, the product can be stapled or screwed into solid PVC or cement boards.

Membrane architecture: the seventh established building material. Designing reliable and sustainable structures for the urban environment.

The composite with tarpaulin can be tailor-made and planted on site (Fig 1. Middelburg project) or it can be made into standard panels measuring 126 cm x 180 cm and pre-cultivated in a greenhouse (Fig 1. Destelbergen office units), and without tarpaulin it can be shipped as a standard product to be cut and planted on site (Fig 1. Brussels project).

The product is typically fed with nutrient-enriched rainwater using a pump unit approximately 3x per day during about 5-10 minutes. The planted composite uses approximately 3-5 L/m²/day of water via evaporation, whilst the fertigation strategy is steered towards reducing the drainwater to a minimum.



Figure 1: three Greentexx® product and installation types illustrated via three existing projects in Middelburg (with tarpaulin and keder on aluminium profiles), Destelbergen (standard-sized panels with tarpaulin and keder in an aluminium/steel structure), and Brussels (without tarpaulin stapled onto a solid board) (© Sioen Industries)

Greentexx® GTS-FR is mounted using keders in combination with hook & loop strips between the different panels. Alternatively, Greentexx® GTX-FR/BL is mounted by stapling the composite onto solid boards. In both scenarios, hook & loop strips at the top & bottom side of each Greentexx® panel allow the vertical garden maintenance crew to periodically check the proper functioning of the dripper lines by opening the dripper line sleeves that are closed using the hook & loop strips.



Figure 2: Artist impression of a vertical garden composite mounted as a tensile architecture project for shading cars in a parking lot. (Picture ©: VGTex)

Conceptually, the implementation of Greentexx® as saddle or more complex tensile architecture structures is conceivable, like in the example of Figure 2. Yet, particular care should be made to orient the pocket patterns in the correct orientation and to include in the design: dripper hoses to all the upper sections and drainwater guiding folds, sleeves, or profiles to all lower sections. Different sections of the Greentexx® GTX-FR/BL composite (without

Membrane architecture: the seventh established building material. Designing reliable and sustainable structures for the urban environment.

waterproof membrane) should be mounted onto the TA membrane after its mounted on site, or beforehand prior to mounting it on site. To date, this innovative concept is theoretical.

The product is expected to have a lifespan of 10 years or more. To date, the longest running Greentexx® vertical garden has been operated for 7.5 years at SIOEN HQ in Ardoois.

3. Project impressions

Since 2019, Greentexx® (formerly called, GreenTecStyle®) has been utilised in both the indoor and outdoor environment. The composite is typically tailormade, confectioned, and shipped from COATEX (Poperinge, Belgium), though most other tensile architecture confectioning workshops should be able to process the composite for any given project.



Figure 3: examples of the Greentexx® composite when applied to the indoor environment, outdoor environment, indoor as a curved surface, in the public space as part of a structure (e-bike shelter), and as a free-standing structure (a hedge). (© Sioen Industries)

4. Mechanisms for combatting urban heat stress

Greentexx® vertical gardens are able to cool the urban environment via two mechanisms: passive and active cooling. Passive cooling (=shading) is obtained by placing the vertical garden in front of the conventional wall, and inherently shading it from direct sunlight. In combination with a ventilated cavity (spacing between the vertical garden and the conventional wall or insulation) the vertical garden also promotes to keep the wall dry, protects it from UV irradiation, and as such, increases the lifetime of the primary structure. Active cooling is achieved through adiabatic cooling, which is the result of water evaporation from both the vegetation and the felts.

Membrane architecture: the seventh established building material. Designing reliable and sustainable structures for the urban environment.

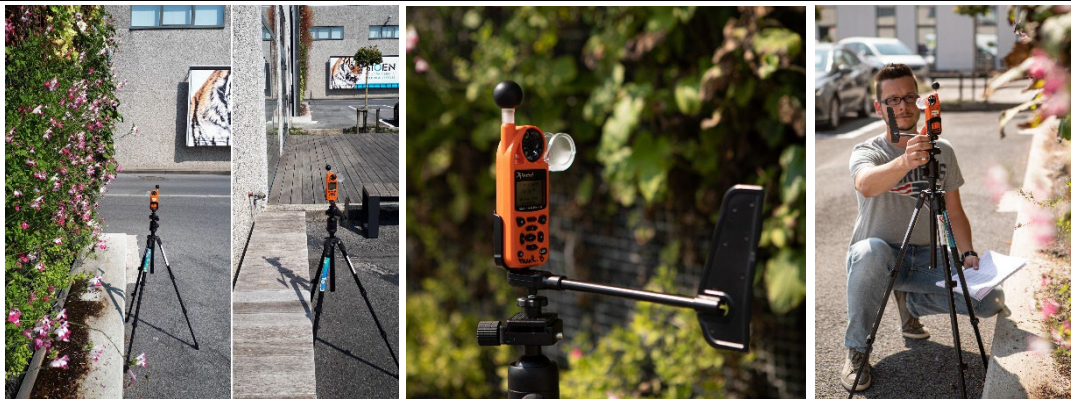


Figure 4. The experimental and control weather station along the vertical garden and conventional wall (left), the Kestrel 5400 weather station on a fixed height and installed with wind vane (middle), and the operator starting the data collection on the weather station (right).

To measure the active cooling potential of Greentexx® vertical gardens, a set-up with three weather stations at three different locations was used (Figure 4). The weather stations used were the Kestrel 54000 Heat Stress Tracker with LiNK installed on tripods at a fixed height from the ground mounted with a wind vane. At all three locations, the weather stations track the WBGT (wet-bulb globe temperature). The WBGT is a heat stress index that is determined to determine the cooling effect of the vertical garden relative to a conventional wall. A weather station takes into account wind direction, wind speed, air temperature, and temperature due to the direct irradiation from the sun at a specific location to calculate the WBGT. One station measures the WBGT at the vertical garden (=experimental location), the second at the convention façade (=control location), and the third in the middle of the parking lot (away from any wall, =reference location). Subsequently, the first two weather stations are placed at different distances from the respective walls to investigate the delta-WBGT, namely at 70 cm, 200 cm, and 350 cm. The reference weather station stays in place elsewhere, far removed from the wall, to investigate the variability in the measurements without the influence of a wall. This third station measures the influence from the pavement (=asphalt) only. The full protocol to determine the heat stress index is available via the Interreg 2-Seas COOL TOWNS project website (www.cooltowns.eu).

During the trials, substantial differences in the WBGT were observed (Figure 5), with up to 5°C lower temperatures observed at 50 cm and the cooling effect of the vertical garden being noticeable even at 200 cm and 350 cm with about 2°C lower temperatures. Closest to the vertical garden the WBGT difference was observed to be lower than at 50 cm. This subdued effect in cooling potential is believed to be due to the wind slowing effect of the vegetation.

Membrane architecture: the seventh established building material. Designing reliable and sustainable structures for the urban environment.



Figure 5. The WBGT decrease observed during the monitoring campaign at two locations (light and dark green) and across different distances (10 – 30 – 50 cm for the first vertical garden and 70 – 200 – 350cm for the second vertical garden).

Additionally, infrared images were taken during the course of the experiment (Figure 6). These images clearly show the differences in temperatures between asphalt (55 - 67°C), the naked concrete wall (52 - 57°C), and the vertical garden (35 - 39 °C).



Figure 6. Infrared images of a vertical garden installed at SIOEN Ardoorie, which illustrates the temperatures differences measured between the cars, asphalt (55 - 67°C), the naked concrete wall (52 - 57°C), and the vertical garden (35 - 39 °C).

4. Conclusion

The Greentexx® composite was deployed in a number of demonstrator projects in Belgium and the Netherlands during the Interreg 2-Seas COOL TOWNS project. During *in situ* experiments Greentexx® vertical gardens were shown to reduce the heat stress index (WBGT) with up to 5°C at 70 cm in front of the vertical garden compared to a conventional (reference) concrete wall during the day. Greentexx® vertical gardens were also observed with infrared cameras to be substantially cooler (35 - 39 °C) compared to the naked concrete wall (52 - 57°C) during the day. Because Greentexx® vertical gardens do not heat up as much as regular walls, it is believed that urban heat stress can contribute to mitigating the urban heat island effect when installed in larger numbers across the city.

Membrane architecture: the seventh established building material. Designing reliable and sustainable structures for the urban environment.

Acknowledgements

The research was conducted with the support of the Interreg 2-Seas programme in the frame of the COOL TOWNS project.

Avoiding identifying any of the authors prior to peer review.

References

www.cooltowns.eu

www.greentexx.com

www.sioen.com

